Genomic Copy Number Alterations In Radiogenic Breast Cancer

A thesis submitted in part requirement for the

degree of Doctor of Philosophy

Mark Alfred Wade

Northern Institute for Cancer Research,

Faculty of Medical Sciences,

Newcastle University

March 2012

Abstract

The aim of this study was to elucidate the underlying molecular genetic mechanisms of radiation-induced breast carcinogenesis. Younger women are more at risk of developing breast cancer than older women following radiation exposure. Circulating oestrogen levels are highest during adolescence and early adulthood and oestrogen has a known transforming effect on breast epithelial cells. One hypothesis suggests that radiation and oestrogen synergise to drive breast cell transformation. There are currently no known genetic markers of radiogenic breast cancer. In order to investigate genetic alterations associated with radiogenic breast cancer *in vitro* models of radiation-induced breast epithelial cell transformation was developed.

The immortalised, non-transformed breast epithelial cell line MCF-10A was exposed to fractionated doses of X-rays in the presence or absence of additional oestrogen. Radiation-treated cells displayed several phenotypic changes some of which provided evidence of cell transformation, including loss of contact inhibition and change to mesenchyme cell morphology. Genomic analysis of radiation treated cells using high-density polymorphism arrays identified a gene deletion of the *POU2F1* transcription factor and amplification of the *c-MYC* proto-oncogene. POU2F1 has a role in cellular stress response and mediates DNA damage response through interactions with BRCA1. Amplification of *c-MYC* has previously been identified in breast cancers of survivors of the atomic bombs during World War II. Genetic alteration in *POU2F1* and *c-MYC* may therefore be linked to radiation-induced breast cell transformation. Changes in gene copy-number were confirmed by fluorescent in situ hybridisation (FISH) and alterations in protein expression by western analysis.

Gene copy number and expression of *POU2F1* and *c-MYC* was investigated in a cohort of radiogenic and sporadic breast cancer tissue samples by FISH analysis and immunohistochemistry. Expression of c-MYC was higher in radiation-induced breast cancers compared to sporadic breast cancers ($p = 0.002$), as was the mean number of copies of *c-MYC* ($p = 0.030$). Loss of expression of POU2F1 was identified in one of 18 radiation-induced breast cancers but was not observed in sporadic breast disease (0/33).

In summary, a cell model of radiation-induced breast cell transformation identified *POU2F1* deletion and *c-MYC* amplification as putative markers of transformation, which were subsequently identified in primary tissue samples, suggesting a role for these alterations in the development of radiogenic breast cancer.

Acknowledgements

Firstly I would like to thank my supervisors Dr Felicity May and Dr James Allan for their expertise and fantastic advice and support in both academic and personal aspects of my life throughout this project. I would also like to thank my colleagues, past and present, in both the Molecular Carcinogenesis group and Solid Tumour Target Discovery group: Dr Claire Worrall, Dr Zoë Davison, Dr Brendan Luey, Dr Nahed Hawsawi, Dr Ahmed Roshdi, Dr Nicola Sunter, Dr Sarah Fordham and Victoria Forster. I would also like to thank Dr Lisa Russell and Dino Masic for all their help in teaching me FISH procedures, Dr Vikki Rand for helping me with bioinformatic analysis of the data I generated, Anna Long for her immonhistochemical expertise and Dr Steve Crosier from the cellular pathology department in the RVI. I would also like to thank Dr Chris Bacon for his timely advice throughout my project, Dr Nick Bown, David Rowe and Chris Lowe from the Northern Genetics Service and all the members of the Northern Institute for Cancer Research who provided advice and help throughout my PhD.

I would also like to greatly thank my family and friends for their support and love throughout my PhD. In particular my wife Rachel who provided the greatest motivation to keep going when times were tough, and the unwavering support of my Mum and Dad. I could not have done this without any of you.

Finally I would like to thank the Medical Research Council for providing the funding which made this project possible.

Table of contents

List of figures

List of tables

Abbreviations

8-oxo-G	8-oxo-guanine
A	Adenine
aCGH	Array-comparative genomic hybridization
ADP	Adenosine diphosphate
AML	Acute myeloid leukaemia
ANOVA	Analysis of variance
AP	Apurinic/apyrimidinic
AS	Angiosarcoma
AVL	Atypical vascular lesion
BAC	Bacterial artificial chromosome
BC	Breast cancer
BCA	Bicinchoninic acid
BER	Base excision repair
BFB	Breakage fusion bridge
BP	Biological Process
bp	base pair
BSA	Bovine serum albumin
C	Cytosine
CC	Cellular component
cDNA	Complementary deoxyribonucleic acid
cGγ	Centi-gray
ChIP	Chromatin immunoprecipitation
Chr	Chromosome
CNV	Copy number variant
CRUK	Cancer research United Kingdom
DAPI	4',6-diamidino-2-phenylindole
dATP	Deoxyadenosine triphosphate
DAVID	Database for Annotation, Visualization and Integrated Discovery
DCC-CS	Dextran coated charcoal-treated calf serum
DCIS	Ductal carcinoma in situ
dCTP	Deoxycytidine triphosphate
del	Deletion
der	Derivative
dGTP	Deoxyguanosine triphosphate
DMEM	Dulbeco's modified eagles medium
DMSO	Diemthyl sulphoxide
DNA	Deoxyribonucleic acid
dNTP	Deoxyribonucleotide
DSB	Double strand break
dTTP	Deoxythymidine triphosphate
dup	Duplication
dUTP	Deoxyuridine triphosphatate
EDTA	Ethylenediaminetetraacetic acid
EGF	Epidermal growth factor

EMT	Epithelial to mesenchymal transition
ER (α,β)	Oestrogen receptor (alpha, beta)
ERR	Excess relative risk
FACS	Flow activated cell sorting
FCD	Fibrocystic disease
Fig.	Figure
FISH	Fluorescent in situ hybridisation
G	Guanine
GO	Gene ontology
Gγ	Gray
HCl	Hydrochloric acid
HJ	Holiday junction
HL	Hodgkin lymphoma
HPA	Health protection agency
HR	Homologous recombination
HRP	Horse radish peroxidase
i	Isochromosome
IDC	Infiltrating ductal carcinoma
IHC	Immunohistochemistry
ILC	Infiltrating lobular carcinoma
Kb	Kilobase
kDa	Kilodalton
kV	Kilovolts
LB	Luria broth
LOH	Loss of heterozygosisty
mA	Miliamps
Mb	Megabase
miRNA	Micro ribonuleic acid
MMR	Mis-match repair
mRNA	Messenger RNA
NAHR	Non-allelic homologous recombination
NCBI	National centre for biotechnology information
NHEJ	Non-homologous end joining
NOS	Not specified carcinoma
OH	Hydroxyl
orf	Open reading frame
PBS	Phosphate buffered saline
PI	Propidium iodide
PR	Progesterone receptor
PRF	Phenol red free
QC	Quality control
qPCR	Quantitative real time polymerase chain reaction
qter	Q arm terminus
RAD(*n*)	Radiogenic breast cancer tissue sample
RIGI	Radiation-induce genetic instability

RIPA	Radioimmunoprecipitation assay
RNA	Ribonucleic acid
RNAi	RNA interference
ROS	Reactive oxygen species
RPM	Revolutions per minute
RT	Reverse transcription
SDS	Sodium dodecyl sulphate
SEM	Standard error of the mean
SPO(*n*)	Sporadic breast cancer tissue sample
SSC	Sodium citrate
T	Thymine
t	translocation
TBS	Tris-buffered saline
TE	Tris-EDTA
TEMED	Tetramethylethylenediamine
TNM	Tumour, node, metastasised
UV	Ultra-violet
v/v	volume / volume
w/v	weight / volume
w/w	weight / weight
x g	Gravity

Chapter 1: Introduction

1.1 Cancer

1.1.1 Cell transformation

The malignant transformation of normal cells results from genomic mutations. The accumulation of these mutations affects protein activity and causes the acquisition of altered phenotypes. Altered phenotypes include the ability to: evade apoptosis, sustain proliferative signalling, be insensitive to anti-growth signals, invade and metastasise, have limitless replicative potential, induce angiogenesis, modify cellular metabolism and avoid immunological destruction (Hanahan and Weinberg, 2011). During transformation cells acquire characteristics which facilitate the acquisition of these phenotypes, such as genetic instability, which increases the occurrence of mutations and thereby increases the acquisition of oncogenic mutations; and immune system-induced inflammation, which exposes cells to proteins and enzymes that promote cell growth and survival and to mutagenic chemicals that induce mutations (Hanahan and Weinberg, 2011).

Genes that encode proteins where altered function predisposes towards cancer can be divided into two groups, oncogenes and tumour suppressor genes. Oncogenes are genes which promote cell transformation. Proto-oncogenes are normal genes which become oncogenes due to activating mutations or increased expression. For example, point mutations in the *RAS* family of genes can cause inappropriate or constitutive activation of the encoded RAS proteins which promote tumourigenesis (Pylayeva-Gupta *et al.*, 2011). Amplification or dysregulation of *c-MYC* results in protein over-expression and has been detected in many cancers (Meyer and Penn, 2008), and a chromosome translocation which creates the constitutively activated fusion protein BCR-ABL in chronic myeloid leukaemia promotes tumourgenesis (Goldman, 2010). Mutations that convert proto-oncogenes to oncogenes are often dominant.

Tumour suppressor genes often encode proteins involved in response to cellular stress or DNA damage and that regulate correct progression through the cell cycle. Loss of the gene product through inactivating mutations or gene deletions can lead to unregulated cell growth and accumulation of DNA mutations. Inactivating mutations in tumour suppressor genes are often recessive, as described in Knudson's "two hit hypothesis"

(Knudson, 1971). Notable tumour suppressor genes include *P53*, *RB* and *APC* (Sherr and McCormick, 2002; Lane and Levine, 2010; Minde *et al.*, 2011).

Genetic alterations which inactivate DNA repair mechanisms are also important in progression to cancer. An inability to repair DNA damage leads to genomic instability and accumulation of transforming mutations. Mutations to genes involved in base excision repair (BER), mismatch repair (MMR) and homologous recombination (HR) have all been implicated in cancer development (Mitchell *et al.*, 2002; Shinmura *et al.*, 2004; Allan and Travis, 2005; Helleday, 2010).

1.1.2 Causes of cell transformation

Cancer can be caused by agents which are directly mutagenic and also by mechanisms that increase the chance of accumulating mutations. Some cancers are hereditary and develop because the affected individual has an increased susceptibility due to the inheritance of an inactive tumour suppressor gene allele. For example, the risk of developing breast cancer by the age of 70 in individuals with hereditary mutations of *BRCA1* or *BRCA2* has been reported to be 65% and 45%, respectively (Antoniou *et al.*, 2003).

Chemicals and other exposures that cause somatic DNA mutations are called mutagens, and many of these are carcinogenic. Smoking is highly correlated with increased risk of lung cancer because tobacco contains several chemical carcinogens (Pfeifer *et al.*, 2002). For example, enzymatic metabolism of benzo(a)pyrene, which is found in tobacco smoke, produces benzo(a)pyrene diol epoxide which can bind covalently to DNA, disrupt DNA replication and introduce mutations.

Ionising radiation is also a mutagenic carcinogen. Ionising radiation causes DNA damage of which the most toxic is double stranded DNA breaks. Most DNA damage is repaired or if not, the damage can result in cell death or mutation. Cell survival and incorrect repair of the DNA damage can lead to chromosome aberrations such as deletions, duplications and translocations (Cornforth, 2006; Natarajan and Palitti, 2008). The effect of ionising radiation will be discussed in more detail in Sections 1.3 and 1.4.

Some carcinogens are not mutagenic via the direct induction of DNA damage. For example, some hormones stimulate cell proliferation which increases DNA replication and the likelihood of errors in replication and reduces the chance of effective DNA

repair. One of the best known examples of this phenomenon is that increased oestrogen levels increase breast cancer risk (Yager and Davidson, 2006).

Infectious agents such as viruses can also cause cancer. A viral genome can be inserted into a host genome which may alter expression of genes which may have a transforming effect. A well-known example is human papillomavirus which is causative in almost all cases of cervical cancer. The human papillomavirus genome contains the *E6* and *E7* genes which are known to act as oncogenes and can integrate into the host genome (Ganguly and Parihar, 2009).

1.2 Breast cancer

1.2.1 Normal breast structure

The breast is made up of a number of lobes and milk ducts. The lobes contain lobules which comprise clusters of alveolar sacs that contain lacocytes that synthesise milk. The lobules are connected to small ducts which join to larger ducts and converge to one main duct per lobe called a lactiferous duct which transports the milk to the nipple (Ramsay *et al.*, 2005). Breast epithelial cells, which are surrounded by connective and adipose tissue, are responsive to hormones, including oestrogen. Breast development is stimulated at the onset of puberty and develops further during pregnancy and lactation.

1.2.2 Breast cancer overview

Breast cancer is the most common cancer in women in the UK and accounted for 31% of all cancer cases in 2008 (Office for National Statistics, Edition: MB1 39). The life-time risk of developing breast cancer for a woman is 1 in 8. The risk of developing breast cancer increases with age and in 2008 81% of cases occurred in women over 50 years old (Office for National Statistics, Edition: MB1 39). Breast adenocarcinoma develops from breast epithelial cells. Non-invasive breast adenocarcinoma includes ducal carcinoma *in situ* and lobular carcinoma *in situ*. Eighty five per cent of invasive adenocarcinomas are described as ductal and 15% are lobular.

1.2.3 Breast carcinogenesis

The majority of breast cancers develop in patients without a family history of breast cancer (sporadically), but approximately 10% have a hereditary contribution (Deng, 2006). Approximately 25% of hereditary breast cancer cases are due to germ-line

mutations in the *BRCA1* or *BRCA2* genes (Weischer *et al.,* 2007; Desrichard *et al.,* 2011). BRCA1 is involved in transcriptional regulation and cell cycle checkpoint regulation following DNA damage and both BRCA1 and BRCA2 are directly involved in homologous recombination repair of DNA double strand breaks (Yoshida and Miki, 2004; Cousineau *et al.,* 2005; Deng, 2006; Rosen *et al.,* 2006). Loss of function of BRCA1 or BRCA2 results in increased genetic instability and the accumulation of genetic mutations which can lead to breast cancer. Low penetrance germ-line mutations in genes such as *CHEK2, PALB2* and *BPIR1* also increase breast cancer susceptibility and cooperate with other hereditary factors to cause breast cell transformation (Seal *et al.,* 2006; Rahman *et al.,* 2007; Weischer *et al.,* 2007; Desrichard *et al.,* 2011).

Numerous studies have demonstrated that high concentrations of circulating oestrogens increase breast cancer risk. Increased breast cancer risk was identified in post-menopausal women with high circulating concentrations of oestrogen and androgens, which can be converted to oestrogen by aromatase. Women who are obese are also at increased risk of developing breast cancer, possibly because of the production of oestrogen by aromatases in the adipose tissue of the breast (Key *et al.,* 2002; Key *et al.,* 2003; Onland-Moret *et al.,* 2003; Walker *et al.,* 2011). Early menarche and late menopause are also associated with increased breast cancer risk and a recent meta-analysis concluded that increased circulating levels of oestrogen in pre-menopausal women increased breast cancer risk (Key *et al.,* 2003; Walker *et al.,* 2011).

The association between exposure to exogenous oestrogen, such as oestrogens in the contraceptive pill, and breast cancer risk has also been studied. A comprehensive analysis by The Collaborative Group on Hormonal Factors in Breast Cancer (CGHFBC) of over 150,000 individuals in 1996 identified that the relative risk (R.R) of developing breast cancer was significantly elevated for current oral contraceptive users compared to individuals who had never taken the pill (R.R = 1.24). The risk decreased with the increased number of years since ceasing to take the contraceptive pill, and no excess risk was observed in individuals who had stopped taking the contraceptive pill more than 10 years previously. Modest increases in breast cancer risk have also been observed in more recent studies (Kumle *et al.,* 2002; Kahlenborn *et al.,* 2006), and Dumeaux *et al.* (2003) observed an association between risk and cumulative exogenous oestrogen dose received by taking the contraceptive pill. However, there have also been numerous studies which have observed no increase in breast cancer risk with oral contraceptive usage (Marchbanks *et al.,* 2002; Vessey and Painter, 2006; Hannaford *et*

al., 2007), and therefore the association between exogenous exposure to oestrogen in the form of oral contraceptives and breast cancer risk is not conclusive.

As well as oestrogen, exposure to other circulating hormones is putatively carcinogenic. For example, insulin and insulin-like growth factor-1 (IGF-I) increases proliferation of normal and transformed breast epithelial cells, promotes mammary tumour growth in animal models and has been associated with increased breast cancer risk (Chappell *et al.*, 2001; Gunter *et al.*, 2009). Higher circulating insulin concentrations in obese women may contribute to the overall increased breast cancer risk in these individuals (Gunter *et al.*, 2009).

1.2.4 Breast cancer classification and treatment

Breast cancers are classified in a number of ways. Classification can help predict disease prognosis and patient management. The TNM classification system describes the clinical stage by tumour size (T), whether it has spread to the lymph nodes (N) and whether the tumour has metastasised (M). The Bloom and Richardson Grade classifies a tumour by histology (Bloom and Richardson, 1957), which includes criteria such as the proportion of ductal structures, the mitotic index and the nuclear morphology. High grade is associated with poor prognosis.

Treatment of breast cancer depends on many factors that include the clinical stage and histological classification of the tumour. Surgery is still the primary treatment option for most breast cancers, and can be a lumpectomy in which the tumour is resected or mastectomy in which the entire breast is resected. Axillary lymph nodes are also removed in many cases to determine if the disease has spread beyond the breast or to remove dissociated disease. Patients are also often treated with adjuvant chemotherapy or radiotherapy. Chemotherapy is often a combination of agents and the choice of chemotherapy depends on the status of the cancer and the age and health of the patient.

Drugs are available to treat breast cancer depending on the molecular classification of the tumour. One of the most important classifications with regard to treatment choice is the receptor status of the cells. Three important receptors that can be expressed by breast cancer cells are the oestrogen receptor (ER), the progesterone receptor (PR) and HER2.

Cells which express the oestrogen receptor may be oestrogen-dependant and may benefit from treatment with anti-oestrogens such as tamoxifen. Tamoxifen is a competitive antagonist that competes with oestrogen for binding to the oestrogen receptor and thereby inhibits oestrogen activation (Jordan, 2006). Progesterone receptor expression is induced by oestrogen and therefore positive PR expression status can be used to identify patients who will benefit from anti-oestrogen therapy (Mohsin *et al.*, 2004). HER2 is a membrane bound tyrosine kinase which is a member of the ERBB family of tyrosine kinase receptors. *HER2* is an oncogene which causes cell proliferation, angiogenesis and cell invasion when over-expressed relative to normal breast epithelial cells (Menard *et al.*, 2003; Menard *et al.*, 2004). HER2 over-expression occurs in 25-30% of breast cancers and is treated with Trastuzumab (Herceptin); a monoclonal antibody which inhibits HER2 (Spector and Blackwell, 2009). Cancers which do not have any of these receptors are referred to as triple-negative breast cancers and have a poor prognosis due in part to limited options for receptor- targeted therapy (Dent *et al.*, 2007).

Treatment can also depend on somatic genetic mutations. For example, poly ADP ribose polymerase (PARP) inhibitors have been developed for the treatment of cancers with somatic *BRCA1* or *BRCA2* mutations. PARP inhibitors lead to the accumulation of DNA strand breaks by inhibition of base excision repair. In *BRCA1* and *BRCA2* wild type cells these breaks are repaired by homologous recombination. Cancer cells with acquired *BRCA1* or *BRCA2* mutations have defective homologous recombination and therefore cannot repair the strand breaks which results in cell death (Weil and Chen, 2011).

Breast cancers have also been classified into subtypes based on their DNA expression profiles. Detailed molecular and genetic classification of tumour sub-types could lead to a more detailed analysis of prognosis and treatment options (Jonsson *et al.*, 2010). Five molecular subtypes of breast cancer were defined and shown to correlate with overall survival (Perou *et al.*, 2000; Sorlie *et al.*, 2003; Geyer *et al.*, 2009). These molecular subgroups include: *luminal A breast cancers*, which have an expression profile similar to normal luminal epithelial cells of the breast, are ER-positive, express high levels of oestrogen responsive genes and are of low grade; *luminal B breast cancers*, which share similar characteristics to luminal A breast cancers but are more proliferative, are of higher grade and have a poorer prognosis; *basal-like breast cancers*, which are always ER-negative, are very often triple-negative for hormone receptor expression, express

genes characteristic of basal epithelial cells, are of high grade, are highly proliferative and often share characteristics with tumours that arise due to *BRCA1* germ-line mutations; *normal-like breast cancers*, which have high expression of genes associated with basal epithelial cells and adipose cells, low expression of genes associated with luminal epithelial cells and often clusters with normal breast cells during expression profiling; and *HER2 enriched breast cancers*, which are usually ER-negative, over-express HER2 and genes associated with the HER2 pathway, often have *HER2* gene amplification and are an aggressive breast cancer subtype.

1.3 Ionising radiation

Ionising radiation is biologically harmful and is a carcinogen. The mechanisms by which ionising radiation causes biological damage and the effect this damage can have on cellular macromolecules will be discussed in section 1.4; however the basic physics of ionising radiation, sources of its exposure to the population and epidemiological evidence of its carcinogenic effect will first be discussed.

1.3.1 Forms of ionising radiation

Ionising radiation has the required energy to remove electrons from an atom or molecule thereby producing a positively charged ion. Ionising radiation can be in the form of particles, such as: α particles (helium nuclei), β particles (electrons and positrons), protons, neutrons and other heavy ions; or high energy photons, such as gamma rays and x-rays.

Different types of ionising radiation react differently when they come into contact with a medium (Fig. 1.1). Charged particles such as α particles and heavy ions ionise molecules along the path that they are travelling. As they ionise atoms they lose energy and the linear distance that the particle travels before all energy is lost is defined as the range of the particle. The range of α particles and heavy ions is relatively short.

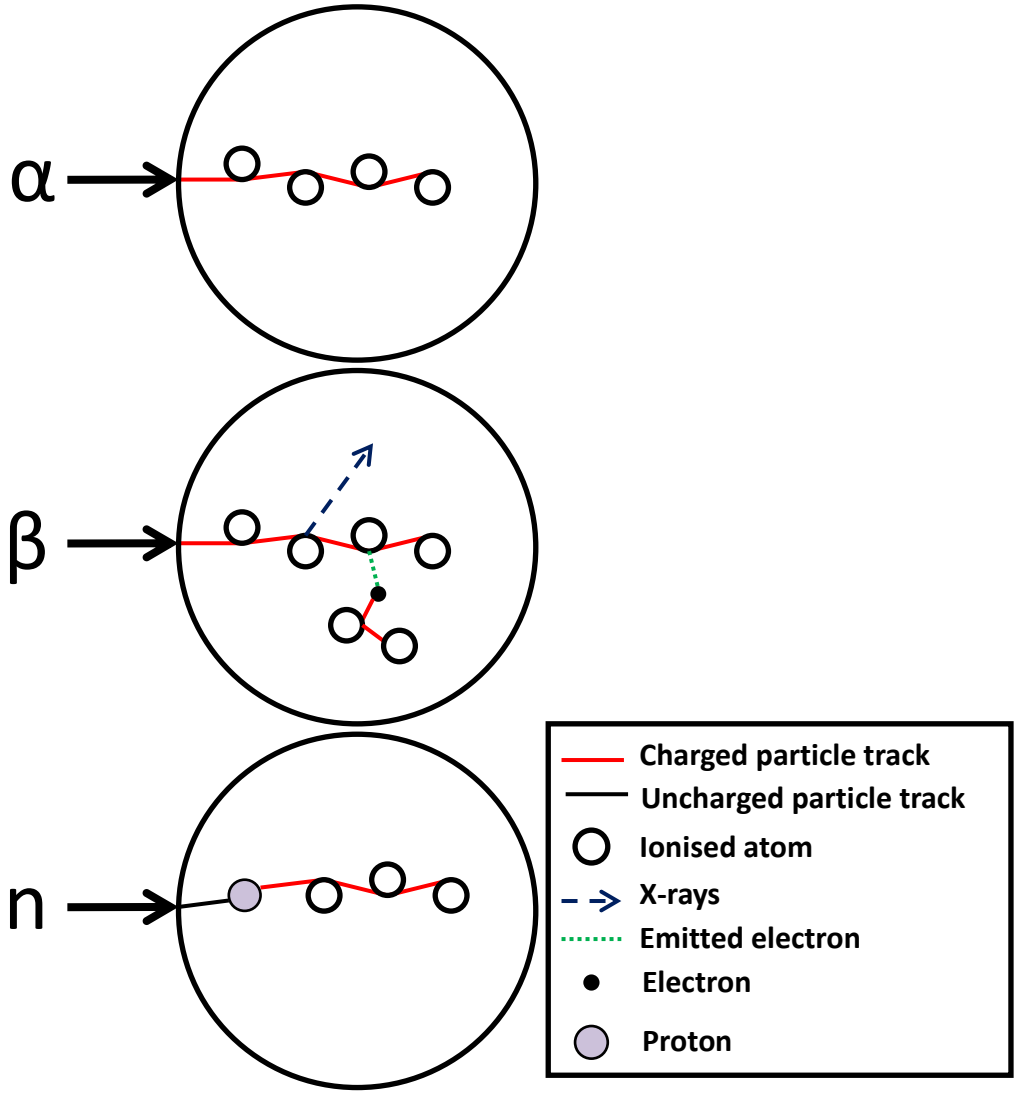

Figure 1.1 Mechanisms of particle ionising radiation.

α, β and neutron (n) particles each move through a medium differently to cause ionisation of atoms or molecules. The figure shows interactions between atoms and different ionising particles as they move through a medium. (N.B figure is not to scale). α particles ionise atoms along its particle track. β particles can release breaking radiation in the form of X-rays as they decelerate when approaching a nucleus and can also eject orbiting electrons from a nucleus, that can go on to ionise other atoms in the medium. Neutrons are uncharged particles which can collide with protons creating an ionising charged particle.

Gamma rays and x-rays (photons) do not ionise along a linear path of trajectory and the range of gamma and X-ray radiation is relatively long. There are 3 ways in which high energy photons ionise when passing through matter (Fig. 1.2): the photoelectric effect, compton scattering and pair production (Simpkin, 1999; Hubbell, 2006).

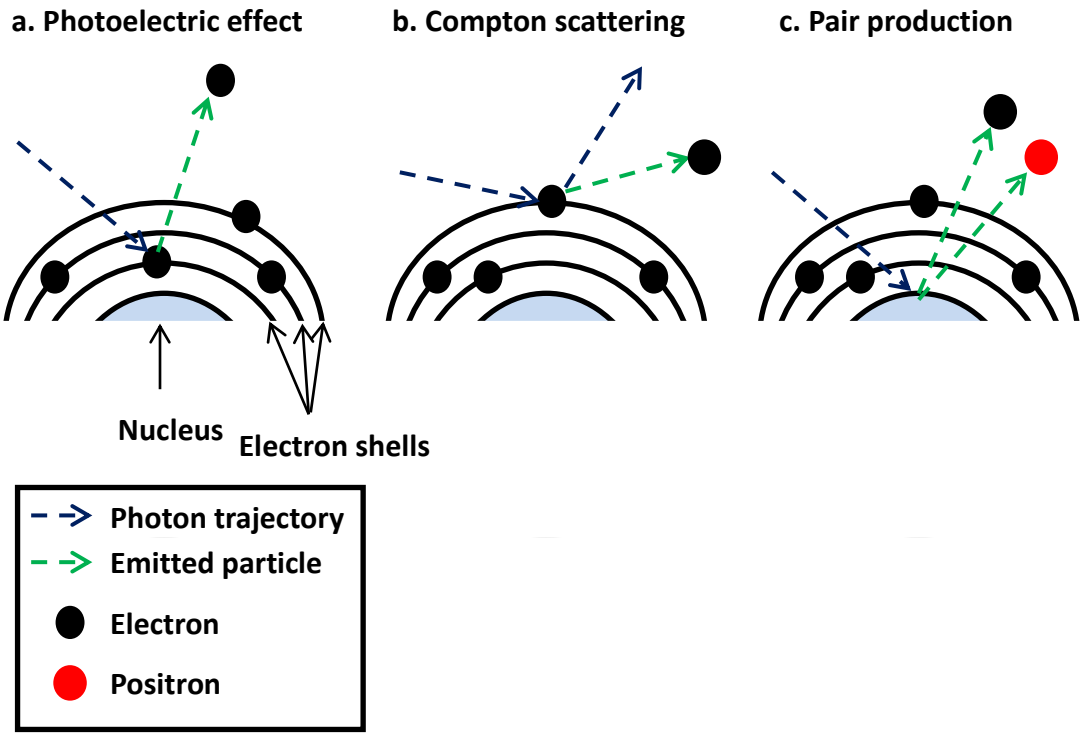

Figure 1.2 Photon ionisation.
High energy photons (e.g. gamma and X-rays) ionise atoms via 3 main mechanisms: **(a)** the photoelectric effect, whereby a photon collides with a tightly bound electron in an atom (an inner shell electron), passes all of its energy to the electron and therefore ceases to exist. The electron escapes its nucleus and ionises molecules around it, acting as a charged particle (a photoelectron). **(b)** compton scattering, whereby a photon collides with a weakly bound electron in an atom (an outer shell electron). The electron is ejected from the nucleus with the energy transferred to it from the photon and can ionise molecules around it. The photon is deflected from the collision and continues its path through the medium in a different trajectory with reduced energy. **(c)** pair production, whereby a photon collides with the nucleus of an atom giving up all of its energy producing an electron and a positron. The electron and positron then act as ionising charged particles within the medium.

Radiation can be defined by the type of particle that constitutes the ionising radiation but also by the type of energy transferred during the radiation. High-linear-energy-transfer (LET) radiation (e.g. α particles, heavy ions and neutrons) releases a high amount of energy along the trajectory (particle track) of the ionising particle resulting in dense regions of ionised atoms (Fig. 1.3a). Low-LET radiation (e.g. gamma rays and x-rays) releases energy along the particle track more sparsely and therefore ionisation of atoms occurs more evenly throughout a medium (Fig. 1.3b). The dose of radiation relates to the total amount of energy deposited within a medium.

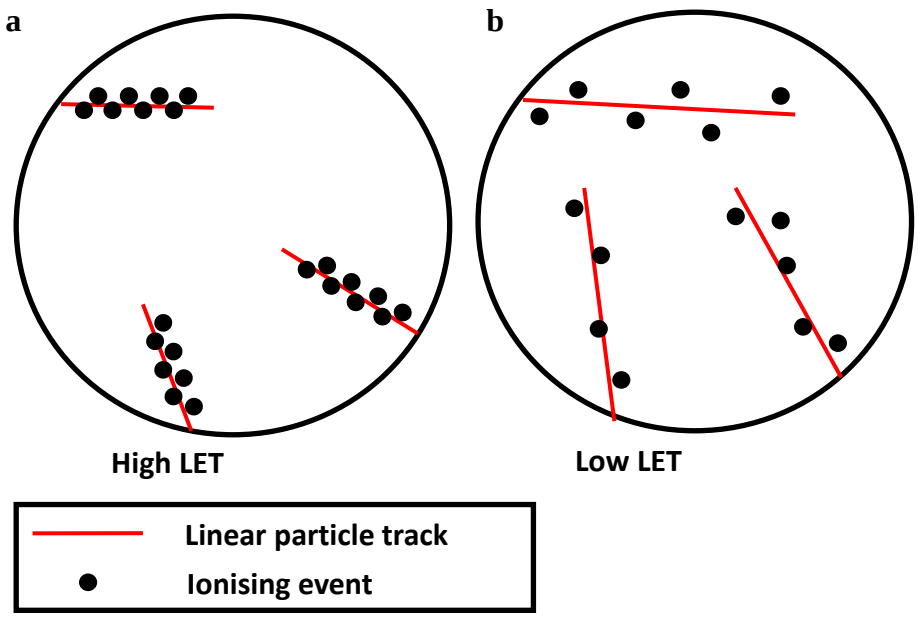

Figure 1.3 High and low-linear-energy transfer (LET).
(a) High-LET radiation induces a high frequency of ionising radiation events along the particle track resulting in dense regions of ionisation within a medium. **(b)** Low-LET radiation releases energy more sparsely along the particle track. As a consequence, low-LET radiation travels farther than high-LET radiation and ionisation occurs more homogenously through the medium.

1.3.2 Sources of ionising radiation

Sources of ionising radiation exposure to the general population can broadly be put into two categories: natural and artificial. In the U.K 84% of the annual ionising radiation exposure to the population is from natural sources and 16% from artificial sources (www.ukradon.org) (Fig. 1.4).

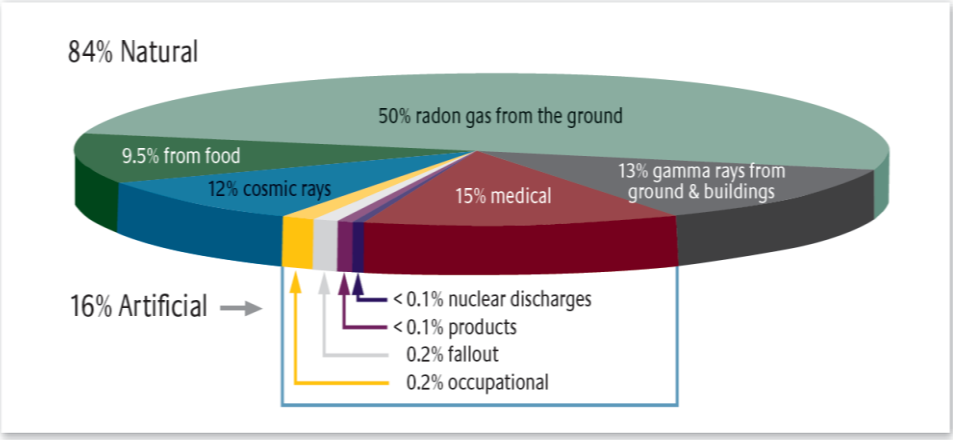

Figure 1.4 Sources of human exposure to ionising radiation in the U.K.
Average annual radiation dose exposed to the UK population. Figure obtained from www.ukradon.org.

Natural sources of ionising radiation exposure include cosmic rays and the external and internal exposure to naturally occurring molecules undergoing radioactive decay (UNSCEAR 2008). Radioactive decay is the spontaneous, random process by which the nucleus of an unstable atom (the radionuclide) loses energy in order to convert to a more stable form. The energy that is lost during this process is ionising radiation.

Cosmic radiation originates from outer space and consists mainly of protons, α particles, heavy ions and electrons. Collisions between these particles and atoms in the atmosphere produce smaller charged particles (secondary radiation) which in turn can interact with atomic nuclei in the atmosphere to produce unstable radionuclides. Cosmic radiation exposure is greater at higher altitudes and at geographical locations closer to the magnetic poles (UNSCEAR 2008; UNSCEAR 2002).

External exposure to ionising radiation originates from gamma ray emission of radionuclides in the soil and in building materials. Internal exposure comes from inhalation and ingestion of radionuclides (UNSCEAR 2008; UNSCEAR 2002). Inhalation of radon gas is a major source of internal exposure to ionising radiation. Radon-222 and radon-220 are gaseous radioactive decay products of the thorium radionuclide and uranium radionuclide series respectively, which are present in soil and

rocks. When radon-222 and radon-220 particles are inhaled they attach to the bronchial walls of the lungs and emit predominantly α particles (UNSCEAR 2008; UNSCEAR 2002). When radon gas is emitted indoors, usually through the floor from the rocks and soil beneath, the build-up of radon gas can cause a significant increase in internal ionising radiation exposure. Radon gas levels are not uniform and depend on the concentration of uranium radionuclides in rocks and soil and the abundance of porous soil and rock deposits in a given area. Maps of radon gas levels in homes in England and Wales illustrate the difference between different geographical areas (Fig. 1.5).

Therapeutic and diagnostic medical radiation and environmental pollution due to nuclear weapons testing, nuclear power plants and fallout from nuclear accidents are examples of artificial sources of radiation exposure (UNSCEAR 2008; UNSCEAR 2002).

X-rays are generated and used for diagnostic purposes in medicine. X-rays penetrate soft tissues and bone to different degrees so can produce images of internal structures on photographic film. (UNSCEAR 2008; UNSCEAR 2002). Ionising radiation is also used to treat cancer. Beams of X-rays, gamma rays or electrons are used to target specific tissues to give lethal doses of irradiation to malignant cells. (UNSCEAR 2008; UNSCEAR 2002).

Artificial nuclear reactions used for power generation and in nuclear bombs are also a source of artificial radiation exposure; however the relative effect of these exposures on the general public is small (UNSCEAR 2008; UNSCEAR 2002). There have however been accidents at nuclear power plants, notably Chernobyl in 1986 and more recently Fukishima in Japan, which released relatively large amounts of radionuclides into the local environment and beyond.

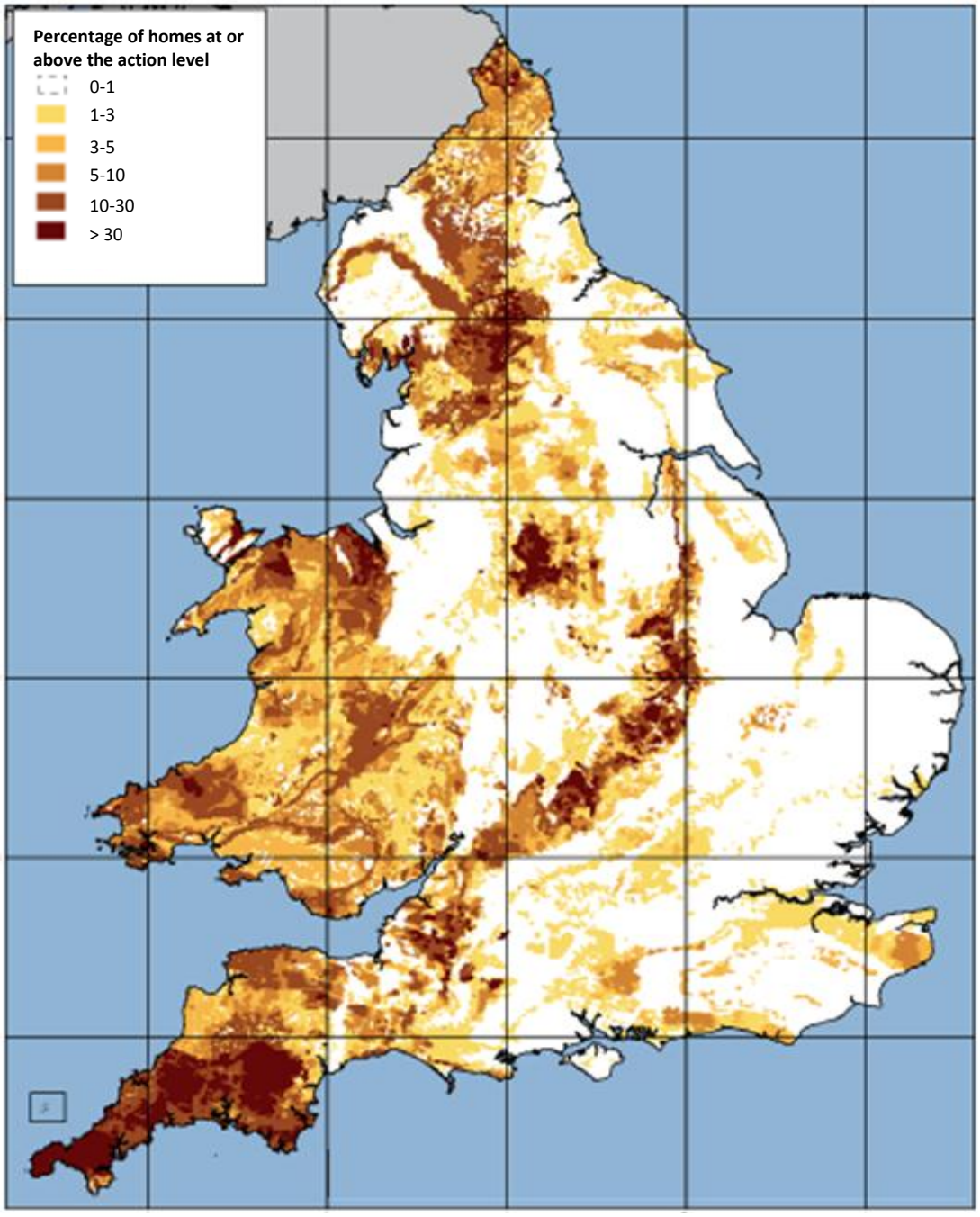

Figure 1.5 Radon gas levels in homes in England and Wales
The map shows the percentage of homes in England and Wales which contain above 200 becquerels per cubic metre (Bq m^{-3}) of radon gas according to the Health Protection Agency (www.hpa.org.uk). The HPA recommends action to remove radon gas from homes with a concentration above 200 Bq m^{-3}. Map obtained from www.ukradon.org.

1.3.3 Ionising radiation and carcinogenesis

Evidence for the carcinogenic effect of ionising radiation in humans largely comes from epidemiological study of atomic bomb survivors who lived in Hiroshima and Nagasaki during the Second World War (1945), populations exposed to medical radiation, and populations exposed to occupational radiation.

Individuals living in Nagasaki and Hiroshima at the time of the atomic bombs were exposed to a range of ionising radiation doses. Detailed estimates of individual radiation dose were generated based on the distance from the hypocentre of the bombs and the amount of shielding each person had (Pierce and Preston, 1993). An increased incidence of leukaemia compared to the general population was identified in survivors as early as 1952 and an elevated risk of leukaemia has since been verified in a life time study of approximately 120,000 bomb survivors (Preston *et al.*, 1994). An increased risk for many solid cancers compared to un-irradiated populations has also been identified; including cancers of the oesophagus, stomach, colon, liver, lung, female breast, bladder, brain, central nervous system, thyroid and skin (non-melanoma) (Preston *et al.*, 2007). A linear relationship between dose and risk was observed for most cancer types. The excess relative risk (ERR – the risk in the exposed group compared to an un-irradiated population) for each cancer reduced as age at the time of exposure increased.

Diagnostic and therapeutic doses of radiation are low but are often given repeatedly, which means that some patients receive a large cumulative dose. Diagnostic and therapeutic radiation has been associated with increased cancer risk in many tissue types. For example, there is an established linear dose relationship for lung and breast cancer risk following radiotherapy for Hodgkin lymphoma (Gilbert *et al.*, 2003; van Leeuwen *et al.*, 2003). An increased risk of thyroid cancer was identified in children, but not adults, exposed to medical radiation (Schonfeld *et al.*, 2011). The relationship between thyroid cancer risk and age has also been observed in atomic bomb survivor studies and children affected by the fallout from Chernobyl (Cardis and Hatch, 2011). There is also an established risk of developing acute myeloid leukaemia (AML) following medical radiation exposure, however only at low doses (Boice *et al.*, 1987). At high therapeutic doses there is evidence that cell kill abrogates AML risk (Allan and Travis, 2005).

Evidence also indicates that occupational exposure to ionising radiation can increase cancer risk. For example, the risks of radon gas inhalation were first identified in uranium miners who had a significantly increased risk of lung cancer compared to the

general population. The association between radon gas exposure and lung cancer risk was extrapolated to the general population and was found to also affect individuals who live in houses with high radon concentrations (Al-Zoughool and Krewski, 2009). A dose dependant increased risk of leukaemia in Chernobyl 'clean up' workers has also been identified (Cardis and Hatch, 2011).

Evidence for the carcinogenic effect of ionising radiation has also been demonstrated using *in vitro* transformation assays. Classically the CH310T1/2 cell transformation assay has been used to establish the transformative effect of a number of carcinogenic agents, including exposure to ionising radiation (Combes *et al.,* 1999). The CH310T1/2 cell line is a non-transformed, immortalised, contact inhibited mouse fibroblast cell line. When CH310T1/2 cells are transformed they form cell foci and the number and morphology of the foci formed in response to a carcinogen allows a semi quantitative measure of cell transforming capability. Different forms of ionising radiation have been shown to transform CH310T1/2 cells and it has been established that the extent of cell transformation is dose dependant (Hieber *et al.,* 1990; Mill *et al.,* 1998). Immortalised human cell lines have also been used to establish the carcinogenic effect of ionising radiation such as the human fibroblast cell line MSU1.0 (Reinhold *et al.,* 1996), which also forms foci when transformed, and a human cell hybrid cell line (HeLa x skin fibroblast) in which transformed cells express a specific cell surface marker and can therefore be identified (Mendonca and Redpath, 1989).

Exposure to ionising radiation is therefore an established carcinogen and a risk factor in developing cancer in many different tissues of the body. The present study will focus on radiation-induced breast cancer. A more detailed review of epidemiological, *in vitro* and *in vivo* studies of radiogenic breast cancer will be discussed in Sections 1.5, 1.6 and 1.7.

1.4 Ionising radiation induced DNA damage

The interactions of ionising radiation within a cell are random and can affect any cellular component; however somatic damage to DNA is believed to be the key mechanism of cell carcinogenesis (Chadwick and Leenhouts, 2011). The following section will concentrate on the mechanisms of radiation-induced DNA damage, how damage is repaired by the cell and how damage can potentially result in mutation.

1.4.1 Mechanisms of DNA damage and repair

Ionising radiation can cause both direct and indirect damage to DNA. Direct ionisation of atoms in the sugar phosphate backbone and nucleosides of DNA can cause DNA strand breaks and abasic sites. The production of free radicals in the nucleus, mainly due to radiolysis which produces reactive oxygen species (ROS) such as hydroxyl radicals (*OH) from water, can cause indirect DNA damage (Fig. 1.6) (Ward, 1985; Goodhead, 1994). For example, hydroxyl radicals can cause strand breaks in the DNA sugar phosphate backbone by hydrogen extraction at the sugar moiety and ROS can cause oxidative damage to bases (Balasubramanian *et al.*, 1998; Cooke *et al.*, 2003).

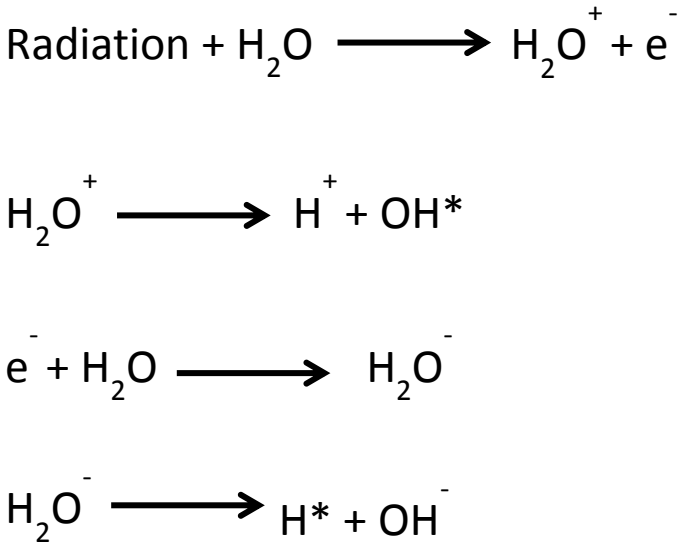

Figure 1.6 Radiolysis of water.

Ionisation causes water molecules to split by a process called radiolysis. Radiolysis causes a cascade of chemical reactions which produces free radicals (signified by an *) which are highly reactive and can damage DNA.

Interactions between nucleotides, free radical species and ROS can create many different base products (Cooke *et al.*, 2003; Ziech *et al.*, 2011). The most common base change due to oxidative damage, and the most studied, is 8-oxo-Guanine (8-oxo-G; also called 8-hydroxyguanine) (Fig. 1.7). Guanine normally base pairs with cytosine, however 8-oxo-G preferentially pairs with adenine during replication. If un-repaired, base mis-pairing can result in a G:C to T:A substitution in the genome following DNA replication (Cooke *et al.*, 2003) (Fig. 1.8).

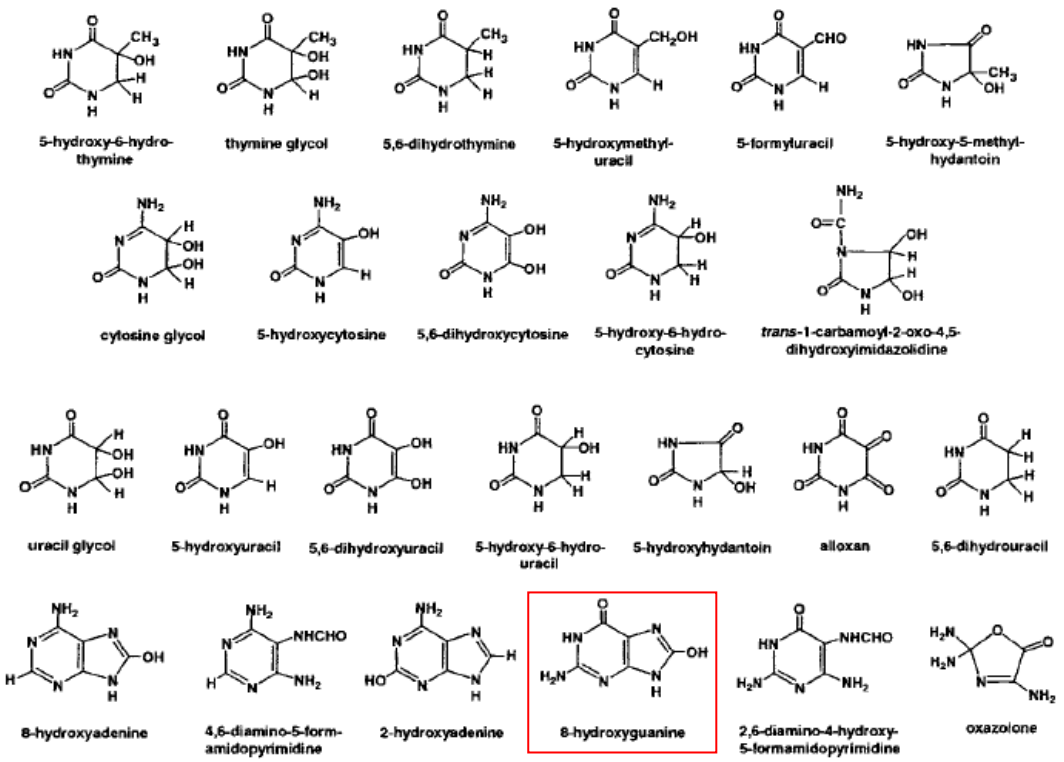

Figure 1.7 DNA base products following interaction with free radical species and reactive oxygen.
Free radicals and reactive oxygen species can interact with numerous atoms in DNA, resulting in the formation of damaged DNA bases, including 8-oxo-Guanine (highlighted by the red box)
Figure from Cooke *et al* (2003).

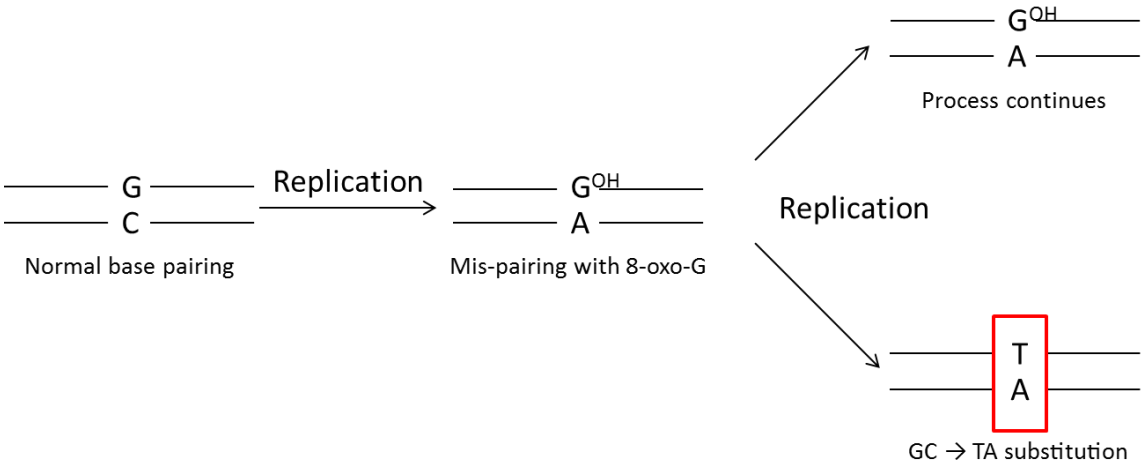

Figure 1.8 Base substitutions due to base mis-pairing with 8-oxo-Guanine mediated by DNA polymerase during DNA replication.

Oxidative damage of guanine generates 8-oxo-Guanine (G^{OH}), which can induce mis-pairing with adenine (A) instead of cytosine (C) following replication. If unrepaired, at the next round of replication, the mis-paired adenine is paired with thymine, ultimately resulting in a G:C→T:A substitution at the site of the original 8-oxo-Guanine lesion (highlighted by the red box).

Single strand breaks, abasic sites and oxidised bases are repaired by different stages of the BER pathway (Fig. 1.9). Briefly, repair begins with the detection and excision of the damaged base by DNA glycosylases (e.g. OGG1, NTHL1) which generates an AP site (apurinic/apyrimidinic site). AP endonucleases (e.g. APEX1/2) cleave the DNA strand backbone at the AP site creating a single base gap (repair begins at this stage for radiation-induced abasic sites and single strand breaks). DNA polymerases (e.g. polβ) use the complimentary DNA strand to add the correct base to the AP site, and finally DNA ligases (e.g. LIGI, LIGIII and cofactor XRCC1) repair the DNA strand break (Fromme and Verdine, 2004; Zharkov, 2008).

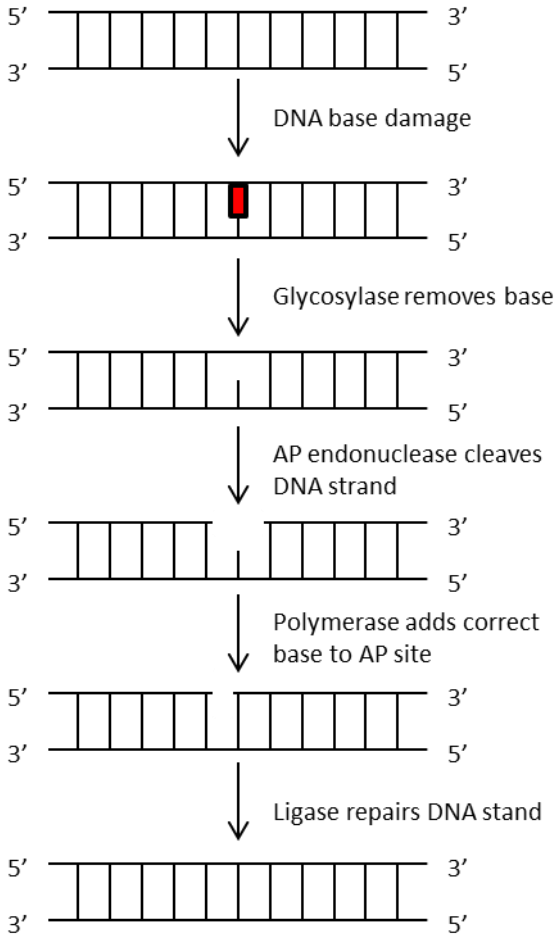

Figure 1.9 Base excision repair pathway.

Horizontal lines represent the DNA strand backbone and vertical lines represent base pairing between the DNA strands. The red box represents a damaged base. DNA bases damage can be repaired by the BER pathway. The damaged base is removed by glycosylase enzymes and the DNA strand at the newly abasic site is cleaved by endonucleases. Polymerases replace the damaged base and ligases repair the broken DNA strand. DNA damage which directly causes abasic sites or single strand breaks are repaired by BER starting with AP endonuclease activity.

Base excision repair of multiple localised DNA lesions can sometimes cause both strands of DNA to be cleaved which generates a double strand break (Fig. 1.10) (Blaisdell *et al.*, 2001). Both high-LET and low-LET radiation can create clustered DNA damage, either due to the high energy deposition along the particle track (high-LET) or radiolysis of water adjacent to DNA (low-LET) (Blaisdell *et al.*, 2001; Terato and Ide, 2004; Hada and Georgakilas, 2008). It has been demonstrated that clustered DNA damage can lead to complex chromosomal alterations (Singleton *et al.*, 2002). It is also believed that complex clustered DNA damage is more difficult to repair as repair enzymes cannot access the DNA lesions (Asaithamby *et al.*, 2011). It therefore appears that clustered DNA damage is a key biological consequence of ionising radiation.

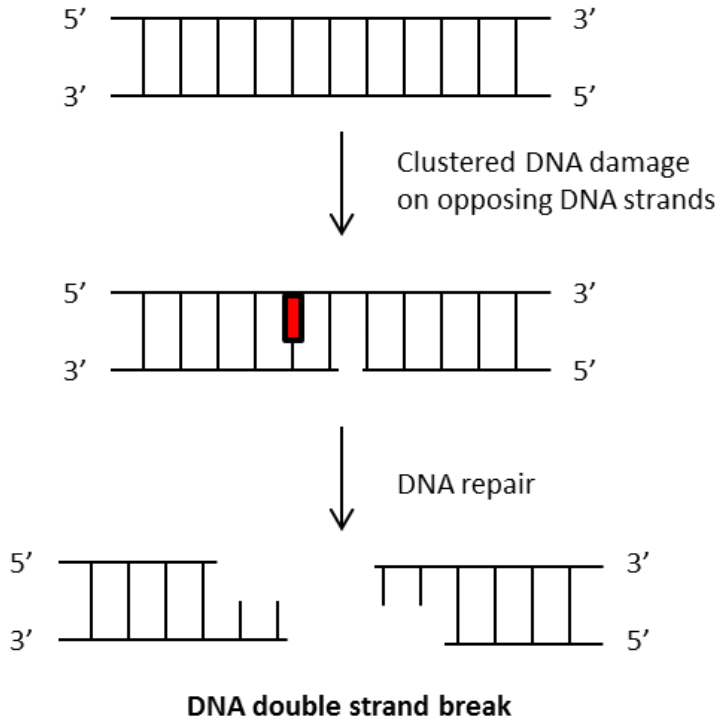

Figure 1.10 Clustered DNA damage causing DNA double strand breaks.
Horizontal lines represent the DNA strand backbone and vertical lines represent base pairing between the DNA strands. The red box represents a damaged base. Clustering of DNA damage, such as base damage and single strand break on opposing DNA strands, can generate a DNA double strand break due to strand cleavage at the damaged base during DNA repair. Direct induction of single strand breaks in close proximity on opposing DNA strands can also lead directly to DNA double strand breaks due to instability of the double helix.

Double strand breaks which are not generated by BER of clustered DNA damage are caused by localised single strand break events on opposite DNA strands. DNA double strand breaks are repaired either by non-homologous end joining (NHEJ) or homologous recombination (HR) (Fig. 1.11 and Fig. 1.12). ATM detects the presence of a double strand break and begins a cascade of reactions which stop the cell cycle and leads either to cell death or DNA repair (Shiloh, 2003). NHEJ directly binds broken ends of the DNA while HR uses the DNA sequence of a sister chromatid or complementary chromosome as a template for repair (Li and Heyer, 2008; Mahaney *et al.*, 2009; Nagasawa *et al.*, 2010). NHEJ is active throughout the whole of the cell cycle whereas HR is predominantly active in the late S and G2 phases when sister chromatids are present (Natarajan and Palitti, 2008; Nagasawa *et al.*, 2010), although NHEJ is still the dominant repair mechanism.

Many of the proteins required for NHEJ have been identified, although the exact role for some of these is still unclear (Fig1.11). Briefly, NHEJ comprises 3 main stages: i) Detection of the double strand breaks and tethering together of the DNA ends (e.g. by KU70/80 heterodimer and DNA-PKcs); ii) DNA end processing to remove damaged or non-ligatable ends (e.g. by Artemis, DNA polymerase μ and λ, PNK, ARLF and WRN); and iii) ligation of the DNA ends (e.g. by DNA Ligase IV-XRCC4 complex, XLF). Some of the proteins involved in NHEJ may only be necessary for specific types of double strand break damage, for example; different types of DNA ends that need processing before ligation. The essential kinase activity of DNA-PKcs is also unclear although it is believed that autophosphorylation of the protein is required for disassembly of the protein complex (Mahaney *et al.*, 2009).

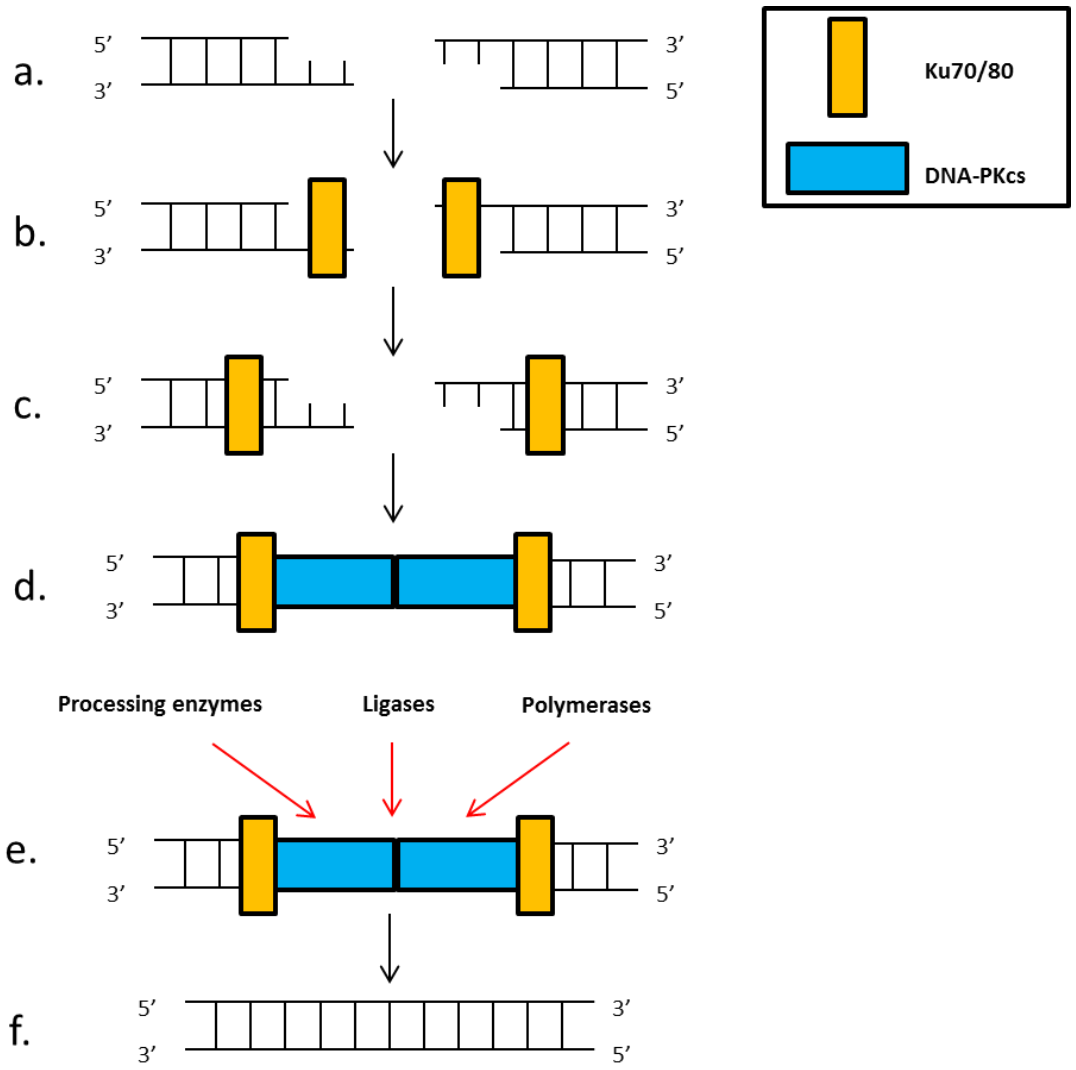

Figure 1.11 Non-homologous end joining (NHEJ).
Horizontal lines represent the DNA strand backbone and vertical lines represent base pairing between the DNA strands. The 5' and 3' orientation of the DNA strands is also shown. Double strand breaks **(a)** induced by ionising radiation can be repaired by NHEJ. The KU heterodimer (comprising KU70 and KU80) binds the ends of the double strand break **(b)** and then translocates along the strand **(c)** allowing space for recruitment of DNA-PKcs to bind to the extreme ends of the break**.** Two DNA-PKcs molecules interact to bring the termini in close proximity **(d)**. Other factors are then recruited to the NHEJ process, including enzymes which remove damaged DNA strand ends, DNA ligases which join the DNA strands and DNA polymerases **(e)**. It is currently unclear what order these factors are recruited to the double strand break, or whether DNA-PKcs dissociates from the double strand break before these factors are recruited. How the factors are released from the process is also unclear.

Like NHEJ, many of the proteins required for HR have been identified, but for some, their specific roles and interactions have not been fully elucidated (Fig. 1.12). Briefly, double strand breaks are identified and processed by the MRN complex (MRE11-RAD50- NBS complex) which produces single stranded 3' overhangs. The single stranded DNA is coated with replication protein A (RPA) before BRCA2/RAD52-mediated replacement by RAD51 filaments (complexes involving RAD51 homologues are also implicated in this process) (Thacker, 2005). RAD51 can search for sequence homology and invade complimentary double stranded DNA, thereby displacing a single strand which is used as a template to repair the double strand break (RAD54 and BRCA1 may also be involved in this process). Strand invasion can be resolved in different ways thereby generating alternative DNA products (Filippo *et al.*, 2008; Li and Heyer, 2008).

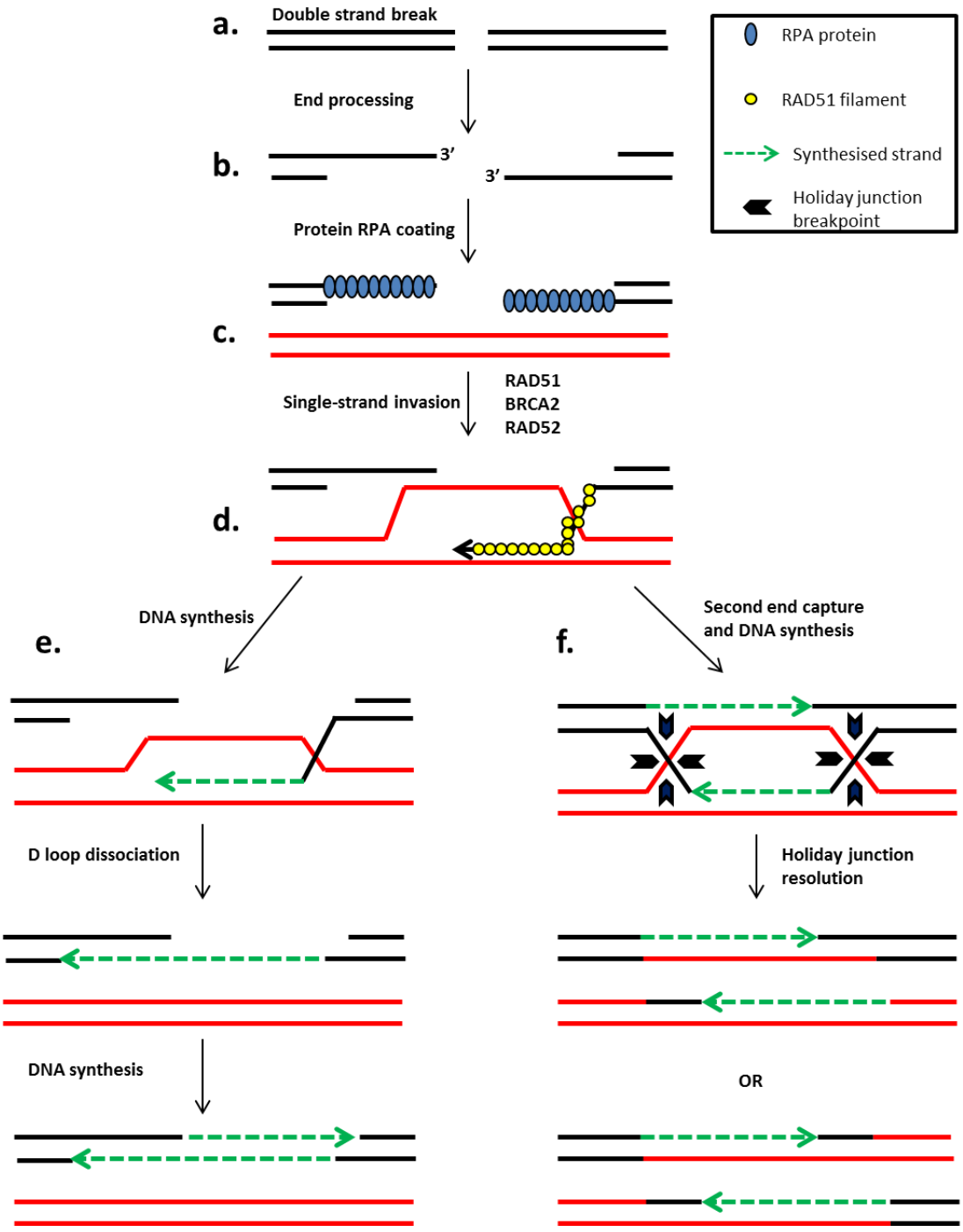

Figure 1.12 Homologous recombination repair of double strand breaks.
Each line represents a single DNA strand. A double DNA strand break occurs **(a),** the ends of which are processed by 5'-3' exonuclease enzymes to produce single strand 3' overhangs **(b)**. The single stranded DNA is coated with RPA protein **(c)** which is then replaced by RAD51 filaments mediated by BRCA1 and RAD52 **(d)**. RAD51 filaments allow the single stranded DNA to invade a homologous DNA strand forming a D-loop **(d)**. Double strand breaks can then be repaired by either synthesis-dependant strand annealing (SDSA) **(e)**, or double strand break repair (DSBR) **(f).** In SDSA **(e)**, synthesis of the invading strand uses the homologous chromosome as a template followed by dissociation of the D-loop and synthesis of the complimentary single DNA strand using the newly synthesised DNA as a template. Newly synthesised DNA strands are indicated by the green arrows. In DSBR **(f)** the D-loop structure from the homologous chromosome is used as a template for the non-invading single DNA strand, thereby forming 2 Holiday junctions. Depending on the resolution of the Holiday junctions by exonucleases different crossover products can be formed. The alternative Holiday junction break points are indicated by the large black arrows.

1.4.2 Consequences of ionising radiation-induced DNA damage

As described in section 1.4.1, ionising radiation can cause an array of DNA damage. Incorrect or absent repair of this damage can have biological consequences ranging from single gene mutations to cell death. Radiation-induced DNA double strand breaks can cause chromosomal alterations that can affect large regions of DNA. The relevance of small scale mutations such as point mutations induced by oxidative damage cannot be ignored however, as the genes affected by these mutations could affect numerous molecular processes, such as DNA repair. The present study will assess copy number alterations induced by ionising radiation in relation to breast cancer. Therefore the following section will describe the mechanisms of copy number alterations induced by radiation-induced DNA double strand breaks.

Chromosomal Aberrations

The classic hypothesis of chromosome aberrations generated by radiation-induced double strand breaks is the 'breakage and reunion' model (Sax, 1940; Bender *et al.*, 1974). The model suggests that double strand breaks are generated at single or multiple sites on multiple chromosomes and low fidelity repair of these breaks (most likely by NHEJ) in different configurations generates multiple chromosome aberrations (Figure 1.13) (Cornforth, 2006; Nagasawa *et al.*, 2010), including: terminal and interstitial deletions, duplications, inversions, translocations, inter-chromosomal exchange, dicentric and acentric fragment formation and ring chromosome formation. Experimentally verified complex chromosomal rearrangements which require 3 or more breakpoints along 2 or more chromosomes can also be generated under the 'breakage and reunion' model (Savage and Simpson, 1994; Cornforth, 2006).

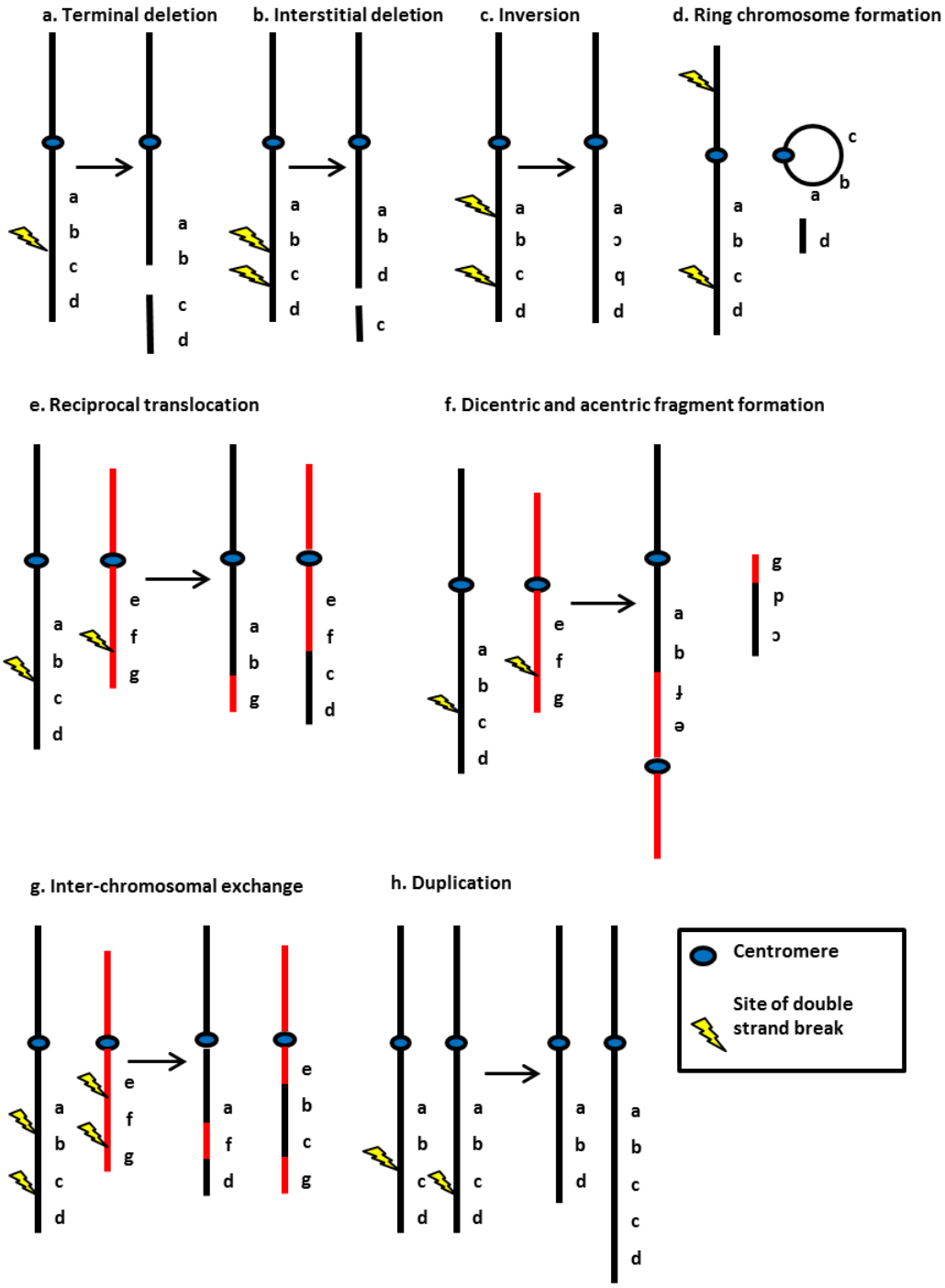

Figure 1.13 Chromosome aberration induction by DNA double strand breaks.
Each line represents a chromosome. Different coloured chromosomes are non-homologous. The alphabetical labels on the chromosome figures represent different regions of the chromosome arm. Inverted regions are represented by inverted letters. Double strand breaks within the same chromosome can lead to a number of different chromosome alterations, such as: terminal deletion generated by one double strand break event **(a**), interstitial deletion **(b)** and inversion of chromosomal regions generated by two simultaneous double strand break events **(c)**, and ring chromosome formation generated by two simultaneous double strand break events either side of a centromere **(d)**. Double strand breaks in two different chromosomes can lead to chromosomal exchanges, such as: reciprocal translocations **(e)** and dicentric (chromosomes with two centromeres) and acentric (chromosomes with no centromere) chromosome formation **(f).** Multiple double strand breaks on different chromosome arms can also lead to inter-chromosomal exchanges **(g)**. Double strand break and chromosomal exchange on homologous chromosomes can cause simultaneous duplication and deletion of DNA **(h)**.

A novel mechanism of gene amplification has also been suggested which could be initiated by radiation-induced double strand breaks (Fig. 1.14). Breakage-fusion-bridge cycles describe a mechanism whereby a double strand break occurs on a chromosome during G0/G1 phase of the cell cycle, causing loss of its telomere. The chromosome is then replicated generating two sister chromatids without telomeric ends. The sister chromatids subsequently fuse creating a dicentric chromosome. During mitotic cell division the centromeres are pulled apart and a double strand break occurs close to the original break site generating a chromosome with an inverted repeat. Multiple rounds of the cycle may then occur causing amplification of the genomic region until a telomere is acquired (Hastings *et al.*, 2009).

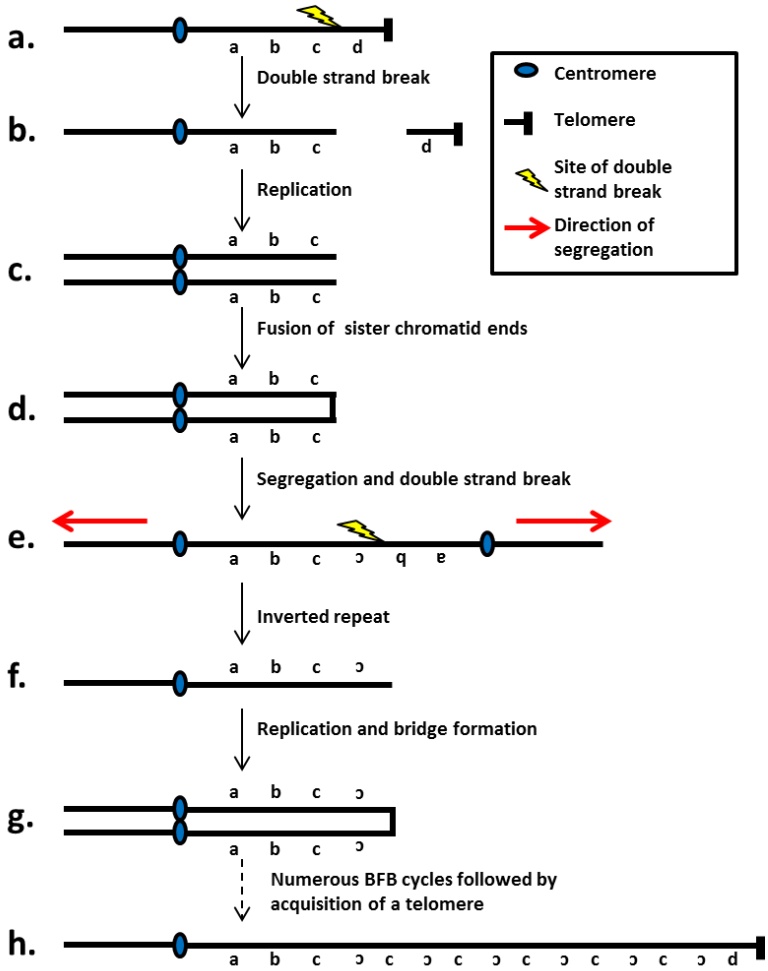

Figure 1.14 Breakage fusion bridge cycle mechanism.
Each line represents a chromosome. The alphabetical labels on the chromosome figures represent different regions of the chromosome arm. Inverted regions are represented by inverted letters. A double strand DNA break on a chromosome arm results in loss of a telomere **(a-b).** Replication of the chromosome occurs followed by fusion of the two telomere free chromosome ends creating a dicentric chromosome **(c-d)**. Mitotic segregation pulls the two centromeres apart during anaphase causing a further double strand break close to the original one **(e)** thereby generating a chromosome with an inverted repeat **(f)**. This chromosome replicates and forms a bridge therefore repeating the cycle **(g-h)**. The cycle can continue until a telomere is acquired; therefore creating a chromosome with numerous inverted repeats **(h)**.

Recombination alterations

Models have been suggested in which errors in HR repair could also lead to chromosome/gene duplication and deletion. As stated in section 1.4.1, HR repair is not actively observed until S and G2 phases of the cell cycle, therefore genetic aberrations caused by HR repair are not likely to occur until later in the cell cycle (Natarajan and Palitti, 2008; Nagasawa *et al.*, 2010).

Non-allelic homologous recombination (NAHR) describes a mechanism by which double strand breaks instigate homologous recombination in homologous chromosomes or sister chromatids at homologous sequences but at non-allelic sites (Fig. 1.15) (Hastings *et al.*, 2009). For example, repeat DNA sequences are present in chromosomes which can cause misalignment during homologous recombination and subsequent loss or gain of DNA on a chromosome arm.

Homologous recombination repair between homologous chromosomes may also lead to copy-neutral loss of heterozygosity (LOH) (also called uniparental disomy), which can be initiated by strand breakage in a heterozygous region of the genome. Homologous recombination repairs the break using the homologous chromosome as a template thereby converting the heterozygous area into a homozygous one, but without a reduction in copy number (Fig. 1.16). This can be biologically relevant if the area used as a template contains a mutated gene which is normally masked by a wild type version. LOH of this gene therefore unmasks the mutated phenotype (Bishop and Schiestl, 2001; O'Keefe *et al.*, 2010).

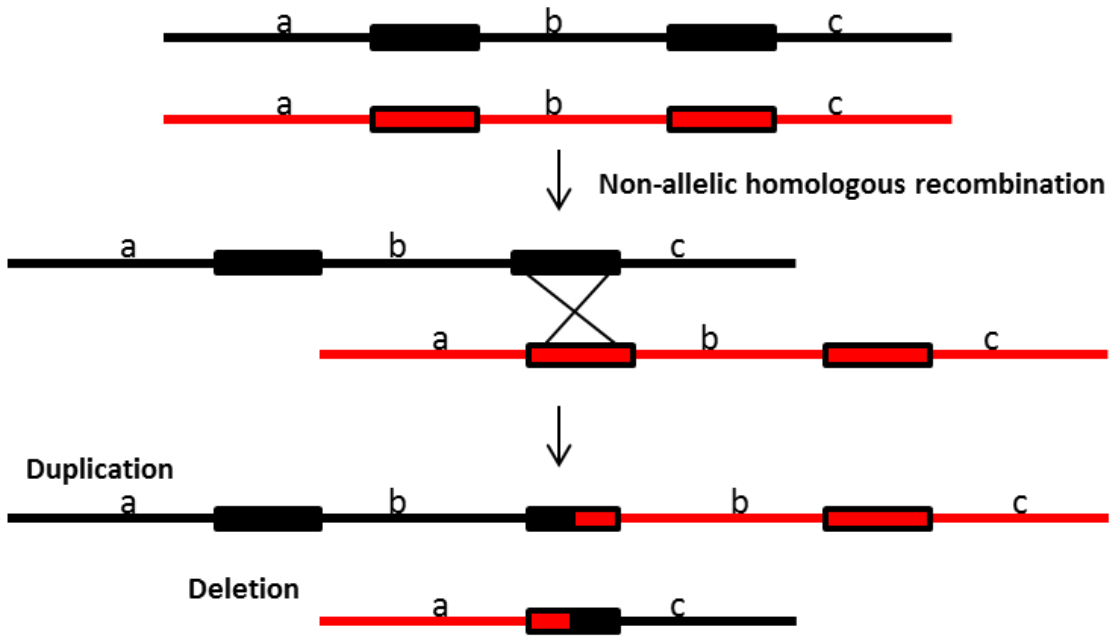

Figure 1.15 Non-allelic homologous recombination leading to interstitial deletion and duplication. Each line represents double stranded DNA. The red and black DNA stands are from homologous chromosomes. The alphabetical labels on the DNA strand represent specific regions of the homologous chromosomes. The red and black boxes represent homologous repeat sequences on the DNA strands. Non-allelic homologous recombination (NAHR) occurs when a double strand break initiates HR repair between two homologous chromosomes at incorrect homologous positions i.e. misaligned repeat sequences. In the above situation the recombination event results in a duplication of region "b" on one chromosome and deletion of region "b" on its homologous chromosome.

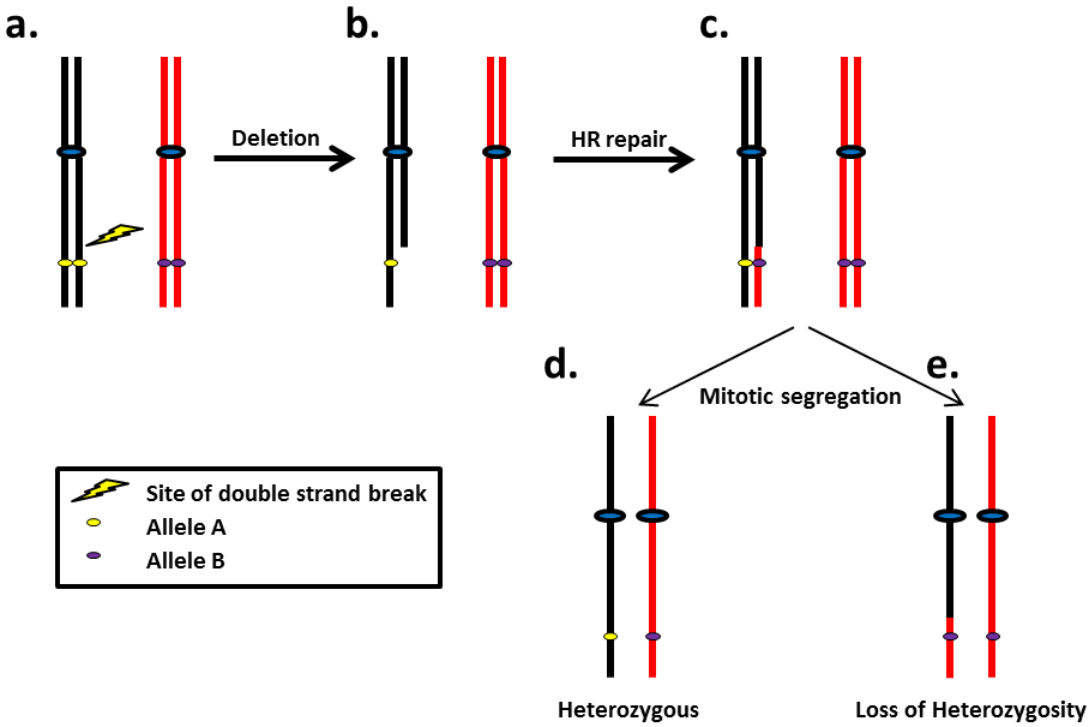

Figure 1.16 Genomic deletion leading to copy-neutral loss of heterozygosity (LOH).
Each line represents a sister chromatid on homologous chromosomes. The position of a heterozygous allele (A and B) is shown on each chromatid arm. A double strand break on a sister chromatid arm containing allele A **(a)** results in a terminal deletion and therefore deletion of one copy of allele A **(b)**. The sister chromatid is repaired using the homologous chromosome as a template, therefore allele A is replaced by allele B on the sister chromatid arm **(c)**. Depending on chromosome segregation during mitosis a daughter cell could be heterozygous for the allele **(d)** or have acquired two copies of allele B therefore becoming homozygous for the allele (LOH) without loss of genetic material (copy-neutral) **(e)**.

Chromatid alterations

Chromosomal aberrations are predominantly identified in cells which have been exposed to ionising radiation in G0/G1 phase of the cell cycle (Nagasawa *et al.*, 2010). During the S and G2 phases chromosomes are undergoing replication or have already been replicated thereby producing genetically identical sister chromatids. Ionising radiation can cause damage to sister chromatids thereby producing chromatid alterations such as chromatid deletions or exchanges between different sister chromatids. It has been demonstrated that cells exposed to ionising radiation in the S and G2 phases of the cell cycle predominantly display chromatid alterations (Nagasawa *et al.*, 2010).

Chromatid breaks are specific lesions defined as inversions or inter-chromatid and terminal deletions of single chromatid arms (Bryant, 2004). It has been demonstrated that single double strand breaks can cause chromatid breaks. For example, chromatid breaks are generated in cells with only one I-SCEI restriction enzyme site and the proportion of breaks increases linearly with radiation dose (Bryant, 1998; Rogers-Bald *et al.*, 2000). Inter-chromatid deletions and inter-chromatid inversions are megabases (Mb) longer than gaps generated by double strand breaks. The fact that large inter-chromatid deletions and inter-chromatid inversions (which would normally require at least two double strand break events) can be generated by a single double strand break suggests that double strand breaks may indirectly cause chromatid breaks (Bryant, 2004).

A model has been proposed which involves disruption of topoisomerase IIα mediated deconcatenation (untangling) of sister chromatids (Terry *et al.*, 2008). Briefly, a double strand break within a looped domain of chromatin on a sister chromatid causes a disruption of the looped structure. This disruption leads to error prone excision and re-joining of the chromatid ends during topoisomerase IIα mediated deconcatenation (Fig. 1.17). The consequence can be loss of the looped domain or inversions caused by mis-joining. It has been postulated that ROS generated by ionising radiation or oxidative damaged bases in the DNA can directly induce error-prone topoisomerase IIα deconcatenation (Li *et al.*, 1999; Sutherland *et al.*, 2000; Terry *et al.*, 2008). Consistent with a role for topoisomerase IIα, lower expression reduces the frequency of chromatid breaks (Terry *et al.*, 2008). It has therefore been suggested that differences in expression of topoisomerase IIα could affect the radio-sensitivity of cells in S and G2 phase of the cell cycle.

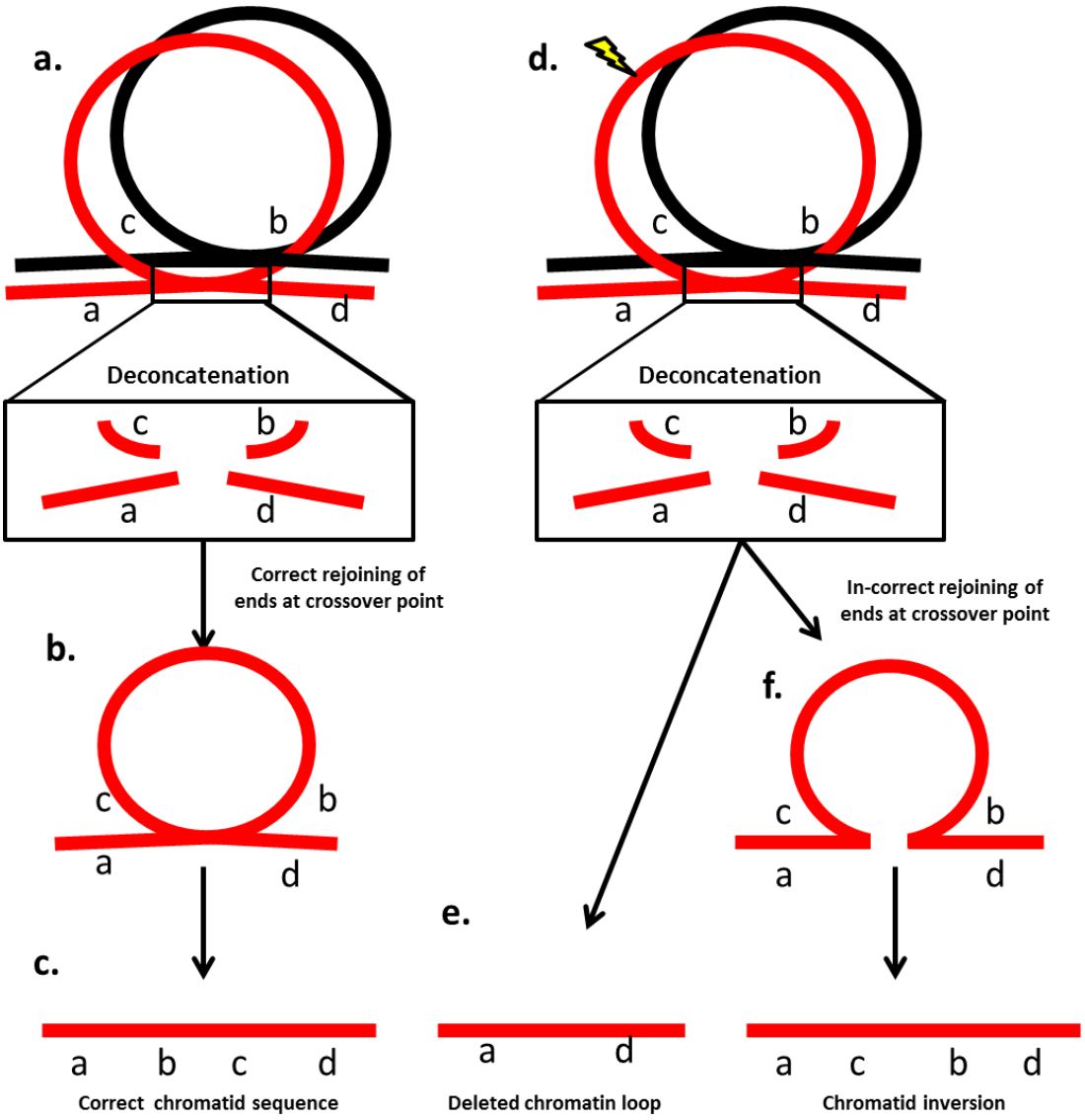

Figure 1.17 Chromatid breaks mediated via error-prone deconcatenation.
Each line represents a sister chromatid within a chromatid pair. The alphabetical labels on the red chromatid represent different regions of the chromatid. Paired sister chromatid loops can become entwined **(a)** and need to be untangled by topoisomeraseII mediated deconcatenation **(b)** which cleaves and re-joins chromatid strands at the crossover point of the chromatin loop. Correct re-joining of the chromatid ends at the crossover point results in unaltered DNA sequence **(c)**. Incorrect re-joining of ends at the crossover point due to an earlier double strand break **(d)** in the chromatin loop which disrupts topoisomeraseII-mediated deconcatenation can cause excision of the loop structure resulting in DNA sequence deletion **(e)** or inversion of the DNA sequence **(f)**.
Figure derived from Bryant (2004).

Some of the mechanisms by which ionising radiation causes genetic mutations that contribute to cell transformation have been described. Point mutations, loss and gain of gene copy number, chromosome rearrangements and copy neutral LOH can affect the activity of both tumour suppressor genes and oncogenes which could in turn lead to cancer. It should be noted however that other hypotheses question the importance of direct induction of DNA damage to ionising radiation-induced carcinogenesis, and suggest that secondary indirect effects of radiation exposure are also important (Section 1.4.3).

1.4.3 Indirect mutagenic effects of ionising radiation

In vitro studies of numerous cell types identified two indirect effects of ionising radiation exposure: radiation-induced genetic instability (RIGI) and radiation-induced bystander effect.

The progeny of irradiated cells can display delayed effects, including cell death and genetic instability (increased rate of chromosomal aberrations) generations after the initial radiation exposure (Morgan, 2003; Wright, 2010). This phenomenon is seen at very low doses and there is no increase in effect with dose (Morgan, 2003; Wright, 2010). Alterations to gene expression and epigenetic regulation such as methylation and histone modification have been postulated as being involved in RIGI (Aypar *et al.*, 2011). Mitochondrial disruption which leads to increased concentrations of ROS has also been implicated, based on an observed association between free radical levels and RIGI (Morgan, 2003; Kim *et al.*, 2006; Wright, 2010; Aypar *et al.*, 2011). A recent study has also suggested that ionising radiation exposure to either the nucleus or cytoplasm of a cell can induce RIGI (Hu *et al.*, 2012).

The radiation-induced bystander effect describes responses observed in cells which were not directly exposed to ionising radiation but which share the same local environment as exposed cells (Morgan, 2003; Wright, 2010). Again, the effect is seen at very low doses and there is no increase in effect with dose. The responses include gene mutations and chromosomal instability but also non-detrimental effects such as cell differentiation, growth inhibition, cell proliferation and the development of radiation-resistance (Wright, 2010). The bystander effect is a result of receiving signals from irradiated cells via soluble factors in the growth medium or via gap junction communication (Hei *et al.*, 2008). It should be noted that not all cell types produce

radiation-induce bystander effects and the nature of the bystander effect also varies (Wright, 2010).

The non-target radiation-induced effects have predominantly been observed *in vitro* and the consequences of these effects *in vivo* are unknown. At very low radiation doses, which are unlikely to directly cause harmful genetic damage, the non-target effects may be biologically relevant; however at higher radiation doses it is speculated that non-target detrimental effects will be overshadowed by direct DNA damage (Hei *et al.*, 2008; Wright, 2010).

1.5 Ionising radiation exposure and breast cancer risk

Ionising radiation acting as a carcinogen has been introduced in section 1.3 and some putative mechanisms of radiation-induced cell transformation have also been detailed. The present study will focus on the molecular mechanisms of radiation-induced breast cell transformation (radiogenic breast cancer). Knowledge regarding radiation exposure and breast cancer risk has largely developed from the study of breast cancer development following radiotherapy for Hodgkin lymphoma. The following sections will therefore discuss the characteristics of radiogenic breast cancer in Hodgkin lymphoma survivors and provide further epidemiological examples of radiation-induced breast carcinogenesis.

1.5.1 Breast cancer and Hodgkin lymphoma

Hodgkin lymphoma is one of the most common cancers in young adults. A combination of targeted radiotherapy and chemotherapy has made the prognosis of the disease very favourable with cure rates currently exceeding 85% in the United Kingdom (Howlander *et al* 2011). However, many studies have shown that young women treated successfully with chest radiotherapy for Hodgkin lymphoma have an increased risk of developing breast cancer (Hancock *et al.*, 1993; Tinger *et al.*, 1997; Travis *et al.*, 2003; van Leeuwen *et al.*, 2003; Basu *et al.*, 2008; El-Din *et al.*, 2008; De Bruin *et al.*, 2009; Elkin *et al.*, 2011). Incidence rates vary between studies. For example, estimates of breast cancer incidence following radiotherapy of women under 30 years of age range between 4-34% after 20-25 years follow up (Travis *et al.*, 2005). The variance in estimates between studies is in part due to alternative methods of risk calculation used by different investigators, and also the inclusion or absence of additional parameters used to calculate the risk (e.g. age, sex, race, type of therapy and magnitude of radiation

dose). It is generally accepted however that radiation exposure increases breast cancer risk in women treated for Hodgkin lymphoma, and that risk is inversely associated with age.

Historically, radiotherapy for Hodgkin lymphoma was administered to the mantle area in approximately 2 Gγ fractionated doses to a mean cumulative dose of 40 Gγ (Fig. 1.18) (Hancock *et al.*, 1993; El-Din *et al.*, 2008; De Bruin *et al.*, 2009). Breast cancer risk in women treated for Hodgkin lymphoma using this method is dose dependant and the risk increases linearly with increased cumulative dose (Travis *et al.*, 2003; van Leeuwen *et al.*, 2003). It should be noted that current methods of radiotherapy aim to limit the area of the breast exposed to radiation and a recent study showed that more targeted methods that avoid direct exposure of the breast tissue can reduce breast cancer risk (De Bruin *et al.*, 2009).

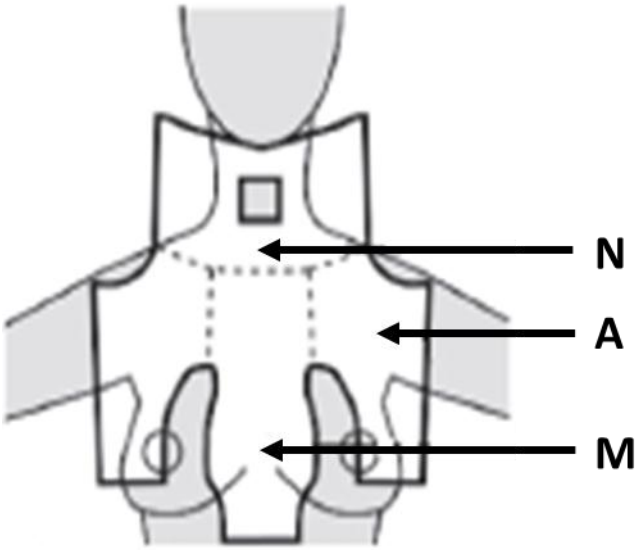

Figure 1.18 Mantle radiotherapy exposure zones.
Areas which are directly exposed to ionising radiation during mantle radiotherapy are shown by the white areas. N, Supraclavicular/neck; A, Axillary; M, Mediastinal. Figure reproduced from De Bruin *et al* 2009.

Many studies have demonstrated that the risk of radiogenic breast cancer is inversely associated with age at exposure (Hancock *et al.*, 1993; Tinger *et al.*, 1997; Travis *et al.*, 2003; van Leeuwen *et al.*, 2003; Basu *et al.*, 2008; El-Din *et al.*, 2008; De Bruin *et al.*, 2009), and some of these studies suggest that there is no increase in risk with exposure over the age of 30 years (Hancock *et al.*, 1993; Travis *et al.*, 2003; Wahner-Roedler *et al.*, 2003). The relationship between age of radiotherapy and breast cancer risk may be related to the higher concentration of circulating oestrogen in younger women compared to older women. This hypothesis derives from the observation that ablation of ovarian function by radiation exposure to the ovaries or concomitant treatment with alkylating

agents during radiotherapy abrogates the increased risk of breast cancer in Hodgkin lymphoma patients (Travis *et al.*, 2003; van Leeuwen *et al.*, 2003). Consistent with a role for oestrogen in driving radiogenic breast cancer, risk decreases as the duration between radiotherapy and menopause decreases (van Leeuwen *et al.*, 2003). Data therefore suggests that exposure to ionising radiation and oestrogen has a synergistic relationship in driving breast epithelial cell transformation. The putative mechanisms of how oestrogen contributes to radiogenic breast cancer are discussed in section 1.6.

The average latency between radiotherapy for Hodgkin lymphoma and breast cancer diagnosis is between 15 and 20 years, depending on the study (Hancock *et al.*, 1993; Tinger *et al.*, 1997; Travis *et al.*, 2003; van Leeuwen *et al.*, 2003; Basu *et al.*, 2008; El-Din *et al.*, 2008; De Bruin *et al.*, 2009). The risk of breast cancer increases from approximately 15 years post-exposure and there is no evidence that risk decreases thereafter. (Travis *et al.*, 2003; van Leeuwen *et al.*, 2003). For example, a Hodgkin lymphoma survivor treated at age 25 years with 40 Gγ of irradiation without alkylating agents has an estimated risk of developing breast cancer by 35, 45 and 55 of 1.4%, 11.1% and 29% respectively. A woman in the general population has a risk of developing breast cancer by 30, 40, 50 and 60 of 0.4%, 0.5%, 2% and 4.3% (Travis *et al.*, 2005).

The long latency between radiation exposure and breast cancer development may be due to an initiating mutation inducing a "mutator phenotype" that increases genetic instability in breast cells, therefore causing a gradual accumulation of transforming mutations (Fig. 1.19) (Bielas and Loeb, 2005). Circulating oestrogen may also play a role in the accumulation of mutations initiated by ionising radiation (discussed in section 1.6).

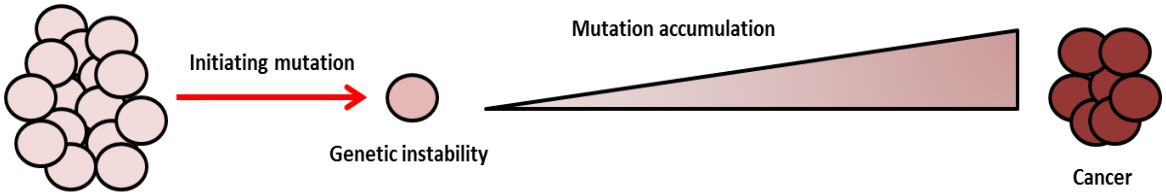

Figure 1.19 Ionising radiation induced genetic instability
Exposure to ionising radiation causes a mutation which increases genetic instability within a cell (initiating mutation). The increase in genetic instability allows the accumulation of mutations over time, ultimately resulting in cell transformation and the development of cancer.

1.5.2 Epidemiological evidence of radiogenic breast cancer

Studies of populations other than Hodgkin lymphoma survivors have also demonstrated the relationship between radiation exposure and breast cancer risk. For example, breast cancer risk was higher in American female radiological workers who worked before 1940 compared to after 1970, presumably due to the advances in shielding technology after 1940. The risk increased with the number of years worked before 1940 and was higher in women who began working before the age of 17 (Doody *et al.*, 2006). A study of female Icelandic airplane cabin crew (who are exposed to higher doses of cosmic radiation) identified a reduced mean age of breast cancer compared to the general population. The risk of developing breast cancer also increased with longer duration of employment (Rafnsson *et al.*, 2001).

Analysis of women who received numerous chest fluoroscopies during pneumothorax therapy identified an 86% increased risk of developing breast cancer compared to the general population. Women who received a higher cumulative dose were more likely to develop breast cancer and the risk was greatest for women exposed before they were 30 years of age. In these patients, putative radiogenic cancer appeared at least 15 years after first exposure (Davis *et al.*, 1989; Hrubec *et al.*, 1989). Breast cancer incidence was twice as high in Scoliosis patients (who received numerous X-rays to monitor the curvature of the spine) compared to the general population and cancer risk increased with increased cumulative dose (Hoffman *et al.*, 1989). Ma *et al.* (2008) also found that women exposed to 9 or more diagnostic chest X-rays for any condition were twice as likely to develop breast cancer relative to patients not exposed.

A study investigating breast cancer risk following therapy for benign breast disease identified an ERR of 3.26 (compared to the general population) in individuals treated with radiotherapy compared to 1.01 for non-radiotherapy treated individuals. The risk was higher in women exposed to radiation under 40 years of age and remained above general population levels 40 years after initial exposure (Mattsson *et al.*, 1993). Radiotherapy for postpartum mastitis (inflammation of the breast) also increased the risk of developing breast cancer 3.2 fold compared to the general population (Carmichael *et al.*, 2003).

Study of atomic bomb survivors identified a linear relationship between breast cancer risk and radiation dose to the breast (Tokunaga *et al.*, 1994; Land *et al.*, 2003; Preston *et al.*, 2007), and also that risk was inversely associated with age (Land *et al.*, 2003).

In summary, epidemiological study of different radiation exposed populations has identified some important characteristics of radiogenic breast cancer development. The risk of breast cancer increases with cumulative dose of radiation and decreases with increasing age of initial exposure; the latter may be mediated by exposure to oestrogen. Radiogenic breast cancer risk increases 10-15 years after initial exposure, which may indicate a role for acquired genetic instability as a result of an initiating genetic mutation. The potential role of oestrogen in radiogenic breast cancer will be discussed in section 1.6.

1.6 Oestrogen and radiogenic breast cancer

A role for oestrogen in breast cancer development has been recognised for some time (see Section 1.2.3). Epidemiological evidence also suggests that oestrogen plays an important role in radiogenic breast cancer development (Section 1.5). A number of *in vitro* and *in vivo* animal studies have demonstrated that concomitant exposure to ionising radiation and oestrogen exposure increases risk of cell transformation.

1.6.1 Putative mechanisms of oestrogen carcinogenesis

Two predominant mechanisms have been proposed to explain the role of oestrogen in breast carcinogenesis: a receptor mediated cell proliferation mechanism and a non-receptor mediated genotoxic mechanism (Yager and Davidson, 2006; Chang, 2011).

Receptor mediated mechanism

Oestrogen has been shown to stimulate proliferation and inhibit apoptosis in a number of *in vitro* and *in vivo* studies (Cohen and Ellwein, 1990; Pike *et al.*, 1993; Yared *et al.*, 2002; Travis and Key, 2003; Butt *et al.*, 2007; Mense *et al.*, 2008). Oestrogen interacts with two ligand dependant nuclear transcription factors, oestrogen receptor alpha (ERα) and oestrogen receptor beta (ERβ). After interaction with oestrogen, ERα and ERβ form homodimers which bind to oestrogen response elements in oestrogen-responsive genes and alter gene expression through interactions with co-activators and co-repressors (Yager and Davidson, 2006; Chang, 2011). Oestrogen bound receptors have also been identified in non-nuclear cell locations such as plasma and mitochondria implicating a role in mitochondrial DNA transcription (Govind and Thampan, 2003; Chen and Yager, 2004). Cross-talk with other signal-transduction pathways such as the epidermal growth factor signal pathway may also occur (Levin, 2003; Liao, 2003).

Oestrogen-induced cell proliferation may contribute to radiogenic breast cancer development because increased cell proliferation causes inaccurate DNA replication and repair which facilitates the accumulation of transforming mutations (Bielas and Heddle, 2000). If ionising radiation induces a mutation that increases spontaneous genetic instability then oestrogen-induced cell proliferation may facilitate the accumulation of transforming mutations.

Genotoxic mechanism

A non-receptor mediated mechanism of oestrogen carcinogenesis has also been proposed (Fig. 1.20). In this model oestrogens are metabolised by cytochrome P-450 enzymes CYP1A1 and CYP1B1 to catechol oestrogen metabolites (Hayes *et al.*, 1996; Liehr, 2000). CYP1A1 is expressed predominantly in the liver while CYP1B1 is found in other tissues including the breast (Chang, 2011). Oxidation of these metabolites produces quinones which can generate unstable DNA adducts with adenine and guanine that are then more prone to depurination and could lead to mutation (Cavalieri and Rogan, 2004; Chang, 2011). Reduction of quinones to catechol oestrogens also produces ROS which can cause oxidative DNA damage (Section 1.4) (Liehr, 2000; Yager and Davidson, 2006; Chang, 2011).

Detoxification pathways that remove oestrogen metabolites are active in breast tissue (Yager and Davidson, 2006; Chang, 2011). Catechol O-methyltransferase (COMT) methylates catechol oestrogen metabolites to methyl catechols which are not genotoxic therefore preventing quinone formation. Non-genotoxic glutathione conjugates are also produced by reactions between quinones and glutathione mediated by glutathione S-transferase (GST) enzymes.

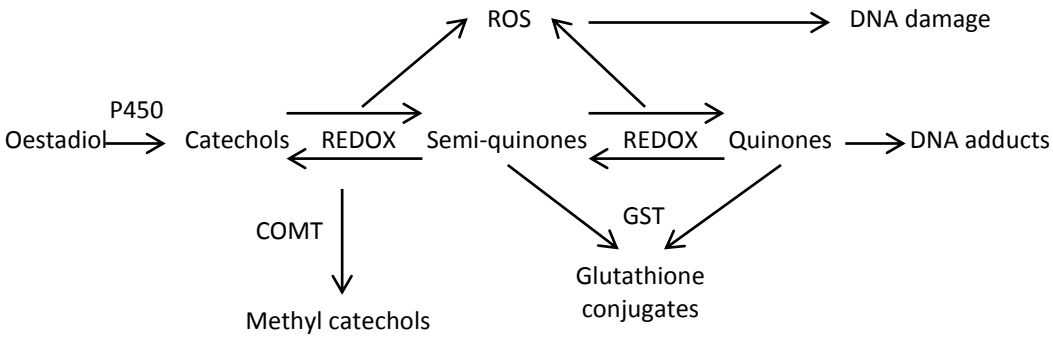

Figure 1.20 Genotoxic mechanism of oestrogen carcinogenesis.

The oxidative pathway of oestrogen metabolism resulting in the production of reactive oxygen species (ROS) and quinones that causes direct DNA damage. REDOX = Reduction and oxidation, P450 = CYP1A1 and CYP1B1 enzymes. COMT = Catechol O-methyltransferase, GST = glutathione S-transferase enzymes. Methyl catechols and glutathione conjugates are non-toxic. The direction of the arrows indicates the direction of the reactions through the pathway.

Oestrogen-associated DNA adducts have been identified in human breast cancers (Embrechts *et al.*, 2003; Markushin *et al.*, 2003) and *in vivo* and *in vitro* studies have demonstrated that the genotoxic activity of oestrogen and its metabolites can be carcinogenic. For example, oestrodiol treatment in a rat model system induced oxidative stress in mammary tissue and evidence of oxidative stress was found in renal tumours induced by oestrodiol exposure in hamsters (Mense *et al.*, 2008). The MCF-10A and MCF-10F breast epithelial cell lines, which are both ERα negative and have very low expression of ERβ, were transformed with oestrodiol and non-steroidal oestrogenic agents (Liu and Lin, 2004; Fernandez *et al.*, 2006; Russo *et al.*, 2006; Huang *et al.*, 2007; Lu *et al.*, 2007). Transformed MCF-10F cells contained mutations associated with breast cancer, such as LOH at the *BRCA1* locus and a 5bp deletion in exon 4 of *P53* (Fernandez *et al.*, 2006). Further experiments with the MCF-10F cell line demonstrated that inhibition of COMT increased the number of DNA adducts prone to depurination, which is consistent with a genotoxic effect of oestrogen (Lu *et al.*, 2007).

Polymorphisms of genes involved in oestrogen metabolism are also associated with increased breast cancer risk (Ritchie *et al.*, 2001; Mitrunen and Hirvonen, 2003; Park *et al.*, 2004; Diergaarde *et al.*, 2008). For example, a variant of *CYP1B1* that has increased catalytic activity and thereby metabolises oestrogen more readily, was associated with increased breast cancer risk in postmenopausal women (Diergaarde *et al.*, 2008). However, association of gene variants with breast cancer risk has been inconsistent, possibly due to small study size and the low penetrance of individual genetic variants (Yager and Davidson, 2006).

Direct DNA damage by oestrogen metabolites may contribute to radiogenic breast cancer development by increasing the amount genetic mutation. If ionising radiation induces a mutation that increases genetic instability, then the subsequent sustained presence of ROS or depurinating metabolites caused by prolonged oestrogen exposure may lead to cell transformation.

Exposure of oestrogen receptor positive MCF-7 breast cancer cells with exogenous oestrogen increased cell proliferation and plating efficiency but also increased DNA damage (Yared *et al.*, 2002). Proliferation of mammary tissue and an increase in oxidative stress in response to oestrodiol treatment was also observed in an *in vivo* rat model (Mense *et al.*, 2008). It therefore appears that both the receptor mediated and genotoxic mechanisms of oestrogen carcinogenesis occur simultaneously.

1.6.2 The role of oestrogen in radiogenic breast cancer

A number of *in vivo* studies have demonstrated that mammary cancer risk is increased following ionising radiation exposure in the presence of exogenous oestrogens. Inano *et al.* (1995) showed that ovariectomised rats (that lack endogenous oestrogen production) developed more radiation-induced mammary cancers if they were injected with estradiol-3-benzoate than un-injected rats. Bartstra and colleagues demonstrated that rats exposed to a single dose of ionising radiation (maximum 2 Gγ) had increased risk of mammary cancer compared to un-irradiated rats. Risk declined if rats were exposed after 36 weeks of age (Bartstra *et al.*, 1998b). Oestrodiol treatment 2 weeks prior to radiation exposure increased cancer risk further, but there was no increased risk if rats were older than 36 weeks (Bartstra *et al.*, 1998a). In a fractionated dose experiment with sustained exogenous oestrodiol exposure from an early age, mammary cancer risk remained elevated up to 64 weeks of age (Bartstra *et al.*, 2000). The authors speculated that the prolonged increase in cancer risk was due to continued proliferation of mammary cells due to sustained oestrodiol treatment.

An *in vitro* study of non-transformed MCF-10F breast epithelial cells, demonstrated that concomitant exposure to high-LET α-particles and oestrodiol generated cell populations with more aggressive transformed phenotypes than radiation on its own (Calaf and Hei, 2000). Changes in morphology, an increase in cell proliferation and anchorage independent growth developed in cells exposed to one or two doses of ionising radiation (60 cGγ). Cells irradiated and cultured in the presence of oestrodiol had enhanced anchorage independent growth and enhanced invasive capabilities compared to cells not

cultured in the presence of oestrodiol, and also produced tumours in mice (Calaf and Hei, 2000). As well as phenotypic changes, combined radiation and oestrogen exposed cells had greater allelic imbalance (expressed as microsatellite instability or LOH at microsatellite markers), expressed more growth factors and expressed greater levels of the onco-proteins c-MYC, HRAS and c-JUN than cells exposed only to radiation (Calaf and Hei, 2001; Roy *et al.*, 2001a; Calaf *et al.*, 2006). It is possible that oestrogen contributed to cell transformation via a genotoxic mechanism in these studies because MCF-10F cells are ERα negative.

Epidemiological, *in vivo* and *in vitro* studies therefore support the notion that combined exposure to ionising radiation and oestrogen increases the risk of the development of mammary cancer than exposure to either carcinogen alone and that this relationship may be synergistic. Both carcinogens are able to transform cells *in vitro* on their own; however in human and animal systems it appears that exposure to oestrogen is an important factor in radiogenic breast cancer development. Two potential mechanisms for the contribution of oestrogen to radiogenic breast transformation have been discussed, and it is probable that both are operating. If a mutation induced by ionising radiation increases genetic instability, oestrogen exposure would increase the subsequent accumulation of transforming mutations.

1.7 Genetic susceptibility to radiogenic breast cancer

Inheritable genetic variants have been identified that appear to increase the risk of developing radiogenic breast cancer and have therefore been termed risk alleles. Risk alleles have been identified in a number of genes associated with DNA damage repair.

ATM is an important regulator of DNA damage response. Bernstein *et al.* (2010) observed that individuals with constitutional deleterious variants of *ATM* were at greater risk of contralateral breast cancer following radiotherapy for a primary tumour; however the specific variants were only present in very small fraction of women. Individuals who are carriers of a low penetrance breast cancer susceptibility variant of *CHEK2* (1100delC) (which is phosphorylated by ATM during DNA damage response) were also observed to be at higher risk of radiogenic breast cancer (Bernstein *et al.*, 2006). A similar result was found in women who had received therapeutic radiation for breast cancer and developed secondary contralateral breast cancer (Broeks *et al.*, 2004). *BRCA1* and *BRCA2* mutation carriers were also identified to be at greater risk of radiogenic breast cancer following chest x-rays (Andrieu *et al.*, 2006).

In a study by Broeks *et al.* (2007), a cohort of women who developed contralateral breast cancer following treatment for primary breast cancer were analysed for breast cancer risk variants of *BRCA1, BRCA2, CHEK2* and *ATM*. Women with a pathogenic mutation for at least one of the genes had a significant increase in contralateral breast cancer risk after radiotherapy for primary breast disease compared to women who were not carriers of a pathogenic mutation.

Variants of genes that are not involved in DNA damage repair have also been identified as risk alleles for radiogenic breast cancer. For example, variants of *FGFR2* were over-represented in Hodgkin lymphoma survivors that developed breast cancer. FGFR2 over-expression has oncogenic effects; therefore a highly active variant may contribute to radiogenic breast cancer development (Ma *et al.*, 2012). A genetic variant that reduced the expression of the transcriptional repressor PRDM1 also associated with Hodgkin lymphoma survivors that developed breast cancer compared to those who did not develop breast cancer following radiation exposure (Best *et al.*, 2011). A variant of the miRNA gene *H19* was also associated with increased breast cancer risk in American female radiological workers (Bhatti *et al.*, 2008).

Understanding the genetic susceptibility to radiation-induced cancer can help inform on the type of treatment an individual should have when radiotherapy is being considered as therapy.

1.8 Molecular genetics of radiogenic breast cancer

Analyses of cancer tissue from radiogenic breast cancer patients and from *in vitro* breast epithelial cell transformation models have identified few putative somatically acquired radiation-induced genetic alterations and gene expression profiles associated with radiation-induced carcinogenesis. The identification of somatically acquired genetic markers of radiogenic breast cancer would further understanding of the molecular mechanisms that drive radiation-induced carcinogenesis, and may help identify initiating mutation(s) that increase genetic instability. Section 1.8 will discuss somatically acquired genetic alterations and gene expression changes that have been identified in radiogenic breast cancer tissues, and somatically acquired genetic alterations that have been identified in radiation-induced breast epithelial cell transformation models.

1.8.1 Molecular genetic study of radiogenic breast cancer tissues

Study of radiogenic cancer has suggested that specific radiation-induced genetic alterations are acquired that can drive cell transformation or are molecular markers for radiation-induced carcinogenesis. For example, a recent study compared chromosomal copy number and gene expression changes in an age matched cohorts of papillary thyroid carcinomas (PTC) that developed either sporadically or following exposure to radioactive iodine as a consequence of the Chernobyl disaster. Copy number gain on chromosome 7 (7q11.22-11.23) was observed in 39% of radiation-induced PTC, but was not seen in the sporadic cohort. Over-expression of *CLIP2*, which encodes a protein that mediates the interaction between membranous organelles and microtubules, was also associated with radiation induced PTC (Hess *et al.*, 2011). Mouse models of radiation-induced acute myeloid leukaemia also identified consistent hemizygous loss on chromosome 2 which included the *PU.1* gene, a candidate susceptibility gene for leukaemogenesis (Suraweera *et al.*, 2005).

To date a somatically acquired molecular genetic marker for radiogenic breast cancer has not been identified. Array based genetic analysis has however identified somatic alterations and gene expression changes common to radiogenic breast cancer populations. For example, sporadic and radiogenic breast cancers (developed after therapy for Hodgkin lymphoma) clustered separately following micro-array gene expression profiling. Radiogenic breast cancers were more likely to be of the HER2 or basal-like breast cancer subtypes (Broeks *et al.*, 2010). Separate clustering indicated that radiogenic breast cancers may have specific gene expression signatures. A recent study using array based comparative genomic hybridisation (aCGH) techniques to analyse copy number alterations in radiogenic breast cancers from atomic bomb survivors also reported greater genetic instability in radiation-induced cancers compared to sporadic disease. The study observed significantly more copy number alterations on average in radiation exposed individuals, although there was considerable variability between patients (Oikawa *et al.*, 2011).

Studies have attempted to identify somatically acquired genetic alterations specifically associated with radiogenic breast cancer. For example, Behrens *et al.* (2000) identified a greater frequency of allelic losses on chromosome 6q13-14, 9p21 and in Hodgkin lymphoma breast cancer cases compared to sporadic breast cancer cases. Varma *et al.* (2005) analysed copy number alterations using aCGH in breast cancer samples from

pre-menopausal women in New York (20 cases) and Belarus (22 cases). The authors hypothesised that the Belarusian cohort may have included cases with radiation aetiology due to exposure that resulted from the Chernobyl disaster. The two populations clustered separately (using somatic copy number alterations) and there were more copy number alterations in the Belarusian cohort compared to the New York cohort. Somatically acquired alterations identified in the study included copy number gain of *MDM4* (at 1q32.1) and *SULT1A3* (at 16p11.2). The authors conceded however that the aetiological role of radiation in the Belarusian cohort was unknown and other exogenous and genetic differences between the two populations may have contributed to the observed heterogeneity. Finally, a study by Miura *et al.* (2008) identified a higher frequency of *HER2* and *c-MYC* amplification (2 fold increase in gene copy number compared to chromosome copy number) in a cohort of breast cancer cases from survivors of the atomic bombs at Nagasaki compared to sporadic breast cancer cases. The frequency of cases with amplification increased with increased radiation dose which was estimated by the distance the individual was from the hypocentre of the bomb.

1.8.2 Molecular genetics of radiation-induced breast cell transformation

The study of genetic changes induced by ionising radiation in cell line models is a useful tool for identifying genetic alterations that may contribute to radiogenic carcinogenesis in different tissue types (Riches *et al.*, 1997; Gamble *et al.*, 1999; Riches *et al.*, 2001; Zitzelsberger *et al.*, 2001; Zitzelsberger *et al.*, 2004).

In studies using the MCF-10F cell line (discussed in section 1.6.2) radiation- and oestrogen- exposed cell populations were characterised for genetic alterations. Chromosome 6q, 17p and 17q were analysed for LOH and microsatellite instability (allelic imbalance) (Roy *et al.*, 2001a). A progressive amount of allelic imbalance was observed for all 3 chromosome regions as the populations analysed displayed more transformation phenotypes. Allelic imbalance of chromosomes 6q, 17p and 17q is implicated in breast cancer development and the frequency of allelic imbalance on regions of 6q and 17q was reported to be higher in radiogenic breast cancer compared to sporadic breast cancer (Behrens *et al.*, 2000) (Section 1.8.1). A similar pattern of progressive allelic imbalance was observed for chromosome regions 11q15.5-15.4 and 11q23-q24; the latter region includes the *ATM* gene *(Roy et al., 2003; Roy et al., 2006)*. Expression analysis of 190 proto-oncogenes and tumour suppressor genes identified

altered expression of 49 genes in cells with transformed phenotypes compared to un-irradiated MCF-10F (Roy *et al.*, 2001b). Seventeen genes were differentially expressed in all irradiated populations that displayed transformed phenotypes. Of the 17 genes 15 were up-regulated and 2 were down-regulated. Up-regulated genes included: *c-MYC*, *IGF1R*, *TEL*, *c-JUN*, *PUF*, *MNDA*, *LUCA1*, *FRA-1*, *FAK*, *CDC25B*, *GSK3*, *c-MYC* binding protein, *E2F1*, *WNT-5A* and *c-YES*. The two down regulated genes were *P48* and *EB1*.

Unger and colleagues identified chromosomal rearrangements in immortalised human mammary epithelial cells transformed with fractionated doses of gamma irradiation to a cumulative dose of 40 Gγ (Unger *et al.*, 2010), including translocations involving chromosomes 7, 8, 10 and 12. Genes identified in the breakpoints of these rearrangements included: *HAS2*, *GRID1*, *RET*, *CPM*, *TBX3*, *TBX5*, *TUBA1A*, *WNT1* and *ARF*. Concomitant deregulation of gene expression was identified for each gene except *TBX3* and *TBX5*. Rearrangements of *HAS2, GRID1* and *RET* were identified in primary human breast cancer samples by fluorescent *in situ* hybridisation (FISH) and differential expression of the genes was identified in breast cancer cases by *in silico* expression analysis of a publicly available gene expression dataset. The study demonstrated that genetic rearrangements identified by *in vitro* models of radiation-induced cell transformation could also be identified in primary breast cancer samples.

In summary, a limited analysis of primary human breast cancer tissues suggests that radiogenic cancer has a "recognisable" somatic genetic signature. This conclusion is also supported by data from *in vitro* studies using radiation-exposed cell lines. Identification of specific frequently acquired somatic genetic alterations could help diagnose breast cancer with radiation aetiology and will aid understanding of the molecular mechanisms of radiation-induced carcinogenesis.

1.9 Breast epithelial cell line MCF-10A

The present study has utilised the breast epithelial cell line MCF-10A as a model for radiation-induced cell transformation. The following section will therefore briefly introduce the characteristics of this cell line.

The MCF-10A cell line was first described by Soule and colleagues (Soule *et al.*, 1990) as an immortal, non-transformed cell line that arose spontaneously from mortal diploid

human mammary epithelial cells following extended culture in low calcium medium. MCF-10A cells are ERα negative and have very low expression of ERβ.

MCF-10A displays numerous characteristics consistent with a non-transformed phenotype, including dependence upon hormones and growth factors for growth; contact inhibition of cell growth; anchorage dependant growth; lack of invasiveness across a semi-permeable membrane; inability to produce tumours in immuno-compromised mice and acini formation in 3D matrix culture (Underwood *et al.*, 2006). These characteristics make MCF-10A useful for transformation studies because their loss, concomitant with the acquisition of phenotypic characteristics associated with transformation, can be monitored. Loss of characteristics associated with the non-transformed phenotype have been identified in MCF-10A cells transformed by various means, such as over-expression of proto-oncogenes and exposure to genotoxic agents such as benzo(a)pyrene (Maeda *et al.*, 2005; Kim *et al.*, 2007; Zientek-Targosz *et al.*, 2008; Imbalzano *et al.*, 2009; Kim *et al.*, 2009a; Botlagunta *et al.*, 2010; Cho *et al.*, 2010; Meng *et al.*, 2010).

The karyotype of MCF-10A is near diploid with the major cytogenetic rearrangement a translocation t(3;9)(p13;p22). MCF-10A also has an unbalanced translocation of chromosome 5 to the derivative chromosome 9, a duplication of chromosome 8q, one extra copy of chromosome 1q plus a further copy of the section chr1:198136766-qter and trisomy for chromosome 20 (Cowell *et al.*, 2005).

A study of the t(3;9)(p13;p22) translocation by FISH and aCGH analysis revealed a bi-allelic deletion at the locus encompassing the *CDKN2A/CDKN2B* genes. The homozygous loss of *CDKN2A/CDKN2B* genes might be a contributing factor to the immortalisation of MCF-10A (Cowell *et al.*, 2005). CDKN2A is involved in regulation of the cell cycle and loss of function is an established event in tumourigenesis. Loss of function mutations of CDKN2A are common in melanoma, head, neck, pancreatic and gastric cancers and are frequently seen in cancer cell lines (Liggett and Sidransky, 1998). Inactivation of CDKN2A is suggested to be an early event in carcinogenesis due to the high frequency of inactivation in many primary cancers. CDKN2A heterodimerises with CDK4 and CDK6 which blocks downstream phosphorylation of the Rb protein, subsequently inhibiting release of E2F and cell proliferation (Liggett and Sidransky, 1998). Therefore, even though MCF-10A cells are not transformed this cell line does contain genetic changes that are common to transformed cells.

1.10 Hypothesis and Aim

Exposure to ionising radiation increases breast cancer risk, and this risk is inversely proportional to age at exposure. Radiogenic breast cancers often have a long latency and usually develop over 10 years after the initial exposure, suggesting that ionising radiation causes an initiating mutation in breast cells that increases genetic instability and predisposes to the acquisition of co-operating mutations. The molecular genetic mechanisms that cause radiogenic breast cancer are unclear, however some studies have suggested that radiogenic breast cancers share common gene expression profiles and may share common genetic alterations. The identification of a common specific genetic alteration in radiogenic breast cancer would help elucidate the molecular genetic mechanisms that underlie radiation carcinogenesis and would help identify breast cancers caused by radiation exposure.

Hypothesis: Exposure to ionising radiation induces specific genetic alterations in breast epithelial cells that initiate cell transformation.

The primary objective of this project was to investigate radiation-induced copy number alterations using an *in vitro* model of radiation-induced breast epithelial cell transformation, and to determine if identified alterations were common to radiogenic breast cancer. The strategies for achieving this were:

- To irradiate the non-transformed breast epithelial cell line MCF-10A with fractionated doses of X-rays. *In vitro* transformation models have previously been shown to induce genetic alterations also seen in primary human cancers.
- To identify copy number alterations and regions of copy neutral LOH caused by radiation exposure in irradiated MCF-10A cells using high density polymorphism arrays, and to investigate the effect of identified copy number alterations on gene and protein expression.
- To compare the protein expression and copy number state of gene targets identified in irradiated MCF-10A cells in radiogenic and sporadic breast cancer tissue samples.

Chapter 2: Materials and Methods

2.1 Tissue Culture

2.1.1 Cell lines

MCF-10A and MCF-7 cell lines were purchased from the American Type Culture Collection (ATCC, VA, USA). Cells were cultured in sterile tissue culture flasks from Corning-Costar (supplied by VWR International Ltd, Leicestershire, UK) with growth surface areas of 25, 75 and 175cm^2 (T25, T75, T175).

2.1.2 Routine cell culture

All cell culture was carried out in a class II microbiological safety cabinet (BIOMAT-2, Medical Air Technology Ltd, Oldham, UK). All chemicals and reagents were purchased from Sigma-Aldrich Co. Ltd. (Dorset, UK) unless otherwise stated.

MCF-10A cells were maintained in Dulbeco's Modified Eagle's Medium: Nutrient Mixture F-12 (DMEM-F12) containing 5% (v/v) horse serum, 20ng/ml epidermal growth factor, 0.5μg/ml hydrocortisone, 100ng/ml cholera toxin, 10μg/ml insulin and 1 % (v/v) penicillin/streptomycin. MCF-7 cells were maintained in Dulbeco's Modified Eagle's Medium (DMEM) containing 10% (v/v) foetal bovine serum, 1μg/ml insulin. Both cell lines were incubated at 37°C in a humidified 5% CO_2 incubator (Heraeus Equipment Ltd., Essex, UK).

To detach cells from the tissue culture flasks the cells were washed twice with autoclaved phosphate buffered saline (PBS) prepared from PBS tablets (Invitrogen Life Technologies, Paisley, UK) and incubated in a trypsin-EDTA (50mg/ml porcine trypsin-20mg/ml EDTA) solution (trypsinisation). MCF-7 cells were incubated in a trypsin-EDTA solution diluted 1:3 in PBS. Following detachment, cells were centrifuged for 5 minutes at 1500 rpm (Beckman Allegra X-12 R rotor SX 4750) in sterile BD Falcon™ tubes (BD Biosciences, Oxford, UK) and seeded into new flasks at dilutions between 1:2 and 1:20 with fresh tissue culture medium. Cell lines were tested at 2 month intervals for mycoplasma by E. C. Matheson using a MycroAlert kit (Lonza Biologics, Slough, UK).

2.1.3 Cryopreservation of cells

Cells were trypsinised and re-suspended in the appropriate freezing medium: MCF-10 - Horse serum supplemented with 8% (v/v) dimethyl sulphoxide (DMSO); MCF-7 – DMEM supplemented with 20% (v/v) foetal bovine serum and 10% (v/v) DMSO. Cell suspension was added to sterile polypropylene cryo-vials (Invitrogen Life Technologies, Pailsley, UK) in 0.5ml aliquots. Each aliquot contained an appropriate number of cells to be seeded onto a T25 flask. Cells were stored at -70°C for 24 hours and then transferred to liquid nitrogen for long term storage.

When cryopreserved cells were needed, aliquots were rapidly thawed and transferred to the appropriate pre-warmed cell culture medium in T25 flasks. The medium was replaced 24 hours after seeding.

2.1.4 Cell withdrawal

MCF-10A cells were grown in phenol-red free Dulbeco's Modified Eagle's Medium (PRF-DMEM) containing 10% dextran coated charcoal-treated calf serum (DCC-CS) for some phenotype characterisation assays. This medium was termed 'withdrawal medium' as it was steroid depleted and contained no additional cytokines.

2.1.5 Preparation of dextran coated charcoal-treated calf serum – (DCC-CS)

Twenty grams of acid washed and neutralised charcoal and 0.2g of dextran T70 (Pharmacia Biotech, Sweden) were mixed with 250ml deionised water in a 250ml centrifuge bottle and incubated for 10 minutes at room temperature, creating dextran coated charcoal (DCC). The DCC was recovered by centrifugation at 7000 rpm for 15 minutes at 4°C (JA17 rotor, Beckman J2-21 centrifuge), re-suspended in 250ml of deionised water and centrifuged again under the same conditions. The DCC was then re-suspended in 200ml of new born calf serum (Invitrogen Life Technologies, Pailsley, UK), transferred to 500ml conical flasks and incubated at 55°C for 40 minutes whilst shaking. The DCC was then removed from the serum by centrifugation at 10000 rpm for 30 minutes at 4°C (JA17 rotor, Beckman J2-21 centrifuge). The serum was transferred to clean centrifuge tubes and centrifuged again under the same conditions to remove any remaining charcoal. Finally the serum was filtered through a 0.45μm

disposable filter (Corning-Costar - supplied by VWR International Ltd, Leicestershire, UK) and stored at -20°C until ready for use.

2.2 Generation of ionising-radiation exposed cell populations

MCF-10A cells were exposed to fractionated doses of X-irradiation to generate cell populations that had been exposed to different cumulative doses of ionising-radiation. The cell populations were used in a stochastic model of the accumulation of radiation-induced copy number alterations and cell transformation (Chapter 3).

Cells were irradiated using a D3300 X-ray system (Gulmay Medical Ltd., Surrey, UK). The D3300 X-ray system was calibrated by Prof. Mike Tilby using Frike dosimetry so that the dose rate at the bottom of a tissue culture vessel (where adherent cells are present) could be calculated depending on the depth of the cell culture medium above the cell monolayer. These calculations were based on the cells being a set distance from the X-ray tube. In all irradiation conditions in the present study the depth of medium above the cells was 2.5 mm. The dose rate at the bottom of the tissue culture vessels was calculated as 2.5 Gγ/min.

An experiment was required to determine the optimum dose to be used in the fractionated dose regimen. Doses were chosen depending on the extent of growth inhibition induced by the radiation exposure. Cells were irradiated using a D3300 X-ray system (Gulmay Medical Ltd., Surrey, UK).

2.2.1 Determination of fractionated doses for dosing regimen

MCF-10A cells were seeded in nine 6 well plates (Corning-Costar - supplied by VWR International Ltd, Leicestershire, UK) at 15% confluence. Cells were grown in 2.47ml of growth medium per well. Twenty four hours after seeding, each 6 well plate was exposed to different doses of ionising radiation. The doses used and the appropriate amount of time cells were exposed to X-rays to deliver the required dose is shown in table 2.1.

Radiation dose cells were exposed to (Gγ)	Amount of time exposed to deliver appropriate dose (min)
0	0
1	0.4
2	0.8
5	1.9
10	3.7
20	7.4
40	14.8
60	22.2
80	29.6

Table 2.1 Doses used to determine the optimum fractionated dose.
Radiation doses cells were exposed to and the exposure time required to deliver the appropriate dose to cells grown in 6 well plates in 2.47ml of growth medium or T75 flasks in 20ml of growth medium (dose rate 2.5 Gγ/min).

Four days after irradiation 3 wells of each 6 well plate were tested for growth inhibition by cell count. Five days after radiation exposure the remaining 3 wells of each 6 well plate were tested for growth inhibition by DNA quantification.

2.2.2 Growth inhibition assay – cell count

Cells in 3 wells of each 6 well plate were trypsinised. Cells from each well were re-suspended in 5ml of growth medium. Ten microliters of cell suspension was loaded onto a Neubauer haemocytometer (VWR International Ltd.) and triplicate counts of the number of cells from each well were recorded.

2.2.3 Growth inhibition assay –DNA quantitation

Cells in the remaining 3 wells of each 6 well plate were lysed with 2ml/well of 0.15M NaCl, 17mM sodium citrate, adjusted to pH 7.0 with NaOH (SSC) and 0.02% (w/v) sodium dodecyl sulphate for 30 min at 37°C on a rotary shaker (KS 250, Janke and Kunkel Laboratories). The DNA was sheared by passing through a 25 gauge needle 5 times. Calf thymus DNA (stock - 1mg/ml) was dissolved in SSC-0.02%SDS solution to concentrations of 2.0, 1.0, 0.5, 0.25, 0.125 and 0.063μg/ml to generate a standard curve. One hundred microliter aliquots from each cell lysate and standard curve solution were placed into duplicate wells of a black 96 well plate (Grenier Bio-One, Gloucester, UK) and mixed 1:1 with Quant-iT PicoGreen dsDNA reagent (Invitrogen Life Technologies, Pailsley, UK) diluted 1:200 in Tris-EDTA (TE) buffer, pH7.5 (10 mM Tris-HCL pH 7.5, 1 mM Na_2EDTA). The plate was covered in foil and incubated for 5 minutes with shaking. The Quant-iT PicoGreen dsDNA reagent fluoresces when bound to DNA, and

is detected at 520nm following excitation with light at a wavelength of 480nm. The Dynex Revelation Reader spectrofluorimeter was used to excite and detect the fluorescent emission of Quant-iT PicoGreen stained DNA. The fluorescent values of the known concentrations of the calf thymus DNA were used to generate a standard curve and the unknown DNA concentrations were calculated from these measurements.

2.2.4 Fractionated dose regimen

MCF-10A cells were irradiated with fractionated doses of 5 Gγ and 10 Gγ to a cumulative dose of 80 Gγ. Cells were irradiated at approximately 40% confluency in T75 flasks that contained 20ml of medium. Dosing times are shown in table 2.1. Once cells began to grow again following exposure to ionising radiation, cells were trypsinised and seeded into a new T75 flask to allow continued cell recovery. Before confluence was reached in these flasks cells were trypsinised and seeded into a new T75 flask to receive the next dose of irradiation. Cells were also seeded into a T175 flask to be grown for cryopreservation (section 2.1.3) so that cells were stored after each fractionated dose. Cell populations from the fractionated dose regimens were termed the 'First 5 Gγ' and 'First 10 Gγ' irradiation series. An un-irradiated MCF-10A population was also grown to the same number of passages as cells that had received a cumulative dose of 80 Gγ in 5 Gγ fractionated doses to act as a reference population for acquired phenotypic and genetic changes. This cell population was termed the 'passage control population'.

Following the generation of the First 5 Gγ and 10 Gγ irradiation series the fractionated dose regimens were repeated with un-irradiated low passage MCF-10A cells, but with 10^{-8}M of 17β oestrodiol added to the medium throughout cell culture. Cell populations from these fractionated dose regimens were termed the 'Second 5 Gγ' and 'Second 10 Gγ' irradiation series. A second passage control population was generated with 10^{-8}M of 17β oestrodiol added to the medium throughout cell culture. When cryopreserved cells from the Second irradiation series were thawed for further study they were grown in normal MCF-10A growth medium without additional oestrodiol.

2.3 Cell cycle analysis

The proportion of cells in different phases of the cell cycle was analysed in sub-confluent and confluent populations of MCF-10A and MCF-7 cells by fluorescence activated flow cytometry. DNA from fixed cells was stained with the intercalating dye

propidium iodide (PI). The amount of fluorescence emitted by PI when excited by blue or UV light reflects the amount of DNA within a cell and therefore what stage of the cell cycle the cell was in when it was fixed. For example, cells in G2 phase of the cell cycle have double the DNA content as cells in G0 or G1. The FACScan (Becton Dickenson) machine was used to excite and detect the fluorescent emission of PI stained cells. The ModFit LT software (Verity Software House) was used to calculate the percentage of cells in each phase of the cell cycle using generated cytometric data.

2.3.1 Cell fixation and PI staining

Cells in T25 flasks were trypsinised, washed in cold PBS and then fixed in 2ml of 70% (v/v) ethanol in PBS. The fixed cells were incubated for at least 24 hours at 4°C. Following incubation the fixed cells were pelleted and re-suspended in 500µl of staining buffer (10µg/µl RNase A, 40µg/µl PI in PBS). The samples were incubated for 15 minutes at 37°C and then passed through a 23G needle to remove clumps. The samples were transferred to 5ml round bottomed FACS tubes (BD Biosciences, Oxford, UK) ready for analysis.

2.3.2 Fluorescence activated flow cytometry

Samples were measured using the FACScan machine (Becton Dickenson), together with CellQuest software (Beckton Dickenson). The FL2 detector was used to detect PI fluorescence. Scatter plots of FL2-A (the total fluorescence emitted from a cell) vs. FL2-W (the transit time of the cell through the argon laser beam) were used to optimise instrument settings. For each sample, 10000 events were collected. Cell aggregates and doublets could be identified on the FL2-A vs. FL2-W scatter plot as they have a longer transit time (FL2-W) through the argon laser than single cells. Aggregates and doublets in the 10000 events detected were excluded from subsequent analysis.

2.3.3 Analysis

Flow cytometric data was analysed using ModFit LT software (Verity Software House). Cytometric data of single cell events were used to generate cell count vs. FL2-A histograms. The proportion of cells in G1, S, and G2 was calculated by the software.

2.4 Cell phenotype assays

Cells from the First and Second 5 Gγ series were phenotypically characterised using a number of *in vitro* assays (Chapter 3). Cell populations analysed from the First 5 Gγ series had received cumulative doses of 10, 25, 40, 55 and 80 Gγ of ionising radiation. Cell populations analysed from the Second 5 Gγ series had received cumulative doses of 10, 20, 40, 60 and 80 Gγ of ionising radiation. Both series were tested and analysed separately. For each *in vitro* assay described, a low passage un-irradiated MCF-10A cell population and the appropriate passage control population for the series tested was also tested.

In all phenotype assays that utilised the PicoGreen fluorimetric DNA quantitation assay the protocol differed slightly from that detailed in section 2.2.3: only 1ml/well SSC-0.02%SDS solution was used to lyse the cells and only 50µl aliquots of cell lysate was placed into the black 96 well plates and mixed 1:1 with Quant-iT PicoGreen dsDNA reagent.

All digital photographs of cells were taken using the Visicam 5.0 (VWR International Ltd, Leicestershire, UK) mounted on an Olympus CK40 microscope.

2.4.1 Cell proliferation rate assay

Cell populations from the First 5 Gγ series were each plated in triplicate wells of 12 well plates (Corning-Costar - supplied by VWR International Ltd, Leicestershire, UK) at a cell density of $2x10^4$ cells per well. Each 12 well plate corresponded to a specific time point. All plates were incubated at 37°C/5% CO_2 and growth medium was replaced in every well each day of the experiment. Twenty four, 33, 48, 56, 72 and 80 hours after seeding, the DNA concentration of triplicate wells for each cell population was measured using the PicoGreen assay (section 2.2.3). Growth curves were generated for each population and growth rate, defined as the number of cell doublings per hour, was calculated from this data by exponential regression using available online software (http://www.doubling-time.com/compute.php).

For the Second 5 Gγ series populations, cells were plated in 24 well plates (Corning-Costar - supplied by VWR International Ltd, Leicestershire, UK) at a cell density of 10^4 cells per well, and DNA concentration was analysed after 24, 34, 48, 56 and 78 hours.

2.4.2 Contact inhibition assay – Cell cycle analysis

Low passage un-irradiated MCF-10A cells and cells from the First 5 Gγ series that had received a cumulative dose of 80 Gγ of radiation were seeded in 21 T25 flasks at 4 x 10^5 cells per flask. Forty eight hours after seeding, cells in 3 flasks per population were fixed for fluorescence activated flow cytometry as described in section 2.3. Three flasks were fixed every 24 hours thereafter for a further 6 days. MCF-10A growth medium was replaced in the flasks daily.

All the fixed cell populations were stained with PI and analysed using the FACScan machine and CytoCell software (both Becton Dickenson) (section 2.3). The mean percentage of cells in each phase of the cell cycle at each time point was calculated from triplicate fixed cell populations using the ModFIT LT software (Verity Software House) (section 2.3). The percentage of cells in S-phase of the cell cycle in confluent cell cultures was used as an indication of how many cells were still cycling and had therefore lost contact inhibition.

2.4.3 Contact inhibition assay – DNA quantitation

Cell populations from the First 5 Gγ series were plated in triplicate wells of 12 well plates at a cell density of 2x10^4 cells per well. All plates were incubated at 37°C/5% CO_2 and growth medium was replaced in every well each day. Nine days after seeding DNA concentration was measured using the PicoGreen assay and the mean DNA concentration per population was calculated using measurements taken from triplicate wells. The experiment was performed 4 times and the mean DNA concentration for each population was calculated using results from each experiment. DNA concentration for each population was expressed relative to the mean DNA concentration of the un-irradiated MCF-10A population. Relative difference in DNA concentration was used to indicate whether cell populations had continued to grow after they had reached confluency.

For the Second 5 Gγ series cells were plated in 24 well plates at a cell density of 10^4 cells per well.

2.4.4 Radiation resistance assay – 96-well cytotoxicity assay

A 96 well clonogenic assay was used to assess the cytotoxicity of ionising radiation on cell populations from the First and Second 5 Gγ series. The technique was first used to

determine the mutability of suspension cell lines at low density (Furth *et al.*, 1981) and was adapted for use in assessment of cytotoxicity in the present study.

Cell populations were trypsinised, counted using a haemocytometer and re-suspended in MCF-10A growth medium at a cell concentration of 10^5 cells/ml. From this, cell suspensions at a concentration of 10 cells/ml were prepared by 10 fold serial dilution. Two hundred microliters of cell suspension for each population was added to each well of duplicate 96-well plates, thereby seeding 2 cells/well. Twenty four hours after seeding one plate per population was exposed to 5 Gγ of ionising radiation by irradiation for 2.7 minutes while the remaining plate was used as an un-irradiated control. In all cases, cells were incubated at 37°C/5% CO_2 for 14 days.

Following the 14 day growth period the number of wells that had a cell colony containing at least 50 cells was recorded in both the irradiated and un-irradiated plates. The number of wells which contained cell colonies from the irradiated plates was expressed as a percentage of the number of wells that contained cell colonies from the same population in the un-irradiated plates. The higher the percentage the less cytotoxic ionising radiation was for that cell population. The experiment was repeated 3 times for the First 5 Gγ series and twice for the Second 5 Gγ series.

2.5 SNP array analysis

High-density polymorphism arrays can detect both copy number alterations and copy neutral LOH across the whole genome using probes for single nucleotide polymorphisms (SNPs) and copy number variants (CNVs) hybridised to a chip. SNPs are single nucleotides within the genome for which two distinct bases appear in a significant proportion of the population. Copy number variants (CNVs) are regions of chromosomes that vary in copy number in humans and are used in polymorphism array technology to look for patterns of copy number variation (Feuk *et al.*, 2006).

The Affymetrix Human SNP 6.0 Array contains more than 906,600 SNP probes and more than 946,000 CNV probes which can be used to interrogate the entire human genome (McCarroll et al., 2008). When sample DNA is hybridized to the oligonucleotide probes on the array a fluorescent signal is emitted. Computational algorithms are used to calculate the relative amounts of fluorescent signal detected and therefore the relative amount of sample DNA that was bound to the oligonucleotides. Data can be generated on the genotype of a SNP (homozygous for allele "A",

heterozygous or homozygous for allele "B") and the copy number state at each probe hybridization site. This allows for the construction of a highly informative integrated map of heterozygosity and copy number state across the entire cancer genome.

Genomic DNA from low passage MCF-10A, First 5 Gγ and 10 Gγ series, Second 5 Gγ and 10 Gγ series and relevant passage control populations were sent to Almac Diagnostics Ltd (Craigavon, UK) to be analysed using the Affymetrix Human SNP 6.0 Array platform. Samples were sent in 3 separate batches. DNA from the low passage MCF-10A and First irradiation series population was sent in the first batch. DNA from the Second irradiation series populations was sent in the second batch and DNA from the passage control populations was sent in the third batch.

2.5.1 Preparation of DNA for SNP array analysis

Genomic DNA was extracted from low passage MCF-10A and First irradiation series cell populations growing in culture using the QIAmp DNA Mini Kit (Qiagen). All buffers were provided by the kit and buffer constitutions are unknown. All centrifugation was done using the Hettich Mikro 22R centrifuge.

Cell populations were trypsinised, counted and re-suspended in MCF-10A growth medium at a concentration of $5x10^6$ cells/ml. One millilitre of cell suspension was added to a 1.5ml eppendorf tube and centrifuged for 5 minutes at 300 x g. The supernatant was removed and the cell pellet was re-suspended in 200µl of PBS followed by the addition of 20µl of proteinase K to digest proteins within the sample. To remove RNA, 4µl of RNaseA (stock 100mg/ml) was added to the sample. The sample was mixed with 200µl of lysis buffer (buffer AL) and incubated for 10 minutes at 56°C. The sample was mixed with 200µl of ethanol and loaded onto a QIAmp Mini spin column that contains a silica gel membrane to which DNA binds. The spin column was centrifuged for 1 minute at 6000 x g, the flow through discarded and 500µl of was buffer (AW1) was added to the spin column. The spin column was centrifuged for 1 minute at 6000 x g, the flow through discarded and 500µl of a second wash buffer (AW2) was added to the spin column. The column was then centrifuged for 3 minutes at 20000 x g. The column was transferred to a new 1.5ml eppendorf and 200µl of elution buffer (AE) (10 mM Tris-HCl, 0.5 mM EDTA, pH 9.0) was added to the spin column. The column was incubated for 1 minute at room temperature and then centrifuged for 1 minute at 6000 x g to elute the DNA.

DNA contained in the flow through was quantified using a NanoDrop® ND-1000 spectrophotometer which measures the absorbance of UV light at 260 nm passed through a 1µl aliquot of extracted DNA, and performs the necessary calculations to provide DNA concentration (in ng/µl). For each sample a minimum of 1µg of DNA was sent to Almac Diagnostics Ltd (Craigavon, UK) to be analysed using the Affymetrix Human SNP 6.0 Array platform.

Genomic DNA was extracted using the same protocol for the Second irradiation and passage control samples, except DNA was extracted directly from pelleted cryopreserved cells.

2.5.2 Data analysis

Raw-array data was received from Almac Diagnostics Ltd (Craigavon, UK). Initial processing of raw data was kindly performed by Dr V. Rand (NICR) using Genotyping Console v4.0 software to allow subsequent copy number and LOH analysis of samples (Affymetrix, California, USA). Briefly, SNP genotype calls were generated by an unpaired comparison to 270 samples from the international Hapmap project, a dataset provided by Affymetrix. The birdseed v2 algorithm was used on all samples within an array batch to maximise efficiency of the clustering algorithm, followed by quantile normalisation of the data. Copy number and LOH analysis was performed using the software's default settings. The detection threshold of copy number alterations was set to exclude regions of copy number change smaller than 100 kb and involving fewer than 5 markers. Quality control assessment of data was performed by determination of the call rate of control SNPs for each sample batch. Call rate of QC SNPs should be above 86%. (Batch 1 – median 95.17%, range 90.27 – 97.12; Batch 2 – median 96.16%, range 92.36% - 97.98%; Batch 3 – median 94.39, range 92.65 – 96.13).

Genome copy number differences between samples was analysed using the Affymetrix Genotyping Console Browser (v1.1.12). Copy number data was expressed as a log2 ratio of the relative signal intensity of each SNP. Copy number alterations smaller than 100 kb were identified by manual interrogation of the data by scanning log2 ratio maps of each chromosome. Log2 ratio's for each SNP could be exported and analysed to determine the putative copy number state of altered regions smaller than 100 kb.

Regions of copy number change from a diploid state and regions of LOH identified by the software that were not present in the low passage un-irradiated MCF-10A genome

were recorded. Identified copy number alterations in irradiated populations were then compared with copy number alterations in the appropriate passage control population and any common alterations were excluded from subsequent analysis.

2.5.3 Analysis of identified regions of copy number change

For large regions of copy number change comprising many genes a literature search for links between the region of the chromosome (i.e. Chromosome 11q) and 'cancer', 'breast cancer' and 'radiation' was performed using the PubMed literature database search engine (http://www.ncbi.nlm.nih.gov/pubmed/)

For regions of copy number change that comprised less than 10 genes, each gene in the region was individually reviewed in the literature for links with 'cancer', breast cancer' and 'radiation' using PubMed.

2.6 Gene expression analysis

The Illumina HT12 v4 expression array was used to analyse the gene expression profile of un-irradiated MCF-10A, First and Second 5 Gγ series and passage control populations. The HT12 v4 array is a whole genome direct-hybridisation BeadChip array which simultaneously profiles 47231 putative transcript sequences using 50-mer probe sequences attached to a 29-mer bead address sequence. Biotin labelled sample RNA binds to the probe sequences. The signal intensity for each probe is relative to the amount of biotin labelled RNA bound to the probe and therefore the abundance of that transcript sequence within the sample tested. Probe sequences were designed *in silico* to cover content from the NCBI RefSeq Release 38 including well established and provisional annotations of coding and non-coding transcripts. The arrays also include internal control sequences which analyse hybridisation efficiency and background signal.

RNA was extracted from growing cell populations and sent to Gen-probe (Manchester, UK) who labelled the RNA with biotin and performed the arrays. Signal intensity data sent back from Gen-probe was analysed for expression changes between irradiated samples and un-irradiated MCF-10A using Ilumina® GenomeStudio V2010.3 software.

2.6.1 Preparation of RNA for gene expression analysis

RNA was extracted using the RNeasy mini kit (Qiagen) according to the manufacturer's instructions. All buffers were provided by the kit and buffer constitutions are unknown. All centrifugations were done using the Hettich Mikro 22R centrifuge.

RNA was extracted from cell populations growing in T75 flasks. Cell populations were trypsinised, re-suspended in 1ml PBS and transferred to a 1.5ml eppendorf tube. The cell suspensions were centrifuged for 3 minutes at 300 x g to generate a cell pellet. Cell pellets were lysed by re-suspension in 350µl of lysis buffer (RLT). Lysate was homogenised by passing through a 21G needle 5 times and 350µl of 70% ethanol was added. The lysate was loaded onto an RNeasy spin column (which contains a silica gel membrane that binds RNA) to which a further 350µl of wash buffer (RW1) was added. The spin column was centrifuged for 15 seconds at 8000 x g and the flow through was discarded. To remove DNA, 80µl of a DNase I solution (10µl DNase I and 7 µl Buffer RDD) was added directly to the spin column membrane and incubated at room temperature for 15 minutes. Following incubation, 350µl of wash buffer was added to the spin column and centrifuged for 15 seconds at 8000 x g. The flow through was discarded, 500µl of a second wash buffer (RPE) was added to the spin column and centrifuged for 15 seconds at 8000 x g. This step was repeated but with a centrifuge time of 2 minutes. The RNeasy spin column was placed in a new 1.5ml eppendorf, 50µl of RNase free water was added directly to the spin column membrane and the RNA was eluted following centrifugation for 1 minute at 8000 x g.

Eluted RNA was quantified using a NanoDrop® ND-1000 spectrophotometer which measures the absorbance of UV light at 260 nm passed through a 1µl aliquot of extracted RNA, and performs the necessary calculations to provide RNA concentration (in ng/µl).

All RNA samples were sent to Gen-probe (Manchester, UK) in a volume of 25µl with a minimum concentration of 50ng/µl to be analysed using the Illumina HT12 v4 expression array.

2.6.2 Data analysis

Raw array-generated probe intensity data files were received by Gen-probe and analysed using Ilumina® GenomeStudio V2010.3 software. The data was normalised

using quantile normalisation algorithms. All samples passed sample independent and sample dependant quality control assessment.

The software calculates a detection p-value which determines the probability that the signal of a given probe is greater than the average signal from internal negative controls. Some genes are assessed by more than one probe. The undetected probe may represent a splice variant or represent a probe sequence that has not been experimentally verified and therefore doesn't represent expression of the gene it was designed for. Lack of detection of one probe within a gene probe set in which all other probes were detected could affect subsequent differential expression analysis for that gene. Therefore all probes that did not have a detection p-value < 0.05 were removed from subsequent analysis.

Probe intensity data from the First and Second 5 Gγ series samples and appropriate passage control samples were compared with probe intensity data from un-irradiated MCF-10A to identify any gene expression changes. The 'Illumina Custom' differential expression algorithm was used to identify differentially expressed genes. Briefly, the algorithm assumes that probe signal intensity is normally distributed and calculates the variation of signal intensity using three components: sequence specific biological variation, non-specific signal variation and technical error variation. The differential expression p-value is calculated depending on the difference in signal intensity of a probe between 2 samples while taking into account the signal variation of that probe in each sample. In the present study there were no replicate samples; therefore specific biological variation and technical error variation could not be estimated and variation could only be assessed by negative control sequences (non-specific signal variation). If the software was not confident that there was a difference in expression for a probe between the samples based on this algorithm then a differentiation p-value of 1 was attributed to the probe in question. If the software was confident of a difference in expression a p-value < 1 was attributed to the probe; however the significance of the difference in expression varied.

A differentiation score was calculated for each probe by the software based on the confidence in the difference of expression between samples and the magnitude of this difference. For genes with more than one probe, the differentiation score of corresponding probes were averaged. A differentiation score was only attributed to probes that had a differentiation p-value < 1. In the present study a differentially

expressed gene was identified as any gene that had been attributed a differentiation score, regardless of the significance of this expression change.

2.7 Functional clustering analysis

Genes that were attributed a differentiation score in the 55 Gγ population of the First 5 Gγ series but were not attributed a differentiation score in the passage control population were assessed for functionally related gene clusters using the **D**atabase for **A**nnotation, **V**isualization and **I**ntegrated **D**iscovery (DAVID) (Huang *et al.*, 2009a; Huang *et al.*, 2009b), an online gene function clustering tool (http://david.abcc.ncifcrf.gov/).

DAVID identifies genes that share common functions as defined by gene ontology (GO) database annotations. Gene ontology terms have a hierarchy from broad to specific functional annotations. A list of differentially expressed genes form the 55 Gγ population was analysed against the GO FAT database (which filters out the broadest functional terms in the hierarchy) for gene clusters attributed to biological process (BP), cellular component (CC) and molecular function (MF) gene ontology annotations (http://www.ebi.ac.uk/QuickGO/).

DAVID uses a modified Fisher Exact Test to calculate the probability that an identified functionally related gene cluster within a given gene list is not present in that gene list by random chance. Briefly, the software compares the proportion of genes in the given gene list that clusters to the biological function in question to the number of genes in the human genome which are related to the biological function. Gene clusters which were not significantly associated with a biological function were excluded from the analysis (p value threshold = 0.05).

Due to the redundant nature of GO annotations in the GO database, DAVID groups GO annotations that share common genes between their respective gene clusters. Briefly, DAVID compares the clustered genes in each identified cluster with every other gene cluster and measures the degree of similarity between the clusters using kappa statistics. A score is attributed to each pair of gene clusters between 0 and 1 to indicate how closely the clusters agree (0 = no agreement, 1 = perfect agreement). A threshold similarity score of 0.85 was set in the present study. Gene clusters which fell below this threshold were not grouped together.

2.8 Fluorescent *in situ* hybridisation (FISH) analysis of *POU2F1* and *c-MYC* loci

In order to confirm copy number alterations identified by SNP array analysis in the irradiated series, FISH was performed on fixed cells. Low-passage un-irradiated MCF-10 cells were assessed for both *POU2F1* and *c-MYC.* First 5 Gγ series populations and the appropriate passage control population were only assessed for *POU2F1* deletion, the Second 5 Gγ series populations and appropriate passage control population were only assessed for *c-MYC* copy number increase.

2.8.1 POU2F1 FISH probe preparation

A commercial FISH probe was not available for the *POU2F1* locus so a probe had to be designed using bacterial artificial chromosome (BAC) clones purchased from the Roswell Park Cancer Institute (New York, USA). Appropriate BAC clones were chosen using the Ensemble Genome Browser. BAC clones were chosen that were within the deleted region on chromosome 1, encompassed the *POU2F1* locus, had overlapping sequences and were from the 30k clone set (Fig. 2.1). The chosen clones were Chr1tp-8H10, Chr1tp-8H11 and Chr1tp-8H12.

Clones were received as bacterial stabs which had to be cultured so that the probe DNA could be extracted for labelling with an appropriate fluorochrome.

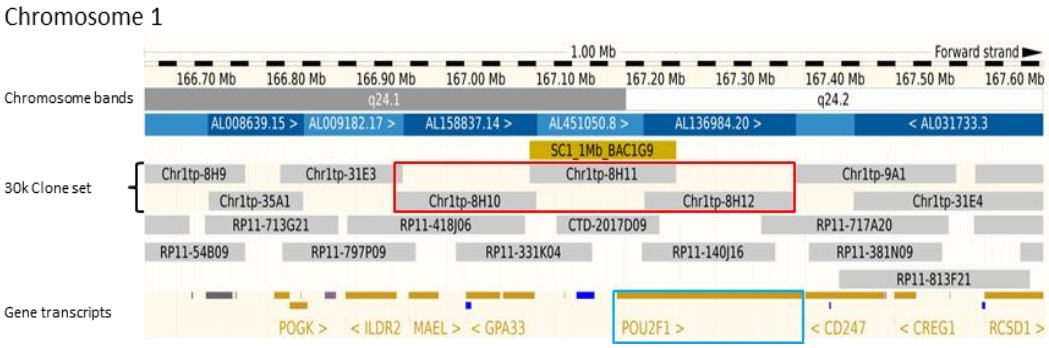

Figure 2.1 BAC clones chosen to asses *POU2F1* copy number
The image above is from the Ensemble genome browser and shows the region of chromosome 1 which contains *POU2F1* (shown in the blue box) and the clones chosen from the 30k clone set to generate a FISH probe to assess *POU2F1* copy number (clones chosen shown in the red box).

2.8.2 Culture of BAC clones

Clones were streaked using a sterile inoculation loop onto individual LB agar plates (1% (w/v) tryptone, 0.5% (w/v) yeast extract, 1% (w/v) NaCl, 1.5% (w/v) agar in deionised water) containing 12.5µg/ml chloramphenicol. The plates were incubated overnight at 37°C. The following day a single colony was picked from each plate and inoculated in

separate conical flasks containing 200ml of LB medium (1% (w/v) tryptone, 0.5% (w/v) yeast extract, 1% (w/v) NaCl) supplemented with 12.5µg/ml chloramphenicol. The cultures were incubated at 37°C overnight in a shaking incubator (C24 Incubator Shaker – Edison, NJ, USA).

2.8.3 Extraction of bacterial DNA for use as FISH probes

DNA was extracted using the NucleoBond® XtraMidi Kit (Macherey-Nagel). All buffers were provided by the kit and buffer constitutions are unknown. The 200ml bacterial cultures were split into 4 separate 50ml Falcon™ tubes and centrifuged for 15 minutes at 5000 x g at 4°C (Heraeus Multifuge 35R+, Thermo Scientific). The supernatant was discarded and the cell pellet re-suspended in 4ml of re-suspension buffer. The contents of 2 of the tubes were then combined into one single tube resulting in two tubes with 8ml of re-suspended material to which 8ml of lysis buffer was added. The suspensions were incubated for 5 minutes at room temperature. Following incubation, 8ml of neutralising buffer was added to the suspensions and mixed by inverting the tubes 15 times. The lysates were then centrifuged at 4°C for 15 minutes at 5000 x g (Heraeus Multifuge 35R+, Thermo Scientific).

The lysates were passed through a nucleobond column which has a silica membrane that binds DNA and a filter which binds the lysed bacteria. The nucleobond column was first equilibrated by applying 12ml of equilibration buffer. Following centrifugation of the lysate the supernatant of both tubes was added to the nucleobond column and flow through was allowed to pass through the column by gravity flow. The column was then washed by applying 5ml of equilibration buffer. The column filter was removed and the column washed with 8ml of wash buffer. DNA was then eluted into a fresh 50ml Falcon™ tube using 5ml of a high salt elution buffer.

DNA was precipitated out of the elution buffer. Isopropanol (3.5ml) was added to the elute and incubated for 2 minutes at room temperature. The elute was then centrifuged at 4°C for 30 minutes at 12000 rpm (Heraeus Multifuge 35R+, Thermo Scientific). Following centrifugation the supernatant was removed and 2ml of 70% ethanol (diluted in deionised water) was added to the pellet. The pellet was centrifuged at room temperature for 5 minutes at 12000 rpm (Heraeus Multifuge 35R+, Thermo Scientific). Following centrifugation the pellet was allowed to air dry and then reconstituted in 200µl of distilled water.

2.8.4 Fluorescent labelling of extracted DNA

DNA extracted from the BAC clones was fluorescently labelled using a Nick Translation Kit (Abbott Molecular, Berkshire, UK). Equal amounts of dATP, dCTP and dGTP were first mixed together to create a dNTP mix. dTTP was diluted separately in nuclease free water at a ratio of 1:2. In an eppendorf tube 10µl dNTP, 5µl dTTP, 5µl of NT buffer and 2.5µl of green labelled (5-Fluorescein) dUTP (Enzo Life Sciences, Exeter, UK) was mixed per DNA sample to be labelled. To this mix 17.5µl of extracted DNA was added followed by 10µl of Nick Translation enzyme mix (exact constitution unknown but most likely contains DNase to nick DNA strands and E.coli polymerase 1 to add fluorescently labelled nucleotides to the nicked DNA). The mixture was incubated at 15°C overnight on a chilling block (PCH-1, Grant-Bio).

The following day the reaction was stopped by the addition of 3µl of 0.5M EDTA. Unlabelled probe was removed by passing through quant Sephadex™ columns (GE Healthcare, Buckinghamshire, UK). The columns purify DNA by gel filtration which does not allow unbound probe to be eluted. First the resin in Sephadex™ columns was re-suspended by vortexing, centrifuged, and the flow through discarded. The labelled DNA sample (50µl) was pipetted into the centre of the resin within the column and the column was centrifuged for 2 minutes at 4000 rpm (Centrifuge 5419, Eppendorf). Ten microliters of human cot-1 DNA was then added to the eluted DNA to bind repetitive sequences present in the probe DNA. A 1 in 10 volume of 3M sodium acetate was added followed by 2.5 times the volume of ice cold ethanol. The samples were incubated at -20°C for 3 hours and then centrifuged for 30 minutes at 13000 rpm at 4°C (Centrifuge 5415, Eppendorf). The supernatant was removed and the pellet re-suspended in 14µl of hybridisation buffer (Cytocell, Cambridge, UK) and 6µl of nuclease free water. The probes were then stored at -20°C until ready for use.

2.8.5 Preparation of c-MYC and centromere 8 probes

For copy number analysis of *c-MYC* the Vysis LSI SpectrumOrange Probe (Abbott Molecular, Berkshire, UK – Cat#:05J545-011) which hybridises a 120kb region spanning the *c-MYC* gene and the CEP8 SpectrumGreen Probe (Abbott Molecular, Berkshire, UK – Cat#:06J37-018) which hybridises to the 8p11.1-q11.1 region of chromosome 8 were used.

Each probe was diluted 1:5 in hybridisation buffer (delivered with each probe) and then mixed together in a 1:1 ratio (*c-MYC/CEP8* probe mix).

2.8.6 Preparation of POU2F1 and centromere 1 probes

For copy number analysis of *POU2F1* the 3 green fluorophore labelled probes (Chr1tp-8H10, Chr1tp-8H11 and Chr1tp-8H12) (section 2.8) which hybridise to DNA within the focal deleted region on chromosome 1q and the Spectrum Red Chromosome 1 Classic Satellite Probe (Cytocell, Cambridge, UK – Cat#LPE001R) which hybridises to the centromere of chromosome 1 were used.

The 3 green fluorophore labelled probes were mixed in equal quantitates. The Spectrum Red Chromosome 1 Classic Satellite Probe was diluted 1:10 with hybridisation buffer provided with the probe. The *POU2F1* probe mix and centromere probe was then mixed in a 1:1 ratio ready for FISH (*POU2F1* probe mix).

2.8.7 Cell line fixation protocol

Cells were grown to approximately 60% confluence in T25 flasks. At the time of fixation growth medium was replaced with 7ml of normal MCF-10A growth medium containing 70µl of KaryoMAX colcemid solution (10µg/ml stock concentration – Invitrogen, Paisley, UK) and incubated for 1 hour at 37°C/5% CO_2 in an attempt to arrest cells in metaphase. Following incubation cells were trypsinised, centrifuged for 5 minutes at 1500 rpm (Beckman Allegra X-12 R rotor SX 4750) and then re-suspended in 1 ml of 0.75M KCl. The suspension was incubated for 10 minutes at 37°C to cause the cells to swell, and then centrifuged for 3 minutes at 1000 rpm (Beckman Allegra X-12 R rotor SX 4750). The supernatant was discarded and 1ml of fixative (3:1 methanol:acetic acid) was added slowly, followed by a further 4ml of fixative. The fixed cells were then pelleted, re-suspended in 1ml of fixative, transferred to 2ml micro tubes (Sarstedt, Leicester, UK) and stored at -20°C until ready for use.

2.8.8 Preparation of samples for FISH

Samples were centrifuged for 2 minutes at 13000 rpm (Centrifuge 5419, Eppendorf). The fixative was removed and the cells re-suspended in fresh fixative (3:1 methanol:acetic acid). Three microliters of sample was added onto a Superfrost microscope slide (Thermo Scientific, West Sussex, UK) and allowed to air dry for 10-15 minutes at 60°C (REC, Digital Heating Ceramic Plate).

2.8.9 Probe hybridisation

Once the cell spots had dried (section 2.9.2) 2µl of appropriate probe mix was added to a round coverslip (VWR International Ltd, Leicestershire, UK) and the coverslip placed over the cells. The edges around the coverslip were sealed with rubber cement. Slides were placed on a humidified hybridisation block (HYBrite™, Abbott Molecular, Berkshire, UK) and heated to 72°C for 5 minutes to denature the probe and nuclear DNA. The slides were then incubated for 24 hours (*c-MYC/CEP8* probe mix) or 48 hours (*POU2F1* probe mix) in the humidified hybridisation chamber at 37°C to allow hybridisation of probe to its target sequence.

2.8.10 Processing of slides following FISH

The slides were taken from the humidified hybridisation blocks after the appropriate length of time and the rubber cement surrounding the coverslips removed. To remove the coverslips the slides were soaked in 20X SSC solution (3M NaCl, 300mM trisodium citrate – Invitrogen) diluted 1:10 in deionised water. The slides were then soaked in Wash 1 solution (2% (v/v) 20X SSC, 0.3% (v/v) NP40 in deionised water) for 2 minutes at 72°C followed by being soaked in Wash 2 solution (10% (v/v) 20X SSC, 0.1% NP40 in deionised water) for a further 2 minutes at room temperature. The slides were removed from the wash, allowed to dry and then 3µl of DAPI (Vector Laboratories, Peterborough, UK) was loaded onto the slide at each cell spot as a nuclear counterstain. The cell spots were then covered with a cover slip ready for analysis.

2.8.11 Analysis of FISH

Cells were analysed using an Olympus BX61 fluorescent microscope with an X-cite 120 mercury bulb and CytoVision camera and imaging software (Leica Microsystems, Newcastle Upon Tyne, UK). Filters allowing the appropriate wavelengths of light through to excite each probe were used to visualise probe staining and DAPI counterstaining (Table 2.2).

For each sample analysed 100 nuclei were scored and the combination of probe signals per nuclei recorded. Blind second scoring of 6/14 samples produced results that were not different to the first scoring (χ^2: $p>0.05$). Photographs were taken using the CytoVision image capture system (Leica Microsystems, Newcastle Upon Tyne, UK) at x40 magnification for use as representative images of the different genotypes observed.

Probe	Filter	Excitation wavelength	Emission wavelength
DAPI	DAPI	359	461
POU2F1	Spectrum Green	497	524
c-MYC	Spectrum Orange	559	588
CEP8	Spectrum Green	497	524
Centromere 1	Spectrum Orange	559	588

Table 2.2 Excitation and emission wavelengths for each probe and counterstain used during FISH.

2.9 G-band karyotyping and metaphase FISH

Fixed cell preparations with metaphase chromosome spreads were generated by David Rowe (Institute of Genetic Medicine, Newcastle, UK) from low passage un-irradiated MCF-10A cells and cells from the Second 5 Gγ series that had received a cumulative dose of 80 Gγ. David Rowe also karyotyped the samples.

2.9.1 Fixed cell preparation

Briefly, growing cells were treated with colcemid and incubated for 4 hours at 37°C/5% CO_2. The cells were then trypsinised, suspended in 0.075 KCl for 7 minutes and then re-suspended in fixative (3:1 - methanol:acetic acid).

Fixed cells were re-suspended in fresh fixative to a suitable cell density and a single drop of sample was dropped at one end of a Superfrost® microscope slide and allowed to run down to the end of the slide (Thermo Scientific, West Sussex, UK). For G-band karyotyping the slides were incubated overnight at 60°C.

2.9.2 G-band karyotyping

Preparations were made of banding trypsin (0.5g of trypsin powder in 10 ml distilled water), saline solution (0.9% (w/v) NaCl in distilled water) and staining solution (8 ml Giemsa stain, 0.5 ml Leishmans stain and 40 ml Gurr buffer).

Slides were soaked and agitated in trypsin solution (2 ml banding trypsin, 25 ml saline solution, 25 ml Gurr buffer) for 7-10 seconds and then immediately transferred and twice soaked in saline solution. The slides were rinsed in distilled water and placed in staining solution for 3 minutes. The slides were then rinsed thoroughly in distilled water and mounted with a coverslip using DPX Mountant.

Twenty metaphase chromosome spreads were analysed for each population and the G-band karyotypes recorded.

2.9.3 Metaphase FISH

Slides with metaphase chromosomes were analysed using FISH. The low-passage MCF-10A sample was analysed for *c-MYC* and *POU2F1* using the protocols outlined in section 2.9. The Second 5 Gγ series 80 Gγ population was only analysed for *c-MYC* copy number. Twenty metaphase chromosome spreads were analysed for each population.

2.10 Western transfer analysis

Protein expression of POU2F1 was analysed in protein extracts from the First 5 Gγ series and c-MYC expression in protein extracts from the Second 5 Gγ series to determine if expression change was concomitant with change in copy number. Protein extracts were made from cells growing in T25 flasks. Three independent extracts were made per cell population analysed. Relative expression between each population was analysed for each extract by western transfer and densitometric analysis. Expression of GAPDH was analysed in each population as a protein loading control as it was not expected that expression of GAPDH would differ between populations.

2.10.1 Protein extraction

Cells were grown in T25 flasks to at least 60% confluence. Cells were first washed with cold PBS and then lysed with 1ml of radioimmunoprecipitation assay buffer (RIPA) (50mM Tris-HCl pH 7.5, 150mM NaCl, 1mM EDTA, 1% (w/v) NP-40 and 0.25% (w/v) sodium deoxyxholate) supplemented with 1μg/ml pepstatin, 1μg/ml aprotinin, 1μg/ml leupeptin, 2mM sodium orthovanadate, 2mM sodium fluoride and 2mM phenyl methyl sulphonyl fluoride, which are protease inhibitors. After addition of the RIPA buffer cells were kept on ice with gentle agitation for 30 minutes. The cell lysate was transferred to 1.5ml centrifuge tubes (Sarstedt, Leicester, UK) and centrifuged at 14000 rpm (Hettich Mikro 22R) for 10 minutes at 4°C. The supernatant was collected and stored at -70°C.

2.10.2 Protein quantification

Protein concentration was measured using the Pierce® bicinchoninic acid (BCA) colourimetric assay. Known concentrations of protein ranging from 0.2-2mg/ml were prepared by re-suspending BSA in RIPA buffer and diluted 1:10 in deionised water for later use in generating a standard curve. Lysate aliquots of 0.5µl were also diluted in a 1:10 ratio in deionised water. BCA assay reagents A and B (Thermo Scientific, West Sussex, UK) were mixed at a ratio of 50:1. Ninety five microliters of the mixture was added to 5µl of each protein standard and diluted lysate. The samples were incubated for 30 minutes at 37°C. Following incubation, samples were placed on ice and the absorbance at 562 nm was measured using a spectrophotometer (Beckman DU 640). A standard curve was generated using the protein standards and unknown protein concentrations of the cell lysates were interpolated using the line of best fit from the standard curve (correlation coefficient: $R^2 < 0.98$).

2.10.3 Polyacrylamide gel electrophoresis

Sodium dodecyl sulphate (SDS) polyacrylamide gel electrophoresis was used to separate proteins. The acrylamide to bisacrylamide ratio was 200:1 (w/w) for the separating gel and contained 12% polyacrylamide (v/v), 0.5M Tris-HCl pH 8.8, 0.1% (w/v) SDS, 0.05% (w/v) ammonium persulphate and 0.1% (v/v) N, N, N', N'-tetramethylethylenediamine (TEMED). The acrylamide to bisacrylamide ratio was 20:1 (w/w) for the stacking gel and contained 3% polyacrylamide (v/v), 125mM Tris-HCl pH 6.8, 0.1% (w/v) SDS. The separating gel was applied to a vertical gel cast (Hoeffer) and allowed to polymerise for 45 minutes followed by the stacking gel which was allowed to polymerise for 15 minutes. A lane comb was positioned at the top of the gel cast as the stacking gel was applied to create lane positions in which protein sample could be placed.

Cell lysate aliquots containing 10µg of protein were mixed with 10µl of 124mM Tris-HCl, 25mM Na_2EDTA, 4% (w/v) SDS, 20% (w/v) glycerol, 0.01% (w/v) bromophenol blue and 10% (v/v) β-mercaptoethanol pH 6.8, made up to a total volume of 20µl using RIPA buffer and boiled for 10 minutes. Samples were then placed in the lanes positioned in the stacking gel. Protein markers of known molecular mass (Full Range rainbow Marker – GE Life Sciences) were placed alongside samples.

Protein samples were electrophoresed in Mighty Small II electrophoresis chambers (Amersham Pharmacia) using a running buffer of 0.5M Tris-HCl, 0.38 M glycine, 0.1% SDS (w/v) at a constant current of 10mA per gel.

2.10.4 Western transfer

Proteins separated by polyacrylamide gel electrophoresis were transferred onto Westran 0.45µM nitrocellulose membrane (VWR International Ltd, Leicestershire, UK) using a semi-dry transfer apparatus (S&S CarboGlas, Peglab, PerfectBlue). From anode to cathode the transfer sandwich comprised two sheets of Whatman 3mm chromatography paper soaked in 0.3M Tris, 20% (v/v) methanol, one sheet soaked in 25mM Tris, 20% (v/v) methanol, nitrocellulose membrane soaked in 25mM Tris, 20% (v/v) methanol, the polyacrylamide separating gel the proteins are bound in and three sheets of Whatman 3mm chromatography paper soaked in 25mM Tris, 40mM 6-aminocaproic acid, 20% (v/v) methanol. The transfer sandwich was electrophoresed at 100mA per gel for 45-60 minutes to allow protein transfer.

Following transfer the membranes were dried overnight, rehydrated in deionised water and washed 3 times for 5 minutes in 25ml 20mM Tris-HCl, 140mM NaCl, 0.1% (v/v) Tween 20 (TBS-Tween). The membranes were then blocked in 5% (w/v) milk in TBS-Tween solution for 60 minutes at room temperature with gentle shaking. Following blocking, membranes were washed a further 3 times for 5 minutes in TBS-Tween solution and then incubated with primary antibody for c-MYC (Santa Cruz Biotechnology, California, USA – Cat#: N-262) or POU2F1 (Santa Cruz Biotechnology, California, USA – Cat#: POU51097) (Table 2.3) (depending on the sample analysed) diluted in 5ml 5% milk (w/v) in TBS-Tween in 50ml tubes agitated on rollers overnight at 4°C. Following incubation with primary antibody, membranes were washed a further 3 times in TBS-Tween and then incubated with horse-radish peroxidase conjugated secondary antibody (Thermo Scientific, West Sussex, UK) (Table 2.3) diluted in 5ml 5% milk in TBS-Tween in 50ml tubes agitated on rollers at room temperature for 90 minutes. Following incubation with secondary antibody, membranes were washed a further 3 times in TBS-Tween and once in TBS.

The membranes were incubated in Supersignal West Dura Extended Duration Substrate Chemiluminescent Solutions Luminol/Enhancer mixed with Peroxide buffer in a 1:1 ratio for 5 minutes and exposed to x-ray film (Fuji, SuperRX) and developed. Exposure times varied (Table 2.3).

After analysis of POU2F1 and c-MYC expression, membranes were washed 3 times for 5 minutes in TBS-Tween solution and then analysed for GAPDH (Santa Cruz Biotechnology, California, USA – Cat#: FL-335) expression following the protocol above (beginning at incubation in primary antibody).

1° Antibody	Dilution	2° Antibody	Dilution	Exposure time
POU2F1	1:1000	Mouse	1:1000	< 5 mins
c-MYC	1:5000	Rabbit	1:2500	< 1 min
GAPDH	1:5000	Rabbit	1:5000	< 10 secs

Table 2.3 Antibody dilutions and exposure times

2.10.5 Densitometric analysis

The x-ray film was digitally scanned and the densitometry of each protein band was analysed using the Lab Works 4.0 software. The background of the x-ray film was subtracted from the analysis. Variations in the amount of protein loaded for each sample was normalised using GAPDH densitometry values. Protein expression of c-MYC and POU2F1 for irradiated and passage control samples was expressed as the percentage of expression relative to un-irradiated MCF-10A. Mean expression was calculated from comparative densitometric analysis of 3 independent protein extracts per population.

2.11 Genotoxic stress assays

Growth inhibition was compared between low passage un-irradiated MCF-10A cells and cells from the First 5 Gγ series which had received a cumulative dose of 80 Gγ of radiation following treatment with different concentrations of hydrogen peroxide (H_2O_2) and doxorubicin, both of which cause DNA damage. Resazurin was used to test the relative amount of viable cells in each population at each concentration. These experiments were kindly performed by Dr N. Sunter.

2.11.1 Growth inhibition assay with H_2O_2

Cells were trypsinised, counted using a haemocytometer and re-suspended in 7ml of growth medium at a concentration of 4 x 10^4 cells/ml. Ninety microliters of cell suspension was seeded per well in 60 wells of a 96 well plate and grown for 24 hours at 37°C/5% CO_2. A 1M H_2O_2 solution was prepared by addition of 102µl of 9.8 M H_2O_2 to 898µl of MCF-10A growth medium and a 100mM solution was prepared from this by a 10 fold dilution in MCF-10A growth medium. Using this dilution 9 separate

concentrations of H_2O_2 were prepared using MCF-10A growth medium and 10µl of each concentration was added to 6 wells per concentration (Table 2.4).

Concentration of H_2O_2 (nM)	Final concentration of H2O2 (nM) per well
4500	450
4000	400
3500	350
3000	300
2500	250
2000	200
1500	150
1000	100
500	50
0 (growth medium)	0

Table 2.4 Concentrations of H_2O_2 used in growth inhibition assay

Plates were incubated for 24 hours at 37°C/5% CO_2 and then examined by the resazurin assay (Section 2.12.3).

2.11.2 Growth inhibition assay with doxorubicin

Cells were trypsinised, counted using a haemocytometer and re-suspended in 4ml of growth medium at a concentration of 2 x 10^4 cells/ml for un-irradiated MCF-10A and 3 x 10^4 cells/ml for cells from the First 5 Gγ series that had received a cumulative dose of 80 Gγ. Ninety microliters of cell suspension was seeded per well in 30 wells of a 96 well plate and grown for 24 hours at 37°C/5% CO_2. A 0.1mM doxorubicin solution was prepared by addition of 30µl of 1mM doxorubicin to 270µl of MCF-10A growth medium. Four separate concentrations of doxorubicin were prepared by ten-fold serial dilutions of the 0.1mM solution in MCF-10A growth medium (Table 2.5). A solvent control was also prepared by addition of 0.1% (v/v) DMSO in growth medium as doxorubicin stock solution contains DMSO. Five microliters of each doxorubicin concentration was added to 6 wells per concentration (Table 2.5).

Concentration of doxirubicin (nM)	Final concentration of doxirubicin (nM) per well
100000	10000
10000	1000
1000	100
100	10
DMSO 0.1% (v/v)	Solvent control

Table 2.5 Concentrations of doxirubicin used in growth inhibition assays

Plates were incubated for 72 hours at 37°C/5% CO_2 and then examined by resazurin assay (Section 2.12.3).

2.11.3 Resazurin assay

Resazurin is a non-toxic, cell permeable compound, which upon entering cells is reduced to resorufin. Resorufin is red in colour, is fluorescent and is released into growth medium by cells when it is produced. Metabolically active cells continuously convert resazurin to resorufin so the relative fluorescence and colour of the media surrounding cells can be used to compare the relative number of viable cells between samples.

Ten microliters of 100μg/ml resazurin was added to each well containing cells following treatment with either H_2O_2 or doxorubicin. The cells were incubated for 4 hours at 37°C and then fluorescence of the growth medium was analysed using a FLUOstar Omega microplate reader (BMG Labtech). Resofurin is excited at a wavelength of 560 nm and emission is detected at 580 nm. Fluorescent readings from multiple wells were used to calculate the mean relative amount of viable cells at each concentration of H_2O_2 or doxorubicin treatment as a percentage of the number of viable cells in a non-treated control.

2.12 DNA repair gene expression analysis

Expression of DNA repair genes was compared between low passage un-irradiated MCF-10A cells and cells from the First 5 Gγ series which had received a cumulative dose of 80 Gγ using a RT^2 Profiler PCR Array (SABiosciences, Maryland, USA).

2.12.1 RNA extraction

RNA was extracted from cell populations growing in T75 flasks using the RNeasy mini kit (Qiagen) according to the manufacturer's instructions. The extraction protocol was

the same as in section 2.6 except the cell lysate was homogenised by adding the lysate directly into a QIAshredder spin column which was centrifuged for 2 minutes at 8000 x g (Hettich Mikro 22R). Extracted RNA was quantified using a NanoDrop® ND-1000 spectrophotometer.

2.12.2 First strand cDNA synthesis

cDNA was synthesised from extracted RNA using the RT^2 First Strand Kit (SABiosciences, Maryland, USA) following manufacturer's instructions.

The first step was a genomic DNA elimination procedure whereby 1µg of RNA was mixed with 2µl of 5X genomic DNA elimination buffer, made to a final volume of 10µl with RNAse free water and incubated for 5 minutes at 4°C. Following incubation the genomic DNA elimination mixture was put directly on ice. Ten microliters of a reverse transcription (RT) cocktail containing RT buffer, primers and RT enzyme was added to the genomic DNA elimination mixture and incubated for 15 minutes at 42°C. Following incubation the RT reaction was stopped by heating the samples for 5 minutes at 95°C. The sample was then diluted in 91µl RNAse free water.

2.12.4 DNA repair gene array

A 96 well RT^2 Profiler PCR Array (SABiosciences, Maryland, USA) was used to analyse relative expression of DNA repair genes using synthesised cDNA. The first strand cDNA synthesis mixture was mixed with 1350µl of SABiosciences RT^2 qPCR Master Mix and was made to a total volume of 2700µl with water. Each well of the 96 well RT^2 Profiler PCR Array was loaded with 25µl of sample. The 96 well plate was sealed and centrifuged for 1 minute at 1000 x g (Sigma 4K15C) to remove bubbles and then placed on ice.

The 7300 Real Time PCR System (Applied Biosystems, California, USA) was used to run the real time qPCR using default baseline and threshold settings. The cycling programme used is shown in table 2.6. Cycle time (Ct) values were calculated automatically for each well of the array by the Sequence Detection Software V.1.3.1.21 (Applied Biosystems, California, USA). Data from the array was uploaded to the SABiosciences PCR array data analysis online portal (http://pcrdataanalysis.sabiosciences.com/pcr/arrayanalysis.php) which analyses the array QC and compares gene expression between different arrays. Expression data from the low passage un-irradiated MCF-10A sample was used as the control dataset to

which expression data from the 80 Gγ population was compared. Arrays for both populations passed Reverse Transcription QC ($\Delta C_t \leq 5$) and genomic DNA contamination QC ($C_t^{GDC} \geq 35$).

Stage	Cycles	Duration (minutes)	Temperature (°C)
1	1	10:00	95
2	40	00:15	95
		01:00	60
3	1	00:15	95
		00:30	60
		00:15	95

Table 2.6 qPCR repair gene cycle programme.

2.13 Breast cancer tissue samples

A cohort of paraffin embedded breast cancer tissue samples from 18 women who had received radiotherapy for Hodgkin lymphoma were available from the National Cancer Registries of Finland (n=8) and Sweden (n=10) (radiogenic breast cancer samples) and were kindly provided by Prof. L.B. Travis (University of Rochester Medical Centre). Estimates of the radiation dose delivered to the specific location in the breast where the cancer developed were made following review of relevant tumour and radiotherapy records by a radiation oncologist (M. Gospodarowiscz, Ontario Cancer Institute) and radiation physicist (M. Stovall, The University of Texas M.D. Anderson Cancer Centre) as described by Travis et al. (2003). Briefly, dose estimates were derived using standard radiotherapy techniques and if tumours occurred outside the nearest measurement field, out-of-beam measurements using a water phantom were used (Stovall *et al.*, 1989). Data on age at Hodgkin lymphoma diagnosis, age at breast cancer diagnosis, stage and pathology of breast cancer, quadrant of the breast the tumour developed in and any chemotherapy treatment received by the individual for Hodgkin lymphoma was also available for each case.

An age matched cohort of paraffin embedded breast cancer tissue samples from individuals with no history of prior cancer or therapeutic radiation exposure were provided by Dr F. May (sporadic breast cancer). Age at the time of breast cancer diagnosis was available for these samples.

All tissues samples used were obtained following appropriate ethical approval.

2.14 Protein expression analysis of breast cancer tissue samples

Paraffin wax tissue sections of radiogenic and spontaneous breast cancer samples (section 2.15) were analysed for expression of c-MYC and POU2F1 by immunohistochemistry (IHC). Tissue section preparation and immunohistochemical staining using c-MYC and POU2F1 antibodies was performed by Anna Long (Histopathology Assistant, NICR, Newcastle University). Estimates of the percentage of nuclei in each section which were from tumour cells were also provided by Anna Long.

2.14.1 c-MYC and POU2F1 IHC

Sections were cut from formalin-fixed, paraffin-embedded tissue blocks using a Microm rotary microtome at 5μm thickness. The sections were floated in a water bath heated to 50°C to flatten out the sections and then mounted on to Superfrost™ adhesion slides (Thermo Scientific, West Sussex, UK). The slides were dried in a slide warmer (RA-Lamb) for 90 minutes at 60°C. Following this, slides were soaked in xylene for 5 minutes to de-wax the sections. The slides were then soaked in absolute, 95% (v/v), 70% (v/v) and 50% (v/v) ethanol diluted in distilled water in sequence to re-hydrate the sections. The slides were pressure cooked in TE buffer (p.H 9) for 30 seconds at 125°C using the Menapath Antigen Access Retrieval Unit (A.Menarini Diagnostics) and allowed to cool at 105°C. This step breaks the crosslinks formed during formalin fixation and exposes the target epitopes to staining with the appropriate antibodies. The slides were rinsed in tap water and the sections were incubated for 10 minutes at room temperature in 3% (v/v) hydrogen peroxide solution. The hydrogen peroxide was rinsed off and the slides soaked in TBS-Tween solution (20mM Tris-HCl, 140mM NaCl, 0.1% (v/v) Tween 20).

The sections were soaked in the appropriate antibody for 60 minutes to detect the target epitope. The c-MYC rabbit monoclonal antibody (Epitomics, California, USA – Cat#:1472-1) was diluted in a 1:75 ratio with TBS buffer (pH 7.6), and the POU2F1 rabbit polyclonal antibody (Abcam, Cambridge, UK – Cat#: Ab15152) was diluted in a 1:50 ratio with TBS buffer (pH 7.6). Following incubation in antibody the slides were rinsed twice in TBS-Tween for 5 minutes each and then incubated in Menapath HRP-Polymer (A.Menarini Diagnostics) for 30 minutes at room temperature. The slides were rinsed in running tap water for 10 minutes and then incubated in Menapath DAB (3.3' diaminobenzidine) solution for 5 minutes. The slides were once more rinsed in running water for 10 minutes before the sections were counter-stained in Gills II Haematoxylin

(Thermo Scientific, West Sussex, UK). The slides were soaked in 70% (v/v), 95% (v/v) and absolute ethanol diluted in distilled water in sequence to dehydrate the sections. The slides were finally rinsed in xylene and mounted in DPX for analysis.

2.14.2 IHC analysis

Sections stained with antibody specific to POU2F1 were assessed by Anna Long and samples were designated as POU2F1 positive or negative depending if staining appeared in cancer cell nuclei.

Sections stained with antibody specific to c-MYC were also assessed by Anna Long. Nuclei of 500 cancer cells across 5 independent fields (100 cells per field) per sample were analysed for c-MYC staining. Each nuclei analysed was attributed a score between 0 and 3 depending on the expression of c-MYC. A score of 0 represented no c-MYC staining; a score of 1 represented weak staining for c-MYC; a score of 2 represented moderate staining for c-MYC; and a score of 3 represented strong staining for c-MYC. A histoscore was then calculated for each sample analysed as the sum of the expression scores given to each nucleus within a sample. Results from blind second scoring of 30% of samples were not different compared to results from the first scoring (χ^2: p>0.05).

Images of stained sections were captured using the PALM Microbeam System (P.A.L.M. Microlaser Technologies GmbH, Germany) in conjunction with the Zeiss Axio Observer inverted microscope (Carl Zeiss Ltd., Welwyn Garden City, UK). The microscope was fitted with PALM RoboStage II for precise slide movement and a CCD camera (Hitachi Kokusai Electric Europe GmbH). All components were controlled by the PALM RoboSoftware (version 4.0.0.10). The magnification used for all images was X40.

2.15 FISH in breast cancer tissue samples

In order to determine if copy number increase at the *c-MYC* locus was common to radiogenic breast cancer, FISH was performed on nuclei isolated from paraffin wax tissue sections of radiogenic and spontaneous breast cancer samples (Section 2.15).

2.15.1 Preparation of whole nuclei from paraffin wax tissue sections

Nuclei were isolated from paraffin tissue sections by Dr S. Crosier of the Cellular Pathology Department at the Royal Victoria Infirmary, Newcastle, UK.

Twenty micrometre paraffin curls were cut from paraffin blocks and placed into separate tubes (Reichart Jung microtome). The curls were de-paraffinised by two, 5 minute incubations in Xylene (VWR International Ltd, Leicestershire, UK). The paraffin curls were rehydrated by three 1 minute incubations in 100% ethanol. The alcohol was drained off and the sample was re-suspended in molecular grade distilled water and incubated for 10 minutes at room temperature. The molecular grade distilled water was aspirated off and the sample was re-suspended in 0.5 ml proteinase K solution and incubated for 30 minutes at 37°C to digest proteins surrounding the nuclei (0.005% proteinase K in 0.05M Tris-HCl pH 7.5, 0.01M EDTA, 0.01M NaCl). The protease digestion was stopped by adding 1ml of 2X PBS. Aggregates were broken up by gentle pipetting and then 1ml of molecular grade methanol was added. The samples were placed on a plate shaker for 10 minutes to disaggregate the samples further. One hundred microliters of sample was placed into a cytospin cartridge and cytospun for 5 minutes at 1000 rpm onto labelled superfrost microscope slides. The slides were stored at 4°C until required.

2.15.2 Protease treatment of isolated nuclei

A further protease pre-treatment of the cytospun isolated nuclei was required in order to expose target sequence to FISH probes. Two protocols were used in the present study. All samples were tested by FISH using both pre-treatment protocols. FISH only worked in 20 out of 33 isolated nuclei slides from sporadic breast cancer samples and 9 out of 18 isolated nuclei slides from radiogenic breast cancer samples.

2.15.3 Protease pre-treatment – protocol 1

All 20 of the sporadic and 3 out of 9 of the radiogenic samples for which *c-MYC* FISH worked were pre-treated with protocol 1. All washes and incubations were in coplin jars, unless otherwise stated, with no more than 6 slides per coplin jar.

Slides were soaked in 70% (v/v) acetic acid diluted in distilled water for 20 seconds The slides were then immediately soaked in Methanol for 10 minutes after which the slides were air dried. RNAse (100µg/ml in 2X SSC) was loaded onto the nuclei, covered with a cover slip and incubated for 30 minutes at 37°C in a humidified hybridisation chamber (HYBrite™, Abbott Molecular, Berkshire, UK). Following incubation, slides were washed twice in 2X SSC for 5 minutes each and the cover slips were removed. The slides were then washed for 2 minutes each in 70% (v/v), 90% (v/v) and 100% (v/v)

ethanol diluted in distilled water, after which the slides were air dried. Pepsin at a concentration of 1mg/ml in 0.01M HCl was loaded onto the nuclei, covered with a cover slip and incubated for 30 minutes at 37°C in a humidified hybridisation chamber (HYBrite™, Abbott Molecular, Berkshire, UK). Following incubation, slides were washed three times in 50mM $MgCl_2$ diluted in PBS for 2 minutes each and the cover slips removed. The slides were then washed for 2 minutes each in 70% (v/v), 90% (v/v) and 100% (v/v) ethanol diluted in distilled water, after which the slides were air dried ready for FISH.

2.15.4 Protease pre-treatment – protocol 2

Only 6 out of 9 of the radiogenic samples produced clearer probe staining after pre-treatment with protocol 2 compared to protocol 1. All washes and incubations were in coplin jars with no more than 6 slides per coplin jar.

Slides were soaked in 0.2M HCl for 20 minutes and then washed in water for 3 minutes. Slides were washed in 2X SSC for 3 minutes before being soaked in 1M NaSCN diluted in water for 30 minutes at 80°C. Following incubation, slides were washed in water for 1 minute and then twice in 2X SSC for 5 minutes each. Pepsin was added to saline solution (0.9% NaCl (w/v) in distilled H_2O) to make a final concentration of 4mg/ml. Slides were incubated in the pepsin/saline solution for 15 minutes at 37°C. Following incubation slides were washed twice in 2X SSC for 5 minutes each and air dried ready for FISH.

2.15.5 c-MYC FISH on pre-treated isolated nuclei

The Vysis LSI SpectrunOrange Probe (Abbott Molecular, Berkshire, UK) and CEP8 SpectrumGreen Probe (Abbott Molecular, Berkshire, UK) were each diluted 1:10 in hybridisation buffer provided with each probe. Each probe was analysed separately for each nuclei sample as analysis of the *c-MYC/CEP8* probe mix (section 2.9) did not produce strong enough signal for the probes to be analysed together.

Following dilution of the FISH probes, 2µl of probe was added to a round coverslip (VWR International Ltd, Leicestershire, UK) and the coverslip placed over the nuclei. The edges around the coverslip were sealed with rubber cement. Slides were placed in a humidified hybridisation chamber (HYBrite™, Abbott Molecular, Berkshire, UK) and heated to 85°C for 30 minutes to denature the probe and nuclear DNA. The slides were

then incubated for 48 hours in the humidified hybridisation chamber at 37°C to allow hybridisation of probe to its target sequence.

The *c-MYC*/*CEP8* probe mix (section 2.9) was loaded onto samples SPO15, SPO2, SPO28, SPO18, RAD9 and RAD10 following the same denature and hybridisation protocol as described above to be analysed using the CytoVision image capture system (Leica Microsystems, Newcastle Upon Tyne, UK).

2.15.6 Analysis of FISH

Cells were analysed using the same equipment and filters as cell line samples (section 2.9). For each sample analysed 100 nuclei were scored for each probe and the number of probe signals per nuclei recorded. Blind second scoring of 9/29 samples analysed produced results that were not significantly different to the initial scoring (χ^2: p>0.05).

For samples that were analysed using the *c-MYC*/*CEP8* probe mix, nuclei were not scored but representative images of the different genotypes in the cell population were captured. The CytoVision image capture system (Leica Microsystems, Newcastle Upon Tyne, UK) was sensitive enough to detect the signals for digital photography but was not a viable option for genotype scoring.

Chapter 3: Development of *in vitro* radiation-induced breast epithelial cell transformation models

3.1 Introduction

Exposure to ionising radiation has been shown to be associated with an increased breast cancer risk in a number of epidemiological studies. These have included studies of: female survivors of the atomic bombs dropped in World War II (Tokunaga *et al.*, 1994; Land, 1995; Land *et al.*, 2003), women who have been exposed to ionising radiation through their occupation (Rafnsson *et al.*, 2001; Doody *et al.*, 2006), women who have received multiple therapeutic and diagnostic X-rays (Davis *et al.*, 1989; Hoffman *et al.*, 1989; Mattsson *et al.*, 1993; Ma *et al.*, 2008) and women who have received radiation therapy for Hodgkin lymphoma (Hancock *et al.*, 1993; Travis *et al.*, 2003; van Leeuwen *et al.*, 2003).

The relative risk of breast cancer increases as dose of ionising radiation increases. Also, younger women exposed to ionising radiation are at greater risk of breast cancer than older women exposed to the same level of radiation. This difference is evident particularly in women under the age of 30; women exposed to radiation over the age of 30 have no increased relative risk of breast cancer (Travis *et al.*, 2003; van Leeuwen *et al.*, 2003).

Ionising radiation causes DNA strand breaks which lead to genetic mutations. Increased radiation dose increases the amount of genetic damage caused to a cell and therefore increases the potential for oncogenic mutations.

It has been suggested that the increased risk in younger women compared to in older women is due to the increased levels of oestrogen in younger women. Oestrogen is a known carcinogen that may cause cancer through an oestrogen receptor-mediated mechanism or a genotoxic mechanism (Russo and Russo, 2006; Yager and Davidson, 2006; Mense *et al.*, 2008). It has therefore been hypothesised that ionising radiation and oestrogen act synergistically to drive malignant transformation of the breast in young women.

The molecular genetic mechanisms which underlie radiation-induced breast cell transformation are currently unclear. *In vitro* models provide a means to investigate radiation-induced breast cell transformation and the genetic alterations which underpin

this transformation. The MCF-10A cell line (Section 1.19) is a suitable immortalised non-transformed, non-tumourigenic breast epithelial cell line with which to investigate radiation-induced transformation (Soule *et al.*, 1990). The cell line is near diploid and the largest rearrangement is a translocation t(3;9)(p13;p22). Study of the t(3;9)(p13;p22) translocation by FISH and CGH array analysis revealed that it resulted in deletion of the *CDNK2A/CDNK2B* genes on chromosome 9. The same genes had also been deleted from the normal chromosome 9 (Cowell *et al.*, 2005). The loss of both *CDNK2A/CDNK2B* genes is suggested to contribute to the immortalisation of the MCF-10A cells.

3.1.1 Aim

The aim of the work described in this chapter is the development of *in vitro* transformation models from the MCF-10A cell line. Previous studies with the MCF-10F cell line (Section 1.6) and *in vivo* rat models have shown that ionising radiation can transform mammary epithelial cells and that concomitant radiation and oestrogen exposure is more effective than either on their own (Calaf and Hei., 2000; Roy *et al.*, 2001; Calaf *et al*., 2006; Bartstra *et al.*, 1998a; Bartstra *et al*., 1998b). Therefore two transformation models were developed. A model which used fractionated doses of X-irradiation was created first, followed by a model in which cells were grown continually in the presence of additional oestrogen in cell culture medium and were exposed to the same fractionated dose regimen. The development and phenotypic characterisation of each model are described. The cell line model derived without additional oestrogen in the medium will be called the "First" *in vitro* model and the cell line model derived with additional oestrogen in the medium will be called the "Second" *in vitro* model in the remainder of the thesis.

3.2 Development of the *in vitro* models.

3.2.1 Determination of fractionated doses for dosing regimen.

A fractionated dose regimen was designed with which to develop a model of the progression of breast epithelial cell transformation induced by the accumulation of genetic alterations caused by ionising radiation. The aim was to irradiate MCF-10A cells with fractionated X-ray doses to a cumulative dose of 80 Gγ. The optimal dose for the fractionated dose regimen would cause genetic damage to MCF-10A cells but not to a lethal level. This optimal dose would be determined by demonstration of growth arrest from which the cells were able to recover sufficiently to receive further doses of ionising radiation. Growth arrest occurs following exposure to irradiation and other DNA damaging agents due to cell cycle arrest in the G1 phase of the cell cycle which allows effective DNA repair before the cell re-enters the cell cycle. A cell which has undergone DNA damage that is too extensive to be repaired becomes senescent and is induced to apoptose.

MCF-10A cells were plated in T75 flasks and 6 well plates and grown to a confluence of 50%. The cells were irradiated with 0, 1, 2, 5, 10, 20, 40, 60 and 80 Gγ of X-irradiation. Five days following irradiation, the morphology of the cells in the T75 flasks was observed to allow for qualitative evaluation of cell recovery (Fig. 3.1).

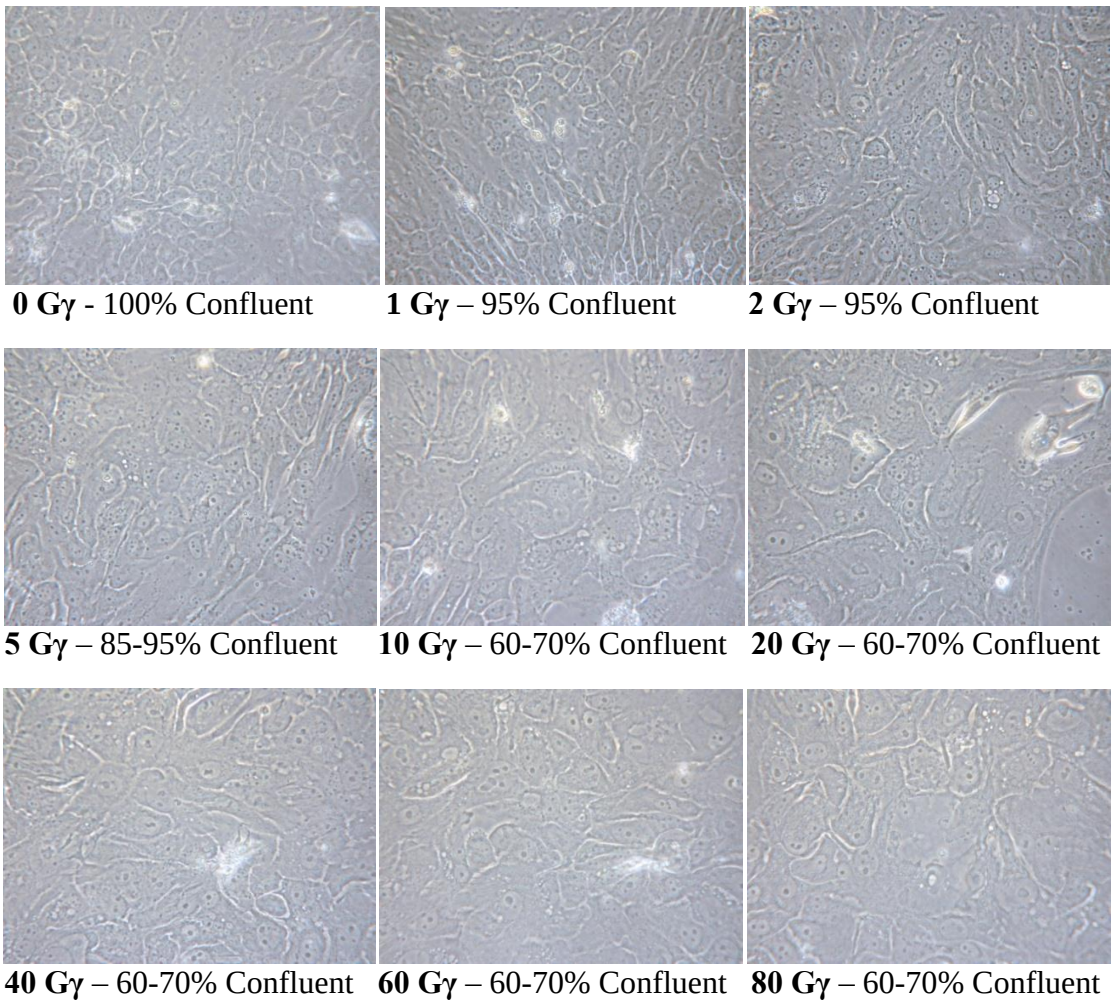

Figure 3.1Effect of ionising radiation on the morphology of MCF-10A cells.
MCF-10A cells were grown to 40-50% confluency in T75 flasks then either left un-irradiated (0 Gγ) or irradiated with either: 1, 2, 5, 10, 20, 40, 60 or 80 Gγ of X-rays. The cells were incubated for 5 days and then the morphology was assessed. The photomicrographs show the morphology of the cells at x40 magnification. The confluency of the cells in the T75 flasks was estimated and is shown beneath the corresponding photomicrographs.

The un-irradiated cells were small, round cells with a cobblestone-like appearance which is the normal morphology of healthy MCF-10A cells. After five days in culture, the cells were 100% confluent and had stopped growing presumably due to contact inhibition. The 1 and 2 Gγ cell populations nearly reached 100% confluency and had a similar morphology to the un-irradiated cells which indicated that these cells had recovered from the initial growth arrest. For cells which had received 5 Gγ and above, the cells appeared to be larger and flatter which is indicative of cell hypertrophy and are characteristics of senescent cells. The cells were sub-confluent which indicated that the cells were still in a stage of growth arrest. The 5 Gγ cell population contained cells that had begun to round up and was slightly more confluent than the population that had received 10 Gγ and above, which indicated that these cells had undergone limited recovery from growth arrest five days after treatment.

Cells that were irradiated in 6 well plates were counted four days after irradiation and the DNA content of cells irradiated in 6 well plates was measured five days after irradiation (Fig. 3.2). Reduced cell numbers and DNA concentration would indicate reduced cell division. The results indicated that the greater the radiation dose the longer the period of growth arrest (Fig. 3.2a) . Up to 5 Gγ this relationship was linear. There was no detectable cell growth after 4 days of cells that had been irradiated with between 5 and 80 Gγ as cell numbers were very similar for each dose within this range. Cell numbers for cells irradiated with 5 Gγ were slightly higher than for cells which had received 10 Gγ and above which may have indicated the beginning of cell growth; however this difference was not significant. Cell numbers were significantly different from un-irradiated cells after 2 Gγ of ionising radiation (Students *t*-test: $p=0.002$).

The results also indicated that irradiation of cells gave rise to growth inhibition in a dose-dependent manner (Fig 3.2b). The DNA content for cells irradiated with 5 Gγ was higher than for cells which received 10 Gγ and above which indicated that by day 5 growth recovery had begun in the 5 Gγ dosed cell population (Paired *t*-test with 10 Gγ sample: $p=0.040$). Overall, the results showed that cell growth was inhibited by irradiation doses between 1 – 80 Gγ after irradiation. The length of time it took for cell growth to recover was dose dependant.

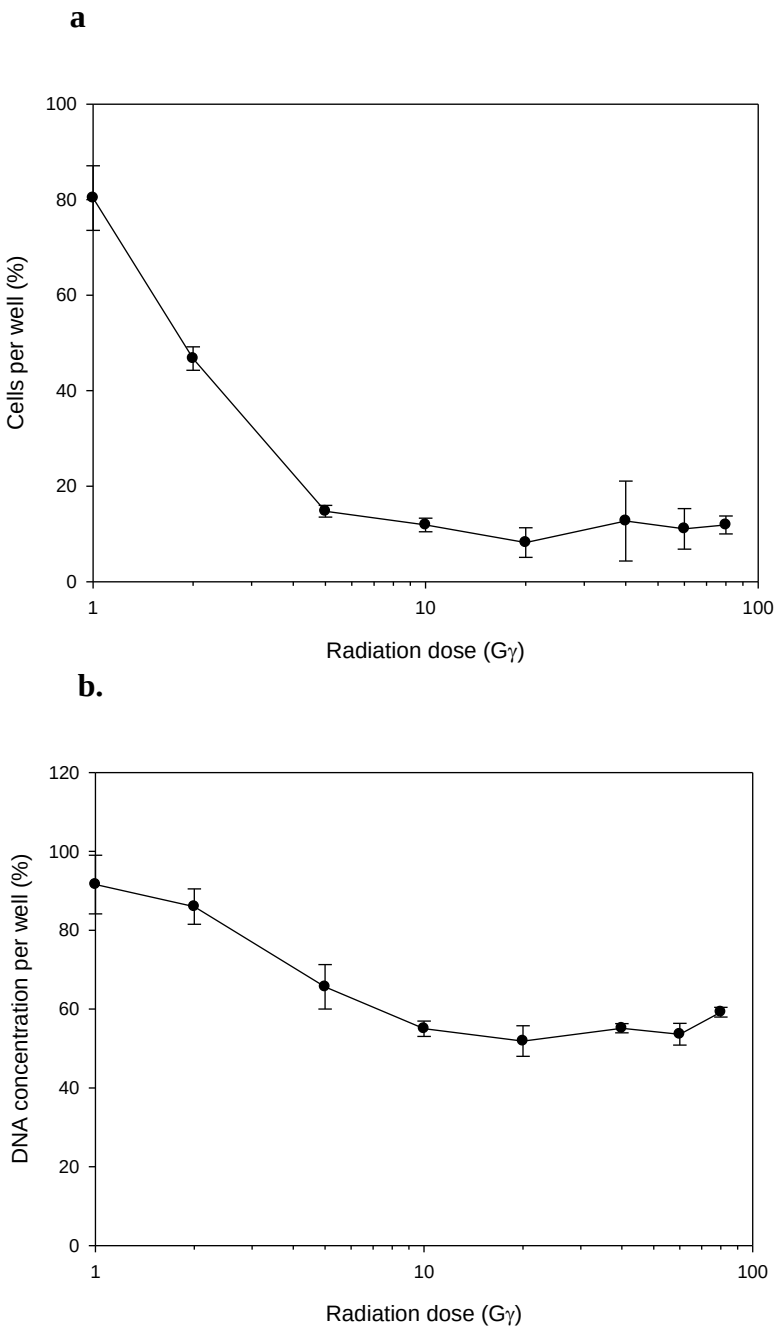

Figure 3.2 Effect of ionising radiation on MCF-10A cell growth.
MCF-10A cells were grown to 40-50 % confluency in 6 well plates and then irradiated with either: 0, 1, 2, 5, 10, 20, 40, 60 or 80 Gγ of X-rays. Four days after irradiation three wells were trypsinised and the cells counted in triplicate (**a)**. The number of cells for the irradiated cells at each dose was calculated as a percentage of the mean un-irradiated number of cells. Five days after irradiation the cells in the remaining three wells of the 6 well plates were lysed and their DNA content measured using a fluorescent pico-green assay **(b)**. The DNA concentration for each radiation dose was expressed as a percentage of the DNA concentration for the un-irradiated cells. Mean percentages +/- SEM of triplicate samples within one experiment are shown.

The MCF-10A cells exposed to 1 and 2 Gγ appeared to recover fully within the five days of the experiment. It was decided that there was probably not enough DNA damage induced to cause cell transformation at these doses and that they would not be suitable for the fractionated dose schedule. Cells exposed to 5 Gγ had shown signs of cell recovery within the five days of the experiment and had recovered fully to have a normal MCF-10A cell morphology after seven days. Cells which received 10 Gγ of X-irradiation recovered after two weeks in culture; they lost their quiescent phenotype and returned to a normal MCF-10A morphology. Cells which received X-irradiation between 20 – 80 Gγ did not recover and remained in a state of cell senescence.

It was decided therefore that MCF-10A cells would undergo fractionated doses of both 5 and 10 Gγ of ionising radiation until they had received a cumulative dose of 80 Gγ.

The dosing regimen outlined in figure 3.3 allowed for future step-wise analysis of genetic alterations and phenotypic changes that had occurred because the cells were frozen after each fractionated dose. During the dosing regimen, the 5 Gγ fractionated dose populations took 5 days to recover and 7 – 9 days elapsed between irradiations. The 10 Gγ fractionated dose populations took 7 days to recover and 10-12 days elapsed between irradiations. MCF-10A cells were grown to the same passage number as the cells that received a cumulative dose of 80 Gγ of ionising radiation in the 5 Gγ fractionated dose series (passage control population). This cell population then acted as reference for any phenotypic changes and genetic alterations observed in the irradiation series.

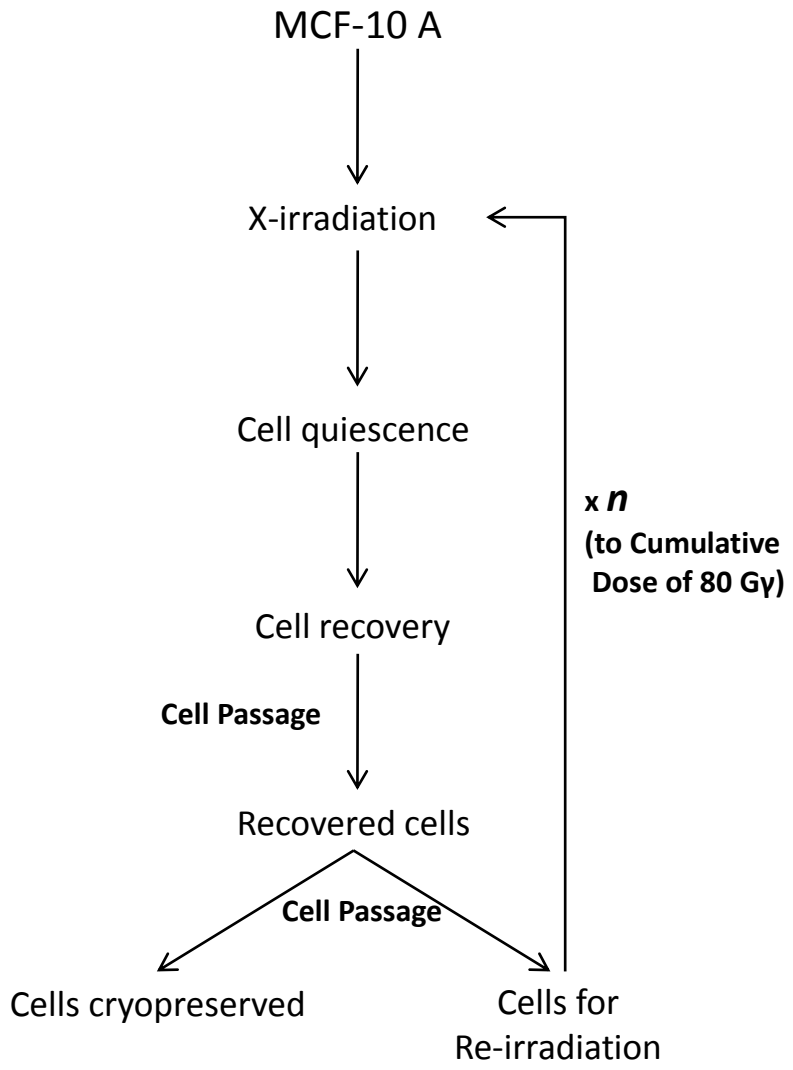

Figure 3.3 Flow diagram for dosing regimens.
Cells were given an initial X-ray dose of 5 or 10 Gγ in the absence and presence of additional oestrogen in their medium in T75 flasks. Cells underwent growth arrest followed by a period of recovery. Once the cells had started to recover they were plated in T75 flasks to allow them space to grow and recover fully. Following full recovery, cells were trypsinised and plated in T75 flasks to receive another dose of X-radiation. Cells were cryopreserved at this stage. Re-irradiation continued until a cumulative dose of 80 Gγ was reached. *n*=number of re-irradiations needed to achieve a cumulative dose of 80 Gγ. This was 15 for the 5 Gγ schedule and 7 for the 10 Gγ schedule.

3.3 Phenotypic characterisation of the First 5 Gγ irradiated series

Several cellular phenotypes are accepted as being characteristics of transformed cells and indicative of cell transformation *in vitro*. Examination of the phenotypic characteristics of the irradiated cells might therefore indicate if the cells had been transformed, and any altered characteristics could be correlated with genetic alterations identified. Phenotypes of the irradiated series were analysed in the 5 Gγ fractionated dose populations. The cumulative dose populations analysed had received 10, 25, 40, 55 and 80 Gγ of irradiation. The remainder of this section describes analysis of cell morphology, proliferation rate, contact inhibition and radiation sensitivity in the First 5 Gγ series.

3.3.1 Changes in cell morphology of the First 5 Gγ irradiated populations

MCF-10A cells had a morphology typical of breast epithelial cells which was characterised by a tight cellular monolayer with a cobblestone like appearance (Fig. 3.4a). Proliferating MCF-10A cells grew in clusters and lamellipodia were often seen which indicated that the cells were motile. Cells from the 40 Gγ population and above had a distinctly different cell morphology to that of un-irradiated MCF-10A cells at both high and low cell density. Cells appeared to cluster into dense cellular islands that retained a cobblestone appearance but had very defined borders and fewer motile cells were visible (Fig. 3.4b). Cells which had received 40 Gγ cumulative dose and above also detached more quickly than un-irradiated MCF-10A cells when incubated in trypsin and appeared to detach more readily when grown in growth factor-depleted medium.

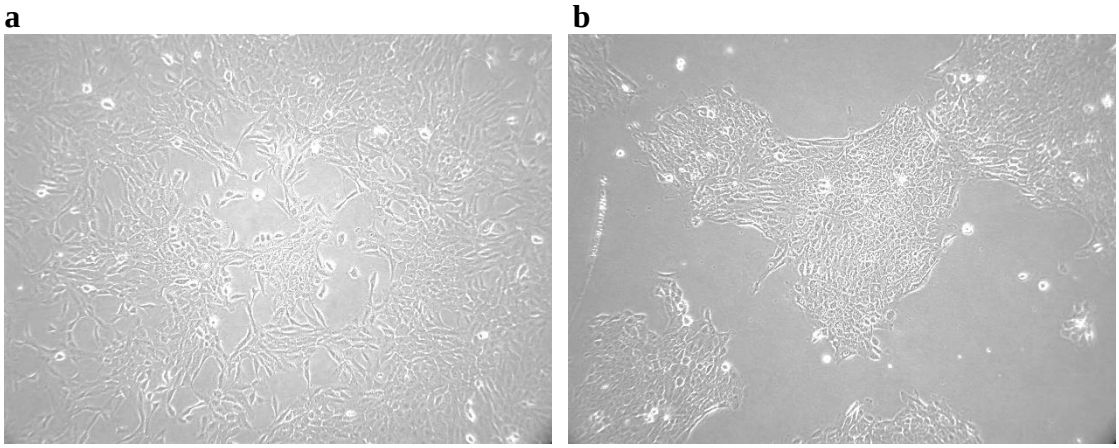

Figure 3.4 Cell morphology of the First 5 Gγ Series
Images shown: un-irradiated MCF-10A cells **(a)** and cells from the First 5 Gγ series which had received a cumulative dose of 55 Gγ **(b)**. Cells from the 55 Gγ population appear to cluster into tight cellular clusters with defined borders and appear less motile that un-irradiated MCF-10A.

3.3.2 Differences in growth rate of the First 5 Gγ irradiated populations

Increased cell proliferation rate has been considered to be indicative of cell transformation. It was noted that the growth rate appeared to slow down as cumulative dose increased and that the 25 Gγ cumulative population had a notably slower growth rate than the other cell populations. The growth rate of the passage control population did not appear to be different from the un-irradiated MCF-10A population. The growth rates of the selected cumulative dose populations of the First 5 Gγ series were analysed in a single experiment. Cells were plated in triplicate wells in 12 well plates and the DNA content of the wells was analysed at specific time points over a period of 4 days.

Growth curves generated for each population indicated that the un-irradiated MCF-10A and 10 Gγ populations had similar growth rates whereas the 25 Gγ population had the slowest growth rate (Fig. 3.5a). The 40, 55 and 80 Gγ populations had similar growth rates which were slower than un-irradiated MCF-10A cells but faster than the 25 Gγ cumulative dose population.

Growth rates for each cell populations, as defined by the number of cell doubling per hour, were determined from the growth curves by exponential regression (Fig. 3.5b). The un-irradiated MCF-10A cell population had the fastest growth rate of 0.048 cell doublings per hour. The trend of the experiment indicated that as cumulative dose increased, growth rate decreased (compared to that of un-irradiated MCF-10A). The 25 Gγ population had a significantly reduced growth rate compared to the un-irradiated and 10 Gγ populations of 0.034 cell doublings per hour (Turkey's test: Un-irradiated MCF-

10A - p=0.04, 10 Gγ population - p=0.022). This growth rate was the lowest of all the cell populations which agreed with observations during cell culture. The growth rate of the 40 Gγ population increased again to 0.043 cell doubling per hour which was lower than un-irradiated MCF-10A but not to a significant level. The growth rate of the 80 Gγ population reduced to 0.038 cell doublings per hour which was significantly lower than the un-irradiated MCF-10A cells (Turkey's test: p=0.048)

Overall results indicated that there may have been two separate events which affected growth rate. The first, which decreased growth rate, may have occurred between the 10 and 25 Gγ cumulative dose populations; the second, which increased growth rate, may have occurred between the 25 and 40 Gγ cumulative dose populations. Further events may have occurred after 40 Gγ cumulative dose which caused the continued gradual reduction in growth rate throughout the remainder of the irradiation series.

a

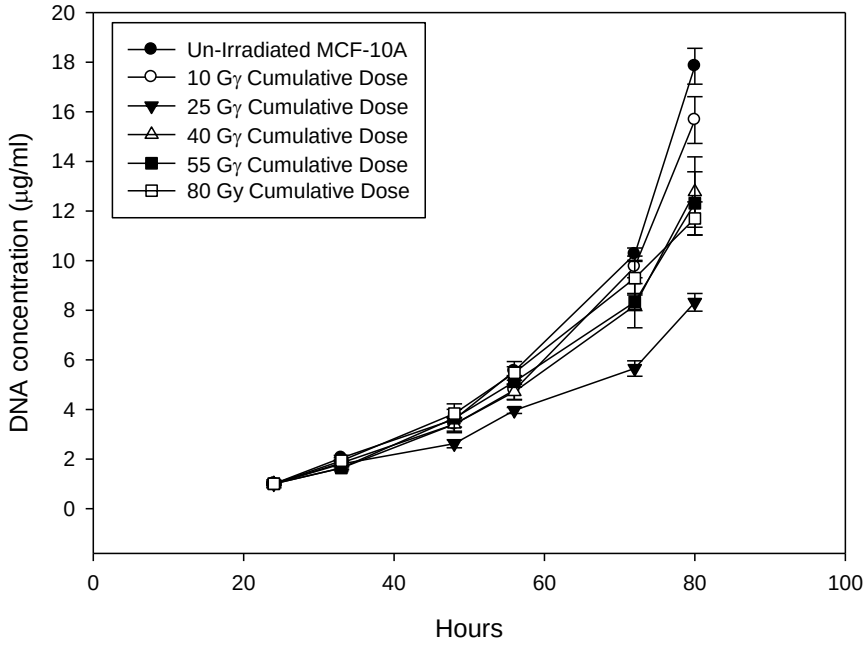

b

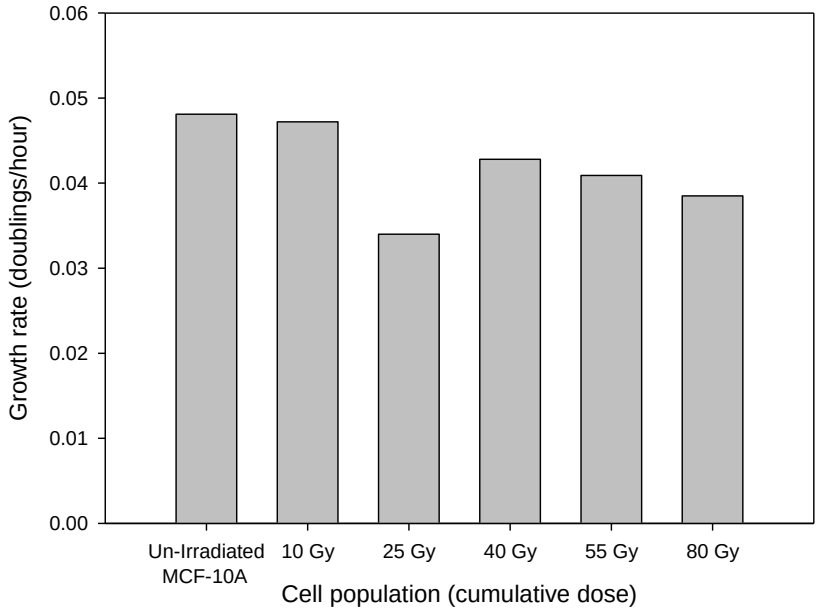

Figure 3.5 Growth rate of the First 5 Gγ series.
Cells from each population were plated in 3 wells of a 12 well plate at a cell density of $2x10^4$ cells per well. Cell culture medium was replaced in the wells each day of the experiment. Cells were lysed for DNA measurement at specific time points over 4 days from 24 hours after plating. The mean DNA concentration of the triplicate samples at each time point was used to calculate growth rate. The DNA concentration from triplicate samples +/- SEM for each cell population at each time point from one experiment normalised to the DNA concentration of the un-irradiated MCF-10A cell population **(a)**. Growth rate, defined as the number of cell doublings per hour, determined from this data **(b)**.

3.3.3 Changes to contact inhibition of the First 5 Gγ irradiated cell populations

Contact inhibition is the inhibition of cell growth that results when cells are in contact with other cells. In normal tissues, contact inhibition helps to prevent uncontrolled cell growth and the loss of this ability is indicative of cell transformation. MCF-10A cells displayed contact inhibition and stopped growing when they had formed a confluent monolayer. Transformed cell lines, such as the breast cancer cell line MCF-7, have lost contact inhibition and continue to proliferate in culture after they have reached 100% confluency which results initially in cells occupying a smaller area and eventually in the cells being piled-up on top of each other.

Cells that display contact inhibition arrest in the G1 phase of the cell cycle (Kuppers *et al.*, 2010). Cell cycle analysis of confluent cell populations therefore provides an indication of whether or not cells are contact-inhibited. Cells which are contact-inhibited will be largely in G0 or G1 phase of the cell cycle. Cell populations which have lost contact inhibition will continue replicating and therefore contain cells in the S-phase of the cell cycle.

Flow cytometric analysis of MCF-10A and MCF-7 cells from 100% confluent populations are shown in figure 3.6. There were fewer MCF-10A cells compared to MCF-7 cells in S-phase of the cell cycle. This difference was evident in both the scatter-graphs (Fig. 3.6 a and b) and subsequent histograms (Fig. 3.6 c and d). The majority of cells in the MCF-10A population were in the G1 phase of the cell cycle which indicated that they had undergone cell cycle arrest and is consistent with the observation that MCF-10A cells displayed contact inhibition when 100% confluent. MCF-7 cells had lost contact inhibition and continued to replicate after they had reached 100% confluency. The loss of contact inhibition was demonstrated by the presence of cells in all phases of the cell cycle.

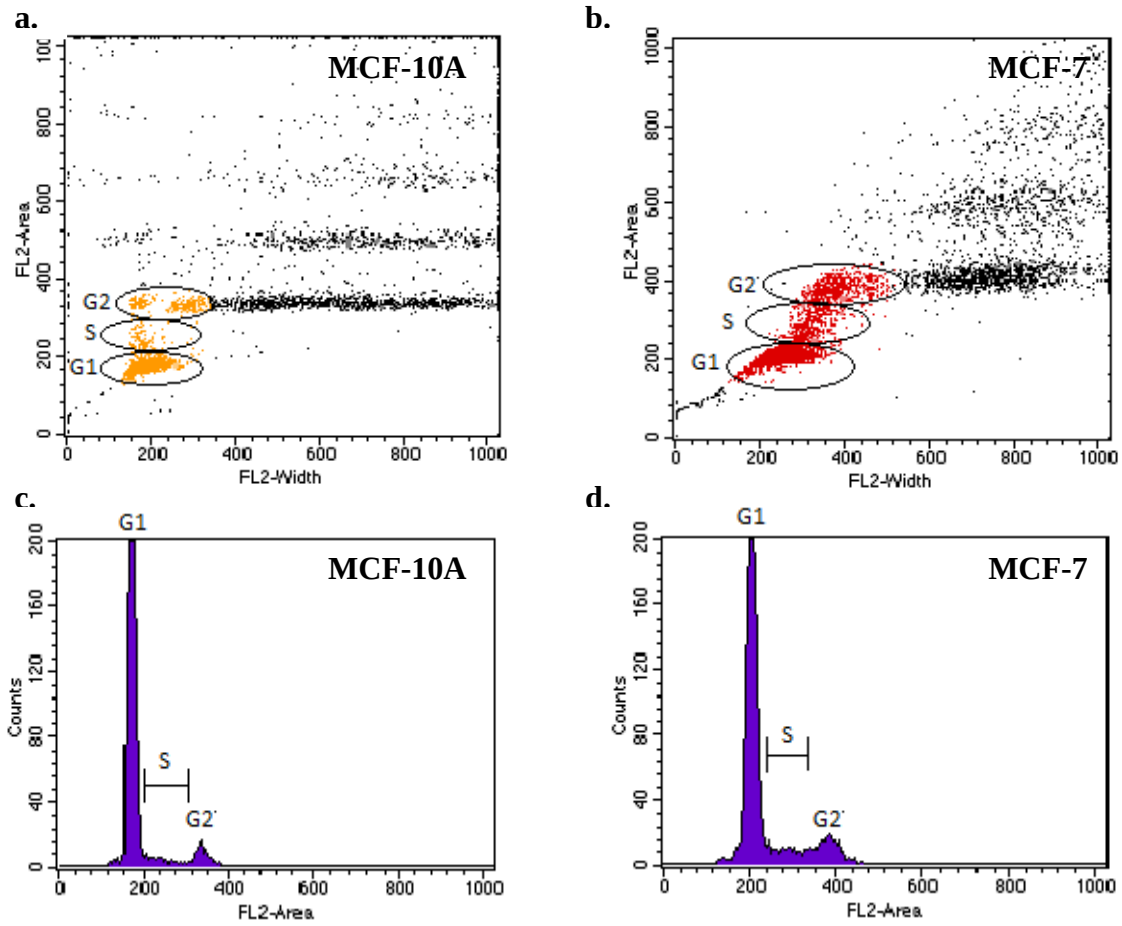

Figure 3.6 Cell cycle analysis of confluent MCF-10A and MCF-7 cells.
MCF-10A **(a** and **c),** and MCF-7 **(b** and **d)** cells were grown to confluence in T25 flasks and prepared for propidium iodide flow cytometric analysis. Ten thousand events were recorded for each cell population. **(a** and **b)**. Areas of the scatter-graphs which represent cells in G1, S and G2 are circled. Cells within these areas are shown in the histograms to demonstrate the proportion of cells in each phase of the cell cycle **(c** and **d)**.

Un-irradiated MCF-10A cells and cells from the First 5 Gγ series that had received a cumulative dose of 80 Gγ were analysed using flow-cytometry on the day the cell populations reached 100% confluency and each day for the subsequent 5 days. Figure 3.7 shows the flow cytometric analyses 24 and 48 hours after cells reached 100% confluency. There were more cells in S-phase of the cell cycle in the 80 Gγ population than the un-irradiated population at both time points, which indicated that more of the 80 Gγ cells were replicating and therefore had reduced contact inhibition. The proportion of cells in S-phase appeared to reduce between 24 and 48 hours for the 80 Gγ cumulative dose population but still remained higher than for un-irradiated MCF-10A cells.

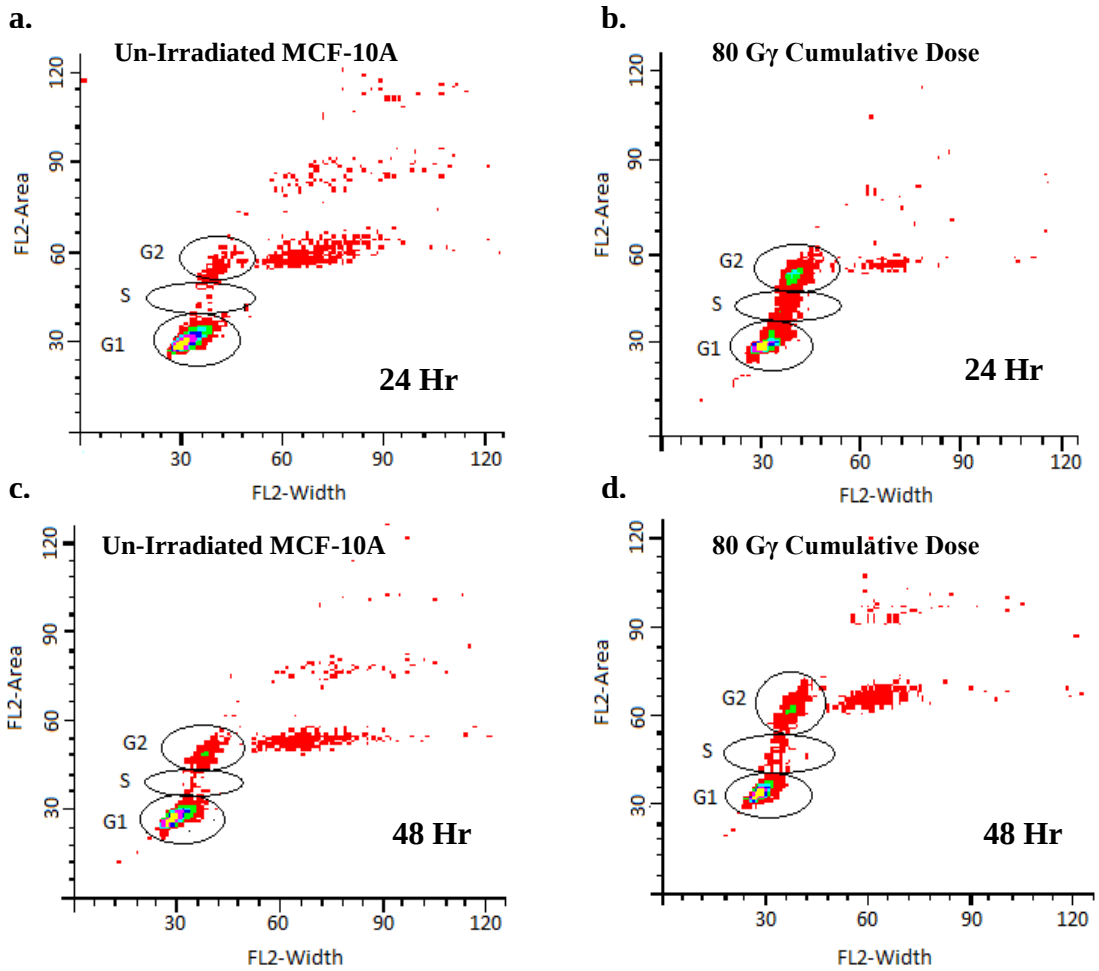

Figure 3.7 Cell cycle distribution of un-irradiated MCF-10A cells and First 5 Gγ series cells that have received a cumulative dose of 80 Gγ.
Un-irradiated cells **(a** and **c)** and cells from the First 5 Gγ series which have received a cumulative dose of 80 Gγ **(b** and **d)** were plated out in T25 flasks at $4x10^5$ cells per flask. Cell populations were trypsinised and fixed for flow cytometry once 100% confluency was reached and at 24 hour intervals for the following 5 days. Growth medium was replaced in all flasks not fixed. Scatter-graphs for the 24 hour time point **(a** and **b)** and the 48 hour time point **(c** and **d)** are shown. Areas of the scatter-graphs which represent cells in G1, S and G2 phase of the cell cycle are circled.

The percentage of cells in S-phase of the cell cycle was calculated for each population at each time point (Fig. 3.8). The 80 Gγ cumulative dose population had a larger percentage of cells in S-phase when they reached 100% confluency than un-irradiated cells. The percentage of cells in S-phase continued to be higher than in un-irradiated cells after 24 hours. Thereafter the difference was smaller but remained significant. These results indicated that the 80 Gγ cumulative dose cells had reduced contact inhibition compared to un-irradiated MCF-10A cells.

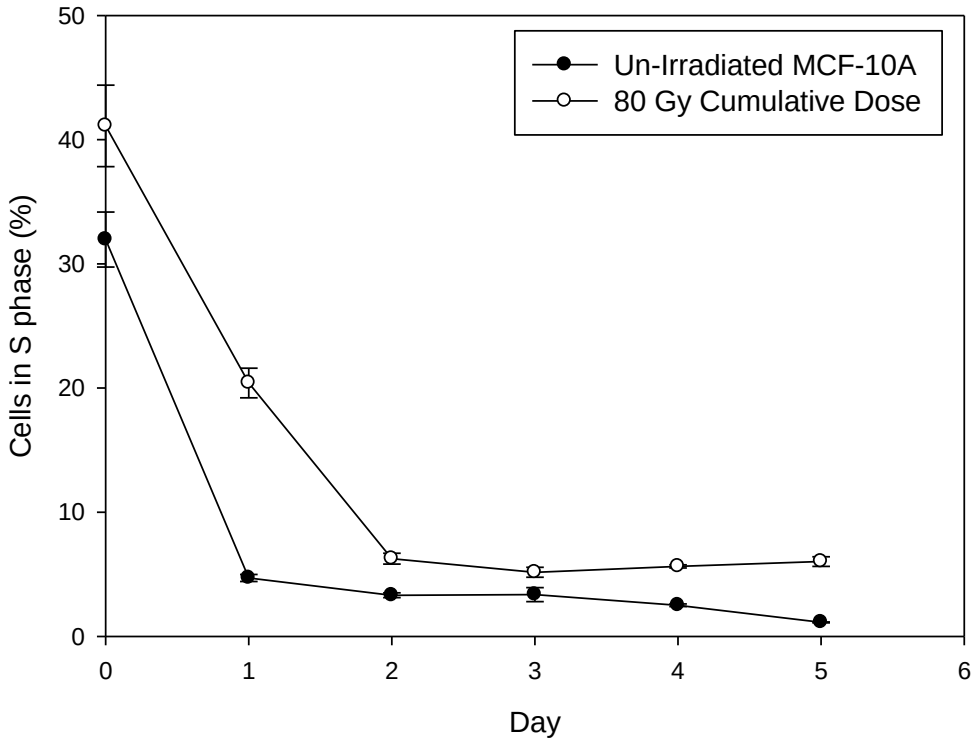

Figure 3.8 Percentage of cells in S-Phase of Un-Irradiated MCF-10A cells and First 5 Gγ Series cells that have received a cumulative dose of 80 Gγ.
The percentage of cells in S-Phase of the cell cycle was calculated with ModFit LT software. Day 0 represents the day when the populations reached 100% confluency. The mean percentages +/- SEM from triplicate analyses are shown. The statistical significance between each population below the 5% confidence level at each time point was tested (Students T-test): Day 0 p=0.021, Day 1 p=0.001, Day 2 p=0.003, Day 3 p=0.014, Day 4 p<0.001, Day 5 p=0.002

The percentage of cells in G2 and M phase of the cell cycle was also analysed (Fig 3.9). The 80 Gγ cell population had significantly fewer cells in G2 and M phase of the cell cycle when the cells reached 100% confluency. A greater proportion of cells in the 80 Gγ population continued to replicate at this time point (Fig. 3.8) which indicated that the 80 Gγ cells were moving through the G2/M checkpoint faster than un-irradiated MCF-10A cells. The day after they had reached 100% confluency, the number of cells in G2 and M phases of the cell cycle in the un-irradiated population was significantly lower than for the 80 Gγ population. This difference was most likely because fewer cells were entering S-phase as they had been arrested in G1 phase of the cell cycle. The increased proportion in cells in G2 and M phases of the cell cycle in the 80 Gγ population compared to un-irradiated MCF-10A was observed throughout the remainder of the experiment.

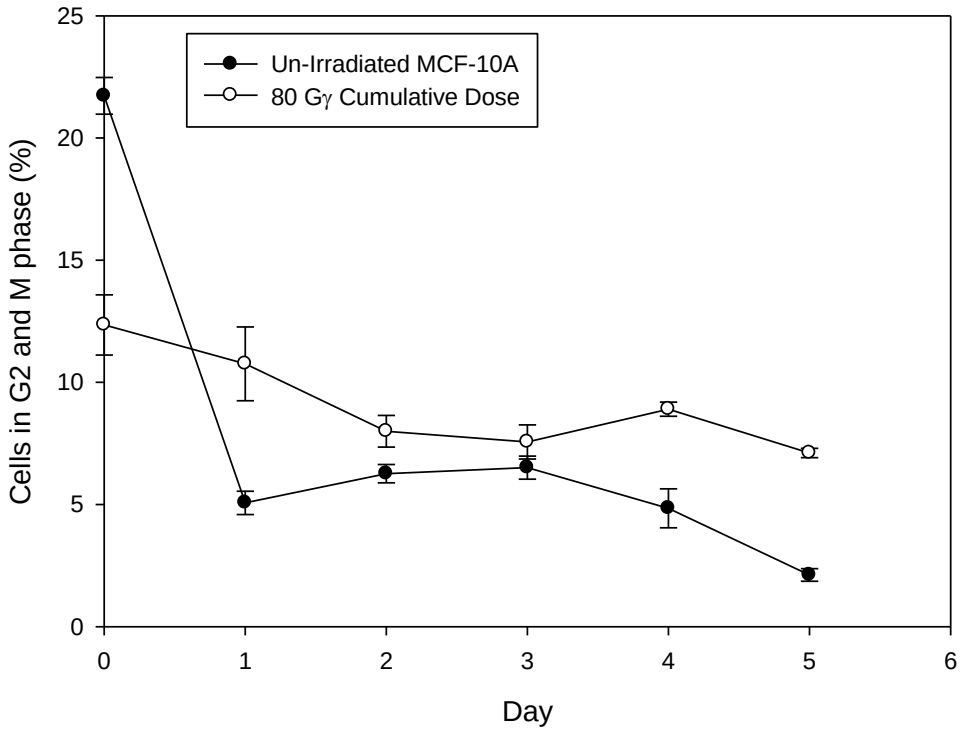

Figure 3.9 G2/M phase cell cycle analysis of Un-Irradiated MCF-10A cells and First 5 Gγ Series cells that have received a cumulative dose of 80 Gγ.
The percentage of cells in G2/M-Phase of the cell cycle was calculated with ModFit LT software. Day 0 represents the day when the populations reached 100% confluency. The mean percentages +/- SEM of triplicate samples are shown. The statistical significance between each population below the 5% confidence level at each time point was tested (Students T-test): Day 0 p=0.001, Day 1 p=0.015, Day 2 p=0.024, Day 3 p=0.105, Day 4 p=0.007, Day 5 p<0.001.

To test for loss of contact inhibition in all the cumulative dose populations in the First 5 Gγ series, cell populations were allowed to grow in 12 well plates for 5 days after they had reached 100% confluency. Figure 3.10 shows representative images of the First 5 Gγ series cell populations 5 days after they had reached 100% confluency. It appeared that as cumulative dose increased, more cells were piling on top of each other which indicated that the populations were continuing to replicate. The 80 Gγ cumulative dose population also showed cells that were piling up and then detaching from the other cells. The passage control population showed a similar phenotype to un-irradiated MCF-10A cells (image not shown).

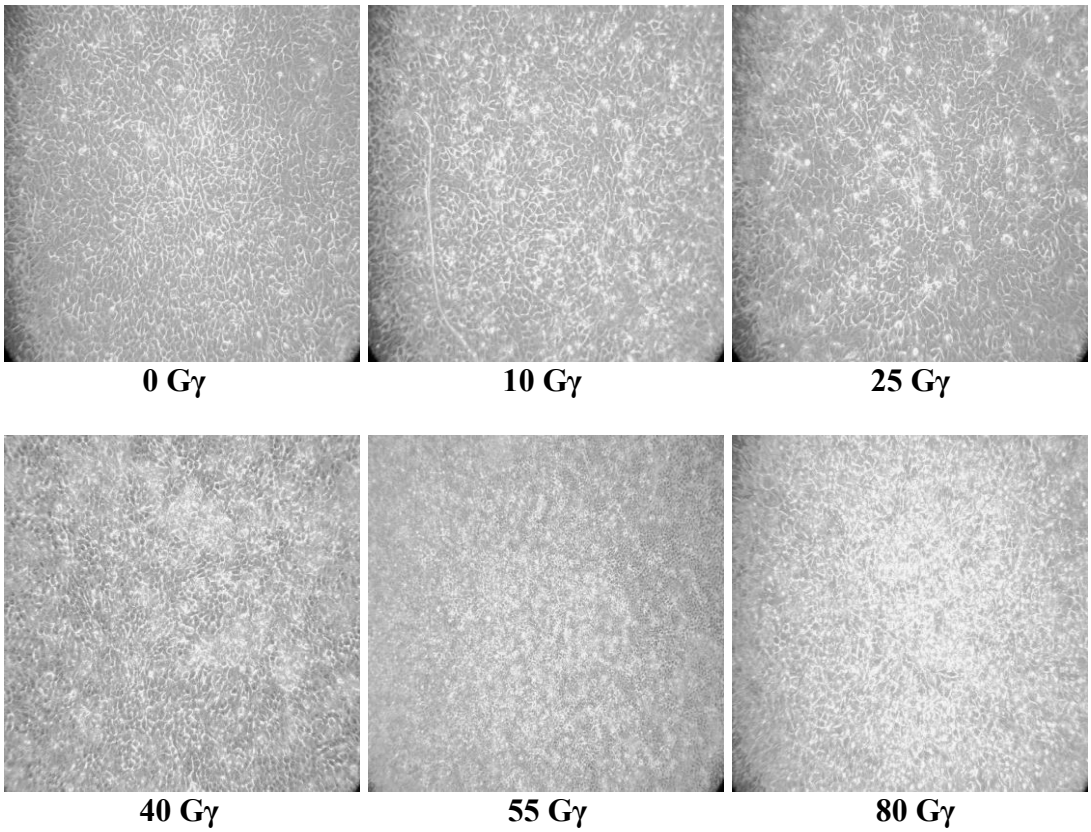

Figure 3.10 The effect of confluency on the First 5 Gγ series.
Cells from each cumulative dose population were plated in 3 wells of a 12 well plate at a cell density of $2x10^4$ cells per well. The medium was replaced on the cells each day for 9 days. Photomicrographs were taken of each cell population after 9 days at x10 magnification. Cumulative dose that had been received by each cell population is indicated below each image.

The DNA concentration of the cells was measured 5 days after they had reached 100% confluency and the relative concentration compared to un-irradiated MCF-10A cells was calculated (Fig. 3.11). If cells had lost contact inhibition then they would have continued to replicate, more cells would be present and therefore the DNA concentration would be higher than un-irradiated MCF-10A.

The DNA concentration of the 80 Gγ cumulative dose population was 2.14 fold higher than un-irradiated MCF-10A and was the only DNA concentration different from un-irradiated MCF-10A (Turkey's test: p=0.002). The relative DNA concentration of the 80 Gγ cumulative dose population was also significantly higher than the 10, 25, 40 Gγ and passage control cell populations (Turkey's test: p=0.008, 0.004, 0.15 and 0.002, respectively). This increased cell number indicated that the 80 Gγ cumulative dose population had reduced contact inhibition compared to the other cell populations. The 55 Gγ cumulative dose population had a 1.47 fold increase in DNA concentration compared to un-irradiated MCF-10A but this did not reach significance (Turkey's test: p=0.490). There was an increase in DNA concentration for the 10, 25 and 40 Gγ cumulative dose populations compared to un-irradiated MCF-10A (1.15, 1.07 and 1.21 fold respectively) but again this was not significant. The passage control population did not differ from un-irradiated MCF-10A (p=1.00).

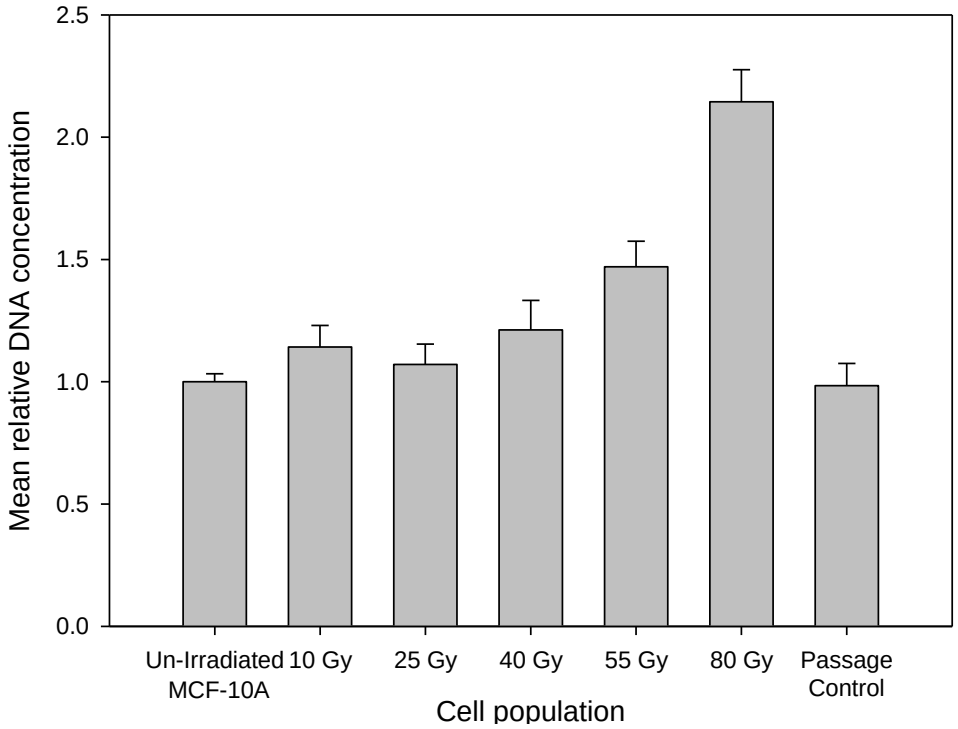

Figure 3.11 DNA concentration of the First 5 Gγ Series 5 days after 100% confluency was reached. Cells from each cumulative dose populations were plated in triplicate wells of a 12 well plate at a cell density of $2x10^4$ cells per well. The medium was replaced on the cells each day for 9 days. The DNA content of the cells was measured with pico-green after 9 days. The mean DNA concentration from triplicate wells relative to the mean DNA concentration of un-irradiated MCF-10A cells +/- SEM from four experiments is shown. Statistical significance for each population within the experiments below the 5' confidence level was tested (ANOVA): p=0.002.

These results, coupled with images of increasing numbers of cells appearing to pile on top of each other as cumulative dose increases (Fig. 3.10), and the difference in the cell cycle profile of confluent un-irradiated and 80 Gγ cumulative dose populations indicated that cells from the First 5 Gγ series had reduced contact inhibition. The passage control population did not display these phenotypes and therefore loss of contact inhibition was not likely to be passage related.

3.3.4 Radiation resistance of the First 5 Gγ irradiation populations

As a cell population receives fractionated doses of ionising irradiation there may be selection for genetic alterations which make the cells more resistant to the effects of ionising radiation. Cells with such alterations would no longer undergo growth arrest induced by ionising radiation, or would recover earlier from growth arrest. Radiation resistant cells would therefore become the dominant cell population. During the development of the First 5 Gγ series it did not appear that cells were becoming more or less radiation-resistant. Cells from the First 5 Gγ series were tested explicitly to investigate if they had become radiation-resistant.

Single cells of the First 5 Gγ series populations were irradiated and the proportion of cells which survived the irradiation and grew into multi-cellular colonies was evaluated. The rational was that the number of single cells which could produce cell colonies after irradiation reflects the radiation-resistance of the cell population. Cells from the chosen cumulative dose populations were plated at 2 cells per well in 96 well plates and either not irradiated or irradiated with 5 Gγ of X-rays. The number of wells which contained cell colonies from cells which had received 5 Gγ was counted and expressed as a percentage of the number of wells with colonies formed from cells of the same population which had not been irradiated. If the percentage of recovered cells was lower for any of the First 5 Gγ series populations than for the un-irradiated MCF-10A population then this would indicate that the cells had become less radiation resistant.

The un-irradiated MCF-10A cells, 10 Gγ cumulative dose cells and passage control cells had between 35% and 40% of radiation-recovered colonies and therefore had a similar radiation-resistance (Fig 3.12). Cell populations which had received between 25 and 80 Gγ cumulative doses of X-irradiation all had a significantly lower percentage of radiation recovered colonies than un-irradiated MCF-10A which indicates that they were less radiation-resistant than un-irradiated MCF-10A cells (Turkey's test: 25 Gγ - p=0.009, 40 Gγ - p=0.002, 55 Gγ - p=0.015, 80 Gγ - p=0.029). The 40 Gγ cumulative dose population had a lower radiation-resistance than the 10 Gγ and passage control populations (Turkey's test: 10 Gγ: p=0.023, Passage control: p=0.024). The 25-80 Gγ cumulative dose populations had between 11% and 20% of radiation recovered colonies and were not significantly different from each other.

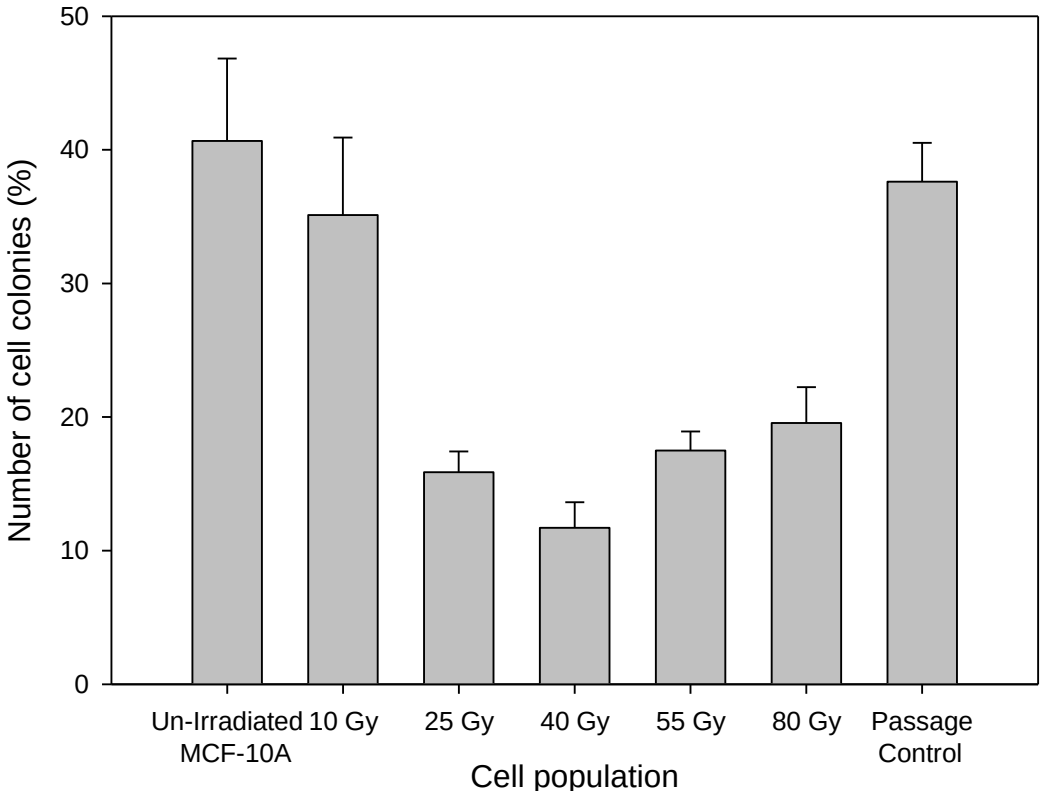

Figure 3.12 Radiation resistance of the First 5 Gγ Series.
Cells from each cumulative dose population were plated at 2 cells per well in two 96 well plates in 200µl of medium. Cells received either no irradiation or were irradiated with 5 Gγ of X-rays. The cells were cultured for a further 14 days and then the number of wells which contained a distinct colony of cells was counted in each 96 well plate. The number of wells with colonies from cells of each population which had received 5 Gγ of irradiation was expressed as a percentage of the number of wells with colonies from cells of the same population which had received no irradiation. Mean values from four experiments for un-irradiated cells, three experiments for the First 5 Gγ series and two experiments for the passage control +/- SEM are shown (ANOVA: p=0.001).

Results therefore indicated that cell populations which had received a cumulative dose of 25 Gγ of ionising radiation and above were more radiation-sensitive than un-irradiated MCF-10A cells and the 10 Gγ cumulative dose cell population. The reduction in radiation-resistance was not observed during the development of the First 5 Gγ series; the cells appeared to recover at the same rate throughout the dosing regimen. The increase in radiation-sensitivity did not appear to be passage-related.

3.4 Development and phenotypic characterisation of the Second *in vitro* model

For the Second *in vitro* model 10^{-8} M of 17β oestrodiol was present in the medium for the duration of the dosing regimen. An oestrodiol concentration of 10^{-8} M is used frequently to stimulate maximal oestrogen response *in vitro* and is equivalent to the high concentrations of oestrogen reached in the plasma of adolescent females (Styrt and Sugarman, 1991). Because MCF-10A cells are ERα negative, any carcinogenic role of oestrogen in these cells will most likely be via a genotoxic rather than a receptor mediated mechanism. To provide a reference cell population for the Second 5 Gγ series, MCF-10A cells were grown in the presence of 10^{-8} M 17β oestrodiol but without irradiation for the same number of passages as were required to reach a cumulative dose of 80 Gγ of ionising radiation (passage control population).

Initially, during the Second dosing series, the 5 Gγ populations took approximately 5 days to recover and 7 – 9 days elapsed between irradiations. After 50 Gγ cumulative dose the cells took only 3-5 days to recover. For the 10 Gγ series, cell recovery took 7 days and 10-12 days elapsed between irradiations; cells did not recover faster as the cumulative dose increased.

Phenotypes of the Second *in vitro* model were analysed in the 5 Gγ irradiation series. The cumulative dose populations analysed were 10, 20, 40, 60 and 80 Gγ. The following sections of this chapter describe cell morphology, proliferation rates, contact inhibition and radiation-sensitivity of this series.

3.4.1 Changes in cell morphology of the Second 5 Gγ irradiated populations

The cell morphology of the Second 5 Gγ series was characteristic of cells undergoing epithelial to mesenchymal transition (EMT), which occurs during epithelial cell transformation. Cells which have undergone EMT have a spindle-like or fibroblastic appearance, less tight cellular junctions with adjacent cells and are more motile. Previous studies have indicated that at low density MCF-10A cells have morphological and gene expression properties similar to cells that are undergoing EMT; however these similarities are lost at high density (Maeda *et* al 2005; Sarro *et al.* 2008). Figure 3.13a shows un-irradiated MCF-10A cells at low density. There were some spindle like cells and other cells were clustered into cell cobblestone-like islands typical of epithelial cells. Cells from the Second 5 Gγ series showed a similar morphology however the spindle cell morphology was more prominent and there was less evidence of the cobblestone

morphology (Figure 3.13b). As cell density increased, un-irradiated MCF-10A cells lost the spindle cell morphology and had traditional epithelial cell morphology (Figure 3.20c). More cells from the Second 5 Gγ series at high density however maintained spindle morphology, and compared to un-irradiated MCF-10A there was a reduced cobblestone appearance to the cell population. The maintenance of EMT-like cell morphology at high cell density may therefore be an indication of cell transformation of the Second 5 Gγ series.

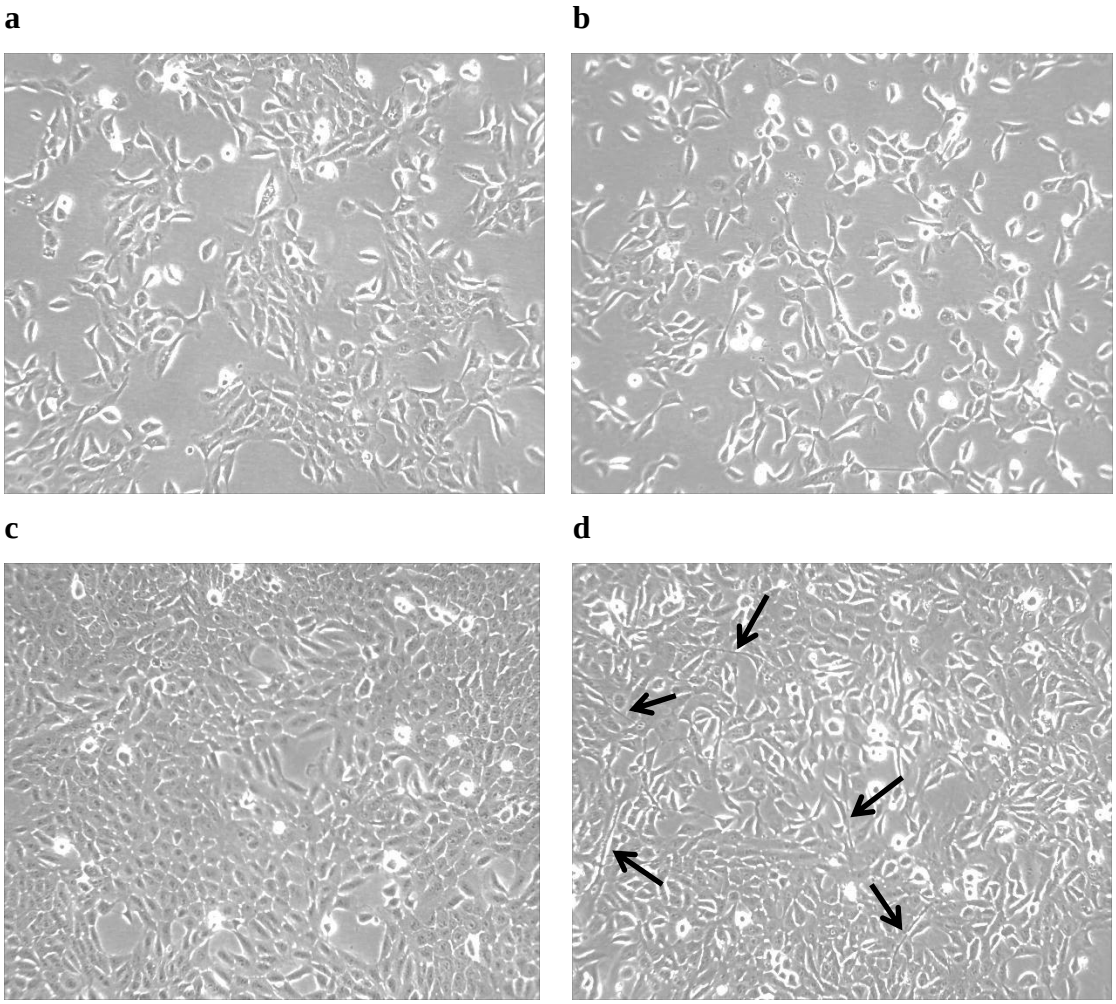

Figure 3.13 Cell morphology of the Second 5 Gγ Series
Cells were plated in T75 flasks and grown to different cell densities. Cell morphology was assessed at x10 magnification. The cell populations shown are: un-irradiated MCF-10A cells at cell confluency of ~ 40% **(a)** and ~ 90% **(c)** and cells from the Second 5 Gγ series which have received a cumulative dose of 60 Gγ at cell confluency of ~ 40% **(b)** and ~ 90% **(d)**. Examples of spindle-like or fibroblastic cell morphology in the Second 5 Gγ series are shown by black arrows.

3.4.3 Growth rate of the Second 5 Gγ irradiated populations

The proliferation rates in the Second 5 Gγ series populations did not differ obviously from each other during routine cell culture. To compare proliferation rates, cells were plated in 24 well plates and the DNA content of the cells was measured over 3 days before the cells had become confluent. There were no apparent differences in growth rate between the different cell populations (Fig.3.14a).

The growth rates of the cell populations were compared by exponential regression. The growth rate was approximately 0.05 cell doublings per hour for un-irradiated MCF-10A cells. The cells grew in all cell populations at similar rates (ANOVA: p=0.144).

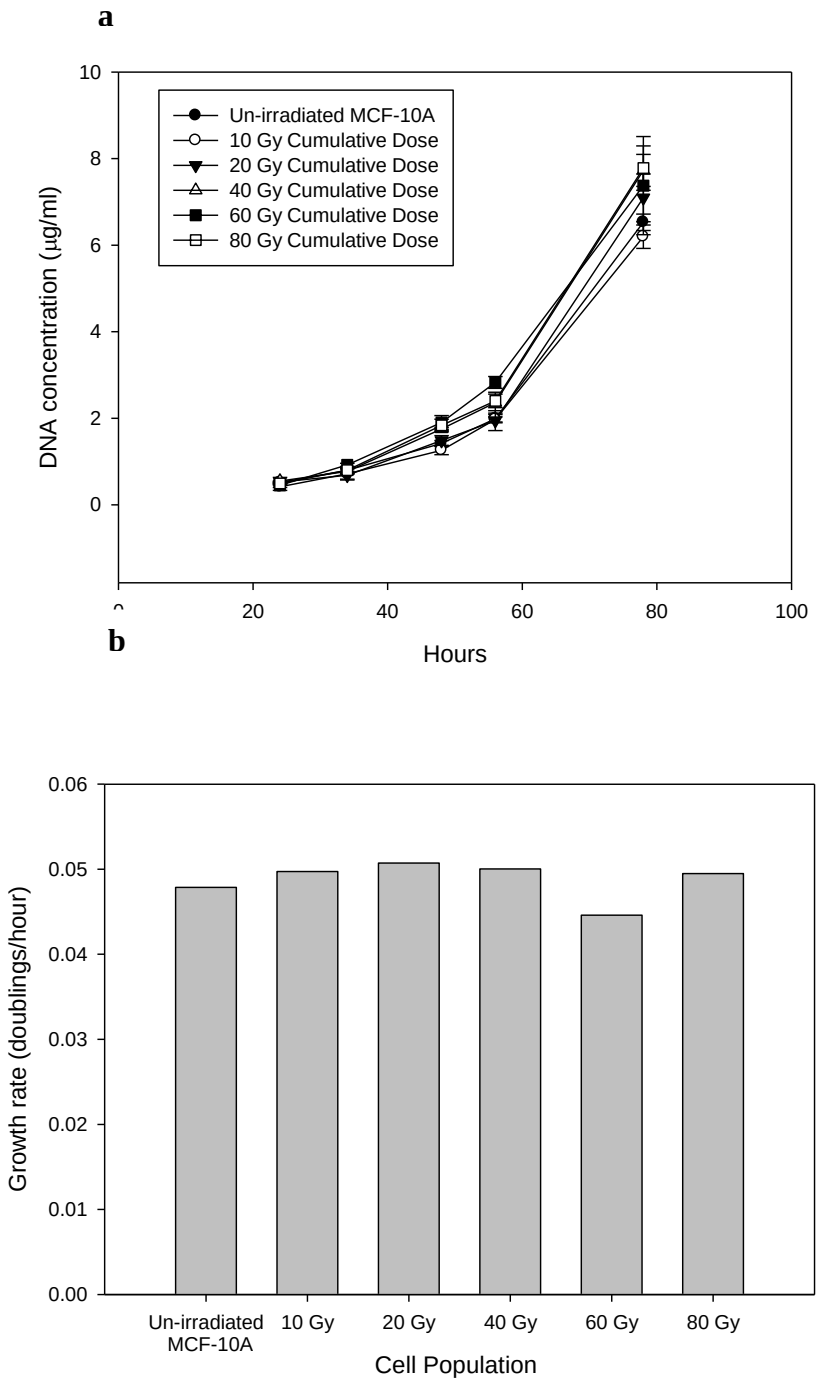

Figure 3.14 Growth rate of the Second 5 Gγ Series.
Cells from each population were plated in 3 wells of a 24 well plate at a cell density of $1x10^4$ cells per well. Cell culture medium was replaced in the wells every day. Cells were lysed for DNA measurement at the indicated times after plating. The mean DNA concentrations of triplicate samples +/- SEM for each cell population was normalised to the DNA concentration of the un-irradiated MCF-10A cell population **(a)**. Growth rate, which is expressed as the number of cell doublings per hour was determined from this data **(b)**.

3.4.4 Contact inhibition of the Second 5 Gγ irradiated populations

The extent to which the Second 5 Gγ series demonstrated contact inhibition was analysed. Cell populations from un-irradiated MCF-10A cells and from chosen cumulative dose populations of the Second 5 Gγ series were allowed to grow in 24 well plates past the point of 100% confluency. Un-irradiated MCF-10A cells, 10 Gγ, 20 Gγ, 40 Gγ, 60 Gγ and 80 Gγ and equivalent high passage MCF-10A cells (data not shown) all appeared as a crowded monolayer with no evidence of cells growing on top of other cells five days after confluency had been reached (Fig 3.15). The observation indicated that all the cell populations had retained contact inhibition.

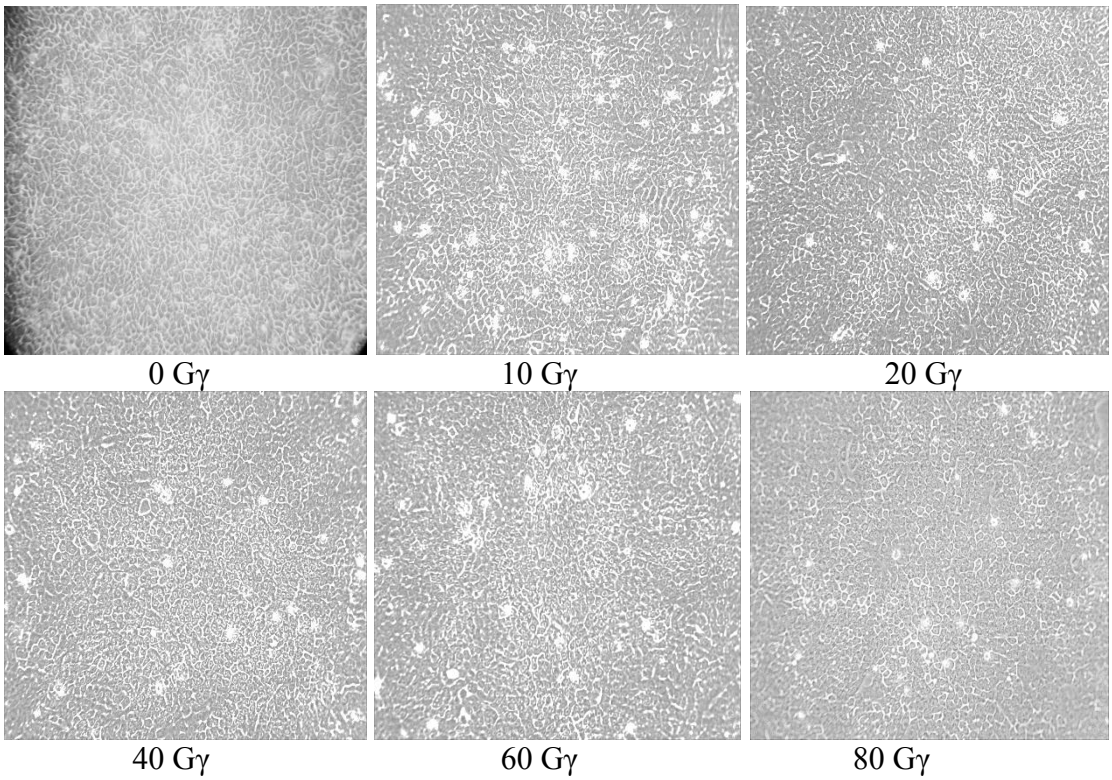

Figure 3.15 Images of the Second 5 Gγ Series 5 days after 100% confluency was reached.
Cells from each cumulative dose population were plated in 3 wells of a 24 well plate at a cell density of $1x10^4$ cells per well. The medium was replaced on the cells each day for 9 days. Photomicrographs were taken of each cell population after 9 days at x10 magnification. Cumulative dose that had been received by each cell population is indicated below each image.

To confirm these observations the DNA concentration of cells was measured 5 days after they had reached 100% confluency. The DNA concentration was similar in un-irradiated cells and in all cumulative dose cell populations (Fig. 3.16) which demonstrated that the cells did not replicate after they had reached 100% confluence and had not lost contact inhibition. There was a slight increase in DNA content as cumulative dose increased but the difference was not significant (ANOVA: p=0.427).

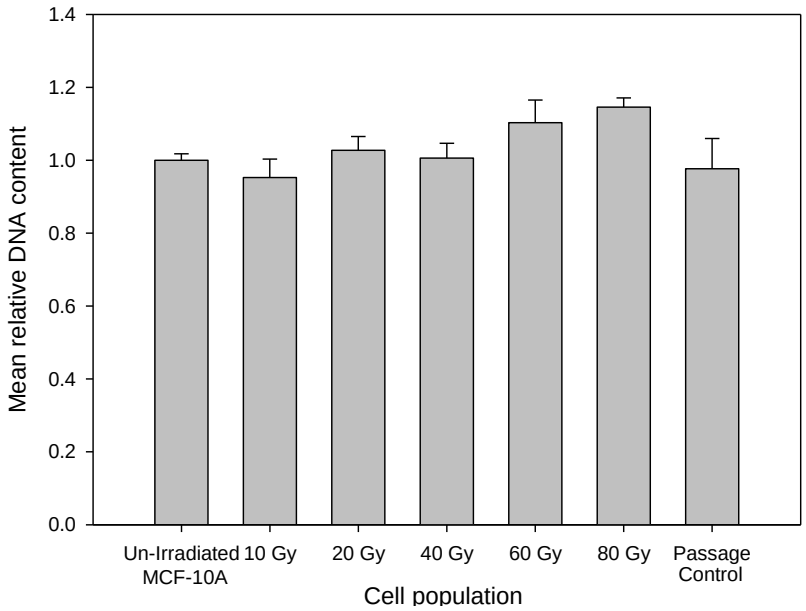

Figure 3.16 DNA content of the Second 5 Gγ Series 5 days after 100% confluency was reached.
Cells from each cumulative dose population were plated in triplicate wells of a 24 well plate at a cell density of $1x10^4$ cells per well. The medium was replaced on the cells each day for 9 days. The DNA content of the cells was measured with pico-green after 9 days. The mean DNA concentration from triplicate samples expressed relative to the mean DNA concentration of un-irradiated MCF-10A cells +/- SEM from one experiment is shown.

3.4.5 Radiation resistance of the Second 5 Gγ irradiation populations

After 10 fractionated doses cells from the Second 5 Gγ series appeared to recover faster from irradiation. This more rapid recovery was not due to an increased growth rate because the growth rate did not change as the cumulative dose increased (Section 3.4.3) and may be indicative of increased radiation-resistance. Cells from the Second 5 Gγ series were therefore tested to investigate if they had become radiation-resistant.

The Second 5 Gγ series populations were plated at low density in 96 well plates and the proportion of single cells which survived irradiation and grew into multi-cellular colonies was evaluated as described in section 3.3.4.

There appeared to be a decrease in radiation resistance as cumulative dose increased, which is contrary to what had been inferred from the cell recovery during the

development of the series (Fig. 3.17). It is also noteworthy that the equivalent high passage MCF-10A cells appeared to have reduced radiation resistance compared to the un-irradiated MCF-10A population. The decrease in radiation resistance between the un-irradiated MCF-10A cells and cells from the Second 5 Gγ series did not reach the 5% confidence level (ANOVA: p=0.092)

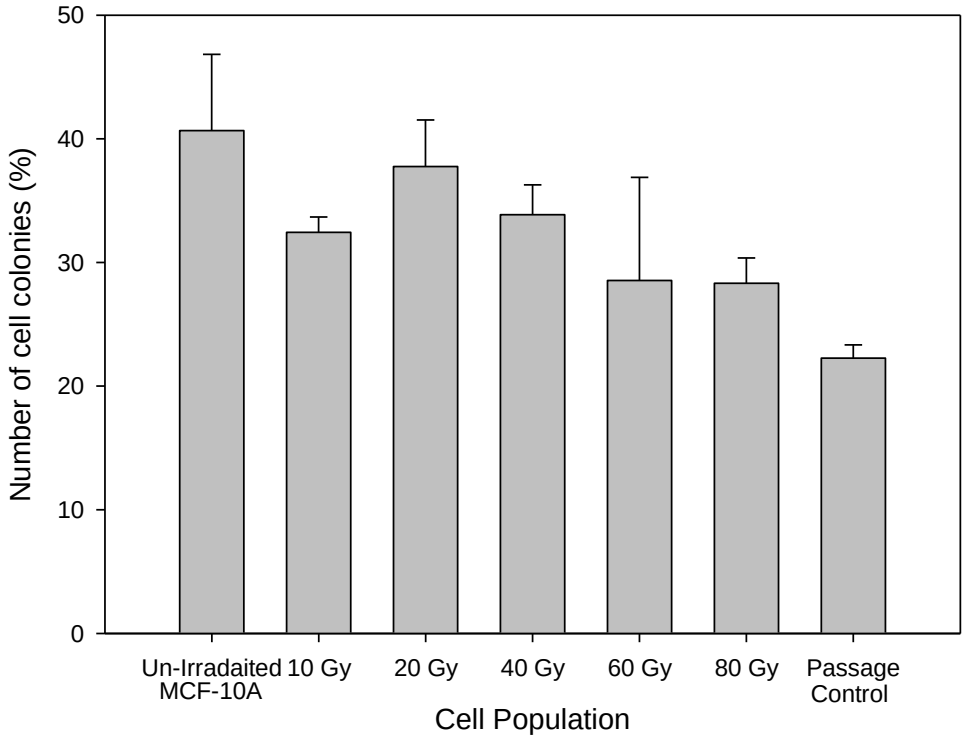

Figure 3.17 Radiation resistance of the Second 5 Gγ series.
Cells from each cumulative dose population were plated at 2 cells per well in two 96 well plates in 200 µl of medium. Cells received either no irradiation or were irradiated with 5 Gγ of X-rays. The cells were cultured for a further 14 days and then the number of wells which contained a distinct colony of cells was counted in each 96 well plate. The number of wells with colonies from cells of each population which had received 5 Gγ of irradiation was expressed as a percentage of the number of wells with colonies from cells of the same population which had received no irradiation. Mean values from two experiments +/- SEM are shown.

3.5 Discussion

The molecular genetics that underlie radiogenic breast cancer are unclear and there are currently no reliable somatically acquired genetic markers that distinguish radiation-induced breast cancer. The development of *in vitro* models which aim to replicate conditions that lead to cell transformation should allow the molecular genetic signatures caused by different mutagens or carcinogens to be discerned. We have developed models of irradiated breast epithelial cells with the non-transformed breast epithelial cell line MCF-10A to investigate the genetic alterations caused by ionising radiation.

Four *in vitro* models of irradiated breast epithelial cells have been developed. The *in vitro* models are divided into two series. In the "First" irradiation series, cells received fractionated doses of X-rays of either 5 Gγ or 10 Gγ to a cumulative dose of 80 Gγ to create two separate *in vitro* models. Cells in the "Second" irradiation series underwent the same fractionated dosing regimens but with 10^{-8} M 17-β oestrodiol present in the cell culture medium throughout the dosing schedule. Epidemiological evidence has suggested that younger women exposed to ionising radiation have a greater risk of developing breast cancer than older women (Hrubec *et al.*, 1989; Land *et al.*, 2003; Travis *et al.*, 2003). It has been hypothesised that this may be due to the increased levels of oestrogen present in younger women (van Leeuwen *et al.*, 2003). The presence of high levels of oestrogen when cells are exposed to ionising radiation may therefore be a relevant factor when developing a radiation exposed *in vitro* model.

This chapter has described the phenotypic characterisation of the First 5 Gγ irradiation series and the Second 5 Gγ irradiation series. Changes in phenotype would indicate that the cell populations have undergone genetic alterations and could provide evidence of cell transformation. Cell morphology, growth rate, radiation sensitivity and contact inhibition were analysed.

3.5.1 First 5 Gγ Series

Cells in the First 5 Gγ series display differences from normal MCF-10A cells in all of the phenotypes analysed. These changes do not appear to be passage related and are therefore consequences of genetic alterations caused by the radiation regimen. Because the irradiated MCF-10A cell populations are heterogeneous, the genetic alterations that lead to phenotypic changes are likely to have occurred in sub-populations of cells which have subsequently become established throughout the population. The establishment of

cell populations with phenotypic changes could occur through chance or because the new phenotype causes a selective advantage to the cells.

3.5.2 Cell morphology

Cells from the First 5 Gγ series appear to become more densely packed and to be less motile than un-irradiated MCF-10A cells. These changes in cell phenotype are observed first in the 40 Gγ cumulative dose cell population. Varied cell morphologies have been reported for transformed MCF-10A cells but the cells often become more spindle-like, lose their normal epithelial-like cobblestone appearance and appear more motile than non-transformed MCF-10A cells (Maeda *et al.*, 2005; Kim *et al.*, 2007; Botlagunta *et al.*, 2008; Kim *et al.*, 2009a; Botlagunta *et al.*, 2010; Cho *et al.*, 2010; Meng *et al.*, 2010). Most studies which describe this altered cell morphology have used targeted cell transformation approaches such as increased expression of oncogenes or growth factors known to stimulate EMT. Cells which have undergone EMT have a spindle-like cell morphology (Maeda *et al.*, 2005; Kim *et al.*, 2007; Kim *et al.*, 2009a; Cho *et al.*, 2010; Meng *et al.*, 2010).

Exposure to ionising radiation is not a specific or single gene alteration approach and the phenotypes induced might be expected to be more varied. Transformation of MCF-10A cells with the ICR191 mutagen, which is also not a specific or single gene approach, did not induce a spindle-like cell morphology but the cells did form tumours in immune-compromised mice (Zientek-Targosz *et al.*, 2008). A spindle like cell morphology may therefore be indicative of MCF-10A cell transformation but is not a pre-requisite for cell transformation. Likewise, cells transformed by transfection with the *HRAS* oncogene did not have a spindle-like morphology but they did form tumours in immune-compromised mice. Subsequently cells cultured from the tumours had a spindle-like morphology (Imbalzano *et al.*, 2009). In the present study, there is the potential for there to be transformed cells within the cell populations, although cells have not been selected for transformation status.

3.5.3 Growth rate

Cells from the First 5 Gγ series show a gradual reduction in growth rate compared to un-irradiated MCF-10A cells as the cumulative dose received by the cells increases. This pattern is interrupted at the 25 Gγ cumulative dose population which has a significant reduction in growth rate but the growth rate increases again by the 40 Gγ

cumulative dose population. Growth rate does not reduce to a significant level again compared to un-irradiated MCF-10A cell population until the 80 Gγ cumulative dose population. The growth rate results indicate that more than one genetic event which affects growth rate has occurred in the First 5 Gγ series. Multiple genetic alterations are expected during a fractionated dose regimen which means that a given phenotype may be altered more than once and potentially in different directions throughout an irradiation series.

Both increases and decreases in growth rate of transformed MCF-10A cells have been reported. Cell populations transformed by *HER2* transfection and *IGF-IR* transfection both had a reduced growth rate (Kim *et al.*, 2007; Meng *et al.*, 2010). MCF-10A cells transformed by transfection with *HRAS* or by exposure to ionising radiation combined with cigarette smoke had an increased growth rate (Imbalzano *et al.*, 2009; Botlagunta *et al.*, 2010). Populations of MCF-10A cells transformed by treatment with the ICR191 mutagen had both increased and reduced growth rates. These cells were capable of growing as tumours in immune-compromised mice irrespective of whether their growth rate was increased or decreased (Zientek-Targosz *et al.*, 2008). Cumulatively, these results indicate that the growth rate of MCF-10A cells may not be a reliable indicator of cell transformation.

3.5.4 Radiation-resistance

Individuals with cancer who have undergone radio-therapy often acquire resistance to irradiation and show evidence of accelerated re-population of the tumours between fractionated doses of irradiation (Phillips *et al.*, 2006). In the present study, we investigated whether the fractionated X-ray dose regimen would select for a radiation-resistant cell population. The First 5 Gγ series showed increased radiation-sensitivity compared to the un-irradiated MCF-10A and equivalent passage number populations. Increased radiation sensitivity was observed in cell populations that had received 25 Gγ cumulative dose of X-rays and above. A current favoured hypothesis for radiation resistance *in vivo* is that radiation-resistant cancer stem cells are present in the tumour cell population and that these cells allow re-growth and repopulation of tumours following ionising radiation therapy (Vlashi *et al.*, 2009). Studies of these cells in a number of cancer types have reported increased activity of DNA damage checkpoint genes (Rich, 2007), increased expression of the developmental pathway proteins, JAGGED-1 and NOTCH-1 (Phillips *et al.*, 2006), and over-expression of the WNT/β-

CATENIN pathway (Woodward *et al.*, 2007). These changes in activity and expression have been reported to be involved in increased radiation-resistance. These studies used cancer cell lines or primary tumour cell populations to confirm that fractionated doses of irradiation enrich the cell populations for cells with radiation-resistant cancer stem cell properties. Results in the present study are consistent with absence of a cancer stem cell population in the original MCF-10A cell population and that cells with cancer stem cell properties were not developed during the dosing schedule.

An increase in radiation sensitivity could be caused by genetic alterations that affect the DNA damage response or DNA damage repair. Loss or altered function of genes involved in these processes would cause cells to become more radiation sensitive. For example, loss of function of a number of DNA damage checkpoint genes such as *ATM* (Collis *et al.*, 2003) and *CHEK1* (Koniaras *et al.*, 2001) have been shown to cause an increase in radiation sensitivity (Pawlik and Keyomarsi, 2004). Loss of DNA repair genes such as *RAD54* in a mouse study (Essers *et al.*, 1997) and *RAD51* in an osteosarcoma *in vitro* study (Du *et al.*, 2010a) have also resulted in elevated radiation sensitivity.

Disruption of the G2/M checkpoint has also been shown to cause increased sensitivity to radiation (Strunz *et al.*, 2002). In the present study there were fewer cells in G2/M phase of the cell cycle in the 80 Gγ cumulative dose population than in the un-irradiated MCF-10A cell population (Section 3.3.3). This finding indicates that the 80 Gγ cumulative dose cells pass through the G2/M checkpoint faster than un-irradiated MCF-10A cells and provides some evidence of G2/M checkpoint disruption. Genetic alterations in genes involved in maintenance of the G2/M checkpoint may therefore be the cause of increased radiation sensitivity in the First 5 Gγ series.

3.5.5 Contact inhibition

The First 5 Gγ series displayed gradual loss of contact inhibition, as represented by an increase in the number of cells present in confluent cell populations, which reached statistical significant in the 80 Gγ population. There was also evidence of loss of contact inhibition in the 40 Gγ and 55 Gγ cumulative dose cell populations, demonstrated by cells growing on top of each other after they have become confluent. This phenotype became more pronounced as the cumulative dose increased. The loss of contact inhibition phenotype observed in the present study differs slightly than those reported in other MCF-10A studies. In the present study, cells appeared to pile on top of each other

evenly across the whole cell population when confluent which indicates that cells with reduced contact inhibition are distributed evenly throughout the population. Transformed cells in other MCF-10A studies formed foci of cells within the cell population (Caruso *et al.*, 2001; Kim *et al.*, 2007; Zientek-Targosz *et al.*, 2008; Meng *et al.*, 2010).

A study by Kim *et al.* (2009b) reported that contact inhibition in MCF-10A cells is mediated by a balance between the level of growth stimulation by EGF and level of growth inhibition by E-Cadherin mediated cell contact. The study reported that at low EGF concentrations, cell replication was observed only at the edge of low density cell clusters. At higher EGF concentrations, replicating cells were observed uniformly throughout the cell clusters. In densely packed cell clusters, cell replication was observed only at the edge of clusters even at high EGF concentrations. After E-Cadherin expression had been silenced, cell replication was observed uniformly throughout the densely packed cell clusters. The authors concluded that a balance exists between EGF concentration and cell-cell contact that determines whether or not cells grow. In the present study, high EGF concentrations were maintained throughout the experiment and cells were packed very densely at confluence. It is therefore possible that the evenly-distributed piling up of cells observed in irradiated cell populations in the present study may be due to a reduction in cell-cell contact compared to in un-irradiated MCF-10A cells.

3.5.6 Second 5 Gγ Series

Cell populations in the Second 5 Gγ series displayed fewer phenotypic changes compared to un-irradiated MCF-10A cells than those of the First 5 Gγ series. The only phenotypic change observed was in cell morphology. The lack of phenotypic changes indicates that fewer genetic alterations have occurred in the Second 5 Gγ series than in the First 5 Gγ series. This result is not consistent with the conclusions from previous studies which have reported that radiation and oestrogen exposure together caused greater allelic imbalance and more phenotypic changes in cells than exposure with either on their own (Bartstra *et al.*, 1998b; Bartstra *et al.*, 1998a; Calaf and Hei, 2000; Roy *et al.*, 2001a).

Cells from the Second 5 Gγ irradiation series appeared to have less tight cellular junctions at high cell densities, did not form epithelial-like cobblestone islands and were more spindle-like in appearance than un-irradiated MCF-10A cells. This cell

morphology is akin to cells undergoing EMT which is an accepted stage in cell transformation (Huber *et al.*, 2005) and has been observed in transformed MCF-10A cells in numerous studies (Maeda *et al.*, 2005; Kim *et al.*, 2007; Botlagunta *et al.*, 2008; Kim *et al.*, 2009a; Botlagunta *et al.*, 2010; Cho *et al.*, 2010; Meng *et al.*, 2010). EMT has been shown to be induced by expression of oncogenes such *as c-MYC, HRAS* and *HER2* (Kim *et al.*, 2009a; Liu *et al.*, 2009; Cho *et al.*, 2010) and by treatment with growth factors such as insulin-like growth factors (IGFs) and transforming growth factor-β (TGF-β) (Morali *et al.*, 2001; Maeda *et al.*, 2005; Kim *et al.*, 2007). 17-β oestrodiol has been shown also to induce EMT transition in MCF-10F cells (Huang *et al.*, 2007). The change in cell morphology in the Second 5 Gγ series indicates that genetic alterations have occurred and may be indicative of cell transformation.

3.5.3 Conclusion

Changes to cell phenotypes in the X-ray treated *in vitro* models analysed suggest that genetic alterations have been caused by the ionising radiation regimen. The loss of contact inhibition by the First 5 Gγ is a transformed phenotype. Other phenotypic changes in the First 5 Gγ series were not typical of the phenotypes of transformed MCF-10A cells reported in the literature. A spectrum of changes is observed in transformed MCF-10A cells and lack of a particular transformed phenotype does not necessarily indicate cells are not transformed. It should be noted however that there is little evidence that the cells in the First 5 Gγ series are transformed.

The findings in this chapter also suggest that the First 5 Gγ series has undergone more phenotypic changes and hence more genetic alterations that the Second 5 Gγ series. This difference is surprising as the literature suggests that the conditions of the Second irradiation regimen should cause more genetic alterations. The Second 5 Gγ series does display cell morphology similar to cells which have undergone EMT. Cells which have undergone this transition are more motile and invasive and investigation of these phenotypes in the Second 5 Gγ series would be interesting (Huber *et al.*, 2005).

Overall, evidence for cell transformation of the *in vitro* models is in-conclusive. There is however compelling evidence that radiation-induced genetic alterations have occurred. Analysis of these genetic alterations could provide information on the genetic basis for the phenotypic changes observed, and may identify potential radiation-induced genetic alterations.

Chapter 4: Gene copy number analysis of radiation-treated MCF-10A cells using a high-density polymorphism array

4.1 Introduction

Ionising radiation causes DNA damage which can lead to mutation following incorrect DNA repair or DNA replication without DNA repair. Ionising radiation can cause damage to individual nucleotides or induce single and double DNA strand breaks (Section 1.4). Damage to nucleotides and single strand breaks can normally be effectively repaired by mechanisms such as base excision repair (Zharkov, 2008). Double strand breaks can be repaired by non-homologous end joining and homologous recombination (Mahaney *et al.*, 2009; Barker and Powell, 2010).

Incorrect repair of DNA double strand breaks can lead to chromosome rearrangements and translocations, and regions of chromosome/gene deletion or duplication (Section 1.4). Some of the main genetic alterations caused by ionising radiation are therefore gene copy number alterations. Loss or gain of copies of genes can subsequently change the level of expression which, depending on the function of the gene, can contribute to cell transformation. For example, copy number loss of a tumour suppressor gene could reduce protein expression and activity which could lead to cancer due to haploinsufficiency. Copy number loss could also induce a state of LOH whereby only one version of the allele remains. Unmasking recessive mutations can contribute to cellular transformation. Alternatively, copy number gain of an oncogene could lead to increased protein expression and activity which again could lead to cancer.

Ionising radiation-induced DNA damage can also induce copy neutral LOH, where a deleted allele can be re-constituted from a homologous chromosome. This process re-establishes the diploid state (copy neutral) but the affected region becomes homozygous. Recessive mutations can also be unmasked through this process and can also contribute to cellular transformation, and has been identified as a mechanism operating in human cancers, such as acute myeloid leukaemia (Gupta *et al.*, 2008; O'Keefe *et al.*, 2010).

High-density polymorphism arrays can detect both copy number alterations and copy neutral LOH across the whole genome using markers for single nucleotide polymorphisms (SNPs) and copy number variants (CNVs). The Affymetrix Human SNP 6.0 Array contains more than 906,600 SNP probes and more than 946,000 CNV

probes which can be used to interrogate the entire human genome (McCarroll *et al.*, 2008) (Section 2.5).

4.1.1 Aim

The aim of the work described in this chapter was to analyse copy number alterations and copy neutral LOH in the un-irradiated MCF-10A cell population and populations from the "First" and "Second" irradiation series (described in chapter 3.1) using the Affymetrix Human SNP 6.0 Array. The pathogenesis of radiation-induced breast cancer remains to be fully elucidated, and somatically acquired genetic alterations that contribute to disease development following radiation exposure have yet to be identified. As such, the *in vitro* model of breast epithelial cells exposed to ionising radiation will be used to identify putative radiation-induced genetic alterations.

4.2 Copy number analysis of parental MCF-10A

In order to identify ionising radiation-induced copy number alterations, the copy number profile of MCF-10A cells before irradiation was analysed. The global copy number state of MCF-10A was determined using Genotyping Console software following data generation using the Affymetrix Human SNP 6.0 Array (Figure 4.1). Some copy number alterations and chromosome rearrangements have previously been published for MCF-10A and these were confirmed by the SNP 6.0 array analysis. However, previously unreported copy number alterations were also identified using this array platform.

4.2.1 Published copy number alterations in MCF-10A

The MCF-10A cell line is a near diploid cell line but its genome contains several established somatic genetic alterations, previously identified using metaphase FISH and aCGH (Cowell *et al.*, 2005).

MCF-10A cells have an extra copy of chromosome 1q (including chromosome 1 centromere) plus a duplication of the region 198136766-qter to create an overall copy number of 4 for this region (Cowell *et al.*, 2005). This alteration was confirmed by SNP 6.0 data analysis, although the duplicated region is shown to be 199265027-qter (Fig 4.2a).

SNP 6.0 analysis also confirmed previously described copy number gains on chromosome 5q (Chr 5: 118383183-qter) and chromosome 8q (Chr 8: 100271658-qter)

to give a copy number of 3 (Fig 4.2b and 4.2c). Copy number gain of chromosome 5q has previously been identified as arising due to a nonreciprocal translocation with a derivative of Chromosome 9 (which will be discussed in section 4.2.2) (Cowell *et al.*, 2005). Previously unreported alterations identified by the SNP 6.0 array will be discussed in section 4.2.3.

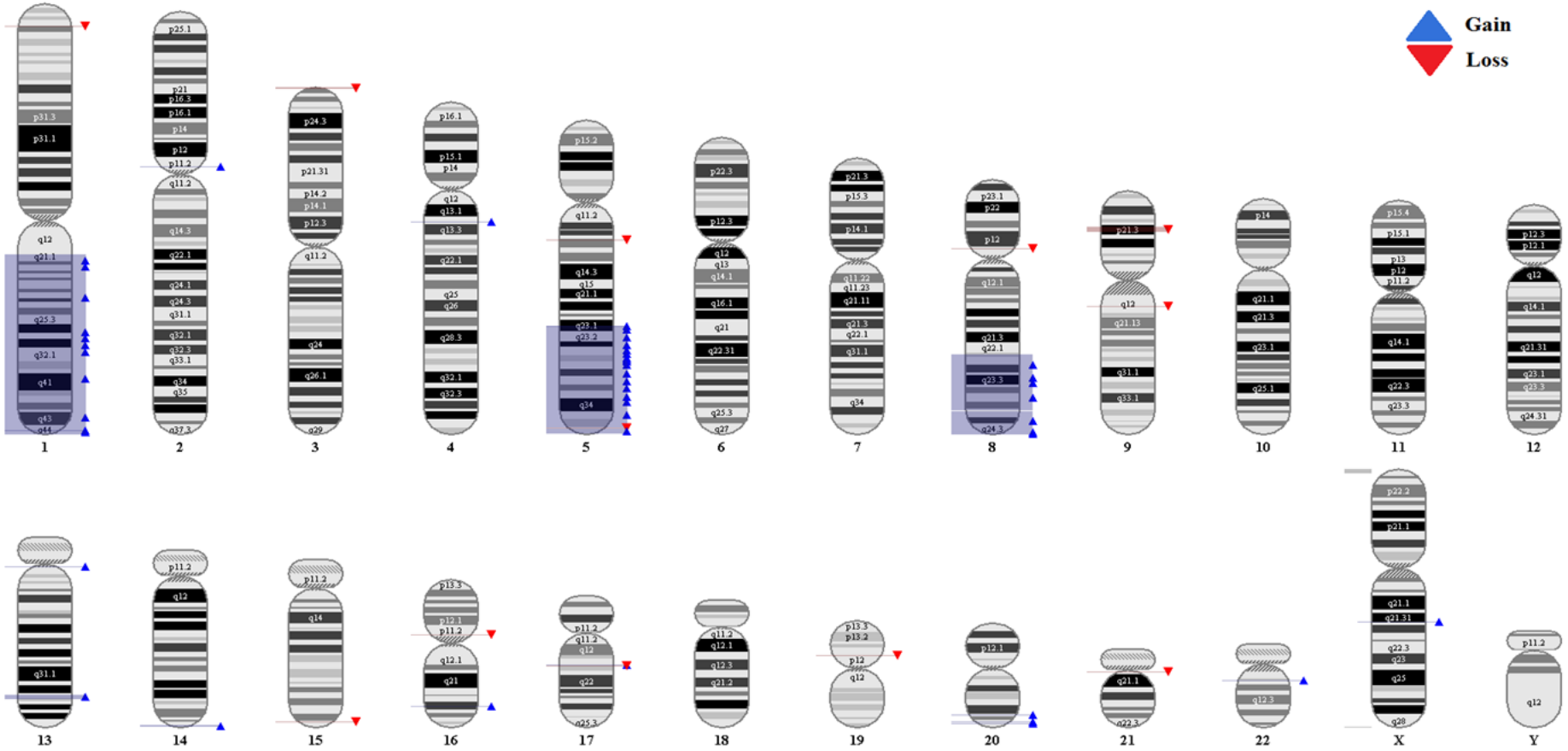

Figure 4.1 Copy number analysis of MCF-10A.
An overview of the copy number alterations identified by the Genome Console software of the parental MCF-10A genome. Blue arrows indicate regions of chromosomes with a copy number greater than 2 and red arrows indicate regions of chromosomes with a copy number less than 2. Regions of the chromosome covered by a block of blue indicate that this whole region has a copy number greater than 2.

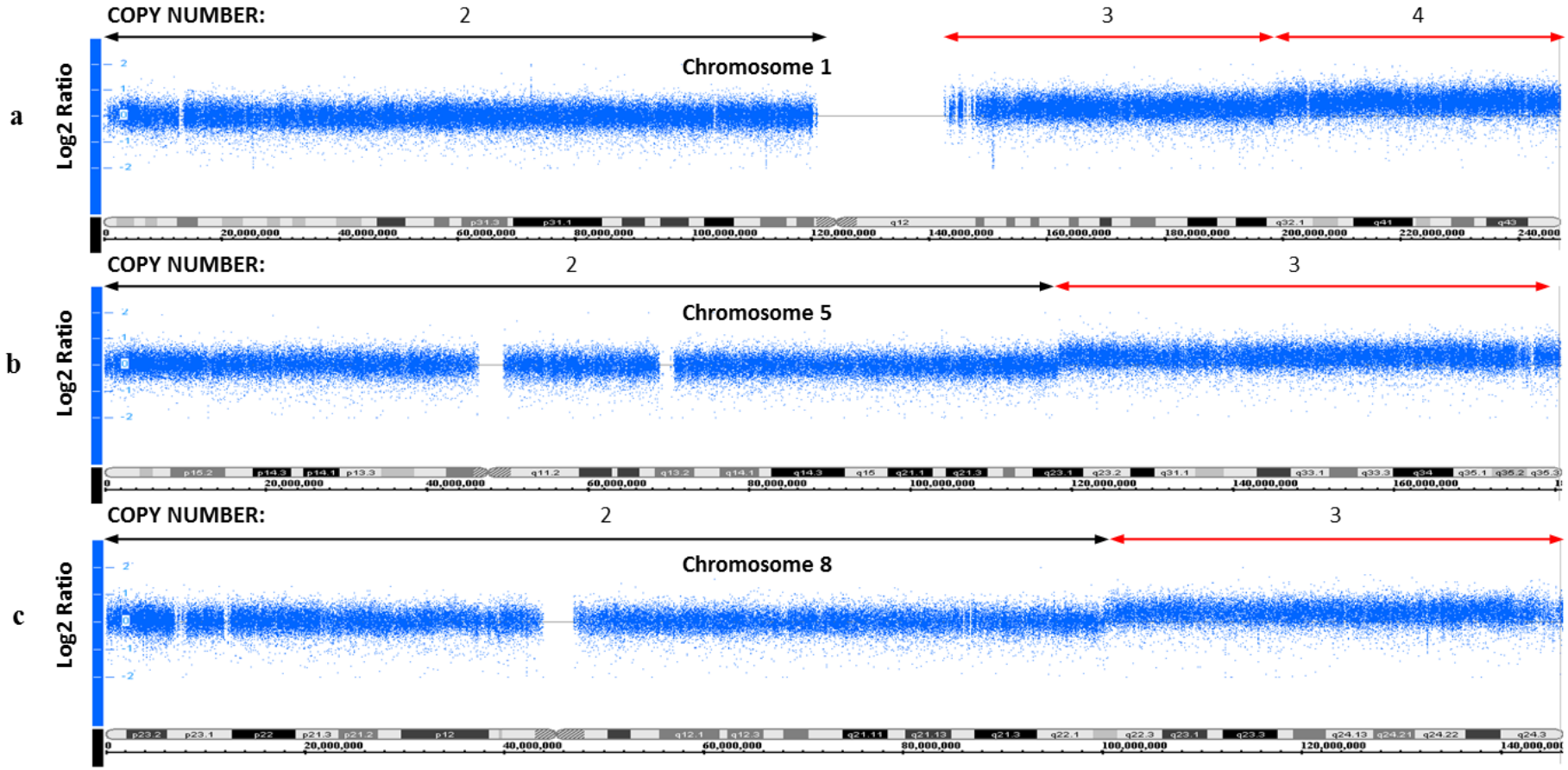

Figure 4.2 Previously reported major alterations of MCF-10A.

The copy number profiles of Chromosome 1 **(a)**, Chromosome 5 **(b)**, and Chromosome 8 **(c)** are shown. The log2 ratio of each marker as calculated by the Genotyping Console software is shown for each chromosome. The calculated copy number of each region of the chromosome is shown above each log2 ratio map. Regions which are not diploid are indicated by a red arrow. A representation of each chromosome along with chromosome position is below each log2 ratio map.

G-band karyotyping of un-irradiated MCF-10A cells by David Rowe (Institute of Genetic Medicine, Newcastle upon Tyne, UK) provided further detail of the somatic alterations identified by the SNP array (Fig. 4.3). The karyotype was defined as 47, XX, i(1)(q10),+del(1)(q12q32), der(3)t(3;9)(p14;p21), der(8)t(8;8)(q22;p23), der(9)t(3;9;5)(p14;p21;q23). The chromosome 1 rearrangement incorporated an isochromosome of 1q which provides the extra copy of 1q identified by the SNP array. A derivative chromosome 1, +del(1)(q12q32), with a deletion between regions q12 and q32 provides the fourth copy of the 199265027-qter region identified by the SNP array (Fig 4.3). SNP array data shows that MCF-10A has 3 copies of the chromosome 1 centromere. The +del(1)(q12q32) chromosome does not have a centromere and it was not identified in any other location; therefore the i(1)(q10) may be dicentric.

The duplication of the chromosome 8q region (Chr 8: 100271658-qter) is positioned on the end of the p arm of the derivative chromosome 8 (Fig. 4.3). The 8q duplication and rearrangement has been described as a translocation in the karyotype definition but in reality the mechanism is unknown. The rearrangement between chromosomes 3, 9 and 5 are as previously described in the literature and will be discussed in section 4.2.2 (Cowell *et al.*, 2005).

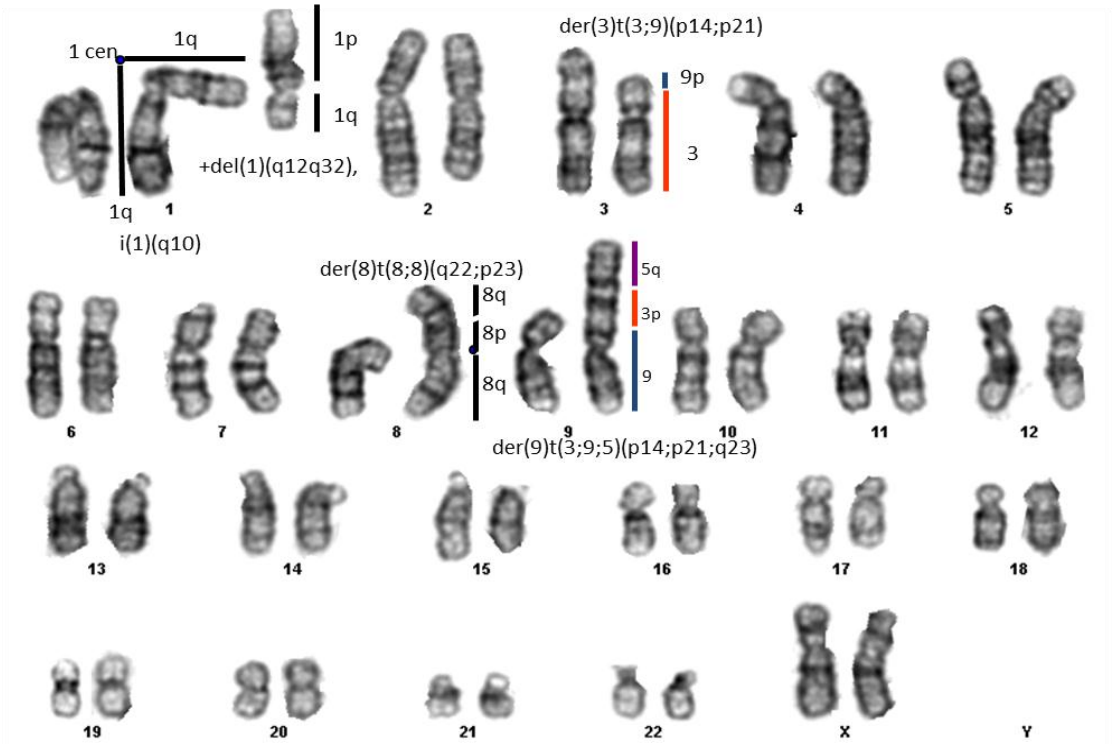

Figure 4.3 G-banding karyotyping of un-irradiated MCF-10A metaphase chromosomes.

Chromosomal rearrangements constitutive to MCF-10A are labelled with the chromosomal regions that constitutes the rearrangement and the karyotype definition of the chromosome. Two derivatives of chromosome 1 and derivative chromosomes 3, 8 and 9 are labelled.

4.2.2 t(3;9) affecting cyclin-dependant kinase inhibitor 2A (CDKN2A)

The major MCF-10A genomic rearrangements described by Cowell *et al* (2005) include a reciprocal translocation between chromosomes 3 and 9 and a non-reciprocal translocation of the end of the q arm of chromosome 5 to the derivative chromosome 9. The site of the reciprocal translocation on chromosome 9 is in the p21.3 region and resulted in a 3.2Mb mono-allelic deletion, reducing the copy number state to 1 (Fig 4.4a). Cowell and colleagues also identified a deletion on the non-translocated chromosome 9 located within the larger area of mono-allelic deletion which contains the *MTAP, CDKN2A* and *CDKN2B* loci, which gave rise to bi-allelic deletion of these loci in MCF-10A.

Cowell *et al.* (2005) suggested the breakpoint of the reciprocal translocation on chromosome 3 to be within the *FAM19A1* gene and showed that expression of this gene is lost in MCF-10A. However, the aCGH approach used in their study was not sufficiently sensitive to identify the exact area of the deletion. SNP analysis in the present study identified a putative mono-allelic deletion of approximately 35Kb in the second intron of *FAM19A1* which may be the sight of the breakpoint suggested by Cowell et al (Fig. 4.4b).

Validation of previously described MCF-10A copy number alterations in the present study confirms that the cell line being used is MCF-10A. The benefit of using high density SNP arrays is demonstrated by the identification of the putative chromosome 3 breakpoint in the t(3:9) rearrangement.

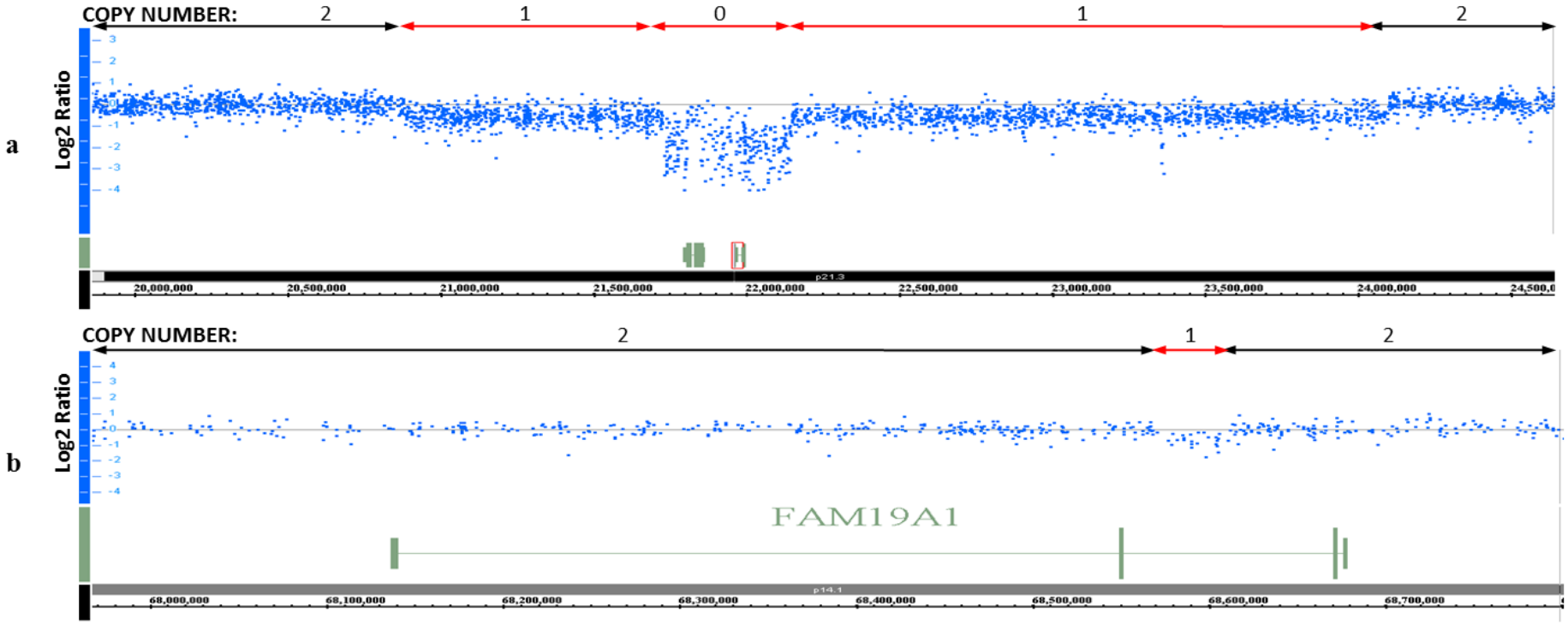

Figure 4.4 Analysis of the breakpoints of t(3:9) in MCF-10A cells.

Log2 ratio map of markers in the regions containing the postulated breakpoints of the reciprocal translocation between chromosome 9 **(a)** and chromosome 3 **(b)**. The copy number of each region is shown above each log2 ratio map. Non-diploid regions are indicated by a red arrow. A representation of the exons (green boxes) and introns (green lines) of any genes in the affected regions are positioned under each log2 ratio map. *CDKN2A* is indicated by a red box surrounding the gene **(a)**. A representation of the region of the chromosome and chromosome base position is displayed under each log2 ratio map. The region on Chromosome 3 is shown at a higher magnification than Chromosome 9.

4.2.3 Previously unreported copy number alterations in MCF-10A

Affymetrix Human SNP 6.0 Array analysis identified previously unreported copy number alterations in MCF-10A. Copy number alterations over 100Kb were identified by the Genotyping Console software and alterations under 100Kb were identified via manual interrogation of the data. Previously unreported regions which have a copy number greater or less than 2 are shown in Table 4.1. Some regions with altered copy number state appear not to include any coding sequence but may include regulatory regions, such as microRNA's. Only regions that include known coding sequences have been included in Table 4.1.

Chromosome	Chromosome Band(s)	Start Pos (bp)	End Pos (bp)	Alteration Size (kb)	# Markers	Start Marker	End Marker	Genes Affected	Copy Number State
1	p36.1-p36.2	12805146	13081658	276.512	14	SNP_A-8502362	CN_450688	9	1
1*	p36.1	25468522	25519521	50.999	22	CN_482243	CN_484335	*RHD*	0/1
1*	q21.3	150822318	150853188	30.87	34	CN_452249	CN_453516	*LCE3C, LCE3B*	0
2*	q22.1	141511213	141573074	61.861	47	CN_817202	CN_178424	*LRP1B*	1
3	p26.3	35333	1249728	1214.395	1016	CN_1037129	CN_978018	*CHL1, CNTN6*	1
3*	p14.1	68577193	68611105	33.912	24	CN_1044605	CN_1044620	*FAM19A1*	1
4	q13.2	69027195	69171918	144.723	65	CN_1109543	CN_1111671	*TMPRSS11E, TMPRSS11E2, UGT2B17*	3
5	q35.3	177047056	177160145	113.089	9	CN_1140773	CN_1140787	*Ny-REN-7*	1
7*	q34	141416100	141438564	22.464	39	CN_1221384	CN_1221421	*MGAM*	0/1
13	q32.1-q32.2	94798750	97213537	2414.787	1401	SNP_A-2175789	SNP_A-8494303	8	3
15	q26.3	97061218	97230719	169.501	117	CN_717196	SNP_A-8702108	*IGF1R*	1
16	q23.1	76357963	76782749	424.786	416	SNP_A-4285424	SNP_A-8703888	*KIAA1576, CLEC3A, WWOX*	3
17	q21.31	41521621	41717774	196.153	126	SNP_A-2043797	CN_739254	*KIAA1267*	3
17	q21.31-q21.32	41719935	42107467	387.532	44	CN_739256	CN_739354	*ARL17, LRRC37A, LRRC37A2, NSF*	1
20	q13.33	59305141	59550658	245.517	197	CN_888475	CN_890585	*CDH4*	3
20	q13.33	60288845	60477622	188.777	73	CN_894900	SNP_A-1841748	6	3
21	q11.2	13534468	14070001	535.533	216	CN_890707	SNP_A-1968961	*ANKRD21, LOC441956*	1
22*	q11.23	22680517	22726802	46.285	17	CN_915263	CN_915281	*GSTT1*	0/1

Table 4.1 Previously unreported regions of the MCF-10A genome which are not diploid.

Regions of the MCF-10A genome which are not diploid were detected by the Genotyping Console software and by manual interrogation of the log2 ratio data of each chromosome. Only copy number altered regions affecting known coding sequence are shown. Alterations identified by manual interrogation of the data are indicated by an (*) in the "Chromosome" column. For manually identified alterations. if the copy number state of all the markers in the region is not conclusive then the two potential copy number states are given in the "Copy Number State" column. If the number of genes in an altered region is under 5 they have been named, otherwise the number of genes in the region has been given.

N.B. *GSTT1* on chromosome 22 is known to be deleted in a high percentage of the population, with 20% of Caucasians being homozygous for the deletion (Nelson *et al* 1995).

4.3 Copy number analysis of the First 5 Gγ series

To identify novel copy number alterations and areas of LOH induced by ionising radiation, MCF-10A populations from the First irradiation series were analysed using the Affymetrix Human SNP 6.0 Array and copy number state was compared to un-irradiated MCF-10A.

Cell populations which had received a cumulative dose of 10, 25, 40, 55 and 80 Gγ were analysed from the 5 Gγ fractionated series and populations which had received a cumulative dose of 10, 20, 40 and 80 Gγ were analysed from the 10 Gγ fractionated series. An MCF-10A cell population which had been cultured to the same passage as the cells that received a cumulative radiation dose of 80 Gγ in the 5 Gγ irradiation series was also analysed as a reference population (passage control population).

Copy number alterations identified in the First 5 Gγ series, First 10 Gγ series and passage control populations which were not present in the un-irradiated MCF-10A genome are shown in Table 4.2, 4.3 and 4.4, respectively. Many of the alterations were large scale and contained many genes; therefore only genes in focal alterations (fewer than 10 genes affected) have been named.

The same genomic region can undergo multiple copy number alterations during a fractionated dosing regimen. Therefore, for each copy number alteration the copy number state of the region in the un-irradiated MCF-10A population, the population prior to when the alteration is identified and the population the alteration was identified in is displayed. This enables the temporal acquisition of successive copy number changes to be discerned.

Complex copy number alterations can develop when a single large copy number change encompasses a region of a chromosome which contains multiple pre-existing smaller and presumably independent regions of different copy number state. In these instances those regions which were altered due to the same single large copy number change are grouped together in red. Table 4.2 shows four instances where this has occurred, on chromosome 1, 5, 11 and 15. The complexity of the alterations on chromosome 1, 5 and 11 will be discussed in section 4.3.2. Chromosomal deletions which extend to the ends of chromosomes are indicated by green shading in Table 4.2.

Chromosome	Chromosome Band(s)	Start Position (bp)	End Position (bp)	Alteration Size (kb)	# Markers	Start Marker	End Marker	Genes Within the Region	Dose Alteration Identified (Gy)	Un-Irradiated MCF-10A Copy Number	Copy Number At Previous Cumulative Dose	Copy Number After Alteration
1	q24.1-24.2	165154658	165756926	602.268	428	CN_437966	CN_008060	*C1orf32, MAEL, GPA33, DUSP27, POU2F1, CD247*	40	3	3	2
1	q25.2-q31.3	176867954	193499072	16631.118	11107	SNP_A-8490238	CN_456733	69	40	3	3	2
1	q21.1-q24.1	143183331	165145938	21962.607	12450	CN_433861	CN_437965	>100	80	3	3	2
1	q24.1-24.2	165154658	165756926	602.268	428	CN_437966	CN_008060	*C1orf32, MAEL, GPA33, DUSP27, POU2F1, CD247*	80	3	2	1
1	q24.2-q25.2	165760448	176863452	11103.004	7319	SNP_A-2109808	CN_437050	>50	80	3	3	2
1	q25.2-q31.1	176867954	193499072	7241.126	4953	SNP_A-8490238	CN_467550	50	80	3	2	1
2	p23.1-22.3	31176346	36986182	5809.836	4208	CN_859406	CN_857277	18	40	2	2	1
2	q31.1	176169514	176771255	601.741	335	SNP_A-2006850	CN_809228	*KIAA1715, EVX2, HOXD1,2,4,8-13*	55	2	2	1
4	p16.3 - p14	56707	37078497	37021.79	24398	CN_1076141	SNP_A-8312396	>100	40	2	2	1
5	q15 - q23.1	93621043	118427111	24806.068	55864	SNP_A-1923724	SNP_A-2151750	>100	40	2	2	3
5	q23.1-q35.3	118432195	180652396	62220.201	39948	SNP_A-8714800	CN_295812	>50	40	3	3	4
5	q23.3 - q35.3	129632118	180652396	51020.278	32858	SNP_A-1983462	CN_295812	>100	55	3	4	3
5	q22.2	112200585	112380304	179.719	119	CN_1099458	CN_1099538	*SRP19, REEP5, DCP2*	80	2	3	4
7	q21.13	88668206	88771110	102.904	62	CN_1241342	SNP_A-8351139	ZNF804B	40	2	2	3
10	p15.1	5536697	5692243	155.546	97	SNP_A-176240	SNP_A-2181218	CALML3	55	2	2	3
11	q22.3 - q23.3	103769002	116689124	12920.122	8635	CN_534299	SNP_A-2020895	>100	40	2	2	1
11	q12.3-q22.3	62318238	103754855	41436.617	25951	CN_559593	CN_534295	>100	55	2	2	3
11	q23.3-q25	116689846	134449982	17760.136	13157	CN_540985	SNP_A-2246844	>100	55	2	2	3
12	q21.1	70892777	72832799	1940.022	1111	CN_607747	SNP_A-8493037	*TRHDE*	55	2	2	1
14	q22.3	54914289	55027066	112.777	88	CN_690754	SNP_A-8608018	*KIAA0831, TBPL2*	40	2	2	3
15	q24.2-q26.3	74222695	97059840	22837.145	15484	SNP_A-8370325	SNP_A-8466948	>100	80	2	2	3
15	q26.3	97061218	97264155	202.937	146	CN_717196	SNP_A-8473478	*IGF1R*	80	1	1	2
15	q26.3	97269028	100276767	3007.739	2200	CN_717265	CN_674320	20	80	2	2	3
16	p13.3	765	1985736	1984.971	726	CN_724789	CN_708789	>50	80	2	2	1
18	q21.2 - q22.3	48080079	70114155	22034.076	15649	CN_777481	CN_161922	>100	40	2	2	1
19	p13.3	41898	4609892	4567.994	1214	CN_7769500	CN_798453	>100	80	2	2	1
20	Whole Chromosome								10	2	2	3
20	p13	9293	4428933	4419.64	3292	CN_884158	CN_903312	>100	80	2	3	2
22	q13.2	39820139	39905513	85.374	195	CN_939737	CN_906914	*EP300*	10	2	1	1
X	p22.2	10392905	10625012	232.107	139	CN_933501	CN_913801	*MID1*	40	2	2	3

Table 4.2 Copy number alterations of the First 5 Gγ series.

Copy number alterations identified by the Genotyping Console software and by manual interrogation of the array data. The table shows the position of the copy number alterations on each chromosome affected and information of the markers used to detect the copy number alteration. Red shaded rows indicate copy number alterations which span a number of regions with different copy number states. Green shaded rows indicate copy number losses affecting telomeric regions. For green shaded copy number alterations the start base position is the position of the first marker on that particular chromosome. Base positions are based upon the annotation build hg18.

Chromosome	Chromosome Band(s)	Start Pos (bp)	End Pos (bp)	Alteration Size (kb)	# Markers	Start Marker	End Marker	Genes	Dose Alteration First Seen (Gy)	Un-Irradiated MCF-10A Copy Number	Copy Number At Time Of Alteration	Copy Number After Alteration	Copy Number After 80 Gy
2	q33.3	206560040	206699229	139.189	64	CN_838437	SNP_A-2203352	FLJ20309, NDUFS1	80	2	2	1	1
4	p16.3-p16.1	56707	6573579	6516.872	3611	CN_1076141	SNP_A-1862292	>50	40	2	2	1	1
9	p24.3-p21.3	36587	5071941	5035.354	5224	SNP_A-8451753	CN_389851	>100	40	2	2	3	3
9	p21.3	5072983	21725930	16652.947	14015	CN_1331569	CN_1322130	>100	40	1	1	2	2
9	p21.3	22149622	24095970	1946.348	1311	CN_1324404	SNP_A-1848109	>100	40	1	1	2	2
9	p21.3-p13.2	24101280	36549683	12448.403	8488	SNP_A-2288480	CN_1302228	>100	40	2	2	3	3
10	p14	8802113	9179270	377.157	314	CN_546701	SNP_A-8286264	0	80	2	2	3	3
10	911.23	28428290	28483377	55.087	42	CN_506488	SNP_A-1999471	MPP7	40	2	2	1	1
12	q24.31-q24.33	120606484	132287718	11681.234	7948	CN_608489	SNP_A-4219877	>100	80	2	2	1	1
18	q23.3	75798195	76009174	210.979	122	CN_797712	CN_797778	PQLC1, TXNL4A, C18orf22, ADNP2	80	2	2	3	3
20	Whole Chromosome								10	2	2	3	3
22	q13.2	39829375	39905513	76.138	187	CN_939746	CN_906914	EP300	10	2	2	1	1
X	q22.3	105900223	106395258	495.035	270	CN_920433	SNP_A-8544165	TBC1D8B, CLDN2, MORC4, RBM41, NUP6CL2	80	2	2	1	1
X	q23.3	114276787	114389568	112.781	48	CN_935881	SNP_A-8497102	LRCH2	80	2	2	1	1

Table 4.3 Copy number alterations of the First 10 Gγ series.

Copy number alterations identified by the Genotyping Console software and by manual interrogation of the array data. The table shows the position of the copy number alterations on each chromosome affected and information of the markers used to detect the copy number alteration. Red shaded areas indicate copy number alterations which span a number of regions with different copy number states. Base positions are based upon the annotation build hg18.

Chromosome	Chromosome Band(s)	Start Pos (bp)	End Pos (bp)	Alteration Size (kb)	# Markers	Start Marker	End Marker	Genes Affected	Un-Irradiated MCF-10A Copy Number	Passage Control Copy Number
1	q23.2-q23.3	159635021	161154482	1519.461	996	SNP_A-4274930	CN_007220	44	3	4
1	P23.3-p25.3	161161869	185709131	24547.262	17026	CN_437923	CN_010876	>100	3	2
19	q13.2-13.31	43268611	43549002	280.391	123	CN_774528	CN_776669	PSG1/6/7/11	2	3
20	Whole Chromosome								2	3
22	q13.2	39843857	39905513	61.656	172	CN_939766	CN_906914	EP300	2	1

Table 4.4 Copy number alterations of the high passage MCF-10A cells (passage control population).

Copy number alterations identified by the Genotyping Console software and by manual interrogation of the array data. Base positions are based upon the annotation build hg19.

Following a cumulative dose of 80 Gγ the First 5 Gγ series had accumulated 24 separate copy number alterations compared to 11 in the First 10 Gγ series. The decision was made to pursue alterations in the First 5 Gγ series rather than the 10 Gγ series due to the increased number of targets for subsequent investigation and the fact that the First 5 Gγ series had undergone *in vitro* phenotypic characterisation (Chapter 3).

Irradiated cell populations were also interrogated for areas of copy neutral LOH. In the First 5 Gγ series and passage control populations there were no areas of copy neutral LOH that were not constitutional to the un-irradiated MCF-10A genome.

4.3.1 Passage related copy number alterations in the First 5 Gγ Series

The passage control population had 5 copy number alterations (Table 4.4), two of which were also found in the First 5 Gγ series: these were a mono-allelic gain of Chromosome 20 and a mono-allelic deletion of *EP300* (Table 4.1). It can therefore be concluded that these alterations are passage related rather than induced by ionising radiation. It should also be noted that both of these alterations were present in the First 10 Gγ series (Table 4.2). The fact that the same alterations were seen in irradiated and passage control populations suggests that passage of the cells can either induce these alterations, presumably due to underlying genomic instability, or that the alterations were already present within a sub-population of un-irradiated MCF-10A cells. Selection during passage would suggest that these alterations conferred a growth advantage.

4.3.2 Complex copy number alterations

There were a number of large scale copy number alterations in the First 5 Gγ series which encompassed millions of bases and many genes. Some of these large scale copy number alterations were complex with more than one event occurring in the same genomic region at independent time points. Complex alterations were identified in Chromosome 1q, 5q and 11q (Table 4.2).

As stated previously, chromosome 1q includes regions of triploidy and tetraploidy constitutional to MCF-10A cells (Fig 4.5a). Two apparently independent mono-allelic deletions were observed in the triploid region of chromosome 1q in the 40 Gγ cumulative dose population (Fig. 4.5b), reducing the copy number state to 2. These were a relatively focal 602Kb deletion (termed “40 Gγ-Deletion 1”) between positions 165154658:165756926, and a 16631 kb deletion (termed “40 Gγ-Deletion 2”) between positions 176867954:193499072.

A large scale mono-allelic deletion was subsequently identified in the 80 Gγ population between positions 1431883331:184109080 (termed “80 Gγ-Deletion”) (Fig. 4.5c). This deletion spanned 40 Gγ-Deletion 1 and encompassed 7241 kb of 40 Gγ-Deletion 2 which further reduced the copy number states of these regions to 1. Centromeric regions not previously affected in the 40 Gγ population but subsequently affected by the 80 Gγ-Deletion reduced copy number state from 3 to 2.

SNP 6.0 array analysis does not inform which allele each copy number alteration occurred on. It can however be concluded that the 80 Gγ-Deletion must have occurred on a different allele than either of the deletions observed in the 40 Gγ population. If the 80 Gγ-Deletion had occurred on the same allele of either of the 40 Gγ deletions then the copy number state of these regions would have remained at 2.

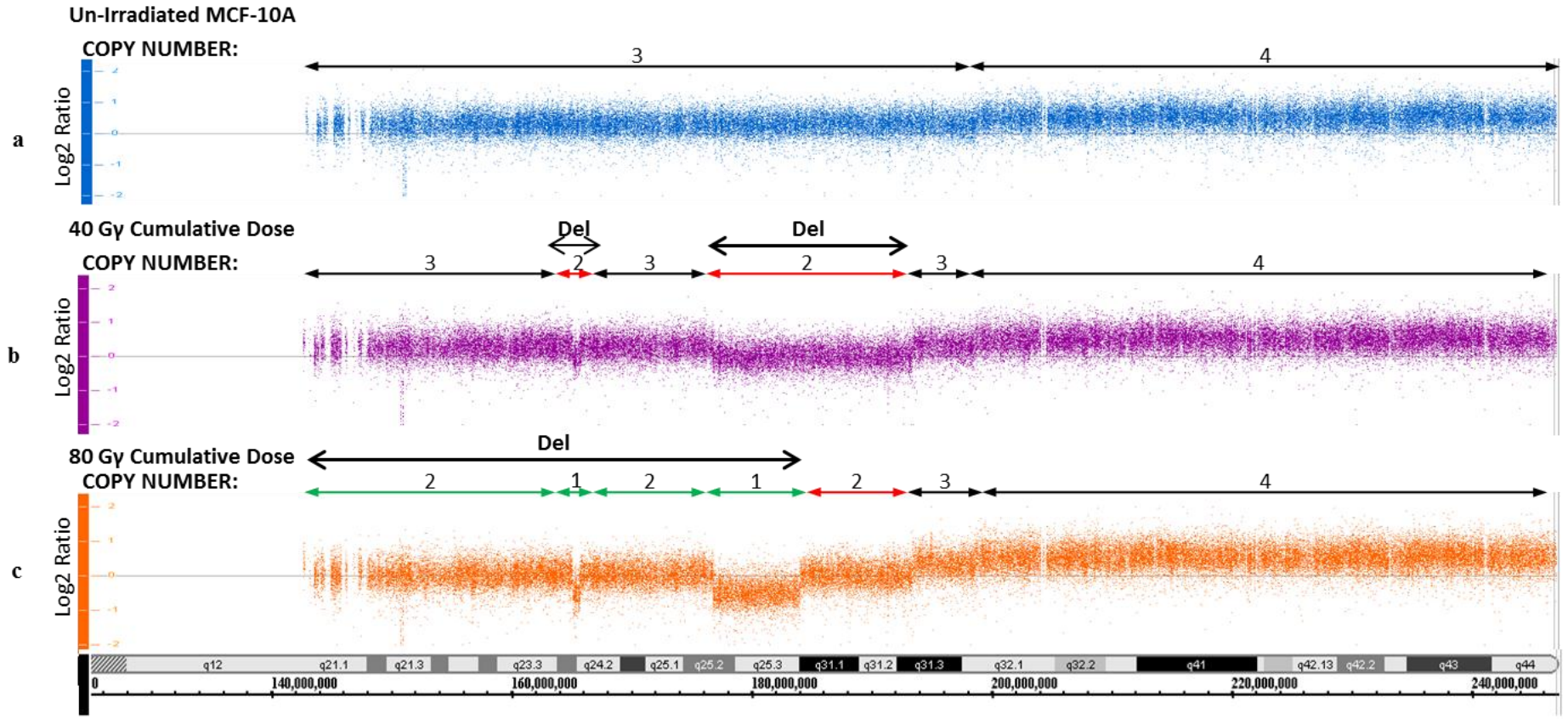

Figure 4.5 Complex copy number alterations– Chromosome 1q.

The copy number profile of chromosome 1q for the un-irradiated MCF-10A (**a**), 40 Gγ cumulative dose (**b**) and 80 Gγ cumulative dose (**c**) populations of the First 5 Gγ series. The copy number of each region of chromosome 1q is shown above each log2 ratio map. Black arrows indicate a region which has not changed from the un-irradiated MCF-10A population. Red arrows indicate copy number alterations that were first identified in the 40 Gγ population. The green arrows indicate copy number alterations that were first identified in the 80 Gγ population. Above the copy number states is an arrow indicating the copy number change event(s) identified in each population (Del = deletion). A representation of the q arm of Chromosome 1, including base positions, is at the bottom of the log2 ratio maps.

Figure 4.6 shows the progression of the complex alteration on chromosome 5q. A mono-allelic copy number gain was identified in the 40 Gγ cumulative dose population between positions 93621043-qter (Fig 4.6b). The start position of this copy number gain was centromeric of a triploid region on chromosome 5 (118383183-qter), which is constitutive to the un-irradiated MCF-10A population. The copy number gain therefore increased the constitutional triploid region to a copy number state of 4 and the constitutional diploid region (93621043:118427111) to a copy number state of 3. An additional mono-allelic deletion was identified in the 55 Gγ cumulative dose population between positions 129632118-qter (Fig 4.6c). The deletion restored the copy number of this region from 4 down to 3. Finally, a small region of copy number gain was observed in the 80 Gγ cumulative dose population between positions 112200585:112380304 encompassing the *SRP19, REEP5* and *DCP2* loci, which was within the triploid region identified in the 40 Gγ cumulative dose population (Fig 4.6d). This increased the copy number state of this smaller region to 4. It is not discernible from the SNP 6.0 data which alleles were affected by these alterations.

Deletions on chromosome 5q have been linked with a number of cancers including ER negative breast cancers and AML (Loo *et al.*, 2004; Wang *et al.*, 2004b; Fang *et al.*, 2011; Sekeres *et al.*, 2011). Genes located in this region have therefore been suggested to be involved in cancer, such as *EGR1* (Ronski *et al.*, 2005). Copy number gains, as seen in this *in vitro* model, have not been linked with cell transformation; yet large scale copy number alterations do suggest an increase in chromosomal instability which often characterises transformed cells (discussed in section 4.5).

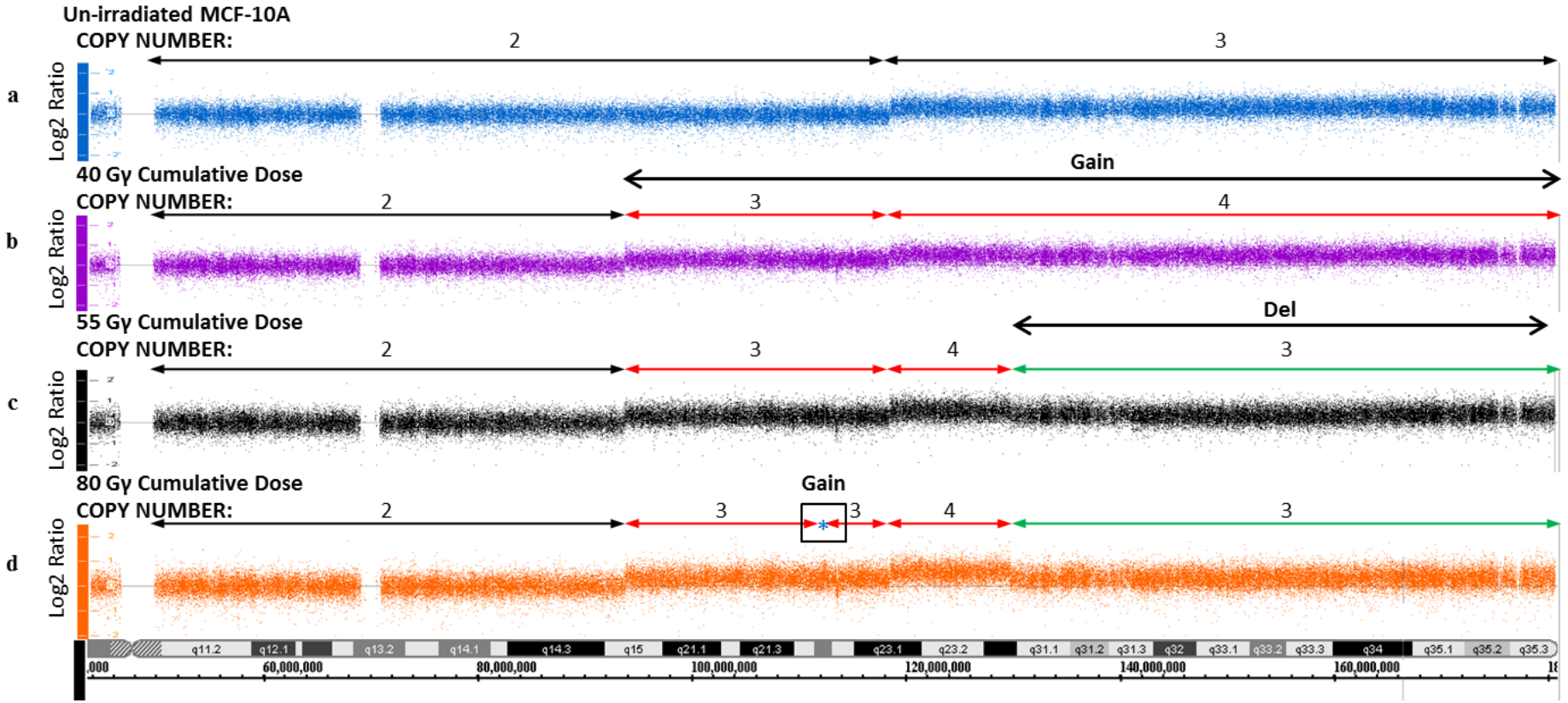

Figure 4.6 Complex copy number alterations– Chromosome 5q.

The copy number profile of chromosome 5q for the un-irradiated MCF-10A **(a)**, 40 Gγ cumulative dose **(b)**, 55 Gγ cumulative dose **(c)** and 80 Gγ cumulative dose **(d)** populations of the First 5 Gγ series. The copy number of each region of chromosome 5q is shown above each log2 ratio map. Black arrows indicate a region which has not changed from the un-irradiated MCF-10A population. Red arrows indicate copy number alterations that were first identified 40 Gγ population. The green arrows indicate copy number alterations that were first identified in the 55 Gγ population. . The blue "*" above the log2 ratio map for the 80 Gγ population **(d)** represents a small gain to a copy number state of 4. Above the copy number states is an arrow indicating the copy number change event identified in each population (Del = Deletion). A representation of Chromosome 5q, including base positions, is below the log2 ratio maps.

Figure 4.7 shows the progression of the complex copy number alteration on chromosome 11. A mono-allelic deletion between positions 103769002:116689124 was observed in the 40 Gγ cumulative dose population which reduced the copy number state of this region to 1 (Fig. 4.7b). A larger mono-allelic gain between positions 62318238-qter which spanned the mono-allelic deletion observed in the 40 Gγ population was then detected in the 55 Gγ population (Fig. 4.7c). The copy number state of the 40 Gγ mono-allelic deleted region was unaffected by this gain, while the rest of the region increased to a copy number state of 3, indicating that the copy number gain must have occurred on the same allele as the 40 Gγ deletion.

Loss of heterozygosity in this area of chromosome 11 is common in a number of cancers, including 40% of primary breast cancers (Carter *et al.*, 1994; Lee *et al.*, 2000; Nagahata *et al.*, 2002; Zhang *et al.*, 2005b). It has also been shown that ionising radiation can induce LOH in this region of chromosome 11 (Roy *et al.*, 2006; Du *et al.*, 2010a). Candidate tumour suppressor genes or loci with a putative role in carcinogenesis located in this region include *CADM1* and *CUL5* (Fay *et al.*, 2003; Murakami, 2005). DNA damage signal and repair genes on chromosome 11, such as *ATM, MRE11A* and *H2AFX*, have also been linked with transformation (Shiloh, 2003). *ATM, CADM1* and *CUL5* are found in the region of deletion identified in the present study. The relevance and potential consequences of deletion of these genes, and deletions of genes in other copy number affected regions, will be discussed in section 4.5.

There was also evidence of shortened telomeres in the First 5 Gγ series indicated by mono-allelic loss of telomeric regions on chromosomes 4p, 16p, 19p and 20p (Table 4.2, highlighted in green). Shortened telomeres can cause chromosomal instability, or in itself be an indication of chromosomal instability (Gollin, 2005; Sabatier *et al.*, 2005; Jefford and Irminger-Finger, 2006). Again, the relevance of these alterations will be discussed in section 4.5.

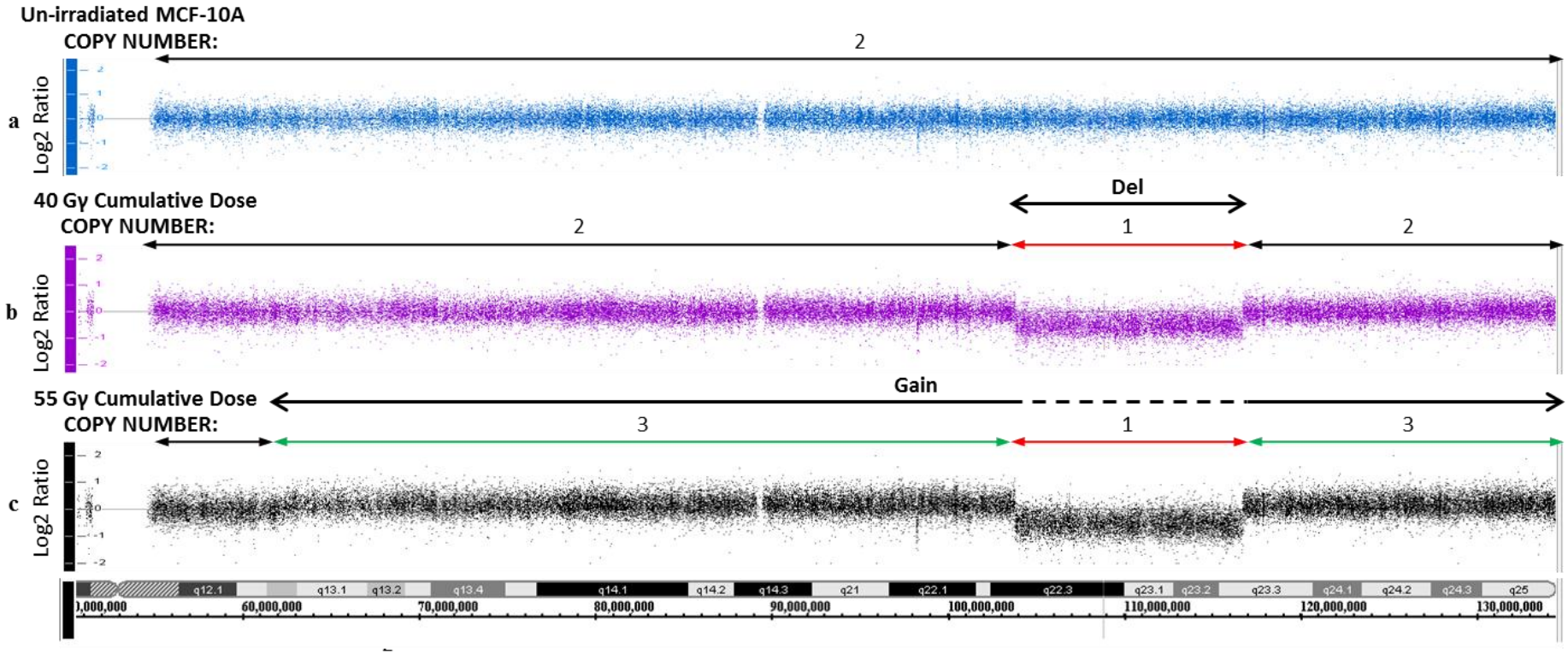

Figure 4.7 Complex copy number alterations– Chromosome 11q.

The copy number profile of chromosome 11q for the un-irradiated MCF-10A (a), 40 Gγ cumulative dose (b) and 55 Gγ cumulative dose (c) populations of the First 5 Gγ series. The copy number of each region of chromosome 11q is shown above each log2 ratio map. Black arrows indicate a region which has not changed from the un-irradiated MCF-10A population. Red arrows indicate copy number alterations that were first identified the 40 Gγ population. The green arrows indicate copy number alterations that were first identified in the 55 Gγ population. Above the copy number states is an arrow indicating the copy number change event identified in each population (Del = deletion). The hashed part of the arrow above the log2 ratio map of the 55 Gγ population indicates a region of the chromosome not affected by the copy number change event, in this case because the deleted region is on a different allele. A representation of Chromosome 11q, including base positions, is below the log2 ratio maps.

4.3.3 Identification of genes in focal regions for further investigation

In order to prioritize candidate genes for further investigation only loci in relatively focal regions of copy number change (<10 affected genes) were considered. Following a literature review of genes within these regions (as described in section 2.5.3) *POU2F1* was chosen for further investigation. *POU2F1* (*OCT-1*) is located within the mono-allelic 602Kb deletion on Chromosome 1q (Section 4.3.2). This 602Kb region contains 6 loci in total: *C1orf32*, *MAEL*, *GPA33*, *DUSP27*, *POU2F1* and *CD247* (Fig. 4.8). As described in section 4.3.2, a mono-allelic deletion of this region was first identified in the 40 Gγ cumulative dose population (Fig. 4.9b). The region is located within a constitutional trisomic region of chromosome 1q in MCF-10A and successive deletion events reduced the copy number state of *POU2F1* from 3 to 1 (Fig. 4.9c). An overview of the copy number alterations on chromosome 1q can be seen in figure 29.

Briefly, POU2F1 is a transcription factor which has a role as a stress sensor and transcriptional regulator of stress response genes (Tantin *et al.*, 2005). POU2F1 also has specific roles in BRCA1 mediated transcriptional regulation of DNA repair genes and genes involved in DNA damage response (Jin *et al.*, 2001; Fan *et al.*, 2002; Maekawa *et al.*, 2008; Saha *et al.*, 2010). The fact that POU2F1 is involved in these processes and was focally deleted in the First 5 Gγ series makes it an interesting gene to investigate further. Further investigation of POU2F1 will be discussed in chapter 6.

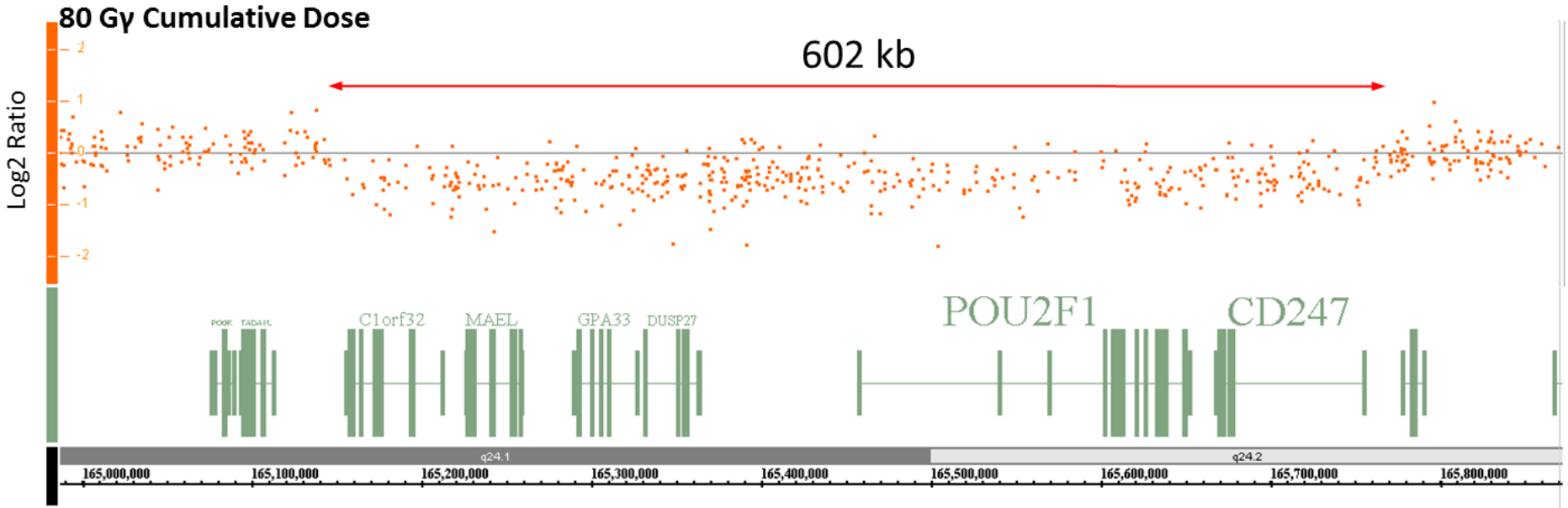

Figure 4.8 602Kb mono-allelic deletion of Chromosome 1q.

The log2 ratio map of a region on Chromosome 1q in the 80 Gγ cumulative dose population genome which contains a 602Kb deletion. The red arrow above the log2 ratio map indicates the position of the 602Kb deletion. The deleted region contains the loci for *POU2F1*, *C1orf32*, *MAEL*, *GPA33*, *DUSP27* and *CD247*. Underneath the log2 ratio map is a representation of the genes within the region. Green boxes represent the exons and green lines represent the introns of the genes. Underneath the genes is a representation of the chromosome arm and base positions of the region.

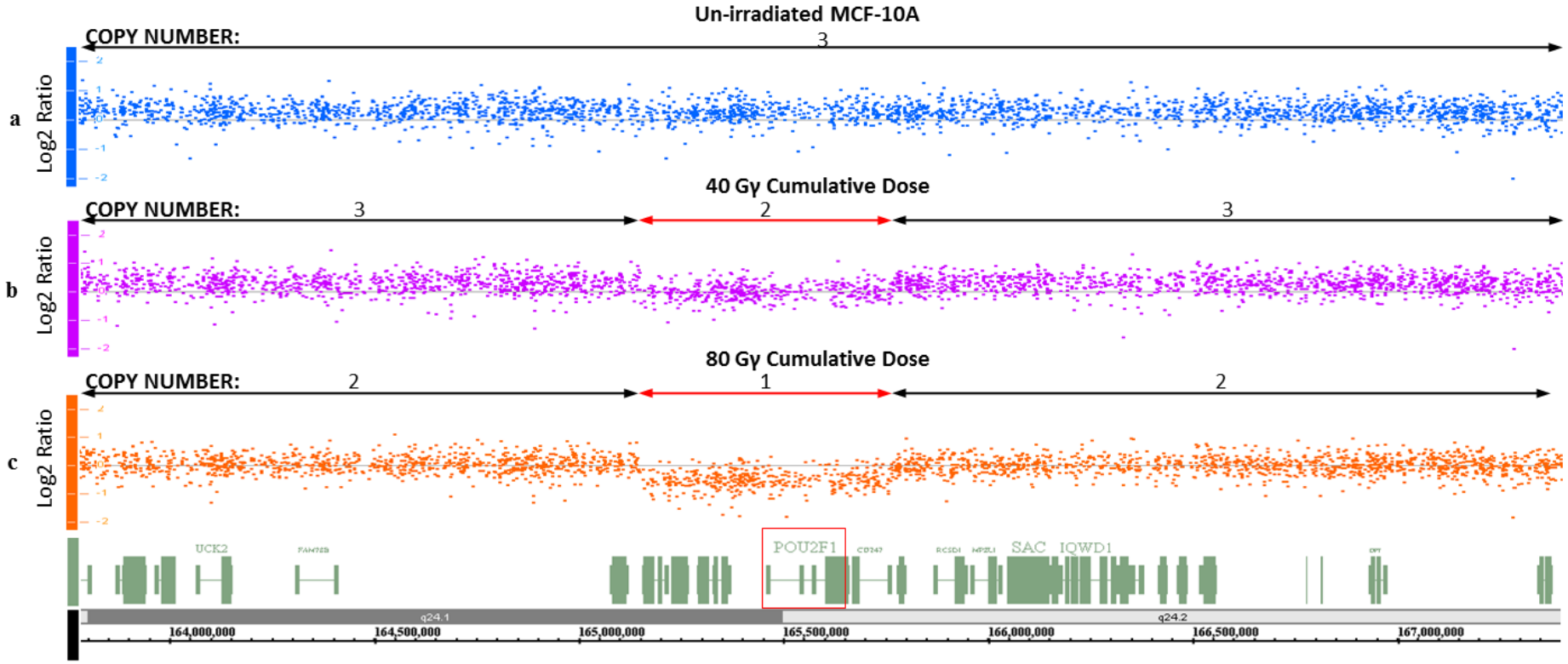

Figure 4.9 Progression of the *POU2F1* copy number alteration in the First 5Gγ Series.

The copy number profile of the region of chromosome 1q containing *POU2F1* for the un-irradiated MCF-10A (**a**), 40 cumulative dose (**b**) and 80 Gγ cumulative dose (**c**) populations of the First 5 Gγ series. The copy number of each region is shown above each log2 ratio map. The red arrow indicates a 602Kb mono-allelic deletion containing *POU2F1* identified in the 40 Gγ population. A larger mono-allelic deletion spanning the 602Kb deletion is then identified in the 80 Gγ cumulative dose population which reduces the copy number state of the 602Kb deletion to 1 and flanking regions to 2. Underneath the log2 ratio maps is a representation of the genes within the region. *POU2F1* is highlighted by the red box. A representation of the chromosome arm, including base positions, is below the gene representations.

4.4 Copy number analysis of the Second 5 Gγ Series (Oestrogen)

Cells from the Second Irradiation series (section 3.5) were also analysed using the Affymetrix SNP 6.0 Array. Cells which had received a cumulative dose of 10, 20, 40, 60 and 80 Gγ of ionising radiation in the presence of exogenous oestrogen were analysed for both the 5 Gγ and 10 Gγ fractionated dosing regimens. Copy number state in these cell populations was compared to un-irradiated MCF-10A cells and an 17β-oestrodiol treated passage control population, to identify copy number alterations caused by ionising radiation.

There were considerably fewer copy number alterations in the Second Irradiation series compared to the First Irradiation series. There were no observed copy number alterations in the Second 10 Gγ series and only 5 copy number alterations in the Second 5 Gγ series. The passage control population on the other hand had 6 copy number alterations. All of the alterations in the passage control population were whole chromosome copy number gains of one extra copy, involving chromosomes 7, 8, 11, 13, 19 and 20. As in the First Irradiation series there were no areas of copy neutral LOH detected in the Second Irradiation series or passage control population which were not constitutional to the un-irradiated MCF-10A genome.

Two of the alterations acquired in the Second 5 Gγ series were trisomy of chromosome 20 and mono-allelic deletion of *EP300*, which were also identified in the First 5 Gγ series. Furthermore, both of these alterations were identified in the passage control population of the First Irradiation series. As such, evidence suggests that these alterations were selected for during passage of the cells and were not in fact caused by ionising radiation.

4.4.1 Novel copy number alterations of the Second 5 Gγ series

Three novel copy number alterations were identified in the Second 5 Gγ series. Two were focal alterations that each affected only one gene. Specifically, these were a mono-allelic deletion of *BMPR1A* and a copy number gain of *c-MYC*. A large copy number gain on chromosome 8q which affected the *c-MYC* locus was also identified.

BMPR1A is located on Chromosome 10 and the mono-allelic deletion occurs between positions 88501217:88649027. Mono-allelic deletion of *BMPR1A* is first identified in the 40 Gγ cumulative dose population. The deletion reduces the copy number state from 2 to 1 (Fig. 4.10). The function of *BMPR1A* and its potential role in cancer will be briefly discussed in section 4.5.

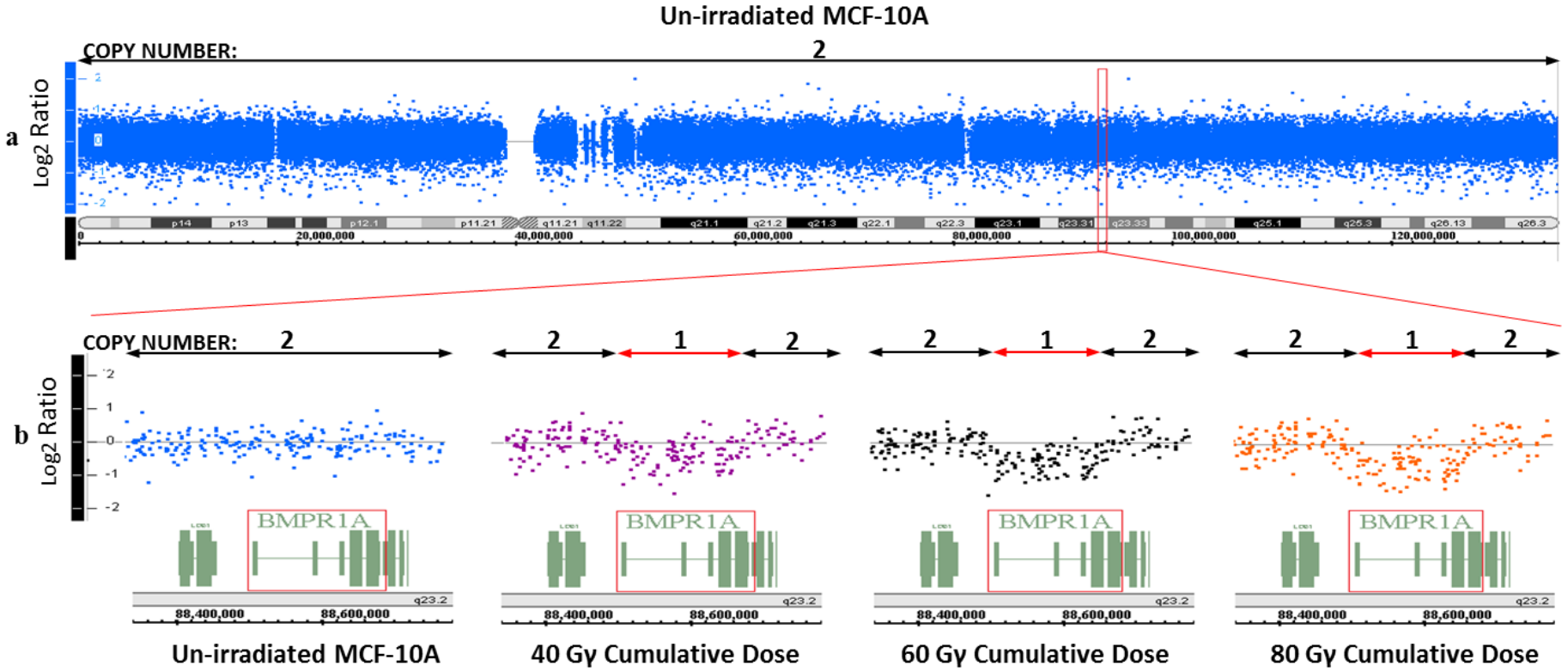

Figure 4.10 Progression of the *BMPR1A* copy number alteration in the Second 5Gγ Series.

The copy number profile of chromosome 10 for the un-irradiated MCF-10A cell population **(a)**. The region containing *BMPR1A* is highlighted by a red box and magnified underneath for the un-irradiated MCF-10A, 40 Gγ cumulative dose, 60 Gγ cumulative dose and 80 Gγ cumulative dose populations **(b)**. The copy number state of each region is shown above each log2 ratio map. Red arrows indicate the area of mono-allelic deletion containing *BMPR1A*. Underneath the magnified log2 ratio maps is a representation of the genes within the region. *BMPR1A is* highlighted by a red box. A representation of the chromosome arm, including base positions, is below each log2 ratio map.

The copy number gain of *c-MYC* occurred within a constitutionally trisomic region of Chromosome 8q (described in section 4.2.1) between positions 127621008:130125337 and was first identified in the 40 Gγ cumulative dose population (Fig. 4.11b). The copy number state of *c-MYC* increased from 3 to 4.

A large region of copy number gain was identified on 8q in the 60 Gγ population between positions 71160976:130125337 which increased the constitutionally diploid and triploid regions to a copy number state of 3 and 4 respectively (Fig 4.11c). The large region of copy number gain ended at the telomeric position of the *c-MYC* copy number gain which therefore increased the copy number state of *c-MYC* above 4. Both copy number alterations on chromosome 8q appeared to share a breakpoint which implied that this point was fragile to double strand breaks in the Second 5 Gγ series. It also appeared that both alterations become more prominent as cumulative dose increased, which indicated that the proportion of cells the alterations were present in increased with cumulative dose (Fig. 4.11). It is impossible to discern from the polymorphism array whether both alterations occurred on the same chromosome and therefore the mechanisms which led to the alterations are unclear. Other techniques will be utilised to investigate the cytogenetic nature of the alterations and their relative abundance in the different irradiated cell populations (described in Chapter 7). The passage control population also had a single copy number increase of *c-MYC* but this was via a whole chromosome copy number gain.

c-MYC is an established proto-oncogene which plays a role in a number of different cellular processes including cell proliferation and apoptosis (Xu *et al.*, 2010). Copy number increase of *c-MYC*, converting it to an oncogene, is an established event in cell transformation and amplification has been reported in 15% of putative sporadic breast cancers (Deming *et al.*, 2000). Furthermore, *c-MYC* amplification was reported in breast cancers that developed in radiation-exposed survivors of the Hiroshima and Nagasaki atomic bombs (Miura *et al.*, 2008). The fact that *c-MYC* is focally altered in the present study and has previously been linked with radiation induced breast cancer makes it an interesting gene for further investigation (Chapter 7).

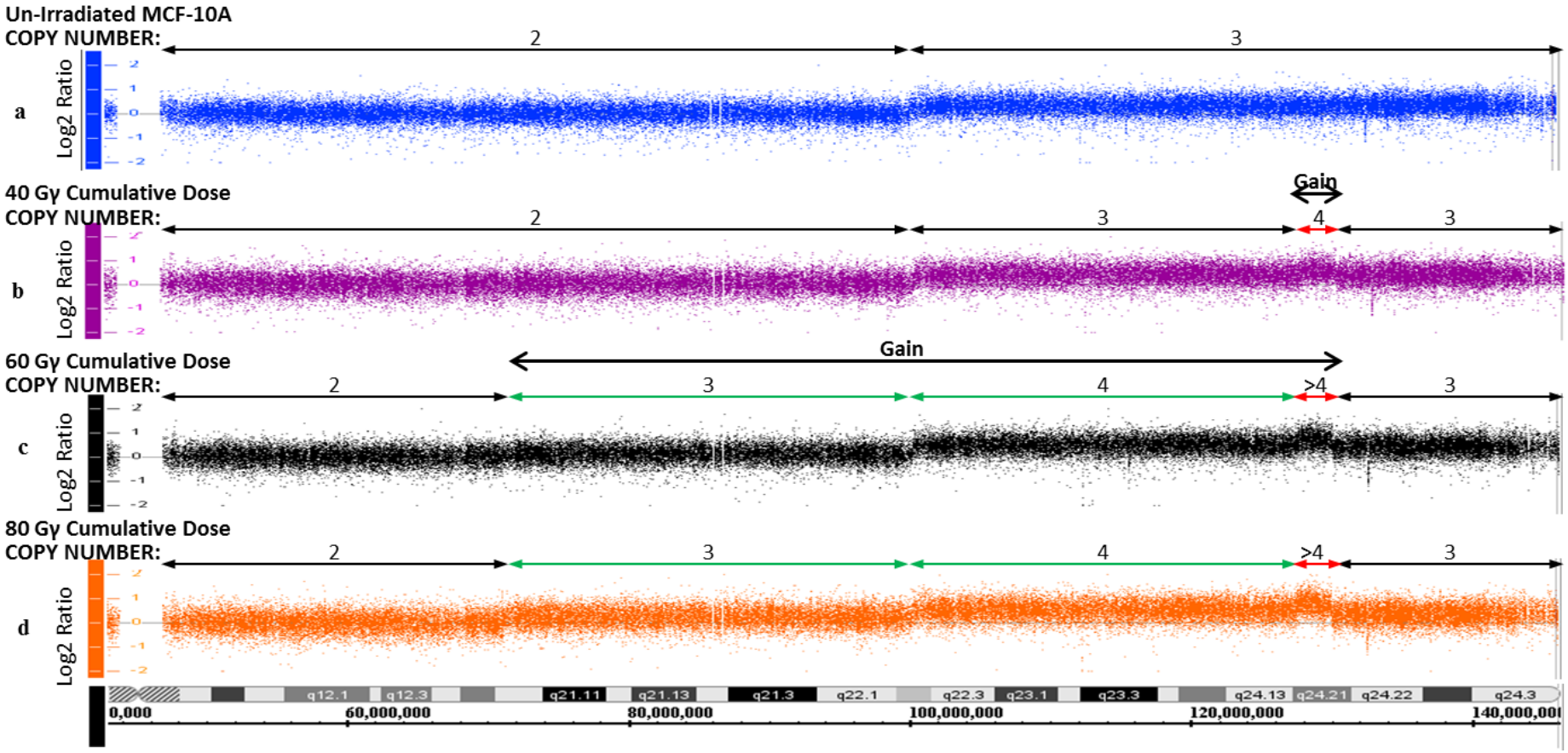

Figure 4.11 Copy number alterations – Chromosome 8q

Copy number profile of chromosome 8q for the un-irradiated MCF-10A (**a**), 40 Gγ cumulative dose (**b**) 60 Gγ cumulative dose (**c**) and 80 Gγ cumulative dose (**d**) populations of the Second 5 Gγ series. The copy number of each region of chromosome 8q is above each log2 ratio map. Black arrows indicate a region which has not changed from the un-irradiated MCF-10A population. Red arrows indicate copy number alterations that were first identified in the 40 Gγ population. The green arrows indicate copy number alterations that were first identified in the 60 Gγ population. Above the copy number states is an arrow indicating the copy number change event(s) identified in each population. A representation of the q arm of Chromosome 8, including base positions, is at the bottom of the log2 ratio maps.

4.5 Discussion

The genetic alterations that contribute to breast cancer development following radiation exposure have yet to be identified. In the present study we have used the breast epithelial cell line MCF-10A to develop two *in vitro* models of radiation-induced breast epithelial cell transformation. The "First" model exposed MCF-10A cells to fractionated doses of 5 Gγ and 10 Gγ of ionising radiation up to a cumulative dose of 80 Gγ allowing for cell recovery between fractionated doses. The 5 Gγ fractionated dose series displayed evidence of phenotypic changes including: changes to cell morphology, reduction of growth rate, loss of contact inhibition and increased sensitivity to ionising radiation. The "Second" model exposed MCF-10A cells to the same radiation dosing regimen but in the presence of exogenous 17-β oestrodiol (10^{-8} M). The 5 Gγ fractionated dose series only displayed changes in cell morphology, with the development of an epithelial to mesenchymal transition (EMT) morphological phenotype.

4.5.1 First irradiation Series

The 5 Gγ fractionated dose series had more than twice the number of copy number alteration events compared to the 10 Gγ fractionated dose series. The amount of DNA damage caused by ionising radiation in a cell is proportional to the dose of radiation received (Chadwick and Leenhouts, 2011). A high dose of ionising radiation causes more genetic damage and is therefore more likely to be lethal to the cell. Lower doses of radiation can cause sub-lethal DNA damage which allows recovery and repopulation of cells which may then fix DNA damage as genetic mutations (Boice *et al.*, 1987; Allan and Travis, 2005; Chadwick and Leenhouts, 2011). The higher cytotoxicity of the 10 Gγ fractionated dose regimen may therefore have not allowed cells to accumulate sub-lethal DNA damage, resulting in fewer overall copy number alteration events in the irradiated populations. The 5 Gγ series had been phenotypically characterised in the previous chapter therefore only alterations in the 5 Gγ series were analysed further.

The First 5 Gγ series had radiation-induced copy number alterations on chromosome 1p, 1q, 2p, 2q, 4p, 5q, 7q, 10p, 11q, 12q, 14q, 15q, 16p, 18q, 19p, 20p and chromosome X (Table 4.2, section 4.3). High density polymorphism array analysis allows the whole genome to be interrogated for copy number alterations. Previous studies have analysed specific chromosome regions and have identified LOH and microsatellite instability (MSI) on chromosomes 6q, 11q and 17p in a radiation-induced *in vitro* breast

transformation model (Roy *et al.*, 2001a; Roy *et al.*, 2006), and on chromosomes 6q, 9p and 17p in breast and lung cancer tissue samples from Hodgkin lymphoma patients (Behrens *et al.*, 2000). Interestingly no copy number alterations or areas of copy neutral LOH were identified on chromosome 6q or 17p in the present study. These regions are known to contain important tumour suppressor genes such as *IGF2R, BRCA1* and *P53* which are commonly affected in breast cancer (Niederacher *et al.*, 1997; Rodriguez *et al.*, 2000).

All of the radiation-induced copy number alterations in the First 5 Gγ series were identified after a cumulative dose of 40 Gγ, and these were generally large regions of deletion or copy number gain, which is a hallmark of chromosomal instability (Jefford and Irminger-Finger, 2006). Two models could explain the apparent lack of copy number alterations between 0 and 25 Gγ of irradiation:

i) Copy number alterations had occurred before 25 Gγ of irradiation but were not in a large enough population of cells to be identified by the SNP array software. SNP analysis of heterogeneous cell populations only identifies copy number alterations which are present in the majority of cells. Therefore a sub-population which accumulated copy number alterations and was gradually clonally selected for would not be detected until later in the irradiation series (Fig. 4.12a)

ii) Between 0 and 25 Gγ of irradiation the DNA damage repair mechanisms were successful in repairing or killing cells with DNA damage. A mutation may have occurred between the 25 Gγ and 40 Gγ populations which led to an increase in chromosomal instability and/or dysregulation of DNA damage response. This led to a rapid clonal selection of a cell population with numerous chromosomal alterations (Fig. 4.12b).

A combination of the two models is also possible.

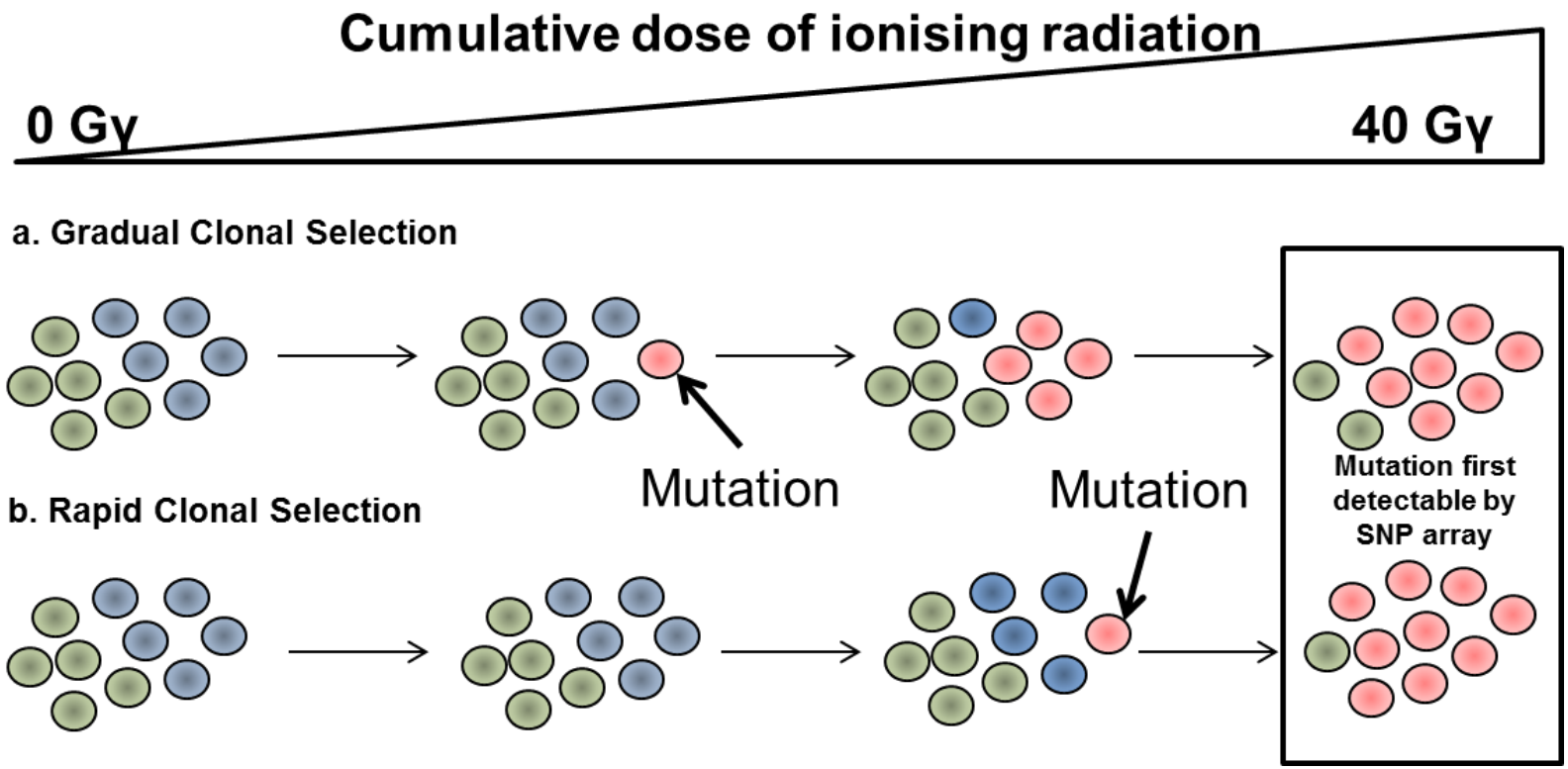

Figure 4.12 Model of copy number accumulation in irradiated MCF-10A cells.
Two models to explain the apparent rapid accumulation of copy number alterations identified between the 25 Gγ and 40 Gγ populations. The figure shows a representation of the genetically heterogeneous MCF-10A cell population with green and blue sub-populations. In the gradual clonal selection model (**a**), mutation or mutations occur relatively early in the irradiation series (red cell). The mutations confer a modest but discernible growth advantage and the sub-population(s) grows as cumulative dose increases until it is of sufficiently high proportion for acquired copy number alterations to be detected by the SNP 6.0 array. In the rapid clonal selection model (**b**), mutations are not fixed in the cell population until temporally later during the irradiation series (red cell) and the acquired mutation(s) confer a strong selective growth advantage. The sub-population which acquired the mutations is therefore rapidly selected for and comprises a sufficiently high population for acquired copy number alterations to be detected by the SNP 6.0 array. A combination of these models may occur in which mutations are acquired early in the irradiation series, but are not detected, followed by a mutation which causes rapid growth and accumulation of copy number alterations.

The mono-allelic loss of chromosome 11q22.3-23.3 identified in the 40 Gγ population contains the gene *ATM,* which encodes a protein kinase involved in DNA damage response and plays an important role in regulating chromosome stability (Shiloh, 2003; Gollin, 2005). The deletion of this region may therefore contribute to the accumulation of copy number alterations in the First 5 Gγ series. ATM was discovered by the identification of inactivating mutations in patients with the genetic disorder ataxia-telangiectasia (Savitsky *et al.*, 1995). Individuals that have the disorder display high levels of genomic instability and sensitivity to double strand break-inducing agents such as ionising radiation (Crawford, 1998; Shiloh, 2003). Briefly, ATM protein kinase rapidly initiates cell-cycle arrest and activation of cell-cycle checkpoints in G1, S and G2 phase of the cell cycle in response to double strand breaks. ATM mediates this activation by phosphorylation of a number of substrates, the full extent of which has not yet been determined. Phosphorylation can directly stimulate or inhibit the action of these proteins, which function as mediators of cell cycle checkpoint activation (Shiloh, 2003). (Fig. 4.13).

ATM has also been implicated as a direct activator of DNA repair. Loss of ATM causes sub-optimal assembly of protein complexes involved in homologous recombination and ATM has been shown to directly bind to sites of double strand breaks (Andegeko *et al.*, 2001; Shiloh, 2003; Shiloh, 2006). ATM is also functionally linked to the maintenance of telomere length and integrity and is involved in the apoptotic response to shortened telomeres (Pandita, 2001; Pandita, 2002; Shiloh, 2003; Silva *et al.*, 2004). The First 5 Gγ series had areas of mono-allelic loss at the telomeres of chromosomes 4p, 16p, 19p and 20p. Shortened telomeres can cause end-to-end fusions which can initiate chromosome breakage and increase chromosome instability, giving rise to gene deletion and amplification (Jefford and Irminger-Finger, 2006). Three of the four chromosomes affected by telomere shortening were not identified until the 80 Gγ cumulative dose population, therefore earlier acquired genetic events, such as ATM loss, may promote the survival of cells with shortened telomeres.

The loss of one copy of *ATM* does not significantly increase the risk of cancer if a functioning allele remains (Gatti *et al.*, 1999). However, under conditions of repeated exposure to ionising radiation and the resultant DNA strand breaks, reduced expression of *ATM* through haploinsufficiency may attenuate repair function and predispose cells to chromosomal damage. A reduced capacity to effectively deal with elevated levels of double strand breaks via ATM haploinsufficiency may explain the increased sensitivity

to ionising radiation shown by the First 5 Gγ series (section 3.3.4). It remains to be determined whether the remaining copy of *ATM* produces functioning protein.

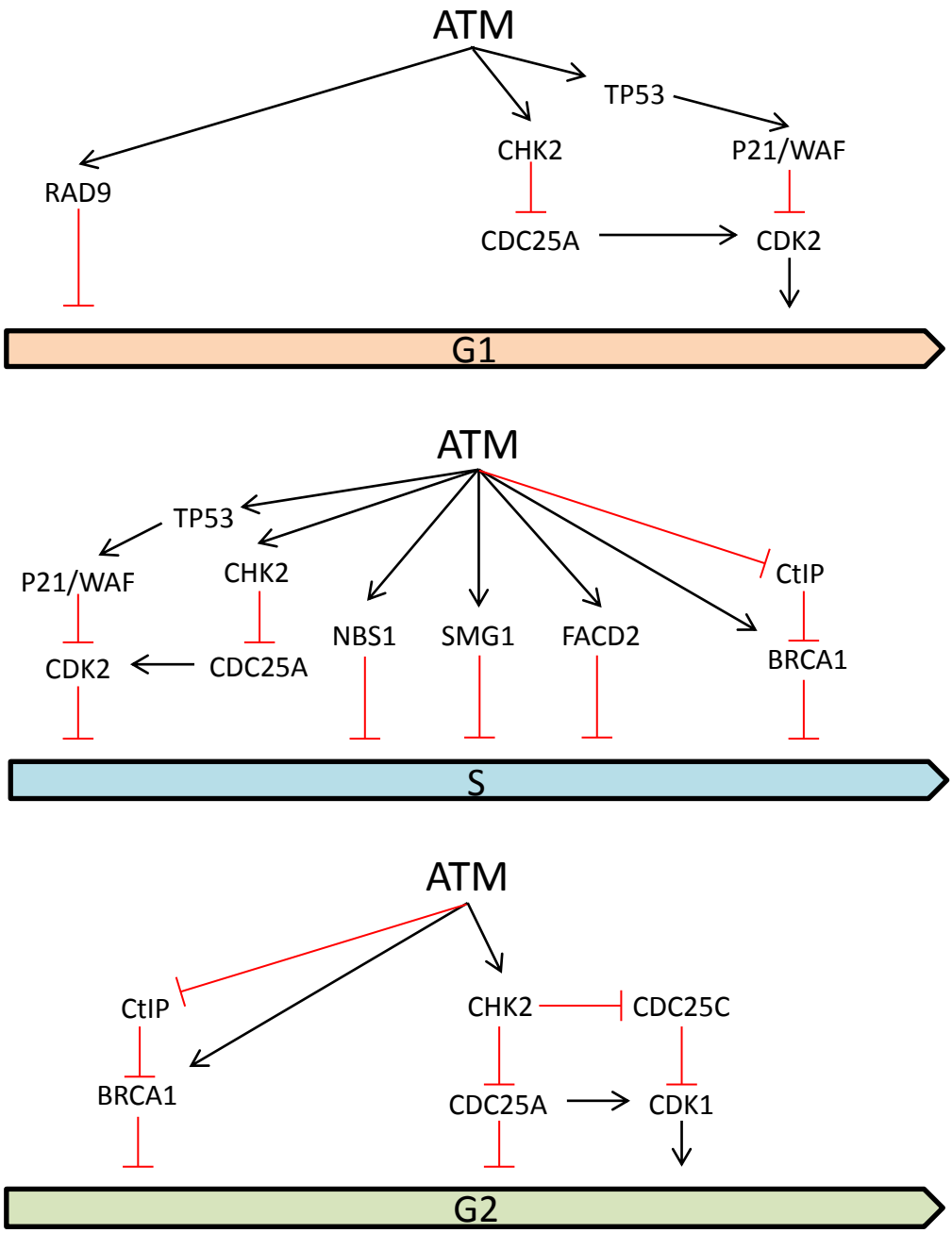

Figure 4.13 ATM mediated activation of cell cycle checkpoints following DNA damage
ATM mediates the activation of G1, S and G2 cell cycle checkpointing in reaction to double strand breaks. The figure above shows each of these phases of the cell cycle. An approximation of at which point in each phase of the cell cycle the checkpoints are activated in is shown. The temporal direction of each phase of the cell cycle is from left to right. ATM mediates checkpointing via phosphorylation of a number of target proteins which can either activate (black arrows) or inhibit (red T shapes) the action of that protein. The activating or inhibitory affect of these target proteins on other proteins in the checkpoint pathway is also shown. The figure is adapted from Shiloh (2003).

ATM is not the only interesting gene in the region of chromosome 11 affected by mono-allelic deletion. The putative tumour suppressor genes *CUL5* and *CADM1* were also affected in the present study. Expression of *CUL*5 was shown to be approximately 2.2 times lower in primary breast cancer cases compared to matched normal tissue, indicating it as a potential tumour suppressor (Fay *et al.*, 2003). The tumour suppressor role of this protein has so far not been fully determined but over-expression of the gene has been shown to inhibit cell proliferation in several cell lines (Lewis *et al.*, 2011).

CADM1 has both extra-cellular and cytoplasmic binding domains. The protein plays an important role in cell-cell adhesion via its extra-cellular domain (Masuda *et al.*, 2002; Liang *et al.*, 2011). Reduction in cell-cell adhesion in cancer can lead to cell invasion and metastasis, and loss of CADM1 promotes transformation to an invasive phenotype (Goto *et al.*, 2005; Murakami, 2005; Liang *et al.*, 2011). Cells in the First 5 Gγ series display reduced contact inhibition which may be due to reduced cell-cell adhesion mediated by loss of *CADM1*. A direct link between contact inhibition specifically and CADM1 has not been reported but loss of CADM1 abrogates recruitment of E-cadherin to cell-cell attached sites and E-cadherin cell-cell contact is an important mediator of contact inhibition (Kim *et al.*, 2009a; Sakurai-Yageta *et al.*, 2009).

CADM1 has also been shown to act as a tumour suppressor via its cytoplasmic binding domain. CADM1 modulates cell cycle progression (Sussan *et al.*, 2005), inhibits tumour growth by inducing cell cycle arrest (Lung *et al.*, 2006), induces apoptosis after re-expression in *CADM1*$^{-/-}$ cells (Mao *et al.*, 2004), and is also involved in modulating immunological surveillance (Murakami, 2005; Liang *et al.*, 2011). Reduced expression of *CADM1* has been reported in a wide variety of cancers including non-small cell lung cancer, breast cancer, nasoasophageal, esophageal, gastric, prostate, pancreatic, colorectal and cervical cancer (Liang *et al.*, 2011). CADM1 protein expression is also inversely proportional to the stage of many of these cancers (Uchino *et al.*, 2003). Loss or reduced expression of CADM1 via promoter silencing due to hyper-methylation can occur in many cancer cases but not all. For example, 70% of primary breast cancers in the study by Takahashi *et al.* (2011) had low *CADM1* expression but only 46% of cancers displayed promoter methylation. Therefore, copy number loss of *CADM1* may represent an alternative and important mechanism by which CADM1 expression is lost in some cancers. It is also possible that LOH and methylation of the promoter of *CADM1* co-operate to reduce *CADM1* expression.

Loss of heterozygosity at the deleted region of chromosome 11 has been reported in a number of malignancies, including breast cancer (40% of cases), colorectal cancer, head and neck squamous cell carcincoma and cervical cancer (Carter *et al.*, 1994; Lee *et al.*, 2000; Nagahata *et al.*, 2002; Zhang *et al.*, 2005b; Parikh *et al.*, 2007). Loss of heterozygosity at this region, and reduced expression of tumour suppressor genes therein, may therefore be a key event in tumour development. Ionising radiation has also been shown to induce LOH in this region in *in vitro* studies (Roy *et al.*, 2006; Du *et al.*, 2010b). The region may therefore be vulnerable to copy number loss due to ionising radiation.

Other areas of large copy number alteration identified in the present study also contain genes which have been identified as potentially having a role in cancer. LOH on Chromosome 4p has been reported in a number of cancers (Polascik *et al.*, 1995; Shivapurkar *et al.*, 1999a; Shivapurkar *et al.*, 1999b; Zheng *et al.*, 2008). *SLIT2*, a putative tumour suppressor gene on chromosome 4p and is silenced or has reduced expression in a number of cancers, including breast cancer (Dallol *et al.*, 2002; Kim *et al.*, 2011b). Ectopic expression of *SLIT2* inhibits tumour cell proliferation, suggesting that loss could promote tumour cell division (Kim *et al.*, 2008; Tseng *et al.*, 2010). *SLIT2* is located in the area of mono-allelic deletion identified in the present study (Table 4.2).

LOH on chromosome 18q has been heavily linked with colorectal cancer (Fearon *et al.*, 1990; De Angelis *et al.*, 1999; Migliore *et al.*, 2011). Chromosome 18q contains the putative tumour suppressor gene *DCC*, which is implicated in cell apoptosis and whose expression is lost in the majority of colorectal cancers (Fearon *et al.*, 1990; Mehlen and Fearon, 2004; Shin *et al.*, 2007; Castets *et al.*, 2011). *DCC* was affected in the region of mono-allelic deletion on 18q identified in the present study (Table 4.2).

Hundreds of genes were affected in the large chromosomal alterations observed in the First 5 Gγ series. Copy number alteration of a subset of these genes will have had an effect on cell transformation and the acquired phenotypic changes (driver mutations), while the effect of alteration on the majority of genes will have been neutral (carrier mutations). A few genes that have been affected by copy number alteration that may play a role in cell transformation have been discussed. To focus the direction of the study, only genes in focally affected regions were considered for further investigation.

Following a literature review of potential gene targets *POU2F1* was chosen for more detailed analysis.

4.5.2 POU2F1

POU2F1 is a member of the POU domain transcription factors. The protein binds to the octamer motif "5'ATGCAAAT3'" through the DNA binding POU domain (Herr *et al.*, 1988; Klemm *et al.*, 1994). The octamer motif is found in the promoters of a number of genes such as: *H2B* (Fletcher *et al.*, 1987), immunoglobulin genes expressed in B cells (Jenuwein and Grosschedl, 1991), *TIE2* (Fadel *et al.*, 1999), *GnRH* (Eraly *et al.*, 1998), the von Willebrand factor gene (Schwachtgen *et al.*, 1998) and the vascular cell adhesion molecule gene (Iademarco *et al.*, 1992). POU2F1 is involved in transcriptional regulation of these genes and either activates or represses gene expression depending on the gene.

Tantin *et al.* (2005) showed that expression of the housekeeping gene *H2B* was not altered in POU2F1 deficient fibroblasts, suggesting that POU2F1 was not essential for basal gene expression. *POU2F1* deficient fibroblasts did however respond abnormally to cellular and genotoxic stress. The cells were hypersensitive to ionising radiation, hydrogen peroxide and doxorubicin, had increased levels of reactive oxygen species, increased incidence of double strand breaks and displayed dysregulation of genes involved in oxidative and metabolic stress pathways Tantin *et al.* (2005), suggesting a role for POU2F1 as a stress sensor and modulator of stress related genes. Previous studies had indicated that DNA damaging exposures such as ionising radiation, ultra-violet (UV) radiation and methyl methanesulfonate induced increased POU2F1 protein levels (Meighan-Mantha 1999; Zhao 2000). DNA damage did not alter mRNA levels of POU2F1 and therefore the induction of POU2F1 was postulated to be mediated via post-translational modification. The promoter binding activity of POU2F1 was also enhanced after DNA damage (Zhao 2000).

Following induction of DNA double strand breaks POU2F1 can be post-translationally modified by DNA-PK (Schild-Poulter *et al.*, 2003; Schild-Poulter *et al.*, 2007). The DNA-PK complex is activated following strand breakage, and is composed of a KU70/80 heterodimer and catalytic subunit (DNA-PKcs) required for DNA repair by non-homologous end joining (Mahaney *et al.*, 2009). DNA-PK phosphorylates 13 serine and threonine residues on the NH_2 terminus of POU2F1 which stabilizes the protein to allow protein accumulation (Schild-Poulter *et al.*, 2007). Phosphorylated POU2F1 plays

a crucial role in p53 mediated transcriptional regulation of the cell cycle checkpoint gene *CDKN1A* following ionising radiation, and also functions to repress the function of *H2B* as a mediator of cell cycle arrest, allowing DNA repair to take place (Schild-Poulter *et al.*, 2003). POU2F1 expression is not up-regulated following ionising radiation in cells deficient for KU70/80 or DNA-PK indicating that phosphorylation by the DNA-PK complex is needed for POU2F1 to promote cell survival transcriptional modifications following double strand breaks (Schild-Poulter *et al.*, 2003). This interaction was also confirmed *in vivo* (Kang *et al.*, 2009). There is also evidence that POU2F1 might directly play a role in non-homologous end joining as it was observed that a POU2F1/KU complex can associate with DNA ends (Schild-Poulter *et al.*, 2001). DNA-PK is activated in response to double strand breaks but POU2F1 activity is also induced following other forms of DNA damage. Wang and Jin (2010) showed that the oxidising agent hydrogen peroxide caused an increase in levels of nuclear POU2F1 and stimulated the kinase activity of DNA-PK and JNK. As such, DNA-PK or JNK complexes may phosphorylate POU2F1 in response to genotoxic stress other than double strand breaks.

POU2F1 plays a major role in transcriptional regulation mediated by BRCA1. *BRCA1* is a tumour suppressor gene which is mutated in 40-50% of hereditary breast cancers (Miki *et al.*, 1994). BRCA1 has many functions such as a direct role in cell cycle regulation, apoptosis, DNA damage response and also functions as a transcriptional regulator of genes involved in these processes (Rosen *et al.*, 2006). POU2F1 has a crucial role in BRCA1-mediated regulation of *GADD45* following induction by DNA damaging agents (Jin *et al.*, 2001; Fan *et al.*, 2002; Maekawa *et al.*, 2008). GADD45 promotes genetic stability of cells following DNA damage and can be induced in a TP53 dependant and independent manor (Liebermann and Hoffman, 2008). POU2F1 along with NF-YA is required for TP53 independent induction of *GADD45* by BRCA1 following DNA damage. Depletion of BRCA1 or POU2F1, or disruption of POU2F1 binding sites abrogates *GADD45* induction (Jin *et al.*, 2001; Fan *et al.*, 2002).

POU2F1 was also shown to interact with BRCA1 to transcriptionally regulate genes in the base excision repair (BER) pathway (Saha *et al.*, 2010). Following oxidative DNA damage BRCA1 induced the expression of BER genes: *OGG1, NTHL1, APEX1* and *XRCC1*. Reduced expression of BRCA1 inhibited BER activity following oxidative damage. RNA interference of POU2F1 abrogated induction of OGG1, NTH1, APEX1 and XRCC1 by BRCA1, indicating the important role POU2F1 has in this process.

Impaired induction of BER following oxidative damage would result in impaired DNA repair and promote the acquisition of mutations. POU2F1 is also important in BRCA1 mediated induction of the spindle checkpoint gene *MAD2*, whose loss causes chromosomal abnormalities and genetic instability (Wang *et al.*, 2004a), and the transcription of ERα (Hosey *et al.*, 2007; Harte *et al.*, 2010).

Loss or reduced expression of POU2F1 may therefore have an effect on many cellular processes, but in particular on response to genotoxic stress. Dysregulation of stress response could result in genetic instability and incorrect repair of DNA damage which could result in oncogenic mutations. The fact that POU2F1 is involved in these processes and was focally deleted in the First 5 Gγ series makes it an interesting gene to investigate further (Chapter 6 and Chapter 8).

4.5.3 Second irradiation series

The Second irradiation series had comparatively fewer copy number alterations than the First irradiation series after both the 5 Gγ and 10 Gγ fractionated dose regimens, which correlates with fewer phenotypic changes observed in the Second 5 Gγ series compared to the First 5 Gγ series (Chapter 3). Whole chromosome copy number increases were identified for 6 chromosomes in the oestrogen exposed passage control population, however only 3 copy number alterations were identified for the irradiated populations. Fewer chromosomal alterations imply that concomitant 17β-oestrodiol and ionising radiation exposure had a protective effect against DNA damage that could initiate copy number alterations. This however contradicts *in vitro*, *in vivo* and epidemiological evidence which suggests that exposure to increased levels of both ionising radiation and oestrogen is more genotoxic than either on their own (reviewed in Chapter 1).

It remains possible that mutations in genes which promote chromosome instability had not occurred in the Second irradiation series and therefore few chromosomal alterations were generated in these cell populations. However, considering the genotoxicity of both ionising radiation and oestrogen exposure this seems unlikely. It is also possible that mutations early on in the irradiation series may have conferred a resistance to DNA damage; for example up-regulation of DNA repair genes or genes which remove ROS. Ultimately however, it is unknown why the Second 5 Gγ series had relatively few copy number alterations.

Radiation/oestrodiol-induced copy number alterations identified in the Second 5 Gγ series were restricted to a mono-allelic deletion of *BMPR1A* on chromosome 10q, a copy number increase of *c-MYC* on chromosome 8q and copy number gain of a large region of chromosome 8q. Both focal alterations were identified in the 40 Gγ cumulative dose population and the large alteration was identified in the 60 Gγ cumulative dose population. The focal *c-MYC* copy number gain and large region of copy number gain on chromosome 8q appeared to share a breakpoint position. Cytogenetic study of these alterations and the relevance of a common breakpoint will be discussed in Chapter 7.

Bone morphogenic protein receptor type 1 (A) (BMPR1A) is a membrane bound receptor which heterodimerizes with type 2 BMPR's on binding with bone morphogenic proteins (BMP's). Ligand bound BMPR1A phosphorylates downstream molecules SMAD1, 5 and 8 which in turn bind to SMAD4 promoting interaction with transcription factors to regulate expression of downstream target genes. BMP signalling plays a role in a number of functions such as bone and cartilage formation and neural crest development (Chen *et al.*, 2004).

Dysregulated BMP signalling has been implicated in promotion of a number of cancers, such as breast cancer, colon cancer and B-cell chronic lymphocytic leukaemia (Helms *et al.*, 2005; Katsuno *et al.*, 2008; Dzietczenia *et al.*, 2010; Slattery *et al.*, 2012), although there is evidence that BMPs can also function as tumour suppressors in other tissues (Edson *et al.*, 2010; Shirai *et al.*, 2011). Mutations in *BMPR1A* have been implicated in colon cancer and juvenile polyposis (Nieminen *et al.*, 2011; Dahdaleh *et al.*, 2012). The molecular mechanisms of BMP signalling are complex and its role in malignant transformation remains to be fully elucidated.

4.5.4 c-MYC

c-MYC is a well-established proto-oncogene which is amplified or over-expressed in a number of cancers, including, but not exclusively: Burkitt's lymphoma, Non-Burkitt's lymphoma, breast cancer, prostate cancer, gastrointestinal cancer, melanoma and small cell lung cancer (Nesbit *et al.*, 1999). c-MYC is a transcription factor which regulates up to 15% of all human genes (Dang *et al.*, 2006). c-MYC has a helix-loop-helix leucine zipper domain at the C-terminal region and binds to form a heterodimer with the protein MAX. This heterodimer binds specifically to E-box elements with the consensus sequence 'CACGTG' to positively or negatively regulate target gene expression

(Blackwood and Eisenman, 1991). Transcriptional activation involves the recruitment of co-activators to the E-box elements, however the mechanism of transcriptional repression is not well understood (Adhikary and Eilers, 2005).

c-MYC is involved in regulating many different cell processes (Dang *et al.*, 2006). Over-expression of c-MYC can lead to deregulation of these processes and to cell transformation and cancer. Over-expression of c-MYC results in increased proliferation by inhibiting cell cycle checkpoint genes and CDK inhibitors, such as GADD45 and $p21^{Cip1}$ and activating cyclins D/D2/E1,A2, CDK4, CDC25A, E2F1 and E2F2, which induces G1 to S phase transition (Obaya *et al.*, 1999; Meyer and Penn, 2008; Xu *et al.*, 2010). c-MYC overexpression has also been reported to block cell differentiation (Wu *et al.*, 2003; Meyer and Penn, 2008), lead to cell immortalization by activation of telomerase reverse transcriptase (TERT) (Wu *et al.*, 1999), promote angiogenesis by regulation of vascular endothelial growth factor VEGF expression (Baudino *et al.*, 2002), and induce apoptosis in the absence of survival factors by activation of p53 apoptotic pathways (Evan *et al.*, 1992; Zindy *et al.*, 1998). Overcoming the apoptotic effects of c-MYC is an essential step in c-MYC induced cell transformation (Xu *et al.*, 2010).

c-MYC overexpression has also been implicated in increasing genetic instability *in vitro* by the induction of ROS and DNA strand breaks (Vafa *et al.*, 2002; Prochownik and Li, 2007). Increased *c-MYC* copy number does not appear to have increased genetic instability in the present study but this characteristic may be relevant for radiogenic breast cancer development.

Over-expression of c-MYC has been associated with increased *c-MYC* copy number (Chrzan *et al.*, 2001a; Blancato *et al.*, 2004), however overexpression can also occur in breast cancers without a *c-MYC* copy number increase, suggesting other mechanisms responsible for c-MYC overexpression (Chrzan *et al.*, 2001a). TGF-β represses transcription of *c-MYC* via a SMAD3, SMAD4, E2F4, E2F5, DP-1 and p107 protein complex at the gene promoter (Frederick *et al.*, 2004). The RAS/RAF/MAPK pathway antagonises TGF-β repression, stabilises the c-MYC protein and represses c-MYC degradation by inhibition of GSK-3β (Sears *et al.*, 1999; Adhikary and Eilers, 2005; Sekimoto *et al.*, 2007). Increased activity by the RAS/RAF/MAPK pathway can therefore increase c-MYC protein levels.

c-MYC is also a downstream target of both the WNT/β-CATENIN signalling and NOTCH signalling pathways, activation of which results in increased *c-MYC* expression (Xu *et al.*, 2010). The relationship between WNT/β-CATENIN signalling and cancer has been investigated and established in colorectal cancer and increased β-CATENIN expression has been observed in breast carcinomas with a poor prognosis (He *et al.*, 1998; Khramtsov *et al.*, 2010; Lopez-Knowles *et al.*, 2010). c-MYC also works in a positive feedback loop with the WNT/β-CATENIN signalling pathway as c-MYC suppresses the WNT inhibitors DKK1 and SFRP1 (Cowling and Cole, 2007; Cowling *et al.*, 2007). The association between the NOTCH signalling pathway and c-MYC expression has been studied in less detail but it has been shown that the *c-MYC* promoter is a direct target of the transcriptional activator NICD, which is released during NOTCH signalling (Klinakis *et al.*, 2006; Xu *et al.*, 2010). NICD accumulates in breast carcinoma cells and one study reported that up-regulation of c-MYC was observed in NICD-induced murine mammary cancer (Klinakis *et al.*, 2006; Stylianou *et al.*, 2006).

Amplification of *c-MYC* is an established event in breast carcinogenesis. A meta-analysis of 29 breast cancer *c-MYC* amplification studies by Deming *et al.* (2000) classified an amplification of *c-MYC* as at least a 2-fold increase in copy number. The analysis reported that 15.7% of breast cancers were *c-MYC* amplified and that amplification had a weak association with tumour grade and prognosis. Subsequent studies have also reported associations between *c-MYC* amplification with high tumour grade and poor prognosis, and that *c-MYC* amplification is more common in invasive breast carcinoma than carcinoma *in situ* (Deming *et al.*, 2000; Robanus-Maandag *et al.*, 2003; Schlotter *et al.*, 2003; Al-Kuraya *et al.*, 2004; Blancato *et al.*, 2004).

There is some evidence in the literature that there is an association between exposure to ionising radiation and amplification of *c-MYC*. Studies of secondary angiosarcoma (AS) which arose after radiotherapy for primary cancers, such as breast cancer, indicated a high incidence of *c-MYC* amplification (55% - 100% of cases) compared to no evidence of *c-MYC* amplification in primary AS (Manner *et al.*, 2010; Guo *et al.*, 2011). *c-MYC* amplification was also reported in AS that developed following lymphoedema in patients not exposed to radiation, so a direct link with ionising radiation cannot be made.

A study of Japanese atomic bomb survivors compared the incidence of *c-MYC* amplified breast cancer in radiation-exposed women and a control group of Japanese

women without exposure (Miura *et al.*, 2008). *c-MYC* amplification was identified in 56.5% of cases from women exposed to high doses of irradiation, 29.4% from women exposed to a lower dose and 14.3 % of women not exposed to ionising radiation. Moreover, *c-MYC* was reported in breast cancers with a concomitant *HER2* amplification. The results from this study therefore suggest that *c-MYC* amplification can be induced by ionising radiation. The focal *c-MYC* copy number increase in MCF-10A reported in the present study, and the increased incidence of *c-MYC* amplified breast cancers in radiation-exposed atomic bomb survivors, identifies *c-MYC* amplification as a putative marker of radiation-induced breast carcinogenesis.

4.5.4 Conclusion

High density SNP array analysis of ionising radiation treated MCF-10A cells (with and without added oestrogen) has identified regions of copy number change which may be linked to radiation-induced breast epithelial cell transformation. These include a mono-allelic deletion of a region on chromosome 11, a focal deletion of the stress response gene *POU2F1* and a copy number increase of the proto-oncogene *c-MYC.*

Further phenotypic characterisation of *POU2F1*-deleted MCF-10A cells, and the prevalence of *POU2F1* deletion in sporadic and radiation-induced breast cancer will be investigated in Chapter 6 and Chapter 8. Likewise, further genotypic characterisation of *c-MYC*-amplified MCF-10A cells will be investigated in chapter 7, along with an assessment of *c-MYC* amplification in sporadic and radiation-induced breast cancer tissue samples (Chapter 8).

First however, the effect of the acquired copy number alterations in the First and Second 5 Gγ series on gene expression will be discussed (Chapter 5).

Chapter 5: Genome-wide expression analysis of irradiated MCF-10A populations

5.1 Introduction

High-density polymorphism analysis of the First and Second 5 Gγ series identified copy number alterations in both irradiation series. Copy number alterations can alter the expression of those genes directly affected by the copy number change and also genes which are transcriptionally regulated by directly affected genes. The First 5 Gγ series had extensive copy number alterations and the expression profile of these irradiated cell populations is predicted to be different to un-irradiated MCF-10A as a consequence. The Second 5 Gγ series only had three copy number alterations, but genes affected by these alterations (*c-MYC* and *BMPR1A*) are known to transcriptionally regulate numerous downstream target genes. The exogenous oestrogen added to the culture media during irradiation of the Second 5 Gγ series can also cause oxidative DNA damage and therefore mutations that can alter gene expression. Analysing the expression profile of cells from the First and Second 5 Gγ series will help to understand the effect of ionising radiation.

In order to investigate the effect of radiation-induced genetic alterations on gene expression the Illumina HT12 v4 expression array was used to analyse RNA extracted from un-irradiated MCF-10A cells and radiation-treated cells from the First and Second 5 Gγ series. Briefly, the array uses 50-mer oligonucleotide probe sequences which are designed, *in silico,* to hybridise with transcript sequences of genes in the human genome. When transcript sequence is bound to the probes a signal for the probe can be detected. The signal intensity for each probe corresponds to the amount of gene-specific transcript that is present in the sample and therefore the relative expression of that gene. For some genes there are multiple probes which are specific to different regions of the gene or to splice variants of the gene. Therefore, within the same gene some probes can generate a signal while others probes might not, depending on which splice variants are transcribed or if the probe sequence is present in the transcript of the gene within that sample.

5.1.1 Aim

The aim of the work described in this chapter was to investigate the expression of genes affected by copy number alteration in irradiated MCF-10A cells (described in Chapter 4), which genes were most differentially expressed and whether differentially expressed genes can be grouped according to cellular function.

5.2 Gene expression analysis of the First 5 Gγ series

The Illumina HT12 v4 expression array was used to analyse RNA extracted from un-irradiated MCF-10A, First 5 Gγ series and passage control cell populations. Expression data was not available for the 10 Gγ and 80 Gγ cumulative dose populations, which limited the subsequent analysis. Expression data was analysed using the Illumina Genome Studio software which compares the signal intensity of each probe in each population to a chosen control population. A differentiation *p*-value was calculated based on the difference in signal intensity between the test and control samples and the variation of internal controls, which in turn was computed into a Differentiation Score for each probe (section 2.6.2). For probes where the software was not confident of a difference between the test and control samples a Differentiation Score was not given. Some probes which were attributed a differentiation score had differentiation *p*-values > 0.05. Due to the lack of replicates for the gene expression analysis the differentiation *p*-value was artificial and therefore may not have reflected the true significance of any expression difference. As such, for subsequent analyses the attribution of a differentiation score was used as the sole indicator of differential expression, regardless of the differential *p*-value. From here on, when the term differentially expressed is used it refers to genes which have been attributed a differentiation score.

It should be noted that due to the lack of repeats and the caveats discussed above that the data is limited and has to be analysed with some caution. Nevertheless, comparisons between gene expression, copy number and phenotypic changes are still possible.

5.2.1 Expression analysis of specific copy number altered genes from the First 5 Gγ series

Genes affected by copy number changes (described in section 4.3) were analysed for concomitant changes in gene expression. Genes analysed were: *CADM1, CUL5, ATM, SLIT2, DCC* and *POU2F1* (Table 5.1). For each probe, Genome Studio calculates a detection *p*-value which indicates whether the signal from that gene is detected above

background as determined by negative controls on the array. Two of the four probes for *ATM* were not detected above background in un-irradiated MCF-10A cells and were therefore discarded from subsequent analysis.

Gene	Chromosome	Copy number change by SNP analysis	Resulting number of copies	Number of expression probes	Number of probes detected
POU2F1	1q	-1	2	1	1*
SLIT2	4p	-1	1	1	1
CADM1	11q	-1	1	1	0
CUL5	11q	-1	1	1	1
ATM	11q	-1	1	4	2
DCC	18q	-1	1	1	0

Table 5.1 Genes affected by copy number alteration analysed for changes in gene expression.
Genes affected by copy number changes which were highlighted in Chapter 4. The chromosomal location of the selected loci and the overall copy number change in the 55 Gγ cell populations relative to un-irradiated MCF10-A is shown (-1 = mono-allelic loss of the gene). The number of probes on the array and the number of probes detected above background for each locus are also detailed.* The POU2F1 probe was not detectable above background in 55 Gγ MCF10-A cells, and only marginally detectable above background in un-irradiated MCF-10A.

Expression of *ATM, CUL5* and *SLIT2* was over 2 fold lower in the 40 Gγ and 55 Gγ populations compared to the un-irradiated MCF-10A cell population (Fig. 5.1). Mono-allelic deletion of these loci was detected in the 40 Gγ and 55 Gγ populations (chapter 4), suggesting that expression of these genes was reduced due to allelic loss. Expression of each selected locus was similar in passage control and un-irradiated MCF-10A cell populations.

CADM1, POU2F1 and *DCC* were each represented by only one probe in the array. Probe signal for *CADM1* and *DCC* were not detected above background in un-irradiated MCF-10A (Detection p-value > 0.05), and signal for *POU2F1* was only slightly higher than background. Non-detection of these probes may indicate that the target transcript was not expressed, or expressed at very low level. However, as the probes are designed *in silico* and have not all been validated in a laboratory setting it could be that some do not hybridise to their target transcripts as expected. It has also been shown that some of the Illumina probe sets hybridise to non-target genomic regions, including intergenic regions (Barbosa-Morais *et al.*, 2010). As only one probe matches to each of these genes, a defective or un-informative probe would give the false impression of absent expression of target transcript. As such, there is a lack of information for these genes rather than definitive proof of lack of expression.

a *ATM* Expression **b *CUL5* Expression**

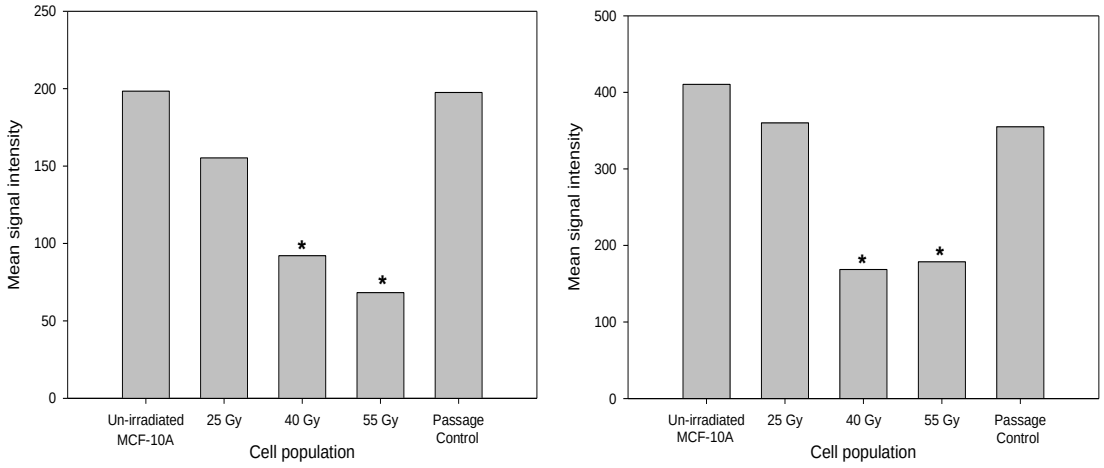

c *SLIT2* Expression

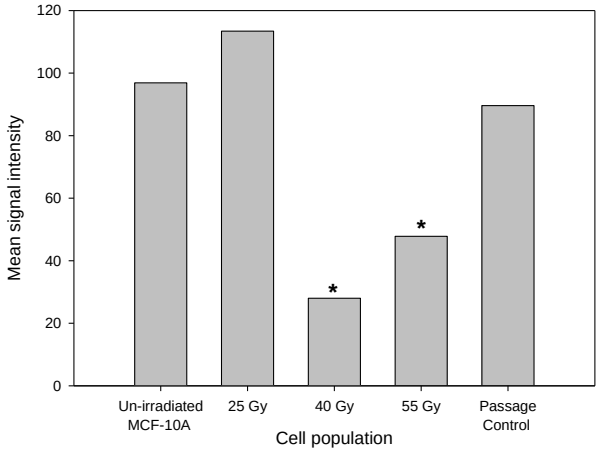

Figure 5.1 Expression analysis of *ATM, CUL5* and *SLIT2* in the First 5 Gγ series.
The mean signal intensity of probes which hybridise to transcripts of *ATM*, *CUL5* and *SLIT2* in un-irradiated MCF-10A, 25 Gγ, 40 Gγ, 55 Gγ and passage control populations is shown. For genes which have more than one probe which hybridises to the gene transcript the average signal intensity is shown. Probe signal intensity that is at least 2 fold lower than that seen in un-irradiated MCF-10A is indicated by an * on the graph.

5.2.2 Analysis of differentially expressed genes of the First 5 Gγ series

Genes that were differentially expressed (attributed with a differentiation score) in the First 5 Gγ series and passage control populations compared to the un-irradiated MCF-10A cell population were identified following analysis with Genome Studio. Probes which were not detected above background (Detection *p*-value > 0.05) in un-irradiated MCF-10A cells were discarded from the analysis.

Differentially expressed genes in each irradiated population that were also differentially expressed in the passage control population were deemed to be passage related expression changes. Differentially expressed genes that were not identified in the passage control population were deemed to be radiation-induced expression changes. The number of radiation-induced and passage related differentially expressed genes in each irradiated population are shown in figure 5.2. The proportion of passage related expression changes reduced as cumulative dose increased, from 44% in the 25 Gγ population, to 24% and 18% in the 40 and 55 Gγ populations, respectively. Genes that were differentially expressed in both radiation-treated and passage control cell populations relative to un-irradiated MCF-10A were removed from subsequent analysis of the First 5 Gγ series in order to focus on radiation-induced alterations.

There was a 10 fold increase in the number of radiation-induced differentially expressed genes in the 40 Gγ population compared to the 25 Gγ population, which approximately corresponded with the observed increase in the number of copy number alterations (discussed in section 4.3) (Fig. 5.2). There was a further increase in the number of radiation-induced differentially expressed genes in the 55 Gγ population, which again approximately corresponded with an increase in the number of copy number alterations. Copy number alterations may directly affect gene expression, as seen for *ATM, CUL5* and *SLIT2* (section 5.2.1), but may also indirectly affect expression of other genes via deletions or amplifications of genes which regulate gene transcription or DNA methylation, for example. Also, copy number alterations will not account for all gene expression changes. Non-copy number related alterations such as point mutations in promoter regions of genes for example will also affect the expression of genes, although these and other mechanisms have not been investigated in this study.

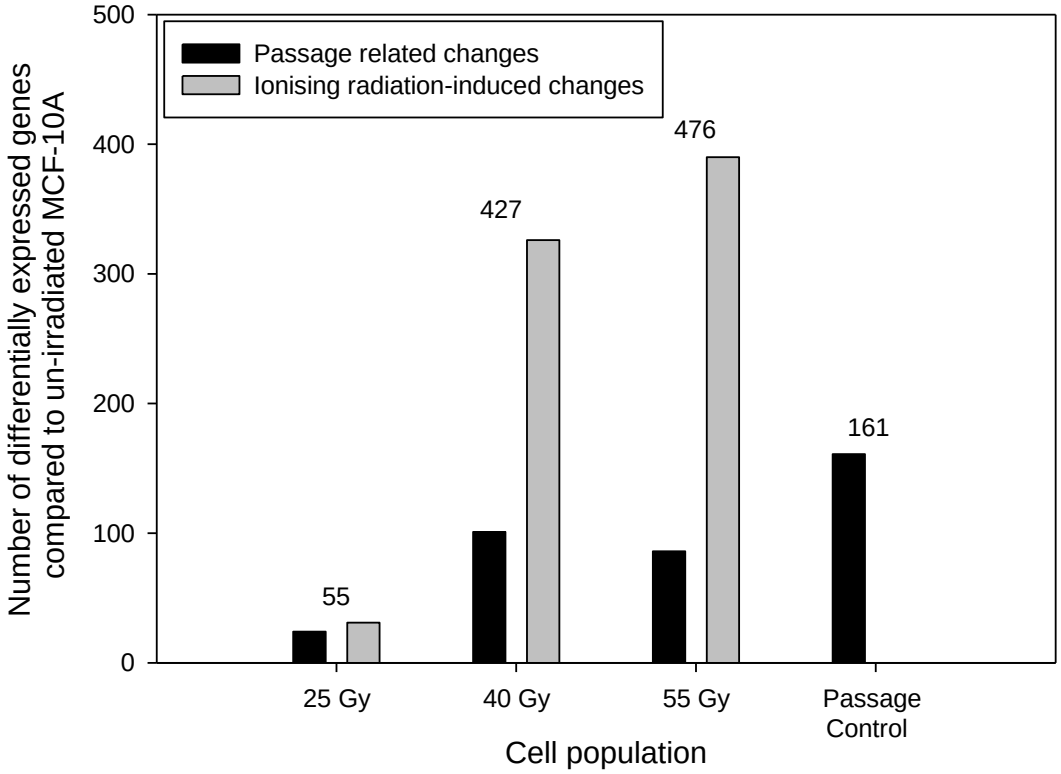

Figure 5.2 Number of differentially expressed genes in the First 5 Gγ series.
The number of genes which are differentially expressed in the 25 Gγ, 40 Gγ, 55 Gγ and passage control populations compared to un-irradiated MCF-10A. The number of differentially expressed genes which are also identified in the passage control population are represented by black bars (passage related expression changes). The number of differentially expressed genes in radiation-exposed MCF-10A, but not affected in the passage control cells, are represented by grey bars (radiation-induced expression changes). The total number of differentially expressed genes is above each pair of bars for each population. The percentage of differentially expressed genes which were passage related for each population was: 25 Gγ – 44%, 40 Gγ – 24%, 55 Gγ – 18%.

The 55 Gγ population had the highest number of differentially expressed genes and had received the highest cumulative dose of irradiation. Therefore only differentially expressed genes from the 55 Gγ population were used in subsequent analysis. The 55 Gγ population had over 200 down-regulated genes and over 150 up-regulated genes compared to the un-irradiated MCF-10A population (Fig. 5.3). In order to reduce the number of genes to analyse in more detail, only the top 10 most differentially expressed genes (according to differentiation score) in each expression group were used in subsequent analysis (Table 5.2a and 5.2b).

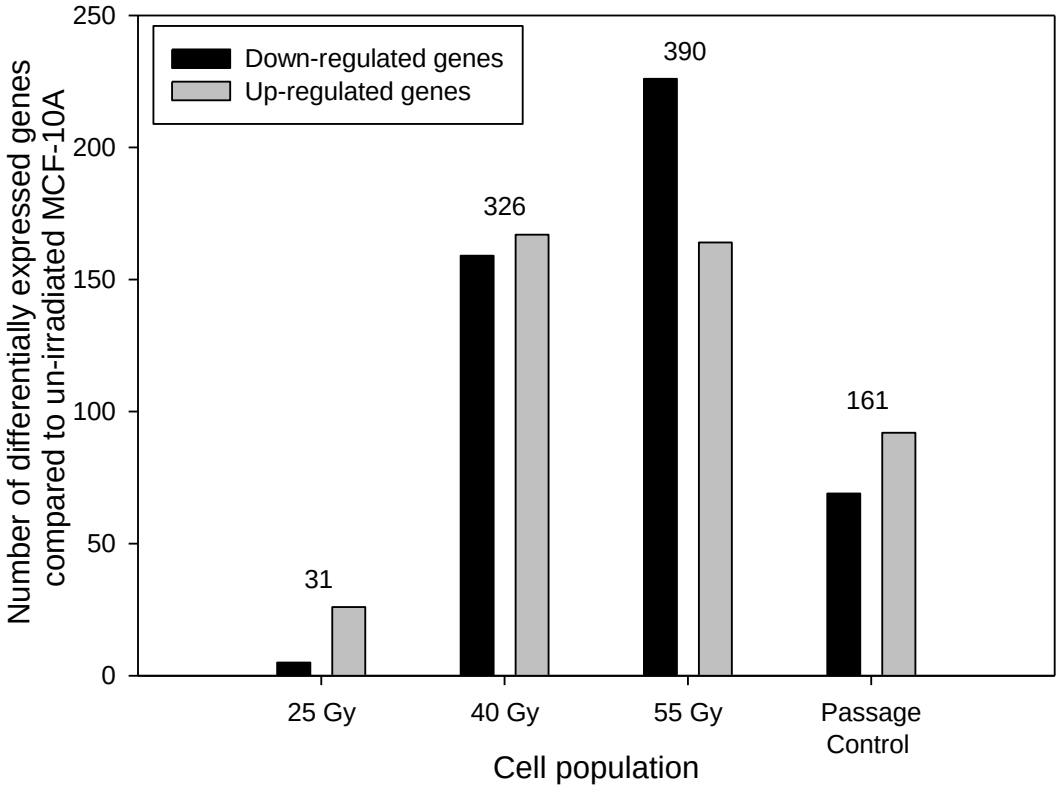

Figure 5.3 The number of down-regulated and up-regulated genes in the First 5 Gγ series.
The number of genes which are down-regulated **(**black bars**)** and up-regulated **(**grey bars**)** in the 25 Gγ, 40 Gγ, 55 Gγ and passage control populations compared to the un-irradiated MCF-10A cell population. The number of differentially expressed genes for the 25 Gγ, 40 Gγ and 55 Gγ populations does not include genes which were also differentially expressed in the passage control population. The total number of differentially expressed genes displayed on the graph is shown above each pair of bars for each population.

a

Reduced Expression				
Gene Name	**Differentiation Score**	**Copy Number Change by SNP Analysis**	**Resulting Number of Copies**	**Gene Function**
FLJ12684	-51.79	None	2	Calcium uptake in mitochondria
ASAP3	-30.88	None	2	Promotes cell proliferation
BCL6	-30.88	None	2	Transcriptional repressor
C14orf147	-27.44	None	2	Unknown
SNCA	-27.26	None	2	Regulation of dopamine release and transport
SIDT2	-24.78	-1	1	Unknown
IFI44L	-24.65	None	2	Unknown
MGMT	-24.46	None	2	DNA repair: Repairs alkylated guanine
HADH	-22.02	None	2	Mitochondrial oxidation of short chain fatty acids
SMOX	-21.86	+1	3	Catalyzes the oxidation of spermin to spermidine

b

Increased Expression				
Gene Name	**Differentiation Score**	**Copy Number Change by SNP Analysis**	**Resulting number of copies**	**Gene Function**
CCND2	66.12	None	2	Regulates progression between G1 and S phase of the cell cycle
LOC100008589	39.25	None	2	Un-annotated gene coding a ribosomal RNA repeating unit
LOC100133565	34.38	None	2	Un-annotated gene
AKAP12	30.46	None	2	Anchoring protein
LOC441763	27.75	None	2	Un-annotated gene
SRP19	25.29	+1	3	Part of the signal-recognition-particle complex
IL24	23.98	None	3	Induces apoptosis in various cancer cells
CHORDC1	22.66	+1	3	Chaperone protein: regulates centrosome duplication
LMTK3	22.45	None	2	Phosphorylates ERα leading to tamoxifen resistance
ADRB2	21.39	None	3	Beta-2-andrenic receptor: smooth muscle relaxation

Table 5.2 Top 10 differentially expressed genes in the 55 Gγ cumulative dose population.
The top 10 down-regulated (**a**) and top 10 up-regulated genes (**b**) (as determined by differentiation score) in the 55 Gγ population compared to the un-irradiated MCF-10A population were identified using Genome Studio. The name and differentiation score (as calculated by Genome Studio: Section 2.6.2) for each of the 20 genes is shown in the table. Negative differentiation scores indicate a reduction in expression and positive differentiation scores indicate an increase in expression. The more negative/positive a score, the larger the difference in expression compared to un-irradiated MCF-10A. The copy number change between the un-irradiated MCF-10A and 55 Gγ population as determined by the SNP 6.0 array is also shown for each gene. None = no change, +*n* = number of copies gained and -*n* = number of copies lost. The resulting copy number state of the gene in the 55 Gγ population is also shown. Genes to be discussed further in section 5.4 are highlighted in red.

Of the 20 most differentially expressed genes only 3 had a gene copy number change which correlated with a reduction or increase in expression (*SIDT2*, *SRP19*, *CHORDC1*; Table 5.2a and b). *SMOX* is in a region of copy number increase but expression of the gene decreased. The lack of correlation between gene expression change and copy number change in the 20 gene cohort suggests that other mechanisms affecting gene expression may be operating.

Genes in the 20 gene cohort that may be relevant to cell transformation or alterations in cell phenotype observed in the First 5 Gγ series included *ASAP3, BCL6, MGMT, CCND2 IL24,* and *LMTK3*. Change in expression of these genes throughout the First 5 Gγ series was analysed as a function of cumulative radiation dose (Fig. 5.4 and Fig. 5.5). Both *ASAP3* and *BCL6* were differentially expressed in the 40 Gγ and 55 Gγ cell populations, however there was also a modest decrease in expression in the 25 Gγ population (Figure 5.4). The expression of *ASAP3* was also reduced in the passage control population but was not identified as differentially expressed by Genome Studio. The expression of *MGMT* dropped substantially between the 40 Gγ and 55 Gγ populations indicating that a genetic event between these two populations caused the decrease in expression (Figure 5.4).

CCND2 expression was differentially increased in all of the irradiated populations analysed compared to un-irradiated MCF-10A (Figure 5.5). *IL24* expression was only differentially expressed in the 55 Gγ population however there is a smaller increase in expression in the 40 Gγ population also. *LMTK3* expression increased more than 4 fold between the 25 Gγ and 40 Gγ populations indicating that a genetic event between these two populations may have caused a sudden increase in expression.

The implications and relevance of altered expression of these genes will be discussed in section 5.4.3.

a *ASAP3* Expression **b *BCL6* Expression**

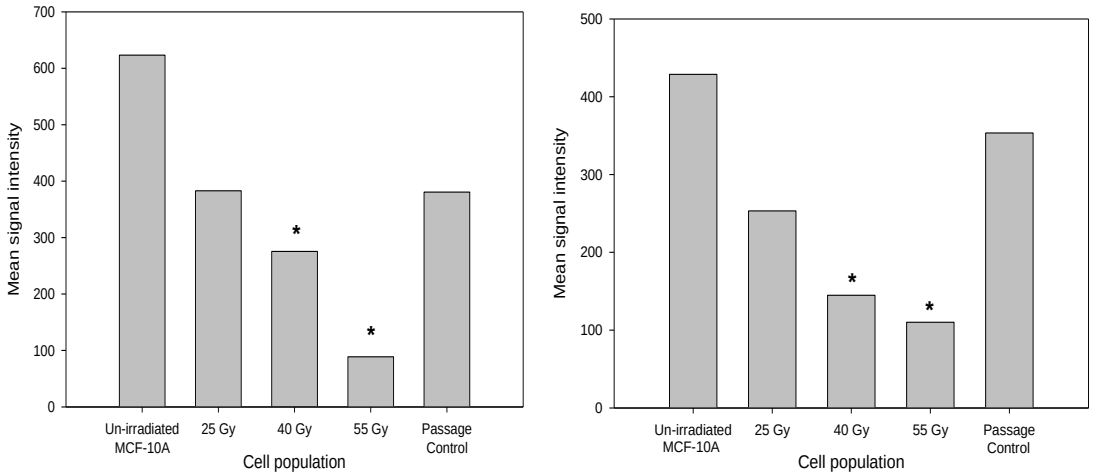

c *MGMT* Expression

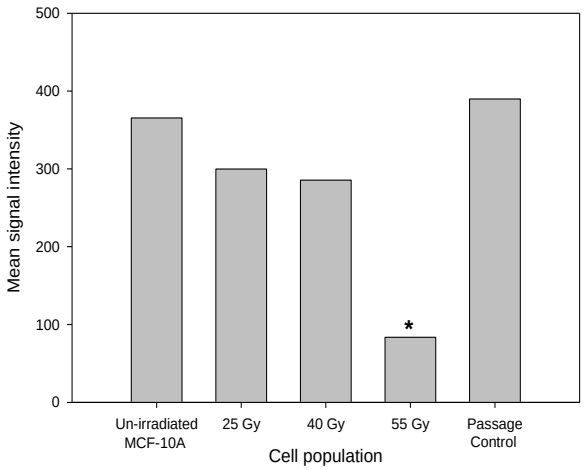

Figure 5.4 Gene expression of *ASAP3, BCL6* and *MGMT* in the First 5 Gγ series.
The average signal intensity of probes which hybridise to transcripts of *ASAP3*, *BCL6* and *MGMT*, in the un-irradiated MCF-10A, 25 Gγ, 40 Gγ, 55 Gγ and passage control population is shown. For genes which have more than one probe which hybridises to the gene transcript the mean signal intensity of the probes is shown. Cell populations whose probe signal intensity is differentially expressed compared to the un-irradiated MCF-10A population as calculated by GenomeStudio is identified by an * on the graph.

a *CCND2* Expression **b *IL24* Expression**

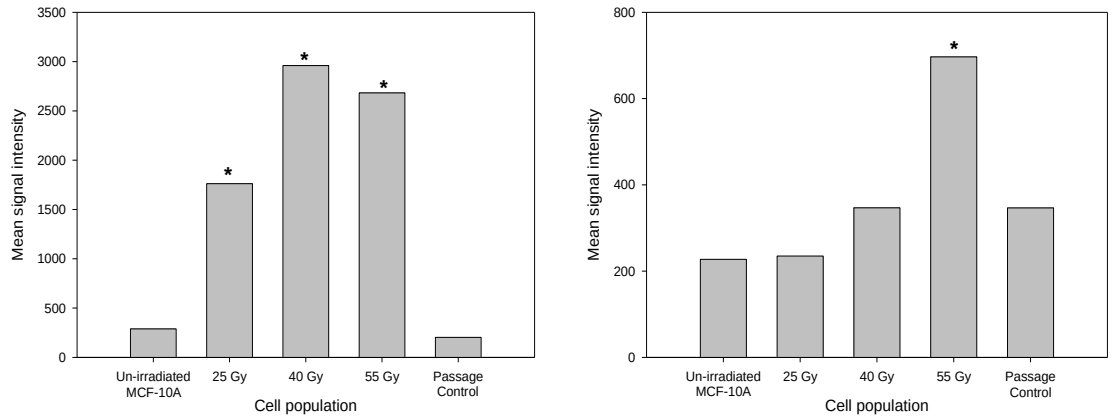

c *LMTK3* Expression

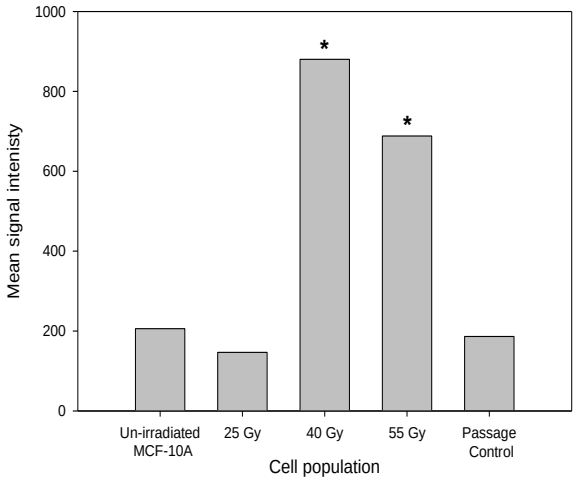

Figure 5.5 Gene expression of *CCND2, IL24* and *LMTK3* in the First 5 Gγ series.
The average signal intensity of probes which hybridise to transcripts of *CCND2, IL24* and *LMTK3* in the un-irradiated MCF-10A, 25 Gγ, 40 Gγ, 55 Gγ and passage control population is shown. For genes which have more than one probe which hybridises to the gene transcript the mean signal intensity of the probes is shown. Cell populations whose probe signal intensity is differentially expressed compared to the un-irradiated MCF-10A population as calculated by GenomeStudio is identified by an * on the graph.

5.2.3 Functional clustering analysis of the First 5 Gγ series

Radiation-induced gene expression changes identified in the 55 Gγ cumulative dose population were used to elucidate biological processes that were enriched for differentially expressed genes. To identify affected processes an online gene function clustering tool (The **D**atabase for **A**nnotation, **V**isualization and **I**ntegrated **D**iscovery - DAVID) was used to cluster differentially expressed genes into functionally related groups defined by Gene Ontology (GO) Database annotations (Huang *et al.*, 2009a; Huang *et al.*, 2009b). DAVID calculated the probability that identified gene clusters were not present in the differentially expressed gene list by chance (Section 2.7). Cellular pathways significantly enriched for differentially expressed genes were more likely to be affected by gene expression changes. DAVID also grouped together gene clusters that shared genes and had similar biological functions.

DAVID identified 10 functional groups which contained multiple gene clusters that were significantly enriched for differentially expressed genes from the 55 Gγ population ($p<0.05$) (Table 5.3). The gene cluster with the lowest *p*-value within each functionally related group is shown in table 5.3. Changes to these 10 processes may have affected the phenotypes observed in the First 5 Gγ series. The specific consequence of the changes to the processes identified cannot be determined as it is unclear whether the activity of the process would be reduced or enhanced by the expression changes. Nevertheless, changes in the expression of genes in these pathways can be considered in the context of the phenotypic changes observed in the First 5 Gγ series. Cellular pathways likely to have been affected by expression changes include: cell death (with 3 of the 10 processes outlined in table 5.3 being related to apoptosis), cell migration, cell growth and cellular response to steroid hormones. The potential implications of changes to these processes in relation to the First 5 Gγ series will be discussed in section 5.4.4.

Database Resource	Gene Group Function (Annotation Term)	Number of Genes	*p* value
GOTERM_BP_FAT	GO:0008219~cell death	27	0.0015
GOTERM_BP_FAT	GO:0042981~regulation of apoptosis	28	0.0036
GOTERM_BP_FAT	GO:0048545~response to steroid hormone stimulus	12	0.0013
GOTERM_MF_FAT	GO:0004252~serine-type endopeptidase activity	9	0.0101
GOTERM_BP_FAT	GO:0045926~negative regulation of growth	8	0.0054
GOTERM_BP_FAT	GO:0043065~positive regulation of apoptosis	16	0.0199
GOTERM_BP_FAT	GO:0016485~protein processing	7	0.0213
GOTERM_BP_FAT	GO:0016477~cell migration	12	0.0184
GOTERM_BP_FAT	GO:0007599~hemostasis	7	0.0182
GOTERM_BP_FAT	GO:0008585~female gonad development	5	0.0349

Table 5.3 Biological processes enriched for differentially expressed genes from the 55 Gγ population of the First irradiation series.
Functional clustering results for genes which were differentially expressed in the 55 Gγ population given by the online functional annotation tool DAVID (http://david.abcc.ncifcrf.gov/). Gene clusters that share a common cellular function and are unlikely to be present in the differentially expressed gene list by chance ($p < 0.05$) are shown. The lower the *p* value the more probable the associated functional group is affected in the assayed cell population. The number of differentially expressed genes associated to each biological process is given. The nomenclature in the Database Resource column refers to the nature of the biological function: BP = Biological process, MF = Molecular Function (Section 2.7). The annotation term relates to a description of the biological function that the gene group is attributed to in the Gene Ontology (GO) database (http://www.ebi.ac.uk/QuickGO/).
It should be noted that some of the biological processes may have overlapping genes within their gene clusters.

5.3 Gene expression analysis of the Second 5 Gγ series

The Illumina HT12 v4 5.3 expression array was used to analyse RNA extracted from the Second 5 Gγ series (irradiated with the addition of exogenous oestrogen). The 10 Gγ, 20 Gγ, 40 Gγ, 60 Gγ and 80 Gγ cumulative dose populations of the Second 5 Gγ series were analysed for gene expression, as was the exogenous oestrogen exposed passage control population.

5.3.1 Expression analysis of specific copy number altered genes from the Second 5 Gγ series

Genes identified by the SNP 6.0 array which had an altered copy number state compared to un-irradiated MCF-10A (*c-MYC* and *BMPR1A*, section 4.4) were specifically analysed for changes in gene expression.

A focal copy number increase of *c-MYC* was identified in the 40 Gγ cumulative dose population (section 4.4.2). A second larger copy number gain on chromosome 8q increased the copy number of *c-MYC* further in the 60 Gγ and 80 Gγ populations. Copy number of the *c-MYC* locus also increased in the passage control population due to a whole chromosome copy number gain of chromosome 8. *c-MYC* was not attributed a differentiation score in any of the populations compared to un-irradiated parental MCF-10A. However, there was a trend for an increase in signal intensity for these probes in the 40 Gγ population compared to un-irradiated MCF-10A which continued to increase as cumulative dose increased, which is consistent with increasing copy number in these cell populations (Fig 5.6a).

Mono-allelic deletion of *BMPR1A* was observed in the 40 Gγ, 60 Gγ and 80 Gγ populations using SNP array analysis. However, *BMPR1A* was not attributed a differentiation score in any of the populations compared to un-irradiated MCF-10A (Fig 5.6b). Again a trend was observed that the signal intensity of the probe was reduced in the 40 Gγ, 60 Gγ and 80 Gγ populations.

Taken together, these data suggest that an increase in *c-MYC* copy number and mono-allelic deletion of *BMPR1A* may be associated with increased and reduced expression respectively.

a ***c-MYC*** **Expression**

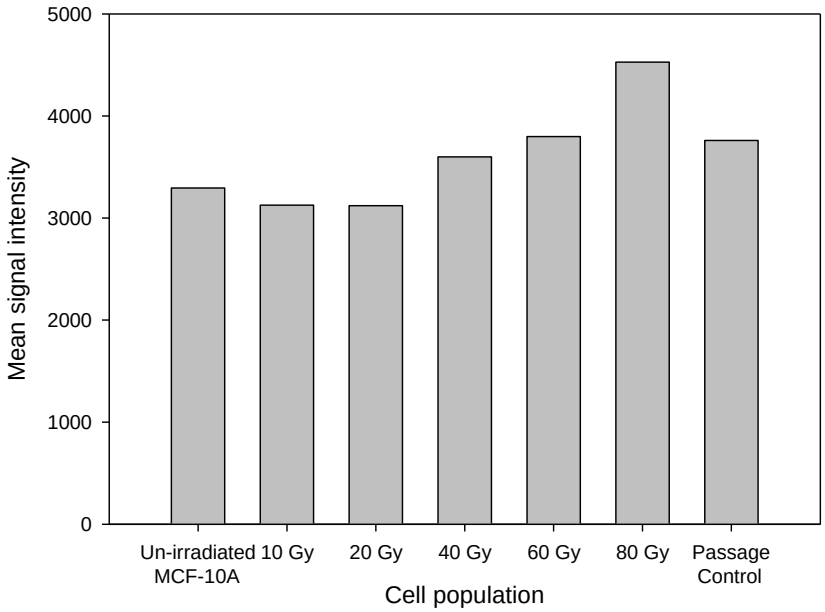

b ***BMPR1A*** **Expression**

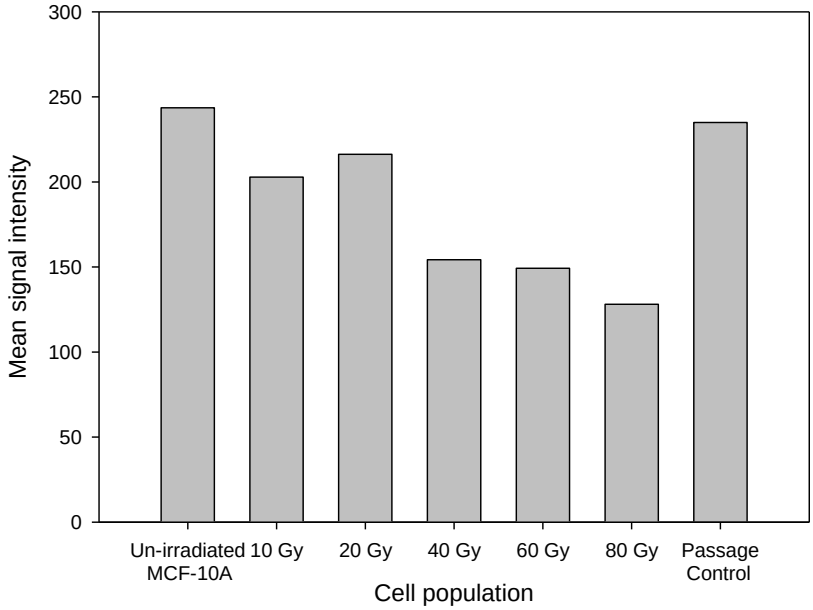

Figure 5.6 Expression of *c-MYC* and *BMPR1A* in the Second 5 Gγ series.
The average signal intensity of probes which hybridise to transcripts of *c-MYC* **(a)** and *BMPR1A* **(b)** in the un-irradiated MCF-10A, 10 Gγ, 20 Gγ, 40 Gγ, 60 Gγ, 80 Gγ and passage control population is shown. For genes which have more than one probe which hybridises to the gene transcript the mean signal intensity of the probes is shown. The genes were not differentially expressed in any population compared to un-irradiated MCF-10A.

5.3.2 Analysis of differentially expressed genes of the Second 5 Gγ series

As described in section 5.2.2, probes which were not expressed above background in un-irradiated parental MCF-10A cells were discarded from the analysis. The SNP 6.0 data indicated that there were only 2 focal copy number alterations and 1 large copy number gain in the Second 5 Gγ series not present in un-irradiated MCF-10A cells. In contrast, there were 5 whole chromosome copy number gains in the passage control population (section 4.4). The relative number of genes affected by copy number alterations in the irradiated cell populations and passage control cells was reflected in the number of differentially expressed genes identified by Genome Studio in these populations. Specifically, in total there were 1540 differentially expressed genes in the passage control population, 857 of which were up-regulated and 683 which were down-regulated. In contrast, the total number of differentially expressed genes in the 80 Gγ population was 46. The passage control population had novel copy number gains of chromosomes 7, 8, 11, 13, and 19. The majority of the differentially up-regulated genes compared to un-irradiated MCF-10A were located on those chromosomes affected by trisomy (Fig. 5.7a). Conversely, these chromosomes carried relatively few differentially down-regulated genes (Fig. 5.7b). The large numbers of genes which increased in copy number in the passage control population may have also had an indirect effect on expression of other genes in the genome.

a Number of up-regulated genes

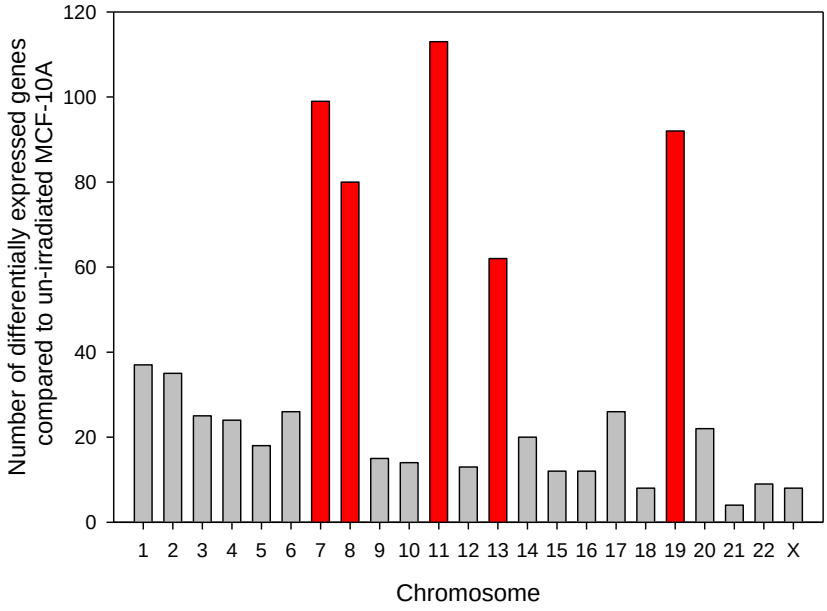

b Number of down-regulated genes

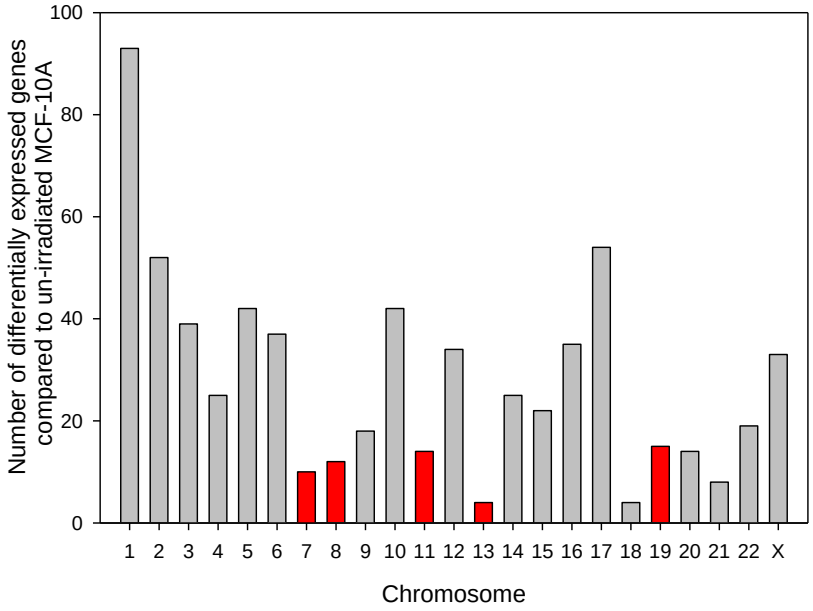

Figure 5.7 Location of differentially expressed genes in the passage control population of the Second 5 Gγ series.
The number of genes which were up-regulated **(a)** and down-regulated **(b)** on each chromosome of the passage control population compared to the un-irradiated MCF-10A population. Trisomic chromosomes identified by the SNP 6.0 array in the passage control population are highlighted in red.

Differentially expressed genes identified in the passage control population were removed from subsequent analysis of the Second 5 Gγ series in order to concentrate on genes whose expression was affected by alterations specific to the irradiated populations. The number of radiation-induced differentially expressed genes increased 3 fold between the 20 Gγ and 40 Gγ populations (Fig. 5.8). Amplification of *c-MYC* and mono-allelic deletion of *BMPR1A* were both first identified in the 40 Gγ population. c-MYC and BMPR1A are both transcriptional regulators which may partly explain the observed increase in the number of differentially expressed genes. An elevated number of differentially expressed genes compared to un-irradiated MCF-10A were maintained in the 60 Gγ and 80 Gγ populations (Fig. 5.8). As there are relatively few differentially expressed genes in the 60 Gγ and 80 Gγ populations, genes identified from both of these populations were analysed further. Specifically, there were 31 differentially expressed genes in total between the two populations. Thirteen genes were differentially expressed in both populations (Fig. 5.9a), 12 genes were only differentially expressed in the 60 Gγ population (Fig. 5.9b) and 6 genes were only differentially expressed in the 80 Gγ population (Fig. 5.9c). Differentiation score rather than signal intensity is shown for each gene in figure 5.9. It is noteworthy that none of these genes were affected by copy number alterations.

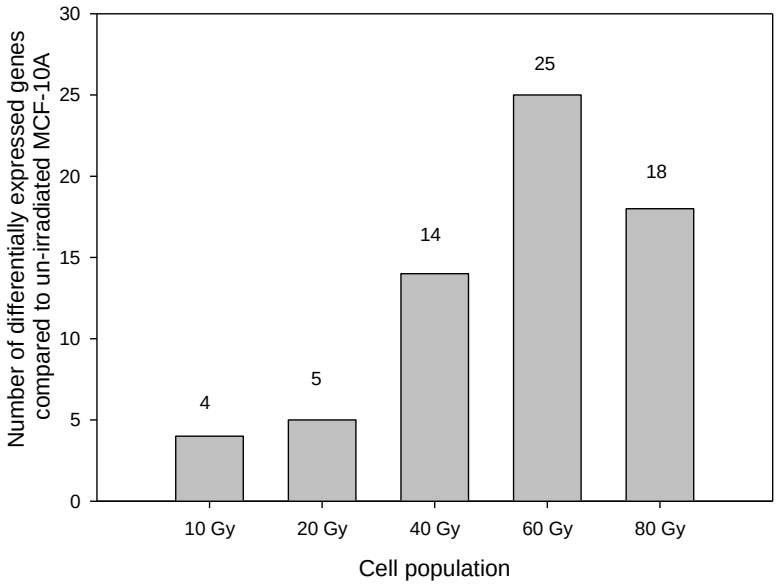

Figure 5.8 Number of differentially expressed genes in the Second 5 Gγ series.
The number of genes which were differentially expressed in the 10 Gγ, 20 Gγ, 40 Gγ, 60 Gγ and 80 Gγ populations compared to un-irradiated MCF-10A. The number of differentially expressed genes for the irradiated populations does not include genes which were also differentially expressed in the passage control population. The number of differentially expressed genes displayed on the graph is shown above each bar for each population.

a. Differentially expressed genes in both the 60 Gγ and 80 Gγ populations

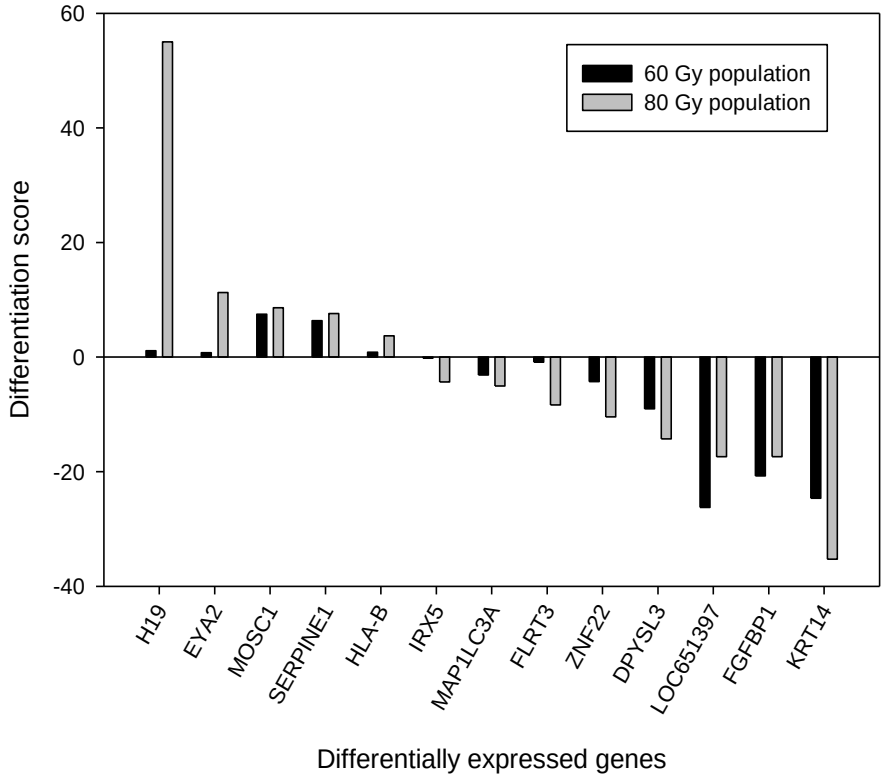

b. 60 Gγ population

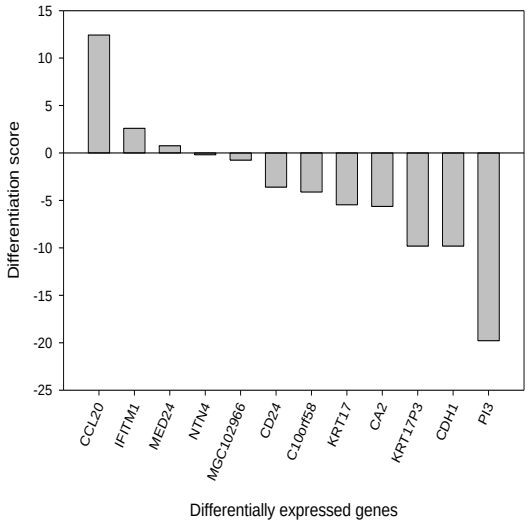

c. 80 Gγ population

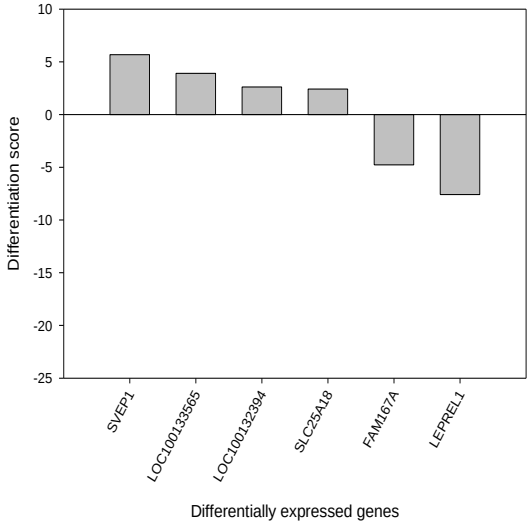

Figure 5.9 Differentially expressed genes of the 60 and 80 Gγ cumulative dose populations.
Genes differentially expressed in both the 60 Gγ (black bars) and 80 Gγ (grey bars) cumulative dose populations (**a**), only in the 60 Gγ population (**b**) and only in 80 Gγ population (**c**) compared to the un-irradiated MCF-10A cell population. Genes are ordered from left to right by differentiation score. In the graph displaying genes differentially expressed in both populations (**a**) genes are ordered from left to right by differentiation score in the 80 Gγ population. A positive score indicates up-regulation of a gene and a negative score indicates down-regulation of a gene relative to un-irradiated MCF-10A. The more positive/negative the score, the greater the difference in expression of the gene compared to the un-irradiated MCF-10A population.

A number of the expression changes identified in the 60 Gγ population correlate with expression changes in cells which undergo epithelial mesenchymal transition (EMT). For example, one very well established marker for EMT is down-regulation of *CDH1* (E-cadherin) which is often concomitant with up-regulation of *CDH2* (N-cadherin). *CDH1* was down-regulated in the 60 Gγ population (Fig 5.9b), and *CDH2* showed increased expression compared to un-irradiated MCF-10A but was not attributed a differentiation score (Fig. 5.10). *CDH1* was not down-regulated in the 80 Gγ population and the expression of *CDH2* did not increase compared to un-irradiated MCF-10A either (Fig. 5.10).

Other genes which are down-regulated in cells undergoing EMT and were also down-regulated in the 60 Gγ population include *KRT14*, *PI3*, *FGFBP1*, *KRT17P3* and *CD24* (Thiery, 2003; Vincent-Salomon and Thiery, 2003; Huber *et al.*, 2005; Higashikawa *et al.*, 2008; Mani *et al.*, 2008; Cho *et al.*, 2010; Micalizzi *et al.*, 2010; Asiedu *et al.*, 2011; Hanahan and Weinberg, 2011) (Fig. 5.9a and b). Down-regulation of *CD24* is also a marker for cancer stem cells which are highly tumourigenic (Reya *et al.*, 2001; Al-Hajj *et al.*, 2003), and which share properties with cells undergoing EMT (Mani *et al.*, 2008). *KRT14* and *FGFBP1* were also down regulated in the 80 Gγ population (Fig. 5.9a). *SERPINE1*, which is an expression marker for EMT and is up-regulated in a number of cancers was also up-regulated in both 60 and 80 Gγ cell populations (Samarakoon *et al.*, 2009; Hesling *et al.*, 2011) (Fig 5.9a).

The identification of some EMT expression markers in the 60 Gγ population and not the 80 Gγ population may be natural fluctuations in the expression profile of these genes or may reflect other molecular processes that are affecting the EMT expression profile (discussed in section 5.4.2).

Other genes which were differentially expressed in the 60 Gγ or 80 Gγ populations and have putative roles in cancer include *H19*, *LEPREL1*, *CCL20* and *EYA2*; each of which will be discussed in section 5.4.2.

Due to the small number of genes that were differentially expressed in the Second 5 Gγ series it was not appropriate to use gene function clustering analysis.

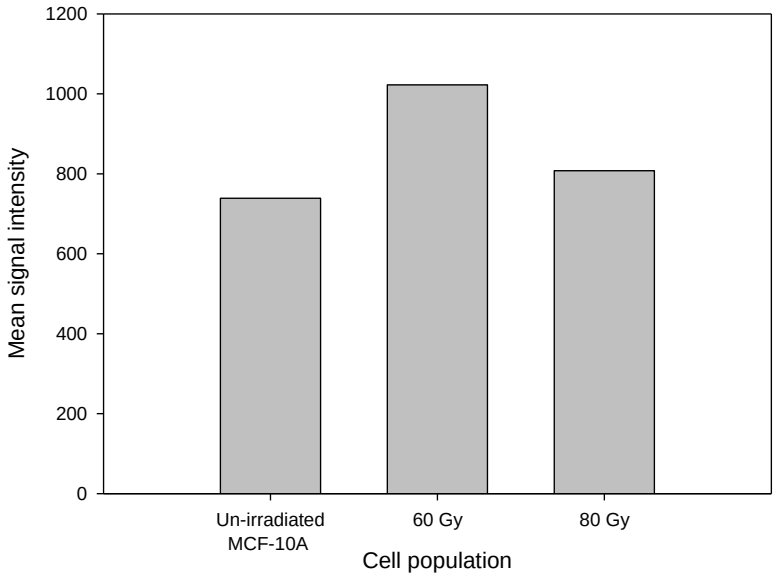

Figure 5.10 Expression analysis of *CDH2* in the Second 5 Gγ series.
The average signal intensity of the single probe which hybridises to the transcript of *CDH2* in the un-irradiated MCF-10A, 60 Gγ and 80 Gγ populations.

5.4 Discussion

High density SNP array analysis of irradiated MCF-10A populations detected numerous copy number alterations induced by ionising radiation. Change in gene copy number can affect cellular phenotype by affecting gene expression. As such, a genome-wide expression array was used to generate a gene expression profile of the First and Second 5 Gγ series. This approach could be used to identify cellular functions affected in irradiated cells, and which might be responsible for radiation-induced phenotypic changes. Furthermore, expression array analysis was also used to investigate the expression of those genes specifically affected by gene copy number alterations.

5.4.1 First 5 Gγ series

Three hundred and ninety putative radiation-induced differentially expressed genes were identified in the 55 Gγ population compared to un-irradiated MCF-10A. The number of differentially expressed genes increased as cumulative dose increased which approximately corresponded to an increase in the number genes with an altered copy number state. This association therefore indicates that copy number alterations directly affect gene expression in the First 5 Gγ series. Similar associations have been made in other *in vitro* studies which have analysed the gene expression profile of cell populations with differing amounts of copy number alteration (Russo and Russo, 2006).

ATM, CUL5 and *SLIT2,* which underwent mono-allelic deletion in the First 5 Gγ series (Chapter 4), showed a concomitant loss of expression. The potential relevance of loss or reduced function of these genes was discussed in section 4.5. Other deleted genes identified in chapter 4 (*CADM1, DCC* and *POU2F1*) were not detected above background in the array and therefore changes in expression could not be analysed. As stated in section 5.2.1, non-detection of probes designed to hybridise to specific transcripts may indicate low expression of the gene, or conversely, that the probes may not bind to the relevant transcript (Barbosa-Morais *et al.*, 2010).

Reduced gene expression often results in reduced protein product. Whether the potential reduction of ATM, CUL5 and SLIT2 transcript is biologically significant in the present study is unknown. The presence of only one functioning copy of *ATM* has been reported to have no effect on cancer risk in mice (Spring *et al.*, 2002); however the functionality of the remaining gene in the present study is unknown. Loss or reduced function of ATM may explain the sudden accumulation of copy number alterations in the 40 Gγ population of the First 5 Gγ series (section 4.5).

Due to the large number of differentially expressed genes in the First 5 Gγ series only the top 10 differentially up-regulated and down-regulated genes (based on their differentiation score) were analysed further. The differentiation score is not a direct representation of the amount of differential expression but is based on the probability that the difference in expression between the test and control samples is real. The probability is however dependant on the difference in signal intensity of the probes between samples (section 2.6.2).

5.4.2 Alternative mechanisms affecting gene expression

Only 3 of the top 20 differentially expressed genes had a concomitant copy number alteration. Therefore 85% of the genes were differentially expressed via other mechanisms. For example, expression or functional changes to transcriptional regulatory proteins such as transcription factors, or epigenetic regulatory proteins can potentially affect the expression of numerous downstream target genes not directly affected by copy number alterations (Sharma *et al.*, 2010; Kanwal and Gupta, 2011). Changes to the methylation profile of the genome which can affect gene expression have been observed *in vivo* and *in vitro* following exposure to ionising irradiation (Raiche *et al.*, 2004; Pogribny *et al.*, 2005; Aypar *et al.*, 2011). Possible radiation-induced alterations to the methylation profile of cells in the present study may therefore

have contributed to expression changes of genes not directly affected by copy number alterations.

Point mutations or small deletions/insertions, which cannot be detected by the SNP 6.0 array, in gene transcription regulatory regions could also affect gene expression. Ionising radiation exposure generates ROS cells which can cause point mutations via oxidative damage. Mutations in promoter regions or other cis-regulatory elements may therefore affect gene expression in the First 5 Gγ series.

Chromosomal translocations can also cause up-regulation or down-regulation of genes while not affecting gene copy number by positioning genes under the influence of strong promoter regions. Translocation of cis-acting transcriptional regulatory elements or translocation breakpoints positioned in non-coding regions which contain cis-acting transcriptional regulatory elements may also affect gene expression (Harewood *et al.*, 2010). Balanced translocations would not be detected by the SNP 6.0 array and it is unknown if cis-regulatory elements have been affected by copy number alterations in non-coding regions of the genome in the present study. Either of these mechanisms could therefore contribute to differential expression of genes not directly affected by copy number change.

5.4.3 Differentially expressed genes in the First 5 Gγ series

Genes of interest in the 20 most differentially expressed genes identified in the First 5 Gγ series included *ASAP3, BCL6, MGMT* (down-regulated) *CCND2 IL24* and *LMTK3* (up-regulated).

ASAP3 is a member of the ARF GTP-ase activating protein (GAP) family, which are involved in the regulation of different cytoskeletal structures important for cell migration and invasion (Randazzo *et al.*, 2007). Reduced expression of ASAP3 was shown to reduce cell migration and invasion (Ha *et al.*, 2008). Down-regulation of this gene may therefore contribute to the apparent reduction in cell migration observed in the First 5 Gγ series (Chapter 3).

BCL6 is a transcriptional repressor that is important for normal antibody response in B and T lymphoid cells (Wagner *et al.*, 2011). BCL6 has at least 500 transcriptional targets (Parekh *et al* 2007) and can interact with at least 61 other proteins (Miles *et al.*, 2005). Expression of BCL6 is also observed in 68% of high grade ductal breast carcinomas and was shown to have an anti-apoptotic role in these cells (Logarajah *et al.*,

2003). Reduced expression of this transcription factor may have affected expression of those genes identified as differentially expressed in the present study, but which were not affected by copy number alterations. A significant reduction in *BCL6* is first identified in the 40 Gγ population, which correlates with a 10 fold increase in differentially expressed genes.

MGMT plays a role in defence against alkylating agents which can form DNA lesions such as O^6-methylguanine (O^6MeG) and O^4-methylthymine (O^4MeT). The O^6MeG and O^4MeT DNA adducts are mispaired during replication and can induce point mutations, sister chromatid exchange and chromosomal aberrations when not effectively repaired (Kaina *et al.*, 2007). MGMT repairs these lesions via non-enzymatic transfer of the methyl group from DNA to a cysteine residue within its own structure, which inactivates MGMT (Kaina *et al.*, 2007). Reduced expression of *MGMT* is predicted to reduce the number of MGMT molecules available for repair of DNA methyl lesions, and could facilitate the accumulation of point mutations. Furthermore, reduced *MGMT* expression could also contribute to the accumulation of copy number alterations by invoking futile DNA mismatch repair of un-repaired O^6MeG lesions, which is thought to induce DNA double strand breaks (Ochs and Kaina, 2000).

Expression of *CCND2* was increased in all analysed irradiated populations relative to un-irradiated MCF-10A. *CCND2* (*cyclin D2*) is involved in regulating progression between G1 and S phase of the cell cycle. D cyclins activate CDK4/6 to phosphorylate retinoblastoma (RB) which releases repression of the transcription factor E2F. Downstream transcriptional targets of E2F in turn stimulate progression of the cell cycle (Ortega *et al.*, 2002). Overexpression of D-type cyclins can therefore accelerate the G1/S transition of the cell cycle (Quelle *et al.*, 1993). Increased expression of *CCDN2* has been observed in cancers such as lymphocytic leukaemia and gastric cancer, but is not seen in the majority of breast cancers (Takano *et al.*, 1999; Igawa *et al.*, 2011). Interestingly, *CCND2* expression is negatively regulated by BCL6 (Shaffer *et al.*, 2000), and the observed reduced expression of *BCL6* may therefore have contributed to increased expression of *CCND2*.

IL24 is a putative tumour suppressor gene which is known to inhibit growth and invasive capabilities and induce apoptosis and radio-sensitivity in cancer cells, including breast cancer cells (Gupta *et al.*, 2006; Patani *et al.*, 2010). Increased

expression of *IL24* may therefore contribute to the radiosensitive phenotype reported in high cumulative dose populations of the First 5 Gγ series (Chapter 3).

LMTK3 has recently been identified as a kinase whose overexpression leads to increased ERα mediated transcription and protection of ERα from proteosomal degradation (Giamas *et al.*, 2011). The protein is over expressed in more aggressive breast cancers and inversely correlates with survival and sensitivity to ERα targeting cancer therapy (Giamas *et al.*, 2011; Stebbing *et al.*, 2011). In the present study the activity of LMTK3 may not be relevant as MCF-10A cells are reported to be ERα negative and ERα gene expression was not detected above background in the expression array (data not shown). However, one hypothesis suggests that ionising radiation and oestrogen synergise to induce breast cancer in young women. If ionising radiation does increase *LMTK3* expression the subsequent effect on ERα activity could be important in this relationship.

5.4.4 Biological processes affected by gene expression changes

Although potentially interesting genes were identified in the 20 gene cohort it is quite hard to infer what effect altered expression would have on biological process in the First 5 Gγ series. All of the identified radiation-induced differentially expressed genes in the 55 Gγ population were therefore used in clustering analysis which identified 10 biological processes potentially affected by gene expression changes. Three of these biological processes were involved in regulation of apoptosis. Dysregulation of programmed cell death is a well-established hallmark of cancer (Lowe and Lin, 2000; Hanahan and Weinberg, 2011). Dysregulated apoptosis allows cells to continue to proliferate when normally they would die, for example at high cell density, and also allows the accumulation of sub-lethal mutations. In the First 5 Gγ series contact inhibition was lost at high cell density and populations accumulated numerous copy number alterations (chapter 3 and chapter 4). Although the direct effect of gene expression change on the apoptotic processes identified by cluster analysis is not determined, loss of contact inhibition provides evidence that cells of the First 5 Gγ series may have acquired a pro-survival phenotype.

Other biological processes potentially affected by expression changes that may be relevant to cell transformation or responsible for the phenotypes observed in the First 5 Gγ series include:

i) Response to steroid hormone and insulin stimulus - The irradiated cell populations appeared to be less tolerant of growth factor withdrawal than un-irradiated MCF-10A. Altered response to steroid hormones and insulin in the First 5 Gγ series may have caused the MCF-10A cells to be more dependent on these stimuli for growth.

ii) Cell migration - The irradiated populations appeared to be compromised in their migratory capabilities compared to un-irradiated MCF-10A cells.

iii) Negative regulation of cell growth - The irradiated populations had a slower rate of growth than un-irradiated MCF-10A cells.

Overall, expression analysis of the First 5 Gγ series has demonstrated that the accumulation of copy number alterations affected the expression of numerous genes. Regulatory mechanisms controlling gene expression may have been affected in the First 5 Gγ series, indicated by the accumulation of differentially expressed genes not directly affected by copy number change. Some of the most differentially expressed genes have roles in cancer and potential phenotypic consequences in the First 5 Gγ series were suggested. The biological processes potentially affected by altered gene expression that may also have had phenotypic consequences in the First 5 Gγ series were also discussed. Alterations to genes involved in DNA repair such as *ATM, MGMT* and *POU2F1,* and dysregulation of programmed cell death may have contributed to the observed accumulation of copy number alterations. The effect of copy number loss on *POU2F1* expression could not be determined from the expression array but will be assessed in chapter 6.

5.4.5 Second 5 Gγ Series

The Second 5 Gγ series had remarkably fewer differentially expressed genes that the First 5 Gγ series. This is likely due to fewer copy number alterations in the Second 5 Gγ series than the First 5 Gγ series (section 4.5). The oestrogen treated passage control population had a large number of differentially expressed genes which reflects the large number of genes which have changed copy number state due to trisomy involving several chromosomes. Other regulatory mechanisms of gene expression (discussed in section 5.4.2) will undoubtedly have been affected in the passage control population also. The large number of differentially expressed genes in the passage control population may have caused an under-estimation of radiation-induced changes in the

Second 5 Gγ series, as changes seen in both irradiated and passage control populations were removed from the analysis.

The two focal copy number alterations identified in the Second 5 Gγ series were a mono-allelic deletion of *BMPR1A* and a copy number gain of *c-MYC*. Altered expression of these genes was consistent with the observed copy number change of the gene, however neither genes were attributed a differentiation score. Both *BMPR1A* and *c-MYC* are involved in transcriptional regulation (Chen and Yager, 2004; Dang *et al.*, 2006). Altered expression of these genes may therefore impact on expression of their transcriptional targets. The increase in the number of differentially expressed genes in the 40 Gγ population coincides with the first appearance of copy number changes to both *BMPR1A* and *c-MYC*.

Of the 32 differentially expressed genes in the 60 Gγ and 80 Gγ populations, 7 were expression changes that have been reported to be differentially expressed during EMT, including down-regulation of *CDH1*, *KRT14*, *PI3*, *FGFBP1*, *KRT17P3* and *CD24* and up-regulation of *SERPINE1* (Thiery, 2003; Vincent-Salomon and Thiery, 2003; Huber *et al.*, 2005; Higashikawa *et al.*, 2008; Ke *et al.*, 2008; Mani *et al.*, 2008; Sarrio *et al.*, 2008; Samarakoon *et al.*, 2009; Cho *et al.*, 2010; Micalizzi *et al.*, 2010; Asiedu *et al.*, 2011; Hanahan and Weinberg, 2011; Hesling *et al.*, 2011). Overexpression of *c-MYC* has been shown to induce EMT in MCF-10A cells (Liu *et al.*, 2009; Cho *et al.*, 2010). Differential expression of genes which associate with EMT may therefore have been due to the copy number increase of *c-MYC* observed in irradiated populations in the present study. The identification of a copy number increase of *c-MYC*, which has been shown to induce EMT *in vitro*, strengthens the hypothesis from chapter 3 that cells in the Second 5 Gγ series were undergoing EMT (Cowling and Cole, 2007; Liu *et al.*, 2009; Smith *et al.*, 2009; Cho *et al.*, 2010).

5.4.6 Epithelial to mesenchymal transition in the Second 5 Gγ series

Epithelial to mesenchymal transition is the cellular switch between a polarised epithelial phenotype to a motile fibroblastic mesenchymal phenotype and is an important process during embryonic development (Thiery, 2002; Huber *et al.*, 2005). EMT is required for morphogenic movements, endoderm formation, gastrulation and the formation of organs and tissues (Thiery, 2002; Huber *et al.*, 2005). EMT is also important during tumourigenesis as it allows cells to invade and metastasise to other areas of the body and has been observed in many cancer types, including breast cancer (Thiery, 2002;

Thiery, 2003; Vincent-Salomon and Thiery, 2003; Huber *et al.*, 2005; Micalizzi *et al.*, 2010; Hanahan and Weinberg, 2011). EMT is characterised by the loss of epithelial cell markers, the most widely reported being E-Cadherin (CDH1), the acquisition of mesenchymal cell markers such as N-Cadherin (CDH2), Vimentin (VIM) and Fibronectin (FIN), a transition from an epithelial cobblestone appearance to a spindle morphology, increased cell motility and increased invasion capability (Thiery, 2002; Thiery, 2003; Vincent-Salomon and Thiery, 2003; Huber *et al.*, 2005; Micalizzi *et al.*, 2010; Hanahan and Weinberg, 2011). EMT is not instantaneous and intermediate phenotypes and expression profiles are observed depending on the model system used and the factors inducing the EMT switch (Figure 5.11) (Huber *et al.*, 2005; Kalluri and Weinberg, 2009; Hanahan and Weinberg, 2011). Numerous proteins and signalling pathways have been identified which induce EMT in cell line studies including, RAS (Liu *et al.*, 2009), TGF-β (Zavadil and Bottinger, 2005), WNT (Kim *et al.*, 2002), SNAIL (Huber *et al.*, 2005), SLUG (Savagner *et al.*, 1997) and TWIST (Yang *et al.*, 2004). None of these genes underwent a copy number alteration in the Second 5 Gγ series.

c-MYC can also induce EMT *in vitro* and *in vivo* (Cowling and Cole, 2007; Trimboli *et al.*, 2008; Liu *et al.*, 2009; Smith *et al.*, 2009; Cho *et al.*, 2010). Specifically, overexpression of c-MYC induces the EMT morphological phenotype, down-regulates the epithelial marker CDH1, up-regulates EMT inducers SNAIL and TWIST, and also up-regulates mesenchymal markers VIM and FIN (Liu *et al.*, 2009; Smith *et al.*, 2009; Cho *et al.*, 2010). SNAIL transcriptionally represses *CDH1* by binding to E-boxes in the promoter region of the gene (Huber *et al.*, 2005). c-MYC was shown to directly induce transcription of *SNAIL1* (SNAIL) through co-operation with DNA bound SMAD proteins following TGF-β induction (Smith *et al.*, 2009), and also through activation of ERK and NF-κB which activates GSK-3β mediated activation of SNAIL (Cho *et al.*, 2010). *CDH1* was down-regulated in the 60 Gγ population in the present study however the expression of *SNAIL1* was not detected above background (although this does not necessarily mean *SNAIL1* was not expressed).

c-MYC is a relatively poor at inducing EMT and very high expression of c-MYC was required to induce a full complement of gene expression and phenotypic changes (Liu *et al.*, 2009; Cho *et al.*, 2010). Therefore although it has been demonstrated c-MYC expression can drive EMT, the amount of c-MYC expressed in the Second 5 Gγ series may not have been enough to induce full transition to the EMT phenotype. Intermediate

phenotypes and gene expression profiles exist during EMT (Fig. 5.11), so it is possible that cells in the Second 5 Gγ series have been induced into entering EMT by c-MYC but are at an early stage of the transition.

Only 3 expression markers of EMT were identified in the 80 Gγ population compared to 7 in the 60 Gγ population. If functional c-MYC expression had reduced in the 80 Gγ population through inactivating mutations or changes to other genes involved in translation or protein stability then a reversal of the EMT expression profile may be explained. The relative levels of c-MYC expression in the Second 5 Gγ series will be investigated in chapter 7.

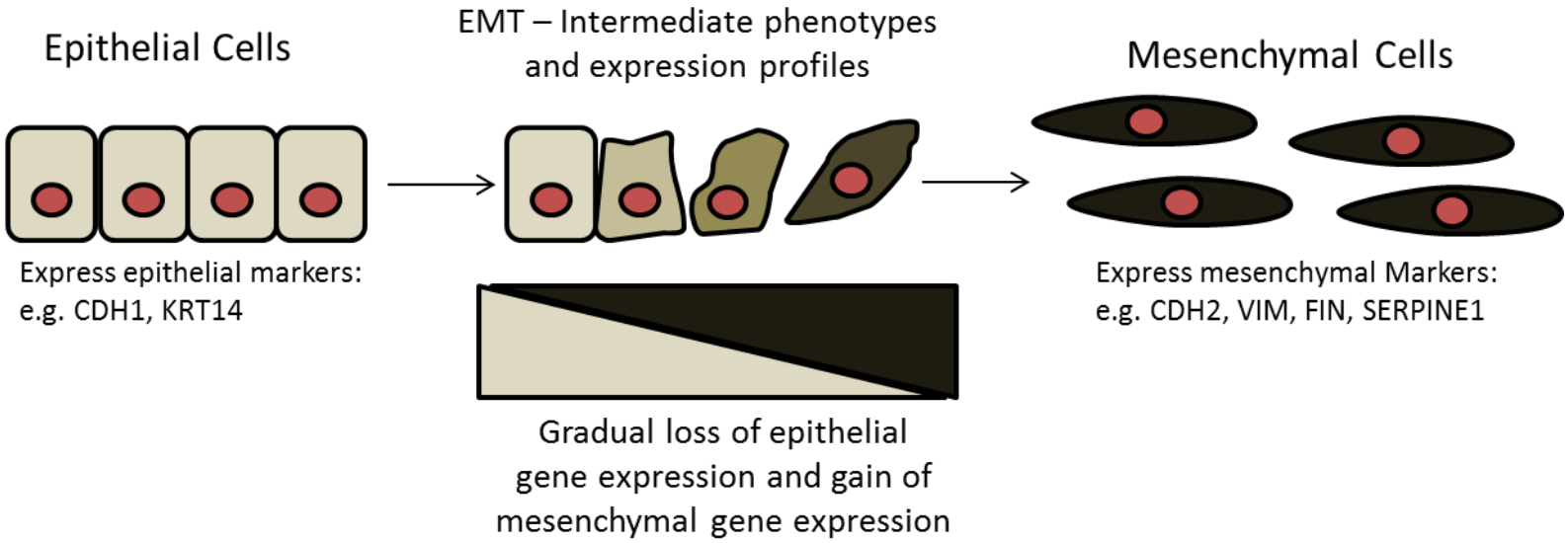

Figure 5.11 Epithelial mesenchymal transition.

The transition from an epithelial cell phenotype to a mesenchymal cell phenotype is not instantaneous and there are intermediate stages between the two cell states. The gradual loss of expression of epithelial cell genes such as *CDH1* and gain of expression of mesenchymal genes such as *VIM* (Vimentin) and *FIN* (Fibronectin) mediate the gradual acquisition of the mesenchymal phenotype. Some cells can therefore acquire a partial EMT-like phenotype without completing the transition. Figure adapted from Kaluri and Weinberg, 2009.

5.4.7 Non-EMT related differentially expressed genes of the Second 5 Gγ series

Other genes which were differentially expressed in the 60 Gγ and 80 Gγ populations of the Second 5 Gγ series which have been implicated in cancer are *H19, EYA2, CCL20* and *LEPREL1*. Although these genes are not reported to be directly related to EMT some of their cellular functions may relate to the EMT phenotype.

H19 was the most differentially up-regulated gene in the 80 Gγ population but was only slightly up-regulated in the 60 Gγ population. *H19* is a non-coding RNA that has been heavily linked with increased tumourigenicity and acquisition of transformed phenotypes *in vitro* (Lottin *et al.*, 2002). Conversely, knockdown of *H19* reduces clonegenicity and anchorage dependant growth (Barsyte-Lovejoy *et al.*, 2006). Consistent with a role as a putative oncogene, *H19* is also up-regulated in a number of cancers, including breast, lung, endometrial, bladder and colorectal cancer (Ariel *et al.*, 2000; Tanos *et al.*, 2004; Barsyte-Lovejoy *et al.*, 2006; Tsang *et al.*, 2010).

c-MYC directly induces *H19* transcription and c-MYC/H19 transcript levels were strongly correlated in breast and lung cancer samples (Barsyte-Lovejoy *et al.*, 2006). Up-regulation of *H19* in the present study may therefore have been due to c-MYC copy number increase. It is also noteworthy that *H19* was the highest differentially expressed gene and *TWIST1* the second highest expressed gene in tumours derived from metastatic cancer cell lines (Yang *et al.*, 2004). As discussed previously, increased TWIST expression and the acquisition of an invasive phenotype are key characteristics of cells undergoing EMT; therefore up-regulation of *H19* may also be an expression marker of EMT. This finding, and the transcriptional link between *H19* and c-MYC, further enhances the case that c-MYC has induced EMT in the present study.

EYA2 is a member of a family of transcriptional co-activators which have key roles in mediating SIX1 transcriptional activation (Farabaugh *et al.*, 2012). SIX1 can induce EMT and stem cell-like phenotypes by up-regulating TGF-β signalling pathways (McCoy *et al.*, 2009; Micalizzi *et al.*, 2010). Loss of EYA2 abrogates SIX1 up-regulation of TGF-β signalling, EMT and stem cell phenotypes in the breast cancer cell line MCF-7 indicating that EYA2 is a critical co-activator of SIX1 induced EMT (Farabaugh *et al.*, 2012). EYA2 has been reported to be over expressed in a number of cancers including ovarian cancer (Zhang *et al.*, 2005a; Farabaugh *et al.*, 2012). Over expression of EYA2 can increase proliferation, migration, invasion and metastasis in

mammary carcinoma cells (Pandey *et al.*, 2010). Up-regulation of *EYA2* observed in the present study may therefore also be an expression marker of EMT.

CCL20 is a chemokine ligand which binds to the chemokine receptor CCR6. *CCL20* was up-regulated in the 60 Gγ population and is also up-regulated in a number of cancers including colorectal cancer and prostate cancer (Beider *et al.*, 2009; Ghadjar *et al.*, 2009; Rubie *et al.*, 2010). Up-regulation of *CCL20* has been implicated in increased cell proliferation and acquisition of a metastatic phenotype (Ghadjar *et al.*, 2009). Up-regulation of *CCL20* has not been implicated in breast cancer or EMT directly, but its established role in mediating metastasis suggests a role in the EMT phenotype.

LEPREL1 is required for collagen synthesis and assembly (Vranka *et al.*, 2004). *LEPREL1* was reported to be epigenetically silenced in breast cancer cell lines, but not in other epithelial cancer cell lines, and was down-regulated in the 80 Gγ population in the present study (Shah *et al.*, 2009). Loss of collagen expression is important in the invasive properties of epithelial cancer (Ikeda *et al.*, 2006). Reduced expression of LEPREL1, and therefore impaired assembly of collagen, may also play a role in the invasive or metastatic phenotype. Again there is no direct link to EMT, however loss of *LEPREL1* is potentially implicated in acquisition of phenotypic characteristics of cells undergoing EMT.

Expression analysis of the Second 5 Gγ series provides strong evidence that irradiated MCF-10A cells have at least initiated EMT, and that this transition is likely to be mediated by the copy number increase of c-MYC. Specifically, expression markers of EMT have been identified in the 60 Gγ and 80 Gγ populations concomitant with increased *c-MYC* copy number. Differentially expressed genes implicated in carcinogenesis but not currently related to EMT could also putatively play a role in EMT as there is a common link with cell invasion and metastasis in their functions. The present study may have therefore identified new putative markers for EMT.

5.4.8 c-MYC, EMT and stem cell phenotypes

Mani *et al.* (2008) recently reported a link between EMT and stem cells. Stem cells can self-renew while also being able to differentiate and generate progenitor cells. Cells with stem cell characteristics have been found in a number of tumours, including breast cancer, and are termed cancer stem cells (Reya *et al.*, 2001). Stem cells are identified by surface expression of CD44 and reduced surface expression of CD24 ($CD24^{-/low}/CD44^{+}$)

(Al-Hajj *et al.,* 2003). Mani et al. (2008) showed that populations which have been induced to undergo EMT become enriched for $CD24^{-/low}/CD44^{+}$ cells and that these cells share properties with normal and cancer stem cells. The $CD24^{-/low}/CD44^{+}$ cells generated also had an EMT expression profile. The study reported that isolated murine and human stem cells which had not been generated by induced EMT shared phenotypic and gene expression characteristics with EMT cells. The study concluded that EMT promotes the generation of cancer stem cells. *CD24* was down-regulated in the 60 Gγ population while CD44 expression remained unaffected. Whether the down-regulation of *CD24* resulted in reduced expression of its protein product in the present study is unknown; however it is possible that cells in the Second 5 Gγ series which have been induced to undergo EMT by c-MYC may share some characteristics with stem cells.

Stem-cell phenotypes include ionising radiation-resistance and a reduction of mutations and double strand breaks induced by ionising radiation (Phillips *et al.,* 2006; Diehn *et al.,* 2009; Vlashi *et al.,* 2009). Diehn et al. (2009) showed that stem cells had fewer intracellular ROS than non-stem cells. Stem cells also had increased expression of anti-oxidant and ROS metabolism genes, as well as increased expression of transcription factors which regulate these genes. Following ionising radiation, which increases intracellular ROS and induces DNA double strand breaks, stem cells had lower levels of ROS and therefore fewer double strand breaks (Diehn et al. 2009; Phillips et al. 2006). Cells in the Second 5 Gγ series had few copy number alterations, which may be partly due to the acquisition of a stem cell DNA damage resistant phenotype conferred by c-MYC-induced EMT. Increased *c-MYC* copy number may therefore be implicated in acquired radiation DNA damage resistance.

5.4.3 Conclusion

The expression analysis of the First and Second 5 Gγ is somewhat limited by the lack of repeats for each sample in the array and the problems this causes when identifying biologically relevant gene expression changes. If expression changes due to radiation exposure were to be investigated further in these populations then further repeats would be needed. Methods such as qPCR could also be used for specific gene targets.

Nevertheless, expression analysis of both the First and Second 5 Gγ series has shed some light on the expression changes which may have contributed to phenotypic changes observed in the different cell populations. Importantly, the expression analysis provides one possible explanation for the disparity in acquired copy number alterations

between the First and Second 5 Gγ series. The First 5 Gγ series appears to have acquired copy number and expression changes which have caused increased chromosomal instability, for example alterations to DNA repair genes and to apoptosis pathways; however the Second 5 Gγ series acquired a specific copy number alteration at the c-MYC locus which may have promoted development of a phenotype similar to that seen in stem cells, and which includes resistance to ionising radiation-induced DNA damage.

Acquisition of a radiation-resistance phenotype may also have implications for the mechanism by which breast cells are transformed by radiation *in vivo*. If ionising radiation induces *c-MYC* amplification, and the evidence from atomic bomb survivors supports this assumption (Miura et al. 2008), then the acquisition of a radiation-resistant phenotype is predicted to result in the enrichment of *c-MYC* amplified cells with subsequent radiation exposure. *c-MYC* amplification on its own may not be sufficient to transform the cells but gene amplification will increase the proportion of cells at risk of acquiring secondary and higher order mutations required for complete transformation. As such, the probability of breast cancer developing in a radiation exposed individual would now be greater as fewer additional mutations would be required for transformation. Increased oestrogen levels in young women with an enrichment of *c-MYC* amplified cells would further increase the chance of transforming "hits" due to its carcinogenic effects; which may explain the putative synergistic relationship seen between ionising radiation and oestrogen.

Chosen genes from each irradiation series (*POU2F1* – First 5 Gγ series; *c-MYC* – Second 5 Gγ series) will be analysed further to assess what significance the copy number and expression changes had on protein level and to assess the relative abundance of each copy number alteration within the heterogeneous cell populations (chapter 6 and chapter 7). The relevance of these alterations in sporadic and radiation-induced breast cancer samples will also be investigated (chapter 8).

Chapter 6: Investigation of the deleted transcription factor *POU2F1* in irradiated MCF-10A (First 5 Gγ series)

6.1 Introduction

The *POU2F1* locus is located in a constitutively trisomic region of chromosome 1q in the un-irradiated MCF-10A genome. Mono-allelic deletion of a 602 Kb region on chromosome 1q which included the *POU2F1* locus was detected in the 40 Gγ cumulative dose population of the First 5 Gγ series. A second deletion on chromosome 1q, which also included the *POU2F1* locus, in the 80 Gγ population resulted in bi-allelic loss of this gene, reducing copy number state from 3 to 1 in the First 5 Gγ series.

POU2F1 is a member of the POU domain transcription factors and is involved in transcriptional regulation of a number of genes including regulation of stress response genes (Tantin *et al.*, 2005). DNA damaging agents which cause oxidative damage, single and double strand breaks induce increased expression of POU2F1 protein levels and enhanced DNA binding activity (Meighan-Mantha *et al.*, 1999; Zhao *et al.*, 2000). POU2F1 regulates promoter binding of BRCA1, and expression of its downstream target genes. Specifically, POU2F1 and BCRA1 co-operate to regulate *GADD45* expression following DNA damage (which helps to maintain genetic stability), and base excision repair (BER) genes following oxidative stress (Jin *et al.*, 2001; Fan *et al.*, 2002; Maekawa *et al.*, 2008; Saha *et al.*, 2010). These findings indicate that POU2F1 plays a major role in cellular response to genotoxic stress. Dysregulation of stress response could result in genetic instability, incorrect repair of DNA damage and the acquisition of oncogenic mutations. The fact that POU2F1 is involved in DNA damage response and that its locus was focally deleted in the First 5 Gγ irradiated series makes it an interesting candidate for further investigation. If *POU2F1* deletion is prevalent in breast cancer that develops following ionising radiation it would identify this lesion as potentially important in the molecular pathogenesis of radiogenic breast disease.

6.1.1 Aim

The aim of the work described in this chapter was to confirm the copy number state of *POU2F1* in cell populations from the First 5 Gγ series using fluorescent *in situ* hybridisation (FISH) and to investigate the effect that gene deletion has on protein level using western transfer. Given that *POU2F1* plays a role in DNA damage response, and in particular *BRCA1* mediated transcriptional regulation of BER genes, the response of

cells from the First 5 Gγ series to oxidative stress was investigated. The expression of DNA repair genes in the 80 Gγ population was also investigated to see what effect, if any, loss of POU2F1 had on BER and other DNA repair pathways.

6.2 In vitro confirmation of *POU2F1* copy number state in the First 5 Gγ series

POU2F1 copy number was investigated in the First 5 Gγ series using FISH. A red fluorescent chromosome 1 centromere probe and a green fluorescent probe mix consisting of 3 BAC probes which map to *POU2F1* were used for cytogenetic analysis (section 2.8). Confirmation that these probes map to the correct chromosome and in the correct region was shown using metaphase chromosomes, prepared by David Rowe (Institute of Genetic Medicine, Newcastle upon Tyne, UK), from un-irradiated MCF-10A cells (Fig. 6.1). Specifically, the green centromere probe hybridised to the centromere of chromosome 1 and the *POU2F1* probe hybridised to a region at the centromeric end of 1q. FISH analysis confirmed that the i(1)(q10) chromosome in MCF-10A was a dicentric chromosome (section 4.2.1).

Figure 6.2a shows the percentage of cells which have 3, 2 and 1 copies of *POU2F1* in each cell population as determined by counting 100 cells for each population. Over 95% of the cells in each cell population displayed 3 chromosome 1 centromere probes consistent with the established copy number state in un-irradiated MCF-10A. The centromere counts are therefore not included on the graph. Standard FISH scoring protocols classify alterations that are seen in less than 5% of all cells scored as "not reportable," and such alterations have therefore not been included in Figure 6.2. FISH images illustrating *POU2F1* copy number in the un-irradiated MCF-10A, 40 Gγ cumulative dose and 80 Gγ cumulative dose cell populations are shown in figure 6.2 b, c, and d.

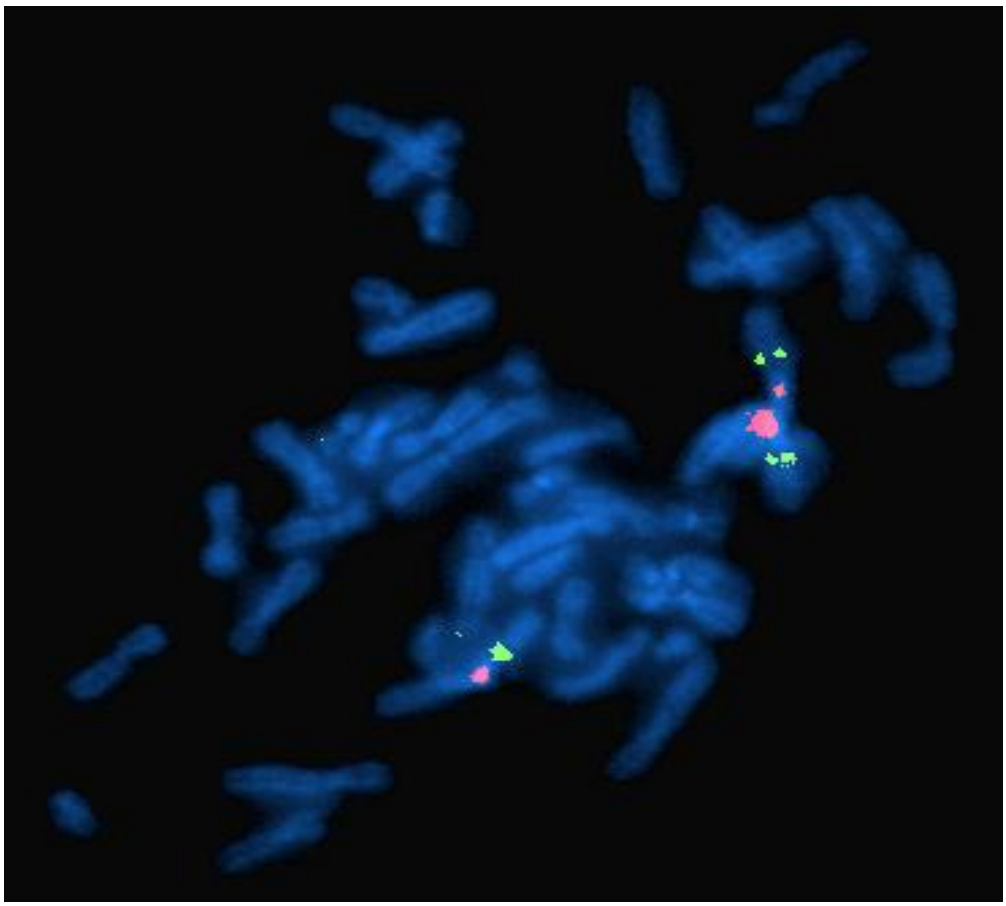

Figure 6.1 Cytogenetic analysis of *POU2F1* in MCF-10A cells.
FISH probes are specific to the centromere of chromosome 1 (red) and the *POU2F1* locus (green). Metaphase chromosomes of un-irradiated MCF-10A were counterstained with DAPI. The probe for *POU2F1* hybridises to the q arm of the same chromosomes as the centromere 1 probe, specifically on a normal chromosome 1 and the dicentric i(1)q(10) chromosome, which is consistent with its position in the genome.

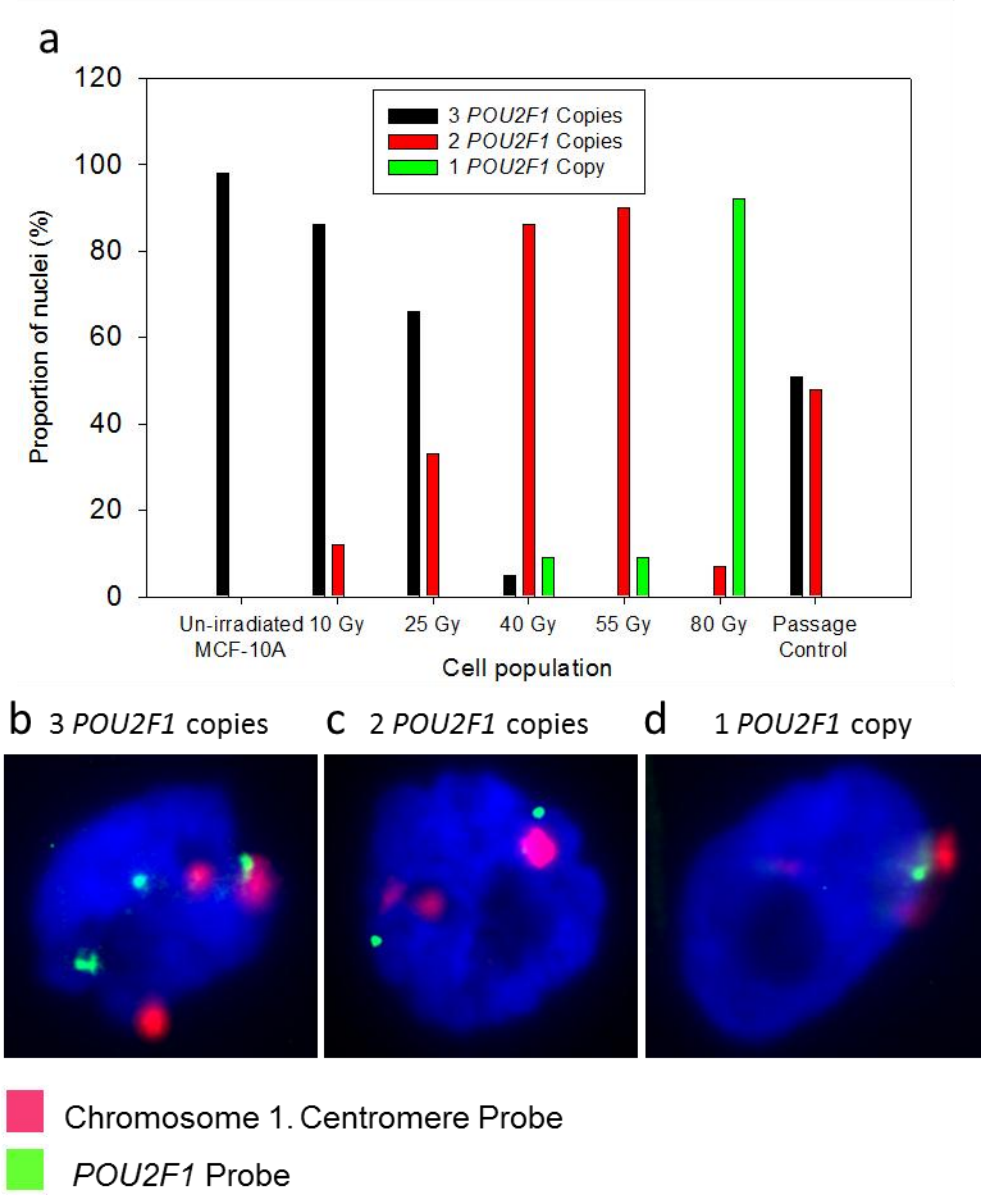

Figure 6.2 Cytogenetic analysis of *POU2F1* in the First 5 Gγ series.
The probes are specific to the centromere of chromosome 1 (red) and the *POU2F1* locus (green) and the cells was counterstained with DAPI. Following FISH on cells in the First 5 Gγ series the percentage of cells with 1 (green bar), 2 (red bar) and 3 (black bar) copies of *POU2F1* could be calculated from counts of 100 cell nuclei in each cell population **(a**). Examples of FISH of the dominant sub-populations in the un-irradiated MCF-10A **(b)**, 40 Gγ cumulative dose **(c)**, and 80 Gγ cumulative dose cell populations **(d)** are also shown.

FISH data agrees with copy number data generated using the SNP 6.0 array. Specifically, in the un-irradiated cell populations and those established following 10 Gγ and 25 Gγ cumulative doses, cells with 3 copies of *POU2F1* represent the dominant cell population, comprising 98%, 86% and 66% of all cells, respectively. In the 40 Gγ cumulative dose population, cells with 2 copies of *POU2F1* represent the dominant population (86% of all cells). The proportion of cells with this genotype persists until the 80 Gγ cumulative dose population when cells with one copy of *POU2F1* represent the dominant population (92% of all cells). The passage control population has approximately equal amounts of cells with 3 and 2 copies of *POU2F1*, which reflects the large mono-allelic deletion on chromosome 1q encompassing the *POU2F1* locus (Table 4.4).

FISH results also illustrate the heterogeneity of the cell populations and the potential for selection of sub-populations with certain genotypes. For example, mono-allelic deletion of *POU2F1* was first identified in the 40 Gγ population by the SNP 6.0 array, however 12% of cells had two copies of *POU2F1* in the 10 Gγ population which rose to 33 % in the 25 Gγ population. These data demonstrate that the mono-allelic deletion of *POU2F1* carried by the majority of cells in the 40 Gγ population may have actually occurred earlier and was then subsequently selected for, and is consistent with the gradual clonal selection model described in section 4.5 and illustrated in figure 4.12. However, it cannot be conclusively determined that the sub-populations with 2 copies of *POU2F1* in the 10 Gγ and 25 Gγ populations contain the same specific *POU2F1* deletion as identified in the 40 Gγ population, because FISH does not discriminate between deletions affecting the same locus but with different breakpoints. As such, it is possible that the *POU2F1* deletion identified in the 40 Gγ population is unique to that population.

Similarly, bi-allelic deletion of *POU2F1* was first identified in the 80 Gγ population by the SNP 6.0 array, however 7% of cells in the 40 Gγ population also had only one copy of *POU2F1*. A rapid increase in the number of cells with one copy of *POU2F1* at the 80 Gγ population indicates that either the population observed in the 40 Gγ population was selected was for or that the bi-allelic deletion of *POU2F1* identified in the 80 Gγ population is unique to that population.

FISH analysis demonstrates that each cell population is genetically heterogeneous. Without SNP analysis data of all sub-populations it is hard to map the true genesis of a

copy number alteration and its subsequent selection, which would require sub-populations to be sorted and purified.

SNP analysis measures the mean copy number of the entire population. Overall the SNP genotype of the *POU2F1* locus in each cell population agrees with the dominant genotype identified by FISH in each population of the First 5 Gγ series.

6.3 Protein expression of POU2F1 in the First 5 Gγ series

In order to determine the effect of *POU2F1* copy number on protein expression POU2F1 protein levels in un-irradiated MCF-10A, First 5 Gγ series and passage control cells were analysed by western transfer and immunoblot (section 2.10). Representative images of the immunoblot analysis are shown in figure 6.3a and b. A strong band of the correct mass for POU2F1 (95 kDa) was observed in the un-irradiated MCF-10A cell population. POU2F1 expression in the First 5 Gγ series was reduced in the 40 Gγ and 55 Gγ cumulative dose cells compared to the un-irradiated, 10 Gγ and 25 Gγ cells, and is almost undetectable in the 80 Gγ cells (Fig. 6.3a). POU2F1 expression is also noticeably lower in the passage control cells compared to un-irradiated MCF-10A, consistent with mono-allelic deletion in a significant fraction of the cells (Fig. 6.3b; Turkey's Test: p=0.042).

POU2F1 expression was quantified by densitometric analysis of 3 independent experiments and normalised using GAPDH expression (Fig. 6.3c). Expression of POU2F1 in the 40 Gγ and 55 Gγ cell populations is more than two fold lower than expression in un-irradiated MCF-10A cells (Turkey's Test: p=0.017; p=0.006). In the 80 Gγ population expression of POU2F1 has fallen to 2% of the level in un-irradiated MCF-10A cells (Turkey's Test: p<0.001).

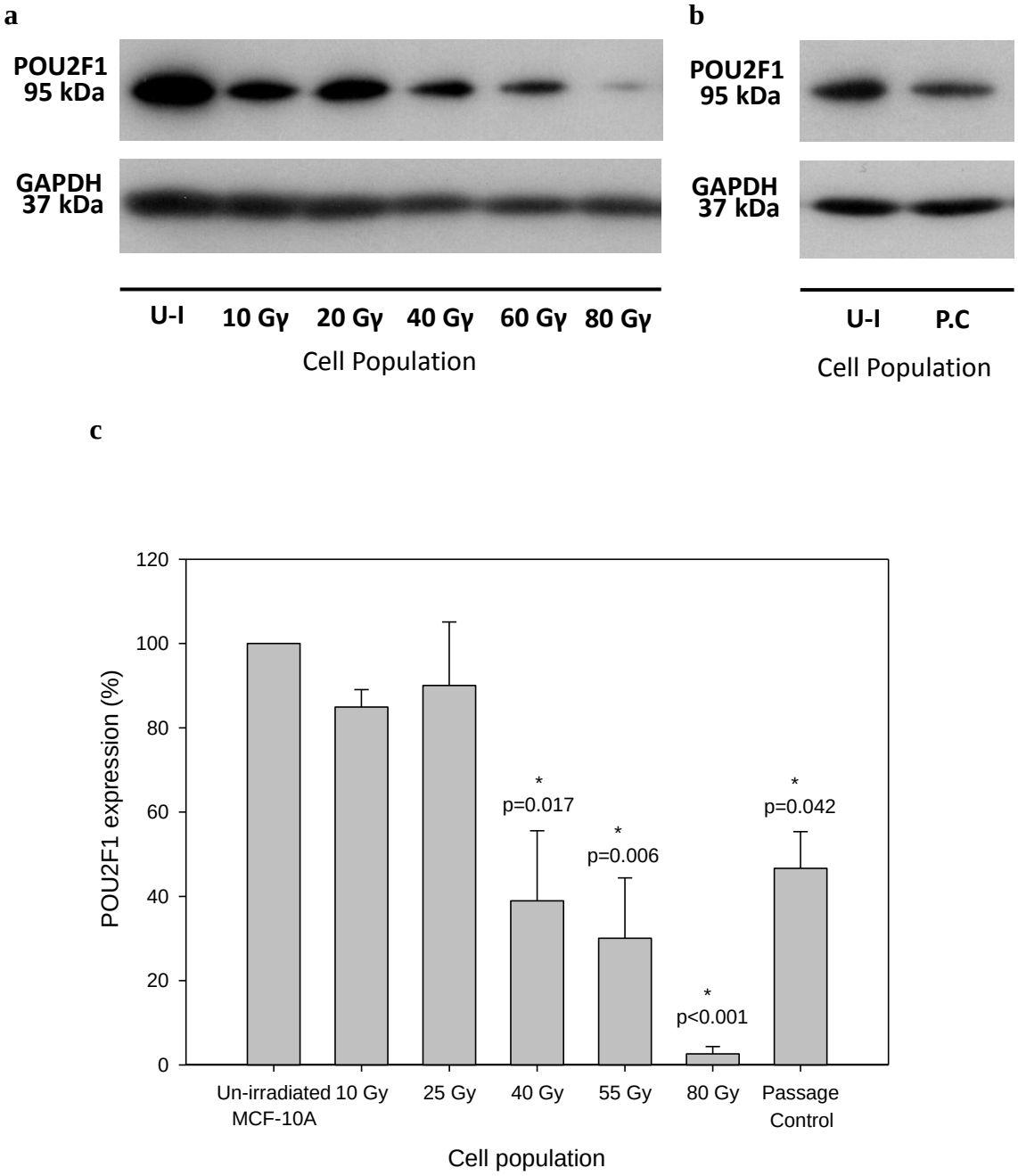

Figure 6.3 POU2F1 expression in the First 5 Gγ series.
Western transfer analysis of the First 5 Gγ series **(a)** and passage control population **(b)** with antibodies specific for the 95kDa protein POU2F1 and 37kDa protein GAPDH. Densitometric analysis of 3 independent western transfers was used to quantify the expression of POU2F1 for each cell population as a percentage of the expression of POU2F1 in un-irradiated MCF-10A cells (which was set at 100% expression) **(c)**. U-I = un-irradiated MCF-10A and P.C = passage control in cell population lane identifiers below each image in **(a)** and **(b)**. 10 μg of protein was used for each cell population in each experiment. Although irradiated and passage control populations were analysed separately the same un-irradiated MCF-10A protein extracts were used and expression was expressed as a percentage of the expression of c-MYC in un-irradiated MCF-10A cells within these experiments. To calculate the relative protein expression of POU2F1, band intensity was normalised against GAPDH band intensity within each experiment. Difference in expression between populations below the 5% confidence level was tested (ANOVA: $p<0.001$). A post hoc Turkey's test was then used to assess the difference in expression between individual populations below the 5% confidence level. (*) indicates populations whose POU2F1 protein expression was significantly different from un-irradiated MCF-10A.

The reduction in POU2F1 expression corresponds to when the deletions of POU2F1 are detected in the SNP 6.0 Array. This relationship indicates that the amount of POU2F1 protein expressed is directly affected by the copy number state of the gene. The 80 Gγ cumulative dose cells have 1 copy of POU2F1 which almost completely removes POU2F1 expression. Complete loss of expression may indicate that loss of only one POU2F1 allele in cells diploid for POU2F1 is sufficient to almost completely abrogate POU2F1 expression, or that the protein is unstable at low concentrations. The dramatic reduction in POU2F1 expression may also be due to other mutations, either in POU2F1 itself or other genes, which affect POU2F1 transcription, transcript stability or protein stabilisation.

6.4 Response of cells from the First 5 Gγ Series to DNA damage

POU2F1 plays a role in response to DNA damage caused by numerous DNA damaging agents (Meighan-Mantha *et al.*, 1999; Zhao *et al.*, 2000; Jin *et al.*, 2001; Fan *et al.*, 2002; Tantin *et al.*, 2005; Maekawa *et al.*, 2008). In particular, POU2F1 deletion has been shown to dysregulate oxidative stress response genes (Tantin *et al.*, 2005) and is directly involved in BRCA1 mediated transcriptional induction of BER genes in response to oxidative damage (Saha *et al.*, 2010). The 80 Gγ cumulative dose cell population expresses negligible amounts of POU2F1 and therefore response to oxidative damage may be compromised. In order to test this, the response of un-irradiated MCF-10A cells and 80 Gγ cumulative dose cells to oxidative damage by hydrogen peroxide (H_2O_2) was tested. Cells were seeded at $4x10^3$ cells per well in 96 well plates and treated with 0-450 μM of hydrogen peroxide. Twenty-four hours after hydrogen peroxide treatment, the number of cells in each well was determined using the Resazurin assay for cell viability (Section 2.11). The mean number of hydrogen peroxide treated cells was expressed as a percentage of the mean number of vehicle-only treated cells over the same time period (Fig. 6.4). Reduced cell number after hydrogen peroxide treatment would indicate reduced cell growth and therefore increased sensitisation to oxidative stress.

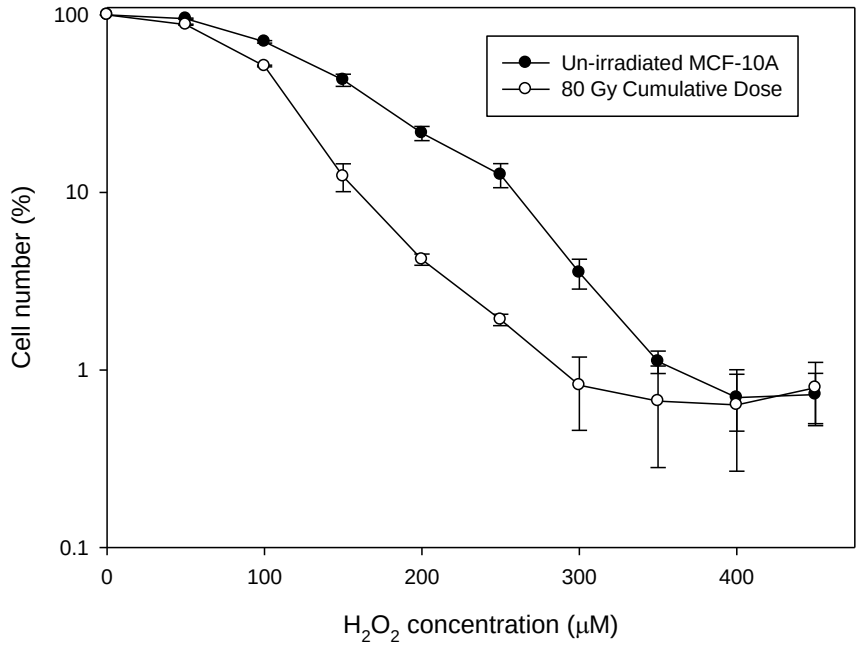

Figure 6.4 Response of un-irradiated MCF-10A cells and 80 Gγ cumulative dose cells (First 5 Gγ series) to hydrogen peroxide.
Cells were treated with 1-450uM H_2O_2 for 24 hours. The surviving cell number for each concentration of H_2O_2 is expressed as a percentage of the number of vehicle-only treated cells. Mean values of surviving cell numbers from multiple experiments are expressed +/- SEM (un-irradiated MCF-10A *n*=5; 80 Gγ cumulative dose *n*=4). An ANOVA test was used to assess statistical significance of cell number percentage between each H_2O_2 concentration within each cell population: un-irradiated MCF-10A p<0.001; 80 Gγ cumulative dose p<0.001. A post-hoc Turkey's test was used to asses at which concentrations cell number percentage was significantly different within the same cell population. A paired T-test was used to test for significant differences in growth inhibition at each concentration of H_2O_2: 0 μM p=1; 50 μM p=0.005; 100 μM p=0.020; 150 μM p=0.001; 200 μM p-0008; 250 μM p=0.025; 300 μM p=0.028, 350 μM p=0.352; 400 μM p=0.846; 450 μM p=0.579.

In both populations cell number reduced as hydrogen peroxide concentration increased. Significant reduction in cell number occurred after treatment with 50 μM of hydrogen peroxide in the 80 Gγ population (Turkey's test: p<0.001) and after 100 μM in the un-irradiated MCF-10A population (Turkey's test: p<0.001). The working range of the assay does not go below approximately 98% growth inhibition (2% cell number). Both populations reached this threshold after treatment with 350-450 μM of hydrogen peroxide. The 80 Gγ population had fewer cells compared to the un-irradiated MCF-10A population 24 hours after treatment with 50-300 μM of H_2O_2 (Paired T-Test: p < 0.050) (Un-irradiated MCF-10A GI50 = 135 μM, GI90 = 254 μM; 80 Gγ population GI50 = 101 μM, GI90 = 157 μM). The difference was most pronounced after treatment with 250 μM of H_2O_2 (6.5 fold difference in cell number). The results indicate that the 80 Gγ cumulative dose cell population was more sensitive to hydrogen peroxide than the un-irradiated MCF-10A cell population.

The response of un-irradiated MCF-10A cells and 80 Gγ cells to DNA damage by doxorubicin was also investigated (Fig. 6.5). Doxorubicin undergoes redox cycling which generates reactive oxygen species and induces DNA damage similar to that induced by hydrogen peroxide. However, its main cytotoxic mechanism is through interference with topoisomerase II which generates DNA strand breaks. There was a doxorubicin dose-dependent reduction in cell growth in both cell populations, with significant reductions in cell number following treatment with 100-1000 μM doxorubicin (Turkey's test: $p<0.001$). The 80 Gγ cell population was significantly more sensitive to 100 μM doxorubicin than un-irradiated MCF-10A cells (Paired T-test: $p=0.029$), although the difference in sensitivity was relatively modest (Un-irradiated MCF-10A GI50 = 340 μM; 80 Gγ population GI50 = 112 μM). The 80 Gγ cumulative dose population therefore appeared to be more sensitive to doxorubicin than the un-irradiated MCF-10A cell population but the sensitivity was not as pronounced as with hydrogen peroxide treatment.

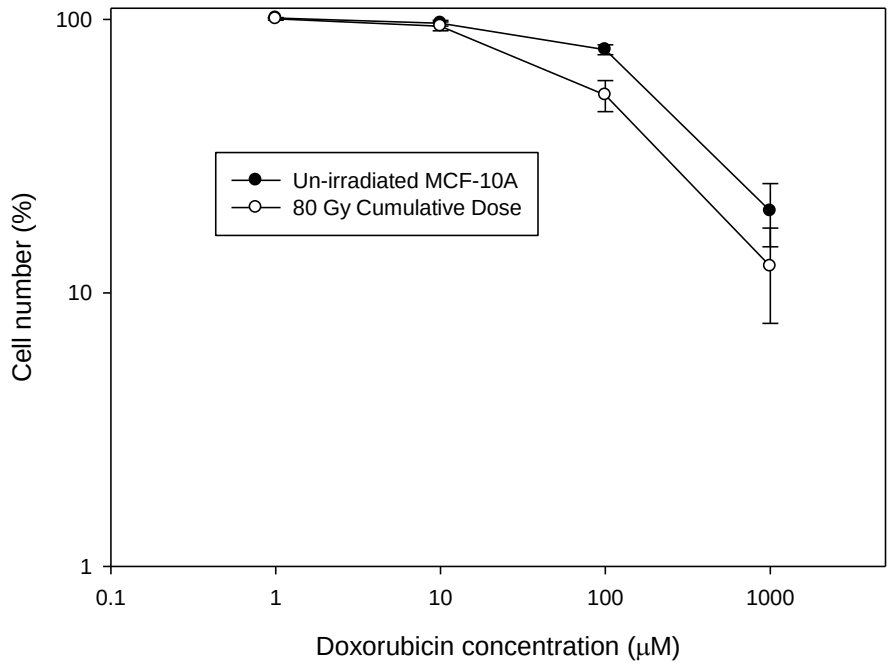

Figure 6.5 Response of un-irradiated MCF-10A cells and 80 Gγ cumulative dose cells (First 5 Gγ series) to doxorubicin.
Cells were treated with 1-1000uM doxorubicin for 72 hours The surviving cell number for each concentration of doxorubicin is expressed as a percentage of the number of vehicle-only treated cells. Mean values from multiple experiments are expressed +/- SEM (un-irradiated MCF-10A $n=5$; 80 Gγ cumulative dose $n=4$). An ANOVA test was used to assess statistical significance of cell number percentage between each doxorubicin concentration within each cell population: un-irradiated MCF-10A $p<0.001$; 80 Gγ cumulative dose $p<0.001$. A post-hoc Turkeys test was used to asses at which concentrations cell number percentage was significantly different within the same cell population. A paired T-test was used to test for significant differences in growth inhibition at each concentration of doxorubicin: 0 μM p=1; 1 μM p=0.600; 10 μM p=0.264; 100 μM p=0.029; 1000 μM p-0078.

6.5 Expression of DNA repair genes in the 80 Gγ cumulative dose population of the First 5 Gγ series

Sensitivity to the cytotoxic effects of hydrogen peroxide and doxorubicin in the 80 Gγ population (section 6.4) suggests a deficiency in DNA repair and in particular base excision repair of oxidative DNA lesions. In order to test whether DNA repair expression is affected in POU2F1-deleted cells a Real-Time PCR array of DNA repair genes was used to analyse basal gene expression of un-irradiated MCF-10A cells and 80 Gγ cumulative dose cells. BER genes known to be transcriptionally regulated by POU2F1 and BRCA1 were also specifically investigated (section 6.5.3).

6.5.1 Expression of DNA repair genes in the 80 Gγ cumulative dose population

DNA repair genes that have a minimum two fold increase or decrease in gene expression in the 80 Gγ cumulative dose population compared to the un-irradiated MCF-10A population under basal conditions are shown in table 6.1. Fold decreases are shown in blue and fold increases in red. The copy number changes of the genes between the un-irradiated MCF-10A cell population and the 80 Gγ cumulative dose cell population are also shown.

Gene expression changes may occur due to changes in the copy number of that gene, changes in the transcriptional mechanisms/regulation of the gene or mutations in the genes themselves which dysregulate transcription (for review see section 5.4). Two genes identified by the DNA repair gene array show gene expression changes and a corresponding copy number alteration; these are *ATM* which has been discussed previously (section 4.5) and *MPG,* which encodes a 3-methladenine DNA glycosylase. Specifically, mono-allelic deletion of *MPG* (located on chromosome 16p), is associated with a three-fold reduction in gene expression (Table 6.1), suggesting a direct association between copy number and expression. Conversely, however, a single copy gain at the locus for *NEIL1* on chromosome 15q is inconsistent with the observed two-fold decrease in gene expression.

Gene	Fold Increase/Decrease	Copy Number Change	Resulting copy number of copies in 80 Gγ population
MGMT	-4.5065	none	2
RAD50	-3.487	none	3
MPG	-3.0147	-1	1
MSH4	-2.9322	none	2
NEIL1	-2.7741	+1	3
RAD51D	-2.5704	none	2
MLH3	-2.5175	none	2
ATM	-2.3817	-1	1
PARP3	-2.2377	none	2
NTHL1	-2.0028	none	2
NEIL3	2.0111	none	2
RPA3	2.0534	none	2

Table 6.1 Differentially expressed DNA repair genes in the 80 Gγ cumulative dose cells compared to un-irradiated MCF-10A cells.
Genes which show at least a 2 fold increase or decrease in expression in the 80 Gγ population compared to the un-irradiated MCF-10A population are listed. Decrease in expression is shown in blue and increase is shown in red. The copy number change of the gene in the 80 Gγ population compared to the un-irradiated MCF-10A population is also shown. none = no change, +*n* = number of copies gained and -*n* = number of copies lost. The resulting copy number state in the 80 Gγ population is also displayed.

Of the 12 genes listed in table 6.1, only *MGMT* and *ATM* showed differential gene expression in other cell populations of the First 5 Gγ series following analysis with the Illumina HT12 v4 expression array (chapter 5). Specifically, *MGMT* had reduced in expression in the 55 Gγ population and *ATM* had reduced expression in both the 40 and 55 Gγ populations. There was also reduced expression of *PARP3* in the 55 Gγ population but this was not attributed a differentiation score (data not shown). Four of the remaining 9 genes were not detected above background by the Illumina HT12 v4 expression array (*MPG, MSH4, NEIL1* and *MLH3*). For genes detected above background (*RAD50, RAD51D, NTHL1, NEIL3* and *RPA3*) expression did not change between the 25 Gγ and 55 Gγ populations compared to un-irradiated MCF-10A; it is therefore likely that genetic alterations between the 55 Gγ and 80 Gγ populations affected expression of these genes.

6.5.2 Expression of BER genes transcriptionally regulated by POU2F1 and BRCA1

Saha et al. (2010) showed that POU2F1 was essential for BRCA1 mediated up-regulation of the BER genes *NTHL1, APEX1, XRCC1* and *OGG1* following oxidative damage; however complete loss of POU2F1 expression only affected basal expression of *NTHL1*, whereas a reduction in expression of BRCA1 reduced basal expression of all four genes. Saha and colleagues concluded that BRCA1 was the limiting factor of *NTHL1, APEX1, XRCC1* and *OGG1* basal expression, but that POU2F1 was an

essential component of the BRCA1 complex that induces up-regulation of these genes in response to genotoxic stress. The basal expression of *NTHL1, APEX1, XRCC1, OGG1* and *BRCA1* was assessed in the POU2F1-deleted 80 Gγ population (Table 6.4).

Gene	Fold Increase/Decrease
NTHL1	-2.0028
APEX1	-1.9346
XRCC1	-1.3213
OGG1	-1.0367
BRCA1	-1.3213

Table 6.2 Relative expression of BER genes transcriptionally regulated by POU2F1 and BRCA1. The fold decrease in gene expression of *NTHL1, APEX1, XRCC1, OGG1* and *BRCA1* in the 80 Gγ cumulative dose population compared to expression in the un-irradiated MCF-10A population.

Only *NTHL1* had at least a 2 fold decrease in basal expression although the expression of *APEX1* was also close to a 2 fold reduction. Expression of *NTHL1* and *APEX1* was not affected in other populations of the First 5 Gγ series (data not shown). The difference in basal expression of *XRCC1, OGG1* and *BRCA1* between the un-irradiated MCF-10A and 80 Gγ population was relatively small. The expression profile of *NTHL1, APEX1, XRCC1* and *OGG1* under basal conditions in the POU2F1 deleted 80 Gγ population therefore agreed with the findings by Saha et al. (2010); however data from the present study also suggested that basal expression of *APEX1* may be affected by POU2F1 loss.

6.6 Discussion

POU2F1 is a transcription factor involved in regulation of genes following genotoxic stress; including DNA repair and other genes involved in maintaining genetic stability (Meighan-Mantha *et al.*, 1999; Zhao *et al.*, 2000; Jin *et al.*, 2001; Fan *et al.*, 2002; Schild-Poulter *et al.*, 2003; Wang *et al.*, 2004a; Maekawa *et al.*, 2008; Saha *et al.*, 2010) (Reviewed in section 4.5.2). A focal mono-allelic deletion of the *POU2F1* locus was detected using SNP array analysis in the 40 Gγ cumulative dose population of the First 5 Gγ series (chapter 4). The *POU2F1* locus is in a constitutively triploid region of chromosome 1q in MCF-10A cells, therefore the focal deletion reduced the copy number state of *POU2F1* to 2. A further non-focal deletion on chromosome 1q was detected in the 80 Gγ population which reduced the copy number state of *POU2F1* to 1.

The following sections will discuss the relevance of *POU2F1* deletion and concomitant loss of protein expression on DNA damage response and the accumulation of DNA damage in the First 5 Gγ series.

6.6.1 POU2F1 copy number state and protein expression

FISH analysis of the *POU2F1* locus confirmed that in every population of the First 5 Gγ series where SNP data suggested a deletion, a deleted genotype was present in the dominant sub-population. FISH analysis also implied that the deletions of *POU2F1* may have occurred earlier in the irradiation series than when detected by the SNP 6.0 array and those sub-populations with *POU2F1* deletions were subsequently selected for, although it is not possible to determine whether POU2F1 deletion directly conferred a growth advantage. Further, it cannot be confirmed that the deletions of *POU2F1* detected by FISH in the non-dominant sub-populations of the First 5 Gγ series were the same specific deletions detected by the SNP 6.0 array in the 40 Gγ and 80 Gγ populations.

Expression analysis of *POU2F1* by the Illumina HT12 v4 expression array was un-informative as the probe representing *POU2F1* was only marginally detected above background in un-irradiated MCF-10A cells (chapter 5). Protein expression analysis by Western transfer and immunoblot however confirmed that POU2F1 is expressed in MCF-10A cells and that reduced expression is concomitant with deletion of the gene. Almost complete loss of expression in the 80 Gγ cells implies that either transcription from a single allele is not sufficient to maintain significant expression levels (possibly due to protein instability at low levels), or that a further mutation occurred in the 80 Gγ population which affected expression of the remaining allele.

Saha et al. (2010) showed that the expression of the BER gene *NTHL1* was only reduced in *POU2F1*$^{-/-}$ fibroblasts and not in cells with approximately 60 % reduced protein concentration. In the present study a Real-Time PCR array, used to compare basal expression of DNA repair genes in the un-irradiated MCF-10A and 80 Gγ cell populations, identified a unique 2 fold reduction in expression of *NTHL1* in the 80 Gγ population. Other genetic alterations may have affected *NTHL1* expression but the result indicates that expression of POU2F1 in the present study may have conferred the same effect as seen in null (*POU2F1*$^{-/-}$) cells, and therefore provides further evidence that POU2F1 expression was effectively lost in the 80 Gγ population.

The amount of POU2F1 expressed under basal conditions may be a limiting factor in POU2F1-mediated response to genotoxic stress as loss of protein expression under basal conditions has been shown to attenuate the DNA damage response. For example, reduced basal expression of POU2F1 attenuates induction of *CDNK1A* transcription

following ionising radiation (Nenoi *et al.*, 2009). Studies have also shown that increase in POU2F1 levels after genotoxic stress is not mediated by an increase in transcription but by kinase-mediated post-translational stabilization of the protein (Meighan-Mantha *et al.*, 1999; Zhao *et al.*, 2000; Tantin *et al.*, 2005; Schild-Poulter *et al.*, 2007; Wang and Jin, 2010). For example, POU2F1 induction after DNA damage induced by ionising radiation is abrogated when the kinase activity of DNA-PK is lost (Schild-Poulter *et al.*, 2007), although this has no effect on basal levels of POU2F1 (Schild-Poulter *et al.*, 2007). Loss of POU2F1 expression in the present study may therefore have attenuated DNA damage response. The concentration of POU2F1 directly after ionising radiation treatment would need to be assessed in the First 5 Gγ series to investigate whether reduced basal expression affected protein induction following ionising radiation however.

6.6.2 POU2F1 and DNA damage response

As described previously, POU2F1 expression is essential for the BRCA1 mediated up-regulation of the BER genes *NTHL1, APEX1, XRCC1* and *OGG1* (Saha *et al.*, 2010). Loss of BRCA1/POU2F1 induction of these genes increased sensitivity to oxidative damage by hydrogen peroxide. Increased sensitivity to oxidative stress in cells with reduced POU2F1 activity has been observed in a number of other studies (Tantin *et al.*, 2005; Wang and Jin, 2010). An increase in sensitivity to hydrogen peroxide and doxorubicin in the present study has been demonstrated, which could be due to POU2F1 loss.

Reduced POU2F1 activity also leads to increased sensitivity to ionising radiation (Zhao *et al.*, 2000; Tantin *et al.*, 2005). Loss of POU2F1 could affect BER of oxidative damage caused by ROS generated following radiation exposure. POU2F1 has also been implicated as having a direct role in non-homologous end joining, which is responsible for repairing double strand DNA breaks (Schild-Poulter *et al.*, 2001). The gradual reduction in loss of POU2F1 in the First 5 Gγ series may therefore have contributed to the apparent increase in radio-sensitivity in irradiated populations (chapter 3).

POU2F1 is also part of a BRCA1/NF-κB complex which is an important transcriptional regulator of *p53* independent induction of GADD45 following DNA damage (Jin *et al.*, 2001; Fan *et al.*, 2002; Maekawa *et al.*, 2008). Loss of POU2F1 activity reduced transcription of GADD45A following genotoxic stress (Jin *et al.*, 2001; Fan *et al.*, 2002). GADD45A coordinates numerous cellular responses through interactions with partner

proteins in response to genotoxic stress, including DNA damage repair, cell cycle arrest and activation of stress response kinases (Liebermann and Hoffman, 2008). *GADD45A*$^{-/-}$ mice developed mammary tumours and displayed increased mutation frequency in response to ionising radiation (Liebermann and Hoffman, 2008). Loss of GADD45A induction due to POU2F1 loss may therefore increase DNA damage, mutation and genetic instability. POU2F1 also plays a role in BRCA1-mediated transcription of the spindle checkpoint gene *MAD2* (Wang *et al.*, 2004a). The spindle checkpoint is important for maintaining chromosomal integrity. Loss of *MAD2* expression abrogates the spindle checkpoint, promotes chromosome mis-segregation and therefore the accumulation of DNA damage.

Loss of POU2F1 expression in the present study may therefore have contributed to the accumulation of copy number alterations and gene expression changes identified in the First 5 Gγ series following ionising radiation treatment (chapter 4 and 5). The increase in genetic instability and accumulation of potentially advantageous mutations may have led to the apparent selection of cell sub-populations with a *POU2F1* deletion identified by FISH analysis.

It should also be noted that there was a two-fold change in the expression of 12 DNA damage repair genes which may also have contributed to the increased sensitivity to genotoxic stress and the accumulation of copy number alterations and gene expression changes in the First 5 Gγ series.

Genes which showed reduced expression included: *MGMT* which repairs the O^6-alkylguanine DNA lesion caused by alkylating agents (discussed in section 5.4.1), *MSH4* and *MLH3* which have roles in DNA mismatch repair (Santucci-Darmanin *et al.*, 2002; Jaafar and Flores-Rozas, 2009), *RAD50* which is involved in DNA double strand break response, *RAD51D* which plays a role in homologous recombination and telomere maintenance (D'Amours and Jackson, 2002; Shiloh, 2006; Czornak *et al.*, 2008) and *ATM* which is also involved in double strand break stress response (Shiloh, 2003). Reduced expression of *RAD50, RAD51D* and *ATM* may have contributed to the accumulation of copy number alterations, increase in radiation sensitivity and telomere loss due to the abrogation of DNA double strand break repair and telomere maintenance. Of the genes with increased expression *NEIL3* is implicated in BER (Liu *et al.*, 2010) and *RPA3* is postulated to have a role in repair of single strand DNA (Salas *et al.*, 2009).

Four of the 10 down-regulated genes have a role in the BER pathway (*MPG, NEIL1, PARP3,* and *NTHL1*). Reduction in the basal levels of expression of *MPG, NEIL1, PARP3,* and *NTHL1* may therefore play a role in increased sensitivity to oxidative DNA damage in the 80 Gγ population (Section 6.4).

Reduced expression of at least 6 of the genes was unique to the 80 Gγ population which indicates that a genetic mutation between the 55 Gγ and 80 Gγ cell populations affected their expression. It is possible that loss of POU2F1 expression in the 80 Gγ population could have affected expression of these DNA repair genes considering the established role of POU2F1 in DNA damage response. Both *ATM* and *NTHL1* have previously been shown to be down-regulated in cells with reduced POU2F1 expression (Tantin et al., 2005; Saha et al., 2010). Regulation of the DNA damage repair genes by POU2F1 could be confirmed by reconstitution of POU2F1 expression in the 80 Gγ population to assess if DNA repair gene expression is restored. Techniques such as ChIP, which would assess if POU2F1 is part of transcriptional complexes which regulate these genes, could also be used to investigate this hypothesis further.

6.6.4 Conclusion

In summary, a focal deletion of *POU2F1* was identified in the First 5 Gγ series following exposure to ionising radiation. This deletion was confirmed by cytogenetic analysis and caused a concomitant loss in protein expression. POU2F1 has known roles in response to genotoxic stress and a POU2F1-deleted population in the present study displayed increased cytotoxicity due to oxidative stress and reduced expression of a number of DNA repair genes. However, current data has not conclusively proved that loss of POU2F1 expression caused these changes. Due to the known function of *POU2F1* in maintaining genetic stability and the radiation-mediated deletion of the gene in MCF-10A, POU2F1 expression will be investigated in a cohort of radiogenic and sporadic breast cancer tissue samples to assess if loss of expression is a feature of radiogenic breast cancer (chapter 8).

Chapter 7: Investigation of the copy number increase of *c-MYC* in the Second 5 Gγ series

7.1 Introduction

c-MYC is a transcription factor which regulates up to 15 % of all human genes and is involved in cell growth, proliferation, metabolism, differentiation and apoptosis (Dang *et al.*, 2006). Increased c-MYC expression is an established event in cancer development and progression and can cause uncontrolled cell proliferation, immortalisation of cells, epithelial to mesenchymal transition, angiogenesis, reduced cell differentiation and ultimately cell transformation (Xu *et al.*, 2010). *c-MYC* amplification (2 fold increase in *c-MYC* copy number over chromosome 8 copy number) is associated with over-expression of mRNA and protein product and it is reported to occur in 15% of all breast cancers (Deming *et al.*, 2000).

The *c-MYC* locus is in a constitutively trisomic region of chromosome 8q in the un-irradiated MCF-10A genome. A focal copy number increase of *c-MYC* was detected in the 40 Gγ cumulative dose population of the Second 5 Gγ series. A larger region of copy number increase on chromosome 8, ending at the telomeric breakpoint of the focal alteration, was detected in the 60 Gγ population and further increased the copy number state of *c-MYC* (section 4.4.2). Gene expression analysis of the Second 5 Gγ series identified expression changes in genes transcriptionally regulated by *c-MYC*, including the putative oncogene *H19* and genes involved in epithelium to mesenchymal transition (chapter 5). The incidence of *c-MYC* amplification has been reported to be higher in breast cancer cases from individuals exposed to ionising radiation during the atomic bombs of Hiroshima and Nagasaki compared to breast cancers in the general population (Miura *et al.*, 2008). The established oncogenic properties of amplified *c-MYC* and the previous links with radiogenic cancer therefore make the copy number increase event identified in MCF-10A cells a high priority candidate for investigation in radiogenic breast cancer.

7.1.1 Aim

The aim of the work described in this chapter was to investigate *c-MYC* copy number alterations in cells from the Second 5Gy series using fluorescent *in situ* hybridisation (FISH), and to investigate the effect increased copy-number has on c-MYC expression using western transfer and immunoblot.

7.2 *In vitro* confirmation of *c-MYC* copy number alterations

c-MYC copy number alterations were investigated in the Second 5 Gγ series using FISH. A commercially available green fluorescent chromosome 8 centromere probe and a commercially available orange fluorescent probe which maps to *c-MYC* were used for cytogenetic analysis (section 2.8). Confirmation that these probes map to the correct chromosome and in the correct region was made using metaphase chromosomes, prepared by David Rowe (Institute of Genetic Medicine, Newcastle upon Tyne, UK), from un-irradiated MCF-10A cells (Fig. 7.1). As expected, the green centromere probe hybridised to the centromere of the constitutively normal chromosome 8 and the der(8)t(8;8)(q22;p23) chromosome. The *c-MYC* probe hybridised to the q arm of these two chromosomes in positions consistent with the MCF-10A karyotype described in section 4.2.1.

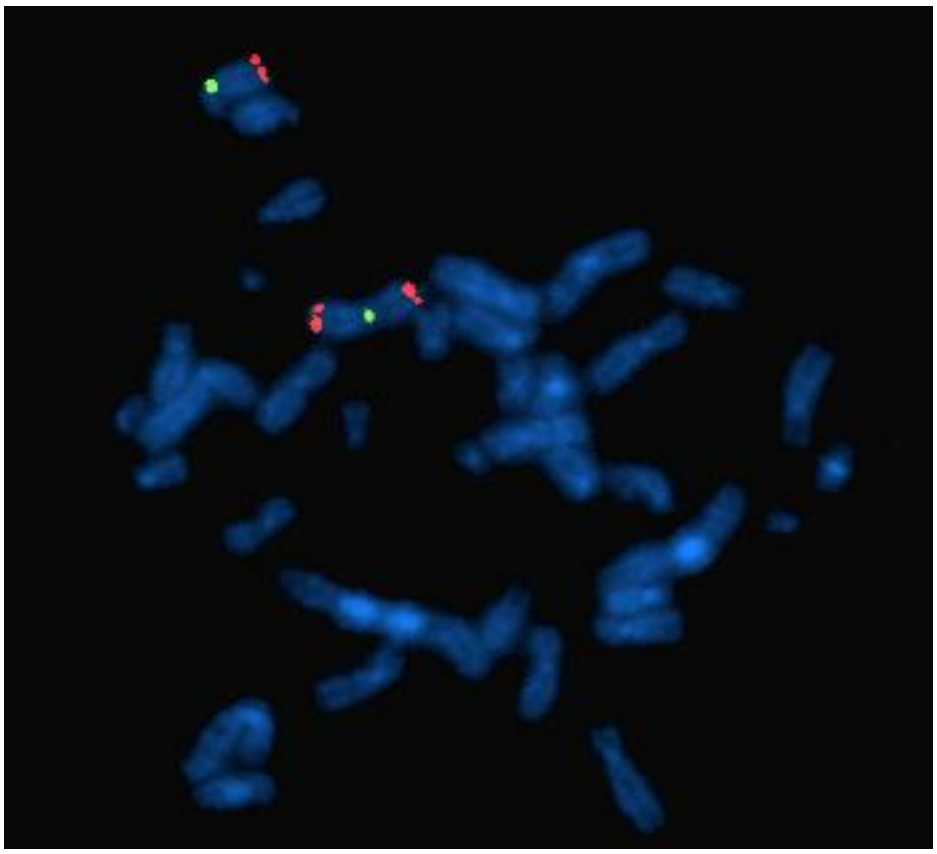

Figure 7.1 Cytogenetic analysis of *c-MYC* in un-irradiated MCF-10A cells.
FISH probes are specific to the centromere of chromosome 8 (green) and the *c-MYC* locus (red) and the metaphase chromosomes of un-irradiated MCF-10A were counterstained with DAPI. The probe for *c-MYC* hybridises to the q arm of the same chromosomes as the centromere 8 probe, specifically on a normal chromosome 8 and the der(8)t(8;8)(q22;p23) chromosome, which is consistent with its established position in the genome.

7.2.1 c-MYC copy number alterations in the 80 Gγ population determined using metaphase cells

Copy number alterations of the *c-MYC* locus were investigated using metaphase chromosomes from the 80 Gγ cumulative dose population from the Second 5 Gγ series. Metaphase chromosome spreads were not available for the other populations of the Second 5 Gγ series.

G-band analysis of the 80 Gγ population identified that the large region of copy number gain on chromosome 8q (between positions 71160976:130125337; section 1.4.2) was attached to the end of the constitutively normal chromosome 8q, creating the derivative chromosome dup8(q12-q24) (Fig. 7.2). All 20 cells analysed by G-band karyotyping contained the dup8(q12-q24) chromosome. SNP 6.0 analysis showed that the *c-MYC* locus was at the telomeric end of the duplicated region (section 1.4.2). FISH analysis of metaphase chromosomes from the 80 Gγ population showed that the *c-MYC* locus was at the telomeric end of the dup8(q12q24) chromosome q arm which confirmed that the duplicated region was not inverted (Fig 7.3a).

Sub-populations were identified that had multiple copies of *c-MYC* on the q arm of the dup8(q12q24) chromosomes (Fig 7.3 b and c). Multiple copies of *c-MYC* appeared to be present at the *c-MYC* locus on both constitutive 8q and the duplicated region. The *c-MYC* genotype observed in this sub-population most likely represented the focal *c-MYC* amplification identified by the SNP 6.0 array (Section 4.4.2).

Despite all chromosomes analysed by G-band karyotyping containing the dup8(q12-q24) chromosome, alternative karyotypes with different alterations that incorporated the *c-MYC* locus were also observed by FISH analysis (albeit at a much lower frequency than the dup8(q12q24) alterations). For example a translocation of *c-MYC* to an unknown chromosome was identified in cells which did not contain the dup8(q12-q24) chromosome (Fig 7.3d). Cells containing a second duplication on the dup8(q12q24) chromosome and a duplication on one of the q arms of the constitutive der(8)t(8;8)(q22;p23) were also observed (Fig 7.3e and f).

In summary it appeared that numerous chromosome rearrangements occurred on chromosome 8q that involved the *c-MYC* locus and that the focal amplification of *c-MYC* only occurred on the dup8(q12q24) chromosome.

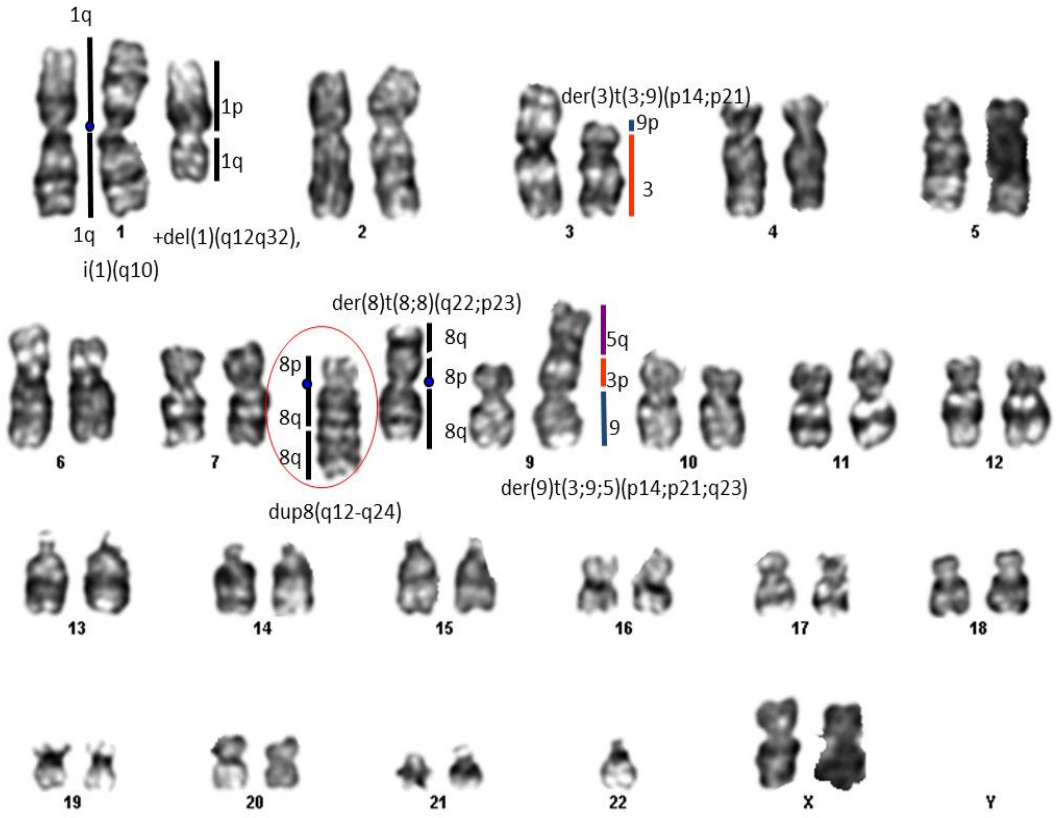

Figure 7.2 G-band karyotyping of metaphase chromosomes from the 80 Gγ population of the Second 5 Gγ series.
Chromosomes which display chromosomal rearrangements are labelled with the chromosomal regions that constitute the rearrangement and the karyotype definition of the chromosome. All rearrangements are constitutive to the MCF-10A cell line except the dup8(q12-q24) chromosome which is circled. The dup8(q12-q24) chromosome is unique to the Second 5 Gγ series.

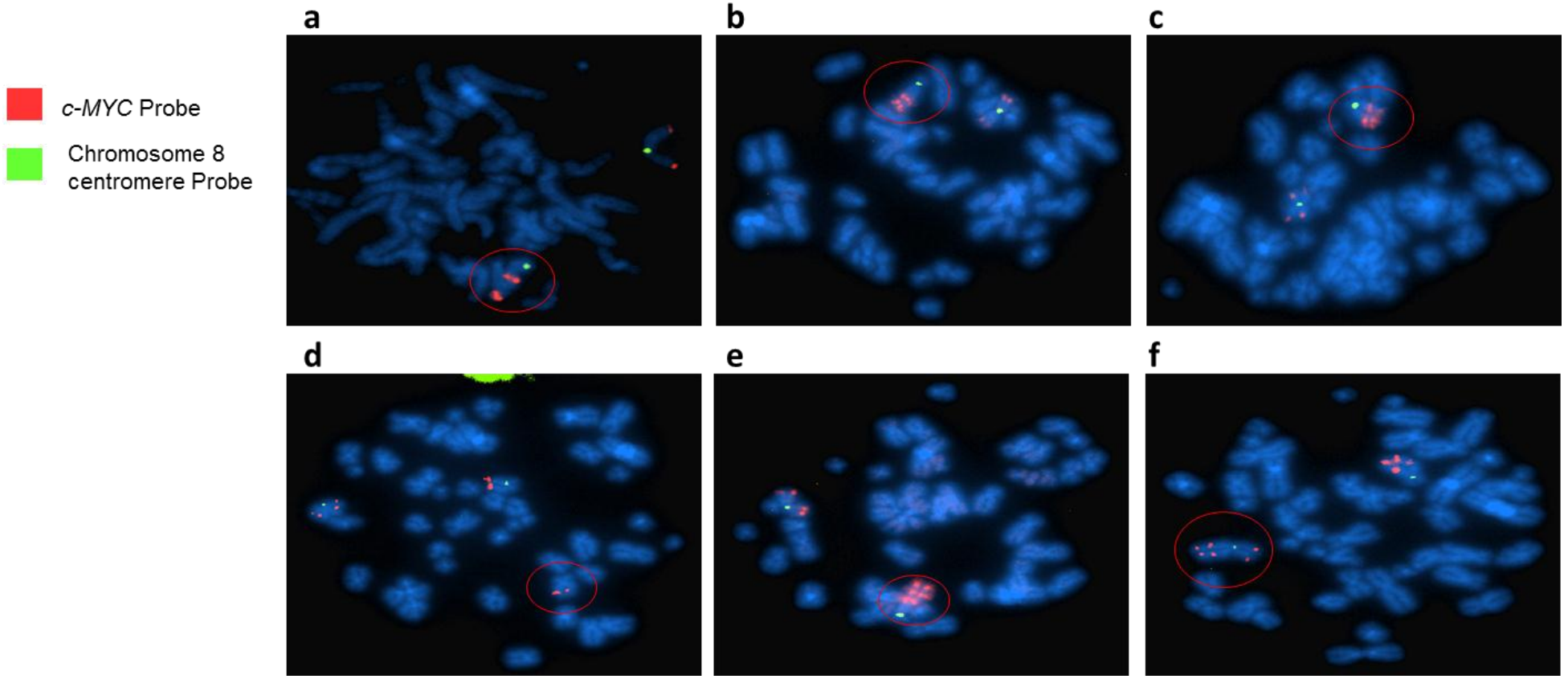

Figure 7.3 Copy number alterations of *c-MYC* in the 80 Gγ population (Second 5 Gγ series).

FISH probes are specific to the centromere of chromosome 8 (green) and the *c-MYC* locus (red) and the metaphase chromosomes were counterstained with DAPI. Examples of different chromosome alterations which incorporate the *c-MYC* locus on metaphase chromosomes from cells of the 80 Gγ population (Second 5 Gγ series) are circled in red: duplication of the 8q21-q24 region with the *c-MYC* locus positioned at the telomeric end of the duplicated region **(a)**, multiple copies of *c-MYC* at the *c-MYC* locus on the constitutive 8q arm and duplicated region of the dup(8)(q21-q24) chromosome **(b) and (c)**, a translocation of the *c-MYC* locus to an unknown chromosome **(d)**, a second duplication on the q arm of the dup(8)(q21-q24) chromosome **(e)** and a duplication of a region of 8q incorporating the *c-MYC* locus on one arm of the constitutive der(8)t(8;8)(q22;p23) chromosome.

7.2.2 c-MYC copy number alterations in the Second 5 Gγ series determined using interphase cells.

FISH analysis of interphase cell populations identified 3 distinct *c-MYC* genotypes in sub-populations from the Second 5 Gγ series. These were:

i. 2 copies of chromosome 8 and 3 copies of *c-MYC*; representing the genotype of un-irradiated MCF-10A cells which has a region of constitutional trisomy on chromosome 8q (section 4.2.1) (Fig. 7.4a).
ii. 2 copies of chromosome 8 and 4 distinct copies of *c-MYC*. Two copies of *c-MYC* appeared to consistently localise to each centromere probe in this cell population indicating that each chromosome now had two copies of *c-MYC* (Fig. 7.4b);
iii. 2 copies of chromosome 8 and multiple copies of *c-MYC* (Figure 7.4c). The nature of the staining of the *c-MYC* locus by the FISH probe meant that cells with multiple copies of *c-MYC* were easy to identify but the exact number of copies of *c-MYC* was sometimes hard to discern. Cells with this pattern of staining were therefore grouped together as *c-MYC* amplified cells (copy number > 4).

There was no evidence of focal *c-MYC* amplification in the passage controls cells. Rather, the dominant *c-MYC* genotype in the passage control cells was 3 copies of chromosome 8 and 4 copies of *c-MYC*, consistent with acquired Trisomy 8 (section 4.4). Only 9% of passage control cells had the un-irradiated MCF-10A *c-MYC* genotype (2 centromere 8 and 3 c-MYC signals). There was no indication of focal *c-MYC* amplification.

The percentage of cells in each cell population with each of the 3 identified *c-MYC* genotypes was calculated after scoring 100 cells in populations of the Second 5 Gγ series (Fig. 7.4d, e and f). Standard FISH scoring protocols classify alterations that are seen in less than 5% of all cells scored as not reportable; therefore such alterations have not been included in the analysis. The proportion of cells with 2 copies of chromosome 8 and 3 copies of *c-MYC* reduced as cumulative radiation dose increased. Reduction in the proportion of cells with this genotype indicated that the un-irradiated MCF-10A genotype was selected against. The proportion of cells with this genotype had reduced almost 3 fold by the 60 Gγ population compared to un-irradiated MCF-10A (Fig. 7.4d).

Cells with 2 copies of chromosome 8 and 4 copies of *c-MYC* were not observed in the un-irradiated MCF-10A cell population. This genotype was observed in 12% of cells in the 10 Gγ population and increased as cumulative dose increased. There was however a reduction in the percentage of cells with this genotype in the 60 Gγ population although the percentage increased again in the 80 Gγ population (Fig. 7.4e).

No cells contained *c-MYC* amplification in the un-irradiated MCF-10A or 10 Gγ cell populations; however 7% of cells contained *c-MYC* amplification in the 20 Gγ population (Figure 7.4f). The percentage of cells with a *c-MYC* amplification increased as cumulative dose increased, becoming the dominant genotype in the 60 Gγ population comprising 46% of all cells. However the number of *c-MYC* amplified cells reduced again to 36 % in the 80 Gγ population. The increasing proportion of cells with *c-MYC* amplification as cumulative dose increased indicated that these cells had been selected for. The reduction in the percentage of *c-MYC* amplified cells in the 80 Gγ population and increase of cells with 2 copies of chromosome 8 and 4 copies of *c-MYC* indicated that a mutation may have occurred which conferred a selective advantage on cells with the latter genotype.

In summary, FISH analysis of the Second 5 Gγ series confirmed that populations of the Second 5 Gγ series were genetically heterogeneous and that the proportion of cells with an increased *c-MYC* copy number increased with cumulative dose. Although the percentage of cells with *c-MYC* amplification reduced in the 80 Gγ population compared to the 60 Gγ population, the percentage of cells with any increase in *c-MYC* copy number compared to the un-irradiated MCF-10A genotype increased.

Speculation as to which *c-MYC* genotypes represented which sub-population observed in the metaphase analysis of the 80 Gγ population will be discussed in section 7.4. Potential mechanisms by which the alterations may have arisen, at what stage of the irradiation series alterations occurred and how this correlates with data form the SNP 6.0 analysis will also be discussed in section 7.4.

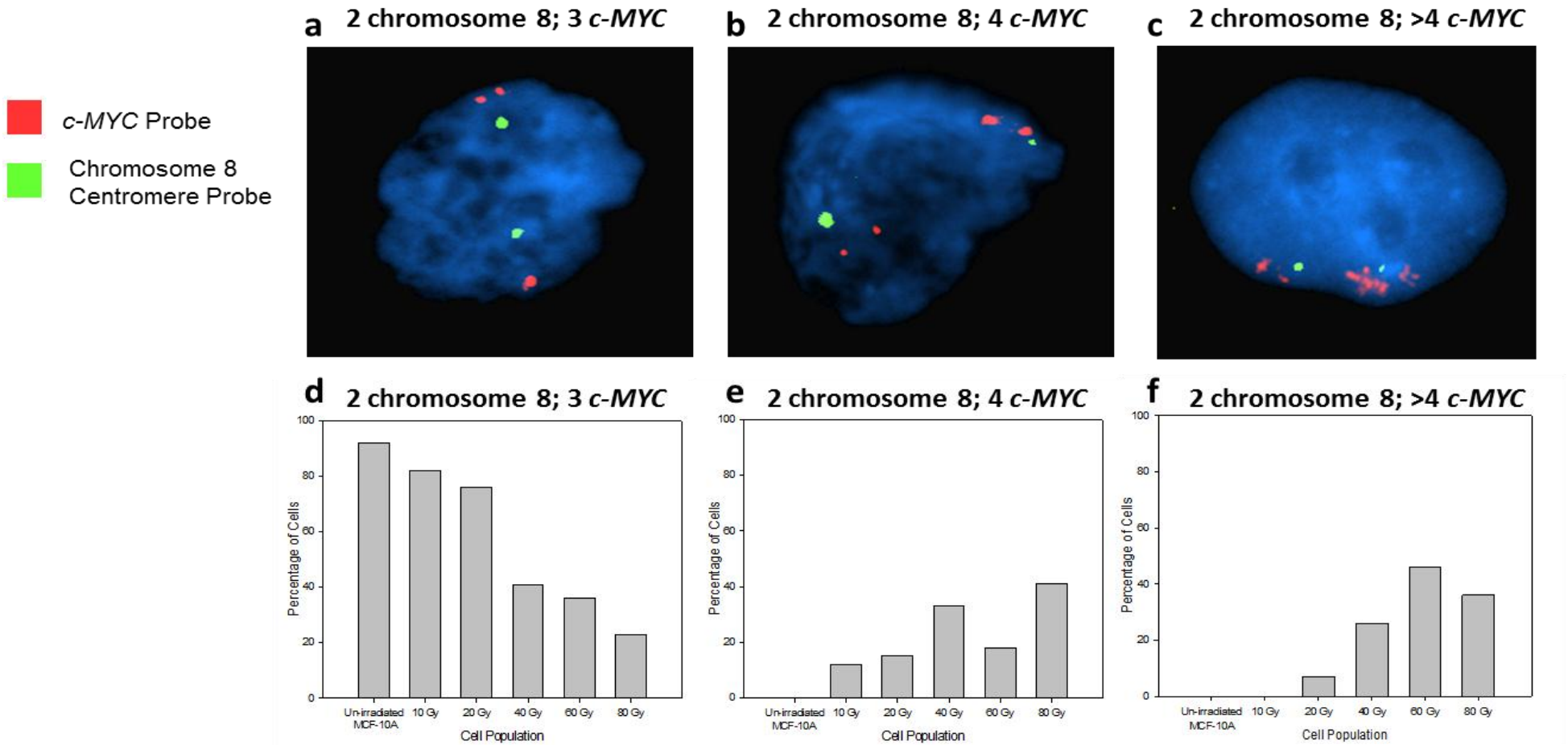

Figure 7.4 *c-MYC* copy number gains in the Second 5 Gγ series

FISH probes specific to the centromere of chromosome 8 (green) and the *c-MYC* locus (red) were used to analyse *c-MYC* copy number in populations of the Second 5 Gγ series. Cells were counterstained with DAPI. Examples of the three dominant *c-MYC* genotypes in cells of the Second 5 Gγ series are shown: 2 copies of chromosome 8 with 3 copies of *c-MYC* **(a)**, 4 copies of *c-MYC* **(b)** and greater than 4 copies of *c-MYC* **(c)**. Underneath the image of each genotype is a graph displaying the percentage of cells with that genotype calculated from counts of 100 nuclei from each cell population: 2 copies of chromosome 8 with 3 copies of *c-MYC* **(d)**, 4 copies of *c-MYC* **(e)** and greater than 4 copies of *c-MYC* **(f)**.

7.3 c-MYC protein expression in the Second 5 Gγ series

Western transfer and immunoblot was used to determine what effect *c-MYC* copy number had on c-MYC protein levels in un-irradiated MCF-10A, Second 5 Gγ series and passage control cells. Representative images of the immunoblot analysis are shown in figure 7.5a and b. A strong band at the correct mass for c-MYC (67 kDa) was observed in the un-irradiated MCF-10A cell population. c-MYC expression in the Second 5 Gγ series was reduced in the 20 Gγ cumulative dose cells compared to un-irradiated MCF-10A cells. Expression increased in the 40 Gγ, 60 Gγ and 80 Gγ cells and was higher than in un-irradiated MCF-10A cells (Fig. 7.5a). Expression of c-MYC appeared to be higher in the passage control population than in un-irradiated MCF-10A cells also (Fig. 7.5b).

c-MYC expression was quantified by densitometric analysis of 3 independent experiments from 3 independent protein extracts and normalised using GAPDH expression (Fig. 7.5c). Expression appeared to reduce in the 20 Gγ population compared to un-irradiated MCF-10A; however the difference was not significant (Turkey's Test: p=0.477). Cell populations with an increased *c-MYC* copy number identified by SNP 6.0 analysis (40 Gγ, 60 Gγ, 80 Gγ and passage control populations) had increased expression of c-MYC compared to un-irradiated MCF-10A; however only the 60 Gγ population had significantly increased expression (Turkey's Test: p=0.002).

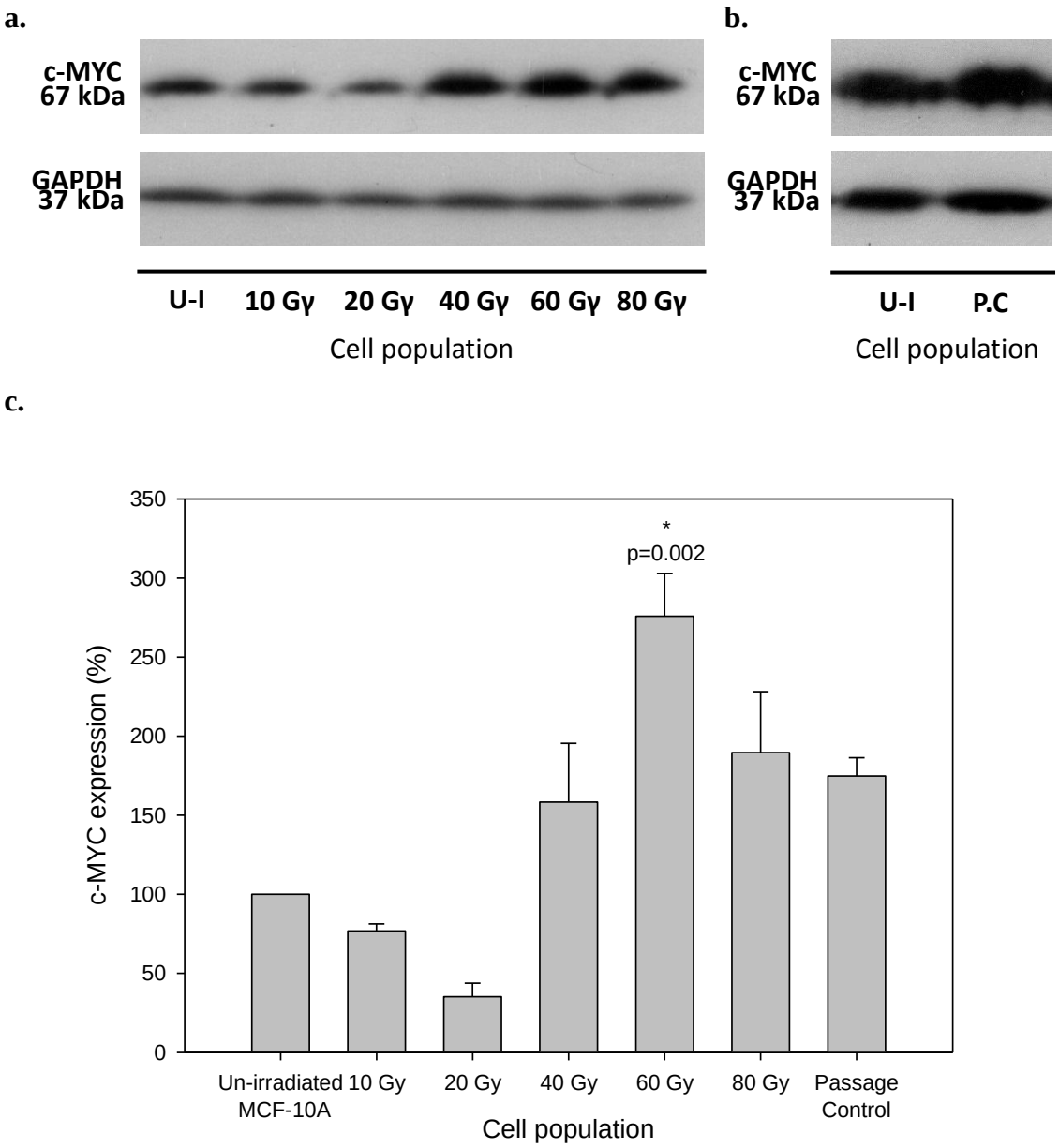

Figure 7.5 c-MYC protein expression in the Second 5 Gγ series
Western transfer analysis of the Second 5 Gγ series **(a)** and passage control population **(b)** with antibodies specific for the 67kDa protein c-MYC and 37kDa protein GAPDH. Densitometric analysis of 3 independent western transfers using 3independant protein extracts was used to quantify the expression of c-MYC for each cell population as a percentage of the expression of c-MYC in un-irradiated MCF-10A cells (which was set at 100% expression) **(c)**. U-I = un-irradiated MCF-10A and P.C = passage control in cell population lane identifiers below each image in **(a)** and **(b)**. 10 µg of protein was used for each cell population in each experiment. Although irradiated and passage control populations were analysed separately the same un-irradiated MCF-10A protein extracts were used and expression was expressed as a percentage of the expression of c-MYC in un-irradiated MCF-10A cells within these experiments. To calculate the relative protein expression of c-MYC the densitometry results for each sample were normalised with densitometry of GAPDH within each experiment. Difference in expression between populations below the 5% confidence level was tested (Kruskal-Wallis: p=0.006). A post hoc Turkey's test was then used to assess the difference in expression between individual populations below the 5% confidence level. * indicates populations whose c-MYC protein expression was significantly different from un-irradiated MCF-10A.

The fluctuations of c-MYC expression in the 40 Gγ, 60 Gγ, 80 Gγ and passage control populations do not directly correlate with the increase in *c-MYC* copy number identified by SNP 6.0 array and FISH analysis. For example, the comparable level of expression in the 40 Gγ and 80 Gγ populations was not expected as the 80 Gγ population had a higher proportion of cells with increased *c-MYC* copy number. It was interesting however that c-MYC expression was highest in the 60 Gγ population as this population had the highest frequency of cells with *c-MYC* amplification (section 7.2.2, Fig. 7.4f).

The apparent fluctuations in c-MYC expression may be due to the inaccuracies of western densitometry which is only semi-quantitative. It is also possible however, that those genes which regulate the expression or stabilisation of c-MYC may have been altered or were acting in different ways in the different cell populations and subsequently caused different levels of expression. The relationship between *c-MYC* copy number and c-MYC expression may therefore not be a simple one. Overall however, the trend in the Second 5 Gγ series was that increased *c-MYC* copy number in the majority of cells led to an overall increase in c-MYC expression.

7.4 Discussion

The incidence of *c-MYC* amplification is increased in breast cancers following exposure to ionising radiation, and chromosomal rearrangements involving the 8q24.2 region have been reported in breast epithelial cells transformed with γ rays (Miura *et al.*, 2008; Unger *et al.*, 2010). It is therefore possible that genetic alterations on chromosome 8q, including *c-MYC* amplification, are common following radiation exposure. The numerous chromosomal re-arrangements of 8q observed in the present study, including c-MYC amplification, is consistent with this model and suggests that 8q is particularly susceptible to radiation-induced instability. The present study also confirmed concomitant increase of c-MYC expression with increase in the proportion of cells containing *c-MYC* copy number gains. Section 7.4.1 will discuss putative mechanisms by which copy number alterations incorporating the *c-MYC* locus occurred on chromosome 8q, followed by discussion of the relevance elevated c-MYC protein expression has on the transformation process.

7.4.1 Copy number alterations on chromosome 8q in the Second 5 Gγ series

Translocation of the *c-MYC* locus was identified in a sub-population of the 80 Gγ population. A reciprocal translocation of *c-MYC* to a location close to enhancers of *IgH*

on chromosome 14 is a well-established driver of transformation in Burkitt lymphoma (Boxer and Dang, 2001). Translocation breakpoints in relation to *c-MYC* in Burkitt lymphoma include sites within, immediately 5' and distant to the gene (Boxer and Dang, 2001). Breakpoints for the observed translocations in the present study have not been determined. Further large copy number gains incorporating the *c-MYC* locus on the dup8(q12q24) and der(8)t(8;8)(q22;p23) chromosomes were also observed. The genomic regions involved in these rearrangements are also unknown.

The two dominant alterations incorporating *c-MYC* in the 80 Gγ population identified by both SNP analysis and FISH analysis of the 80 Gγ population were a focal amplification of *c-MYC* and a duplication of the q21-q24 region of chromosome 8. SNP array analysis of these two alterations indicated that they share a common breakpoint (section 4.4.2).

Amplification of *c-MYC* appeared to only occur on the dup8(q12q24) chromosome and was identified at the *c-MYC* locus on both the constitutive q arm and on the duplicated region (Fig. 7.3b and c). It therefore appears that both the duplication and amplification were initiated on the same chromosome and that the amplification occurred before the duplication. This model correlates with the temporal acquisition of the genetic alterations identified by the SNP 6.0 array which first identified the focal amplification in the 40 Gγ population and the duplication in the 60 Gγ population (section 4.4.2).

The molecular mechanisms generating the derivative chromosome are likely to be complex; however a model has been proposed which could generate this rearrangement (Fig. 7.6). Early in the irradiation series a radiation-induced double strand break at the telomeric end of the focal amplification may have induced a BFB cycle (described in section 1.4.2) which caused focal *c-MYC* copy number increase (Fig 7.6 a-f). At a later point a second double strand break centromeric to the amplification caused a chromatid rearrangement to the end of the sister chromatid at the site of the focal amplification, creating the dup8(q12q24) chromosome (Fig 7.6 g-h). At some point during subsequent cell division a chromosome 8 telomere was added to the end of the dup8(q12q24) chromosome, perhaps via homologous recombination repair using the der(8)t(8;8)(q22;p23) chromosome as a template (Fig 7.6 i). Cells with the amplified dup8(q12q24) chromosome were then subsequently selected for.

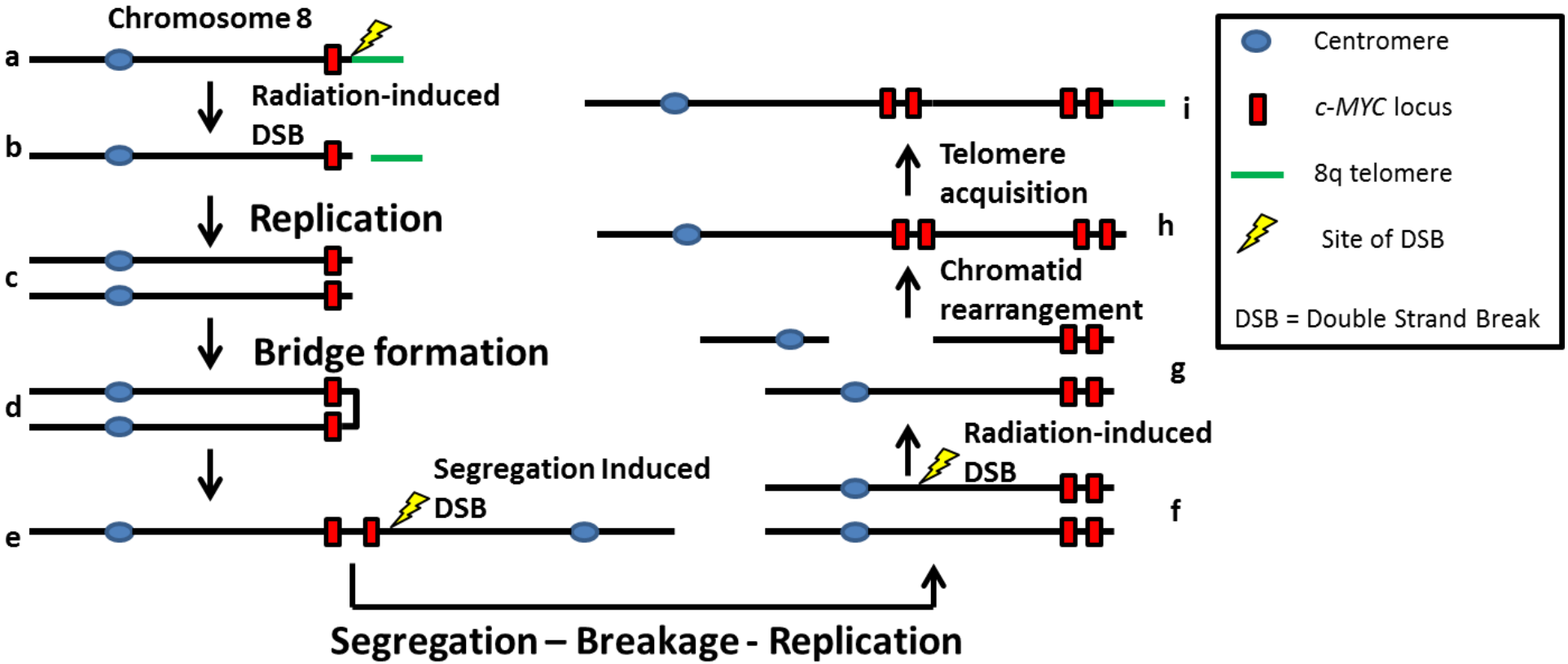

Figure 7.6 Potential mechanism generating the *c-MYC* amplified dup(8)(q21-q24) chromosome.

A radiation-induced double strand break occurs telomeric to the *c-MYC* locus **(a)**, which removes the 8q telomere **(b)**. Replication of the chromosome results in two broken sister chromatids **(c)**. The chromatids fuse to form a dicentric chromosome **(d)**. Mitotic segregation of the centromeres results in a second break centromeric to the *c-MYC* locus , creating a chromosome with 2 copies of *c-MYC* **(e)**. The derivative chromosome replicates and this cycle could continue creating multiple copies of *c-MYC*. In the above figure however only one cycle is shown. A second potentially radiation-induced double strand break occurs on one chromatid of the replicated chromosome prior to sister chromatid fusion **(f – g)**. The broken fragment of the chromatid containing the *c-MYC* amplification attaches to its sister chromatid creating a tandem duplication with *c-MYC* at the terminal end of the chromosome arm **(h)**. Acquisition of a telomere, potentially via homologous recombination with the der(8)t(8;8)(q22;p23) chromosome halts further breakage fusion bridge cycles **(i)**.

The proposed model would derive alterations which appear to have the same breakpoint. No telomere deletion would be detected in chromosome 8q by SNP array analysis as the proportion of cells with the telomere deletion would represent too small a percentage of cells early in the irradiation series. Amplification caused by BFB cycles are identified by a series of inverted repeats (Hastings *et al.*, 2009). Sequence analysis of the *c-MYC* locus in amplified chromosomes could therefore confirm if BFB cycles generated the amplification.

There is some evidence that the duplication event may have occurred before the focal amplification. For example: some dup(q12q24) chromosomes did not appear to contain multiple copies of *c-MYC*, suggesting that duplication occurred prior to amplification (Fig. 7.3a); FISH analysis of the Second 5 Gγ series identified a genotype of 2 chromosome 8 centromeres and 4 distinct copies of *c-MYC* in a substantial proportion of cells in certain populations; and the first copy number increase of *c-MYC* identified by FISH in the Second 5 Gγ series was a single distinct copy number gain in the 10 Gγ population, implying a duplication event (section 7.2.2). It should be noted that some of the cells observed with 4 distinct *c-MYC* copies may actually contain alternative alterations which incorporate *c-MYC*, or may in fact be *c-MYC* amplified cells in which the resolution of the FISH staining is not good enough to identify multiple *c-MYC* copies close together in the cell. This latter point could relate to both metaphase and non-metaphase FISH.

It is theoretically possible that the duplication could have occurred before the focal amplification but be detected subsequent to the amplification by the SNP 6.0 array. The duplication was only a single copy number gain, therefore in heterogeneous cell populations this alteration may be masked when not present in over 50% of cells. The focal amplification on the other hand appears to be an increase of multiple copies. This would cause a relatively large increase in signal intensity at the *c-MYC* locus and may be detected by the SNP array even when in a minor sub-population of cells. This could therefore lead to a situation whereby the focal amplification occurs after the duplication event, but is detected first.

Two double strand break events in the same chromatid or in a sister chromatid could generate the dup(q12q24) chromosome (Fig 7.7). A translocation from the der(8)t(8;8)(q22;p23) could also cause the duplication but won't be described in this example. Double strand break events in the same chromatid would lead to *c-MYC* being

positioned at the terminal end of the chromosome which could lead to BFB cycles and therefore *c-MYC* amplification (Fig. 7.7a). Separate double strand break events would allow a telomere to be positioned at the end of the dup(q12q24) chromosome and *c-MYC* amplification would require a further strand break event and most likely occur by an alternative mechanism (Fig 7.7b). The position of the telomere is unclear from G-band analysis of the 80 Gγ population.

Examples of alternative amplification mechanisms include: non-allelic homologous recombination (NAHR) (described in section 1.4.2) which relies on a measure of sequence homology either side of the amplified region (Hastings *et al.*, 2009), double rolling circle replication, or fold-back priming which both rely on inverted repeats either side of the amplified region (Rattray *et al.*, 2005; Watanabe and Horiuchi, 2005). The "duplication first" model however would not explain the observation that both loci of *c-MYC* on the dup(q12q24) chromosome appeared to have amplified regions.

In summary, with the data currently available it is very difficult to determine a mechanism by which the genetic alterations on chromosome 8q were generated in the Second 5 Gγ series. It is very possible that mechanisms other than those proposed resulted in focal *c-MYC* amplification and q21-q24 duplication. Metaphase analysis of early populations of the Second 5 Gγ series may help determine the temporal acquisition of the alterations; however this analysis was not possible. Overall, the spectrum of alterations incorporating the *c-MYC* locus seen in the present study indicates a series of complex rearrangements of chromosome 8q which were induced by ionising radiation exposure; therefore suggesting that this region of chromosome 8 contains one or more sites sensitive to radiation-induced breakage.

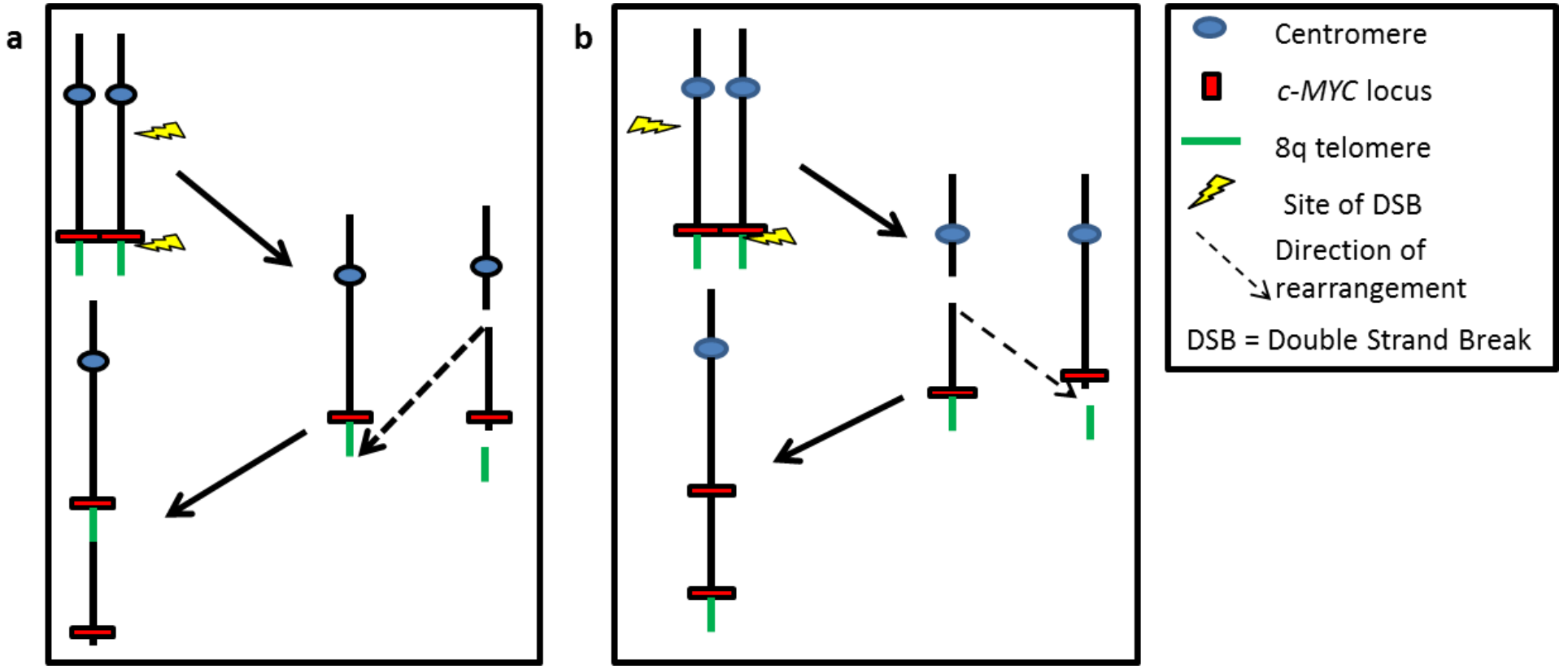

Figure 7.7 Potential mechanisms of the "duplication first model".

Simultaneous radiation-induced DSB events on the same chromatid **(a)** or on different chromatids of the same chromosome **(b)** could generate two slightly different dup(8)(q21q24) chromosomes. **(a):** DSB's on the same chromatid at the breakpoints of the 8q21q24 duplication would create a chromatid fragment which could position itself onto the q arm of a constitutively normal chromatid resulting in the telomere being positioned at an intra-chrmosomal region. A non-telomeric region at the end of this region could conceivably therefore induce a BFB cycle. **(b):** DSB's on different chromatids at the breakpoints of the 8q21q24 duplication would create two broken chromatids that could rearrange so that the centromeric breakpoint of one fragment attaches to the telomeric breakpoint of the other fragment. This could create a tandem duplication with a telomere at the end of the chromosome. Amplification of the *c-MYC* locus would then occur at a later point of the irradiation series.

7.4.2 Potential mechanisms linking c-MYC amplification and ionising radiation

The following section will briefly discuss two potential mechanisms which could cause preferential chromosomal arrangements, including *c-MYC* amplification, on chromosome 8q after exposure to ionising radiation. The role of these potential mechanisms is purely speculative and they have not been shown to affect *c-MYC* or radiation induced alterations in radiogenic breast cancer.

Common fragile sites with a particular propensity to undergo breakage during replication stress (inefficient DNA replication that causes replication to progress slowly or to stall) are known to exist in the human genome (Arlt *et al.*, 2006). Two known common fragile sites, FRA8C and FRA8D, flank the *c-MYC* locus and have been implicated in chromosomal rearrangements in cervical cancer and Burkitt lymphoma (Ferber *et al.*, 2004). It has also been suggested that the FRA8C and FRA8D sites may actually represent one large fragile site and common chromosome breaks at these sites represent peak fragile regions (Arlt *et al.*, 2006). Radiation-induced genotoxic stress, which in turn induces replication stress, has been shown to induce breaks at fragile sites in rats (Camats *et al.*, 2006). Breakage of common fragile sites at the *c-MYC* locus may therefore be indirectly induced by ionising radiation exposure which could lead to *c-MYC* amplification in radiogenic breast cancer. This has not been analysed or shown in previous studies however.

The fragile site mechanism may have contributed to the alterations on chromosome 8q observed in the Second 5 Gγ series. A fragile site would potentially explain how both the focal amplification and duplicated region appeared to share a common breakpoint. The common breakpoint in the present series was positioned between the FRA8C and FRA8D fragile sites. A common fragile breakpoint could explain the spectrum in chromosomal alterations observed in the Second 5 Gγ series.

Transcriptionally active regions of the chromosome (euchromatin) have been shown to be more susceptible to chromosome aberrations due to ionising radiation exposure than transcriptionally inactive regions (heterochromatin) (Nagasawa *et al.*, 2010). For example, radiation-induced genetic alterations were shown to be more common on chromosome 2 in a radiation-susceptible AML strain of mice than radiation-resistant AML strains (Darakhshan *et al.*, 2006). It has been suggested that this was due to differences in chromatin organisation in the different strains of mice (Nagasawa *et al.*, 2010). Differences in chromatin structure on chromosome 8q may therefore make the

region encompassing the *c-MYC* locus particularly susceptible to radiation-induced DNA damage.

Oestrogen has been shown to induce chromatin modifications to facilitate transcriptional activation of target genes (Green and Carroll, 2007). As discussed in chapter 1, breast epithelial cells are hormone sensitive and oestrogen exposure is an important risk factor for radiogenic breast cancer. *c-MYC* is transcriptionally activated by oestrogen bound ERα and histone modifiers have been shown to facilitate oestrogen dependant transcription (Kawazu *et al.*, 2011; Wang *et al.*, 2011); therefore exposure to oestrogen in the breast of young women may cause chromatin modifications at the *c-MYC* locus which may make it susceptible to radiation damage. Alterations of chromosome 8q in the present study were only observed in cells with oestrogen added to the medium. The MCF-10A cell line is ERα negative, but does express ERβ which is 96% homologous to ERα at the DNA binding domain (Yager and Davidson, 2006). It is therefore conceivable that chromatin modification due to oestrogen exposure may have affected chromatin structure at the *c-MYC* locus rendering it susceptible to DNA damage. It should be re-iterated however that the effect of oestrogen on radiation-induced alterations of chromosome 8q is speculative, and development of this hypothesis would require further experimentation.

7.4.2 c-MYC expression

Previous chapters have discussed potential phenotypic and gene expression changes that may be related to a copy number increase of *c-MYC* (chapter 3 and chapter 5). In particular, induction of EMT has been discussed in relation to the Second 5 Gγ series. Phenotypic changes potentially induced by *c-MYC* copy number increase rely on the assumption that copy number gain of *c-MYC* increases c-MYC expression. Protein expression analysis confirmed that expression increased in cell populations with an identified *c-MYC* copy number increase.

Densitometric analysis indicated that expression of c-MYC fluctuated throughout the irradiation series; however this may be due to the semi quantitative nature of the analysis. Therefore speculation as to how fluctuations in expression may have affected different populations of the Second 5 Gγ series has to be appropriately circumspect.

c-MYC expression was highest in the 60 Gγ population. This population was shown to differentially express more markers of EMT following gene expression analysis than

any other population in the Second 5 Gγ series (section 5.3.2). Expression of c-MYC in the 80 Gγ population reduced compared to the 60 Gγ population. A reduction in the number of differentially expressed EMT markers between the 60 Gγ and 80 Gγ populations was also observed (section 5.3.2). Together these data support the hypothesis that c-MYC can induce gene expression changes that can drive EMT, and that reduction of c-MYC expression can reverse these gene expression changes (section 5.4.6).

Potential mechanisms for c-MYC expression changes in the Second 5 Gγ series include a reduction in the number of cells with *c-MYC* copy number gains, or changes to c-MYC regulation and stabilisation throughout the Second 5 Gγ series. FISH analysis of the Second 5 Gγ series implied that the 60 Gγ population had a larger proportion of cells with focal amplification of *c-MYC* than the 80 Gγ population, which had a larger proportion of cells with only a single copy number increase. At face value it is possible that a reduction in *c-MYC* amplified cells and an increase in cells with only a single copy number increase of *c-MYC* in the 80 Gγ population could have caused an overall reduction in c-MYC expression. However, as was discussed in section 7.4.1 accurate analysis of the FISH data is difficult.

As discussed in section 4.5.4 different pathways and proteins can control expression of *c-MYC* and stabilisation of c-MYC protein. For example: the TGF-β complex, the RAS/RAF/MAPK pathway, GSK-3β and the WNT and NOTCH signalling pathways (Sears *et al.*, 1999; Frederick *et al.*, 2004; Adhikary and Eilers, 2005; Sekimoto *et al.*, 2007; Xu *et al.*, 2010). There is no indication by SNP array or gene expression analysis that any of the genes involved in *c-MYC* expression or stabilisation were altered in the 80 Gγ population; however functional and expression changes of proteins involved in these processes could in theory have been affected and may explain fluctuation in c-MYC expression.

7.4.3 Conclusion

In summary, genetic alterations identified by SNP array analysis that affect the *c-MYC* loci have been confirmed in the Second 5 Gγ series using cytogenetic techniques. The mechanisms by which these alterations were generated remain to be determined. Alterations affecting the *c-MYC* locus which were not identified by SNP array analysis were also identified in the 80 Gγ population using FISH which provides further evidence that chromosome 8q may be prone to genetic rearrangement. Increased c-

MYC expression concomitant with increasing *c-MYC* copy number indicates that phenotypic and gene expression changes of the Second 5 Gγ series may have been induced by c-MYC.

Considering these results *c-MYC* copy number and c-MYC expression will be analysed in radiogenic and sporadic breast cancer samples to assess if amplification of *c-MYC* and concomitant increase in expression is a feature of radiogenic breast cancer (chapter 8).

Chapter 8: POU2F1 expression and *c-MYC* amplification in sporadic and radiation-induced primary breast cancer tissues

8.1 Introduction

The established increased risk of breast cancer following exposure to ionising radiation is believed to occur through the gradual accumulation of transforming mutations following an initiation event induced by ionising radiation (Allan and Travis, 2005). Oestrogen and its metabolites are believed to play a role in the accumulation of mutations via genotoxic and receptor mediated mechanisms following initiation (van Leeuwen *et al.*, 2003; Yager and Davidson, 2006). The discovery of a molecular genetic alteration which is common in radiogenic breast cancer may identify early mutation events induced by ionising radiation and would facilitate the understanding of radiogenic breast transformation.

A focal deletion of *POU2F1* has been identified following exposure to ionising radiation in MCF-10A cells and reduced protein expression concomitant with copy number loss has been demonstrated. Previous studies have demonstrated that POU2F21 is an important regulator of DNA damage response genes and sensitivity to genotoxic exposures in POU2F1-deficient cells has been demonstrated in the present study (Meighan-Mantha *et al.*, 1999; Zhao *et al.*, 2000; Jin *et al.*, 2001; Fan *et al.*, 2002; Schild-Poulter *et al.*, 2003; Tantin *et al.*, 2005; Maekawa *et al.*, 2008; Saha *et al.*, 2010; Wang and Jin, 2010). Reduced DNA damage response is an established mechanism of cell transformation due to the concomitant increase in genetic instability and accumulation of potentially oncogenic mutations. Deletion of *POU2F1* and subsequent reduction in expression is therefore a candidate early genetic event in radiogenic breast carcinogenesis.

A radiation-induced focal amplification of *c-MYC* and further alterations of chromosome 8q which incorporate the *c-MYC* locus in radiation exposed MCF-10A cells have been identified and a concomitant increase in protein expression has been demonstrated. c-MYC is an established oncogene, is overexpressed in a number of cancers, is implicated in cell transformation and data from this study has linked copy number increase of *c-MYC* with epithelial to mesenchymal transition (Dang *et al.*, 2006; Meyer and Penn, 2008; Xu *et al.*, 2010). Incidence of *c-MYC* amplification has also been reported to be higher in breast cancer cases from survivors of the atomic bomb at Nagasaki who were exposed to ionising radiation compared to individuals not exposed

to radiation (Miura *et al.*, 2008). The identification of a radiation-induced copy number increase in the present study and previous links with radiogenic breast cancer therefore makes *c-MYC* copy number gain a strong candidate for an early genetic event in radiogenic breast transformation.

8.1.1 Aim

The aim of the work described in this chapter was to compare protein expression of both POU2F1 and c-MYC in spontaneous and radiation-induced breast cancer tissue samples by immunohistochemistry. The copy number state of *c-MYC* was also investigated to determine if *c-MYC* copy number increase is a common event in radiogenic breast cancer.

8.2 Spontaneous and radiation-induced breast cancer cohorts

Two cohorts of paraffin embedded breast cancer tissue samples were available to investigate the role of POU2F1 and c-MYC in sporadic and ionising radiation-induced breast cancer.

Material was available from 18 women who developed breast cancer after treatment with ionising radiation for Hodgkin lymphoma ("radiogenic breast cancers") and 33 women who developed apparent sporadic breast cancer without any antecedent therapeutic radiation exposure ("sporadic breast cancers").

The link between ionising radiation and increased breast cancer risk in Hodgkin lymphoma survivors has been extensively reviewed (chapter 1). Briefly, women who receive ionising radiation treatment for Hodgkin lymphoma have an increased risk of breast cancer which is dose dependant (van Leeuwen *et al.*, 2003). The risk is also dependant on the age of the individual, with a number of studies claiming that there is no increase in relative risk of breast cancer in women who have received ionising radiation treatment for Hodgkin lymphoma over the age of 30 (Travis *et al.*, 2003; van Leeuwen *et al.*, 2003). Treatment with alkylating agents during radiotherapy for Hodgkin lymphoma attenuates the risk of breast cancer, potentially through ablation of ovarian function which reduces circulating oestrogen levels (van Leeuwen *et al.*, 2003).

8.2.1 Radiogenic breast cancer cohort

A summary of the characteristics of the radiogenic breast cancer cases is outlined in table 8.1. The mean cumulative radiation dose received by patients for Hodgkin lymphoma was 19.2 Gγ (Median, 19.2 Gγ; Range, 1.2 Gγ - 42.7 Gγ), the mean age of diagnosis of Hodgkin lymphoma was 21.73 years (Median, 21 years: Range 16 – 29 years), the mean age of breast cancer diagnosis was 37.89 years (Median, 37.89 years; Range 30 – 47 years) and the mean latency between Hodgkin lymphoma diagnosis and breast cancer diagnosis was 15.33 years (Median, 14 years; Range, 7 – 24 years). Most patients developed infiltrating ductal carcinoma (11/18, 61%). There were 2 cases each of infiltrating lobular carcinoma and comedocarcinoma, and 1 case of tubular carcinoma. Breast cancer in the remaining 2 cases was unspecified. Most breast cancers arose in the upper outer quadrant of the breast (12 of 18), 2 arose in the lower outer quadrant, 2 in the lower inner quadrant and 1 in the upper inner quadrant. Half of the cases were stage IIA breast cancers, 5 were stage I, 3 were stage IIB and 1 was stage IIIA. Only 6 of the 18 Hodgkin lymphoma patients received alkylating agents as part of combined modality therapy.

Sample ID	Radiation Dose Received (Gy)	Age of HL Diagnosis (years)	Age of BC Diagnosis (years)	Latency Between Diagnoses (years)	Breast Cancer Pathology	Breast Cancer Quadrant	Breast Cancer Stage	Received Alkylating Agent During HL Treatment
RAD1	24	22	40	17	IDC	LOQ	IIA	NO
RAD2	7.9	23	46	22	ILC	UOQ	IIA	YES
RAD3	11.8	17	30	12	ILC	UIQ	IIA	YES
RAD4	31.5	19	31	11	IDC	UOQ	I	NO
RAD5	1.2	28	39	10	Carcinoma, NOS	other	IIA	NO
RAD6	4.1	16	39	22	IDC	UOQ	IIA	YES
RAD7	31.1	18	28	10	IDC	UOQ	I	NO
RAD8	22.5	22	47	24	IDC	UOQ	IIA	NO
RAD9	3.9	29	46	17	adenocarcinoma, NOS	UOQ	I	NO
RAD10	24.7	26	45	18	IDC	LOQ	I	NO
RAD11	42.7	27	35	7	comedocarcinoma	UOQ	IIB	NO
RAD12	41.7	21	37	12	IDC	UOQ	IIIA	YES
RAD13	40.6	29	42	13	IDC	UOQ	IIA	NO
RAD14	7	21	35	14	IDC	LIQ	IIA	YES
RAD15	7.9	18	41	22	IDC	LIQ	IIA	NO
RAD16	37.9	21	34	13	IDC	UOQ	IIB	NO
RAD17	4.8	16	35	19	tubular adenocarcinoma	UOQ	I	YES
RAD18	4.3	19	32	13	comedocarcinoma	UOQ	IIB	NO
Average	19.42	21.78	37.89	15.33				

Table 8.1 Data for paraffin embedded radiation-induced breast cancer tissue cases.

HL = Hodgkin lymphoma, BC = Breast cancer
IDC = infiltrating ductal carcinoma, ILC = infiltrating lobular carcinoma, NOS = Cancer type not specified
LOQ = Lower Outer Quadrant, UOQ = Upper Outer Quadrant, LIQ = Lower Inner Quadrant, UIQ = Upper Inner Quadrant

There was no correlation between the radiation dose received and age of diagnosis of Hodgkin lymphoma (Pearson's coefficient = 0.226; p = 0.368) or between radiation dose received and age of diagnosis of breast cancer (Pearson's coefficient = -0.270; p = 0.279). There was however a moderate inverse correlation between radiation dose received and latency in years between diagnosis of Hodgkin lymphoma and breast cancer (Pearson's coefficient = -0.459; p = 0.055) (Fig. 8.1).

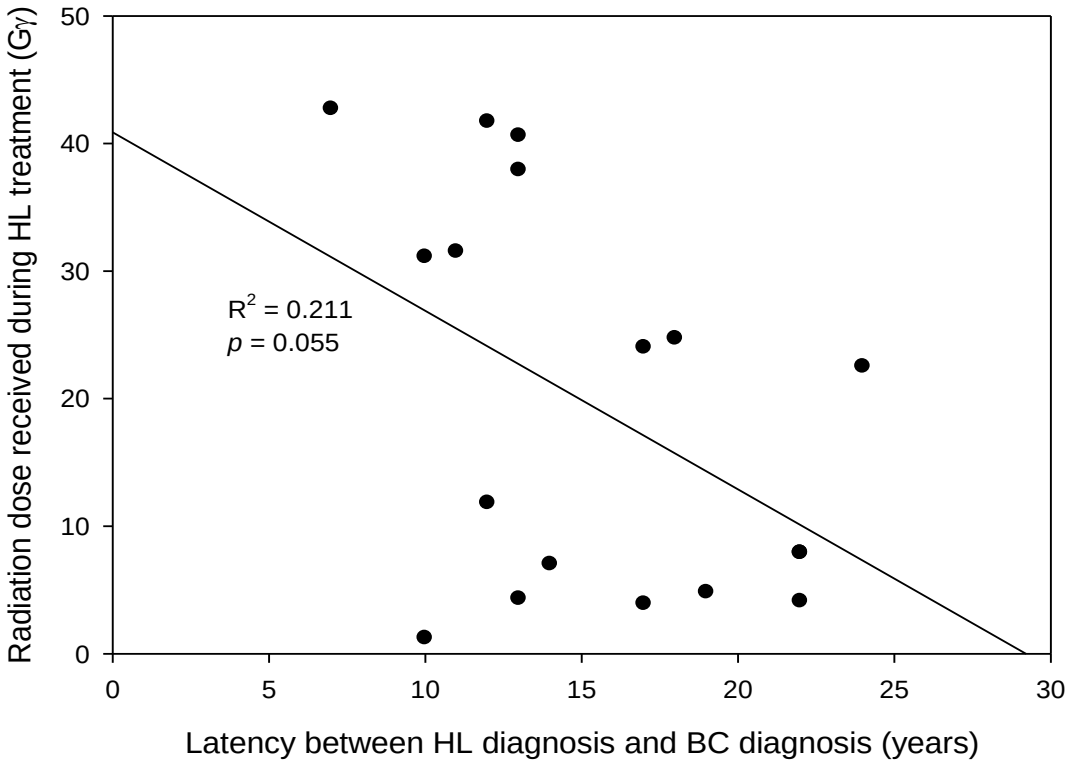

Figure 8.1 Relationship between latency of breast cancer diagnosis following Hodgkin lymphoma and radiation dose received during radiotherapy for Hodgkin lymphoma.
HL = Hodgkin lymphoma, BC = Breast cancer

There was no correlation between the age of Hodgkin lymphoma diagnosis and latency between Hodgkin lymphoma and breast cancer diagnosis (Pearson's coefficient = -0.220; $p>0.05$). There was however a positive correlation between age of Hodgkin lymphoma diagnosis and age of breast cancer diagnosis (Pearson's coefficient = 0.546; $p = 0.019$) and between age of breast cancer diagnosis and latency between diagnosis of Hodgkin lymphoma and breast cancer (Pearson's coefficient = 0.0675; $p = 0.002$). These correlations were expected as the younger a patient is diagnosed with Hodgkin lymphoma the younger they are likely to develop breast cancer and the younger a patient will develop breast cancer the lower the latency between diagnoses (Fig 8.2 a and b).

a

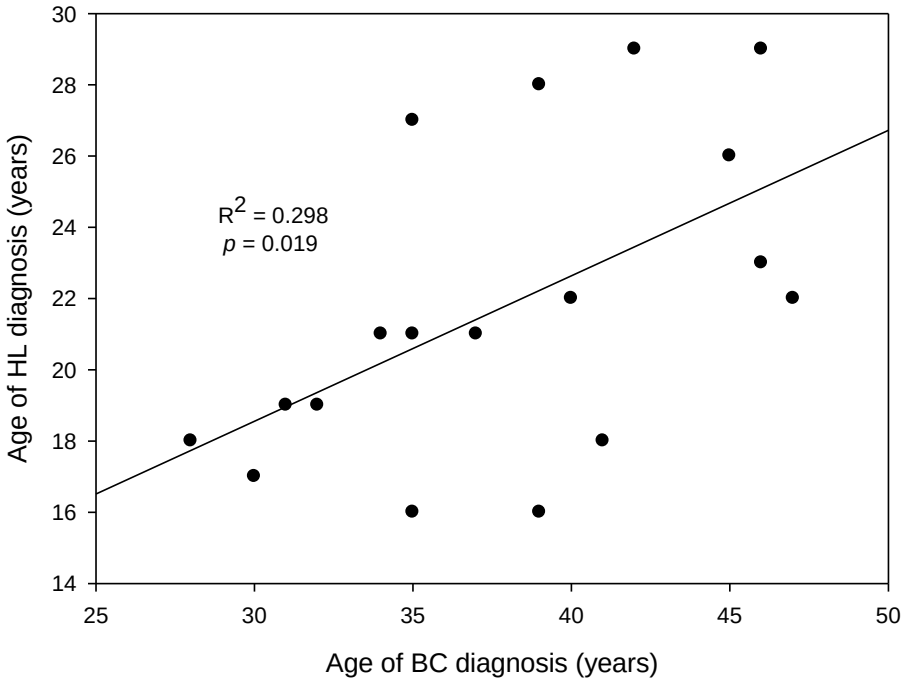

b

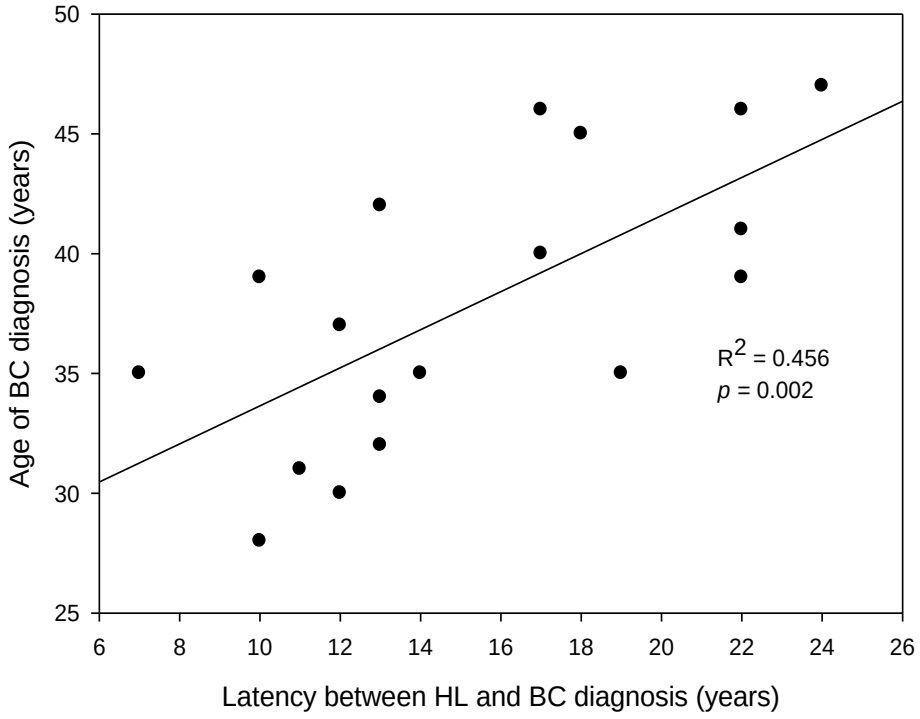

Figure 8.2 Relationship between age of diagnosis of Hodgkin lymphoma and breast cancer (a) and latency between diagnoses and age of breast cancer diagnosis (b).
HL = Hodgkin lymphoma, BC = Breast cancer

There was no significant difference in the age of Hodgkin lymphoma diagnosis, age of breast cancer diagnosis, or latency between cases treated with radiation monotherapy and those treated with combined modality (T-test: $p>0.050$). Within the group of patients who received methylating chemotherapy there was no significant correlation between either the cumulative dose of methylating agent received (Procarbazine dose per m^2) or number of cycles of chemotherapy and age of Hodgkin lymphoma diagnosis, age of breast cancer diagnosis and latency between the diagnoses (Pearson's coefficient: $p>0.050$). However, the small size of the patient cohort limits the statistical power to detect significant associations.

8.2.2 Sporadic breast cancer cohort

A summary of the data for the sporadic breast cancer cases is outlined in table 8.2. An attempt was made to match the radiogenic and sporadic cases by age of diagnosis of breast cancer. The mean age of breast cancer diagnosis in the radiogenic cohort was 37.9 years old with a range between 28 and 47 years. The mean age of breast cancer diagnosis in the sporadic cases was 40.6 years old (Median, 41) with a range between 28 and 49 years. Most cases included areas of infiltrating ductal carcinoma (29 of 33, 88%), 6 cases had areas of ductal carcinoma *in situ*, 3 cases had areas of comedocarcinoma, 2 cases had areas of infiltrating lobular carcinoma, 2 cases had areas of fibrocystic disease and 2 cases had mammary Paget's disease; which is a malignant condition that forms in the skin of the nipple. Information on stage and breast quadrant site was not available for these cases.

Sample ID	Age of BC Diagnosis (years)	Breast Cancer Pathology
SPO1	43	IDC
SPO2	43	IDC
SPO3	36	comedocarcinoma
SPO4	44	IDC
SPO5	39	IDC + DCIS
SPO6	46	IDC
SPO7	42	IDC+DCIS
SPO8	44	IDC
SPO9	38	IDC
SPO10	37	IDC+comedocarcinoma
SPO11	44	IDC
SPO12	47	IDC+FCD
SPO13	35	IDC
SPO14	47	IDC
SPO15	43	IDC
SPO16	38	IDC
SPO17	37	IDC
SPO18	41	ILC + FCD
SPO19	47	IDC + DCIS
SPO20	32	comedocarcinoma
SPO21	49	IDC
SPO22	47	IDC
SPO23	48	IDC
SPO24	33	ILC + IDC
SPO25	32	IDC + DCIS
SPO26	41	IDC
SPO27	34	IDC
SPO28	45	IDC
SPO29	37	IDC
SPO30	39	IDC
SPO31	28	mammary Paget's disease + DCIS
SPO32	39	IDC + mammary Paget's disease + DCIS
SPO33	45	IDC

Table 8.2 Data for paraffin embedded sporadic breast cancer tissue cases.
IDC = infiltrating ductal carcinoma, ILC = infiltrating lobular carcinoma, DCIS = ductal carcinoma *in situ*, FCD = fibrocystic disease.

8.3 Expression of POU2F1 in sporadic and radiogenic breast cancer

Sections of paraffin embedded tumours (detailed in section 8.2) were analysed for expression of POU2F1 by immunohistochemistry (section 2.14). Only nuclei in malignant areas of the sections (identified following pathological review) were assessed for POU2F1 expression. POU2F1 staining was relatively polarised, with nuclei either staining very strongly or not at all. All sporadic breast cancer cases (33/33, 100%) and 17/18 (94%) radiogenic breast cancer cases were strongly positive for POU2F1 expression (Fig. 8.3). There was therefore no significant difference in POU2F1 expression between radiation-induced and sporadic breast cancer cases (Fisher exact test: $p = 0.353$). Tissue from a single radiogenic breast cancer case, RAD7, (table 8.1) was negative for POU2F1 expression (Fig. 8.4). Immunohistochemistry was performed twice for this sample, and showed no expression on both occasions. Sections were simultaneously stained for c-MYC with positive expression seen in sample RAD7 indicating that immunohistochemistry did work on this particular sample.

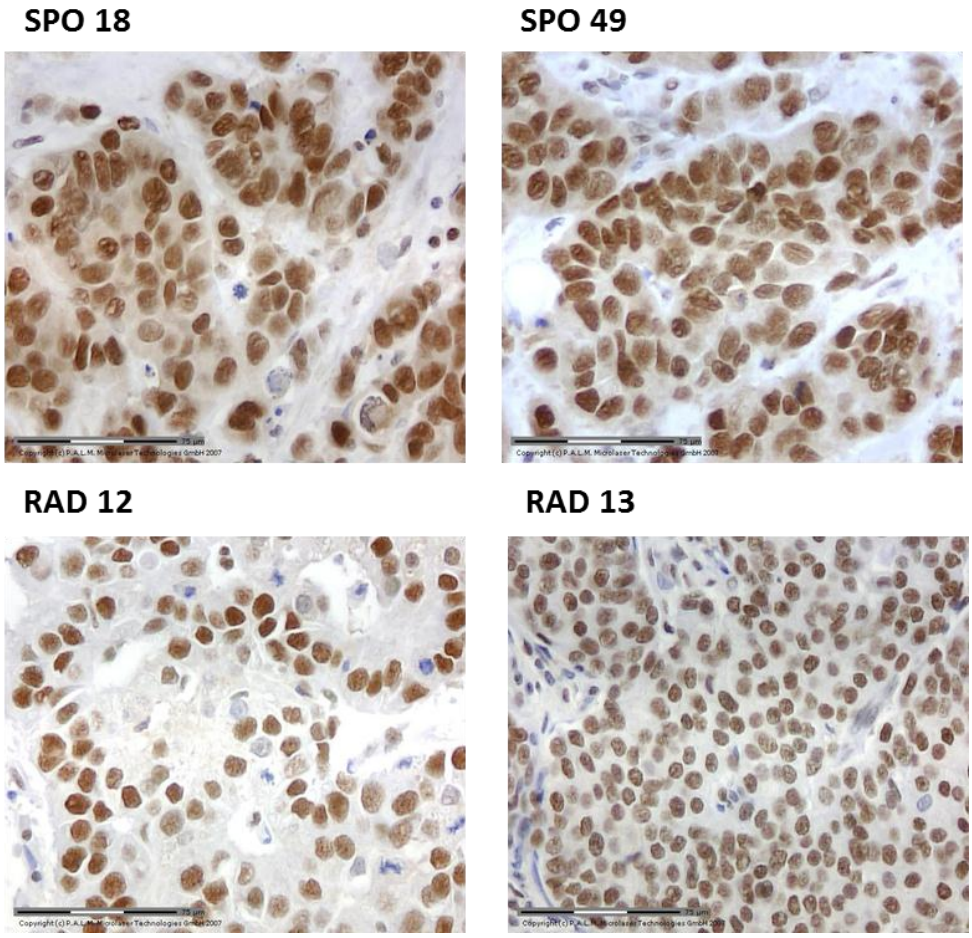

Figure 8.3 Expression of POU2F1 in sporadic and radiogenic breast cancer.
Sections of sporadic and radiogenic breast cancers were tested for POU2F1 expression by immunohistochemistry. Both sporadic and radiogenic breast cancer cases displayed strong expression of POU2F1 in tumour cell nuclei. Example samples shown ar x40 magnification: SPO18, SPO49, RAD12 and RAD13.

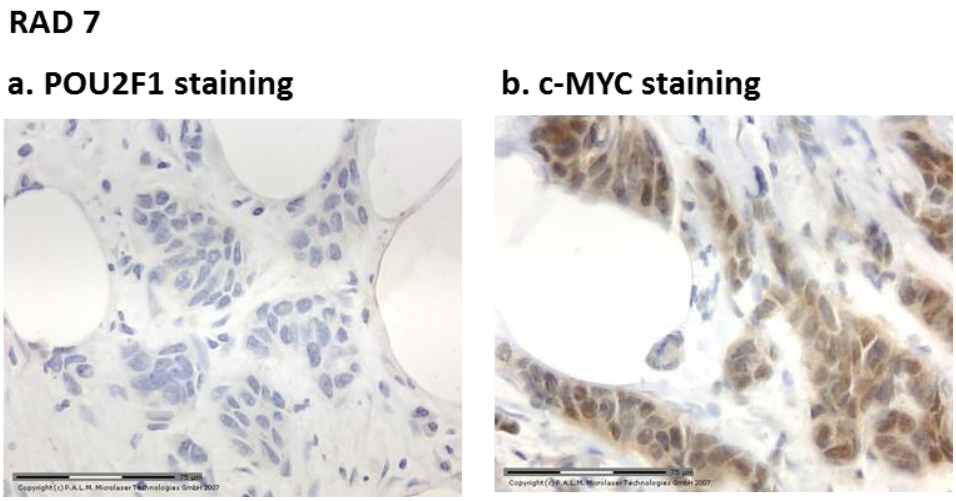

Figure 8.4 POU2F1 negative breast cancer sample.
Sections of sporadic and radiogenic breast cancers were tested for POU2F1 expression by immunohistochemistry. Only RAD7 was negative for POU2F1 expression, indicated by no staining in tumour cell nuclei **(a)**. The sample showed positive staining for c-MYC expression in tumour cell nuclei **(b)** which indicated that negative staining of POU2F1 was not due to the sample being unreceptive to immunohistochemistry. Images were taken at x40 magnification.

8.4 c-MYC expression in radiation-induced and sporadic breast cancer

Paraffin embedded tumour sections (detailed in section 8.2) were analysed for expression of c-MYC by immunohistochemistry (Section 2.14). Only tumour nuclei were analysed for c-MYC expression (identified following pathological review). c-MYC staining was variable within individual tumour sections and heterogeneous between patient samples, necessitating the development of an appropriate scoring system. Five hundred nuclei from 5 independent fields (100 nuclei per field) were analysed for each case. Each nucleus was given a score from 0 - 3 depending on c-MYC staining (0 = no expression, 1 = weak expression, 2 = moderate expression, 3 = strong expression) (Fig. 8.5). A sample was deemed to be negative for c-MYC expression if 90% or more of the nuclei analysed were given an expression score of 0. Eight of the radiation-induced cohort (8/18, 44%) and 16 of the sporadic cohort (16/33, 48%) did not express c-MYC in at least 10% of nuclei counted (χ^2: p = 0.986). Exposure to ionising radiation was not therefore associated with c-MYC-positivity in the cohort of breast cancer patients described in this study. Examples of samples with different levels of c-MYC expression are shown in figure 8.6.

An overall histoscore was calculated for each sample as a quantitative representation of expression. Briefly, the histoscore is the sum of the expression scores given to each nuclei within each sample. Taking all cases together, including those with c-MYC expression in fewer than 10% of nuclei, expression of c-MYC was higher in the radiation-induced cohort than the sporadic cohort (Figure 8.7a) but the difference was not statistically significant (Mann-Whitney test: p=0.072). When samples with c-MYC expression in fewer than 10% of nuclei were removed from the analysis, expression of c-MYC was significantly higher in the radiation-induced cohort (Figure 8.7b) (Mann-Whitney test: p=0.002).

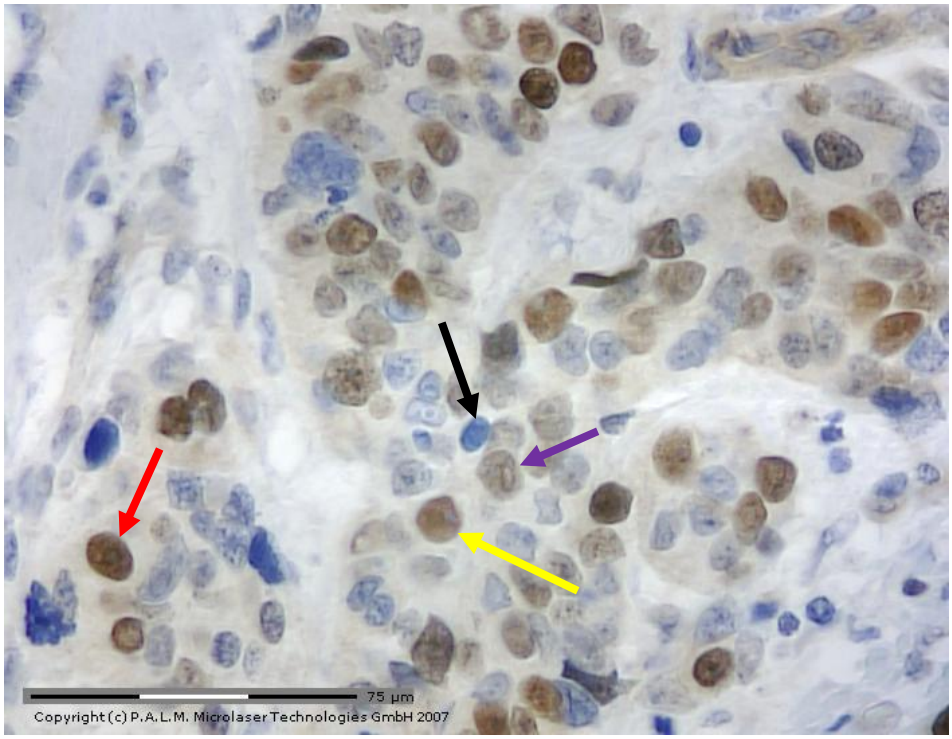

Figure 8.5 c-MYC immunohistochemistry.
Sections of sporadic and radiation-induced breast cancers were tested for c-MYC expression by immunohistochemistry. An example of a sample with heterogeneous levels of c-MYC expression in nuclei of tumour cells is shown (Sample RAD11)**.** Nuclei with no expression (Expression score = 0: black arrow) weak expression (Expression score = 1: purple arrow), moderate expression (Expression score = 2: yellow arrow) and strong expression (Expression score =3: red arrow) of c-MYC are shown. The image is at x40 magnification.

a RAD13

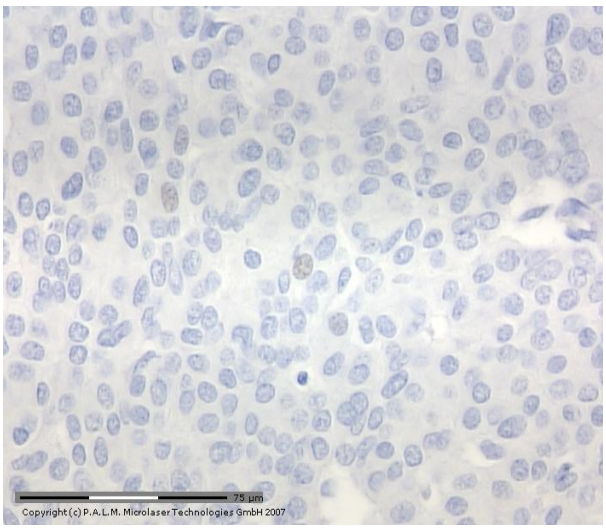

b RAD9

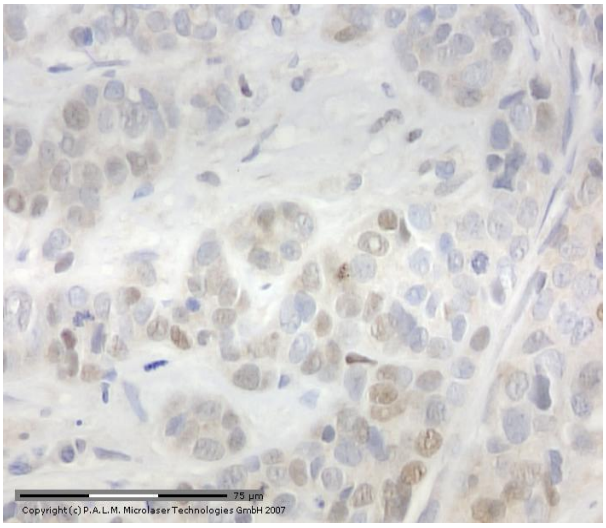

c RAD6

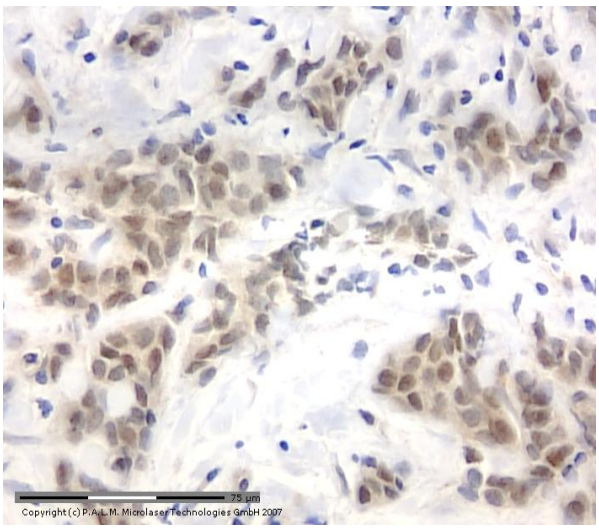

Figure 8.6 c-MYC immunohistochemistry in radiogenic samples.
Sections of sporadic and radiation-induced breast cancers were tested for c-MYC expression by immunohistochemistry. Sample RAD13 has no c-MYC expression in nuclei of tumour cells **(a)** and is therefore c-MYC negative. Sample RAD9 **(b)** shows weak staining and therefore weak c-MYC expression in a number of cell nuclei (Histoscore = 70.4)**.** Sample RAD6 **(c)** shows moderate to strong staining in the majority of cell nuclei and therefore has relatively high expression of c-MYC (Histoscore = 158.8).

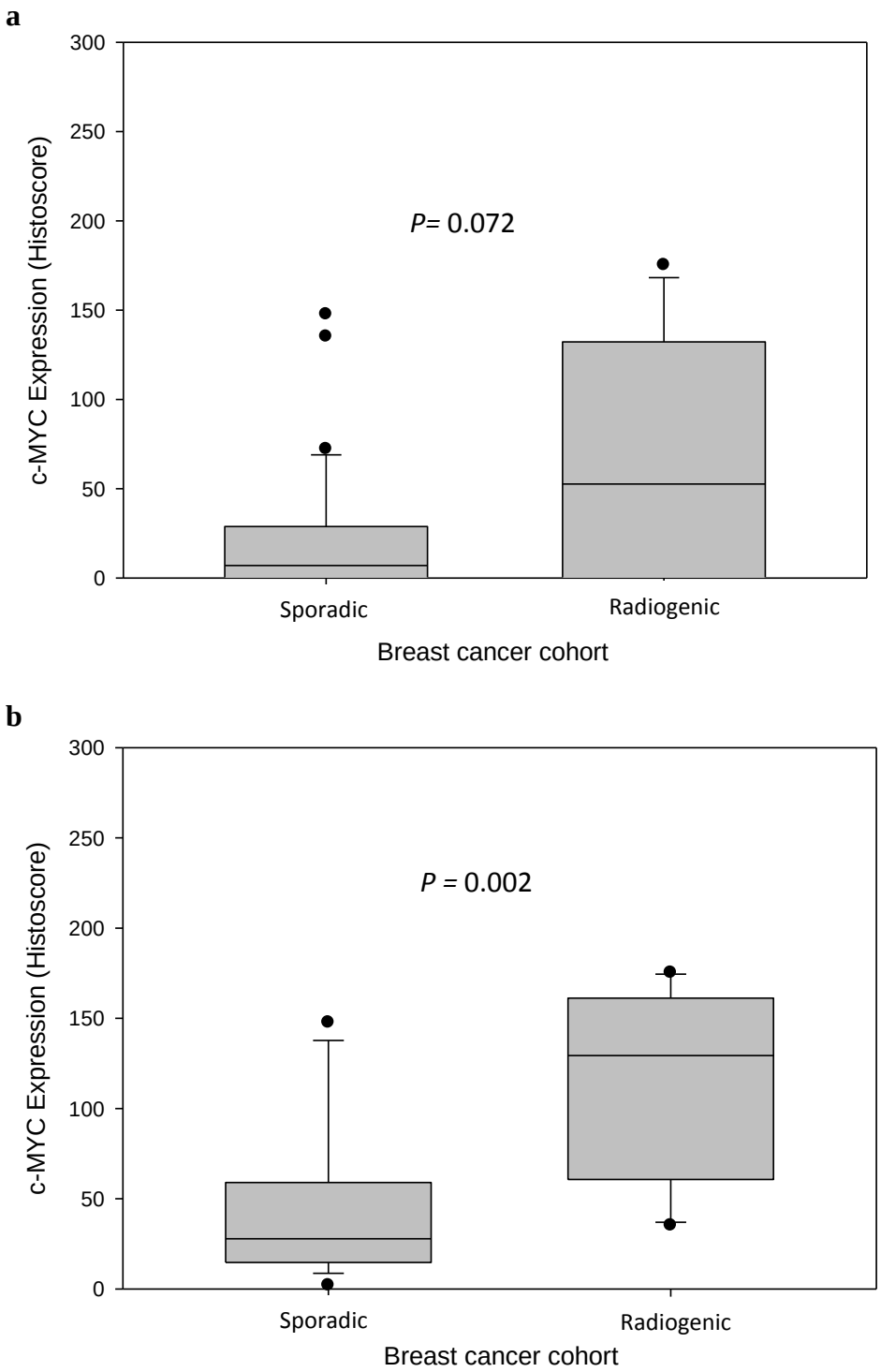

Figure 8.7 c-MYC expression in sporadic and radiogenic breast cancers.
Sections of sporadic (n=33) and radiogenic breast cancers (n=18) were tested for c-MYC expression by immunohistochemistry. The overall histoscore for each sample was calculated and the histoscores between the cohorts were compared **(a)**. The histoscores between the cohorts after the removal of samples which were negative for c-MYC expression (< 10% of nuclei positive for c-MYC) were also compared **(b)**. Horizontal bars represent the median values, the boxes represent the 25th and 75th percentiles of the data, the error bars represent the 10th and 90th percentiles and the black dots represent values outside the 10th and 90th percentile.

Although the proportion of cases positive for c-MYC expression was not significantly different between the radiogenic and sporadic breast cancer cases, the mean c-MYC expression level was higher in radiogenic cases. For the purpose of the analysis samples were split into 4 groups which represented: no c-MYC expression (histoscore = 0), weak expression (histoscore: 1-50), moderate expression (histoscore: 50-100) and high expression (histoscore > 100). The proportion of samples with weak, moderate or high c-MYC expression was calculated (Fig. 8.8). Three fold more radiogenic samples had high c-MYC expression than sporadic samples and 5.5 fold more sporadic samples had weak c-MYC expression compared to radiogenic samples. The difference in the proportion of samples with different scores of c-MYC expression between the two cohorts was significant (χ^2: p = 0.045). The results therefore indicated that mean expression of c-MYC was higher in radiation-induced breast cancer.

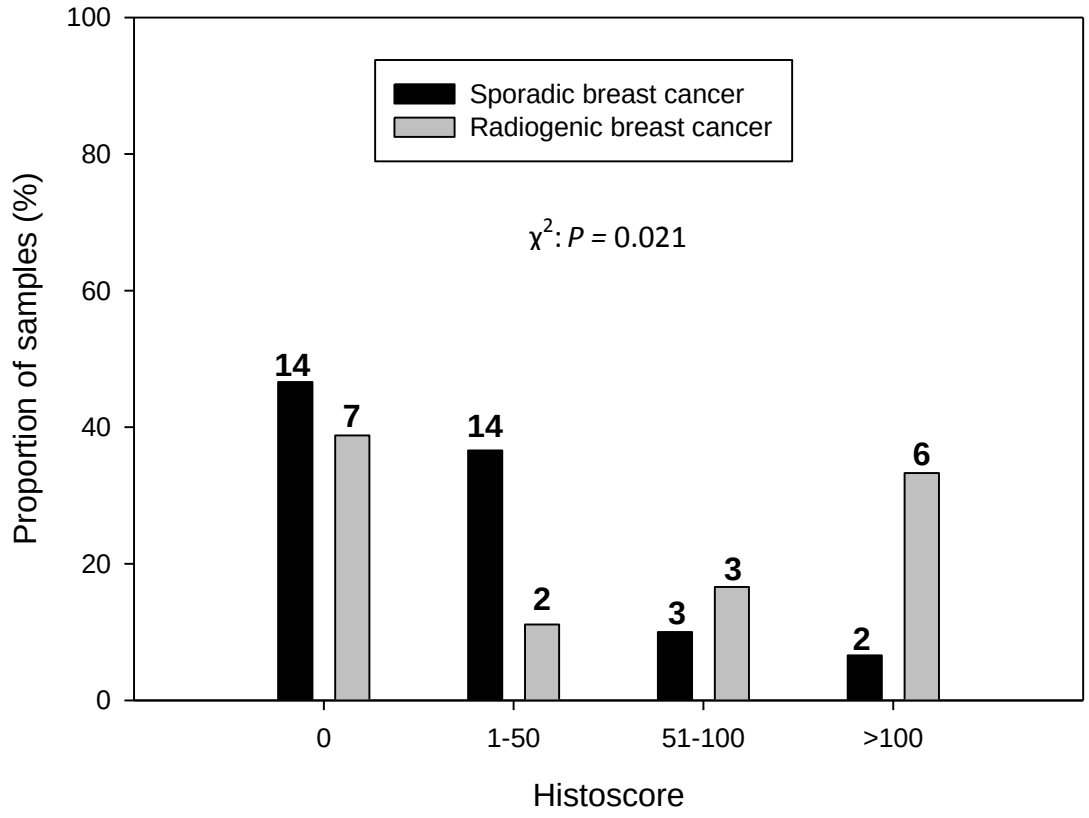

Figure 8.8 Proportion of sporadic and radiogenic breast cancers with different levels of c-MYC expression.
The proportion of samples which have a c-MYC histoscore of: 0, 1-50, 50-100 and >100 in the sporadic (n=33) and radiation-induced cohorts (n=18). Above each bar is the number of samples represented in that group from each cohort.

There was no correlation between c-MYC expression (histoscore) and age of breast cancer diagnosis in the sporadic cohort (Pearson's coefficient: $p = 0.644$). There was also no correlation between c-MYC expression and age of Hodgkin lymphoma diagnosis, age of breast cancer diagnosis or latency between diagnoses in the radiogenic cohort (Pearson's coefficient: $p>0.050$). There was also no relationship between c-MYC expression and pathology of the cancer in either of the cohorts and no relationship between expression and stage of the breast cancer in the radiogenic cohort.

There was however a weak positive correlation between c-MYC expression and radiation dose received during radiotherapy (Fig. 8.9a) (Pearson's coefficient = 0.414; $p = 0.078$). When samples which were deemed negative for c-MYC expression were removed from the analysis the correlation between radiation dose received and c-MYC expression strengthened but was also of borderline significance (Fig. 8.9b) (Pearson's coefficient = 0.544; $p = 0.076$).

In summary, analysis of c-MYC expression in radiogenic and sporadic breast cancer in the present study suggests that exposure to ionising radiation does not influence the proportion of breast cancers positive for c-MYC expression, but prior exposure to radiation associates with higher mean c-MYC expression level; an association which may be radiation dose dependent.

a

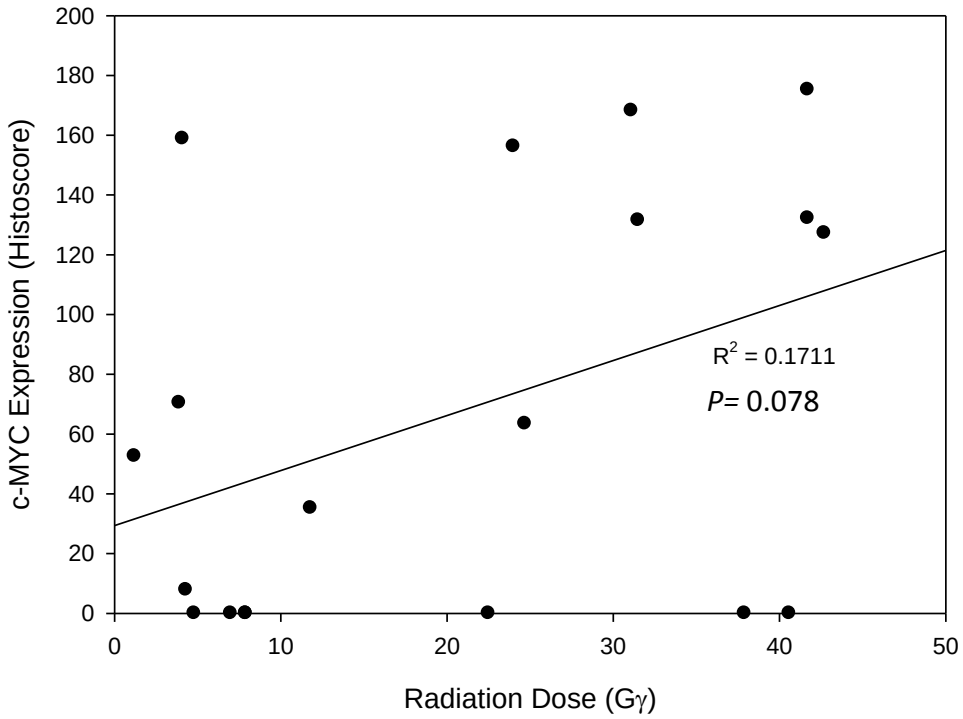

b

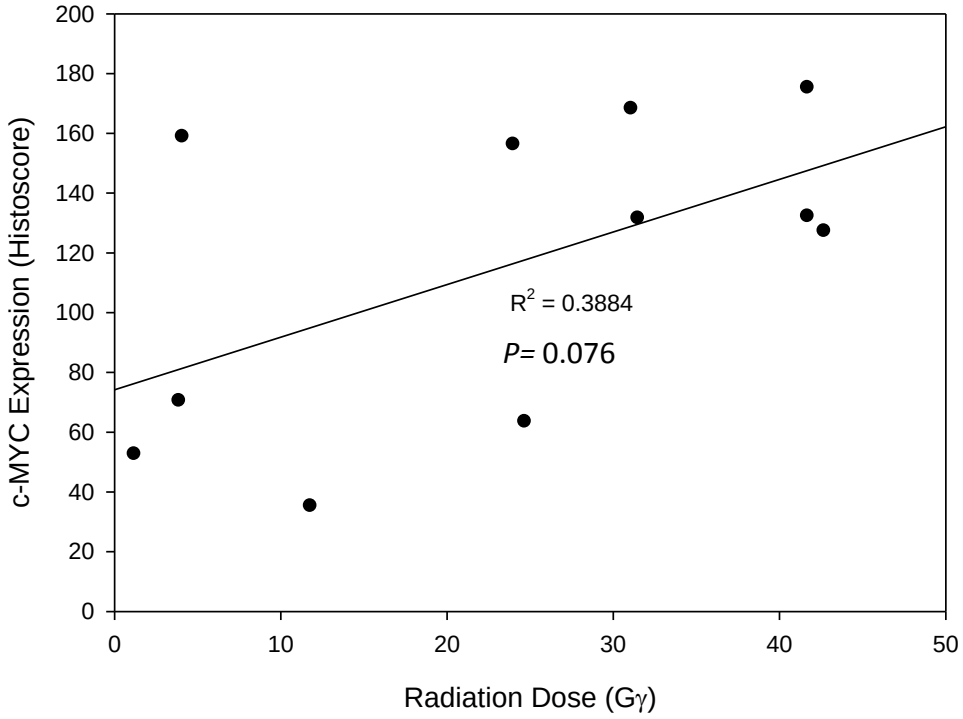

Figure 8.9 Correlation between radiation dose and c-MYC expression in radiogenic breast cancers. c-MYC expression is expressed against radiation dose received during radiotherapy for Hodgkin lymphoma in all tumours of the radiation-induced cohort **(a)** and only in tumours which expressed c-MYC (>10% of nuclei positive for c-MYC expression) **(b)**.

8.5 c-MYC copy number in radiogenic and sporadic primary breast cancer

c-MYC copy number was analysed in isolated nuclei from paraffin embedded tissues by FISH. A green fluorescent probe (Abbott Molecular, Berkshire, UK) which mapped to the centromere of chromosome 8 and an orange fluorescent probe (Abbott Molecular, Berkshire, UK) which mapped to *c-MYC* were used for cytogenetic analysis on slides of isolated nuclei (section 2.15). FISH was successful in 9 out of 18 radiogenic breast cancer cell nuclei samples and 20 out of 33 sporadic breast cancer cell nuclei samples. Hybridisation of both FISH probes on the same slide produced very weak signals in a large proportion of the samples which made reliable simultaneous assessment of *c-MYC* and chromosome 8 copy numbers impossible. However, separate hybridisation of the probes on independent slides from the same tissue sample produced stronger signals which could be counted. The disadvantage of this method of analysis was that the *c-MYC*/chromosome 8 status could not be determined in an individual nucleus.

One hundred nuclei were counted for each probe in each sample (Table 8.3). Copy number is indicated at the top of table 8.2 and the number of nuclei which have that particular copy number for each probe is shown underneath. Copy number analysis for *c-MYC* is indicated by red shaded numbers and copy number analysis for chromosome 8 by green shaded numbers. The intensity of the shading indicates the number of nuclei which contain that particular copy number.

	Copy number of probe													
	1	2	3	4	5	6	7	8	9	10	11	12	13	14
SPO2	5	53	8	6	21	5	2							
	38	62												
SPO5	7	82	10	1										
	7	79	9	5										
SPO6	16	77	4	3										
	17	79	3	1										
SPO7	8	44	13	29	3	3								
	8	48	12	25	3	2	1			1				
SPO10	7	88	3	1		1								
	7	80	9	1	1	1	1							
SPO11		62	5	5	14	9	2	2	1					
		66	7	11	8	6				1	1			
SPO13	16	74		10										
	4	88	6	2										
SPO15	10	89	1											
	9	88	3											
SPO17	4	56	10	14	8	3	5							
	3	49	8	19	13	4	3	1						
SPO18	10	66	18	6										
	7	66	21	6										
SPO21	10	62	12	4	5	4	1	2						
	7	62	23	7		1								
SPO22	15	76	4	4	1									
	17	76	5	2										
SPO24	5	70	15	8	2									
	14	71	13	2										
SPO26	9	39	36	16										
	4	50	43	2	1									
SPO27	8	67	20	1	2	2								
	13	71	12	3		1								
SPO28	4	48	30	18										
	7	83	9	1										
SPO29	5	38	15	42										
	6	44	7	43										
SPO30	15	73	9	3										
	40	52	6	2										
SPO31	12	76	10	1			1							
	7	77	14	2										
SPO32	7	83	6	4										
	17	67	14	2										
RAD1		45	8	32	2	11	2	1						
	7	44	16	18	8	4	3							
RAD2	4	92	2	2										
	9	84	4	3										
RAD3	1	48	48	3										
	17	48	35											
RAD4	5	92	1	2										
	4	94	2											
RAD5		56	4	32	9									
	2	63	25	9	1									
RAD8	1	22	11	40	17	5	1	1	1	1				
	9	35	9	40	2	2	2	1						
RAD9		41	3	15	22	7	7	2		2			1	
	13	79	4	4										
RAD10		53			3	5	1	8	13	6	5	5		1
	11	74	9	5	1									
RAD17	2	56	4	6	20	12								
	2	64	5	14	18			1						

Number of nuclei	0-5	6-20	21-50	51-75	75-100
	0-5	6-20	21-50	51-75	75-100

Table 8.3 Copy number analysis for *c-MYC* and chromosome 8 in radiogenic and sporadic breast cancer samples.

The number of copies of each probe is indicated at the top of the table. For each sample the number of nuclei which contain a particular copy number for *c-MYC* (red) and chromosome 8 centromere (green) is shown. The intensity of each colour is an indicator of the number of nuclei with that particular copy number. The number of nuclei which corresponds to each shade is shown by the key at the bottom of the table, where darker shades represent higher counts. SPO = sporadic; RAD = radiogenic.

A summary of the information in table 8.3 is shown in table 8.4. One of the caveats of copy number analysis using isolated nuclei is that it is not possible to determine whether the nuclei being counted are from tumour or non-malignant breast cells in any particular tissue sample. As an aid to data interpretation, an estimate of the tumour content of each tissue sample was made from histopathalogical analysis of the paraffin embedded tissue blocks. Twenty four of twenty nine (83%) tissue samples had a tumour content of at least 50% and 15/29 (52%) tissue samples had a tumour content of at least 75% (Table 8.4). The mean tumour content in the sporadic breast cancer series (62.5%) was not significantly different from that in the radiogenic breast cancer series (76.6%) (T-test: p=0.080). An estimate of tumour content in each tissue samples is available as a reference but the copy number counts were not adjusted in subsequent analysis using this value.

Sample	*Mean c-MYC* copy number	Mean chromosome 8 copy number	Ratio between *c-MYC* and chromosome 8 copy number	% of nuclei *c-MYC* copy number ≥ 3	% of nuclei chromosome 8 copy number ≥ 3	% of tumour nuclei in each sample
SPO2	3.08	1.62	1.90	42.00	0.00	80
SPO5	2.05	2.12	0.97	11.00	14.00	55
SPO6	1.94	1.88	1.03	7.00	4.00	70
SPO7	2.84	2.84	1.00	48.00	44.00	70
SPO10	2.02	2.16	0.94	5.00	13.00	85
SPO11	3.22	2.95	1.09	38.00	34.00	75
SPO13	2.04	2.06	0.99	10.00	8.00	90
SPO15	1.94	1.91	1.01	1.00	3.00	45
SPO17	2.95	3.19	0.92	40.00	48.00	80
SPO18	2.20	2.26	0.97	24.00	27.00	50
SPO21	2.58	2.34	1.10	28.00	31.00	70
SPO22	2.00	1.92	1.04	9.00	7.00	50
SPO24	2.32	2.03	1.14	25.00	15.00	65
SPO26	2.59	2.46	1.05	52.00	46.00	75
SPO27	2.28	2.09	1.09	25.00	16.00	55
SPO28	2.62	2.04	1.28	48.00	10.00	35
SPO29	2.94	2.87	1.02	57.00	50.00	80
SPO30	2.00	1.70	1.18	12.00	8.00	45
SPO31	2.05	2.11	0.97	12.00	16.00	20
SPO32	2.07	2.01	1.03	10.00	16.00	50
RAD1	3.38	3.00	1.13	55.00	49.00	75
RAD2	2.02	2.01	1.00	4.00	7.00	85
RAD3	2.50	2.18	1.15	51.00	35.00	90
RAD4	2.00	1.98	1.01	3.00	2.00	30
RAD5	2.95	2.44	1.21	45.00	35.00	90
RAD8	3.87	3.10	1.25	77.00	56.00	80
RAD9	3.49	1.99	1.75	59.00	8.00	90
RAD10	5.28	2.11	2.51	47.00	15.00	65
RAD17	3.22	2.91	1.11	42.00	38.00	85

Table 8.4 Copy number analysis for *c-MYC* and chromosome 8 in radiogenic and sporadic breast cancer samples – summary table.

For each sample the mean copy number for *c-MYC* and chromosome 8 was calculated. A mean copy number score greater than 2 indicated that there were nuclei with more than 2 copies of *c-MYC* or chromosome 8. The ratio between these values was calculated by dividing mean *c-MYC* copy number score by mean chromosome 8 copy number score. The percentage of nuclei which have a *c-MYC* and chromosome 8 copy number ≥ 3 was also calculated. The estimated percentage of tumour nuclei counted in each sample was determined following histopathalogical examination of the paraffin embedded tissue samples that the nuclei were extracted from. Green shaded samples show no evidence of a *c-MYC* copy number increase with fewer than 10% of nuclei counted having a *c-MYC* copy number ≥ 3, and red shaded samples show evidence of focal *c-MYC* amplification.

Although probing nuclei samples with two probes at the same time did not allow accurate copy number analysis by eye, some nuclei had strong enough signal for both probes to be detected by digital photography. Dual probe analysis was therefore performed on selected nuclei samples (SPO15, SPO2, SPO28, SPO18, RAD 9 and RAD 10) to obtain example images of *c-MYC*/chromosome 8 copy number status.

Samples that showed no amplification of *c-MYC* could be easily identified following analysis of the raw and summary copy number data. For samples that did not show evidence of *c-MYC* amplification (shaded green in table 8.4) the mean copy number of *c-MYC* and chromosome 8 was close to 2 and the ratio between the mean copy number values was close to 1. Fewer than 10% of the nuclei in these samples had a *c-MYC* copy number ≥ 3. An example of dual probe hybridisation for the non-amplified sample SPO15 is shown in figure 8.10.

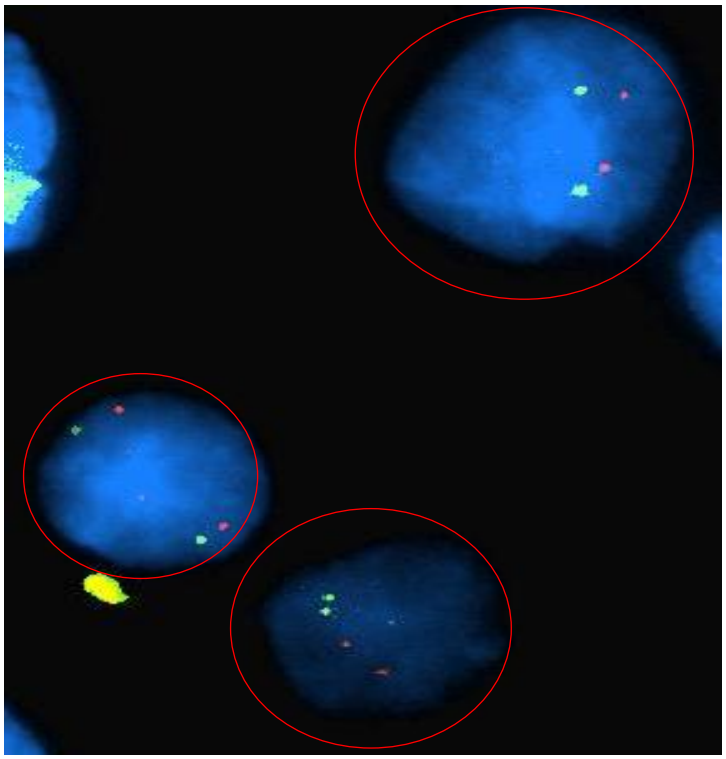

Figure 8.10 Dual probe FISH of sample SPO15.
Nuclei which are diploid for chromosome 8 (green probe) and *c-MYC* (red probe) are circled red.

Samples that showed evidence of a specific, intra-chromosomal, *c-MYC* copy number increase (shaded red in table 8.4) had a mean *c-MYC* copy number greater than 2 which was also greater than the mean copy number for chromosome 8. The ratio between the mean copy number values was greater than one and the proportion of nuclei which had a *c-MYC* copy number ≥ 3 was more than double that for chromosome 8. Examples of nuclei which show a specific copy number increase of *c-MYC* in samples SPO2, SPO28, RAD 9 and RAD 10 are shown in figure 8.11. These samples could be deemed to contain cells with a specific *c-MYC* amplification.

SPO2 appeared to have a monosomy of chromosome 8 and multiple copies of *c-MYC*. Examples of nuclei with 5 and 6 copies of *c-MYC* are shown in figure 8.11a. There was also a population which was diploid for chromosome 8 and had 4 copies of *c-MYC* in sample SPO2. The majority of nuclei from sample SPO28 were diploid for chromosome 8 and had either 3 or 4 copies of *c-MYC* (Fig. 8.11b).

Specific *c-MYC* amplified samples from the radiogenic breast cancer cohort (RAD9 and RAD10) had many more copies of *c-MYC* than the specifically amplified sporadic breast cancer samples (SPO2 and SPO28). RAD9 had a range between 4 and 13 copies of *c-MYC* per cell diploid for chromosome 8 (Table 8.4). Figure 8.11c shows nuclei with increasing copies of *c-MYC* from left to right in nuclei diploid for chromosome 8. The majority of RAD10 amplified nuclei had *c-MYC* copy numbers above 5 and up to 14 copies (Table 8.4). Figure 8.11d shows a range of nuclei diploid for chromosome 8 which have *c-MYC* amplification in this sample.

Many of the breast cancer samples are highly heterogeneous in terms of somatic *c-MYC* and chromosome 8 centromere copy number. This is particularly apparent in the radiogenic breast cancer samples where the number of copies of *c-MYC* varied greatly within the same nuclei population.

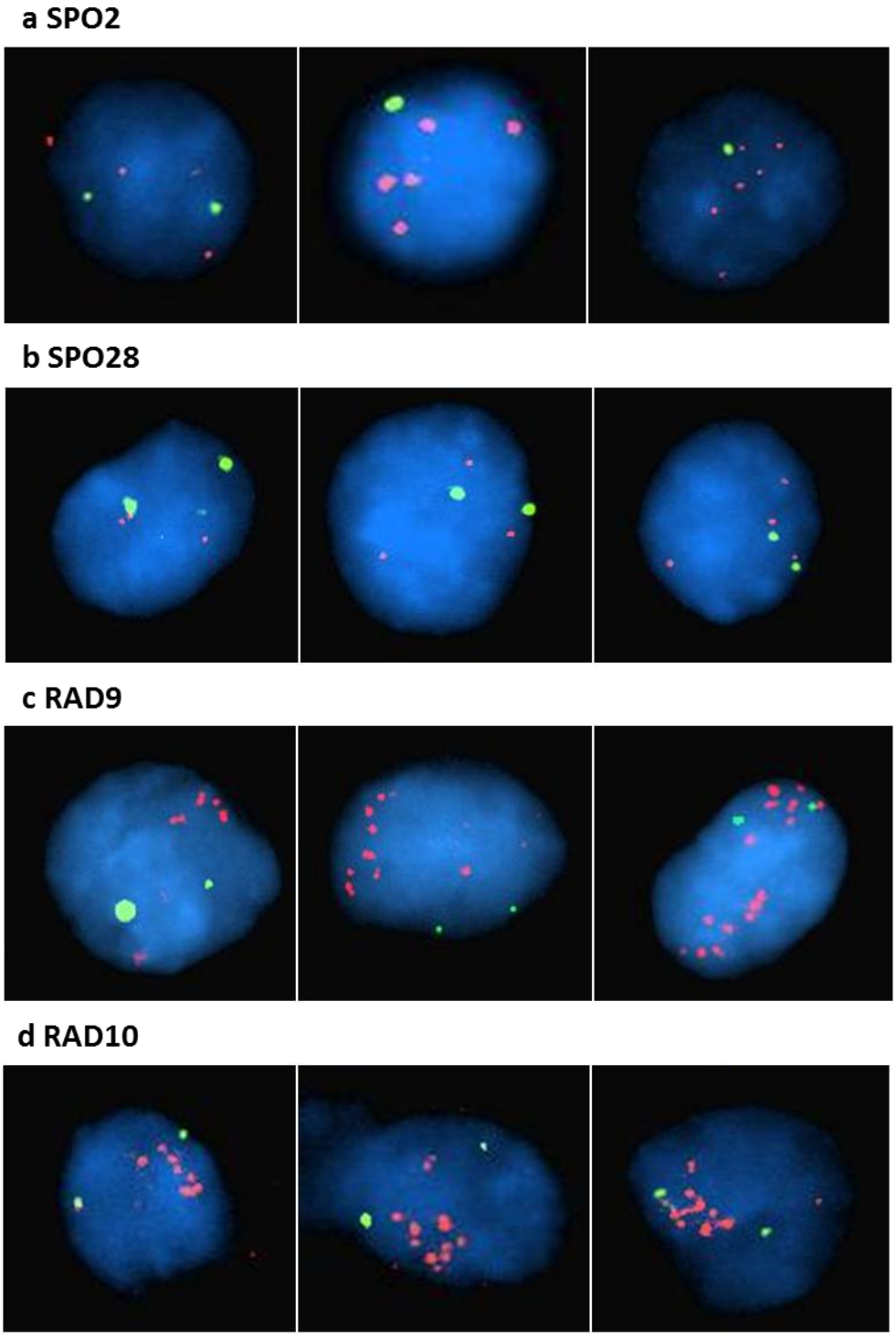

Figure 8.11 Dual probe FISH of samples SPO2, SPO28, RAD9 and RAD10.

Nuclei that show examples of specific, intra-chromosomal, *c-MYC* copy number increase for samples SPO2 **(a)**, SPO28 **(b)**, RAD9 **(c)** and RAD 10 **(d)**. The chromosome 8 FISH probe is green and the *c-MYC* FISH probe is red. The samples all show heterogeneity within the *c-MYC* amplified cell populations with regard to *c-MYC* copy number. The images are therefore arranged left to right for each sample from lowest *c-MYC* copy number to highest *c-MYC* copy number.

Numerous samples can be characterised by an increase in both c-MYC and chromosome 8 centromere copy number (un-shaded samples table 8.4). As such, the *c-MYC* copy number increase observed in these samples, such as SPO7, SPO17, SPO18 and SPO29, is likely due to chromosome 8 aneuploidy rather than specific *c-MYC* amplification. An example of dual probe hybridisation of SPO18 which contains a population with 3 copies of chromosome 8 and 3 copies of *c-MYC* is shown in figure 8.12.

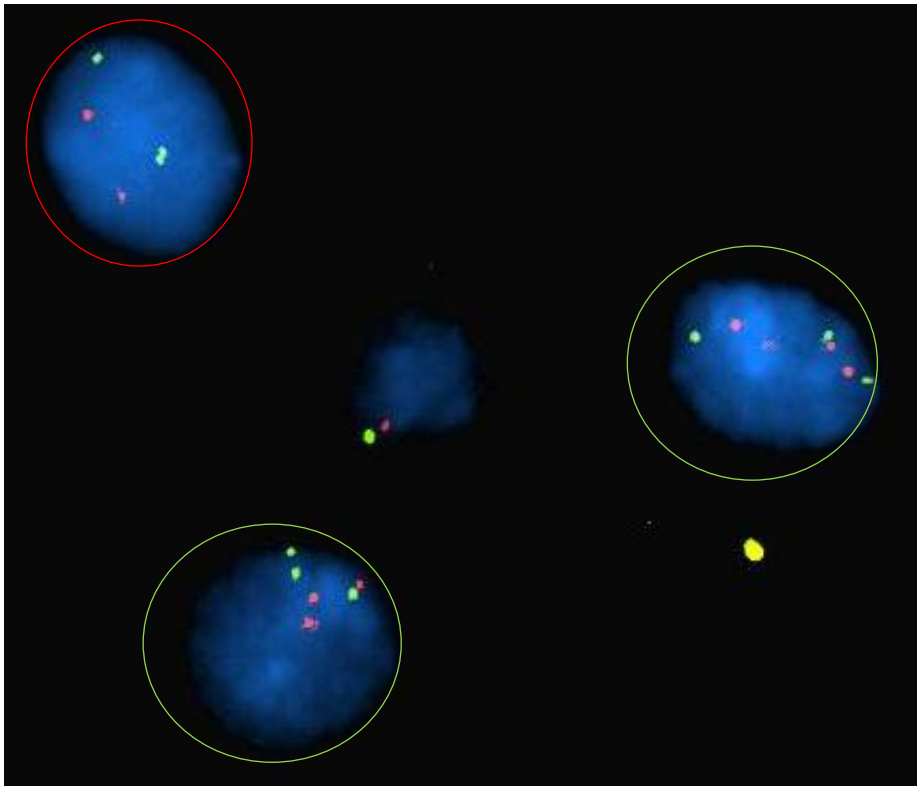

Figure 8.12 Dual probe FISH of sample SPO18.
Nuclei which are diploid for chromosome 8 (green probe) and *c-MYC* (red probe) are circled in red, nuclei which have 3 copies of chromosome 8 and *c-MYC* are circled in green. The un-circled nucleus in the middle of the image appears to have lost a copy of chromosome 8 and therefore a copy of *c-MYC*.

Some of the samples which displayed aneuploid *c-MYC* copy number gains also displayed evidence of specific *c-MYC* copy number increase, including RAD5 (41% of nuclei had greater than 3 copies of *c-MYC* compared to 10% for chromosome 8) and RAD8 (26 % of nuclei had greater than 4 copies of *c-MYC* compared to 7% for chromosome 8). The nature of the *c-MYC* copy number increase is ambiguous in these samples and without data from analysis using both probes in the same nuclei it is difficult to be confident of the mechanisms underlying the increase in *c-MYC* copy number.

Although dual scoring analysis was not available to determine the exact copy number increase mechanism of each sample, the ratio between mean *c-MYC* copy number and mean chromosome 8 copy number alluded to the relative contribution of specific and aneuploid copy number increase within each sample. A ratio of 1 indicated that any increase in *c-MYC* copy number was directly proportional to the copy number of chromosome 8 in the cell population. A ratio above one indicated that there were more copies of *c-MYC* than chromosome 8 and therefore potentially specific *c-MYC* amplification in a sub-population of the cells. Samples identified as having specific *c*-MYC amplifications (SPO2, SPO28, RAD9 and RAD10) had the highest *c-MYC*/chromosome 8 ratios (Table 8.4).

For the purposes of analysis, samples were split into 3 groups depending on the *c-MYC*/chromosome 8 ratio. A ratio $\leq$1.04 was used to identify samples with no evidence of specific *c-MYC* amplification in the sample, a ratio between 1.05-1.14 identified samples with some evidence of specific *c-MYC* amplifications and a ratio $\geq$1.15 identified samples where there was strong evidence of specific *c-MYC* amplification within the cell population. The proportion of samples in each cohort which had a *c-MYC*/chromosome 8 ratio of $\leq$1.04, 1.05-1.14 and $\geq$1.15 was calculated (Fig. 8.13). The radiogenic breast cancer cohort had 38% fewer samples with a *c-MYC*/chromosome 8 ratio of $\leq$1.04 and 40 % more samples with a ratio $\geq$1.15 than the sporadic breast cancer cohort. The difference between the two cohorts did not reach statistical significance but the small sample size will have limited the power of this analysis (χ^2: p = 0.062). Nevertheless, these data suggest that there were a higher proportion of samples focally amplified at the *c-MYC* locus in the radiogenic breast cancer cohort compared to the sporadic breast cancer cohort.

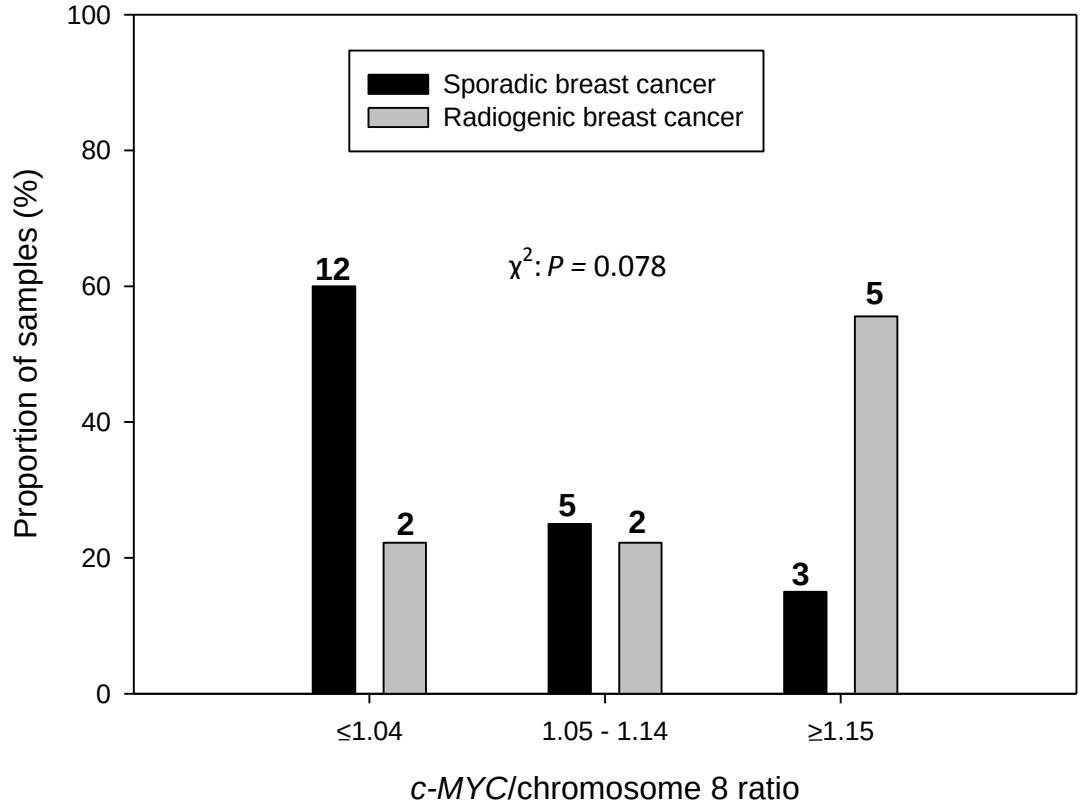

Figure 8.13 *c-MYC*/chromosome 8 ratio analysis.
The graph shows the percentage of cells in each cohort which have a *c-MYC*/chromosome 8 ratio of: <1.04, 1.05-1.14 and >1.15. Above each bar is the number of samples represented in that group from each cohort.

An increase in *c-MYC* copy number would be biologically relevant regardless of the mechanism of amplification. As such, the difference in *c-MYC* copy number between the two cohorts was statistically analysed. A sample was deemed to contain a cell population with a particular *c-MYC* copy number if at least 10 % of the nuclei had that number of copies. The percentage of samples which had cell populations with ≥ 3, 4, 5, 6 or 7 copies of *c-MYC* in each cohort is shown in figure 8.14. For both cohorts approximately 80% of the samples contained cell populations with ≥ 3 copies of *c-MYC*. The proportion of radiogenic samples with populations containing ≥4, 5 and 6 copies however was 15%, 30% and 40% higher than the sporadic breast cancer cohort, respectively. No sporadic breast cancer samples contained populations with ≥7 copies of *c-MYC* whereas 20% of the radiogenic cohort had cell populations with at least 7 copies of *c-MYC*. This analytical approach is affected by the proportion of malignant and non-malignant cells in each tissue sample. However, there was no difference in the mean tumour cell content between the samples from the two cohorts (T-test: p=0.079). As such, samples from the radiogenic breast cancer cohort appeared to have copy number gain events which lead to a higher number of copies of *c-MYC* compared to the sporadic breast cancer cohort; however the difference in the proportion of samples was only significant at ≥ 6 copies of *c-MYC* (Fisher Exact Test: p = 0.022).

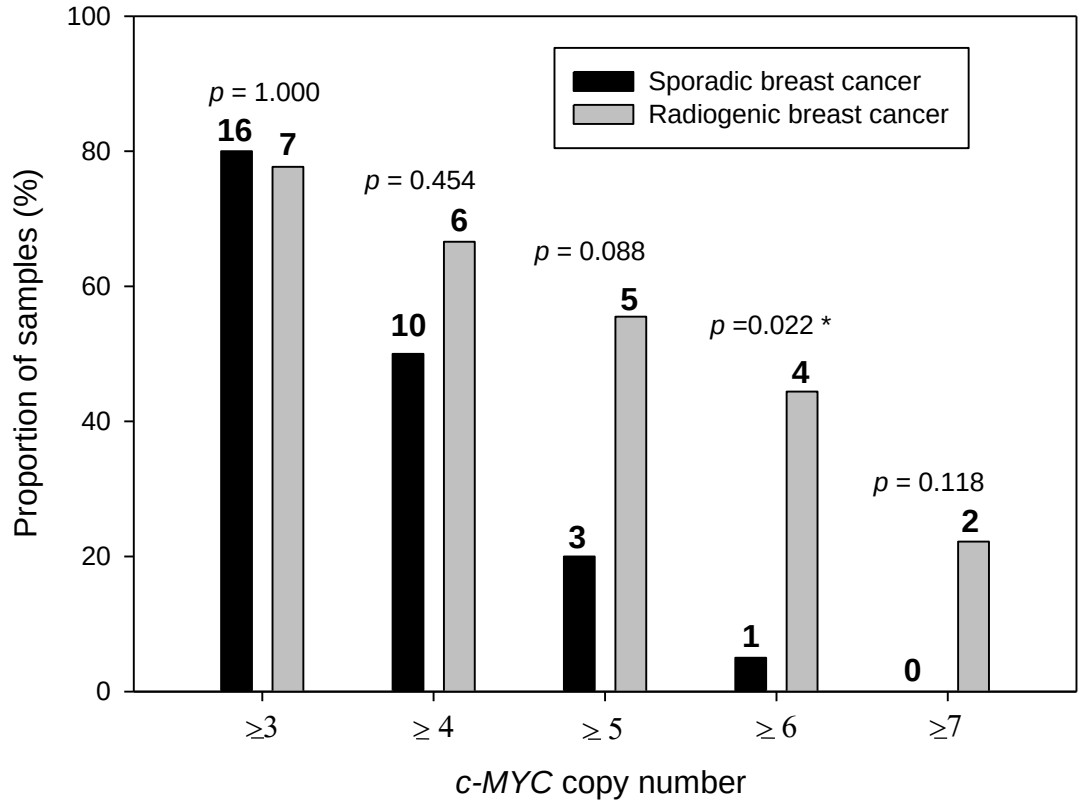

Figure 8.14 The proportion of samples which contained increasing copies of *c-MYC*.
The percentage of samples in which at least 10% of the nuclei counted contained ≥3, 4, 5, 6 and 7 copies of *c-MYC* from both the sporadic (n=20) and radiation-induced (n=9) breast cancer cohorts. Above each group is the Fisher Exact Test *p* value indicating the difference in the proportion of cases between the two cohorts. Above each individual bar is the number of cases for each cohort within that group. Significant differences between the two cohorts is represented by an *.

The difference in the mean *c-MYC* copy number per nuclei between the two cohorts was also analysed. The radiogenic breast cancer cohort had a higher mean *c-MYC* copy number than the sporadic breast cancer cohort which again indicated that exposure to ionising radiation increased the number of *c-MYC* copies in breast cancer cells. (Mann-Whitney test: $p = 0.030$) (Figure 8.15)

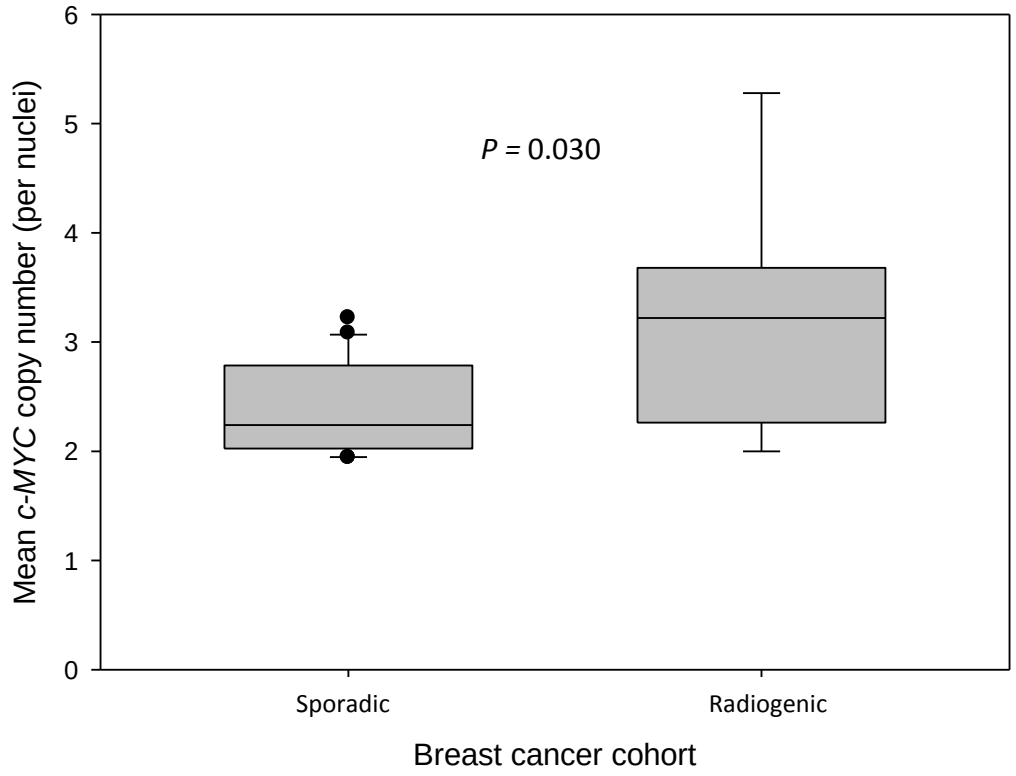

Figure 8.15 Mean *c-MYC* copy number in the sporadic and radiogenic breast cancer cohorts.
A comparison was made between the mean *c-MYC* copy number per nuclei in samples from the sporadic (n=20) and radiogenic (n=9) breast cancer cohorts. Horizontal bars represent the median values, the boxes represent the 25th and 75th percentiles of the data, the error bars represent the 10th and 90th percentiles and the black dots represent the values which lie outside the 10th and 90th percentile.

There was no correlation in either cohort between the mean *c-MYC* copy number and age of breast cancer diagnosis (Pearson's coefficient: Radiation-induced $p = 0.130$; Sporadic $p = 0.411$). There was also no correlation between mean *c-MYC* copy number and radiation dose received during radiotherapy, age of diagnosis of Hodgkin lymphoma or latency in years between Hodgkin lymphoma and breast cancer diagnosis (Pearson's coefficient: $p>0.050$ for all analyses).

Analysis of both cohorts combined revealed that there was no correlation between mean *c-MYC* copy number and c-MYC expression (Pearson's coefficient: $p = 0.141$) (Table 8.5). However when the samples were separated into those which had a mean *c-MYC* copy number ≥ 3, and those which had a mean *c-MYC* copy number < 3 there appeared to be an association with c-MYC expression (Figure 8.16). Seven samples which had a mean *c-MYC* copy number ≥ 3 had a c-MYC histoscore of 64.26 (Median = 63.4) compared to 22.10 (Median = 1) in 22 samples which had a mean *c-MYC* copy number < 3; however the difference was not significant (Mann-Whitney: $p = 0.115$). It is noteworthy that some samples, such as RAD 8, have evidence for increased *c-MYC* copy but are null for c-MYC expression, and others, such as RAD 4, which have no increase in *c-MYC* copy number but have high c-MYC expression.

In summary, those cancers that developed following exposure to therapeutic ionising radiation had a greater proportion of specific copy number increase of *c-MYC* compared to sporadic breast cancers. Exposure to ionising radiation also appeared to increase the absolute number of copies of *c-MYC* however the influence this has on expression of c-MYC is unclear. The implications of these findings will be discussed in section 8.5.

Sample	*c-MYC* Score	Histoscore
SPO2	3.08	147.6
SPO5	2.05	0
SPO6	1.94	2
SPO7	2.84	0
SPO10	2.02	0
SPO11	3.24	12.2
SPO13	2.04	6.6
SPO15	1.94	0
SPO17	2.95	47
SPO18	2.20	0
SPO21	2.58	29.8
SPO22	2.00	0
SPO24	2.32	0
SPO26	2.59	0
SPO27	2.28	27.8
SPO28	2.62	0
SPO29	2.94	17.2
SPO30	2.00	72.2
SPO31	2.05	64.2
SPO32	2.07	0
RAD1	3.37	156.2
RAD2	2.02	0
RAD3	2.53	35.2
RAD4	2.00	131.5
RAD5	2.94	52.6
RAD8	3.87	0
RAD9	3.89	70.4
RAD10	5.28	63.4
RAD17	3.17	0

Table 8.5 *c-MYC* copy number and c-MYC expression results of samples from the sporadic and radiogenic breast cancer cohorts.
Displayed are the calculated mean *c-MYC* copy number scores and c-MYC expression histoscores of samples which were analysed by FISH in the sporadic and radiogenic breast cancer cohorts. SPO = Sporadic breast cancer samples; RAD = Radiogenic breast cancer samples.

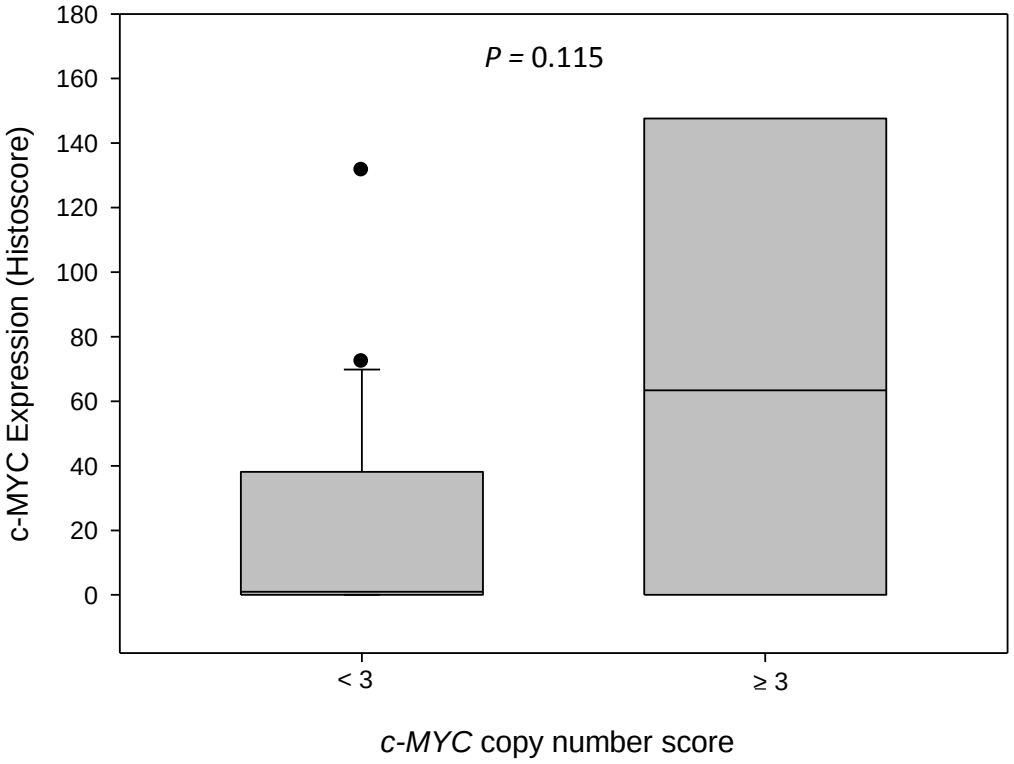

Figure 8.16 Comparison of c-MYC expression between cohorts with different mean *c-MYC* copy number states.
A comparison was made between *c-MYC* expression (histoscore) in breast cancer samples which had a mean *c*-MYC copy number score < 3 (n=22) or ≥ 3 (n=7). Horizontal bars represent the median values, the boxes represent the 25th and 75th percentiles of the data, the error bars represent the 10th and 90th percentiles and the black dots represent the values which lie outside the 10th and 90th percentiles.

8.6 Discussion

In this chapter the expression of POU2F1 and c-MYC, and the copy number state of *c-MYC,* between cohorts of radiogenic and sporadic breast cancer has been compared in an attempt to identify a molecular genetic marker of radiogenic breast cancer.

8.6.1 Breast cancer cohorts

Material was available from 18 patients who developed breast cancer following radiotherapy for Hodgkin lymphoma and 33 age-matched patients who developed sporadic breast cancer.

The mean age of breast cancer diagnosis was 37.89 years in the radiation-induced cohort and 40.6 years in the sporadic cohort. In the United Kingdom 81% of breast cancer cases occur in women aged 50 years and over (Office for National Statistics, Edition: MB1 39). Breast cancer in younger women tends to be more aggressive and invasive with approximately 70 % of cancers being infiltrating ductal carcinomas (Axelrod *et al.,* 2008). In the present study, 87 % of sporadic breast cancer cases contained areas of infiltrating ductal carcinoma, which is consistent with the pathology of breast cancer in younger women. There was no information available other than the age of breast cancer diagnosis and pathology of the cancer for the sporadic cases.

As stated previously, the link between ionising radiation therapy for Hodgkin lymphoma in young women and the subsequent increased risk of breast cancer is well established (reviewed in Chapter 1). The radiogenic breast cancer cohort used in the present study had characteristics consistent with similar cohorts used in previous studies. For example, for the majority of cases, cancer developed following mantle field radiotherapy in the upper outer quadrant of the breast, as this region of the breast is exposed to the largest dose of ionising radiation (Christie *et al.,* 1998). In the present study 66 % of breast cancers in the radiogenic cohort developed in this region and is therefore consistent with previous reports.

The latency between exposure to ionising radiation and development of cancer is a key characteristic of radiation-induced carcinogenesis, and is most likely due to radiation-induced genetic instability which causes subsequent accumulation of cell transforming mutations over time (Allan and Travis, 2005). The mean latency between age of diagnosis of Hodgkin lymphoma and breast cancer in the present study was 15.33 years and was consistent with the mean latency reported in other studies (15-20 years)

(Hancock *et al.*, 1993; Tinger *et al.*, 1997; Travis *et al.*, 2003; van Leeuwen *et al.*, 2003; Wahner-Roedler *et al.*, 2003; Basu *et al.*, 2008; De Bruin *et al.*, 2009; Elkin *et al.*, 2011).

Precise estimates of dose to the affected area of the breast allow detailed analysis of the effects of ionising radiation on breast transformation. In the present study, a borderline significant inverse linear relationship between radiation dose received at the affected area of the breast and latency between radiotherapy for Hodgkin lymphoma and breast cancer diagnosis was identified. Travis *et al.* (2003) showed that 60 % of individuals who had received < 4 Gγ of ionising radiation to the affected area of the breast developed breast cancer more than 20 years after exposure to ionising radiation; however 65.6 % of individuals who had received ≥ 4 Gγ of ionising radiation to the affected area of the breast developed breast cancer within 20 years of exposure to ionising radiation. The present study was the first study to identify a putative linear relationship between radiation dose and latency of breast cancer development following radiotherapy for Hodgkin lymphoma.

Higher radiation doses increase the amount of DNA damage in cells (Chadwick and Leenhouts, 2011). The probability of a cell acquiring multiple mutations therefore increases with increasing radiation dose. Moreover, the probability of inactivating a key gene in a cellular pathway that controls spontaneous mutation frequency also presumably increases as a function of increasing radiation dose. Cells that acquire a mutator phenotype take less time to acquire genetic alterations required for transformation. Taken together, these observations provide a plausible explanation for the inverse relationship between dose and latency in radiogenic cancer.

In the case of mantle field radiotherapy for Hodgkin lymphoma, higher radiation dose also means a greater number of fractionated doses of irradiation (approximately 2 Gγ per fractionated dose) (Hancock *et al.*, 1993; De Bruin *et al.*, 2009). Fractionated dosing is established as a mechanism for selecting cells with a mutator phenotype (Hampson *et al.*, 1997), further promoting and accelerating transformation to the malignant state.

In summary, the radiogenic breast cancer cohort utilised in the present study display characteristics which are consistent with radiation-induced breast cancer.

8.6.2 POU2F1

POU2F1 was an interesting candidate for a molecular genetic marker of radiogenic breast cancer as it was focally deleted following exposure to ionising radiation in MCF-10A cells had with a concomitant reduction in protein expression, and has an established role in cellular DNA damage response (Meighan-Mantha *et al.*, 1999; Zhao *et al.*, 2000; Jin *et al.*, 2001; Fan *et al.*, 2002; Schild-Poulter *et al.*, 2003; Tantin *et al.*, 2005; Schild-Poulter *et al.*, 2007; Maekawa *et al.*, 2008; Saha *et al.*, 2010; Wang and Jin, 2010). In particular, the role played by POU2F1 as a transcriptional regulator of BER genes following oxidative damage was intriguing as both radiation and oestrogen metabolites (which synergise to promote breast transformation) can both induce oxidative DNA damage (Yager and Davidson, 2006). It can therefore be speculated that *POU2F1* deletion, and subsequent reduction in protein expression, may make young women exposed to ionising radiation at greater risk of developing breast cancer.

No spontaneous breast cancer samples lost POU2F1 expression, yet 1 radiation-induced sample (RAD7) displayed complete loss of expression. This sample had received the sixth highest dose of radiation (31.1 Gγ), was from the youngest individual diagnosed with breast cancer (28 years), had only a latency of 10 years between Hodgkin lymphoma and breast cancer diagnosis, was an infiltrating ductal carcinoma and was a low stage cancer (Stage I). However, the identification of only 1 breast cancer case with no POU2F1 expression indicates that loss of POU2F1 expression is not a common event in radiogenic breast cancer.

It is possible that reduced, but not lost, expression of POU2F1 would increase genetic instability in cells. For example, loss of only 60% of basal POU2F1 expression was enough to abrogate BER gene induction (Saha *et al.*, 2010). Due to the strong staining of the IHC antibody in the present study it was only possible to positively or negatively assess POU2F1 expression. It would be interesting to use other methods of protein quantification, or to reanalyse the samples by IHC using different dilutions of the antibody, to assess if more subtle differences in POU2F1 expression between the radiogenic and spontaneous breast cancer cohorts existed. It would also be interesting to assess the incidence of *POU2F1* deletion between radiogenic and spontaneous breast cancer. Irradiated MCF-10A cells showed almost complete loss of POU2F1 expression even though one allele of *POU2F1* remained; however it is also possible that other mutations affected expression of the protein. It is possible that mono-allelic deletion of

POU2F1 in a diploid cell may reduce POU2F1 expression to a mutagenic but non-lethal level through a mechanism involving haploinsufficiency. Unfortunately, due to poor probe hybridisation (data not shown) it was not possible to assess the copy number state of POU2F1 by FISH analysis in primary patient material in the present study.

8.6.3 c-MYC copy number

A focal amplification of *c-MYC* and an associated increase in c-MYC expression in MCF-10A cells following exposure to exogenous oestrogen and ionising radiation was identified in the present study. Amplification of *c-MYC* has previously been linked with radiation-carcinogenesis and in particular has been identified in breast cancer developing in atomic bomb survivors (Felber *et al.*, 1992; Miura *et al.*, 2008; Manner *et al.*, 2010; Guo *et al.*, 2011). *c-MYC* is an established oncogene which initiates cell transformation and increases genetic instability (Prochownik and Li, 2007; Xu *et al.*, 2010). Amplification of *c-MYC* is therefore a strong candidate as an early genetic event and molecular marker of radiogenic breast cancer.

c-MYC copy number state was analysed in isolated nuclei from radiogenic and sporadic breast cancer tissues. One of the caveats of copy number analysis using isolated nuclei is that it is not possible to determine whether the nuclei being counted are from tumour or non-malignant breast cells in any particular tissue sample. Adjusting copy number counts according to relative tumour content would rely on the assumption that only nuclei from malignant cells contain a *c-MYC* copy number increase. Field cancerization theory has demonstrated that non-malignant and malignant cells adjacent to each other in a tissue can share genetic alterations as both cell populations are descended from the same non-transformed, but mutated, cellular ancestor (Slaughter *et al.*, 1953; Braakhuis *et al.*, 2003; Heaphy *et al.*, 2009). If *c-MYC* amplification is an early event in breast carcinogenesis, nuclei from pre-malignant tissue may also contain copy number increase of *c-MYC*. One approach to test this hypothesis is to use laser capture microscopy to purify and analyse malignant and pre-malignant cells separately.

c-MYC copy number analysis indicated that the incidence of cases that contained a specific copy number increase of *c-MYC* was higher in the radiogenic breast cancer cohort than the sporadic breast cancer cohort. Furthermore, the absolute number of copies of *c-MYC* was higher in radiogenic breast cancer compared to sporadic breast cancer indicating a tendency towards the acquisition of higher-copy number gains.

These data therefore indicate that *c-MYC* amplification is more common in radiogenic breast cancer than sporadic breast cancer.

Results from the present study agree with the findings of Miura et al. (2008) which investigated *c-MYC* amplification in breast cancer cases from survivors of the atomic bomb at Nagasaki. The study reported that the incidence of breast cancers with *c-MYC* amplification (at least 2 fold greater number of *c-MYC* copies compared to chromosome 8 copies) was higher in individuals exposed to ionising radiation compared to an age matched control group and that the incidence of *c-MYC* amplification increased as estimated radiation dose increased. We did not observe an association between the incidence of *c-MYC* amplification and radiation dose received by an individual in the present study; however the number of cases analysed was small. Also, the doses received by the Hodgkin lymphoma patients were relatively high compared to atomic bomb survivors. A difference in *c*-MYC incidence was observed by Miura et al. (2008) between groups of individuals who had received < 1.2 Gγ and ≥ 1.2 Gγ. The lowest dose received by a Hodgkin lymphoma patient was 1.2 Gγ. It is therefore possible that the relationship between *c-MYC* amplification incidence and dose is lost at the higher dose range.

Miura et al. (2008) also reported an association between *c-MYC* amplification and *HER2* amplification in atomic bomb survivors. Amplifications of *c-MYC* and *HER2* are closely associated in breast cancer (Park *et al.*, 2005). It has been demonstrated that radiation exposure during breast maturation increases the risk of *HER2* amplification and increased incidence of HER2 positive breast cancer was identified in radiogenic breast cancer from Hodgkin lymphoma patients (Castiglioni *et al.*, 2007; Sanna *et al.*, 2007; Broeks *et al.*, 2010). The increased incidence of *c-MYC* amplification identified in the present study may therefore in part relate to an increase in incidence of HER2 positive breast cancer.

Caution must be exercised when comparing results between the atomic bomb study and the present study as the breast cancer cohorts and circumstances of radiation exposure were very different. For example, the incidence of breast cancer per unit population in Japan is lower than in Western populations, mainly due to lifestyle factors such as contraceptive methods and alcohol intake (Iwasaki and Tsugane, 2011). Differences in genetic background between Asian and European populations may also impact on breast cancer risk, radiation sensitivity or risk of oncogene amplification. Also, although both

cohorts are from populations which have an established increased risk of breast cancer following exposure to ionising radiation, the atomic bomb survivors were exposed to a single dose of irradiation compared to fractionated doses in Hodgkin lymphoma patients.

Despite these differences the incidence of *c-MYC* amplification appears to be elevated in both cohorts compared to spontaneous breast cancer, and the common factor which links the cohorts is exposure to ionising radiation significantly above background levels.

c-MYC amplification has also been implicated in radiation-induced secondary angiosarcoma (AS) following radiotherapy for breast cancer and radiation-induced skin cancer in rats (Felber *et al.*, 1992; Manner *et al.*, 2010; Guo *et al.*, 2011). *c-MYC* amplification was identified in 100% of radiation-induced secondary AS on the breast but was not identified in any radiation-induced atypical vascular lesions (AVL's), which are reported to be pre-malignant precursors to secondary AS (Guo *et al.*, 2011), suggesting that c-MYC amplification is not an initiating event, but develops later during tumour formation. However, the role of AVL's as precursors to AS is not established and AVL's are considered benign entities (Mandrell *et al.*, 2010). The absence of *c-MYC* amplification in AVL's may not therefore rule out *c-MYC* amplification as being an early event in secondary AS.

It is possible that *c-MYC* amplification is a common late stage event in radiogenic breast cancer; however the mechanism by which *c-MYC* could be amplified due to ionising radiation many years after the initial exposure is unclear. The identification of radiation-induced *c-MYC* amplification in MCF-10A cells prior to cell transformation, and increased incidence of amplification in two different cohorts of radiogenic breast cancer implicate *c-MYC* amplification as a common early genetic event. Based on the field cancerization theory discussed previously, the identification of *c-MYC* copy number increases in radiation exposed pre-malignant breast tissue would suggest an early role for *c-MYC* amplification during transformation and would be an interesting line of investigation in future studies.

8.6.4 c-MYC protein expression

Protein expression analysis showed that mean c-MYC expression was higher in the radiogenic breast cancer cohort compared to the sporadic cohort and identified a borderline significant correlation between radiation dose and expression. There was no difference between the cohorts in the proportion of cases which showed no c-MYC

expression; however there was an increase in the proportion of samples with high c-MYC expression. Expression of c-MYC has not previously been analysed in radiogenic cancer.

It has been demonstrated *in vitro* that increased *c-MYC* copy number increases c-MYC expression; however there was no correlation between *c-MYC* copy number and expression in primary breast cancer tissue in the present study. The lack of correlation will in part be due to the low number of cases for which both copy number and expression data was available, however inconsistency between *c-MYC* amplification and protein expression are not uncommon and has been described in breast, pancreatic, bladder and colon cancer studies (Erisman *et al.*, 1985; Sauter *et al.*, 1995; Chrzan *et al.*, 2001b; Schleger *et al.*, 2002). Cases in which protein expression appears inconsistent to gene copy number are likely to be due to gene regulatory mechanisms such as transcriptional activation/repression and mRNA/protein stability affecting expression of the protein (Xu *et al.*, 2010).

Despite this, a non-significant 3 fold increase in mean c-MYC expression in cases with a mean *c-MYC* copy number score > 3 was identified. Likewise, (Blancato *et al.*, 2004) reported a correlation between *c-MYC* amplification and expression in breast cancer. The increased incidence of *c-MYC* amplification and increased tendency of higher copy number gains in radiogenic breast cancer may therefore partly explain increased c-MYC expression in radiogenic breast cancer; however the limited number of radiogenic samples for which there is copy number data makes confirmation of this hypothesis difficult at the present time.

The observed dose dependant increase in c-MYC expression in primary tissue samples may be caused via positive selection of cells which express high levels of c-MYC. Fractionated dose exposure causes multiple cycles of cell death and re-population in the irradiated area (Phillips *et al.*, 2006; Vlashi *et al.*, 2009). If c-MYC expression confers a growth advantage during cycles of cell death and re-population then fractionated dose exposure may select for cells with increasing expression of c-MYC. Over-expression of c-MYC increases cell proliferation which would provide an obvious growth advantage during repopulation of an irradiated area (Dang *et al.*, 2006; Meyer and Penn, 2008; Xu *et al.*, 2010). c-MYC has also been implicated in increasing radiation resistance, which would reduce cell death during repeated exposure to ionising radiation, also leading to an increase of c-MYC expressing cells (Chiang *et al.*, 1998; Davey *et al.*, 2004; Kim *et*

al., 2011a). The present study has demonstrated that *c-MYC* amplified cells have an expression profile with features similar to the cancer stem cell, which is known to be a radiation-resistant cell population and is a favoured candidate for causing radiation-resistance in breast cancer (Vlashi *et al.*, 2009). Over-expression of transcriptional activators of c-MYC such as JAGGED-1, NOTCH-1 and the WNT/β-CATENIN pathway have been reported in radiation-resistant cancer stem cell populations, providing further evidence for a putative role for c-MYC in radiation-resistance (Phillips *et al.*, 2006; Woodward *et al.*, 2007). Selection of cell populations with increasing expression of c-MYC during fractionated radiation exposure may therefore explain the apparent dose dependant relationship in the Hodgkin lymphoma cohort. Selection of cell populations with high levels of c-MYC would also explain the presence of cell populations which over-express c-MYC but do not have *c-MYC* amplification.

It is possible that the radiation induced *c-MYC* amplification model and c-MYC selection model work synergistically in circumstances of repeat exposure to ionising radiation. Ionising radiation may induce amplification of *c-MYC* in a sub-population of cells which is subsequently selected for during cycles of cell death and re-population during repeat radiation exposure.

8.6.5 c-MYC and oestrogen in radiogenic breast cancer

The relationship between oestrogen and *c-MYC* amplification in radiogenic breast carcinogenesis must also be considered, as loss of circulating oestrogen can attenuate the risk of radiogenic breast cancer (Travis *et al.*, 2003; van Leeuwen *et al.*, 2003).

Over-expression of c-MYC is insufficient on its own to induce cell transformation (Land *et al.*, 1983; Xu *et al.*, 2010). Further genetic mutations are therefore needed. Exposure to oestrogen and its metabolites may promote the accumulation of mutations needed for the development of breast cancer. Loss of circulating oestrogen may reduce the probability of accumulating these alterations and therefore attenuate breast cancer risk.

c-MYC is a downstream transcriptional target of ERα and is up-regulated in ERα positive breast cancer. Following *c-MYC* amplification, high circulating oestrogen concentrations may further enhance c-MYC expression and therefore increase genetic instability. Oestrogen has also been reported to stabilise c-MYC protein (Rodrik *et al.*,

2006). It is postulated that stabilisation is mediated by ERα but this yet to be conclusively demonstrated. Loss of oestrogen exposure may therefore lead to c-MYC degradation and attenuation of c-MYC oncogenic activity.

Conversely, previous studies have reported an increased incidence of basal-like breast cancers (which are ERα negative) in radiogenic cohorts compared to age matched sporadic cohorts (Sanna *et al.*, 2007; Broeks *et al.*, 2010). Over-expression of c-MYC is common in the basal-like breast cancer subtype and is believed to mimic a large part of ER transcriptional regulation; suggesting a mechanism via which these cancers attain oestrogen independence (Alles *et al.*, 2009). Epithelial to mesenchymal transition is implicated in the development of basal-like breast cancers and c-MYC over-expression has been shown to induce EMT (Cowling and Cole, 2007; Trimboli *et al.*, 2008; Liu *et al.*, 2009; Smith *et al.*, 2009; Cho *et al.*, 2010). The present study has demonstrated that *c-MYC* amplification induced phenotypic and gene expression changes related to EMT in MCF-10A cells. c-MYC over-expression may therefore be an early event in the induction of basal–like breast cancer. It should be noted however, that although c-MYC over-expression has been associated with basal-like sporadic breast cancer, *c-MYC* amplification was reported to be rare (Rodriguez-Pinilla *et al.*, 2007). The higher incidence of *c-MYC* amplification in radiogenic breast cancer may therefore suggest a novel mechanism for the induction of basal-like breast cancer not observed in sporadic cancer. Investigation of *c-MYC* copy number status in radiogenic basal-like breast cancers would allow this hypothesis to be tested.

In summary, evidence has been provided that the incidence of *c-MYC* amplification and expression of c-MYC is higher in radiogenic breast cancer compared to sporadic breast cancer and may therefore be a molecular marker of radiogenic breast cancer. Whether *c-MYC* amplification occurs early or late during transformation remains unclear; however it is hypothesised that ionising radiation induces *c-MYC* amplification at the time of exposure which contributes to the accumulation of mutations ultimately leading to cancer. Whether *c-MYC* amplification is a common radiation-induced event in all cancer types is also unknown and investigation of other radiogenic cancer types is warranted.

Chapter 9: Final Discussion

The aim of the present study was to develop an *in vitro* model of radiation-induced breast epithelial cell transformation in order to identify copy number alterations induced by ionising radiation exposure, which in turn could be investigated in a cohort of primary human radiogenic breast cancer samples. The overall aim was to identify alterations that could be used as genetic markers to identify radiogenic breast cancer and to gain further understanding of the molecular genetic mechanisms underlying radiogenic breast cancer development. Two *in vitro* models were investigated in detail, where cells were exposed to 5 Gγ fractionated doses of X-rays either with our without the addition of exogenous oestrogen. Cell populations from both models contained radiation-induced copy number alterations and demonstrated phenotypic changes associated with cell transformation. However cell transformation was not fully confirmed in either cell model.

Copy number alterations were identified in cell populations from both models that were putatively related to radiogenic cancer. For example, a region of mono-allelic deletion was observed on chromosome 11q containing *ATM* and putative tumour suppressor genes *CADM1* and *CUL5* that had previously been reported as an area of LOH following radiation-induced breast epithelial cell transformation (Roy *et al.*, 2006; Du *et al.*, 2010b). Copy number loss of this region was not investigated further in primary human radiogenic breast cancers in the present study but may be a region of interest in future work.

Focal copy number alterations which affected the *POU2F1* locus (deletion) and *c-MYC* locus (copy number gain) were selected for further investigation in primary human radiogenic breast samples. POU2F1 was chosen for further study due to its known function in mediating the response to DNA damage and maintaining genetic stability (Meighan-Mantha *et al.*, 1999; Zhao *et al.*, 2000; Jin *et al.*, 2001; Fan *et al.*, 2002; Schild-Poulter *et al.*, 2003; Tantin *et al.*, 2005; Maekawa *et al.*, 2008; Nenoi *et al.*, 2009; Saha *et al.*, 2010). The latent development of breast cancer following radiation exposure has been hypothesised to be due to initiating alterations that increase genetic instability and allow the gradual accumulation of transforming mutations. Loss of POU2F1 function is predicted to cause an increase in genetic instability, identifying deletion of the *POU2F1* locus as an interesting novel target for further investigation. Furthermore, POU2F1 is involved in BRCA1 mediated transcriptional activation of ERα (Hosey *et al.*,

2007). Specifically, POU2F1 was shown to simultaneously occupy the *ESR1* (ERα gene) promoter with BRCA1, suggesting that POU2F1 and BRCA1 heterodimerise to regulate *ESR1*. Consistent with this model, siRNA-mediated depletion of endogenous POU2F1 abrogates BRCA1 binding to the *ESR1* promoter and reduces expression of ERα (Hosey *et al.*, 2007). BRCA1 mutant breast cancers are more likely to be ERα negative (Lakhani *et al.*, 2005). Likewise, radiogenic breast cancer is also more likely to be ERα negative compared to sporadic breast cancer (Foulkes *et al.*, 2004; Broeks *et al.*, 2010; Dores *et al.*, 2010), with loss of POU2F1 via gene deletion as one possible mechanism.

POU2F1 expression was not lost in any sporadic breast cancer tissue samples analysed (n=33) and in only one radiogenic breast cancer tissue sample (n=18) which indicates that POU2F1 expression loss would not be a good marker for identifying radiation-induced breast cancer. Copy number state of the *POU2F1* locus was not analysed in the available primary human breast cancer tissues, although this would be an interesting line of further investigation especially given the observed deletion *in vitro*. However, the low frequency of protein expression loss in the primary human tissue samples makes it unlikely that *POU2F1* deletion is a common event in radiogenic breast cancer.

c-MYC was focally amplified (> 1 copy number increase) in MCF-10A and further chromosomal alterations of chromosome 8q which affected the *c-MYC* locus were also identified. Re-arrangement of chromosome 8q was previously identified in a radiation transformed breast epithelial cell population (Unger *et al.*, 2010) and the incidence of *c-MYC* amplification (2 fold increase in *c-MYC* copy number over chromosome 8 copy number) was reported to be higher in breast cancers from radiation exposed atomic bomb survivors compared to individuals not exposed to irradiation (Miura *et al.*, 2008). The incidence of specific copy number increases of *c-MYC* and the mean number of *c-MYC* copies was higher in the radiogenic breast cancer tissue samples than the sporadic breast cancer tissues analysed in the present study. Evidence therefore suggests that chromosomal rearrangements involving chromosome 8q and the *c-MYC* locus may be induced by ionising radiation exposure, potentially due to the presence of fragile sites that span the *c-MYC* locus, and that copy number gain may be a frequent outcome of these rearrangements (Ferber *et al.*, 2004; Arlt *et al.*, 2006).

A recent study by Best *et al.* (2011) reported that two genetic variants which form a haplotype that reduces basal expression and abrogates radiation-induced expression of

the transcriptional repressor PRDM1, was significantly associated with development of breast cancer following radiotherapy for Hodgkin lymphoma. *PRDM1* is a tumour suppressor in activated diffuse large B cell lymphoma (Calado *et al.*, 2010; Mandelbaum *et al.*, 2010) and is frequently lost in many cancers including solid tumours (Beroukhim *et al.*, 2010). *PRDM1* is located on chromosome 6q; LOH of which was shown to be more common in radiogenic breast cancer than sporadic breast cancer, although markers at the *PRDM1* locus were not specifically investigated (Behrens *et al.*, 2000). PRDM1 is involved in a variety of cellular processes such as proliferation, differentiation and apoptosis and is known to negatively regulate *c-MYC* (Lin *et al.*, 1997; Calame, 2010). Best *et al.* (2011) showed that cells homozygous for the haplotype that reduces PRDM1 expression abrogated *c-MYC* repression following ionising radiation and therefore suggested a role for PRDM1 as a radiation-responsive tumour suppressor. Overall, evidence suggests that dysregulation of c-MYC expression is an important event in the aetiology of radiogenic breast cancer. Loss of PRDM1 expression and amplification of *c-MYC* is predicted to result in the same phenotype. Evidence that *c-MYC* copy number increase is induced by ionising radiation suggests that *c-MYC* amplification may be an important initiator of c-MYC dysregulation in some cases of radiogenic breast cancer.

The value of *c-MYC* amplification as a marker of radiogenic breast cancer is questionable, as *c-MYC* amplification is an established event in sporadic breast cancer and has been reported to be present in approximately 15% of all breast cancer cases (Deming *et al.*, 2000). However, it is possible that a fraction of sporadic breast cancer cases might have a radiation aetiology and that *c-MYC* amplification or c-MYC over-expression in such "sporadic" cases may reflect this. Exposure to ionising radiation is ubiquitous, and is derived from both artificial and natural sources, and although the dose of irradiation for most people is very low, exposure to radiation may still cause DNA damage and could contribute to cancer risk. If the *c-MYC* locus is susceptible to radiation-induced amplification or rearrangement, as evidence suggests, it is possible that a proportion of sporadic cancers that display these genetic events do in fact have a radiation aetiology. Exploring the incidence of *c-MYC* amplification and c-MYC over-expression in other radiogenic solid tumours would be an interesting line of future investigation, and could provide further evidence that c-MYC dysregulation is a common radiation-induced event.

If *c-MYC* amplification is an early event in radiogenic breast cancer, it is theoretically possible that following relatively high doses of radiation exposure monitoring individuals for *c-MYC* amplification or c-MYC expression increase in areas of the breast exposed to radiation may be an early indicator of risk of developing breast cancer later in life; however current technology would make this an invasive and unrealistic procedure to undertake. The development and application of targeted therapy against cells with c-MYC dysregulation could prove efficacious in the treatment of radiogenic breast cancer and might also be of value as prophylaxis to inhibit the outgrowth of c-MYC-deregulated cells following radiation exposure.

Evidence suggests that oestrogen and radiation interact to drive transformation in the breast (Travis *et al.*, 2003; van Leeuwen *et al.*, 2003), although the mechanisms responsible remain to be elucidated. The contribution of the pro-proliferative and genotoxic effects of oestrogen on the accumulation of transforming mutations following a radiation-induced initiating event, such as *c-MYC* dysregulation, remains a robust hypothesis. Interestingly, the *PRDM1* repressive haplotype discovered by Best *et al.* (2011) only associated with breast cancer development in young Hodgkin lymphoma patients that received radiotherapy (median age = 15.6) and not with older Hodgkin lymphoma patients (median age = 24) (although the number of adult cases was smaller). If the repressive effect of PRDM1 mediates radiogenic breast cancer development via c-MYC dysregulation then this result suggests that an interaction between c-MYC over-expression and oestrogen exposure may exist. It should be noted however that repression of PRDM1 will have effects other than dysregulation of c-MYC which might also contribute to radiogenic breast transformation.

In summary, the present study has identified radiation-induced genetic alterations in an *in vitro* model system that was also observed in primary human radiogenic breast tissue samples. Specifically, this study is the first to identify a radiation-induced focal copy number increase of the *c-MYC* locus in breast epithelial cells *in vitro* and the first to implicate increased incidence of *c-MYC* amplification, increased absolute copy number of *c-MYC* and increased c-MYC expression in radiogenic breast cancer samples from Hodgkin lymphoma patients compared to sporadic breast cancer.

9.1 Future directions

A number of further investigations would be desirable following the findings of the present study.

9.1.1 SNP array analysis

A repeat of the irradiation series may be useful to attempt to recreate copy number alterations identified in the present study. Recreation of copy number changes would provide strong evidence that an alteration is preferentially induced by ionising radiation.

9.1.2 POU2F1 function

Evidence suggests that loss of POU2F1 renders cells sensitive to DNA damaging agents. Ectopic expression of POU2F1 following transfection of an expression vector could be used to test whether this phenotype can be rescued in POU2F1-deleted MCF-10A cells. Likewise, *POU2F1* RNAi experiments in un-irradiated MCF-10A cells could elucidate whether loss of POU2F1 expression sensitised cells to DNA damaging agents, including ionising radiation, in a fully controlled isogenic system. Chromatin immunoprecipitation experiments could also determine if POU2F1 interacts with putative POU2F1 binding sites in DNA repair genes which show altered expression. These experiments would further elucidate the role of POU2F1 in cellular response to ionising radiation.

9.1.3 Phenotypic characterisation of c-MYC amplified cells

Further phenotypic characterisation of the Second 5 Gγ series, particularly in populations with increased *c-MYC* copy number and expression could provide further evidence that c-MYC induces EMT. For example, cell migration and invasion assays could potentially reveal further EMT related phenotypes.

9.1.4 Mutation analysis in primary tissue samples

Copy number analysis of the *POU2F1* locus in radiogenic and sporadic breast cancer samples could identify whether deletion of *POU2F1* is common in radiogenic breast cancer.

Re-analysis of *c-MYC* copy number status in tissue sections *in situ* rather than isolated nuclei could also provide more conclusive information on the incidence of *c-MYC*

amplification in breast tumour cells, and allow a more informative correlation with expression of c-MYC using the IHC data. Analysis of *c-MYC* copy number status in primary human pre-malignant cells could identify whether *c-MYC* amplification was an early event in radiogenic breast transformation.

Analysis of *c-MYC* amplification and c-MYC expression in other human tissues susceptible to radiation transformation, such as the pancreas and stomach, by FISH and IHC could provide further information on whether radiation-induced *c-MYC* amplification is common to all tissue types or is a tissue specific phenomenon.

Appendices

1.1 List of genes discussed in text and genes that encode proteins discussed in text.

ABL	Abelson murine leukemia viral oncogene homolog1
APC	Adenomatous polyposis coli
APEX1/2	Apurinic/apyrimidinic endonuclease
ARF	ADP-ribosylation factor
ARLF	Aprataxin- and PNK-Like Factor
ASAP3	ArfGAP with SH3 domain, ankyrin repeat and PH domain 3
ATM	Ataxia-telangiectasia mutated
BCL6	B-cell CLL/lymphoma 6
BCR	Breakpoint Cluster Region
BMP	Bone morphogenetic protein
BMPR1A	Bone morphogenetic protein receptor, type IA
BPIR1	BRCA1 interacting protein C-terminal helicase 1
BRCA1/2	Breast cancer. early onset
CADM1	Cell adhesion molecule 1
CCL20	Chemokine (C-C motif) ligand 20
CCND2/E1/E2/A2	Cyclin
CCR6	chemokine receptor 6
CD24/44/247	Cluster of differentiation
CDC25A/B	Cell division cycle 25 homolog
CDH1	E-cadherin (epithelial)
CDH2	N-cadherin (neuronal)
CDK4	Cyclin dependant kinase 4
CDNK2A/B	Cyclin-dependent kinase inhibitor 2
CHEK1/2	Checkpoint homolog
CHORDC1	Cysteine and histidine-rich domain containing 1
c-JUN	Mitogen-activated protein kinase 9
CLIP2	CAP-GLY domain containing linker protein 2
COMT	Catechol O-methyltransferase
CPM	Carboxypeptidase M
CUL5	Cullin 5
CYP1A1	Cytochrome P450, family 1, subfamily A, polypeptide 1
CYP1B1	Cytochrome P450, family 1, subfamily B, polypeptide 1

DCC	Deleted in colorectal cancer
DCP2	*DCP2* decapping enzyme homolog
DKK1	Dickkopf homolog 1
DNA-PKcs	Protein kinase, DNA-activated, catalytic polypeptide1
DP-1	Rranscription factor *Dp-1*
DUSP27	Dual specificity phosphatase 27
E2F1/2/4/5	E2F transcription factor
EB1	Microtubule-associated protein, RP/EB family, member 1
EGR1	Early growth response 1
EP300	E1A binding protein p300
ERBB	v-erb-b2 erythroblastic leukemia viral oncogene homolog
ERK	Mitogen-activated protein kinase 1
EX01	Exonuclease 1
EYA2	Eyes absent homolog 2
FAK	Focal adhesion kinase
FAM19A1	Family with sequence similarity 19 (chemokine (C-C motif)-like), member A1
FGFBP1	Fibroblast growth factor binding protein 1
FGFR2	Fibroblast growth factor receptor 2
FIN	Fibronectin
FOXO1	Forkhead box O1
FRA-1	Fos-related antigen-1
FRA8C/D	Fragile site
GADD45	Growth arrest and DNA-damage-inducible
GAPDH	Glyceraldehyde-3-phosphate dehydrogenase
GCLM	Glutamate-cysteine ligase, modifier subunit
GPA33	Glycoprotein A33
GRID1	Glutamate receptor, ionotropic, delta 1
GSK3	Glycogen synthase kinase 3
GST	Glutathione S-transferase
H19	H19, imprinted maternally expressed transcript (non-protein coding)
H2AFX	H2A histone family, member X
H2B	Histone cluster 1, H2be

HAS2	Hyaluronan synthase 2
HER2/ErbB2	v-erb-b2 erythroblastic leukemia viral oncogene homolog 2
IGF2R	Insulin-like growth factor 2 receptor
IGF-I	Insulin-like growth factor-1
IGFR1	Insulin-like growth factor 1 receptor
IgH	Immunoglobulin heavy locus
IL24	Interleukin 24
KRT(14,17P3 etc)	Keratin
Ku70/80	X-ray repair complementing defective repair in Chinese hamster cells 6
LCIS	Lobular carcinoma in situ
LEPREL1	Leprecan-like 1
LET	Linear energy transfer
LIG(I/II/II etc)	Ligase
LMTK3	Lemur tyrosine kinase 3
LUCA1	Hyaluronoglucosaminidase 1
MAD2	Mitotic arrest deficient-like2
MAEL	Maelstrom homolog
MAPK	Mitogen-activated protein kinase
MAX	MYC associated factor X
MDM4	Mdm4 p53 binding protein homolog
MGMT	O-6-methylguanine-DNA methyltransferase
MLH3	MutL homolog 3
MNDA	Myeloid cell nuclear differentiation antigen
MPG	N-methylpurine-DNA glycosylase
MRE11	Meiotic recombination 11 homolog
MRN	MRE11/RAD50/NBN
MSH4	MutS homolog 4
MYC	Myelocytomatosis viral oncogene homolog
NBN	Nibrin
NEIL1 /2/3	Nei endonuclease VIII-like
NF-YA	Nuclear transcription factor Y, alpha
NTHL1	Nth endonuclease III-like 1 (E. coli)
OGG1	8-oxoguanine DNA glycosylase

p107	Retinoblastoma-like 1
P48	Pancreas specific transcription factor
P53	Tumour protein 53 gene
PALB2	Partner and localiser of BRCA2
PARP	Poly ADP ribose polymerase
PI3	Peptidase inhibitor 3, skin-derived
PNK	Polynucleotide kinase
POL	Polymerase
POU2F1	POU class 2 homeobox 1
PRDM1	PR domain containing 1, with ZNF domain
PTC	Papillary thyroid carcinomas
PTEN	Phosphatase and tensin homolog
PU.1	Spleen focus forming virus (SFFV) proviral integration oncogene spi1
PUF	Poly-U binding splicing factor
RAD (50, 51 etc)	Radiation sensitivity abnormal
RAF	v-raf-1 murine leukemia viral oncogene homolog
RAS	Rat sarcoma
Rb	Retinoblastoma
REEP5	Receptor accessory protein 5
RET	Ret proto-oncogene
RPA	Replication protein A
SERPINE1	Serpin peptidase inhibitor, clade E member 1
SFRP1	Secreted frizzled-related protein 1
SIDT2	SID1 transmembrane family, member 2
SIX1	SIX homeobox 1
SLIT2	Slit homolog 2
SLUG	Snail homolog 2
SMAD(1,2 etc)	Mothers against decapentaplegic homolog
SNAIL	Zinc finger protein snai1
SNP	Single nucleotide polymorphism
SOD1/2	Superoxide dismutase
SRP19	Signal recognition particle 19kDa

SULT1A3	Sulfotransferase family, cytosolic, 1A, phenol-preferring, member 3
TBX3/5	T-box
TEL	ETS-related protein
TERT	telomerase reverse transcriptase
TGF	Transforming growth factor
TIE2	Tyrosine kinase with immunoglobulin-like and EGF-like domains 2
TRF1/2	Telomeric repeat binding factor
TUBA1A	Tubulin, alpha 1a
TWIST	Class A basic helix-loop-helix protein
VEGF	Vascular endothelial growth factor
VIM	Vimentin
WNT	Wingless-type MMTV integration site family
WRN	Werner syndrome, RecQ helicase-like
XLF	XRCC4-Like-Factor
XPA	Xeroderma pigmentosum, complementation group A
XRCC1	X-ray repair complementing defective repair in Chinese hamster cells 1
XRCC4	X-ray repair complementing defective repair in Chinese hamster cells 4
YES	v-yes-1 Yamaguchi sarcoma viral oncogene homolog
ESR1	Estrogen receptor 1

1.2 Online resources

http://www.doubling-time.com/compute.php - Roth V. 2006

http://david.abcc.ncifcrf.gov/ - Huang *et al* 2009a; 2009b

http://www.ebi.ac.uk/QuickGO/

http://pcrdataanalysis.sabiosciences.com/pcr/arrayanalysis.php

http://www.ensemble.org

http://www.ncbi.nlm.nih.gov/pubmed/

http://www.ukradon.org/

http://www.hpa.org.uk/

References

Adhikary, S. and Eilers, M. (2005) 'Transcriptional regulation and transformation by Myc proteins', *Nat Rev Mol Cell Biol*, 6(8), pp. 635-45.

Al-Hajj, M., Wicha, M.S., Benito-Hernandez, A., Morrison, S.J. and Clarke, M.F. (2003) 'Prospective identification of tumorigenic breast cancer cells', *Proc Natl Acad Sci U S A*, 100(7), pp. 3983-8.

Al-Kuraya, K., Schraml, P., Torhorst, J., Tapia, C., Zaharieva, B., Novotny, H., Spichtin, H., Maurer, R., Mirlacher, M., Kochli, O., Zuber, M., Dieterich, H., Mross, F., Wilber, K., Simon, R. and Sauter, G. (2004) 'Prognostic relevance of gene amplifications and coamplifications in breast cancer', *Cancer Res*, 64(23), pp. 8534-40.

Al-Zoughool, M. and Krewski, D. (2009) 'Health effects of radon: a review of the literature', *Int J Radiat Biol*, 85(1), pp. 57-69.

Allan, J.M. and Travis, L.B. (2005) 'Mechanisms of therapy-related carcinogenesis', *Nat Rev Cancer*, 5(12), pp. 943-55.

Alles, M.C., Gardiner-Garden, M., Nott, D.J., Wang, Y., Foekens, J.A., Sutherland, R.L., Musgrove, E.A. and Ormandy, C.J. (2009) 'Meta-analysis and gene set enrichment relative to er status reveal elevated activity of MYC and E2F in the "basal" breast cancer subgroup', *PLoS One*, 4(3), p. e4710.

Andegeko, Y., Moyal, L., Mittelman, L., Tsarfaty, I., Shiloh, Y. and Rotman, G. (2001) 'Nuclear retention of ATM at sites of DNA double strand breaks', *J Biol Chem*, 276(41), pp. 38224-30.

Andrieu, N., Easton, D.F., Chang-Claude, J., Rookus, M.A., Brohet, R., Cardis, E., Antoniou, A.C., Wagner, T., Simard, J., Evans, G., Peock, S., Fricker, J.P., Nogues, C., Van't Veer, L., Van Leeuwen, F.E. and Goldgar, D.E. (2006) 'Effect of chest X-rays on the risk of breast cancer among BRCA1/2 mutation carriers in the international BRCA1/2 carrier cohort study: a report from the EMBRACE, GENEPSO, GEO-HEBON, and IBCCS Collaborators' Group', *J Clin Oncol*, 24(21), pp. 3361-6.

Antoniou, A., Pharoah, P.D., Narod, S., Risch, H.A., Eyfjord, J.E., Hopper, J.L., Loman, N., Olsson, H., Johannsson, O., Borg, A., Pasini, B., Radice, P., Manoukian, S., Eccles, D.M., Tang, N., Olah, E., Anton-Culver, H., Warner, E., Lubinski, J., Gronwald, J., Gorski, B., Tulinius, H., Thorlacius, S., Eerola, H., Nevanlinna, H., Syrjakoski, K., Kallioniemi, O.P., Thompson, D., Evans, C., Peto, J., Lalloo, F., Evans, D.G. and Easton, D.F. (2003) 'Average risks of breast and ovarian cancer associated with BRCA1 or BRCA2 mutations detected in case Series unselected for family history: a combined analysis of 22 studies', *Am J Hum Genet*, 72(5), pp. 1117-30.

Ariel, I., Sughayer, M., Fellig, Y., Pizov, G., Ayesh, S., Podeh, D., Libdeh, B.A., Levy, C., Birman, T., Tykocinski, M.L., de Groot, N. and Hochberg, A. (2000) 'The imprinted H19 gene is a marker of early recurrence in human bladder carcinoma', *Mol Pathol*, 53(6), pp. 320-3.

Arlt, M.F., Durkin, S.G., Ragland, R.L. and Glover, T.W. (2006) 'Common fragile sites as targets for chromosome rearrangements', *DNA Repair (Amst)*, 5(9-10), pp. 1126-35.

Asaithamby, A., Hu, B. and Chen, D.J. (2011) 'Unrepaired clustered DNA lesions induce chromosome breakage in human cells', *Proc Natl Acad Sci U S A*, 108(20), pp. 8293-8.

Asiedu, M.K., Ingle, J.N., Behrens, M.D., Radisky, D.C. and Knutson, K.L. (2011) 'TGFbeta/TNF(alpha)-mediated epithelial-mesenchymal transition generates breast cancer stem cells with a claudin-low phenotype', *Cancer Res*, 71(13), pp. 4707-19.

Axelrod, D., Smith, J., Kornreich, D., Grinstead, E., Singh, B., Cangiarella, J. and Guth, A.A. (2008) 'Breast cancer in young women', *J Am Coll Surg*, 206(3), pp. 1193-203.

Aypar, U., Morgan, W.F. and Baulch, J.E. (2011) 'Radiation-induced genomic instability: are epigenetic mechanisms the missing link?', *Int J Radiat Biol*, 87(2), pp. 179-91.

Balasubramanian, B., Pogozelski, W.K. and Tullius, T.D. (1998) 'DNA strand breaking by the hydroxyl radical is governed by the accessible surface areas of the hydrogen atoms of the DNA backbone', *Proc Natl Acad Sci U S A*, 95(17), pp. 9738-43.

Barbosa-Morais, N.L., Dunning, M.J., Samarajiwa, S.A., Darot, J.F., Ritchie, M.E., Lynch, A.G. and Tavare, S. (2010) 'A re-annotation pipeline for Illumina BeadArrays: improving the interpretation of gene expression data', *Nucleic Acids Res*, 38(3), p. e17.

Barker, C.A. and Powell, S.N. (2010) 'Enhancing radiotherapy through a greater understanding of homologous recombination', *Semin Radiat Oncol*, 20(4), pp. 267-273 e3.

Barsyte-Lovejoy, D., Lau, S.K., Boutros, P.C., Khosravi, F., Jurisica, I., Andrulis, I.L., Tsao, M.S. and Penn, L.Z. (2006) 'The c-Myc oncogene directly induces the H19 noncoding RNA by allele-specific binding to potentiate tumorigenesis', *Cancer Res*, 66(10), pp. 5330-7.

Bartstra, R.W., Bentvelzen, P.A., Zoetelief, J., Mulder, A.H., Broerse, J.J. and van Bekkum, D.W. (1998a) 'Induction of mammary tumors in rats by single-dose gamma irradiation at different ages', *Radiat Res*, 150(4), pp. 442-50.

Bartstra, R.W., Bentvelzen, P.A., Zoetelief, J., Mulder, A.H., Broerse, J.J. and van Bekkum, D.W. (1998b) 'The influence of estrogen treatment on induction of mammary carcinoma in rats by single-dose gamma irradiation at different ages', *Radiat Res*, 150(4), pp. 451-8.

Bartstra, R.W., Bentvelzen, P.A., Zoetelief, J., Mulder, A.H., Broerse, J.J. and van Bekkum, D.W. (2000) 'The effects of fractionated gamma irradiation on induction of mammary carcinoma in normal and estrogen-treated rats', *Radiat Res*, 153(5 Pt 1), pp. 557-69.

Basu, S.K., Schwartz, C., Fisher, S.G., Hudson, M.M., Tarbell, N., Muhs, A., Marcus, K.J., Mendenhall, N., Mauch, P., Kun, L.E. and Constine, L.S. (2008) 'Unilateral and bilateral breast cancer in women surviving pediatric Hodgkin's disease', *Int J Radiat Oncol Biol Phys*, 72(1), pp. 34-40.

Baudino, T.A., McKay, C., Pendeville-Samain, H., Nilsson, J.A., Maclean, K.H., White, E.L., Davis, A.C., Ihle, J.N. and Cleveland, J.L. (2002) 'c-Myc is essential for vasculogenesis and angiogenesis during development and tumor progression', *Genes Dev*, 16(19), pp. 2530-43.

Behrens, C., Travis, L.B., Wistuba, II, Davis, S., Maitra, A., Clarke, E.A., Lynch, C.F., Glimelius, B., Wiklund, T., Tarone, R. and Gazdar, A.F. (2000) 'Molecular changes in second primary lung and breast cancers after therapy for Hodgkin's disease', *Cancer Epidemiol Biomarkers Prev*, 9(10), pp. 1027-35.

Beider, K., Abraham, M., Begin, M., Wald, H., Weiss, I.D., Wald, O., Pikarsky, E., Abramovitch, R., Zeira, E., Galun, E., Nagler, A. and Peled, A. (2009) 'Interaction between CXCR4 and CCL20 pathways regulates tumor growth', *PLoS One*, 4(4), p. e5125.

Bender, M.A., Griggs, H.G. and Bedford, J.S. (1974) 'Mechanisms of chromosomal aberration production. 3. Chemicals and ionizing radiation', *Mutat Res*, 23(2), pp. 197-212.

Bernstein, J.L., Haile, R.W., Stovall, M., Boice, J.D., Jr., Shore, R.E., Langholz, B., Thomas, D.C., Bernstein, L., Lynch, C.F., Olsen, J.H., Malone, K.E., Mellemkjaer, L., Borresen-Dale, A.L., Rosenstein, B.S., Teraoka, S.N., Diep, A.T., Smith, S.A., Capanu, M., Reiner, A.S., Liang, X., Gatti, R.A. and Concannon, P. (2010) 'Radiation exposure, the ATM Gene, and contralateral breast cancer in the women's environmental cancer and radiation epidemiology study', *J Natl Cancer Inst*, 102(7), pp. 475-83.

Bernstein, J.L., Teraoka, S.N., John, E.M., Andrulis, I.L., Knight, J.A., Lapinski, R., Olson, E.R., Wolitzer, A.L., Seminara, D., Whittemore, A.S. and Concannon, P. (2006) 'The CHEK2*1100delC allelic variant and risk of breast cancer: screening results from the Breast Cancer Family Registry', *Cancer Epidemiol Biomarkers Prev*, 15(2), pp. 348-52.

Beroukhim, R., Mermel, C.H., Porter, D., Wei, G., Raychaudhuri, S., Donovan, J., Barretina, J., Boehm, J.S., Dobson, J., Urashima, M., Mc Henry, K.T., Pinchback, R.M., Ligon, A.H., Cho, Y.J., Haery, L., Greulich, H., Reich, M., Winckler, W., Lawrence, M.S., Weir, B.A., Tanaka, K.E., Chiang, D.Y., Bass, A.J., Loo, A., Hoffman, C., Prensner, J., Liefeld, T., Gao, Q., Yecies, D., Signoretti, S., Maher, E., Kaye, F.J., Sasaki, H., Tepper, J.E., Fletcher, J.A., Tabernero, J., Baselga, J., Tsao, M.S., Demichelis, F., Rubin, M.A., Janne, P.A., Daly, M.J., Nucera, C., Levine, R.L., Ebert, B.L., Gabriel, S., Rustgi, A.K., Antonescu, C.R., Ladanyi, M., Letai, A., Garraway, L.A., Loda, M., Beer, D.G., True, L.D., Okamoto, A., Pomeroy, S.L., Singer, S., Golub, T.R., Lander, E.S., Getz, G., Sellers, W.R. and Meyerson, M. (2010) 'The landscape of somatic copy-number alteration across human cancers', *Nature*, 463(7283), pp. 899-905.

Best, T., Li, D., Skol, A.D., Kirchhoff, T., Jackson, S.A., Yasui, Y., Bhatia, S., Strong, L.C., Domchek, S.M., Nathanson, K.L., Olopade, O.I., Huang, R.S., Mack, T.M., Conti, D.V., Offit, K., Cozen, W., Robison, L.L. and Onel, K. (2011) 'Variants at 6q21 implicate PRDM1 in the etiology of therapy-induced second malignancies after Hodgkin's lymphoma', *Nat Med*, 17(8), pp. 941-3.

Bhatti, P., Doody, M.M., Alexander, B.H., Yuenger, J., Simon, S.L., Weinstock, R.M., Rosenstein, M., Stovall, M., Abend, M., Preston, D.L., Pharoah, P., Struewing, J.P. and Sigurdson, A.J. (2008) 'Breast cancer risk polymorphisms and interaction with ionizing radiation among U.S. radiologic technologists', *Cancer Epidemiol Biomarkers Prev*, 17(8), pp. 2007-11.

Bielas, J.H. and Heddle, J.A. (2000) 'Proliferation is necessary for both repair and mutation in transgenic mouse cells', *Proc Natl Acad Sci U S A*, 97(21), pp. 11391-6.

Bielas, J.H. and Loeb, L.A. (2005) 'Mutator phenotype in cancer: timing and perspectives', *Environ Mol Mutagen*, 45(2-3), pp. 206-13.

Bishop, A.J. and Schiestl, R.H. (2001) 'Homologous recombination as a mechanism of carcinogenesis', *Biochim Biophys Acta*, 1471(3), pp. M109-21.

Blackwood, E.M. and Eisenman, R.N. (1991) 'Max: a helix-loop-helix zipper protein that forms a sequence-specific DNA-binding complex with Myc', *Science*, 251(4998), pp. 1211-7.

Blaisdell, J.O., Harrison, L. and Wallace, S.S. (2001) 'Base excision repair processing of radiation-induced clustered DNA lesions', *Radiat Prot Dosimetry*, 97(1), pp. 25-31.

Blancato, J., Singh, B., Liu, A., Liao, D.J. and Dickson, R.B. (2004) 'Correlation of amplification and overexpression of the c-myc oncogene in high-grade breast cancer: FISH, in situ hybridisation and immunohistochemical analyses', *Br J Cancer*, 90(8), pp. 1612-9.

Bloom, H.J. and Richardson, W.W. (1957) 'Histological grading and prognosis in breast cancer; a study of 1409 cases of which 359 have been followed for 15 years', *Br J Cancer*, 11(3), pp. 359-77.

Boice, J.D., Jr., Blettner, M., Kleinerman, R.A., Stovall, M., Moloney, W.C., Engholm, G., Austin, D.F., Bosch, A., Cookfair, D.L., Krementz, E.T. and et al. (1987) 'Radiation dose and leukemia risk in patients treated for cancer of the cervix', *J Natl Cancer Inst*, 79(6), pp. 1295-311.

Botlagunta, M., Vesuna, F., Mironchik, Y., Raman, A., Lisok, A., Winnard, P., Jr., Mukadam, S., Van Diest, P., Chen, J.H., Farabaugh, P., Patel, A.H. and Raman, V. (2008) 'Oncogenic role of DDX3 in breast cancer biogenesis', *Oncogene*, 27(28), pp. 3912-22.

Botlagunta, M., Winnard, P.T., Jr. and Raman, V. (2010) 'Neoplastic transformation of breast epithelial cells by genotoxic stress', *BMC Cancer*, 10, p. 343.

Boxer, L.M. and Dang, C.V. (2001) 'Translocations involving c-myc and c-myc function', *Oncogene*, 20(40), pp. 5595-610.

Braakhuis, B.J., Tabor, M.P., Kummer, J.A., Leemans, C.R. and Brakenhoff, R.H. (2003) 'A genetic explanation of Slaughter's concept of field cancerization: evidence and clinical implications', *Cancer Res*, 63(8), pp. 1727-30.

Broeks, A., Braaf, L.M., Huseinovic, A., Nooijen, A., Urbanus, J., Hogervorst, F.B., Schmidt, M.K., Klijn, J.G., Russell, N.S., Van Leeuwen, F.E. and Van 't Veer, L.J. (2007) 'Identification of women with an increased risk of developing radiation-induced breast cancer: a case only study', *Breast Cancer Res*, 9(2), p. R26.

Broeks, A., Braaf, L.M., Wessels, L.F., van de Vijver, M., De Bruin, M.L., Stovall, M., Russell, N.S., van Leeuwen, F.E. and Van 't Veer, L.J. (2010) 'Radiation-associated breast tumors display a distinct gene expression profile', *Int J Radiat Oncol Biol Phys*, 76(2), pp. 540-7.

Broeks, A., de Witte, L., Nooijen, A., Huseinovic, A., Klijn, J.G., van Leeuwen, F.E., Russell, N.S. and van't Veer, L.J. (2004) 'Excess risk for contralateral breast cancer in CHEK2*1100delC germline mutation carriers', *Breast Cancer Res Treat*, 83(1), pp. 91-3.

Bryant, P.E. (1998) 'The signal model: a possible explanation for the conversion of DNA double-strand breaks into chromatid breaks', *Int J Radiat Biol*, 73(3), pp. 243-51.

Bryant, P.E. (2004) 'Repair and chromosomal damage', *Radiother Oncol*, 72(3), pp. 251-6.

Butt, A.J., Sutherland, R.L. and Musgrove, E.A. (2007) 'Live or let die: oestrogen regulation of survival signalling in endocrine response', *Breast Cancer Res*, 9(5), p. 306.

Calado, D.P., Zhang, B., Srinivasan, L., Sasaki, Y., Seagal, J., Unitt, C., Rodig, S., Kutok, J., Tarakhovsky, A., Schmidt-Supprian, M. and Rajewsky, K. (2010) 'Constitutive canonical NF-kappaB activation cooperates with disruption of BLIMP1 in the pathogenesis of activated B cell-like diffuse large cell lymphoma', *Cancer Cell*, 18(6), pp. 580-9.

Calaf, G. and Hei, T.K. (2001) 'Oncoprotein expression in human breast epithelial cells transformed by high-LET radiation', *Int J Radiat Biol*, 77(1), pp. 31-40.

Calaf, G.M. and Hei, T.K. (2000) 'Establishment of a radiation- and estrogen-induced breast cancer model', *Carcinogenesis*, 21(4), pp. 769-76.

Calaf, G.M., Roy, D. and Hei, T.K. (2006) 'Growth factor biomarkers associated with estrogen- and radiation-induced breast cancer progression', *Int J Oncol*, 28(1), pp. 87-93.

Calame, K. (2010) 'Blimp-1's maiden flight', *J Immunol*, 185(1), pp. 3-4.

Camats, N., Ruiz-Herrera, A., Parrilla, J.J., Acien, M., Paya, P., Giulotto, E., Egozcue, J., Garcia, F. and Garcia, M. (2006) 'Genomic instability in rat: breakpoints induced by ionising radiation and interstitial telomeric-like sequences', *Mutat Res*, 595(1-2), pp. 156-66.

Cardis, E. and Hatch, M. (2011) 'The Chernobyl accident--an epidemiological perspective', *Clin Oncol (R Coll Radiol)*, 23(4), pp. 251-60.

Carmichael, A., Sami, A.S. and Dixon, J.M. (2003) 'Breast cancer risk among the survivors of atomic bomb and patients exposed to therapeutic ionising radiation', *Eur J Surg Oncol*, 29(5), pp. 475-9.

Carter, S.L., Negrini, M., Baffa, R., Gillum, D.R., Rosenberg, A.L., Schwartz, G.F. and Croce, C.M. (1994) 'Loss of heterozygosity at 11q22-q23 in breast cancer', *Cancer Res*, 54(23), pp. 6270-4.

Caruso, J.A., Reiners, J.J., Jr., Emond, J., Shultz, T., Tainsky, M.A., Alaoui-Jamali, M. and Batist, G. (2001) 'Genetic alteration of chromosome 8 is a common feature of human mammary epithelial cell lines transformed in vitro with benzo[a]pyrene', *Mutat Res*, 473(1), pp. 85-99.

Castets, M., Broutier, L., Molin, Y., Brevet, M., Chazot, G., Gadot, N., Paquet, A., Mazelin, L., Jarrosson-Wuilleme, L., Scoazec, J.Y., Bernet, A. and Mehlen, P. (2011) 'DCC constrains tumour progression via its dependence receptor activity', *Nature*.

Castiglioni, F., Terenziani, M., Carcangiu, M.L., Miliano, R., Aiello, P., Bertola, L., Triulzi, T., Gasparini, P., Camerini, T., Sozzi, G., Fossati-Bellani, F., Menard, S. and Tagliabue, E. (2007) 'Radiation effects on development of HER2-positive breast carcinomas', *Clin Cancer Res*, 13(1), pp. 46-51.

Cavalieri, E.L. and Rogan, E.G. (2004) 'A unifying mechanism in the initiation of cancer and other diseases by catechol quinones', *Ann N Y Acad Sci*, 1028, pp. 247-57.

Chadwick, K.H. and Leenhouts, H.P. (2011) 'Radiation induced cancer arises from a somatic mutation', *J Radiol Prot*, 31(1), pp. 41-8.

Chang, M. (2011) 'Dual roles of estrogen metabolism in mammary carcinogenesis', *BMB Rep*, 44(7), pp. 423-34.

Chappell, J., Leitner, J.W., Solomon, S., Golovchenko, I., Goalstone, M.L. and Draznin, B. (2001) 'Effect of insulin on cell cycle progression in MCF-7 breast cancer cells. Direct and potentiating influence', *J Biol Chem*, 276(41), pp. 38023-8.

Chen, D., Zhao, M. and Mundy, G.R. (2004) 'Bone morphogenetic proteins', *Growth Factors*, 22(4), pp. 233-41.

Chen, J.Q. and Yager, J.D. (2004) 'Estrogen's effects on mitochondrial gene expression: mechanisms and potential contributions to estrogen carcinogenesis', *Ann N Y Acad Sci*, 1028, pp. 258-72.

Chiang, C.S., Sawyers, C.L. and McBride, W.H. (1998) 'Oncogene Expression and Cellular Radiation Resistance: A Modulatory Role for c-myc', *Mol Diagn*, 3(1), pp. 21-27.

Cho, K.B., Cho, M.K., Lee, W.Y. and Kang, K.W. (2010) 'Overexpression of c-myc induces epithelial mesenchymal transition in mammary epithelial cells', *Cancer Lett*, 293(2), pp. 230-9.

Christie, D.R., Wills, R., Drew, J.F. and Barton, M.B. (1998) 'The doses received by the breast during mantle radiotherapy', *Int J Radiat Oncol Biol Phys*, 41(1), pp. 223-6.

Chrzan, P., Skokowski, J., Karmolinski, A. and Pawelczyk, T. (2001a) 'Amplification of c-myc gene and overexpression of c-Myc protein in breast cancer and adjacent non-neoplastic tissue', *Clin Biochem*, 34(7), pp. 557-62.

Chrzan, P., Skokowski, J., Karmolinski, A. and Pawelczyk, T. (2001b) 'Amplification of c-myc gene and overexpression of c-Myc protein in breast cancer and adjacent non-neoplastic tissue', *Clin Biochem*, 34(7), pp. 557-562.

Cohen, S.M. and Ellwein, L.B. (1990) 'Cell proliferation in carcinogenesis', *Science*, 249(4972), pp. 1007-11.

Collis, S.J., Swartz, M.J., Nelson, W.G. and DeWeese, T.L. (2003) 'Enhanced radiation and chemotherapy-mediated cell killing of human cancer cells by small inhibitory RNA silencing of DNA repair factors', *Cancer Res*, 63(7), pp. 1550-4.

Combes, R., Balls, M., Curren, R., Fischbach, M., Fusenig, N., Kirkland, D., Lasne, C., Landolph, J., LeBoeuf, R., Marquardt, H., McCormick, J., Muller, L., Rivedal, E., Sabbioni, E., Tanaka, N., Vasseur, P. and Yamasaki, H. (1999) 'Cell transformation assays as predictors of human carcinogenicity - The report and recommendations of ECVAM Workshop 39', *Atla-Alternatives to Laboratory Animals*, 27(5), pp. 745-767.

Cooke, M.S., Evans, M.D., Dizdaroglu, M. and Lunec, J. (2003) 'Oxidative DNA damage: mechanisms, mutation, and disease', *Faseb Journal*, 17(10), pp. 1195-214.

Cornforth, M.N. (2006) 'Perspectives on the formation of radiation-induced exchange aberrations', *DNA Repair (Amst)*, 5(9-10), pp. 1182-91.

Cousineau, I., Abaji, C. and Belmaaza, A. (2005) 'BRCA1 regulates RAD51 function in response to DNA damage and suppresses spontaneous sister chromatid replication slippage: implications for sister chromatid cohesion, genome stability, and carcinogenesis', *Cancer Res*, 65(24), pp. 11384-91.

Cowell, J.K., LaDuca, J., Rossi, M.R., Burkhardt, T., Nowak, N.J. and Matsui, S. (2005) 'Molecular characterization of the t(3;9) associated with immortalization in the MCF10A cell line', *Cancer Genet Cytogenet*, 163(1), pp. 23-9.

Cowling, V.H. and Cole, M.D. (2007) 'Turning the tables: Myc activates Wnt in breast cancer', *Cell Cycle*, 6(21), pp. 2625-7.

Cowling, V.H., D'Cruz, C.M., Chodosh, L.A. and Cole, M.D. (2007) 'c-Myc transforms human mammary epithelial cells through repression of the Wnt inhibitors DKK1 and SFRP1', *Mol Cell Biol*, 27(14), pp. 5135-46.

Crawford, T.O. (1998) 'Ataxia telangiectasia', *Semin Pediatr Neurol*, 5(4), pp. 287-94.

Czornak, K., Chughtai, S. and Chrzanowska, K.H. (2008) 'Mystery of DNA repair: the role of the MRN complex and ATM kinase in DNA damage repair', *J Appl Genet*, 49(4), pp. 383-96.

D'Amours, D. and Jackson, S.P. (2002) 'The Mre11 complex: at the crossroads of dna repair and checkpoint signalling', *Nat Rev Mol Cell Biol*, 3(5), pp. 317-27.

Dahdaleh, F.S., Carr, J.C., Calva, D. and Howe, J.R. (2012) 'Juvenile polyposis and other intestinal polyposis syndromes with microdeletions of chromosome 10q22-23', *Clin Genet*, 81(2), pp. 110-6.

Dallol, A., Da Silva, N.F., Viacava, P., Minna, J.D., Bieche, I., Maher, E.R. and Latif, F. (2002) 'SLIT2, a human homologue of the Drosophila Slit2 gene, has tumor suppressor activity and is frequently inactivated in lung and breast cancers', *Cancer Res*, 62(20), pp. 5874-80.

Dang, C.V., O'Donnell, K.A., Zeller, K.I., Nguyen, T., Osthus, R.C. and Li, F. (2006) 'The c-Myc target gene network', *Semin Cancer Biol*, 16(4), pp. 253-64.

Darakhshan, F., Badie, C., Moody, J., Coster, M., Finnon, R., Finnon, P., Edwards, A.A., Szluinska, M., Skidmore, C.J., Yoshida, K., Ullrich, R., Cox, R. and Bouffler, S.D. (2006) 'Evidence for complex multigenic inheritance of radiation AML susceptibility in mice revealed using a surrogate phenotypic assay', *Carcinogenesis*, 27(2), pp. 311-8.

Davey, R.A., Locke, V.L., Henness, S., Harvie, R.M. and Davey, M.W. (2004) 'Cellular models of drug- and radiation-resistant small cell lung cancer', *Anticancer Res*, 24(2A), pp. 465-71.

Davis, F.G., Boice, J.D., Jr., Hrubec, Z. and Monson, R.R. (1989) 'Cancer mortality in a radiation-exposed cohort of Massachusetts tuberculosis patients', *Cancer Res*, 49(21), pp. 6130-6.

De Angelis, P.M., Clausen, O.P., Schjolberg, A. and Stokke, T. (1999) 'Chromosomal gains and losses in primary colorectal carcinomas detected by CGH and their associations with tumour DNA ploidy, genotypes and phenotypes', *Br J Cancer*, 80(3-4), pp. 526-35.

De Bruin, M.L., Sparidans, J., van't Veer, M.B., Noordijk, E.M., Louwman, M.W., Zijlstra, J.M., van den Berg, H., Russell, N.S., Broeks, A., Baaijens, M.H., Aleman, B.M. and van Leeuwen, F.E. (2009) 'Breast cancer risk in female survivors of Hodgkin's lymphoma: lower risk after smaller radiation volumes', *J Clin Oncol*, 27(26), pp. 4239-46.

Deming, S.L., Nass, S.J., Dickson, R.B. and Trock, B.J. (2000) 'C-myc amplification in breast cancer: a meta-analysis of its occurrence and prognostic relevance', *Br J Cancer*, 83(12), pp. 1688-95.

Deng, C.X. (2006) 'BRCA1: cell cycle checkpoint, genetic instability, DNA damage response and cancer evolution', *Nucleic Acids Res*, 34(5), pp. 1416-26.

Dent, R., Trudeau, M., Pritchard, K.I., Hanna, W.M., Kahn, H.K., Sawka, C.A., Lickley, L.A., Rawlinson, E., Sun, P. and Narod, S.A. (2007) 'Triple-negative breast cancer: clinical features and patterns of recurrence', *Clin Cancer Res*, 13(15 Pt 1), pp. 4429-34.

Desrichard, A., Bidet, Y., Uhrhammer, N. and Bignon, Y.J. (2011) 'CHEK2 contribution to hereditary breast cancer in non-BRCA families', *Breast Cancer Res*, 13(6), p. R119.

Diehn, M., Cho, R.W., Lobo, N.A., Kalisky, T., Dorie, M.J., Kulp, A.N., Qian, D., Lam, J.S., Ailles, L.E., Wong, M., Joshua, B., Kaplan, M.J., Wapnir, I., Dirbas, F.M., Somlo, G., Garberoglio, C., Paz, B., Shen, J., Lau, S.K., Quake, S.R., Brown, J.M., Weissman, I.L. and Clarke, M.F. (2009) 'Association of reactive oxygen species levels and radioresistance in cancer stem cells', *Nature*, 458(7239), pp. 780-3.

Diergaarde, B., Potter, J.D., Jupe, E.R., Manjeshwar, S., Shimasaki, C.D., Pugh, T.W., Defreese, D.C., Gramling, B.A., Evans, I. and White, E. (2008) 'Polymorphisms in genes involved in sex hormone metabolism, estrogen plus progestin hormone therapy use, and risk of postmenopausal breast cancer', *Cancer Epidemiol Biomarkers Prev*, 17(7), pp. 1751-9.

Doody, M.M., Freedman, D.M., Alexander, B.H., Hauptmann, M., Miller, J.S., Rao, R.S., Mabuchi, K., Ron, E., Sigurdson, A.J. and Linet, M.S. (2006) 'Breast cancer incidence in U.S. radiologic technologists', *Cancer*, 106(12), pp. 2707-15.

Dores, G.M., Anderson, W.F., Beane Freeman, L.E., Fraumeni, J.F., Jr. and Curtis, R.E. (2010) 'Risk of breast cancer according to clinicopathologic features among long-term survivors of Hodgkin's lymphoma treated with radiotherapy', *Br J Cancer*, 103(7), pp. 1081-4.

Du, L.Q., Wang, Y., Wang, H., Cao, J., Liu, Q. and Fan, F.Y. (2010a) 'Knockdown of Rad51 expression induces radiation- and chemo-sensitivity in osteosarcoma cells', *Med Oncol*.

Du, N., Baker, P.M., Do, T.U., Bien, C., Bier-Laning, C.M., Singh, S., Shih, S.J., Diaz, M.O. and Vaughan, A.T. (2010b) '11q21.1-11q23.3 Is a site of intrinsic genomic instability triggered by irradiation', *Genes Chromosomes Cancer*, 49(9), pp. 831-43.

Dumeaux, V., Alsaker, E. and Lund, E. (2003) 'Breast cancer and specific types of oral contraceptives: a large Norwegian cohort study', *Int J Cancer*, 105(6), pp. 844-50.

Dzietczenia, J., Wrobel, T., Jazwiec, B., Mazur, G., Butrym, A., Poreba, R. and Kuliczkowski, K. (2010) 'Expression of bone morphogenetic proteins (BMPs) receptors in patients with B-cell chronic lymphocytic leukemia (B-CLL)', *Int J Lab Hematol*, 32(6 Pt 1), pp. e217-21.

Edson, M.A., Nalam, R.L., Clementi, C., Franco, H.L., Demayo, F.J., Lyons, K.M., Pangas, S.A. and Matzuk, M.M. (2010) 'Granulosa cell-expressed BMPR1A and BMPR1B have unique functions in regulating fertility but act redundantly to suppress ovarian tumor development', *Mol Endocrinol*, 24(6), pp. 1251-66.

El-Din, M.A.A., El-Badawy, S.A. and Taghian, A.G. (2008) 'Breast Cancer after Treatment of Hodgkin's Lymphoma: General Review', *International Journal of Radiation Oncology Biology Physics*, 72(5), pp. 1291-1297.

Elkin, E.B., Klem, M.L., Gonzales, A.M., Ishill, N.M., Hodgson, D., Ng, A.K., Marks, L.B., Weidhaas, J., Freedman, G.M., Miller, R.C., Constine, L.S., Myrehaug, S. and Yahalom, J. (2011) 'Characteristics and Outcomes of Breast Cancer in Women With and Without a History of Radiation for Hodgkin's Lymphoma: A Multi-Institutional, Matched Cohort Study', *Journal of Clinical Oncology*, 29(18), pp. 2466-2473.

Embrechts, J., Lemiere, F., Van Dongen, W., Esmans, E.L., Buytaert, P., Van Marck, E., Kockx, M. and Makar, A. (2003) 'Detection of estrogen DNA-adducts in human breast tumor tissue and healthy tissue by combined nano LC-nano ES tandem mass spectrometry', *J Am Soc Mass Spectrom*, 14(5), pp. 482-91.

Eraly, S.A., Nelson, S.B., Huang, K.M. and Mellon, P.L. (1998) 'Oct-1 binds promoter elements required for transcription of the GnRH gene', *Mol Endocrinol*, 12(4), pp. 469-81.

Erisman, M.D., Rothberg, P.G., Diehl, R.E., Morse, C.C., Spandorfer, J.M. and Astrin, S.M. (1985) 'Deregulation of c-myc gene expression in human colon carcinoma is not accompanied by amplification or rearrangement of the gene', *Mol Cell Biol*, 5(8), pp. 1969-76.

Essers, J., Hendriks, R.W., Swagemakers, S.M., Troelstra, C., de Wit, J., Bootsma, D., Hoeijmakers, J.H. and Kanaar, R. (1997) 'Disruption of mouse RAD54 reduces ionizing radiation resistance and homologous recombination', *Cell*, 89(2), pp. 195-204.

Evan, G.I., Wyllie, A.H., Gilbert, C.S., Littlewood, T.D., Land, H., Brooks, M., Waters, C.M., Penn, L.Z. and Hancock, D.C. (1992) 'Induction of apoptosis in fibroblasts by c-myc protein', *Cell*, 69(1), pp. 119-28.

Fadel, B.M., Boutet, S.C. and Quertermous, T. (1999) 'Octamer-dependent in vivo expression of the endothelial cell-specific TIE2 gene', *J Biol Chem*, 274(29), pp. 20376-83.

Fan, W., Jin, S., Tong, T., Zhao, H., Fan, F., Antinore, M.J., Rajasekaran, B., Wu, M. and Zhan, Q. (2002) 'BRCA1 regulates GADD45 through its interactions with the OCT-1 and CAAT motifs', *J Biol Chem*, 277(10), pp. 8061-7.

Fang, M., Toher, J., Morgan, M., Davison, J., Tannenbaum, S. and Claffey, K. (2011) 'Genomic differences between estrogen receptor (ER)-positive and ER-negative human breast carcinoma identified by single nucleotide polymorphism array comparative genome hybridization analysis', *Cancer*, 117(10), pp. 2024-34.

Farabaugh, S.M., Micalizzi, D.S., Jedlicka, P., Zhao, R. and Ford, H.L. (2012) 'Eya2 is required to mediate the pro-metastatic functions of Six1 via the induction of TGF-beta signaling, epithelial-mesenchymal transition, and cancer stem cell properties', *Oncogene*, 31(5), pp. 552-62.

Fay, M.J., Longo, K.A., Karathanasis, G.A., Shope, D.M., Mandernach, C.J., Leong, J.R., Hicks, A., Pherson, K. and Husain, A. (2003) 'Analysis of CUL-5 expression in breast epithelial cells, breast cancer cell lines, normal tissues and tumor tissues', *Mol Cancer*, 2, p. 40.

Fearon, E.R., Cho, K.R., Nigro, J.M., Kern, S.E., Simons, J.W., Ruppert, J.M., Hamilton, S.R., Preisinger, A.C., Thomas, G., Kinzler, K.W. and et al. (1990) 'Identification of a chromosome 18q gene that is altered in colorectal cancers', *Science*, 247(4938), pp. 49-56.

Felber, M., Burns, F.J. and Garte, S.J. (1992) 'Amplification of the c-myc oncogene in radiation-induced rat skin tumors as a function of linear energy transfer and dose', *Radiat Res*, 131(3), pp. 297-301.

Ferber, M.J., Eilers, P., Schuuring, E., Fenton, J.A., Fleuren, G.J., Kenter, G., Szuhai, K., Smith, D.I., Raap, A.K. and Brink, A.A. (2004) 'Positioning of cervical carcinoma and Burkitt lymphoma translocation breakpoints with respect to the human papillomavirus integration cluster in FRA8C at 8q24.13', *Cancer Genet Cytogenet*, 154(1), pp. 1-9.

Fernandez, S.V., Russo, I.H. and Russo, J. (2006) 'Estradiol and its metabolites 4-hydroxyestradiol and 2-hydroxyestradiol induce mutations in human breast epithelial cells', *Int J Cancer*, 118(8), pp. 1862-8.

Feuk, L., Carson, A.R. and Scherer, S.W. (2006) 'Structural variation in the human genome', *Nat Rev Genet*, 7(2), pp. 85-97.

Filippo, J.S., Sung, P. and Klein, H. (2008) 'Mechanism of eukaryotic homologous recombination', *Annual Review of Biochemistry*, 77, pp. 229-257.

Fletcher, C., Heintz, N. and Roeder, R.G. (1987) 'Purification and characterization of OTF-1, a transcription factor regulating cell cycle expression of a human histone H2b gene', *Cell*, 51(5), pp. 773-81.

Foulkes, W.D., Metcalfe, K., Sun, P., Hanna, W.M., Lynch, H.T., Ghadirian, P., Tung, N., Olopade, O.I., Weber, B.L., McLennan, J., Olivotto, I.A., Begin, L.R. and Narod, S.A. (2004) 'Estrogen receptor status in BRCA1- and BRCA2-related breast cancer: the influence of age, grade, and histological type', *Clin Cancer Res*, 10(6), pp. 2029-34.

Frederick, J.P., Liberati, N.T., Waddell, D.S., Shi, Y. and Wang, X.F. (2004) 'Transforming growth factor beta-mediated transcriptional repression of c-myc is dependent on direct binding of Smad3 to a novel repressive Smad binding element', *Mol Cell Biol*, 24(6), pp. 2546-59.

Fromme, J.C. and Verdine, G.L. (2004) 'Base excision repair', *Adv Protein Chem*, 69, pp. 1-41.

Furth, E.E., Thilly, W.G., Penman, B.W., Liber, H.L. and Rand, W.M. (1981) 'Quantitative assay for mutation in diploid human lymphoblasts using microtiter plates', *Anal Biochem*, 110(1), pp. 1-8.

Gamble, S.C., Cook, M.C., Riches, A.C., Herceg, Z., Bryant, P.E. and Arrand, J.E. (1999) 'p53 mutations in tumors derived from irradiated human thyroid epithelial cells', *Mutat Res*, 425(2), pp. 231-8.

Ganguly, N. and Parihar, S.P. (2009) 'Human papillomavirus E6 and E7 oncoproteins as risk factors for tumorigenesis', *J Biosci*, 34(1), pp. 113-23.

Gatti, R.A., Tward, A. and Concannon, P. (1999) 'Cancer risk in ATM heterozygotes: a model of phenotypic and mechanistic differences between missense and truncating mutations', *Mol Genet Metab*, 68(4), pp. 419-23.

Geyer, F.C., Marchio, C. and Reis-Filho, J.S. (2009) 'The role of molecular analysis in breast cancer', *Pathology*, 41(1), pp. 77-88.

Ghadjar, P., Rubie, C., Aebersold, D.M. and Keilholz, U. (2009) 'The chemokine CCL20 and its receptor CCR6 in human malignancy with focus on colorectal cancer', *Int J Cancer*, 125(4), pp. 741-5.

Giamas, G., Filipovic, A., Jacob, J., Messier, W., Zhang, H., Yang, D., Zhang, W., Shifa, B.A., Photiou, A., Tralau-Stewart, C., Castellano, L., Green, A.R., Coombes, R.C., Ellis, I.O., Ali, S., Lenz, H.J. and Stebbing, J. (2011) 'Kinome screening for regulators of the estrogen receptor identifies LMTK3 as a new therapeutic target in breast cancer', *Nat Med*, 17(6), pp. 715-9.

Gilbert, E.S., Stovall, M., Gospodarowicz, M., Van Leeuwen, F.E., Andersson, M., Glimelius, B., Joensuu, T., Lynch, C.F., Curtis, R.E., Holowaty, E., Storm, H., Pukkala, E., van't Veer, M.B., Fraumeni, J.F., Boice, J.D., Jr., Clarke, E.A. and Travis, L.B.

(2003) 'Lung cancer after treatment for Hodgkin's disease: focus on radiation effects', *Radiat Res*, 159(2), pp. 161-73.

Goldman, J.M. (2010) 'Chronic myeloid leukemia: a historical perspective', *Semin Hematol*, 47(4), pp. 302-11.

Gollin, S.M. (2005) 'Mechanisms leading to chromosomal instability', *Semin Cancer Biol*, 15(1), pp. 33-42.

Goodhead, D.T. (1994) 'Initial events in the cellular effects of ionizing radiations: clustered damage in DNA', *Int J Radiat Biol*, 65(1), pp. 7-17.

Goto, A., Niki, T., Chi-Pin, L., Matsubara, D., Murakami, Y., Funata, N. and Fukayama, M. (2005) 'Loss of TSLC1 expression in lung adenocarcinoma: relationships with histological subtypes, sex and prognostic significance', *Cancer Sci*, 96(8), pp. 480-6.

Govind, A.P. and Thampan, R.V. (2003) 'Membrane associated estrogen receptors and related proteins: localization at the plasma membrane and the endoplasmic reticulum', *Mol Cell Biochem*, 253(1-2), pp. 233-40.

Green, K.A. and Carroll, J.S. (2007) 'Oestrogen-receptor-mediated transcription and the influence of co-factors and chromatin state', *Nat Rev Cancer*, 7(9), pp. 713-22.

Gunter, M.J., Hoover, D.R., Yu, H., Wassertheil-Smoller, S., Rohan, T.E., Manson, J.E., Li, J., Ho, G.Y., Xue, X., Anderson, G.L., Kaplan, R.C., Harris, T.G., Howard, B.V., Wylie-Rosett, J., Burk, R.D. and Strickler, H.D. (2009) 'Insulin, insulin-like growth factor-I, and risk of breast cancer in postmenopausal women', *J Natl Cancer Inst*, 101(1), pp. 48-60.

Guo, T., Zhang, L., Chang, N.E., Singer, S., Maki, R.G. and Antonescu, C.R. (2011) 'Consistent MYC and FLT4 gene amplification in radiation-induced angiosarcoma but not in other radiation-associated atypical vascular lesions', *Genes Chromosomes Cancer*, 50(1), pp. 25-33.

Gupta, M., Raghavan, M., Gale, R.E., Chelala, C., Allen, C., Molloy, G., Chaplin, T., Linch, D.C., Cazier, J.B. and Young, B.D. (2008) 'Novel regions of acquired uniparental disomy discovered in acute myeloid leukemia', *Genes Chromosomes Cancer*, 47(9), pp. 729-39.

Gupta, P., Su, Z.Z., Lebedeva, I.V., Sarkar, D., Sauane, M., Emdad, L., Bachelor, M.A., Grant, S., Curiel, D.T., Dent, P. and Fisher, P.B. (2006) 'mda-7/IL-24: multifunctional cancer-specific apoptosis-inducing cytokine', *Pharmacol Ther*, 111(3), pp. 596-628.

Ha, V.L., Bharti, S., Inoue, H., Vass, W.C., Campa, F., Nie, Z., de Gramont, A., Ward, Y. and Randazzo, P.A. (2008) 'ASAP3 is a focal adhesion-associated Arf GAP that functions in cell migration and invasion', *J Biol Chem*, 283(22), pp. 14915-26.

Hada, M. and Georgakilas, A.G. (2008) 'Formation of clustered DNA damage after high-LET irradiation: a review', *J Radiat Res (Tokyo)*, 49(3), pp. 203-10.

Hampson, R., Humbert, O., Macpherson, P., Aquilina, G. and Karran, P. (1997) 'Mismatch repair defects and O6-methylguanine-DNA methyltransferase expression in acquired resistance to methylating agents in human cells', *J Biol Chem*, 272(45), pp. 28596-606.

Hanahan, D. and Weinberg, R.A. (2011) 'Hallmarks of cancer: the next generation', *Cell*, 144(5), pp. 646-74.

Hancock, S.L., Tucker, M.A. and Hoppe, R.T. (1993) 'Breast cancer after treatment of Hodgkin's disease', *J Natl Cancer Inst*, 85(1), pp. 25-31.

Hannaford, P.C., Selvaraj, S., Elliott, A.M., Angus, V., Iversen, L. and Lee, A.J. (2007) 'Cancer risk among users of oral contraceptives: cohort data from the Royal College of General Practitioner's oral contraception study', *BMJ*, 335(7621), p. 651.

Harewood, L., Schutz, F., Boyle, S., Perry, P., Delorenzi, M., Bickmore, W.A. and Reymond, A. (2010) 'The effect of translocation-induced nuclear reorganization on gene expression', *Genome Res*, 20(5), pp. 554-64.

Harte, M.T., O'Brien, G.J., Ryan, N.M., Gorski, J.J., Savage, K.I., Crawford, N.T., Mullan, P.B. and Harkin, D.P. (2010) 'BRD7, a subunit of SWI/SNF complexes, binds directly to BRCA1 and regulates BRCA1-dependent transcription', *Cancer Res*, 70(6), pp. 2538-47.

Hastings, P.J., Lupski, J.R., Rosenberg, S.M. and Ira, G. (2009) 'Mechanisms of change in gene copy number', *Nat Rev Genet*, 10(8), pp. 551-64.

Hayes, C.L., Spink, D.C., Spink, B.C., Cao, J.Q., Walker, N.J. and Sutter, T.R. (1996) '17 beta-estradiol hydroxylation catalyzed by human cytochrome P450 1B1', *Proc Natl Acad Sci U S A*, 93(18), pp. 9776-81.

He, T.C., Sparks, A.B., Rago, C., Hermeking, H., Zawel, L., da Costa, L.T., Morin, P.J., Vogelstein, B. and Kinzler, K.W. (1998) 'Identification of c-MYC as a target of the APC pathway', *Science*, 281(5382), pp. 1509-12.

Heaphy, C.M., Griffith, J.K. and Bisoffi, M. (2009) 'Mammary field cancerization: molecular evidence and clinical importance', *Breast Cancer Res Treat*, 118(2), pp. 229-39.

Hei, T.K., Zhou, H., Ivanov, V.N., Hong, M., Lieberman, H.B., Brenner, D.J., Amundson, S.A. and Geard, C.R. (2008) 'Mechanism of radiation-induced bystander effects: a unifying model', *J Pharm Pharmacol*, 60(8), pp. 943-50.

Helleday, T. (2010) 'Homologous recombination in cancer development, treatment and development of drug resistance', *Carcinogenesis*, 31(6), pp. 955-60.

Helms, M.W., Packeisen, J., August, C., Schittek, B., Boecker, W., Brandt, B.H. and Buerger, H. (2005) 'First evidence supporting a potential role for the BMP/SMAD pathway in the progression of oestrogen receptor-positive breast cancer', *J Pathol*, 206(3), pp. 366-76.

Herr, W., Sturm, R.A., Clerc, R.G., Corcoran, L.M., Baltimore, D., Sharp, P.A., Ingraham, H.A., Rosenfeld, M.G., Finney, M., Ruvkun, G. and et al. (1988) 'The POU domain: a large conserved region in the mammalian pit-1, oct-1, oct-2, and Caenorhabditis elegans unc-86 gene products', *Genes Dev*, 2(12A), pp. 1513-6.

Hesling, C., Fattet, L., Teyre, G., Jury, D., Gonzalo, P., Lopez, J., Vanbelle, C., Morel, A.P., Gillet, G., Mikaelian, I. and Rimokh, R. (2011) 'Antagonistic regulation of EMT by TIF1gamma and Smad4 in mammary epithelial cells', *EMBO Rep*, 12(7), pp. 665-72.

Hess, J., Thomas, G., Braselmann, H., Bauer, V., Bogdanova, T., Wienberg, J., Zitzelsberger, H. and Unger, K. (2011) 'Gain of chromosome band 7q11 in papillary thyroid carcinomas of young patients is associated with exposure to low-dose irradiation', *Proc Natl Acad Sci U S A*, 108(23), pp. 9595-600.

Hieber, L., Trutschler, K., Smida, J., Wachsmann, M., Ponsel, G. and Kellerer, A.M. (1990) 'Radiation-induced cell transformation: transformation efficiencies of different types of ionizing radiation and molecular changes in radiation transformants and tumor cell lines', *Environ Health Perspect*, 88, pp. 169-74.

Higashikawa, K., Yoneda, S., Taki, M., Shigeishi, H., Ono, S., Tobiume, K. and Kamata, N. (2008) 'Gene expression profiling to identify genes associated with high-invasiveness in human squamous cell carcinoma with epithelial-to-mesenchymal transition', *Cancer Lett*, 264(2), pp. 256-64.

Hoffman, D.A., Lonstein, J.E., Morin, M.M., Visscher, W., Harris, B.S., 3rd and Boice, J.D., Jr. (1989) 'Breast cancer in women with scoliosis exposed to multiple diagnostic x rays', *J Natl Cancer Inst*, 81(17), pp. 1307-12.

Hosey, A.M., Gorski, J.J., Murray, M.M., Quinn, J.E., Chung, W.Y., Stewart, G.E., James, C.R., Farragher, S.M., Mulligan, J.M., Scott, A.N., Dervan, P.A., Johnston, P.G., Couch, F.J., Daly, P.A., Kay, E., McCann, A., Mullan, P.B. and Harkin, D.P. (2007) 'Molecular basis for estrogen receptor alpha deficiency in BRCA1-linked breast cancer', *J Natl Cancer Inst*, 99(22), pp. 1683-94.

Hrubec, Z., Boice, J.D., Jr., Monson, R.R. and Rosenstein, M. (1989) 'Breast cancer after multiple chest fluoroscopies: second follow-up of Massachusetts women with tuberculosis', *Cancer Res*, 49(1), pp. 229-34.

Hu, B., Grabham, P., Nie, J., Balajee, A.S., Zhou, H., Hei, T.K. and Geard, C.R. (2012) 'Intrachromosomal changes and genomic instability in site-specific microbeam-irradiated and bystander human-hamster hybrid cells', *Radiat Res*, 177(1), pp. 25-34.

Huang, D.W., Sherman, B.T. and Lempicki, R.A. (2009a) 'Bioinformatics enrichment tools: paths toward the comprehensive functional analysis of large gene lists', *Nucleic Acids Res*, 37(1), pp. 1-13.

Huang, D.W., Sherman, B.T. and Lempicki, R.A. (2009b) 'Systematic and integrative analysis of large gene lists using DAVID bioinformatics resources', *Nature Protocols*, 4(1), pp. 44-57.

Huang, Y., Fernandez, S.V., Goodwin, S., Russo, P.A., Russo, I.H., Sutter, T.R. and Russo, J. (2007) 'Epithelial to mesenchymal transition in human breast epithelial cells transformed by 17beta-estradiol', *Cancer Res*, 67(23), pp. 11147-57.

Hubbell, J.H. (2006) 'Electron-positron pair production by photons: A historical overview', *Radiation Physics and Chemistry*, 75(6), pp. 614-623.

Huber, M.A., Kraut, N. and Beug, H. (2005) 'Molecular requirements for epithelial-mesenchymal transition during tumor progression', *Curr Opin Cell Biol*, 17(5), pp. 548-58.

Iademarco, M.F., McQuillan, J.J., Rosen, G.D. and Dean, D.C. (1992) 'Characterization of the promoter for vascular cell adhesion molecule-1 (VCAM-1)', *J Biol Chem*, 267(23), pp. 16323-9.

Igawa, T., Sato, Y., Takata, K., Fushimi, S., Tamura, M., Nakamura, N., Maeda, Y., Orita, Y., Tanimoto, M. and Yoshino, T. (2011) 'Cyclin D2 is overexpressed in proliferation centers of chronic lymphocytic leukemia/small lymphocytic lymphoma', *Cancer Sci*, 102(11), pp. 2103-7.

Ikeda, K., Iyama, K., Ishikawa, N., Egami, H., Nakao, M., Sado, Y., Ninomiya, Y. and Baba, H. (2006) 'Loss of expression of type IV collagen alpha5 and alpha6 chains in

colorectal cancer associated with the hypermethylation of their promoter region', *Am J Pathol*, 168(3), pp. 856-65.

Imbalzano, K.M., Tatarkova, I., Imbalzano, A.N. and Nickerson, J.A. (2009) 'Increasingly transformed MCF-10A cells have a progressively tumor-like phenotype in three-dimensional basement membrane culture', *Cancer Cell Int*, 9, p. 7.

Inano, H., Yamanouchi, H., Suzuki, K., Onoda, M. and Wakabayashi, K. (1995) 'Estradiol-17 beta as an initiation modifier for radiation-induced mammary tumorigenesis of rats ovariectomized before puberty', *Carcinogenesis*, 16(8), pp. 1871-7.

Iwasaki, M. and Tsugane, S. (2011) 'Risk factors for breast cancer: epidemiological evidence from Japanese studies', *Cancer Sci*, 102(9), pp. 1607-14.

Jaafar, L. and Flores-Rozas, H. (2009) 'Elucidating the role of human mismatch repair factor hMLH3', *Cancer Biol Ther*, 8(14), pp. 1421-3.

Jefford, C.E. and Irminger-Finger, I. (2006) 'Mechanisms of chromosome instability in cancers', *Crit Rev Oncol Hematol*, 59(1), pp. 1-14.

Jenuwein, T. and Grosschedl, R. (1991) 'Complex pattern of immunoglobulin mu gene expression in normal and transgenic mice: nonoverlapping regulatory sequences govern distinct tissue specificities', *Genes Dev*, 5(6), pp. 932-43.

Jin, S., Fan, F., Fan, W., Zhao, H., Tong, T., Blanck, P., Alomo, I., Rajasekaran, B. and Zhan, Q. (2001) 'Transcription factors Oct-1 and NF-YA regulate the p53-independent induction of the GADD45 following DNA damage', *Oncogene*, 20(21), pp. 2683-90.

Jonsson, G., Staaf, J., Vallon-Christersson, J., Ringner, M., Holm, K., Hegardt, C., Gunnarsson, H., Fagerholm, R., Strand, C., Agnarsson, B.A., Kilpivaara, O., Luts, L., Heikkila, P., Aittomaki, K., Blomqvist, C., Loman, N., Malmstrom, P., Olsson, H., Johannsson, O.T., Arason, A., Nevanlinna, H., Barkardottir, R.B. and Borg, A. (2010) 'Genomic subtypes of breast cancer identified by array-comparative genomic hybridization display distinct molecular and clinical characteristics', *Breast Cancer Res*, 12(3), p. R42.

Jordan, V.C. (2006) 'Tamoxifen (ICI46,474) as a targeted therapy to treat and prevent breast cancer', *Br J Pharmacol*, 147 Suppl 1, pp. S269-76.

Kahlenborn, C., Modugno, F., Potter, D.M. and Severs, W.B. (2006) 'Oral contraceptive use as a risk factor for premenopausal breast cancer: a meta-analysis', *Mayo Clin Proc*, 81(10), pp. 1290-302.

Kaina, B., Christmann, M., Naumann, S. and Roos, W.P. (2007) 'MGMT: key node in the battle against genotoxicity, carcinogenicity and apoptosis induced by alkylating agents', *DNA Repair (Amst)*, 6(8), pp. 1079-99.

Kalluri, R. and Weinberg, R.A. (2009) 'The basics of epithelial-mesenchymal transition', *J Clin Invest*, 119(6), pp. 1420-8.

Kang, J., Gemberling, M., Nakamura, M., Whitby, F.G., Handa, H., Fairbrother, W.G. and Tantin, D. (2009) 'A general mechanism for transcription regulation by Oct1 and Oct4 in response to genotoxic and oxidative stress', *Genes Dev*, 23(2), pp. 208-22.

Kanwal, R. and Gupta, S. (2011) 'Epigenetic modifications in cancer', *Clin Genet*.

Katsuno, Y., Hanyu, A., Kanda, H., Ishikawa, Y., Akiyama, F., Iwase, T., Ogata, E., Ehata, S., Miyazono, K. and Imamura, T. (2008) 'Bone morphogenetic protein signaling enhances invasion and bone metastasis of breast cancer cells through Smad pathway', *Oncogene*, 27(49), pp. 6322-33.

Kawazu, M., Saso, K., Tong, K.I., McQuire, T., Goto, K., Son, D.O., Wakeham, A., Miyagishi, M., Mak, T.W. and Okada, H. (2011) 'Histone demethylase JMJD2B functions as a co-factor of estrogen receptor in breast cancer proliferation and mammary gland development', *PLoS One*, 6(3), p. e17830.

Ke, X.S., Qu, Y., Goldfinger, N., Rostad, K., Hovland, R., Akslen, L.A., Rotter, V., Oyan, A.M. and Kalland, K.H. (2008) 'Epithelial to mesenchymal transition of a primary prostate cell line with switches of cell adhesion modules but without malignant transformation', *PLoS One*, 3(10), p. e3368.

Key, T., Appleby, P., Barnes, I. and Reeves, G. (2002) 'Endogenous sex hormones and breast cancer in postmenopausal women: reanalysis of nine prospective studies', *J Natl Cancer Inst*, 94(8), pp. 606-16.

Key, T.J., Appleby, P.N., Reeves, G.K., Roddam, A., Dorgan, J.F., Longcope, C., Stanczyk, F.Z., Stephenson, H.E., Jr., Falk, R.T., Miller, R., Schatzkin, A., Allen, D.S., Fentiman, I.S., Wang, D.Y., Dowsett, M., Thomas, H.V., Hankinson, S.E., Toniolo, P., Akhmedkhanov, A., Koenig, K., Shore, R.E., Zeleniuch-Jacquotte, A., Berrino, F., Muti, P., Micheli, A., Krogh, V., Sieri, S., Pala, V., Venturelli, E., Secreto, G., Barrett-Connor, E., Laughlin, G.A., Kabuto, M., Akiba, S., Stevens, R.G., Neriishi, K., Land, C.E., Cauley, J.A., Kuller, L.H., Cummings, S.R., Helzlsouer, K.J., Alberg, A.J., Bush, T.L., Comstock, G.W., Gordon, G.B. and Miller, S.R. (2003) 'Body mass index, serum sex hormones, and breast cancer risk in postmenopausal women', *J Natl Cancer Inst*, 95(16), pp. 1218-26.

Khramtsov, A.I., Khramtsova, G.F., Tretiakova, M., Huo, D., Olopade, O.I. and Goss, K.H. (2010) 'Wnt/beta-catenin pathway activation is enriched in basal-like breast cancers and predicts poor outcome', *Am J Pathol*, 176(6), pp. 2911-20.

Kim, B.Y., Kwak, S.Y., Yang, J.S. and Han, Y.H. (2011a) 'Phosphorylation and stabilization of c-Myc by NEMO renders cells resistant to ionizing radiation through up-regulation of gamma-GCS', *Oncol Rep*, 26(6), pp. 1587-93.

Kim, G.E., Lee, K.H., Choi, Y.D., Lee, J.S., Lee, J.H., Nam, J.H., Choi, C., Park, M.H. and Yoon, J.H. (2011b) 'Detection of Slit2 promoter hypermethylation in tissue and serum samples from breast cancer patients', *Virchows Arch*, 459(4), pp. 383-90.

Kim, G.J., Fiskum, G.M. and Morgan, W.F. (2006) 'A role for mitochondrial dysfunction in perpetuating radiation-induced genomic instability', *Cancer Res*, 66(21), pp. 10377-83.

Kim, H.J., Litzenburger, B.C., Cui, X., Delgado, D.A., Grabiner, B.C., Lin, X., Lewis, M.T., Gottardis, M.M., Wong, T.W., Attar, R.M., Carboni, J.M. and Lee, A.V. (2007) 'Constitutively active type I insulin-like growth factor receptor causes transformation and xenograft growth of immortalized mammary epithelial cells and is accompanied by an epithelial-to-mesenchymal transition mediated by NF-kappaB and snail', *Mol Cell Biol*, 27(8), pp. 3165-75.

Kim, H.K., Zhang, H., Li, H., Wu, T.T., Swisher, S., He, D., Wu, L., Xu, J., Elmets, C.A., Athar, M., Xu, X.C. and Xu, H. (2008) 'Slit2 inhibits growth and metastasis of fibrosarcoma and squamous cell carcinoma', *Neoplasia*, 10(12), pp. 1411-20.

Kim, I.Y., Yong, H.Y., Kang, K.W. and Moon, A. (2009a) 'Overexpression of ErbB2 induces invasion of MCF10A human breast epithelial cells via MMP-9', *Cancer Lett*, 275(2), pp. 227-33.

Kim, J.H., Kushiro, K., Graham, N.A. and Asthagiri, A.R. (2009b) 'Tunable interplay between epidermal growth factor and cell-cell contact governs the spatial dynamics of epithelial growth', *Proc Natl Acad Sci U S A*, 106(27), pp. 11149-53.

Kim, K., Lu, Z. and Hay, E.D. (2002) 'Direct evidence for a role of beta-catenin/LEF-1 signaling pathway in induction of EMT', *Cell Biol Int*, 26(5), pp. 463-76.

Klemm, J.D., Rould, M.A., Aurora, R., Herr, W. and Pabo, C.O. (1994) 'Crystal structure of the Oct-1 POU domain bound to an octamer site: DNA recognition with tethered DNA-binding modules', *Cell*, 77(1), pp. 21-32.

Klinakis, A., Szabolcs, M., Politi, K., Kiaris, H., Artavanis-Tsakonas, S. and Efstratiadis, A. (2006) 'Myc is a Notch1 transcriptional target and a requisite for Notch1-induced mammary tumorigenesis in mice', *Proc Natl Acad Sci U S A*, 103(24), pp. 9262-7.

Knudson, A.G., Jr. (1971) 'Mutation and cancer: statistical study of retinoblastoma', *Proc Natl Acad Sci U S A*, 68(4), pp. 820-3.

Koniaras, K., Cuddihy, A.R., Christopoulos, H., Hogg, A. and O'Connell, M.J. (2001) 'Inhibition of Chk1-dependent G2 DNA damage checkpoint radiosensitizes p53 mutant human cells', *Oncogene*, 20(51), pp. 7453-63.

Kumle, M., Weiderpass, E., Braaten, T., Persson, I., Adami, H.O. and Lund, E. (2002) 'Use of oral contraceptives and breast cancer risk: The Norwegian-Swedish Women's Lifestyle and Health Cohort Study', *Cancer Epidemiol Biomarkers Prev*, 11(11), pp. 1375-81.

Kuppers, M., Ittrich, C., Faust, D. and Dietrich, C. (2010) 'The transcriptional programme of contact-inhibition', *J Cell Biochem*, 110(5), pp. 1234-43.

Lakhani, S.R., Reis-Filho, J.S., Fulford, L., Penault-Llorca, F., van der Vijver, M., Parry, S., Bishop, T., Benitez, J., Rivas, C., Bignon, Y.J., Chang-Claude, J., Hamann, U., Cornelisse, C.J., Devilee, P., Beckmann, M.W., Nestle-Kramling, C., Daly, P.A., Haites, N., Varley, J., Lalloo, F., Evans, G., Maugard, C., Meijers-Heijboer, H., Klijn, J.G., Olah, E., Gusterson, B.A., Pilotti, S., Radice, P., Scherneck, S., Sobol, H., Jacquemier, J., Wagner, T., Peto, J., Stratton, M.R., McGuffog, L. and Easton, D.F. (2005) 'Prediction of BRCA1 status in patients with breast cancer using estrogen receptor and basal phenotype', *Clin Cancer Res*, 11(14), pp. 5175-80.

Land, C.E. (1995) 'Studies of cancer and radiation dose among atomic bomb survivors. The example of breast cancer', *Jama*, 274(5), pp. 402-7.

Land, C.E., Tokunaga, M., Koyama, K., Soda, M., Preston, D.L., Nishimori, I. and Tokuoka, S. (2003) 'Incidence of female breast cancer among atomic bomb survivors, Hiroshima and Nagasaki, 1950-1990', *Radiat Res*, 160(6), pp. 707-17.

Land, H., Parada, L.F. and Weinberg, R.A. (1983) 'Tumorigenic conversion of primary embryo fibroblasts requires at least two cooperating oncogenes', *Nature*, 304(5927), pp. 596-602.

Lane, D. and Levine, A. (2010) 'p53 Research: the past thirty years and the next thirty years', *Cold Spring Harb Perspect Biol*, 2(12), p. a000893.

Lee, A.S., Seo, Y.C., Chang, A., Tohari, S., Eu, K.W., Seow-Choen, F. and McGee, J.O. (2000) 'Detailed deletion mapping at chromosome 11q23 in colorectal carcinoma', *Br J Cancer*, 83(6), pp. 750-5.

Levin, E.R. (2003) 'Bidirectional signaling between the estrogen receptor and the epidermal growth factor receptor', *Mol Endocrinol*, 17(3), pp. 309-17.

Lewis, S.P., Willis, A.N., Johnson, A.E., Resau, J. and Burnatowska-Hledin, M.A. (2011) 'Mutational analysis of VACM-1/cul5 exons in cancer cell lines', *APMIS*, 119(7), pp. 421-30.

Li, T.K., Chen, A.Y., Yu, C., Mao, Y., Wang, H.M. and Liu, L.F. (1999) 'Activation of topoisomerase II-mediated excision of chromosomal DNA loops during oxidative stress', *Genes Dev*, 13(12), pp. 1553-1560.

Li, X. and Heyer, W.D. (2008) 'Homologous recombination in DNA repair and DNA damage tolerance', *Cell Res*, 18(1), pp. 99-113.

Liang, Q.L., Chen, G.Q., Li, Z.Y. and Wang, B.R. (2011) 'Function and histopathology of a cell adhesion molecule TSLC1 in cancer', *Cancer Invest*, 29(2), pp. 107-12.

Liao, J.K. (2003) 'Cross-coupling between the oestrogen receptor and phosphoinositide 3-kinase', *Biochem Soc Trans*, 31(Pt 1), pp. 66-70.

Liebermann, D.A. and Hoffman, B. (2008) 'Gadd45 in stress signaling', *J Mol Signal*, 3, p. 15.

Liehr, J.G. (2000) 'Is estradiol a genotoxic mutagenic carcinogen?', *Endocr Rev*, 21(1), pp. 40-54.

Liggett, W.H., Jr. and Sidransky, D. (1998) 'Role of the p16 tumor suppressor gene in cancer', *J Clin Oncol*, 16(3), pp. 1197-206.

Lin, Y., Wong, K. and Calame, K. (1997) 'Repression of c-myc transcription by Blimp-1, an inducer of terminal B cell differentiation', *Science*, 276(5312), pp. 596-9.

Liu, M., Bandaru, V., Bond, J.P., Jaruga, P., Zhao, X., Christov, P.P., Burrows, C.J., Rizzo, C.J., Dizdaroglu, M. and Wallace, S.S. (2010) 'The mouse ortholog of NEIL3 is a functional DNA glycosylase in vitro and in vivo', *Proc Natl Acad Sci U S A*, 107(11), pp. 4925-30.

Liu, M., Casimiro, M.C., Wang, C., Shirley, L.A., Jiao, X., Katiyar, S., Ju, X., Li, Z., Yu, Z., Zhou, J., Johnson, M., Fortina, P., Hyslop, T., Windle, J.J. and Pestell, R.G.

(2009) 'p21CIP1 attenuates Ras- and c-Myc-dependent breast tumor epithelial mesenchymal transition and cancer stem cell-like gene expression in vivo', *Proc Natl Acad Sci U S A*, 106(45), pp. 19035-9.

Liu, S. and Lin, Y.C. (2004) 'Transformation of MCF-10A human breast epithelial cells by zeranol and estradiol-17beta', *Breast J*, 10(6), pp. 514-21.

Logarajah, S., Hunter, P., Kraman, M., Steele, D., Lakhani, S., Bobrow, L., Venkitaraman, A. and Wagner, S. (2003) 'BCL-6 is expressed in breast cancer and prevents mammary epithelial differentiation', *Oncogene*, 22(36), pp. 5572-8.

Loo, L.W., Grove, D.I., Williams, E.M., Neal, C.L., Cousens, L.A., Schubert, E.L., Holcomb, I.N., Massa, H.F., Glogovac, J., Li, C.I., Malone, K.E., Daling, J.R., Delrow, J.J., Trask, B.J., Hsu, L. and Porter, P.L. (2004) 'Array comparative genomic hybridization analysis of genomic alterations in breast cancer subtypes', *Cancer Res*, 64(23), pp. 8541-9.

Lopez-Knowles, E., Zardawi, S.J., McNeil, C.M., Millar, E.K., Crea, P., Musgrove, E.A., Sutherland, R.L. and O'Toole, S.A. (2010) 'Cytoplasmic localization of beta-catenin is a marker of poor outcome in breast cancer patients', *Cancer Epidemiol Biomarkers Prev*, 19(1), pp. 301-9.

Lottin, S., Adriaenssens, E., Dupressoir, T., Berteaux, N., Montpellier, C., Coll, J., Dugimont, T. and Curgy, J.J. (2002) 'Overexpression of an ectopic H19 gene enhances the tumorigenic properties of breast cancer cells', *Carcinogenesis*, 23(11), pp. 1885-95.

Lowe, S.W. and Lin, A.W. (2000) 'Apoptosis in cancer', *Carcinogenesis*, 21(3), pp. 485-95.

Lu, F., Zahid, M., Saeed, M., Cavalieri, E.L. and Rogan, E.G. (2007) 'Estrogen metabolism and formation of estrogen-DNA adducts in estradiol-treated MCF-10F cells. The effects of 2,3,7,8-tetrachlorodibenzo-p-dioxin induction and catechol-O-methyltransferase inhibition', *J Steroid Biochem Mol Biol*, 105(1-5), pp. 150-8.

Lung, H.L., Cheung, A.K., Xie, D., Cheng, Y., Kwong, F.M., Murakami, Y., Guan, X.Y., Sham, J.S., Chua, D., Protopopov, A.I., Zabarovsky, E.R., Tsao, S.W., Stanbridge, E.J. and Lung, M.L. (2006) 'TSLC1 is a tumor suppressor gene associated with metastasis in nasopharyngeal carcinoma', *Cancer Res*, 66(19), pp. 9385-92.

Ma, H., Hill, C.K., Bernstein, L. and Ursin, G. (2008) 'Low-dose medical radiation exposure and breast cancer risk in women under age 50 years overall and by estrogen and progesterone receptor status: results from a case-control and a case-case comparison', *Breast Cancer Res Treat*, 109(1), pp. 77-90.

Ma, Y.P., van Leeuwen, F.E., Cooke, R., Broeks, A., Enciso-Mora, V., Olver, B., Lloyd, A., Broderick, P., Russell, N.S., Janus, C., Ashworth, A., Houlston, R.S. and Swerdlow, A.J. (2012) 'FGFR2 genotype and risk of radiation-associated breast cancer in Hodgkin lymphoma', *Blood*, 119(4), pp. 1029-31.

Maeda, M., Johnson, K.R. and Wheelock, M.J. (2005) 'Cadherin switching: essential for behavioral but not morphological changes during an epithelium-to-mesenchyme transition', *J Cell Sci*, 118(Pt 5), pp. 873-87.

Maekawa, T., Sano, Y., Shinagawa, T., Rahman, Z., Sakuma, T., Nomura, S., Licht, J.D. and Ishii, S. (2008) 'ATF-2 controls transcription of Maspin and GADD45 alpha genes independently from p53 to suppress mammary tumors', *Oncogene*, 27(8), pp. 1045-54.

Mahaney, B.L., Meek, K. and Lees-Miller, S.P. (2009) 'Repair of ionizing radiation-induced DNA double-strand breaks by non-homologous end-joining', *Biochem J*, 417(3), pp. 639-50.

Mandelbaum, J., Bhagat, G., Tang, H., Mo, T., Brahmachary, M., Shen, Q., Chadburn, A., Rajewsky, K., Tarakhovsky, A., Pasqualucci, L. and Dalla-Favera, R. (2010) 'BLIMP1 is a tumor suppressor gene frequently disrupted in activated B cell-like diffuse large B cell lymphoma', *Cancer Cell*, 18(6), pp. 568-79.

Mandrell, J., Mehta, S. and McClure, S. (2010) 'Atypical vascular lesion of the breast', *J Am Acad Dermatol*, 63(2), pp. 337-40.

Mani, S.A., Guo, W., Liao, M.J., Eaton, E.N., Ayyanan, A., Zhou, A.Y., Brooks, M., Reinhard, F., Zhang, C.C., Shipitsin, M., Campbell, L.L., Polyak, K., Brisken, C., Yang, J. and Weinberg, R.A. (2008) 'The epithelial-mesenchymal transition generates cells with properties of stem cells', *Cell*, 133(4), pp. 704-15.

Manner, J., Radlwimmer, B., Hohenberger, P., Mossinger, K., Kuffer, S., Sauer, C., Belharazem, D., Zettl, A., Coindre, J.M., Hallermann, C., Hartmann, J.T., Katenkamp, D., Katenkamp, K., Schoffski, P., Sciot, R., Wozniak, A., Lichter, P., Marx, A. and Strobel, P. (2010) 'MYC high level gene amplification is a distinctive feature of angiosarcomas after irradiation or chronic lymphedema', *Am J Pathol*, 176(1), pp. 34-9.

Mao, X., Seidlitz, E., Truant, R., Hitt, M. and Ghosh, H.P. (2004) 'Re-expression of TSLC1 in a non-small-cell lung cancer cell line induces apoptosis and inhibits tumor growth', *Oncogene*, 23(33), pp. 5632-42.

Marchbanks, P.A., McDonald, J.A., Wilson, H.G., Folger, S.G., Mandel, M.G., Daling, J.R., Bernstein, L., Malone, K.E., Ursin, G., Strom, B.L., Norman, S.A., Wingo, P.A., Burkman, R.T., Berlin, J.A., Simon, M.S., Spirtas, R. and Weiss, L.K. (2002) 'Oral contraceptives and the risk of breast cancer', *N Engl J Med*, 346(26), pp. 2025-32.

Markushin, Y., Zhong, W., Cavalieri, E.L., Rogan, E.G., Small, G.J., Yeung, E.S. and Jankowiak, R. (2003) 'Spectral characterization of catechol estrogen quinone (CEQ)-derived DNA adducts and their identification in human breast tissue extract', *Chem Res Toxicol*, 16(9), pp. 1107-17.

Masuda, M., Yageta, M., Fukuhara, H., Kuramochi, M., Maruyama, T., Nomoto, A. and Murakami, Y. (2002) 'The tumor suppressor protein TSLC1 is involved in cell-cell adhesion', *J Biol Chem*, 277(34), pp. 31014-9.

Mattsson, A., Ruden, B.I., Hall, P., Wilking, N. and Rutqvist, L.E. (1993) 'Radiation-induced breast cancer: long-term follow-up of radiation therapy for benign breast disease', *J Natl Cancer Inst*, 85(20), pp. 1679-85.

McCarroll, S.A., Kuruvilla, F.G., Korn, J.M., Cawley, S., Nemesh, J., Wysoker, A., Shapero, M.H., de Bakker, P.I., Maller, J.B., Kirby, A., Elliott, A.L., Parkin, M., Hubbell, E., Webster, T., Mei, R., Veitch, J., Collins, P.J., Handsaker, R., Lincoln, S., Nizzari, M., Blume, J., Jones, K.W., Rava, R., Daly, M.J., Gabriel, S.B. and Altshuler, D. (2008) 'Integrated detection and population-genetic analysis of SNPs and copy number variation', *Nat Genet*, 40(10), pp. 1166-74.

McCoy, E.L., Iwanaga, R., Jedlicka, P., Abbey, N.S., Chodosh, L.A., Heichman, K.A., Welm, A.L. and Ford, H.L. (2009) 'Six1 expands the mouse mammary epithelial stem/progenitor cell pool and induces mammary tumors that undergo epithelial-mesenchymal transition', *J Clin Invest*, 119(9), pp. 2663-77.

Mehlen, P. and Fearon, E.R. (2004) 'Role of the dependence receptor DCC in colorectal cancer pathogenesis', *J Clin Oncol*, 22(16), pp. 3420-8.

Meighan-Mantha, R.L., Riegel, A.T., Suy, S., Harris, V., Wang, F.H., Lozano, C., Whiteside, T.L. and Kasid, U. (1999) 'Ionizing radiation stimulates octamer factor DNA binding activity in human carcinoma cells', *Mol Cell Biochem*, 199(1-2), pp. 209-15.

Menard, S., Casalini, P., Campiglio, M., Pupa, S.M. and Tagliabue, E. (2004) 'Role of HER2/neu in tumor progression and therapy', *Cell Mol Life Sci*, 61(23), pp. 2965-78.

Menard, S., Pupa, S.M., Campiglio, M. and Tagliabue, E. (2003) 'Biologic and therapeutic role of HER2 in cancer', *Oncogene*, 22(42), pp. 6570-8.

Mendonca, M.S. and Redpath, J.L. (1989) 'Isolation of human cell hybrids (HeLa x skin fibroblast) expressing a radiation-induced tumour-associated antigen', *Br J Cancer*, 60(3), pp. 324-6.

Meng, L., Gabai, V.L. and Sherman, M.Y. (2010) 'Heat-shock transcription factor HSF1 has a critical role in human epidermal growth factor receptor-2-induced cellular transformation and tumorigenesis', *Oncogene*, 29(37), pp. 5204-13.

Mense, S.M., Remotti, F., Bhan, A., Singh, B., El-Tamer, M., Hei, T.K. and Bhat, H.K. (2008) 'Estrogen-induced breast cancer: alterations in breast morphology and oxidative stress as a function of estrogen exposure', *Toxicol Appl Pharmacol*, 232(1), pp. 78-85.

Meyer, N. and Penn, L.Z. (2008) 'Reflecting on 25 years with MYC', *Nat Rev Cancer*, 8(12), pp. 976-90.

Micalizzi, D.S., Farabaugh, S.M. and Ford, H.L. (2010) 'Epithelial-Mesenchymal Transition in Cancer: Parallels Between Normal Development and Tumor Progression', *Journal of Mammary Gland Biology and Neoplasia*, 15(2), pp. 117-134.

Migliore, L., Migheli, F., Spisni, R. and Coppede, F. (2011) 'Genetics, cytogenetics, and epigenetics of colorectal cancer', *J Biomed Biotechnol*, 2011, p. 792362.

Miki, Y., Swensen, J., Shattuck-Eidens, D., Futreal, P.A., Harshman, K., Tavtigian, S., Liu, Q., Cochran, C., Bennett, L.M., Ding, W. and et al. (1994) 'A strong candidate for the breast and ovarian cancer susceptibility gene BRCA1', *Science*, 266(5182), pp. 66-71.

Miles, R.R., Crockett, D.K., Lim, M.S. and Elenitoba-Johnson, K.S. (2005) 'Analysis of BCL6-interacting proteins by tandem mass spectrometry', *Mol Cell Proteomics*, 4(12), pp. 1898-909.

Mill, A.J., Frankenberg, D., Bettega, D., Hieber, L., Saran, A., Allen, L.A., Calzolari, P., Frankenberg-Schwager, M., Lehane, M.M., Morgan, G.R., Pariset, L., Pazzaglia, S., Roberts, C.J. and Tallone, L. (1998) 'Transformation of C3H 10T1/2 cells by low doses of ionising radiation: a collaborative study by six European laboratories strongly supporting a linear dose-response relationship', *J Radiol Prot*, 18(2), pp. 79-100.

Minde, D.P., Anvarian, Z., Rudiger, S.G. and Maurice, M.M. (2011) 'Messing up disorder: how do missense mutations in the tumor suppressor protein APC lead to cancer?', *Mol Cancer*, 10, p. 101.

Mitchell, R.J., Farrington, S.M., Dunlop, M.G. and Campbell, H. (2002) 'Mismatch repair genes hMLH1 and hMSH2 and colorectal cancer: a HuGE review', *Am J Epidemiol*, 156(10), pp. 885-902.

Mitrunen, K. and Hirvonen, A. (2003) 'Molecular epidemiology of sporadic breast cancer. The role of polymorphic genes involved in oestrogen biosynthesis and metabolism', *Mutat Res*, 544(1), pp. 9-41.

Miura, S., Nakashima, M., Ito, M., Kondo, H., Meirmanov, S., Hayashi, T., Soda, M., Matsuo, T. and Sekine, I. (2008) 'Significance of HER2 and C-MYC oncogene amplifications in breast cancer in atomic bomb survivors: associations with radiation exposure and histologic grade', *Cancer*, 112(10), pp. 2143-51.

Mohsin, S.K., Weiss, H., Havighurst, T., Clark, G.M., Berardo, M., Roanh le, D., To, T.V., Qian, Z., Love, R.R. and Allred, D.C. (2004) 'Progesterone receptor by immunohistochemistry and clinical outcome in breast cancer: a validation study', *Mod Pathol*, 17(12), pp. 1545-54.

Morali, O.G., Delmas, V., Moore, R., Jeanney, C., Thiery, J.P. and Larue, L. (2001) 'IGF-II induces rapid beta-catenin relocation to the nucleus during epithelium to mesenchyme transition', *Oncogene*, 20(36), pp. 4942-50.

Morgan, W.F. (2003) 'Non-targeted and delayed effects of exposure to ionizing radiation: I. Radiation-induced genomic instability and bystander effects in vitro', *Radiat Res*, 159(5), pp. 567-80.

Murakami, Y. (2005) 'Involvement of a cell adhesion molecule, TSLC1/IGSF4, in human oncogenesis', *Cancer Sci*, 96(9), pp. 543-52.

Nagahata, T., Hirano, A., Utada, Y., Tsuchiya, S., Takahashi, K., Tada, T., Makita, M., Kasumi, F., Akiyama, F., Sakamoto, G., Nakamura, Y. and Emi, M. (2002) 'Correlation of allelic losses and clinicopathological factors in 504 primary breast cancers', *Breast Cancer*, 9(3), pp. 208-15.

Nagasawa, H., Brogan, J.R., Peng, Y., Little, J.B. and Bedford, J.S. (2010) 'Some unsolved problems and unresolved issues in radiation cytogenetics: a review and new data on roles of homologous recombination and non-homologous end joining', *Mutat Res*, 701(1), pp. 12-22.

Natarajan, A.T. and Palitti, F. (2008) 'DNA repair and chromosomal alterations', *Mutat Res*, 657(1), pp. 3-7.

Nenoi, M., Daino, K., Nakajima, T., Wang, B., Taki, K. and Kakimoto, A. (2009) 'Involvement of Oct-1 in the regulation of CDKN1A in response to clinically relevant doses of ionizing radiation', *Biochim Biophys Acta*, 1789(3), pp. 225-31.

Nesbit, C.E., Tersak, J.M. and Prochownik, E.V. (1999) 'MYC oncogenes and human neoplastic disease', *Oncogene*, 18(19), pp. 3004-16.

Niederacher, D., Picard, F., van Roeyen, C., An, H.X., Bender, H.G. and Beckmann, M.W. (1997) 'Patterns of allelic loss on chromosome 17 in sporadic breast carcinomas

detected by fluorescent-labeled microsatellite analysis', *Genes Chromosomes Cancer*, 18(3), pp. 181-92.

Nieminen, T.T., Abdel-Rahman, W.M., Ristimaki, A., Lappalainen, M., Lahermo, P., Mecklin, J.P., Jarvinen, H.J. and Peltomaki, P. (2011) 'BMPR1A mutations in hereditary nonpolyposis colorectal cancer without mismatch repair deficiency', *Gastroenterology*, 141(1), pp. e23-6.

O'Keefe, C., McDevitt, M.A. and Maciejewski, J.P. (2010) 'Copy neutral loss of heterozygosity: a novel chromosomal lesion in myeloid malignancies', *Blood*, 115(14), pp. 2731-9.

Obaya, A.J., Mateyak, M.K. and Sedivy, J.M. (1999) 'Mysterious liaisons: the relationship between c-Myc and the cell cycle', *Oncogene*, 18(19), pp. 2934-41.

Ochs, K. and Kaina, B. (2000) 'Apoptosis induced by DNA damage O6-methylguanine is Bcl-2 and caspase-9/3 regulated and Fas/caspase-8 independent', *Cancer Res*, 60(20), pp. 5815-24.

Oikawa, M., Yoshiura, K., Kondo, H., Miura, S., Nagayasu, T. and Nakashima, M. (2011) 'Significance of genomic instability in breast cancer in atomic bomb survivors: analysis of microarray-comparative genomic hybridization', *Radiat Oncol*, 6, p. 168.

Onland-Moret, N.C., Kaaks, R., van Noord, P.A., Rinaldi, S., Key, T., Grobbee, D.E. and Peeters, P.H. (2003) 'Urinary endogenous sex hormone levels and the risk of postmenopausal breast cancer', *Br J Cancer*, 88(9), pp. 1394-9.

Office for National Statistics, Edition: MB1 39

Ortega, S., Malumbres, M. and Barbacid, M. (2002) 'Cyclin D-dependent kinases, INK4 inhibitors and cancer', *Biochim Biophys Acta*, 1602(1), pp. 73-87.

Pandey, R.N., Rani, R., Yeo, E.J., Spencer, M., Hu, S., Lang, R.A. and Hegde, R.S. (2010) 'The Eyes Absent phosphatase-transactivator proteins promote proliferation, transformation, migration, and invasion of tumor cells', *Oncogene*, 29(25), pp. 3715-22.

Pandita, T.K. (2001) 'The role of ATM in telomere structure and function', *Radiat Res*, 156(5 Pt 2), pp. 642-7.

Pandita, T.K. (2002) 'ATM function and telomere stability', *Oncogene*, 21(4), pp. 611-8.

Parikh, R.A., White, J.S., Huang, X., Schoppy, D.W., Baysal, B.E., Baskaran, R., Bakkenist, C.J., Saunders, W.S., Hsu, L.C., Romkes, M. and Gollin, S.M. (2007) 'Loss

of distal 11q is associated with DNA repair deficiency and reduced sensitivity to ionizing radiation in head and neck squamous cell carcinoma', *Genes Chromosomes Cancer*, 46(8), pp. 761-75.

Park, K., Kwak, K., Kim, J., Lim, S. and Han, S. (2005) 'c-myc amplification is associated with HER2 amplification and closely linked with cell proliferation in tissue microarray of nonselected breast cancers', *Hum Pathol*, 36(6), pp. 634-9.

Park, S.K., Yim, D.S., Yoon, K.S., Choi, I.M., Choi, J.Y., Yoo, K.Y., Noh, D.Y., Choe, K.J., Ahn, S.H., Hirvonen, A. and Kang, D. (2004) 'Combined effect of GSTM1, GSTT1, and COMT genotypes in individual breast cancer risk', *Breast Cancer Res Treat*, 88(1), pp. 55-62.

Patani, N., Douglas-Jones, A., Mansel, R., Jiang, W. and Mokbel, K. (2010) 'Tumour suppressor function of MDA-7/IL-24 in human breast cancer', *Cancer Cell Int*, 10, p. 29.

Pawlik, T.M. and Keyomarsi, K. (2004) 'Role of cell cycle in mediating sensitivity to radiotherapy', *Int J Radiat Oncol Biol Phys*, 59(4), pp. 928-42.

Perou, C.M., Sorlie, T., Eisen, M.B., van de Rijn, M., Jeffrey, S.S., Rees, C.A., Pollack, J.R., Ross, D.T., Johnsen, H., Akslen, L.A., Fluge, O., Pergamenschikov, A., Williams, C., Zhu, S.X., Lonning, P.E., Borresen-Dale, A.L., Brown, P.O. and Botstein, D. (2000) 'Molecular portraits of human breast tumours', *Nature*, 406(6797), pp. 747-52.

Pfeifer, G.P., Denissenko, M.F., Olivier, M., Tretyakova, N., Hecht, S.S. and Hainaut, P. (2002) 'Tobacco smoke carcinogens, DNA damage and p53 mutations in smoking-associated cancers', *Oncogene*, 21(48), pp. 7435-51.

Phillips, T.M., McBride, W.H. and Pajonk, F. (2006) 'The response of CD24(-/low)/CD44+ breast cancer-initiating cells to radiation', *J Natl Cancer Inst*, 98(24), pp. 1777-85.

Pierce, D.A. and Preston, D.L. (1993) 'Joint analysis of site-specific cancer risks for the atomic bomb survivors', *Radiat Res*, 134(2), pp. 134-42.

Pike, M.C., Spicer, D.V., Dahmoush, L. and Press, M.F. (1993) 'Estrogens, progestogens, normal breast cell proliferation, and breast cancer risk', *Epidemiol Rev*, 15(1), pp. 17-35.

Pogribny, I., Koturbash, I., Tryndyak, V., Hudson, D., Stevenson, S.M., Sedelnikova, O., Bonner, W. and Kovalchuk, O. (2005) 'Fractionated low-dose radiation exposure leads to accumulation of DNA damage and profound alterations in DNA and histone methylation in the murine thymus', *Mol Cancer Res*, 3(10), pp. 553-61.

Polascik, T.J., Cairns, P., Chang, W.Y., Schoenberg, M.P. and Sidransky, D. (1995) 'Distinct regions of allelic loss on chromosome 4 in human primary bladder carcinoma', *Cancer Res*, 55(22), pp. 5396-9.

Preston, D.L., Kusumi, S., Tomonaga, M., Izumi, S., Ron, E., Kuramoto, A., Kamada, N., Dohy, H., Matsuo, T., Matsui, T. and et al. (1994) 'Cancer incidence in atomic bomb survivors. Part III. Leukemia, lymphoma and multiple myeloma, 1950-1987', *Radiat Res*, 137(2 Suppl), pp. S68-97.

Preston, D.L., Ron, E., Tokuoka, S., Funamoto, S., Nishi, N., Soda, M., Mabuchi, K. and Kodama, K. (2007) 'Solid cancer incidence in atomic bomb survivors: 1958-1998', *Radiat Res*, 168(1), pp. 1-64.

Prochownik, E.V. and Li, Y. (2007) 'The ever expanding role for c-Myc in promoting genomic instability', *Cell Cycle*, 6(9), pp. 1024-9.

Pylayeva-Gupta, Y., Grabocka, E. and Bar-Sagi, D. (2011) 'RAS oncogenes: weaving a tumorigenic web', *Nat Rev Cancer*, 11(11), pp. 761-74.

Quelle, D.E., Ashmun, R.A., Shurtleff, S.A., Kato, J.Y., Bar-Sagi, D., Roussel, M.F. and Sherr, C.J. (1993) 'Overexpression of mouse D-type cyclins accelerates G1 phase in rodent fibroblasts', *Genes Dev*, 7(8), pp. 1559-71.

Rafnsson, V., Tulinius, H., Jonasson, J.G. and Hrafnkelsson, J. (2001) 'Risk of breast cancer in female flight attendants: a population-based study (Iceland)', *Cancer Causes Control*, 12(2), pp. 95-101.

Rahman, N., Seal, S., Thompson, D., Kelly, P., Renwick, A., Elliott, A., Reid, S., Spanova, K., Barfoot, R., Chagtai, T., Jayatilake, H., McGuffog, L., Hanks, S., Evans, D.G., Eccles, D., Easton, D.F. and Stratton, M.R. (2007) 'PALB2, which encodes a BRCA2-interacting protein, is a breast cancer susceptibility gene', *Nat Genet*, 39(2), pp. 165-7.

Raiche, J., Rodriguez-Juarez, R., Pogribny, I. and Kovalchuk, O. (2004) 'Sex- and tissue-specific expression of maintenance and de novo DNA methyltransferases upon low dose X-irradiation in mice', *Biochem Biophys Res Commun*, 325(1), pp. 39-47.

Ramsay, D.T., Kent, J.C., Hartmann, R.A. and Hartmann, P.E. (2005) 'Anatomy of the lactating human breast redefined with ultrasound imaging', *J Anat*, 206(6), pp. 525-34.

Randazzo, P.A., Inoue, H. and Bharti, S. (2007) 'Arf GAPs as regulators of the actin cytoskeleton', *Biol Cell*, 99(10), pp. 583-600.

Rattray, A.J., Shafer, B.K., Neelam, B. and Strathern, J.N. (2005) 'A mechanism of palindromic gene amplification in Saccharomyces cerevisiae', *Genes Dev*, 19(11), pp. 1390-9.

Reinhold, D.S., Walicka, M., Elkassaby, M., Milam, L.D., Kohler, S.K., Dunstan, R.W. and McCormick, J.J. (1996) 'Malignant transformation of human fibroblasts by ionizing radiation', *Int J Radiat Biol*, 69(6), pp. 707-15.

Reya, T., Morrison, S.J., Clarke, M.F. and Weissman, I.L. (2001) 'Stem cells, cancer, and cancer stem cells', *Nature*, 414(6859), pp. 105-11.

Rich, J.N. (2007) 'Cancer stem cells in radiation resistance', *Cancer Res*, 67(19), pp. 8980-4.

Riches, A., Peddie, C., Rendell, S., Bryant, P., Zitzelsberger, H., Bruch, J., Smida, J., Hieber, L. and Bauchinger, M. (2001) 'Neoplastic transformation and cytogenetic changes after Gamma irradiation of human epithelial cells expressing telomerase', *Radiat Res*, 155(1 Pt 2), pp. 222-229.

Riches, A.C., Herceg, Z., Bryant, P.E., Stevens, D.L. and Goodhead, D.T. (1997) 'Radiation-induced transformation of SV40-immortalized human thyroid epithelial cells by single exposure to plutonium alpha-particles in vitro', *Int J Radiat Biol*, 72(5), pp. 515-21.

Ritchie, M.D., Hahn, L.W., Roodi, N., Bailey, L.R., Dupont, W.D., Parl, F.F. and Moore, J.H. (2001) 'Multifactor-dimensionality reduction reveals high-order interactions among estrogen-metabolism genes in sporadic breast cancer', *Am J Hum Genet*, 69(1), pp. 138-47.

Robanus-Maandag, E.C., Bosch, C.A., Kristel, P.M., Hart, A.A., Faneyte, I.F., Nederlof, P.M., Peterse, J.L. and van de Vijver, M.J. (2003) 'Association of C-MYC amplification with progression from the in situ to the invasive stage in C-MYC-amplified breast carcinomas', *J Pathol*, 201(1), pp. 75-82.

Rodriguez-Pinilla, S.M., Jones, R.L., Lambros, M.B., Arriola, E., Savage, K., James, M., Pinder, S.E. and Reis-Filho, J.S. (2007) 'MYC amplification in breast cancer: a chromogenic in situ hybridisation study', *J Clin Pathol*, 60(9), pp. 1017-23.

Rodriguez, C., Causse, A., Ursule, E. and Theillet, C. (2000) 'At least five regions of imbalance on 6q in breast tumors, combining losses and gains', *Genes Chromosomes Cancer*, 27(1), pp. 76-84.

Rodrik, V., Gomes, E., Hui, L., Rockwell, P. and Foster, D.A. (2006) 'Myc stabilization in response to estrogen and phospholipase D in MCF-7 breast cancer cells', *FEBS Lett*, 580(24), pp. 5647-52.

Rogers-Bald, M., Sargent, R.G. and Bryant, P.E. (2000) 'Production of chromatid breaks by single dsb: evidence supporting the signal model', *Int J Radiat Biol*, 76(1), pp. 23-9.

Ronski, K., Sanders, M., Burleson, J.A., Moyo, V., Benn, P. and Fang, M. (2005) 'Early growth response gene 1 (EGR1) is deleted in estrogen receptor-negative human breast carcinoma', *Cancer*, 104(5), pp. 925-30.

Rosen, E.M., Fan, S. and Ma, Y. (2006) 'BRCA1 regulation of transcription', *Cancer Lett*, 236(2), pp. 175-85.

Roy, D., Calaf, G. and Hei, T.K. (2001a) 'Frequent allelic imbalance on chromosome 6 and 17 correlate with radiation-induced neoplastic transformation of human breast epithelial cells', *Carcinogenesis*, 22(10), pp. 1685-92.

Roy, D., Calaf, G. and Hei, T.K. (2001b) 'Profiling of differentially expressed genes induced by high linear energy transfer radiation in breast epithelial cells', *Mol Carcinog*, 31(4), pp. 192-203.

Roy, D., Calaf, G. and Hei, T.K. (2003) 'Allelic imbalance at 11p15.5-15.4 correlated with c-Ha-ras mutation during radiation-induced neoplastic transformation of human breast epithelial cells', *Int J Cancer*, 103(6), pp. 730-7.

Roy, D., Calaf, G.M., Hande, M.P. and Hei, T.K. (2006) 'Allelic imbalance at 11q23-q24 chromosome associated with estrogen and radiation-induced breast cancer progression', *Int J Oncol*, 28(3), pp. 667-74.

Rubie, C., Frick, V.O., Ghadjar, P., Wagner, M., Grimm, H., Vicinus, B., Justinger, C., Graeber, S. and Schilling, M.K. (2010) 'CCL20/CCR6 expression profile in pancreatic cancer', *J Transl Med*, 8, p. 45.

Russo, J., Fernandez, S.V., Russo, P.A., Fernbaugh, R., Sheriff, F.S., Lareef, H.M., Garber, J. and Russo, I.H. (2006) '17-Beta-estradiol induces transformation and tumorigenesis in human breast epithelial cells', *Faseb J*, 20(10), pp. 1622-34.

Russo, J. and Russo, I.H. (2006) 'The role of estrogen in the initiation of breast cancer', *J Steroid Biochem Mol Biol*, 102(1-5), pp. 89-96.

Sabatier, L., Ricoul, M., Pottier, G. and Murnane, J.P. (2005) 'The loss of a single telomere can result in instability of multiple chromosomes in a human tumor cell line', *Mol Cancer Res*, 3(3), pp. 139-50.

Saha, T., Rih, J.K., Roy, R., Ballal, R. and Rosen, E.M. (2010) 'Transcriptional regulation of the base excision repair pathway by BRCA1', *J Biol Chem*, 285(25), pp. 19092-105.

Sakurai-Yageta, M., Masuda, M., Tsuboi, Y., Ito, A. and Murakami, Y. (2009) 'Tumor suppressor CADM1 is involved in epithelial cell structure', *Biochem Biophys Res Commun*, 390(3), pp. 977-82.

Salas, T.R., Petruseva, I., Lavrik, O. and Saintome, C. (2009) 'Evidence for direct contact between the RPA3 subunit of the human replication protein A and single-stranded DNA', *Nucleic Acids Res*, 37(1), pp. 38-46.

Samarakoon, R., Higgins, C.E., Higgins, S.P. and Higgins, P.J. (2009) 'TGF-beta1-Induced Expression of the Poor Prognosis SERPINE1/PAI-1 Gene Requires EGFR Signaling: A New Target for Anti-EGFR Therapy', *J Oncol*, 2009, p. 342391.

Sanna, G., Lorizzo, K., Rotmensz, N., Bagnardi, V., Cinieri, S., Colleoni, M., Nole, F. and Goldhirsch, A. (2007) 'Breast cancer in Hodgkin's disease and non-Hodgkin's lymphoma survivors', *Ann Oncol*, 18(2), pp. 288-92.

Santucci-Darmanin, S., Neyton, S., Lespinasse, F., Saunieres, A., Gaudray, P. and Paquis-Flucklinger, V. (2002) 'The DNA mismatch-repair MLH3 protein interacts with MSH4 in meiotic cells, supporting a role for this MutL homolog in mammalian meiotic recombination', *Hum Mol Genet*, 11(15), pp. 1697-706.

Sarrio, D., Rodriguez-Pinilla, S.M., Hardisson, D., Cano, A., Moreno-Bueno, G. and Palacios, J. (2008) 'Epithelial-mesenchymal transition in breast cancer relates to the basal-like phenotype', *Cancer Res*, 68(4), pp. 989-97.

Sauter, G., Carroll, P., Moch, H., Kallioniemi, A., Kerschmann, R., Narayan, P., Mihatsch, M.J. and Waldman, F.M. (1995) 'c-myc copy number gains in bladder cancer detected by fluorescence in situ hybridization', *Am J Pathol*, 146(5), pp. 1131-9.

Savage, J.R. and Simpson, P.J. (1994) 'FISH "painting" patterns resulting from complex exchanges', *Mutat Res*, 312(1), pp. 51-60.

Savagner, P., Yamada, K.M. and Thiery, J.P. (1997) 'The zinc-finger protein slug causes desmosome dissociation, an initial and necessary step for growth factor-induced epithelial-mesenchymal transition', *J Cell Biol*, 137(6), pp. 1403-19.

Savitsky, K., Bar-Shira, A., Gilad, S., Rotman, G., Ziv, Y., Vanagaite, L., Tagle, D.A., Smith, S., Uziel, T., Sfez, S., Ashkenazi, M., Pecker, I., Frydman, M., Harnik, R., Patanjali, S.R., Simmons, A., Clines, G.A., Sartiel, A., Gatti, R.A., Chessa, L., Sanal, O., Lavin, M.F., Jaspers, N.G., Taylor, A.M., Arlett, C.F., Miki, T., Weissman, S.M., Lovett, M., Collins, F.S. and Shiloh, Y. (1995) 'A single ataxia telangiectasia gene with a product similar to PI-3 kinase', *Science*, 268(5218), pp. 1749-53.

Sax, K. (1940) 'An Analysis of X-Ray Induced Chromosomal Aberrations in Tradescantia', *Genetics*, 25(1), pp. 41-68.

Schild-Poulter, C., Pope, L., Giffin, W., Kochan, J.C., Ngsee, J.K., Traykova-Andonova, M. and Hache, R.J. (2001) 'The binding of Ku antigen to homeodomain proteins promotes their phosphorylation by DNA-dependent protein kinase', *J Biol Chem*, 276(20), pp. 16848-56.

Schild-Poulter, C., Shih, A., Tantin, D., Yarymowich, N.C., Soubeyrand, S., Sharp, P.A. and Hache, R.J. (2007) 'DNA-PK phosphorylation sites on Oct-1 promote cell survival following DNA damage', *Oncogene*, 26(27), pp. 3980-8.

Schild-Poulter, C., Shih, A., Yarymowich, N.C. and Hache, R.J. (2003) 'Down-regulation of histone H2B by DNA-dependent protein kinase in response to DNA damage through modulation of octamer transcription factor 1', *Cancer Res*, 63(21), pp. 7197-205.

Schleger, C., Verbeke, C., Hildenbrand, R., Zentgraf, H. and Bleyl, U. (2002) 'c-MYC activation in primary and metastatic ductal adenocarcinoma of the pancreas: incidence, mechanisms, and clinical significance', *Mod Pathol*, 15(4), pp. 462-9.

Schlotter, C.M., Vogt, U., Bosse, U., Mersch, B. and Wassmann, K. (2003) 'C-myc, not HER-2/neu, can predict recurrence and mortality of patients with node-negative breast cancer', *Breast Cancer Res*, 5(2), pp. R30-6.

Schonfeld, S.J., Lee, C. and Berrington de Gonzalez, A. (2011) 'Medical exposure to radiation and thyroid cancer', *Clin Oncol (R Coll Radiol)*, 23(4), pp. 244-50.

Schwachtgen, J.L., Remacle, J.E., Janel, N., Brys, R., Huylebroeck, D., Meyer, D. and Kerbiriou-Nabias, D. (1998) 'Oct-1 is involved in the transcriptional repression of the von willebrand factor gene promoter', *Blood*, 92(4), pp. 1247-58.

Seal, S., Thompson, D., Renwick, A., Elliott, A., Kelly, P., Barfoot, R., Chagtai, T., Jayatilake, H., Ahmed, M., Spanova, K., North, B., McGuffog, L., Evans, D.G., Eccles, D., Easton, D.F., Stratton, M.R. and Rahman, N. (2006) 'Truncating mutations in the Fanconi anemia J gene BRIP1 are low-penetrance breast cancer susceptibility alleles', *Nat Genet*, 38(11), pp. 1239-41.

Sears, R., Leone, G., DeGregori, J. and Nevins, J.R. (1999) 'Ras enhances Myc protein stability', *Mol Cell*, 3(2), pp. 169-79.

Sekeres, M.A., Gundacker, H., Lancet, J., Advani, A., Petersdorf, S., Liesveld, J., Mulford, D., Norwood, T., Willman, C.L., Appelbaum, F.R. and List, A.F. (2011) 'A phase 2 study of lenalidomide monotherapy in patients with deletion 5q acute myeloid leukemia: Southwest Oncology Group Study S0605', *Blood*, 118(3), pp. 523-8.

Sekimoto, G., Matsuzaki, K., Yoshida, K., Mori, S., Murata, M., Seki, T., Matsui, H., Fujisawa, J. and Okazaki, K. (2007) 'Reversible Smad-dependent signaling between tumor suppression and oncogenesis', *Cancer Res*, 67(11), pp. 5090-6.

Shaffer, A.L., Yu, X., He, Y., Boldrick, J., Chan, E.P. and Staudt, L.M. (2000) 'BCL-6 represses genes that function in lymphocyte differentiation, inflammation, and cell cycle control', *Immunity*, 13(2), pp. 199-212.

Shah, R., Smith, P., Purdie, C., Quinlan, P., Baker, L., Aman, P., Thompson, A.M. and Crook, T. (2009) 'The prolyl 3-hydroxylases P3H2 and P3H3 are novel targets for epigenetic silencing in breast cancer', *Br J Cancer*, 100(10), pp. 1687-96.

Sharma, S., Kelly, T.K. and Jones, P.A. (2010) 'Epigenetics in cancer', *Carcinogenesis*, 31(1), pp. 27-36.

Sherr, C.J. and McCormick, F. (2002) 'The RB and p53 pathways in cancer', *Cancer Cell*, 2(2), pp. 103-12.

Shiloh, Y. (2003) 'ATM and related protein kinases: safeguarding genome integrity', *Nat Rev Cancer*, 3(3), pp. 155-68.

Shiloh, Y. (2006) 'The ATM-mediated DNA-damage response: taking shape', *Trends Biochem Sci*, 31(7), pp. 402-10.

Shin, S.K., Nagasaka, T., Jung, B.H., Matsubara, N., Kim, W.H., Carethers, J.M., Boland, C.R. and Goel, A. (2007) 'Epigenetic and genetic alterations in Netrin-1 receptors UNC5C and DCC in human colon cancer', *Gastroenterology*, 133(6), pp. 1849-57.

Shinmura, K., Tao, H., Goto, M., Igarashi, H., Taniguchi, T., Maekawa, M., Takezaki, T. and Sugimura, H. (2004) 'Inactivating mutations of the human base excision repair gene NEIL1 in gastric cancer', *Carcinogenesis*, 25(12), pp. 2311-7.

Shirai, Y.T., Ehata, S., Yashiro, M., Yanagihara, K., Hirakawa, K. and Miyazono, K. (2011) 'Bone morphogenetic protein-2 and -4 play tumor suppressive roles in human diffuse-type gastric carcinoma', *Am J Pathol*, 179(6), pp. 2920-30.

Shivapurkar, N., Sood, S., Wistuba, II, Virmani, A.K., Maitra, A., Milchgrub, S., Minna, J.D. and Gazdar, A.F. (1999a) 'Multiple regions of chromosome 4 demonstrating allelic losses in breast carcinomas', *Cancer Res*, 59(15), pp. 3576-80.

Shivapurkar, N., Virmani, A.K., Wistuba, II, Milchgrub, S., Mackay, B., Minna, J.D. and Gazdar, A.F. (1999b) 'Deletions of chromosome 4 at multiple sites are frequent in malignant mesothelioma and small cell lung carcinoma', *Clin Cancer Res*, 5(1), pp. 17-23.

Silva, E., Tiong, S., Pedersen, M., Homola, E., Royou, A., Fasulo, B., Siriaco, G. and Campbell, S.D. (2004) 'ATM is required for telomere maintenance and chromosome stability during Drosophila development', *Curr Biol*, 14(15), pp. 1341-7.

Simpkin, D.J. (1999) 'The AAPM/RSNA physics tutorial for residents - Radiation interactions and internal dosimetry in nuclear medicine', *Radiographics*, 19(1), pp. 155-167.

Singleton, B.K., Griffin, C.S. and Thacker, J. (2002) 'Clustered DNA damage leads to complex genetic changes in irradiated human cells', *Cancer Res*, 62(21), pp. 6263-9.

Slattery, M.L., Lundgreen, A., Herrick, J.S., Kadlubar, S., Caan, B.J., Potter, J.D. and Wolff, R.K. (2012) 'Genetic variation in bone morphogenetic protein and colon and rectal cancer', *Int J Cancer*, 130(3), pp. 653-64.

Slaughter, D.P., Southwick, H.W. and Smejkal, W. (1953) 'Field cancerization in oral stratified squamous epithelium; clinical implications of multicentric origin', *Cancer*, 6(5), pp. 963-8.

Smith, A.P., Verrecchia, A., Faga, G., Doni, M., Perna, D., Martinato, F., Guccione, E. and Amati, B. (2009) 'A positive role for Myc in TGFbeta-induced Snail transcription and epithelial-to-mesenchymal transition', *Oncogene*, 28(3), pp. 422-30.

Sorlie, T., Tibshirani, R., Parker, J., Hastie, T., Marron, J.S., Nobel, A., Deng, S., Johnsen, H., Pesich, R., Geisler, S., Demeter, J., Perou, C.M., Lonning, P.E., Brown, P.O., Borresen-Dale, A.L. and Botstein, D. (2003) 'Repeated observation of breast tumor subtypes in independent gene expression data sets', *Proc Natl Acad Sci U S A*, 100(14), pp. 8418-23.

Soule, H.D., Maloney, T.M., Wolman, S.R., Peterson, W.D., Jr., Brenz, R., McGrath, C.M., Russo, J., Pauley, R.J., Jones, R.F. and Brooks, S.C. (1990) 'Isolation and characterization of a spontaneously immortalized human breast epithelial cell line, MCF-10', *Cancer Res*, 50(18), pp. 6075-86.

Spector, N.L. and Blackwell, K.L. (2009) 'Understanding the mechanisms behind trastuzumab therapy for human epidermal growth factor receptor 2-positive breast cancer', *J Clin Oncol*, 27(34), pp. 5838-47.

Spring, K., Ahangari, F., Scott, S.P., Waring, P., Purdie, D.M., Chen, P.C., Hourigan, K., Ramsay, J., McKinnon, P.J., Swift, M. and Lavin, M.F. (2002) 'Mice heterozygous for mutation in Atm, the gene involved in ataxia-telangiectasia, have heightened susceptibility to cancer', *Nat Genet*, 32(1), pp. 185-90.

Stebbing, J., Filipovic, A., Ellis, I.O., Green, A.R., D'Silva, T.R., Lenz, H.J., Coombes, R.C., Wang, T., Lee, S.C. and Giamas, G. (2011) 'LMTK3 expression in breast cancer: association with tumor phenotype and clinical outcome', *Breast Cancer Res Treat*.

Stovall, M., Smith, S.A. and Rosenstein, M. (1989) 'Tissue doses from radiotherapy of cancer of the uterine cervix', *Med Phys*, 16(5), pp. 726-33.

Strunz, A.M., Peschke, P., Waldeck, W., Ehemann, V., Kissel, M. and Debus, J. (2002) 'Preferential radiosensitization in p53-mutated human tumour cell lines by pentoxifylline-mediated disruption of the G2/M checkpoint control', *Int J Radiat Biol*, 78(8), pp. 721-32.

Stylianou, S., Clarke, R.B. and Brennan, K. (2006) 'Aberrant activation of notch signaling in human breast cancer', *Cancer Res*, 66(3), pp. 1517-25.

Styrt, B. and Sugarman, B. (1991) 'Estrogens and infection', *Rev Infect Dis*, 13(6), pp. 1139-50.

Suraweera, N., Meijne, E., Moody, J., Carvajal-Carmona, L.G., Yoshida, K., Pollard, P., Fitzgibbon, J., Riches, A., van Laar, T., Huiskamp, R., Rowan, A., Tomlinson, I.P. and Silver, A. (2005) 'Mutations of the PU.1 Ets domain are specifically associated with murine radiation-induced, but not human therapy-related, acute myeloid leukaemia', *Oncogene*, 24(22), pp. 3678-83.

Sussan, T.E., Pletcher, M.T., Murakami, Y. and Reeves, R.H. (2005) 'Tumor suppressor in lung cancer 1 (TSLC1) alters tumorigenic growth properties and gene expression', *Mol Cancer*, 4, p. 28.

Sutherland, B.M., Bennett, P.V., Sidorkina, O. and Laval, J. (2000) 'Clustered damages and total lesions induced in DNA by ionizing radiation: Oxidized bases and strand breaks', *Biochemistry*, 39(27), pp. 8026-8031.

Takahashi, Y., Iwai, M., Kawai, T., Arakawa, A., Ito, T., Sakurai-Yageta, M., Ito, A., Goto, A., Saito, M., Kasumi, F. and Murakami, Y. (2011) 'Aberrant expression of tumor

suppressors CADM1 and 4.1B in invasive lesions of primary breast cancer', *Breast Cancer*.

Takano, Y., Kato, Y., Masuda, M., Ohshima, Y. and Okayasu, I. (1999) 'Cyclin D2, but not cyclin D1, overexpression closely correlates with gastric cancer progression and prognosis', *J Pathol*, 189(2), pp. 194-200.

Tanos, V., Ariel, I., Prus, D., De-Groot, N. and Hochberg, A. (2004) 'H19 and IGF2 gene expression in human normal, hyperplastic, and malignant endometrium', *Int J Gynecol Cancer*, 14(3), pp. 521-5.

Tantin, D., Schild-Poulter, C., Wang, V., Hache, R.J. and Sharp, P.A. (2005) 'The octamer binding transcription factor Oct-1 is a stress sensor', *Cancer Res*, 65(23), pp. 10750-8.

Terato, H. and Ide, H. (2004) 'Clustered DNA damage induced by heavy ion particles', *Biol Sci Space*, 18(4), pp. 206-15.

Terry, S.Y., Riches, A.C. and Bryant, P.E. (2008) 'A role for topoisomerase II alpha in the formation of radiation-induced chromatid breaks', *Br J Cancer*, 99(4), pp. 670-4.

Thacker, J. (2005) 'The RAD51 gene family, genetic instability and cancer', *Cancer Lett*, 219(2), pp. 125-35.

Thiery, J.P. (2002) 'Epithelial-mesenchymal transitions in tumour progression', *Nat Rev Cancer*, 2(6), pp. 442-54.

Thiery, J.P. (2003) 'Epithelial-mesenchymal transitions in development and pathologies', *Current Opinion in Cell Biology*, 15(6), pp. 740-746.

Tinger, A., Wasserman, T.H., Klein, E.E., Miller, E.A., Roberts, T., Piephoff, J.V. and Kucik, N.A. (1997) 'The incidence of breast cancer following mantle field radiation therapy as a function of dose and technique', *Int J Radiat Oncol Biol Phys*, 37(4), pp. 865-70.

Tokunaga, M., Land, C.E., Tokuoka, S., Nishimori, I., Soda, M. and Akiba, S. (1994) 'Incidence of female breast cancer among atomic bomb survivors, 1950-1985', *Radiat Res*, 138(2), pp. 209-23.

Travis, L.B., Hill, D., Dores, G.M., Gospodarowicz, M., van Leeuwen, F.E., Holowaty, E., Glimelius, B., Andersson, M., Pukkala, E., Lynch, C.F., Pee, D., Smith, S.A., Van't Veer, M.B., Joensuu, T., Storm, H., Stovall, M., Boice, J.D., Jr., Gilbert, E. and Gail, M.H. (2005) 'Cumulative absolute breast cancer risk for young women treated for Hodgkin lymphoma', *J Natl Cancer Inst*, 97(19), pp. 1428-37.

Travis, L.B., Hill, D.A., Dores, G.M., Gospodarowicz, M., van Leeuwen, F.E., Holowaty, E., Glimelius, B., Andersson, M., Wiklund, T., Lynch, C.F., Van't Veer, M.B., Glimelius, I., Storm, H., Pukkala, E., Stovall, M., Curtis, R., Boice, J.D., Jr. and Gilbert, E. (2003) 'Breast cancer following radiotherapy and chemotherapy among young women with Hodgkin disease', *Jama*, 290(4), pp. 465-75.

Travis, R.C. and Key, T.J. (2003) 'Oestrogen exposure and breast cancer risk', *Breast Cancer Res*, 5(5), pp. 239-47.

Trimboli, A.J., Fukino, K., de Bruin, A., Wei, G., Shen, L., Tanner, S.M., Creasap, N., Rosol, T.J., Robinson, M.L., Eng, C., Ostrowski, M.C. and Leone, G. (2008) 'Direct evidence for epithelial-mesenchymal transitions in breast cancer', *Cancer Res*, 68(3), pp. 937-45.

Tsang, W.P., Ng, E.K., Ng, S.S., Jin, H., Yu, J., Sung, J.J. and Kwok, T.T. (2010) 'Oncofetal H19-derived miR-675 regulates tumor suppressor RB in human colorectal cancer', *Carcinogenesis*, 31(3), pp. 350-8.

Tseng, R.C., Lee, S.H., Hsu, H.S., Chen, B.H., Tsai, W.C., Tzao, C. and Wang, Y.C. (2010) 'SLIT2 attenuation during lung cancer progression deregulates beta-catenin and E-cadherin and associates with poor prognosis', *Cancer Res*, 70(2), pp. 543-51.

Uchino, K., Ito, A., Wakayama, T., Koma, Y., Okada, T., Ohbayashi, C., Iseki, S., Kitamura, Y., Tsubota, N., Okita, Y. and Okada, M. (2003) 'Clinical implication and prognostic significance of the tumor suppressor TSLC1 gene detected in adenocarcinoma of the lung', *Cancer*, 98(5), pp. 1002-7.

Underwood, J.M., Imbalzano, K.M., Weaver, V.M., Fischer, A.H., Imbalzano, A.N. and Nickerson, J.A. (2006) 'The ultrastructure of MCF-10A acini', *J Cell Physiol*, 208(1), pp. 141-8.

United Nations Scientific Committee on the Effects of Atomic Radiation (2002)

United Nations Scientific Committee on the Effects of Atomic Radiation (2008)

Unger, K., Wienberg, J., Riches, A., Hieber, L., Walch, A., Brown, A., O'Brien, P.C., Briscoe, C., Gray, L., Rodriguez, E., Jackl, G., Knijnenburg, J., Tallini, G., Ferguson-Smith, M. and Zitzelsberger, H. (2010) 'Novel gene rearrangements in transformed breast cells identified by high-resolution breakpoint analysis of chromosomal aberrations', *Endocr Relat Cancer*, 17(1), pp. 87-98.

Vafa, O., Wade, M., Kern, S., Beeche, M., Pandita, T.K., Hampton, G.M. and Wahl, G.M. (2002) 'c-Myc can induce DNA damage, increase reactive oxygen species, and

mitigate p53 function: a mechanism for oncogene-induced genetic instability', *Mol Cell*, 9(5), pp. 1031-44.

van Leeuwen, F.E., Klokman, W.J., Stovall, M., Dahler, E.C., van't Veer, M.B., Noordijk, E.M., Crommelin, M.A., Aleman, B.M., Broeks, A., Gospodarowicz, M., Travis, L.B. and Russell, N.S. (2003) 'Roles of radiation dose, chemotherapy, and hormonal factors in breast cancer following Hodgkin's disease', *J Natl Cancer Inst*, 95(13), pp. 971-80.

Varma, G., Varma, R., Huang, H., Pryshchepava, A., Groth, J., Fleming, D., Nowak, N.J., McQuaid, D., Conroy, J., Mahoney, M., Moysich, K., Falkner, K.L. and Geradts, J. (2005) 'Array comparative genomic hybridisation (aCGH) analysis of premenopausal breast cancers from a nuclear fallout area and matched cases from Western New York', *Br J Cancer*, 93(6), pp. 699-708.

Vessey, M. and Painter, R. (2006) 'Oral contraceptive use and cancer. Findings in a large cohort study, 1968-2004', *Br J Cancer*, 95(3), pp. 385-9.

Vincent-Salomon, A. and Thiery, J.P. (2003) 'Host microenvironment in breast cancer development - Epithelial-mesenchymal transition in breast cancer development', *Breast Cancer Research*, 5(2), pp. 101-106.

Vlashi, E., McBride, W.H. and Pajonk, F. (2009) 'Radiation responses of cancer stem cells', *J Cell Biochem*, 108(2), pp. 339-42.

Vranka, J.A., Sakai, L.Y. and Bachinger, H.P. (2004) 'Prolyl 3-hydroxylase 1, enzyme characterization and identification of a novel family of enzymes', *J Biol Chem*, 279(22), pp. 23615-21.

Wagner, S.D., Ahearne, M. and Ferrigno, P.K. (2011) 'The role of BCL6 in lymphomas and routes to therapy', *Br J Haematol*, 152(1), pp. 3-12.

Wahner-Roedler, D.L., Nelson, D.F., Croghan, I.T., Achenbach, S.J., Crowson, C.S., Hartmann, L.C. and O'Fallon, W.M. (2003) 'Risk of breast cancer and breast cancer characteristics in women treated with supradiaphragmatic radiation for Hodgkin lymphoma: Mayo Clinic experience', *Mayo Clin Proc*, 78(6), pp. 708-15.

Walker, K., Bratton, D.J. and Frost, C. (2011) 'Premenopausal endogenous oestrogen levels and breast cancer risk: a meta-analysis', *Br J Cancer*, 105(9), pp. 1451-7.

Wang, C., Mayer, J.A., Mazumdar, A., Fertuck, K., Kim, H., Brown, M. and Brown, P.H. (2011) 'Estrogen induces c-myc gene expression via an upstream enhancer activated by the estrogen receptor and the AP-1 transcription factor', *Mol Endocrinol*, 25(9), pp. 1527-38.

Wang, P. and Jin, T. (2010) 'Oct-1 functions as a sensor for metabolic and stress signals', *Islets*, 2(1), pp. 46-8.

Wang, R.H., Yu, H. and Deng, C.X. (2004a) 'A requirement for breast-cancer-associated gene 1 (BRCA1) in the spindle checkpoint', *Proc Natl Acad Sci U S A*, 101(49), pp. 17108-13.

Wang, Z.C., Lin, M., Wei, L.J., Li, C., Miron, A., Lodeiro, G., Harris, L., Ramaswamy, S., Tanenbaum, D.M., Meyerson, M., Iglehart, J.D. and Richardson, A. (2004b) 'Loss of heterozygosity and its correlation with expression profiles in subclasses of invasive breast cancers', *Cancer Res*, 64(1), pp. 64-71.

Ward, J.F. (1985) 'Biochemistry of DNA lesions', *Radiat Res Suppl*, 8, pp. S103-11.

Watanabe, T. and Horiuchi, T. (2005) 'A novel gene amplification system in yeast based on double rolling-circle replication', *EMBO J*, 24(1), pp. 190-8.

Weil, M.K. and Chen, A.P. (2011) 'PARP inhibitor treatment in ovarian and breast cancer', *Curr Probl Cancer*, 35(1), pp. 7-50.

Weischer, M., Bojesen, S.E., Tybjaerg-Hansen, A., Axelsson, C.K. and Nordestgaard, B.G. (2007) 'Increased risk of breast cancer associated with CHEK2*1100delC', *J Clin Oncol*, 25(1), pp. 57-63.

Woodward, W.A., Chen, M.S., Behbod, F., Alfaro, M.P., Buchholz, T.A. and Rosen, J.M. (2007) 'WNT/beta-catenin mediates radiation resistance of mouse mammary progenitor cells', *Proc Natl Acad Sci U S A*, 104(2), pp. 618-23.

Wright, E.G. (2010) 'Manifestations and mechanisms of non-targeted effects of ionizing radiation', *Mutat Res*, 687(1-2), pp. 28-33.

Wu, K.J., Grandori, C., Amacker, M., Simon-Vermot, N., Polack, A., Lingner, J. and Dalla-Favera, R. (1999) 'Direct activation of TERT transcription by c-MYC', *Nat Genet*, 21(2), pp. 220-4.

Wu, S., Cetinkaya, C., Munoz-Alonso, M.J., von der Lehr, N., Bahram, F., Beuger, V., Eilers, M., Leon, J. and Larsson, L.G. (2003) 'Myc represses differentiation-induced p21CIP1 expression via Miz-1-dependent interaction with the p21 core promoter', *Oncogene*, 22(3), pp. 351-60.

Xu, J., Chen, Y. and Olopade, O.I. (2010) 'MYC and Breast Cancer', *Genes Cancer*, 1(6), pp. 629-40.

Yager, J.D. and Davidson, N.E. (2006) 'Estrogen carcinogenesis in breast cancer', *N Engl J Med*, 354(3), pp. 270-82.

Yang, J., Mani, S.A., Donaher, J.L., Ramaswamy, S., Itzykson, R.A., Come, C., Savagner, P., Gitelman, I., Richardson, A. and Weinberg, R.A. (2004) 'Twist, a master regulator of morphogenesis, plays an essential role in tumor metastasis', *Cell*, 117(7), pp. 927-39.

Yared, E., McMillan, T.J. and Martin, F.L. (2002) 'Genotoxic effects of oestrogens in breast cells detected by the micronucleus assay and the Comet assay', *Mutagenesis*, 17(4), pp. 345-52.

Yoshida, K. and Miki, Y. (2004) 'Role of BRCA1 and BRCA2 as regulators of DNA repair, transcription, and cell cycle in response to DNA damage', *Cancer Sci*, 95(11), pp. 866-71.

Zavadil, J. and Bottinger, E.P. (2005) 'TGF-beta and epithelial-to-mesenchymal transitions', *Oncogene*, 24(37), pp. 5764-74.

Zhang, L., Yang, N., Huang, J., Buckanovich, R.J., Liang, S., Barchetti, A., Vezzani, C., O'Brien-Jenkins, A., Wang, J., Ward, M.R., Courreges, M.C., Fracchioli, S., Medina, A., Katsaros, D., Weber, B.L. and Coukos, G. (2005a) 'Transcriptional coactivator Drosophila eyes absent homologue 2 is up-regulated in epithelial ovarian cancer and promotes tumor growth', *Cancer Res*, 65(3), pp. 925-32.

Zhang, Z., Gerhard, D.S., Nguyen, L., Li, J., Traugott, A., Huettner, P.C. and Rader, J.S. (2005b) 'Fine mapping and evaluation of candidate genes for cervical cancer on 11q23', *Genes Chromosomes Cancer*, 43(1), pp. 95-103.

Zhao, H., Jin, S., Fan, F., Fan, W., Tong, T. and Zhan, Q. (2000) 'Activation of the transcription factor Oct-1 in response to DNA damage', *Cancer Res*, 60(22), pp. 6276-80.

Zharkov, D.O. (2008) 'Base excision DNA repair', *Cell Mol Life Sci*, 65(10), pp. 1544-65.

Zheng, H.T., Jiang, L.X., Lv, Z.C., Li, D.P., Zhou, C.Z., Gao, J.J., He, L. and Peng, Z.H. (2008) 'Are there tumor suppressor genes on chromosome 4p in sporadic colorectal carcinoma?', *World J Gastroenterol*, 14(1), pp. 90-4.

Ziech, D., Franco, R., Pappa, A. and Panayiotidis, M.I. (2011) 'Reactive oxygen species (ROS)--induced genetic and epigenetic alterations in human carcinogenesis', *Mutat Res*, 711(1-2), pp. 167-73.

Zientek-Targosz, H., Kunnev, D., Hawthorn, L., Venkov, M., Matsui, S., Cheney, R.T. and Ionov, Y. (2008) 'Transformation of MCF-10A cells by random mutagenesis with frameshift mutagen ICR191: a model for identifying candidate breast-tumor suppressors', *Mol Cancer*, 7, p. 51.

Zindy, F., Eischen, C.M., Randle, D.H., Kamijo, T., Cleveland, J.L., Sherr, C.J. and Roussel, M.F. (1998) 'Myc signaling via the ARF tumor suppressor regulates p53-dependent apoptosis and immortalization', *Genes Dev*, 12(15), pp. 2424-33.

Zitzelsberger, H., Bruch, J., Smida, J., Hieber, L., Peddie, C.M., Bryant, P.E., Riches, A.C., Fung, J., Weier, H.U. and Bauchinger, M. (2001) 'Clonal chromosomal aberrations in simian virus 40-transfected human thyroid cells and in derived tumors developed after in vitro irradiation', *Int J Cancer*, 96(3), pp. 166-77.

Zitzelsberger, H., Hieber, L., Richter, H., Unger, K., Briscoe, C.V., Peddie, C. and Riches, A. (2004) 'Gene amplification of atypical PKC-binding PARD3 in radiation-transformed neoplastic retinal pigment epithelial cell lines', *Genes Chromosomes Cancer*, 40(1), pp. 55-9.